Basement-Cover Relationships and Regional Structure in the Transtensional Orcadian Basin

UTLEY, THOMAS,ANDREW,GUY

Durham University
Department of Earth Sciences

Basement-Cover Relationships and Regional Structure in the Transtensional Orcadian Basin

Thomas Andrew Guy Utley (MGeo)

A thesis submitted in partial fulfilment of the requirements for the degree of Doctor of Philosophy at Durham University

Department of Earth Sciences, Durham University (UK)

December 2019

Declaration

No part of this thesis has previously been submitted for a degree at this or any other university. The work described in this thesis is entirely that of the author, except where reference is made to previously published or unpublished work.

Thomas Andrew Guy Utley

University of Durham

Department of Earth Sciences

December 2019

Table of Contents

Declaration **i**

Table of Contents **ii**

Abstract **ix**

Funding **x**

Acknowledgments **x**

---

1. Chapter 1 – Introduction: **1**

1.1. Project Context and Research Rationale 1

1.1.1. Project Aims and Objectives 3

1.1.2. Thesis Outline 6

1.2. Geology of the Orcadian Basin 7

1.2.1. Regional Tectonic Setting 7

1.2.2. Pre-Devonian Basement and Caledonian Igneous Rocks 11

1.2.2.1. Scottish Mainland 11

1.2.2.2. Orkney 18

1.2.2.3. Shetland 18

1.2.3. Devonian Old Red Sandstone 24

1.2.3.1. Stratigraphy and Paleoclimate 24

1.2.3.2. Mainland Scotland 27

1.2.3.3. Orkney 31

1.2.3.4. Shetland 32

1.2.4. The Evolving Models of Devonian Basin Development 33

1.2.5. Post Devonian Geological History 38

1.2.5.1. Mainland Scotland 38

1.2.5.2. Orkney and Shetland 38

1.3. The Clair Field 39

1.3.1. The Geology and Tectonic Evolution of the Clair Field and Clair Basin 41

1.3.2. Precambrian Basement 42

1.3.3. Devonian-Carboniferous Clair Group 45

1.3.4. Post Devonian Geology 50

1.3.5. The Clair Field as a fractured reservoir 51
1.3.6. Clair Field Analogue Research 53
2. Chapter 2 - Techniques and Methodology – a multiscale analysis: 55
2.1. Regional to sub-regional scale analysis – Remote Sensing, Desk Studies and GIS data collation 57
2.1.1. Published maps and other datasets 57
2.1.2. Photogeology and Lineament Analysis - DEM/DTM (Digital Elevation Models/Digital Terrain Models) and Bathymetry 58
2.1.3. Regional Scale Geophysics 60
Structural Analysis 61
2.1.4. Fold Profile Construction: Down Plunge Projection Method 61
2.2. Sub-regional to outcrop scale – Field Based Techniques 62
2.2.1. Field mapping, structural data and sample collection 62
2.2.2. Virtual Outcrop Models 63
2.2.2.1. Development of the Photogrammetric Workflow 64
2.2.2.1.1. Principles of Photogrammetry 64
2.2.2.1.2. Equipment and Software 65
2.2.2.2. Virtual Outcrop Model Workflow 67
2.2.2.2.1. Acquisition 68
2.2.2.2.2. Processing 79
2.2.2.3. Geological Analysis 73
2.2.3. Paleostress Inversion Techniques 75
2.2.4. Fracture Network Analysis 76
2.3. Macro to microscopic scale – laboratory studies 77
2.3.1. Thin section analysis 77
2.3.2. QEMSCAN Analysis 78
2.3.3. Heavy Mineral Analysis 78
2.3.4. Detrital Zircon Geochronology 78
2.4. Key Definitions and geological concepts 79
2.4.1. Geological Contacts and Cross Cutting Relationships 79
2.4.2. Foliations and Lineations 81
2.4.3. Folds 82
2.4.4. Faults, fractures and joints 83

2.4.5. Fault Classification 86
2.4.6. Fault Zone Architecture and Genesis 88
2.4.7. Fault Rocks 91
2.4.8. Deformation Bands 94
2.4.9. Veins and Dykes 95
2.4.10. Kinematic Indicators 96
2.4.11. Structural Reactivation 99
2.4.12. Transtension, Transpression and Oblique Tectonics 102
2.4.13. The Recognition of Transtensional Basins 107

3. Chapter 3– The development of the Devonian Clair Basin, West of Shetland: Insights from Foula, Shetland, an onshore analogue for the Clair Oil Field. 109

Abstract 110

3.1. Introduction - The Clair Oil Field 111
3.2. Regional Framework 113
3.2.1. The Orcadian Basin in Shetland 113
3.2.2. The Clair Basin 117
3.3. The Geology of Foula 119
3.3.1. Introduction and Methodologies 119
3.3.2. Metamorphic Basement and Minor Intrusions 122
3.3.3. Foula Sandstone Group 126
3.3.3.1. Da Ness Formation 126
3.3.3.2. Soberlie Formation 127
3.3.3.3. Blobersburn Formation 128
3.3.3.4. Sneug Formation 129
3.3.3.5. Daal Formation 129
3.3.3.6. Noup Formation 130
3.3.4. Structural Geology 130
3.3.4.1. Structures in Basement Rocks 131
3.3.4.2. Basement-Cover Relationships 133
3.3.4.3. Structures in Devonian Rocks 138
3.3.4.3.1. Faulting and Fracturing 138
3.3.4.3.2. Folding 140

3.4. Geological evolution of the Foula Sandstone Group 142
3.4.1. Basin initiation and evolution 142
3.4.2. Paleostress analysis 143
3.4.3. The age, provenance and detrital zircon geochronology of the Foula Sandstone Group 146
3.5. Discussion 151
3.5.1. Regional tectonics and paleogeography 151
3.5.2. Implications for ORS Basin Development 154
3.5.3. Implications for the Clair Basin and Clair Oil Field 157
3.5.4. Implications for wider resource development 158
3.6. Conclusions 159
4. Chapter 4 – A reappraisal of Devonian Basin Evolution and Basement-Cover Relationships in NE Scotland and Shetland: Analogues for the offshore Clair Oil Field, West of Shetland, UK. 161
Abstract 161
4.1. Introduction 163
4.2. Regional Framework 165
4.2.1. The Orcadian Basin 165
4.2.2. The Clair Basin 169
4.3. Methodologies 169
4.4. Basement-Cover relationships in the Orcadian Basin 170
4.4.1. Shetland 170
4.4.1.1. Western Shetland Basin 172
4.4.1.1.1. Melby and Papa Stour 173
4.4.1.1.2. Eshaness Peninsula 178
4.4.1.1.3. Western Shetland Basin Summary 179
4.4.1.2. Walls Basin 183
4.4.1.2.1. Folding 185
4.4.1.2.2. West Burra Firth and Snarra Ness 188
4.4.1.2.3. Brindister Voe to the Ward of Hostigates 192
4.4.1.2.4. Walls Basin Summary 194
4.4.1.3. South-Eastern Shetland Basin 195

4.4.1.3.1. Folding 196
4.4.1.3.2. Rova Head and Lerwick 199
4.4.1.3.3. Voe of Sound 203
4.4.1.3.4. East Voe of Quarff 204
4.4.1.3.5. Ocraquoy 207
4.4.1.3.6. Southern Shetland 208
4.4.1.3.7. South Eastern Shetland Basin Summary 209
4.4.2. Orkney 209
4.4.2.1. Stromness 212
4.4.2.2. Yesnaby 215
4.4.2.3. Regional Summary of Basement/Cover in Orkney 217
4.4.3. NE Scotland 219
4.4.3.1. Kirtomy Bay 221
4.4.3.2. Portskerra 224
4.4.3.3. Sarclet 227
4.4.3.4. Braemore-Scaraben and Berriedale-Ousdale Synclines 231
4.4.3.5. Strathpeffer Syncline 233
4.4.3.6. Scarfskerry 234
4.4.4. Devonian Outliers and other examples of basement/cover in the Orcadian Basin 238
4.5. Discussion 243
4.5.1. Devonian Basin Evolution 243
4.5.1.1. Shetland 243
4.5.1.2. Orkney 245
4.5.1.3. NE Scotland 246
4.5.1.4. Regional Synthesis 246
4.5.2. Diversity of Basement-Cover Relationships 247
4.5.3. Implications for Resource Development and the Clair Oil Field 251
4.6. Conclusions 253

5. Chapter 5 – An onshore-offshore interpretation of structures in the Devonian rocks of the Caithness/Orkney region of North-East Scotland, UK: Insights from the seabed geomorphology and onshore exposures of the Pentland Firth. 255

Abstract 256

5.1. Introduction 257

5.2. Regional Framework 260

5.3. Bathymetric Data and Methods 263

5.4. The Geology and Submarine Geomorphology of the Pentland Firth 265

5.4.1. Description of Seabed Morphology 265

5.4.2. Stratigraphy 268

5.4.2.1. Onshore 268

5.4.2.2. Offshore 268

5.4.3. Structural Geology 270

5.4.3.1. Folding 271

5.4.3.2. Faulting and Fracturing 274

5.4.3.3. Topology 280

5.5. Fieldwork 282

5.5.1. Brough-Brims-Risa Fault Zone 282

5.5.2. Faulting and Folding 285

5.5.3. Onshore Fracture Networks and Topology 291

5.6. Discussion 294

5.6.1. Structural Evolution 294

5.6.2. Comparison of Fracture Networks 296

5.6.3. Resource Implications 298

5.7. Conclusions 300

6. Chapter 6 – Discussion, Conclusions and Future Work: 301

6.1. Discussion 303

6.1.1. Implications for Devonian Basin Development 301

6.1.2. Suitability of the Orcadian Basin as an analogue to the Clair Basin 311

6.1.3. Implications for the Clair Oil Field and wider resource development 312

6.1.4. Implications for other basins and geological settings 315

6.2. Conclusions 316

6.3. Future Work 318

References **321**

Appendices **343**

Appendix A **345**

- Conference Abstracts and Presentations
- HTML code for ESRI Storymaps

Appendix B **361**

- Exploration, Appraisal and Development History of the Clair Oil Field
- Overview of previous Clair Field Analogue Studies
- References

Appendix C **379**

- Sample Information, Data Tables, Analytical Results and Other Methods

Abstract

Geological evidence suggests that the Orcadian Basin, a thick development of Devonian age continental facies, comprising alluvial, fluvial, lacustrine and aeolian deposits, is analogous to the Clair Group which developed in the smaller, offshore Clair Basin. Studies for the Clair Group to date have focussed on the predominantly fluvial-lacustrine rocks of the central Orcadian Basin in Caithness and Orkney. However, alternatives exist in Shetland and around the margins of the Orcadian Basin which are of a closer affinity to the predominantly fluvial-alluvial rocks of the Clair Group.

Detailed field studies and structural analysis of basement-cover contacts and the overlying Devonian sedimentary sequences were undertaken in Shetland, Orkney and NE Scotland, in order to understand the scale, geometry and distribution of structures, and as an analogue to equivalent features in the subsurface, at sub-seismic to outcrop scales. This was supplemented by the integration of legacy and new multiscale data (topographic, bathymetric, geological and geophysical) and the production of photogrammetric 3D Virtual Outcrop Models.

A diverse range of basement/cover relationships occurs both spatially and temporally in the basin, together with synchronous Middle Devonian syn-sedimentary faulting and growth folding, as observed on Foula. Thus, some folds interpreted as Permo-Carboniferous inversion structures may have instead initiated earlier, as Devonian growth folds. These folds, together with the large-scale structural geometries of the basins in Shetland are consistent with models of regional constrictional strain, related to sinistral transtension along the Walls Boundary and Great Glen Fault Zones during the Middle Devonian. Analysis of high-resolution bathymetric data from offshore Caithness/Orkney has provided new insights into the distribution and scale of structures in the Orcadian Basin that are poorly exposed onshore, with kilometre-scale folds and numerous faults and fracture zones being mapped for the first time. Provenance studies indicate that Foula and Melby in Western Shetland show a stronger affinity with the Clair Group and Orkney successions, suggesting a large, linked depositional system with Foula representing a transitional region located between the Clair and Orcadian basins. These findings suggest that the Devonian basins of Western Shetland and marginal areas of the Orcadian Basin are suitable analogues to the Clair Basin. Models of Devonian basin development used offshore should also consider the role of strike-slip tectonics and sinistral transtension during basin evolution.

Funding

The work contained in this thesis contains work carried out during a PhD study undertaken as part of the Natural Environment Research Council (NERC) Centre for Doctoral Training (CDT) in Oil & Gas [grant number NEM00578X/1] and was funded by Durham University, whose support is gratefully acknowledged. The work was undertaken in the Department of Earth Sciences at Durham University and the underpinning financial, administrative, laboratory and computer support is gratefully acknowledged.

Acknowledgements

My most heartfelt thanks go to my wife, Rachel. You have been through it all with me, the ups and downs and without your unwavering support and love throughout, it would not have been possible to do it! Thank you!

I would next like to thank my supervisory team particularly Bob for your guidance, and support (the purchase of a drone was appreciated and very helpful!). I also would like to thank Ken, Eddie and Rob for all your help, enthusiasm and support. Thank you all for reading the various iterations of my thesis, abstracts, presentations and assorted drafts of other things, coming into the field and ultimately, getting me to the end!

My thanks must also go all of those who have shared my time at Durham, especially for the cups of tea and endless cake! I'd especially like to thank the following past and present members of the Department of Earth Sciences for all of your friendship and advice over the years: Illaria Gaiani, Sarah Clancy, Elizabeth Atar, Sean O'Neill, Olly Sanford, Erin Scott, Matt Funnell, Charlotte Withers, Fienke Nanne, Kit Hardman, Pavlos Farangitakis, Tim Armitage, Miles Wilson, Alex Peace, Jordan Phethean, Cat Hirst, Bob Jamieson, Adam Robinson, Natalia Wasielka, Jack Lee, Chris Ward, Chris Harbord, Edward Inglis, Alex Tamas, Katharine Groves, Eloise Bretagne, Max Franzel, Nico Schliffmaster, Emma Gregory, Kate Heerema, Tom Phillips, Jonny Imber, Dave Selby, Stuart Jones, Mark Allen and Jon Gluyas.

I am grateful to the Clair Joint Venture Group for the ongoing support into research at Durham University and for providing funding for sample preparation and analysis. I'm also grateful to BP for provision of, and permission to publish imagery examples from their archives. My thanks go in particular to Steve Dee, Dave Ashby and Jessica Miller and the

whole of the BP Sunbury STC team for all their help and guidance during my internship and to Hugh Nicholson and the Clair Team in the Aberdeen office for their continued interest in this research.

I would like to thank Shell and TGS for seismic data, to Schlumberger for the donation of Petrel seismic interpretation software licences to Durham University, to ESRI for ArcGIS software licences and to David Hodgetts of Manchester University for the VRGS software licence. I'd like to acknowledge the UKOilandGasData.com website owned by Common Data Access (CDA) administered by Schlumberger, for access to the seismic data volumes and released UK well database and the Oil and Gas Authority (OGA) for offshore data files. I would also like to acknowledge the EDINA Digimap service, the Ordnance Survey, the BGS and Canmore (Historic Scotland) for the provision of basemaps, aerial imagery and topographic information

My brother, James Utley and old boss Richard Worden of Liverpool University are thanked for doing QEMSCAN analysis and being a sounding board for geological ideas and encouraging me to pursue a PhD in the first place. Alja Sasnowski is thanked for sharing her knowledge and parts of her unpublished PhD thesis and Andy Morton is thanked for his assistance and guidance in the world of sediment provenance. My thanks go to Ian Chaplin for the preparation of thin sections to an extremely high standard and Gary Wilkinson is thanked for his assistance with all things data and GIS related. Anna Bird is also thanked for the crash course in zircon geochronology!

A special thanks must go to Anna Clark, Lorna Morrow and John Underhill for the continued support and provision of a world class training scheme to go alongside my academic research as part of the NERC Centre for Doctoral Training in Oil and Gas. The scheme has allowed to me learn so much more, broaden my knowledge and allow my research to go where it required without the financial restrictions research so often comes up against. I also can't forget all my fellow CDT members for sharing this experience with me. I am very lucky to be able call you not only colleagues, but now, lifelong friends.

My thanks must also go to Magnus Holbourn and the residents of Foula for their hospitality and generosity during my time on their island, to Calum Fraser for his assistance with drone photography and Jim and Richard Scott and the crew of LK241 for the use of their boat. Jim Henderson is also thanked for his continued interest and assistance in this project and for rustling up some tasty food!

My penultimate thanks must go to my Sixth Form tutor Julia Stanton, who took a chance on me and encouraged me to pursue my interest in the natural world, to do an A-Level in geography and took me to the mountains of Snowdonia on fieldwork, where I made the decision that I needed to find out how they got there!

My final thanks go my parents who should not be forgotten for instilling an interest in the natural world in me and encouraging and supporting me in all I have done!

Thank you all!

Chapter 1

Introduction

Chapter 1 – Introduction:

1.1. Project Context and Research Rationale:

The hydrocarbon industry continually seeks to improve how reservoirs are characterised and modelled, meaning that onshore, surface analogue studies are still a fundamental way of better understanding the subsurface. The use of suitable analogues allows better characterisation and understanding of rock properties and geometric relationships, improves interpretations of geophysical and petrophysical data and ultimately leads to a more complete understanding of how fluids may behave in the subsurface.

With the continued development of the Clair Field and the development of Clair Ridge during 2015-9, an improved understanding of the Lower Clair Group and its unconformity with the underlying crystalline basement is now required, where the role of faults and fractures will be key to production.

The onshore, broadly extensional, Orcadian Basin has long been used as the classic analogue for the Clair Basin and Clair Oil Field, West of Shetland. They share many similarities, for example, in that they are same age, comprise similar lithology sequences, and have similar fracture networks, fills and fracture types. There are also differences, namely that the Orcadian Basin formed as a separate basin to the Clair Basin, and in a possibly different tectonic setting due to proximity of the former to the Great Glen-Walls Boundary Fault. Furthermore the age of the main hydrocarbon-bearing fractures in the Orcadian Basin are of a different age (Permian onshore vs Mesozoic-Cenozoic offshore), and the source of hydrocarbons are different (Devonian vs Jurassic)(Dichiarante, 2017; Dichiarante et al., 2016; Witt et al., 2010).

With ongoing drilling on Clair, a planned 3rd phase of development with Clair South, other near field exploration, coupled with a number of other significant developments West of Shetland, any advances in the understanding of the structural and sedimentological evolution of the Clair Group and its unconformity with the basement gleaned from analogue research will benefit industry and allow it to make better informed, safer and lower risk decisions.

1.1.1. Project Aims and Objectives:

This project is a reappraisal of the stratigraphy, structure and tectonic evolution of potential alternative onshore analogues to Clair, using the Devonian basins/sub-basins of the Fair Isle-Shetland-Foula region (

Figure 1.1). Analogue studies to date have focused on the NW Highlands and Outer Hebrides as analogues for the Rona Ridge and Clair Basement, and in the Caithness/Orkney region as analogues for the Clair Group.

This study builds on preliminary work carried out during the 1980's and 1990's and on a series of more recent Clair JVG sponsored and supported research, in particular the most recent work of Dichiarante (2017) who established a well constrained and detailed geological history for the Orcadian Basin. Observations are integrated with and compare to the better studied Devonian basins/sub-basins of Caithness-Orkney-Moray Firth region which together are being studied as an analogue for the role of Palaeozoic tectonics during basin development and later Mesozoic reactivation.

The principal aims of this project are:

1. To reappraise the development of the Devonian sedimentary basins in mainland Scotland and Shetland with a focus on the region closest to the Clair Oil Field, i.e. Foula-Shetland. Sampling will be undertaken to determine the provenance and age of the Devonian sequences of Foula and Western Shetland.
2. Undertake detailed field studies of exposed basement-cover contacts and the structure of the overlying sandstone-dominated sequences exposed in large coastal sections throughout the Orcadian Basin in NE Scotland, Orkney and Shetland, in order to better predict the nature of these contacts in the subsurface.
3. Understand the type, scale and distribution of structures in the Orcadian Basin and improve the understanding of sub-seismic and field scale structures.
4. Further develop the structural model proposed by Dichiarante (2017) in other parts of the Orcadian Basin in particular, the evaluation of the role of strike-slip tectonics during Devonian basin development.

Findings will be compared to and contrasted with previous analogue studies and models which concern the stratigraphic and structural architecture of the Clair field and its regional tectonic setting.

Field studies are supplemented with the use of photogrammetry to capture the geology of key localities and allow for analysis of structures in difficult to access areas and develop 3D Virtual Outcrop Models (VOMs) of the stratigraphy and structure in order to extract geological information and enhance traditional fieldwork.

Implications for Palaeozoic hydrocarbon systems are explored and put into the context of the OGA's (Oil and Gas Authority) MER (Maximising Economic Recovery) policy, with a particular focus being how underdeveloped areas and aspects of the UKCS petroleum system may be better explored and ultimately exploited.

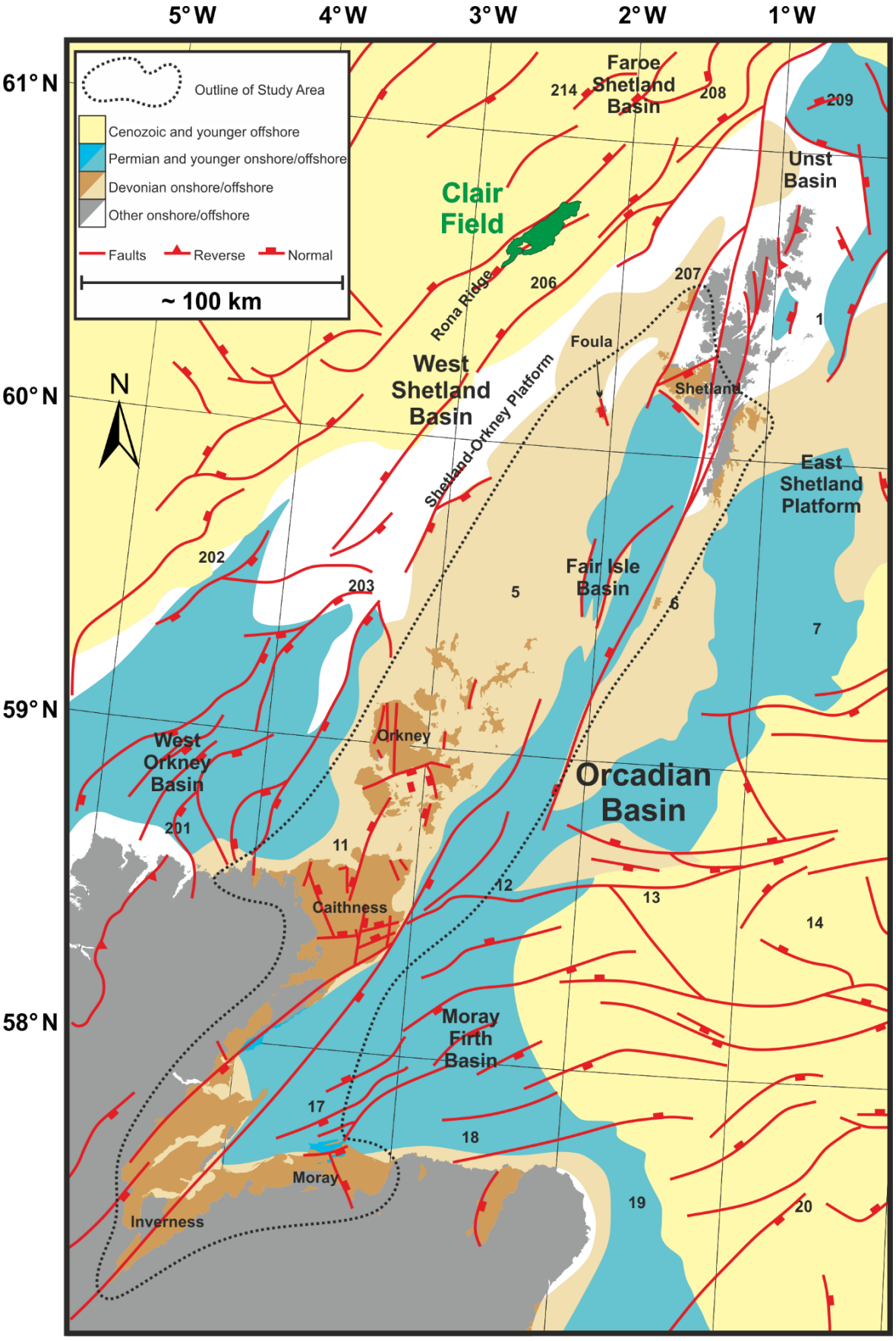

Figure 1.1: Regional geological map of the Orcadian Basin and project study area showing major structures and sub-basins. Note proximity of the island of Foula to the Clair Field. Modified *after* Dichiarante et al., (2016) and Oil and Gas Authority, (2019).

1.1.2. Thesis outline:

Some chapters are standalone manuscripts that have been published and/or will be submitted to peer-reviewed journals. As a result, there is some overlap in the content, as each chapter contains a separate abstract, introduction, a geological setting, the specific data being presented, discussion and conclusions. Each of the published/submitted chapters has been written with several co-authors, however I am the first author and am responsible for primary data collection, interpretations and manuscript writing. Some of the following material has been presented at national and international conferences (see Appendix A).

The following is a description of chapters one to six and the appendices:

- Chapter 1 covers background to the project, the research aims and an overview of the regional geology of the study area and the Clair Field.
- Chapter 2 is an overview of the datasets and key methodologies used and developed during this study. This is followed by a short overview of key definitions and relevant geological concepts.
- Chapter 3 is detailed study of the geology of the island of Foula, a possible analogue for Clair Ridge. New geochronological and provenance data is presented alongside primary field observations and structural analysis. The implications for Devonian basin development, regional tectonics and the Clair Oil field are discussed.
- Chapter 4 builds on the detailed work done on Foula and describes the variety of basement/cover relationships exposed onshore more regionally and explores the role of transtension during the development of the Devonian Basins of Northern Scotland and Shetland. Field data is supplemented with Virtual Outcrop Models to re-examine onshore analogues that have been previously studied. Observations are set in the context of the implications these may have for the evolution of the onshore and offshore Devonian basins and for hydrocarbon exploration, appraisal and development.
- Chapter 5 uses offshore bathymetric and seismic datasets in conjunction with fieldwork and Virtual Outcrop Models to help understand the scale and range of structures in the Orcadian Basin. This study focuses on the geology of the Pentland Firth and links the offshore geology to its immediate onshore equivalent which is

better studied. The implications for offshore petroleum systems, reservoir development and Devonian basin evolution are explored.

- Chapter 6 links the preceding chapters, drawing together key themes and outcomes. In particular, the role of transtension during basin development, the range of basement/cover relationships, and the influence of major strike-slip faults in controlling Devonian paleogeography are discussed. Similarities and differences to existing models of basin development are also explored and the observations made during this study are integrated with these existing models. The conclusions of this study are set in the context of the influence they may have for the appraisal of hydrocarbon resources offshore and for the continued development of the Clair Oil Field. Avenues of enquiry for future work that went beyond the remit/timescale of the project are also presented.
- Appendices containing key supplementary material:
    - Appendix A – Abstracts for conference presentations, talks, posters, fieldtrips. Extracts of HTML code used for presentations. An overview of CDT training undertaken.
    - Appendix B – A review of previous Clair Field analogue studies and a summary of the history of the Clair Field.
    - Appendix C – Data tables, analytical results, results of structural analysis and methodologies for other research that was undertaken.

1.2. Geology of the Orcadian Basin:

1.2.1. Regional Tectonic Setting:

The margins of the North Atlantic adjacent to Northern Scotland, preserve a series of Paleozoic sedimentary basins that developed following the sinistral oblique continental collision of Laurentia, Baltica and Avalonia (Marshall et al., 2003; Ziegler, 1988) as a result of the closure of the Iapetus Ocean (Figure 1.2).

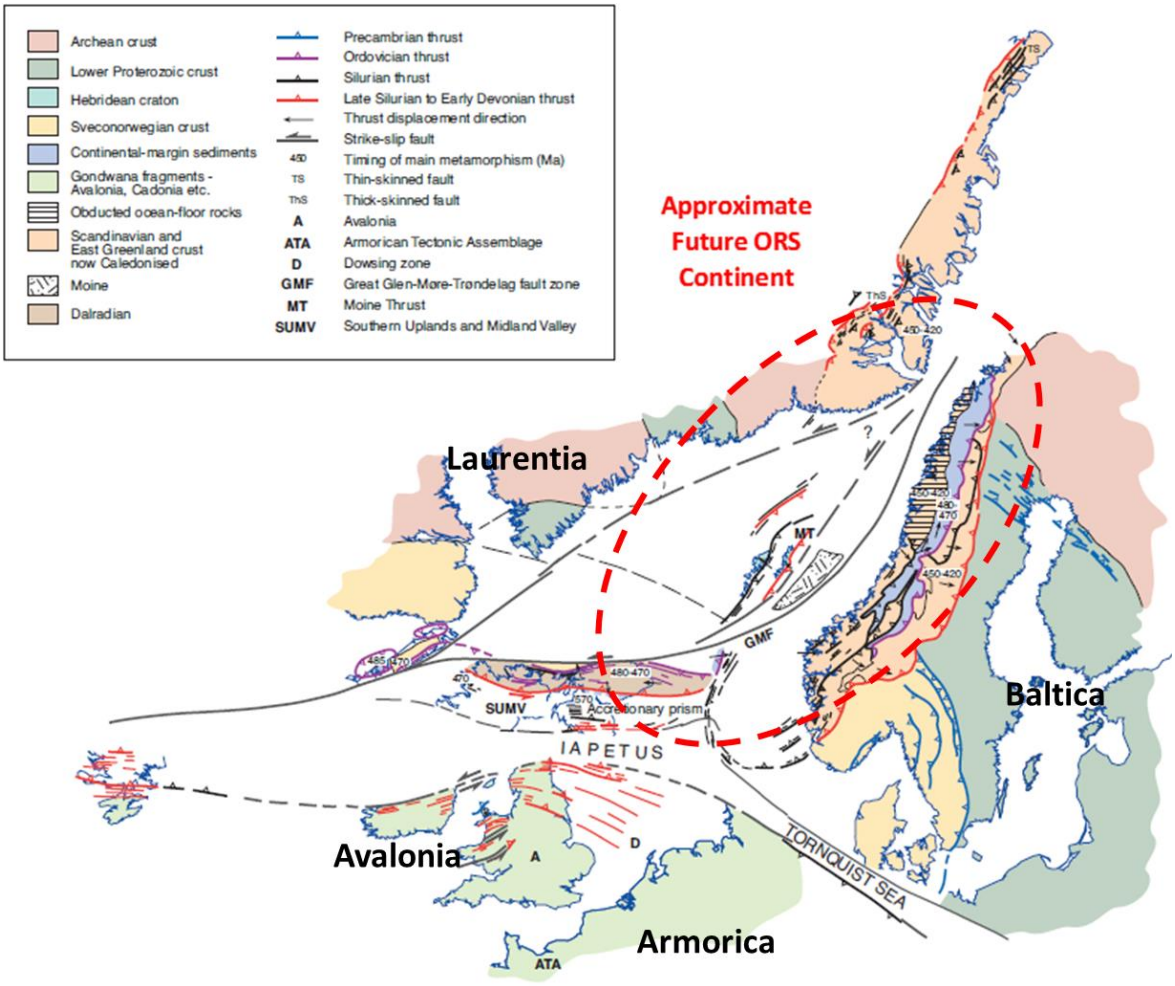

Figure 1.2: Palinspastic map of the Caledonides. Modified *after* Marshall et al. (2003) and references therein. Map shows the approximate position of future ORS continent with reference to the tectonic framework of the North Atlantic at 430Ma and the various basement terranes that were juxtaposed during the Caledonian orogeny.

During closure, a series of orogenic events occurred, including the Caledonian orogen, which led to the formation of the 'Old Red Sandstone' (or ORS) continent during the Silurian and Early Devonian. Following the gravitational collapse of the orogenic belt, coupled with significant left-lateral displacement along major strike-slip faults, a series of arid to semi-arid marginal marine and intra-continental sedimentary basins developed, into which the material being shed from the eroding mountain belt was deposited, e.g. the Orcadian Basin (Figure 1.3). A structural grain imposed on the metamorphic basement during this process has had a strong control on the subsequent structural evolution of the region and is reflected in regional geophysical surveys (Figure 1.4) (Stoker et al., 1993).

The Orcadian Basin is a thick development of Devonian age (Old Red Sandstone or ORS) continental facies, which are predominantly composed of alluvial, fluvial, lacustrine and

aeolian deposits. These sediments were deposited in a series of smaller sub-basins which eventually coalesced to form the much larger Orcadian basin which extended some 600km from Northeast Scotland to the West coast of Norway and as far as Eastern Greenland. The evolving basin was strongly influenced by several major strike-slips faults (the Great Glen Fault Zone, Walls Boundary Fault Zone, and More-Trøndelag Fault Zone) which together accommodated many tens if not hundreds of kilometres of sinistral displacement during its development (Watts et al., 2007 and references therein).

Following the deposition of the Orcadian Basin, a series of pulsed rifting events took place during the Paleozoic, Mesozoic and Cenozoic which would form the North Sea Basin and Atlantic Ocean (Stoker et al., 1993).

Remnant deposits of the Orcadian Basin are now found onshore in the UK in Northern Scotland, around the margins of the Inner Moray Firth, and on the island archipelagos of Orkney and Shetland (Figure 1.3). Deposits also occur onshore in Western Norway, and in Eastern Greenland and have been encountered offshore on the UK and Norwegian continental shelves where they for form the reservoir for numerous oil and gas fields.

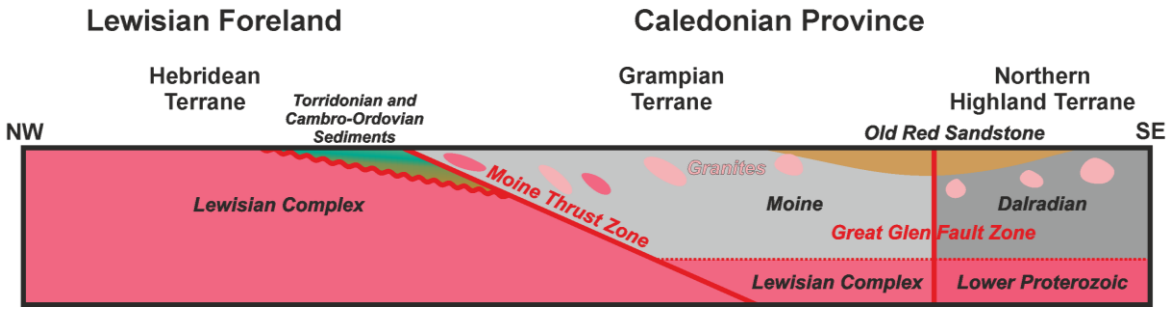

Figure 1.3: Simplified cross section through the Northern Scottish Highlands showing basement terranes and key structures. Modified *after* Stoker et al., (1993)

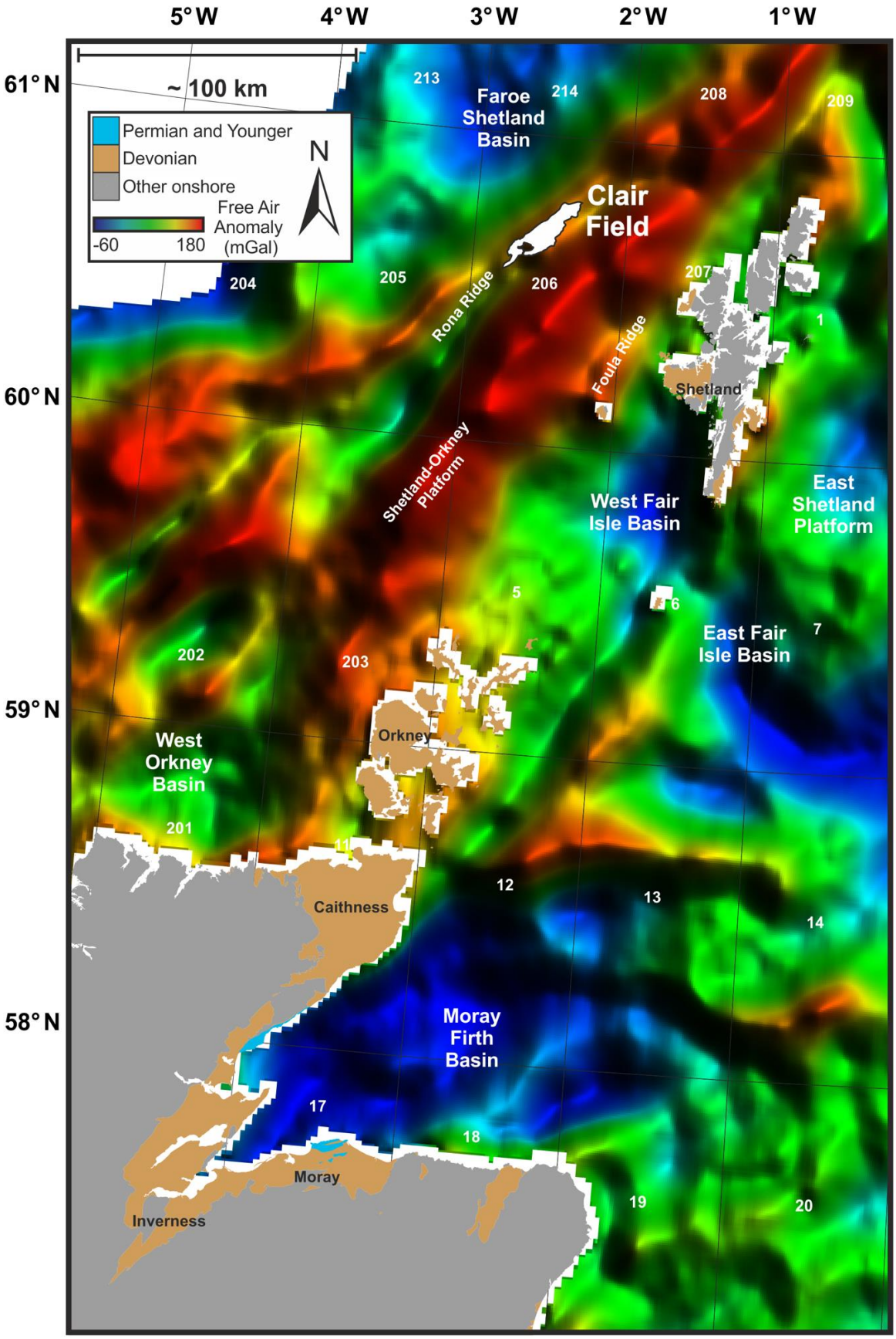

Figure 1.4: Free Air Gravity Anomaly for the study area. Note the strong NE/SW fabric picked out by positive gravitational anomalies highlighting ridges of metamorphic basement (Modified *after* Getech, 2017).

1.2.2. Pre-Devonian Basement and Caledonian Igneous Rocks:

1.2.2.1. Scottish Mainland:

A variety of Pre-Devonian basement rocks underlie and are exposed within, and around the margins of the Orcadian Basin, which reflect the diversity of lithological units that were brought together during the Caledonian Orogeny. The metamorphic basement that underlies the Orcadian Basin is exposed in the inland upland areas of Northeast Scotland within the counties of Sutherland, Caithness, Ross and Cromarty, Inverness-shire, Nairn Banffshire, Moray and Aberdeenshire (Figure 1.5).

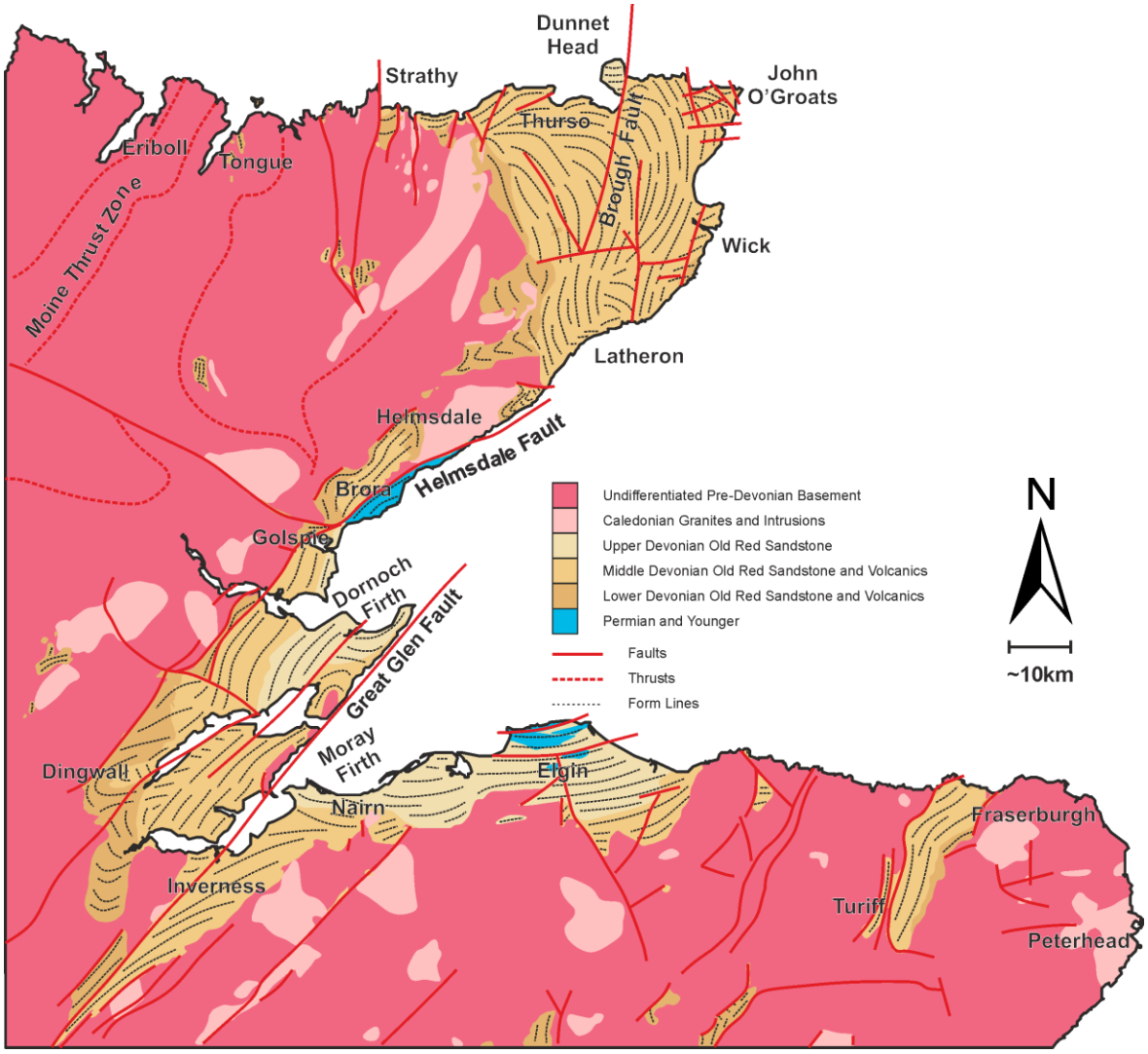

Figure 1.5: Schematic geological map of Caithness, Sutherland and the Moray Firth, showing the extent of ORS deposits and key structural features. Modified *after* (Trewin and Hurst, 2009).

Two major basement terranes are separated by the Moine Thrust Zone (MTZ), an important tectonic boundary which has been traced offshore for some distance (Blumstein et al., 2005; Holdsworth et al., 2007; Ritchie et al., 1987a; Searle et al., 2019) (Figure 1.4 and 1.6).

Further to the West, in what was the foreland to the Caledonian orogeny, rocks of the Lewisian Complex or their age-equivalents are exposed (Holdsworth et al. 2018). In the East, rocks of the Moine Supergroup are exposed in what was the hinterland to the orogeny. The Moine rocks are bound in the East by the Great Glen Fault Zone (GGFZ), a major crustal scale transcurrent fault. This fault system initiated in the mid-Silurian with at least 200km of sinistral offset during the Devonian followed by several punctuated dextral movements during the Palaeozoic and Mesozoic. The GGFZ also marks in part the boundary with the Dalradian basement units of the Grampian Highlands. Overlying the Moine and Grampian rocks are the sediments of the Orcadian Basin (Friend et al., 2000; Seranne, 1992).

The Lewisian Gneiss Complex (Figure 1.6) is a residual fragment of the Laurentian-Greenland continental craton and is comprised of orthogneisses, acid to ultrabasic intrusives and metasediments (Ritchie et al., 2011 and references therein). It is Archean to Proterozoic in age and represents a series of metamorphic terranes that were brought together by approximately 1.7Ga (Johnstone and Mykura, 1989). The Lewisian likely continues to the North of Scotland and West of Shetland but appears to lack any evidence for Proterozoic reworking (Holdsworth et al. 2018).

Figure 1.6 (overleaf): Geological map of the Northwest Highlands showing the Moine Supergroup and Lewisian Gneiss Complex of Northwest Scotland; inset shows location on a larger scale. Abbreviations: LE, Loch Eriboll; T, Tongue; MT, Moine Thrust; NT, Naver Thrust; ST, SwordlyThrust; LB, Loch Borrolan; D, Durcha; OB, Oykell Bridge; CCG, Carn Chuinneag Granite; F, Fannich; CG, Carn Gorm;Sc, Scardroy; SBT, Sgurr Beag Thrust; LM, Loch Monar; Av, Avernish; Dr, Druimnadrochit; FAGG, Fort Augustus Granite Gneiss; G, Glenelg; K, Kinlochourn; SB, Sgurr Breac; L, Lochailort; Ar, Ardnish; LE, Loch Eilt; AGG, Ardgour Granite Gneiss; GSM, Glen Scaddle Metagabbro; Ad, Ardnamurchan; SM, Sound of Mull; RM, Ross of Mull. (Strachan et al., 2010).

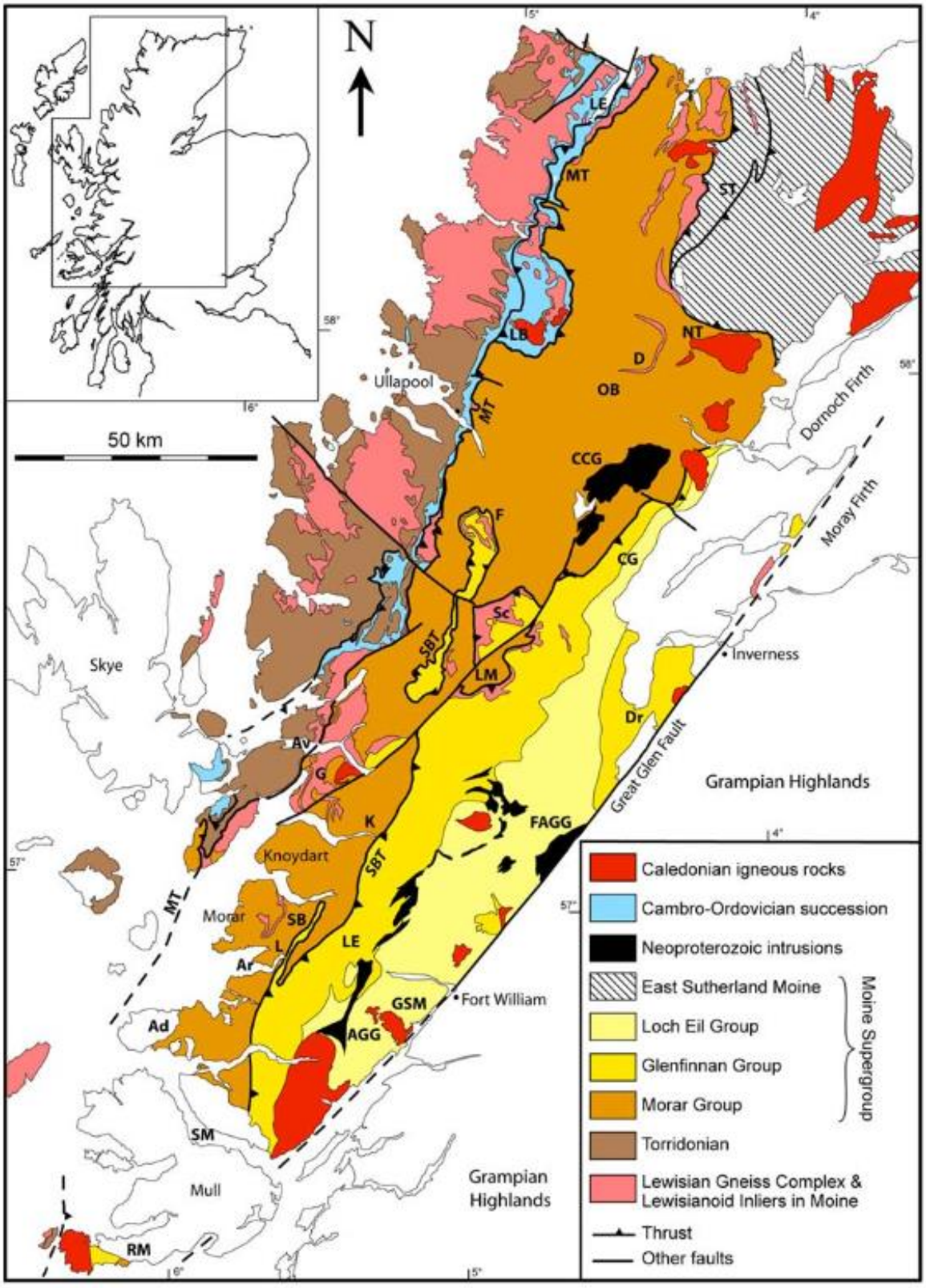

The Lewisian in Scotland is unconformably overlain by the Upper Proterozoic Torridonian Supergroup, which comprises coarse grained continental arkosic sandstones and conglomerates. These are unconformably overlain by Cambro-Ordovician shallow marine carbonates and quartzites. These sediments are largely undeformed and are generally

horizontal to sub-horizontally bedded except within the Moine Thrust Zone where they locally intensely folded and imbricated by thrusting (Parnell et al., 2018).

The Moine Supergroup comprises three major thrust nappes (Holdsworth et al. 1994) of Neoproterozoic (1000-870Ma) amphibolite facies metasedimentary psammitic and pelitic schists, as well as some minor basic and granitic intrusions (Figure 6). These rocks underwent widespread deformation and metamorphism within the core of the orogenic belt and are highly deformed. Three main phases of deformation have been identified; at ~800Ma, ~475-460Ma and ~435-415Ma associated with intense Northwest verging thrusting and folding (Strachan et al. 2010). They have a strong North-South to Northeast-Southwest trending tectonic fabric which dips 15° to the East close to the MTZ but steepens to near vertical further East. Shortening in the Moine is in the order of 100's of kilometres and was likely only a few kilometres thick (Barr et al., 1986). Inliers of Archaean basement within the Moine, e.g. the Strathy Complex, are thought to represent interleaved tectonic slices of the metamorphic basement – possibly Lewisian gneisses - onto which the Moine rocks were deposited (Friend et al., 2008; Strachan, 2003). An extensive review of Moine geology can be found in Strachan et al., (2010).

The Dalradian Supergroup is a ~25km thick Neoproterozoic to early Palaeozoic, heterolithic succession of variable metamorphosed sedimentary and igneous rocks (Cawood et al., 2003; Prave, 1999; Strachan et al., 2013). It is dominated by marine siliciclastic rocks, variable proportions of carbonates and some volcanic rocks. It is locally highly deformed, but sedimentary structures are widely preserved and form the basis for the regional lithostratigraphy.

Throughout the Highlands, a series of Silurian-Devonian granites were emplaced (Lancaster et al., 2017; Lundmark et al., 2018) (Figure 1.7). These granites are thought to be related to the subduction and closure of the Iapetus Ocean, with some emplaced during thrusting and orogenesis. Some younger granites are attributed to later transtension (Lundmark et al., 2018). These granites often underpin localised basement highs, forming rigid and buoyant 'blocks' within the sedimentary basins developed offshore (Donato et al., 1983).

In the basement closest to the onshore margin of the Orcadian Basin, two major granites; the Strath Halladale Complex and Helmsdale Granite are found. The Strath Halladale Complex is a sheeted granite complex that discordantly cuts through the Skinsdale Thrust

Sheet (Kocks et al., 2006). It is dated to 426 Ma (Kocks et al., 2006) and was emplaced during thrusting as evident by reworking of the magmatic foliation. The Helmsdale Granite is fairly representative of many of the granites emplaced during the Caledonian orogeny (Trewin and Hurst, 2009). It was likely emplaced along the line of the Helmsdale Fault, a splay of the Great Glen Fault Zone and is dated to be between 390-420 Ma (BGS, 1998), although the older age is considered more likely as the sedimentary breccia immediately overlying the granite is dated to ~390Ma and comprises k-feldspar phenocrysts derived from the granite indicating that the granite was exhumed before subsequent burial during the Devonian.

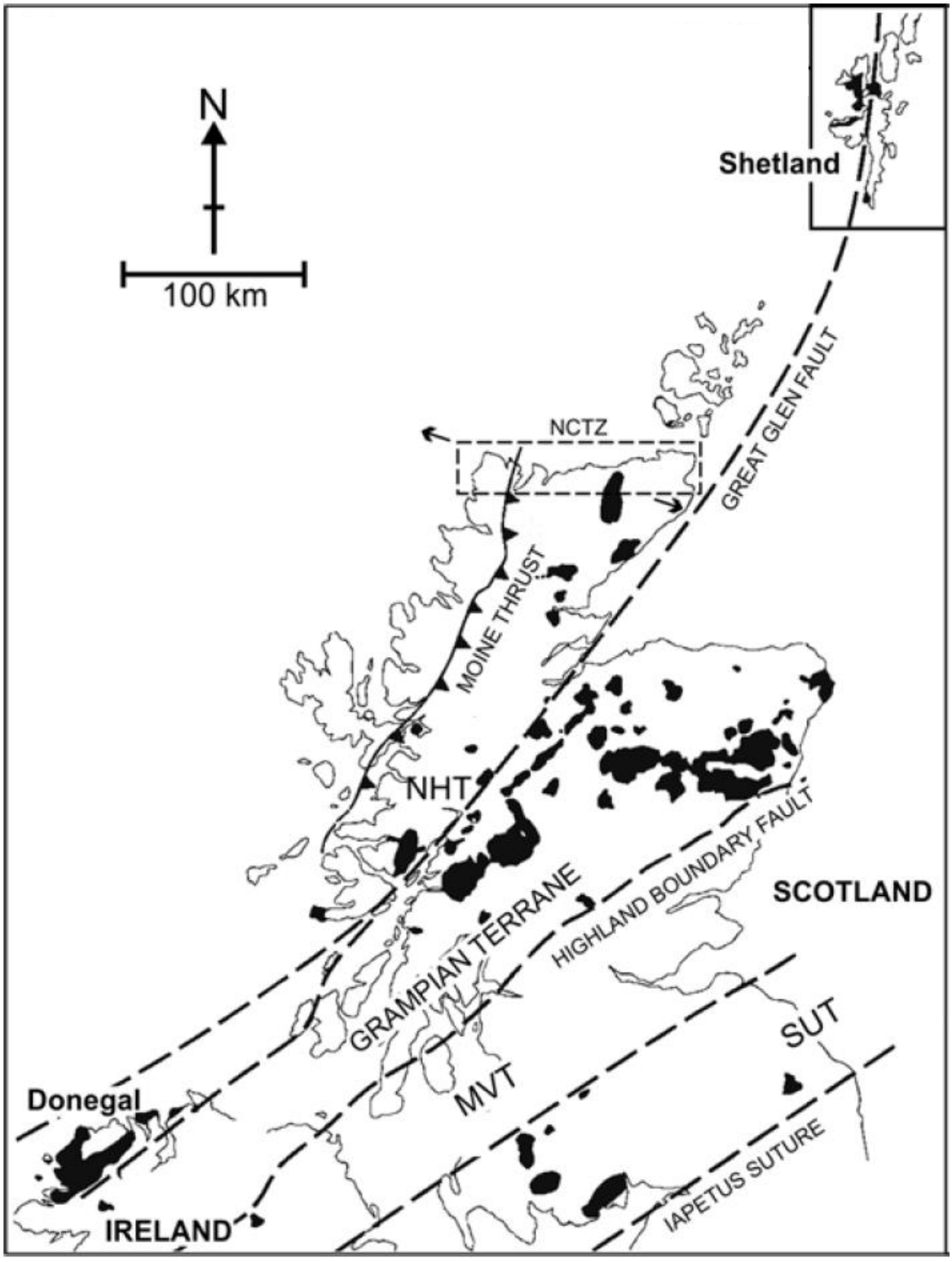

Figure 1.7: Location of Caledonian age granites. Modified *after* Lancaster et al. (2017) and Neilson et al. (2009). Abbreviations: NCTZ = North Coast Transfer Zone, MVT = Midland Valley Terrane, NHT = Northern Highland Terrane, SUT = Southern Uplands Terrane.

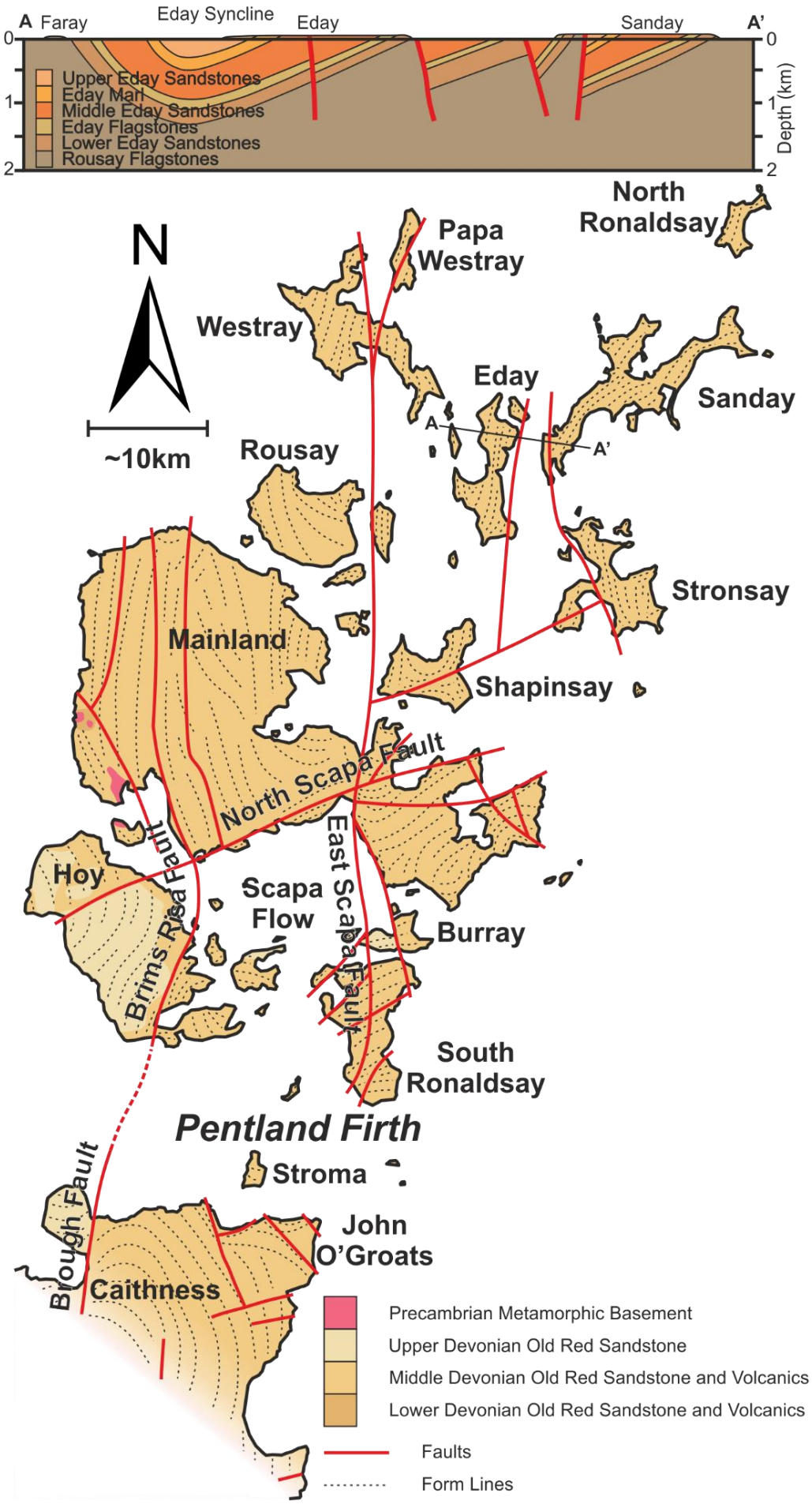
A Faray
Eday Syncline
Eday
Sanday
A'
0
1
2
Depth (km)
Upper Eday Sandstones
Eday Marl
Middle Eday Sandstones
Eday Flagstones
Lower Eday Sandstones
Rousay Flagstones
N
~10km
North Ronaldsay
Papa Westray
Westray
Eday
Sanday
A
A'
Rousay
Stronsay
Mainland
Shapinsay
North Scapa Fault
East Scapa Fault
Brims Ness Fault
Hoy
Scapa Flow
Burray
South Ronaldsay
Pentland Firth
Stroma
Brough Fault
John O'Groats
Caithness
Precambrian Metamorphic Basement
Upper Devonian Old Red Sandstone
Middle Devonian Old Red Sandstone and Volcanics
Lower Devonian Old Red Sandstone and Volcanics
Faults
Form Lines

Figure 1.8 (preceding page): Simplified geological Map of Orkney with key structural features. Modified *After* Mykura et al., (1976a) and BGS (1999). No vertical exaggeration on cross section.

1.2.2.2. Orkney:

The Orkney Isles are situated ~16km north of mainland Scotland and separated from the mainland by the Pentland Firth. The ~90 islands that make up the archipelago largely comprise Middle to Upper Devonian age sedimentary rocks, minor volcanics and several small inliers of metamorphic basement that outcrop near Yesnaby, Stromness and on the island of Graemsay (Mykura et al., 1976a) (Figure 1.8).

The basement in the Orkney Isles form a roughly North to North-Northwest elongate ridge of inliers, which at the time of deposition were a small range of hills onto which the sediments of the Orcadian Basin onlapped and buried. Due to a lack of exposure they are relatively understudied but a comprehensive review can be found in Strachan (2003). The basement inliers can be subdivided into three main rock groups of decreasing age:

1) Paragneisses and amphibolites dominated by psammitic to pelitic gneisses which strongly resemble and are correlated with the Moine Supergroup (Strachan, 2003).
2) Foliated meta-granites which are assigned to the 'Newer Granite' suite of mainland Scotland, are associated with Scandian deformation and dated to c.431-428Ma using U-Pb zircon geochronology (Bjerga, 2017; Lundmark et al., 2018).
3) Later undeformed granites and aplite veins.

1.2.2.3. Shetland:

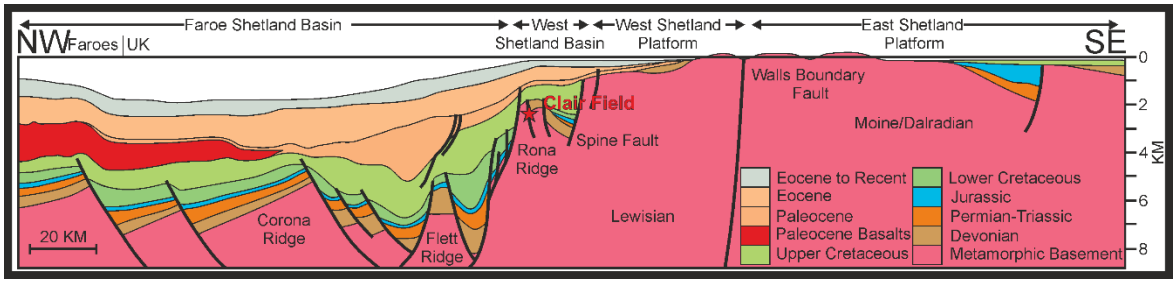

Figure 1.9: Cross section through Shetland and the Faroe Shetland Basin. Modified *after* Stoker et al., (1993).

The Shetland Isles are situated ~170 km northeast of mainland Scotland and ~75km east of the Clair Field. Shetland has a complex geological history and can be simplified into two distinct geological domains; West and East Shetland (Mykura, 1976). The generalised

geology of Shetland consists of a North/South orientated ridge of metamorphic basement comprised of ancient sedimentary rocks which have been metamorphosed and deformed numerous times, and then intruded by a suite of igneous rocks during the Caledonian orogeny (Figure 1.9). This ridge of basement - the Shetland Ridge - is partly overlain by sedimentary and volcanic rocks of Devonian age which are exposed onshore and by a series of younger Mesozoic basins offshore (Figure 1.10).

The two distinct geological domains in Shetland are separated by the Walls Boundary Fault, a major North/South trending, mostly dextral strike slip fault (although significant sinistral motions have been identified) which has a complex tectonic history (Flinn, 1992; Watts, 2001; Watts et al., 2007). This lithospheric scale structure is the proposed northerly continuation of the Great Glen Fault and was likely also linked to the More-Trøndelag Fault Zone in Norway. This structure has been repeatedly reactivated and has had a strong influence on the structural evolution of the area. The Northward continuation of the Moine Thrust is interpreted as lying offshore immediately to the West of Shetland, passing close to the island of Foula (Andrews, 1985; Ritchie et al., 1987b; Ritchie and Hitchen, 1993).

Like in mainland Scotland, the rocks West of the Walls Boundary Fault/Great Glen Fault are generally considered to be of a Moine affinity (excluding the Queyfirth group), and those to the East are deemed broadly equivalent to the Dalradian basement units of the Grampian Highlands (Flinn et al., 2013; Strachan et al., 2013), although there are some key differences e.g. thickness, age and basin evolution (Strachan et al., 2013) which suggest they were deposited in a separate along strike basin.

East of the Walls Boundary Fault, the East Mainland Succession extends from Unst in the North to West of Sumburgh Head in the South. It is cut by a series of faults sub-parallel to the Walls Boundary Fault including the Nesting Fault which has likely accommodated significant strike-slip motion. The East Mainland Succession and is subdivided into four main units (Flinn et al., 1973; Mykura, 1976):

1) Yell Sound Division - migmatised feldspathic psammites
2) Scatsta Division - pelitic and quartzitic schists also variably migmatised
3) Whiteness Division - flaggy micaceous quartz feldspar pasmmites, crystalline limestones and deformed veins of granite and pegmatites.
4) Clift Hills Division - chlorite and biotite muscovite phyllites and hornblende rich rocks.

Other rock units include several shear bound slices of varied basement, including the Quarff Melange and hornblende rich schists at Garths Ness in Southern Shetland. In the Northeast of Shetland, large parts of Yell and Unst are comprised of migmatised metasedimentary gneisses separated by a major thrust from overlying serpentinites, metagabbros and phyllites of the Unst Ophiolite (Walker et al., 2016).

West of the Walls Boundary Fault, the basement rocks form a belt of which extends from North Roe in the North to the Walls Peninsula in the south. In the North, three major groups have been identified (Mykura, 1976):

1) Uyea and Wilgi Geos Group (Western Series) - Archean acid, basic and ultrabasic gneisses, lenses of pyroxene hornblende gneisses and metagabbro which are cut by veins of foliated pegmatite. They are cut by the Uyea Shear Zone in the West and are bound to the east the Wester Keolka Shear Zone, the supposed northward continuation of the Moine Thrust Zone and are provisionally correlated with the Lewisian Complex. However, there is uncertainty and they may in fact represent a slice of Lewisian-like basement with the actual Moine Thrust lying offshore to the West (Armitage, 2019 pers. comm).
2) Sand Voe Group (Fethaland Series) - banded hornblende gneisses, orthogneisses with and bands of impure quartzite. Correlated with the Moine Supergroup.
3) Queyfirth Group (Ollabery Series) - banded quartz and muscovite schists, greenschists, and calcareous rocks ranging from quartzose schist to siliceous limestones which are correlated with the Upper Dalradian.

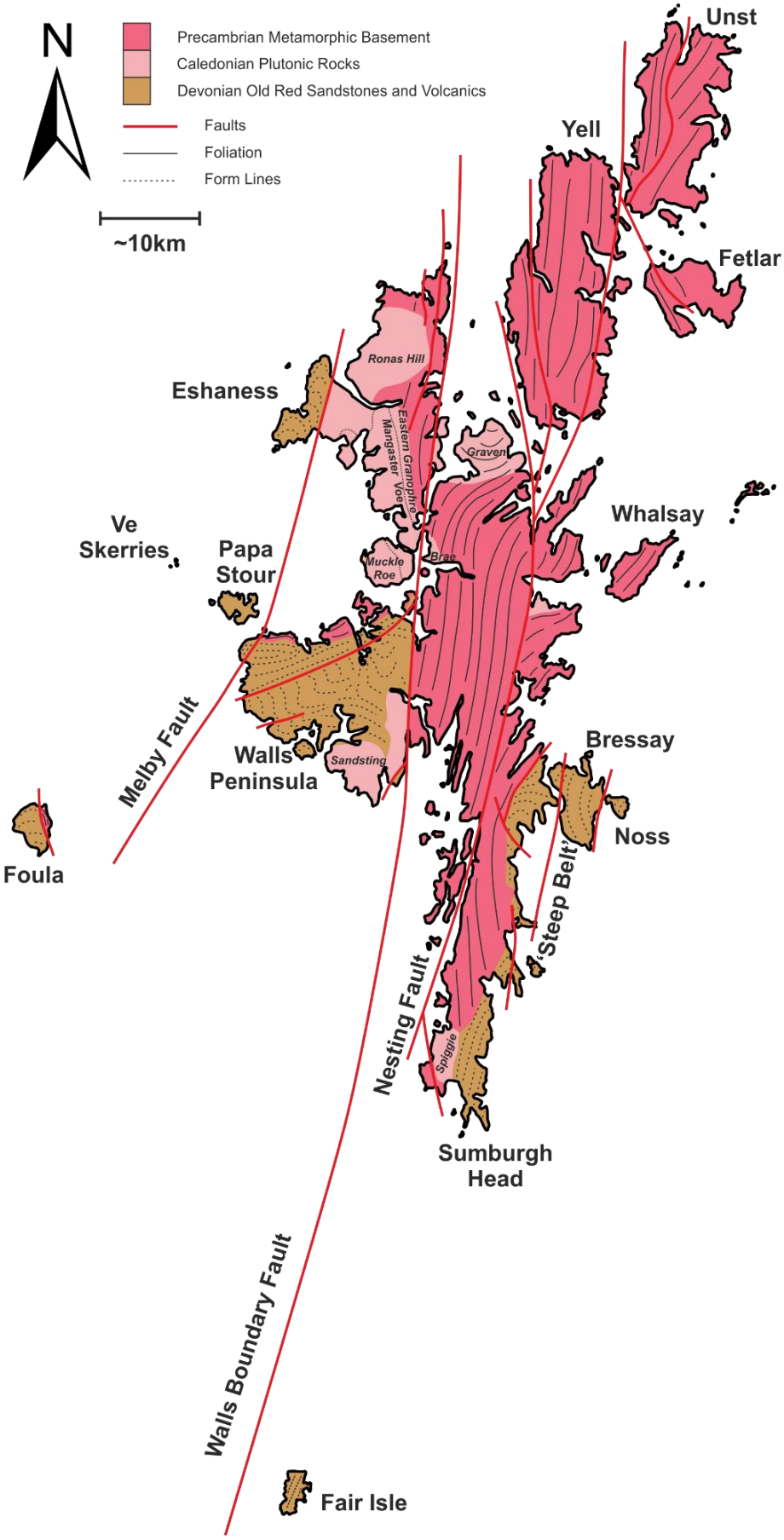

Figure 1.10: Simplified geological map of Shetland with key geological structures. Modified after (Lancaster et al., 2017; Mykura et al., 1976a).

On the Walls Peninsula and islands of Vementry and Papa Little, four lithological units, listed North to South, have been identified (Mykura et al., 1976b):

1) The Vementry Group - hornblende schists, amphibolites, semi-pelites and quartz granulites.
2) Neaans Group - feldspathic muscovite schists, hornblende schists, thin bands of altered limestone and epidote/clinozoisite altered rocks.
3) West Burra Firth Group - tremolite and phlogopite schists, calc-schists and limestones
4) Snarra Ness Group - hornblende and mica schists with lenses of amphibolite.

Mykura et al., (1976b) proposed these units were equivalent to the Sand Voe Group of Northern Shetland based on lithological and deformational similarities, however Flinn et al., (1979) later yielded K-Ar hornblende ages of c.863-366Ma and assigned them to be 'Grenvillian' basement. More recent Rb-Sr white mica ages of c.509Ma and c.451Ma indicate Caledonian deformation and a lack of Neoproterozoic deformation associated with 'Grenvillian' deformation (Walker et al., 2016).

To the West of the Walls Peninsula a thin fault bounded strip of metamorphic basement makes up the eastern coast of the island of Foula and is comprised of garnetiferous mica schists, psammites, pelites, amphibolites, epidote altered rock and a small granite intrusion. A marked similarity in the lithology and structure of the basement on Foula may equate them with the Neaans Group of the Walls Peninsula (Mykura, 1976; Mykura et al., 1976b). To the North of Foula and Northwest of Papa Stour, the small islands of Ve Skerries, are comprised of gneissic material like that found at Uyea. These inliers of gneissic material may be similar to Lewisianoid inliers found in the Moine of mainland Scotland.

Within the basement on Shetland a series of Caledonian plutonic rocks have been emplaced which can be split into two main groups (Lancaster et al., 2017 and references therein) either side of the Walls Boundary Fault (Figures 1.10 and 1.11).

Those to the east of the Walls Boundary Fault include the following units, which have been dated using U-Pb zircon geochronology (Lancaster et al., 2017; Mykura, 1976):

1. Graven Complex - a series of vein complexes that cut the metamorphic country rocks and dated to 440Ma (Lancaster et al., 2017). It is composed of early granites, pegmatites and slightly younger lamprophyres and porphyritic dykes which are cut

by intrusive sheets of diorite, monzonite, granodiorite and granite with mafic enclaves of hornblendite.

2. Brae Complex - a small steep sided intrusion cutting the Yell Sound and East Mainland Succession, dated to 464 Ma (Lancaster et al., 2017) and composed of diorite with subordinate pyroxenites and dunites.

3. Spiggie Complex - composed of granodiorite, porphyritic adamellite, monzonite, pyroxenite and serpentinite which is now largely below sea level.

4. Small areas of granite in Southeast Shetland near to Cunningsburgh and Channerwick with extensive thermal metamorphic aureoles.

The second set, to the West of Walls Boundary Fault form a North/South trending set of intrusions, which extends from the Walls Peninsula in the south to Northmaven in the North. These include the following units which have been dated using U-Pb zircon geochronology (Lancaster et al., 2017; Mykura, 1976):

1. The Sandsting Granite Complex - a large sheet like granite complex that evolved through several pulses of magmatic activity which started with the intrusion of basic dykes, evolving through basic to sub-basic plutonic rocks, acid and sub-basic minor intrusions (Mykura et al., 1976a). It forms the Southeast part of the Walls Peninsula and is intruded into the sedimentary rocks of the Walls Group (section 1.4.2.2.5) and is therefore of Middle Devonian age or younger and confirmed by U-Pb zircon geochronology with an age of c.371Ma (Lancaster et al., 2017)

2. The Northmaven Complex - a much larger intrusion which extends from North Roe in Northern Shetland to Muckle Roe and Vementry on the Northern side of the Walls Peninsula. It is subdivided into the Muckle Roe Granophyre, Ronas Hill Granite, Mangaster Voe Intrusion and Eastern Granophyre which are dated to c.433Ma, c.427Ma, c.389Ma and c.396Ma respectively (Lancaster et al., 2017). It comprises various types of granite, granophyre, diorite, gabbro, some ultrabasic rocks and altered basaltic rocks. The Northmaven Complex appears to have been emplaced over a prolonged period, is Middle to Upper Devonian in age but younger than the Eshaness Volcanics.

Geophysical anomalies offshore, suggest the presence of further buried granitic bodies near the island of Fair Isle, South of the island of Bressay and on the East Shetland Platform (Flinn, 1992; Holloway et al., 1991; Mykura, 1976; Mykura and Harrison, 1972; Patruno et al., 2018; Wilson, 1965).

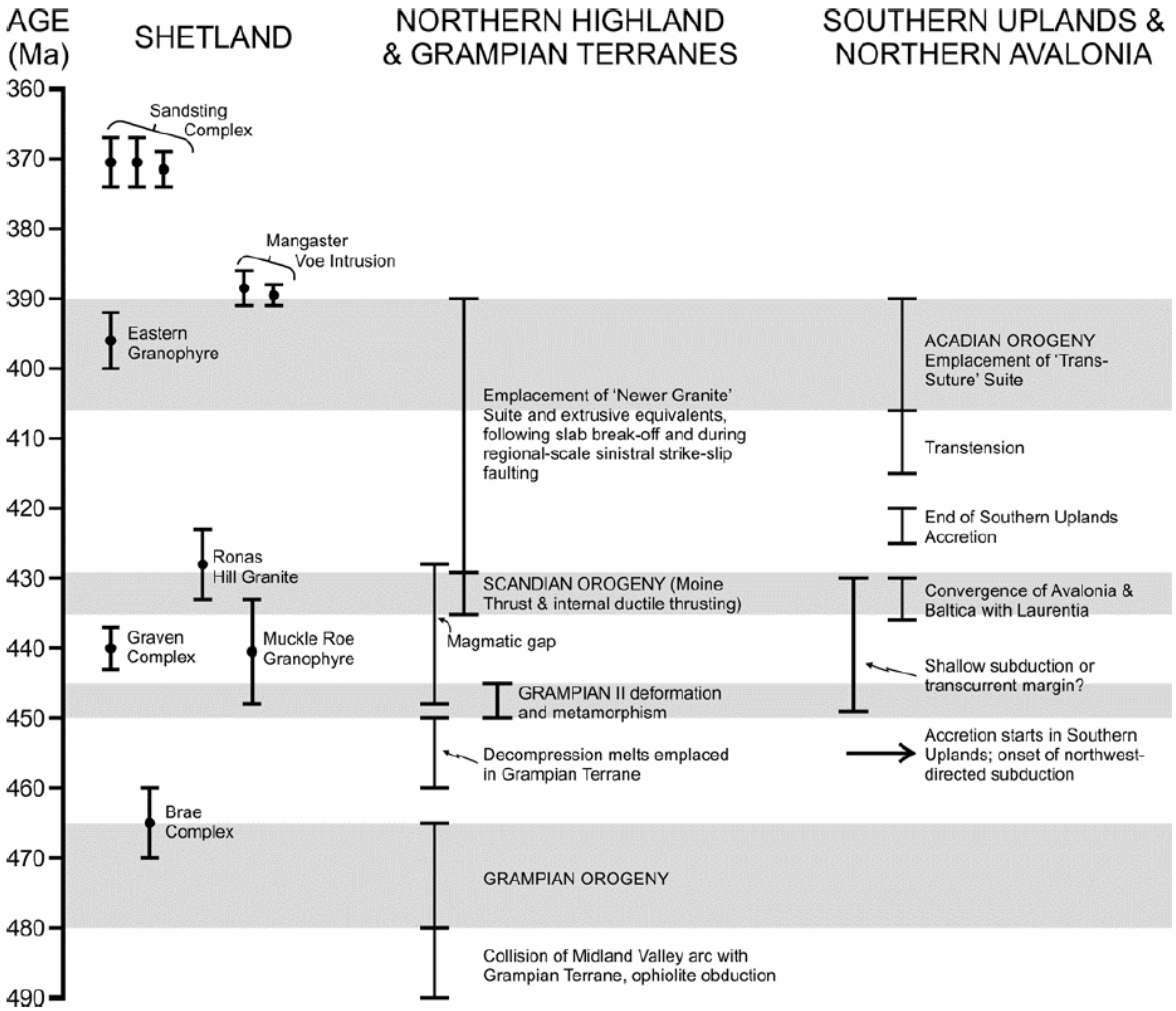

Figure 1.11: Summary of new U-Pb Zircon geochronology data for the 'Newer Granite' suite set in the context of Devonian tectonic events (Lancaster et al., 2017).

1.2.3. Devonian Old Red Sandstone:

1.2.3.1. Stratigraphy and Paleoclimate:

Continental deposits of the Orcadian Basin in the UK, outcrop in mainland Scotland in Caithness and Sutherland, around the coastlines of the Moray Firth and Aberdeenshire and on the archipelagos of the Shetland and Orkney Isles (Figures 1.5, 1.8 and 1.10). A sequence of continental deposits were also deposited in the present day Midland Valley of Scotland and numerous small outliers of ORS are located throughout Scotland, in particularly along

the line of the Great Glen Fault Zone, which may at times have been linked to the greater Orcadian Basin. ORS deposits also subcrop offshore on the UKCS and have been identified during exploration for hydrocarbons during drilling and on seismic.

Paleomagnetic data show that the ORS continent occupied a low-latitude, tropical to sub-tropical position between 15-30° south. The climate was warm to hot and generally arid to semi-arid as indicated by the presence of calcretes (Trewin and Thirlwall, 2002).

The Devonian age strata of the ORS onshore in the British Isles and offshore on UKCS are subdivided into three distinct phases of sedimentation separated by regionally recognised unconformities (Downie, 2009; Marshall et al., 2003; Parnell et al., 1999; Richards, 1990; Trewin and Thirlwall, 2002)(Figure 1.12):

1) The **Lower ORS (LORS) of Lower Devonian (Lochkovian to Emsian) age**, was deposited in small fault-bounded grabens and half grabens in which active faults provided continued coarse alluvial and fluvial sediments.
2) The **Middle ORS (MORS) of Middle Devonian (Eifelian to Givetian) age**, has the widest distribution and saw more prolonged lacustrine conditions and is the major depositional unit in the Orcadian Basin.
3) The **Upper ORS (UORS) of Upper Devonian (Frasnian to Fammenian) age** is predominantly comprised of fluvial and aeolian deposits. It was one of the most widespread ORS units and was potentially continuous from Orkney into the Midland Valley of Scotland or even Northern England and is extensive offshore (Downie, 2009) where it forms the reservoir to several oil fields.

The major controls on deposition in the Orcadian Basin are linked to fluctuations in tectonics and climate leading to variations in the ‘wetness’ of the depositional environment leading to more permanent lacustrine conditions to more ephemeral (Figure 1.13).

Stratigraphic correlation in the Orcadian Basin is based upon several widely developed fossiliferous horizons or ‘fish beds’ such as the Achnarras horizon, which is recognised in Shetland in the North, to the Gamrie Outlier in the South (Parnell et al., 1994).

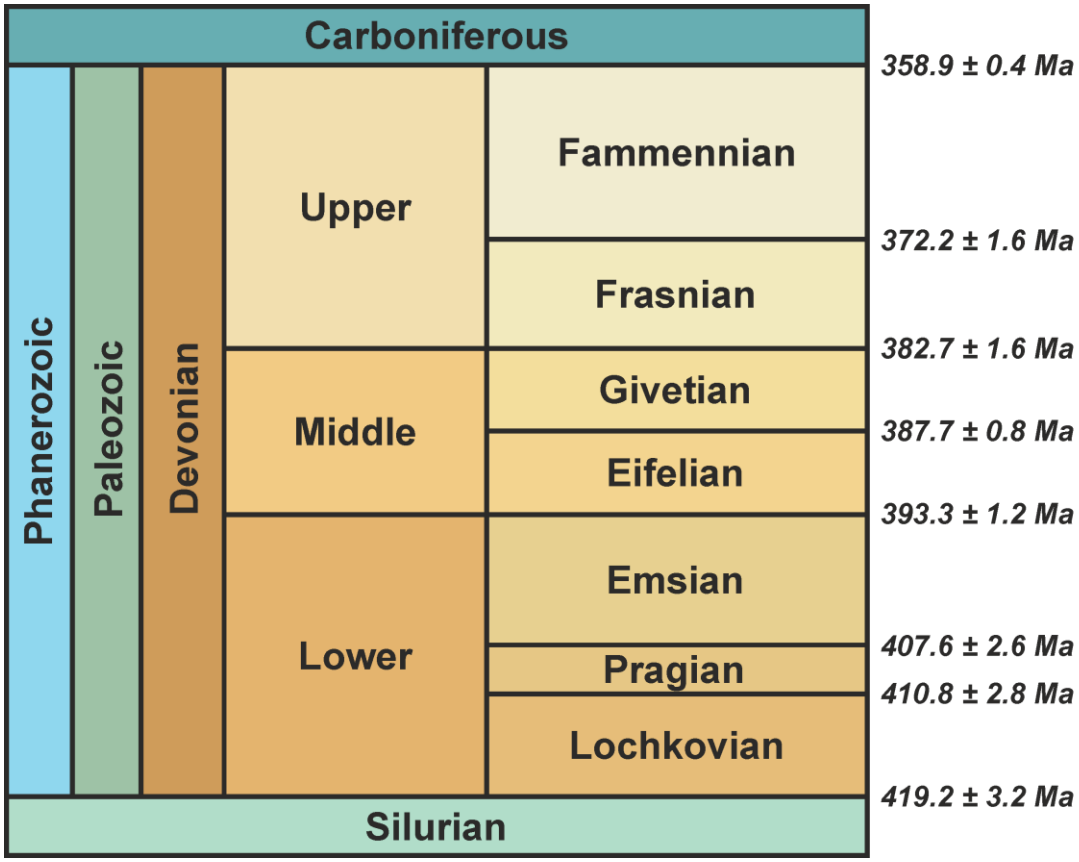

Figure 1.12: Devonian Chronostratigraphic Chart. Modified *after* Cohen et al., (2013).

Figure 1.13 (overleaf): Schematic end member models for the Orcadian Lake and surrounding sedimentary environments from (A) a dry to semi-arid environment with an ephemeral lake, aeolian dune systems, alluvial fans and fluvial systems to (B) a wetter system with more permanent lacustrine conditions (Rogers and Astin, 1991).

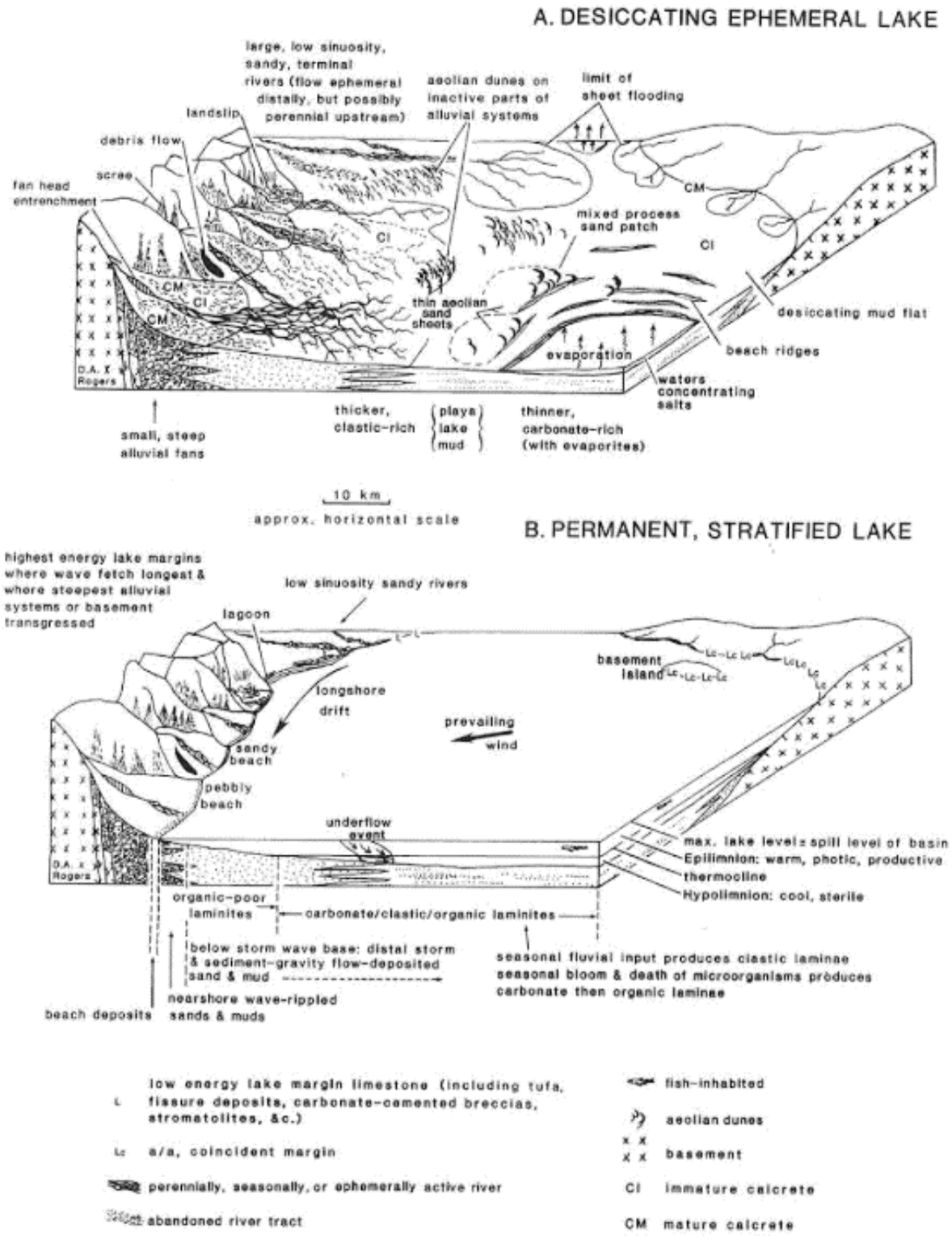

1.2.3.2. Mainland Scotland:

The stratigraphy of the Devonian succession of mainland Scotland are subdivided by age into the Lower, Middle and Upper Devonian, each separated by unconformities (Figure 1.14). The nature of the unconformities varies and reflects local tectonics. The Devonian of mainland Scotland generally dips out to sea, is regionally folded into broad open folds,

and, and locally is highly fractured and faulted with areas of intense deformation, which are attributed to the reactivation and inversion of early structures (Dichiarante 2017).

Middle Devonian sediments comprise most of the Caithness region and form flat-lying moorland, arable pasture and areas of peat bogs with little inland outcrop. Outcrop is largely confined to coastal regions and to upland areas to the South and West where Lower Devonian sediments are also exposed (Figure 5).

Upper Devonian sedimentary and minor volcanic rocks outcrop at Dunnet Head. There is limited Devonian outcrop in Northern Sutherland, with only a few outliers and isolated mini basins of Lower and Middle Devonian deposits on the North coast near to Strathy and Kirtomy (Wilson et al. 2010). More extensive ORS deposits are found in the SE corner of Sutherland and on the Western coastline of the Inner Moray Firth around Easter Ross, the Black Isle, Cromarty and Inverness (Trewin and Hurst, 2009).

The Lower Devonian of mainland Scotland is widely distributed and found around the margins of the Orcadian Basin in addition to several outliers in the Highlands of Northeast Scotland (Blackbourn, 1981a, 1981b). Due to the distributed nature of the Lower Devonian there is a varied stratigraphic nomenclature, but are broadly grouped within the Sarclet or 'Basement Group' (Collins and Donovan, 1977)(Figure 1.14). The basal sediments overlie an irregular basal unconformity which were deposited on alluvial fans, dominated by debris flow processes adjacent to localised topographic highs and driven by active faulting. Elsewhere fluvial/alluvial sandstones were deposited in ephemeral river channels during flash floods on a wide alluvial plain. Evidence of permanent/semi-permanent water is reflected by the presence of flagstones and mudstones containing arthropod trace fossils indicating partial lacustrine conditions. The composition of the basal deposits strongly reflect the underlying basement. For example, they are highly arkosic in proximity to the Helmsdale Granite, whereas elsewhere contain abundant fragments of foliated Moine basement.

The Middle Devonian of mainland Scotland largely is subdivided into the Lower and Upper Caithness Flagstone Groups (Figure 1.14), which are separated by a regionally important transgressive unit, the Achnarras Horizon which represents more persistent lacustrine conditions. The flagstones are comprised of rhythmically bedded, grey, fissile, thinly bedded sandstones, siltstones, mudstones and limestones.

Around the margins of the Orcadian Lake and in more isolated basins, localised conglomerates and other, more coarse clastic sediments (Millbuie Sandstone Group, Strathrory Group) were deposited in fluvial/alluvial systems flowing towards the Orcadian Lake (Johnstone and Mykura, 1989). The Caithness Flagstones are overlain by the John O'Groats Sandstone Group which are a predominantly fluvial sequence comprising pebbly sandstones laid down in braided rivers and finer grained fluvial overbank and alluvial plain deposits (Johnstone and Mykura, 1989).

The Upper Devonian of mainland Scotland is predominantly comprises red-yellow sandstones of fluvial and aeolian origin with thin intercalations of mudstone and shale (Johnstone and Mykura, 1989). The transition into the Upper Devonian marks the extension of braid plains, alluvial plains, fluvial systems and aeolian dunes out into the basin. Rare fish deposits are found, but this period represents a dryer phase with less permanent or only localised lacustrine conditions.

Deposits of Upper Devonian age are found at Dunnet Head (Dunnet Head Sandstone Group) (Figure 1.14) where they are faulted against and overly Middle ORS deposits of the Eday Group, although this contact is not observed. Greater thicknesses of UORS deposits can be found on the Black Isle, around the Dornoch Firth and on the Southern coast of the Moray Firth where they are termed the Balnagown Group (Johnstone and Mykura, 1989).

A laterally extensive and significant thickness of equivalent fluvial and aeolian Upper Devonian clastic sediments of generally good reservoir quality, known as the Buchan Formation (Tang et al,. 2017), form the reservoir for several hydrocarbon fields offshore, where it passes conformably upwards into Lower Carboniferous deltaic sandstones and shales.

The nature of the contact between the Middle and Upper Devonian is uncertain, with several authors disputing it. Early workers (Mykura et al., 1976a) favour widespread uplift and erosion whereas later workers including Underhill and Brodie (1993) and Rogers et al., (1989) favour Devonian rifting followed by subsidence, with no regional break in sedimentation and only more localised transpression related instead, to later Permo-Carboniferous inversion.

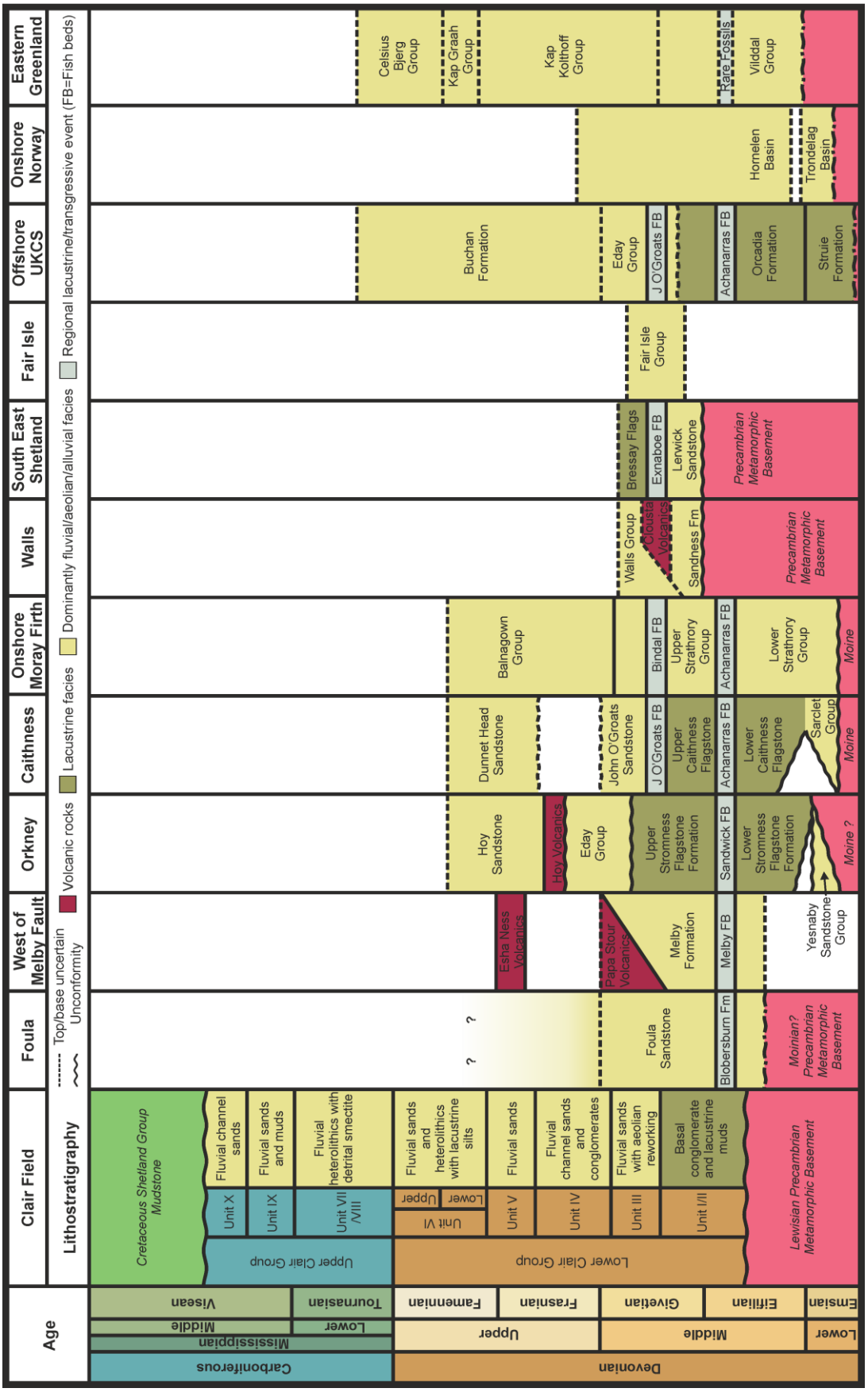

Figure 1.14: Regional Devonian stratigraphic correlation chart and stratigraphy of the Clair Field. *After* Allen and Mange-Rajetzky, (1992); Barclay et al., (2005); Barr et al., 2007; Gautier et al., (2011); House, (2000); Marshall et al., (2003); Ogilvie et al., (2015); Trewin and Thirlwall, (2002).

1.2.3.3. Orkney:

The stratigraphy of the Orkney Isles is predominantly Middle Devonian (Figure 1.8 and 1.14) with minor Lower Devonian deposits located in West Mainland, Orkney. The Lower Devonian ORS sediments of the Yesnaby Sandstone Group are comprised of coarse breccias, well rounded and compositionally immature conglomerates which are interbedded with thin sandstones and some large scale cross bedded sandstones of aeolian origin, which onlap onto metamorphic basement. Lower Devonian sediments of Orkney are equivalent to the Sarclet Group of mainland Scotland.

The Middle Devonian of Orkney is correlated with the Lower and Upper Caithness Flagstones and John O'Groats Sandstone of mainland Scotland and is subdivided into three major groups:

1) The Stromness Flagstones, a cyclic sequence of lacustrine siltstones, fine grained sandstones and carbonate rich siltstones with abundant fish fossils, which overlie breccias, conglomerates and pebbly sandstones.
2) The Rousay Flagstones, a further sequence of cyclic lacustrine sediments which are difficult to distinguish from the Stromness Flagstones apart from some differences in weathering (Mykura et al., 1976a). Detailed paleontological studies have further defined the boundary based on biozones and fossil fish (Leather, 2017)
3) The Eday Group, including the Eday Flagstones, Eday Volcanics, Lower and Middle Eday Sandstones and Eday Marls is a highly variable unit comprised of a thick sequence of sandstones, alternating with marls and minor basic lavas and tuffs. Sediments were deposited in three interacting environments; sandy braided rivers flowing over wide alluvial fans, aeolian dunes and lacustrine beaches (Astin, 1985)

Intrusive Middle Devonian dolerites are associated with extrusive alkaline lava flows and tuffs within the Eday Group flagstones (Kellock, 1969; Mykura et al., 1976a). The basal Devonian Hara Ebb formation has intraformational rhyolites which are dated to 390±0.41Ma (Bjerga, 2017) using U-Pb zircon geochronology.

Upper Devonian rocks of Orkney are restricted to the island of Hoy and comprises parts of the Eday Group, the Hoy Volcanics, and Hoy Sandstones. The Upper Eday Sandstone consists of beds of soft cross bedded sandstones interbedded with carbonate rich shales which were deposited in fluvial channels, lacustrine deltas and on broad alluvial fans and

floodplains. The Hoy Volcanics are comprised of basaltic lavas, tuffaceous sediments and reworked volcanic material. They have a variable thickness and reflect deposition on the undulating, folded and faulted Eday Sandstones they overlie. Recent work by Svebo, (2018) has identified stratigraphic continuity between the Eday Sandstone and the Hoy Volcanics and give an uppermost Givetian age to Frasnian U-Pb zircon age of 378-382±0.22Ma. The Hoy Sandstone comprises medium grained sandstones, thin carbonate rich shales and conglomerates. The Hoy Sandstones are equivalent in age to the Dunnet Head Sandstones of Caithness and therefore Upper Devonian in age, however this age is uncertain due to a paucity of biostratigraphic data throughout the sequence (Trewin and Thirlwall, 2002).

The rocks of Orkney are folded into broad, open, gentle dipping folds with a general northerly trend, although locally are intensely folded, indurated and associated with mineralised breccias (Figure 1.8). These zones of more intense damage generally form monoclinal structures sub-parallel to major faults (Mykura et al., 1976a). Minor folding in the Yesnaby Sandstone Group gives rise to an angular unconformity of ~10° with the overlying Stromness Flagstones, reflecting syndepositional tectonics. Three major fault trends can be identified (Mykura et al., 1976a):

1) East-northeast to Northeast major faults, e.g. North Scapa Fault,
2) North orientated faults (North-northeast to-North-Northwest) and sub-ordinate sub-parallel step faults in West Mainland
3) Uncommon NW faults.

Many of the faults record syn-sedimentary movement, controlling the deposition of units, with significant thicknesses of sediment being deposited in the hangingwalls of some faults e.g. North Scapa Fault (Astin, 1985). Like much of the ORS, the rocks of Orkney are also highly fractured.

1.2.3.4. Shetland:

In Shetland the Devonian age sedimentary and volcanic rocks can be subdivided into three distinct basins separated by large strike-slip faults (Figure 1.10). From East to West these are: 1) E Shetland and Fair Isle, 2) Walls Basin and 3) Foula, Melby, Papa Stour and Eshaness(Figure 1.14). The present-day juxtaposition of the three Devonian basins of Shetland does not reflect their position during the Devonian and instead reflects

subsequent predominantly dextral strike-slip motion offsets along the Walls Boundary, Melby and Nesting Faults (Watts, 2001 and references therein).

The three Devonian basins differ in age, sedimentological and volcanological development, tectonic history and intrusive history. As such they do not represent a continuous sequence, although some horizons have been correlated and may indicate some connection with the Orcadian Basin (Donovan et al., 1978; House, 1977; Marshall, 2000). The stratigraphy of the Devonian successions of the Shetland Isles is further sub-divided into 6 main regions: 1) Foula, 2) Melby and Papa Stour, 3) Eshaness, 4) Walls Peninsula, 5) Eastern Shetland and 6) Fair Isle. All units are unconformable on the underlying basement, but display a variety of basement/cover relationships (Flinn et al., 1979). Despite some general similarities in lithology and depositional environment, variations in the structure, in burial history (yielded from analysis of vitrinite reflectance data and diagenetic studies), and sedimentary provenance data, reflect somewhat different tectonics and basin evolution (Allen and Marshall, 1981; Astin, 1982; Hillier and Marshall, 1992; Marshall et al., 1985; Mykura et al., 1976a; M. Seranne, 1992).

The Westernmost basin containing the regions of Foula, Eshaness and Melby and Papa Stour was the furthest south and likely on the fringes of the major Orcadian Basin (Mykura et al., 1976a) as the sediments are of a closer affinity to those on Orkney and in Caithness and is supported by fossil evidence indicating direct faunal communication (Marshall, 1988). The Walls Basin was likely deposited further north in a tectonically and volcanologically active basin, and is quite different to the other basins (Melvin, 1985). The East Shetland Basin was probably furthest North and bound to West by mountainous terrain but had access to a large open lake to the South and East and may have also been in direct faunal communication with the Eday Basin of Orkney (House, 1977) and recent paleontological analysis has identified a link with the Devonian basins of the Baltic (Newman and Den Blaauwen, 2018).

1.2.4. The Evolving Models of Devonian Basin Development:

Models for the origin of the Orcadian Basin and other offshore Devonian age basins such as the West Orkney Basin have been the matter of some debate. Interpretation of early commercial shallow and deep crustal 2D seismic surveys offshore suggested the presence of series of half grabens bounded by easterly dipping normal faults (Enfield and Coward,

1987) (Figure 1.15). Early interpretations suggested that these basins were Devonian in age and formed as a result of the extensional collapse of the Caledonian orogenic belt and that faults rooted down and were extensionally reactivating Caledonian thrusts (Coward et al., 1989; McClay et al., 1986; Norton et al., 1987). Later studies cast doubt on these models (Stoker et al., 1993) with the identification of Permian to Triassic sediments offshore in the West Orkney Basin, and with evidence of basement reactivation (Roberts and Holdsworth, 1999; Wilson et al., 2010) onshore in Northern Scotland.

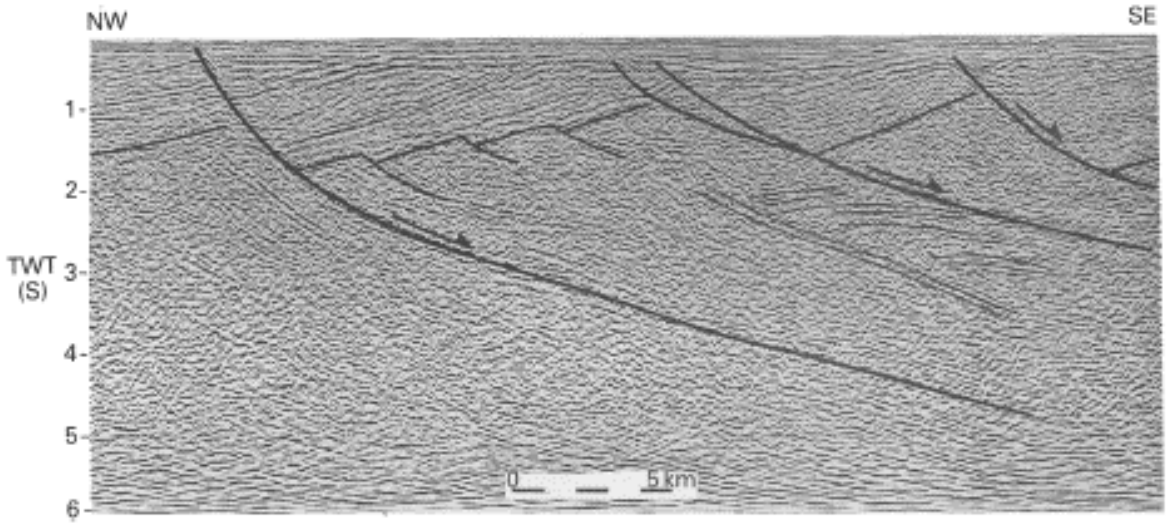

Figure 1.15: Interpreted seismic section through the West Orkney Basin, showing highly reflective basement structures and supposedly syn-rift Devonian half grabens (Coward et al., 1989).

Transtension was first postulated as an alternative model for Devonian basin development by Seranne (1992) who identified the role of strike slip tectonics after working on the Devonian basins of Norway where transtension was becoming an accepted hypothesis (Séguret et al., 1989; Seranne, 1992; Seranne et al., 1991; Seranne and Seguret, 1987). Yet, in a review by Friend et al. (2000) of ORS basin development, the role of transtension and strike-slip tectonics in the development of some of the ORS basins of the North Atlantic was only noted, with the development of the Orcadian Basin still being largely attributed to the purely extensional collapse of the Caledonian mountains. Significant doubt in the purely extensional collapse model was cast by Dewey & Strachan (2003) and later by Fossen (2010)(Figure 1.16 and 1.17) which guided further research and led to the recognition of strike slip and oblique tectonics in the Orcadian Basin, throughout its history (Dichiarante, 2017; Dichiarante et al., 2016; Wilson et al., 2010). In more recent work, the role of the Great Glen and Walls Boundary Faults during basin development and

subsequent reactivation has been identified as a key influence on the tectonic evolution of the basin, as well as the recognition of three distinct phases of deformation during its history (Dichiarante, 2017) (Figure 1.18).

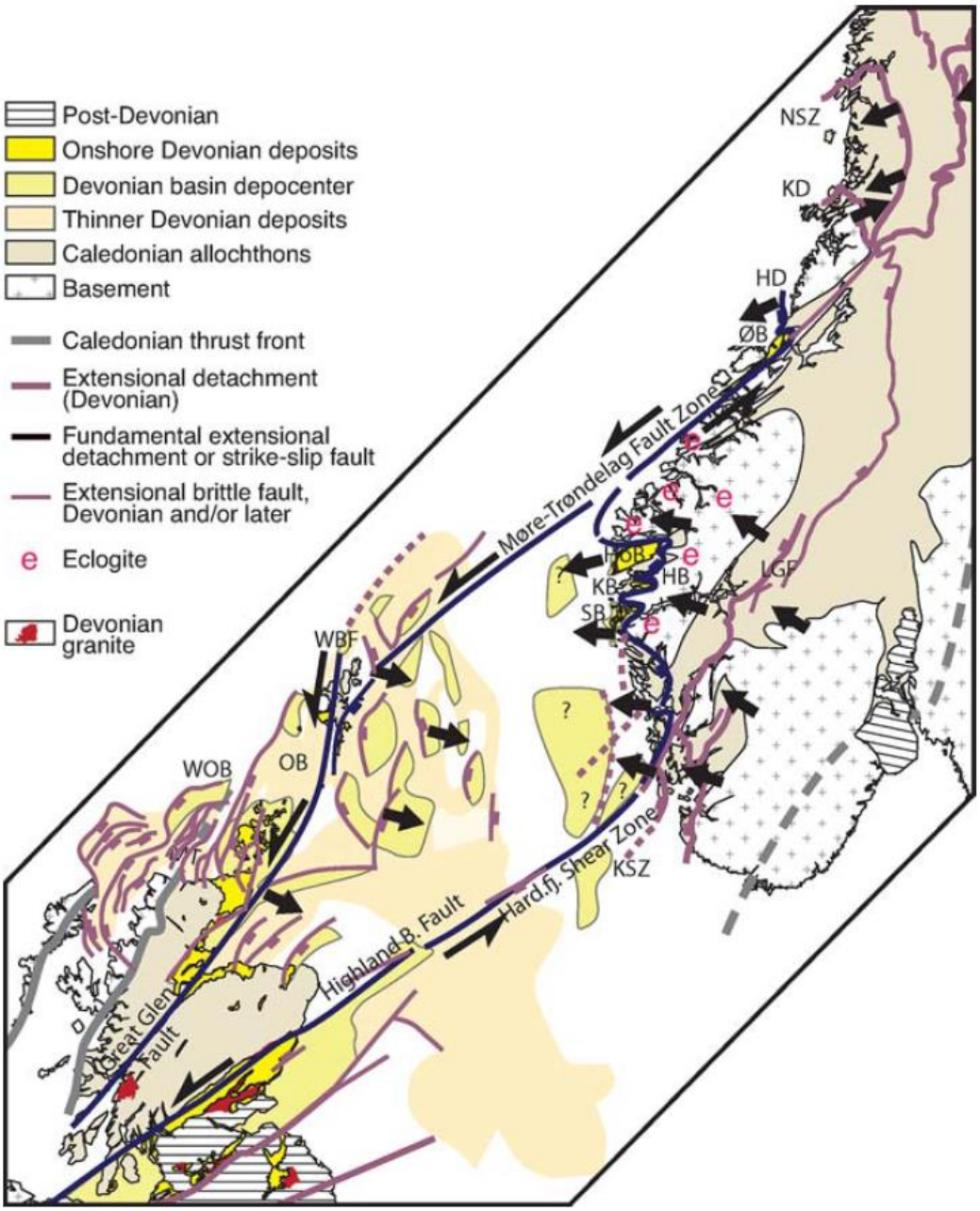

Figure 1.16: Illustration of the strike-slip overstep model for the Devonian extensional system between Southern Norway and Northern Britain. Black faults indicate the main faults in this system, and arrows indicate kinematics. Abbreviations: BASZ, Bergen Arc Shear Zone; HD, Høybakken Detachment; HSZ, Hardangerfjord Shear Zone; KD, Kollstraumen Detachment; LGF, Lærdal-Gjende Fault; GLSZ, Germania Land Deformation Zone; KSZ, Karmøy Shear Zone; MF, Minch Fault; MT, Moine Trust; MTFZ, Møre-Trøndelag Fault Zone; NSDZ, Nordfjord-Sogn Detachment Zone; NSZ, Nesna Shear Zone; OIF, Outer Isles Fault; RD, Røragen Detachment; WGR, Western Gneiss Region; UHP, ultra-high pressure; WOB, West Orkney Basin; OB, Orcadian Basin (Fossen, 2010).

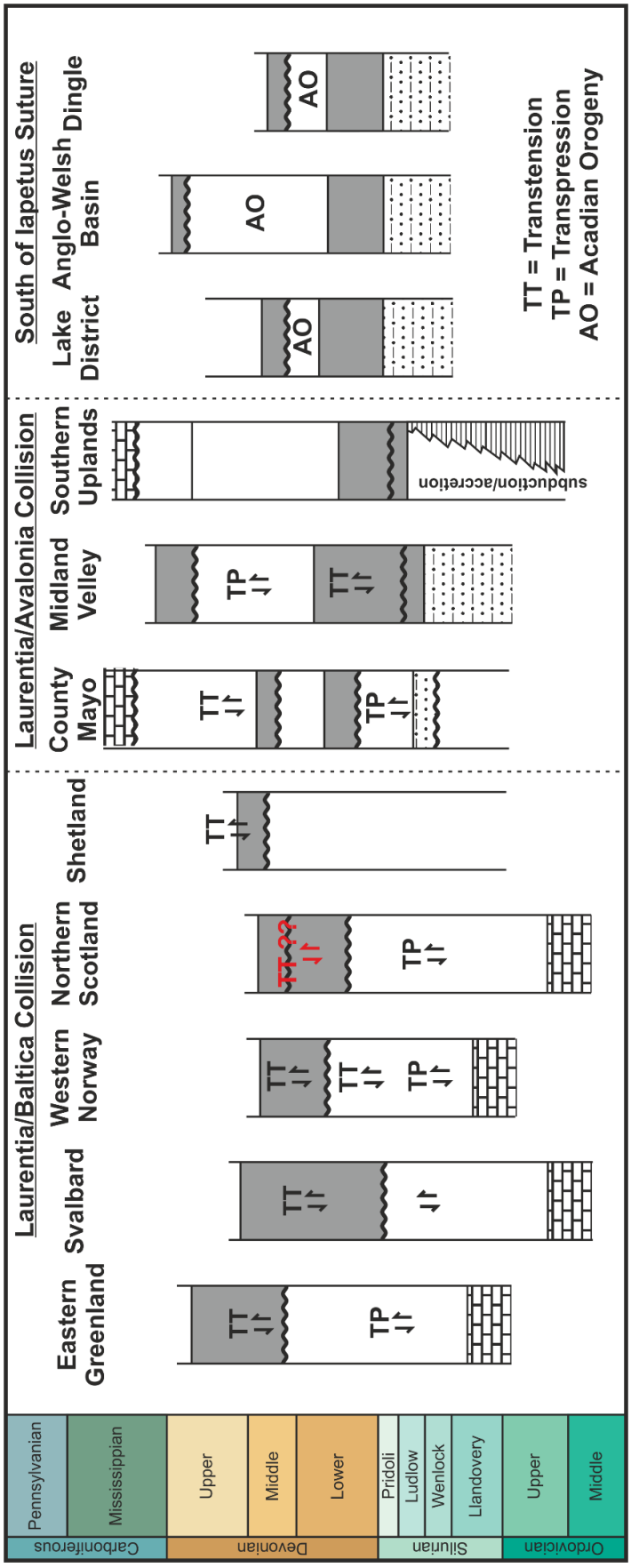

Figure 1.17: Structural Time Chart for the ORS basins of the North Atlantic after (Dewey and Strachan, 2003)

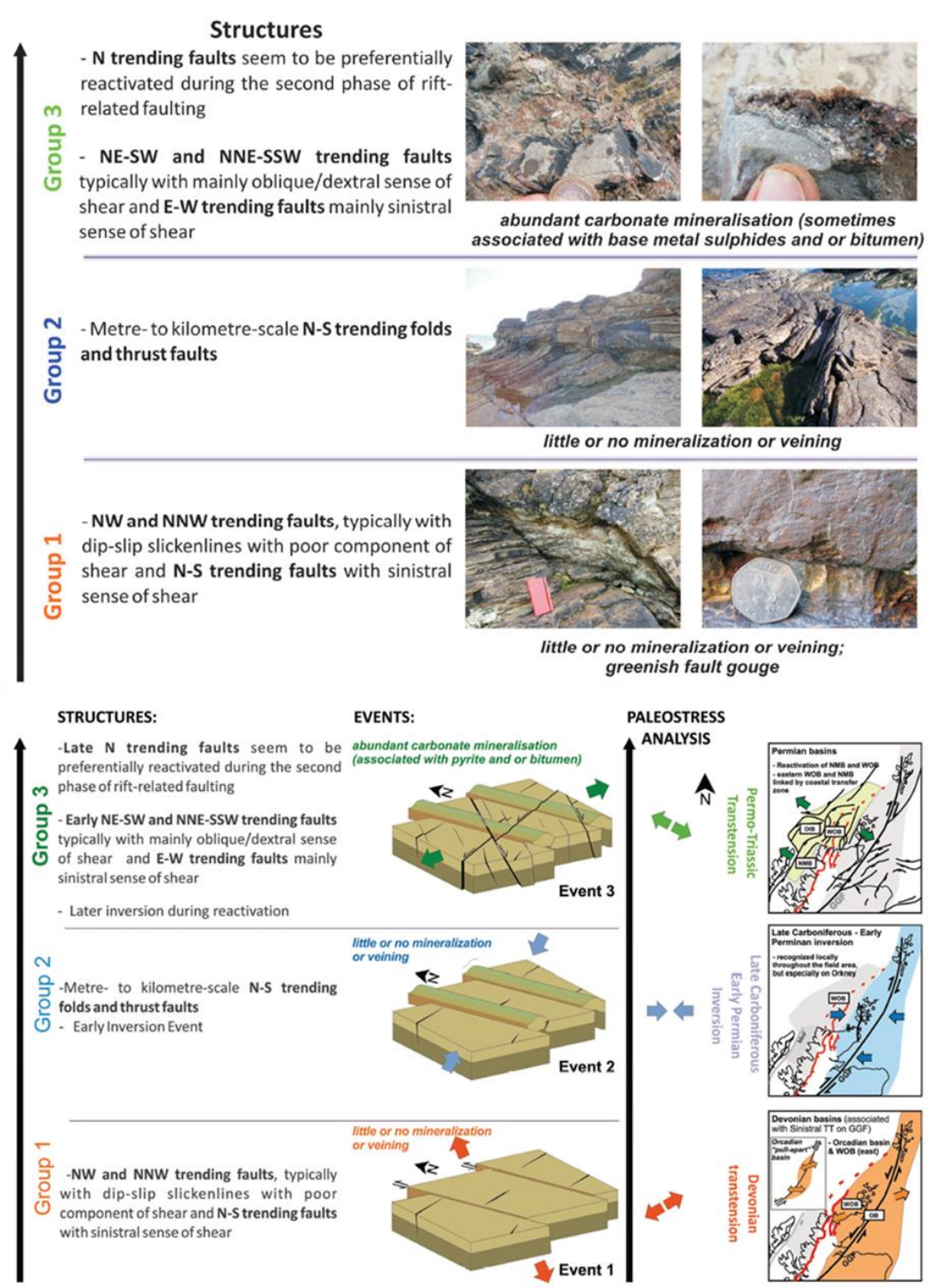

Figure 1.18: Summary structural history for the Orcadian Basin *after* Dichiarante (2017). As a result of this study, three distinct sets of structures related to regional scale events were identified: 1) Devonian transtension, 2) Late Carboniferous to Early Permian Inversion and 3) Permian to Triassic Transtension.

1.2.5. Post Devonian Geological History:

1.2.5.1. Mainland Scotland:

In Caithness, a period of uplift and inversion during the Carboniferous (Figure 1.18) was followed by rifting in the Permian and Triassic and the deposition of a further sequence of arid continental, fluvial, alluvial, aeolian, and lacustrine deposits, localised volcanics. This includes a series of ENE to WSW orientated camptonite/monchiquite dykes, which are particularly well exposed on the North Coast at Castletown (Dichiarante et al., 2016). Several small volcanic vents are also present on the North coast near Dunnet Head and at Duncansby and are described in detail by Crampton et al., (1914). These vents are largely filled with basalt, but also contain agglomerates and clasts of local sedimentary rock, and basement and are Late Permian in age, c.249-270Ma, based on whole rock K/Ar dating (Baxter and Mitchell, 1984; BGS, 1986, 1985a; Macintyre et al., 1981).

During the Jurassic, rifting renewed and sequences of fluvial, paralic and marine sediments were deposited as river systems and deltas delivered sediment into the North Sea rift. Limited outcrops of these rocks are seen onshore at Brora and Elgin. Cretaceous rocks and younger strata do not outcrop onshore but are evident in offshore data and indicate continued subsidence in the Moray Firth Basin, with deposition of the Upper Cretaceous Chalk and Cenozoic sediments. Tertiary fluvial and deltaic deposits are not preserved onshore but are found offshore. It is likely that some or all of these rocks were deposited over Northern Scotland but Paleogene uplift related to the development of the Iceland plume, in conjunction with glaciation have eroded much of this material (Holford et al., 2010) with Wilkinson (2017) estimating that approximately 1900-2400m of post-Caledonian sedimentary rocks have been eroded during the Cenozoic. A detailed overview of the Post-Devonian stratigraphy can be found in Trewin and Hurst (2009).

1.2.5.2. Orkney and Shetland:

The post Devonian geological history of Shetland and Orkney is poorly constrained due to a lack of younger deposits preserved onshore but may be similar to that of mainland Scotland (Mykura et al., 1976). Exposed on Orkney are a series of camptonite, monchiquite, bostonite, Late- Carboniferous to Permian age dykes, sills and basaltic volcanic vents (Healy et al., 2018; Lundmark et al., 2011). The volcanic vents are closely associated with the monchiquite dykes and are partially filled with monchiquitic basalts and sedimentary

breccias which resemble similar breccias in the Eastern Shetland 'steep belt' (Mykura et al., 1976a) and are most numerous in the south and west of the Orkney Isles. These volcanic rocks are broadly equivalent in age to those exposed in Northern Caithness and to Permo-Triassic dykes that are widely distributed through the Scottish Highlands and Northern England (Baxter and Mitchell, 1984; Brown, 1975). In Eastern Shetland and on the islands of Bressay and Noss, two northward trending belts of steeply inclined strata, associated with tuffsitic breccias, tuffsites and carbonate mineralisation cut the ORS and are thought to be of Permo-Carboniferous age (Mykura, 1972, 1976). An undeformed basic dyke of unknown age also cuts the metamorphic basement on Ve Skerries (Mykura et al., 1976b).

Further evidence for post Devonian geological activity may be inferred from the nearby sedimentary basins that have developed offshore (Stoker et al., 1993). Permo-Triassic basins are found offshore on the Orkney-Shetland platform into which thick deposits of continental clastic sediments were deposited. Younger sediments are largely missing, although minor quantities of Jurassic and Cretaceous rocks are preserved in some smaller basins around the margins of the Orkney Shetland Platform which are equivalent in age to the thick sequences preserved in the Northern North Sea and Faro-Shetland Basin. Like mainland Scotland, the Orkney-Shetland platform has undergone exhumation and uplift associated with the Iceland plume (Wilkinson, 2017).

Throughout this time the basement that underlies the Orkney-Shetland platform which separates the North Sea from the Atlantic, has acted as a buoyant structure and resisted burial despite protracted rifting and basin development since the Palaeozoic. Structures such as the Shetland Ridge can thus be seen as analogous to many other basement highs/ridges that are seen in the adjacent sedimentary basins such as the Rona Ridge. These structures are important regional features and have had a key role in controlling sedimentary basin evolution both structurally, but also as sources of sediment into the nearby basins.

1.3. The Clair Field:

The Clair Oil Field is located 75km west of the Shetland Isles, on the North-East Atlantic margin (Figure 1.19). It is the largest known resource on the UKCS, with a closure of 250 km² (Ogilvie et al., 2015; Witt et al., 2010; Wylde et al., 2005) and has an estimated 7 Billion BOE STOIIP (Barrels of Oil Equivalent, Stock Tank Oil Originally In Place), which makes Clair

a key component of future hydrocarbon production from the UKCS (Wylde et al., 2005) and for meeting future UK energy demands.

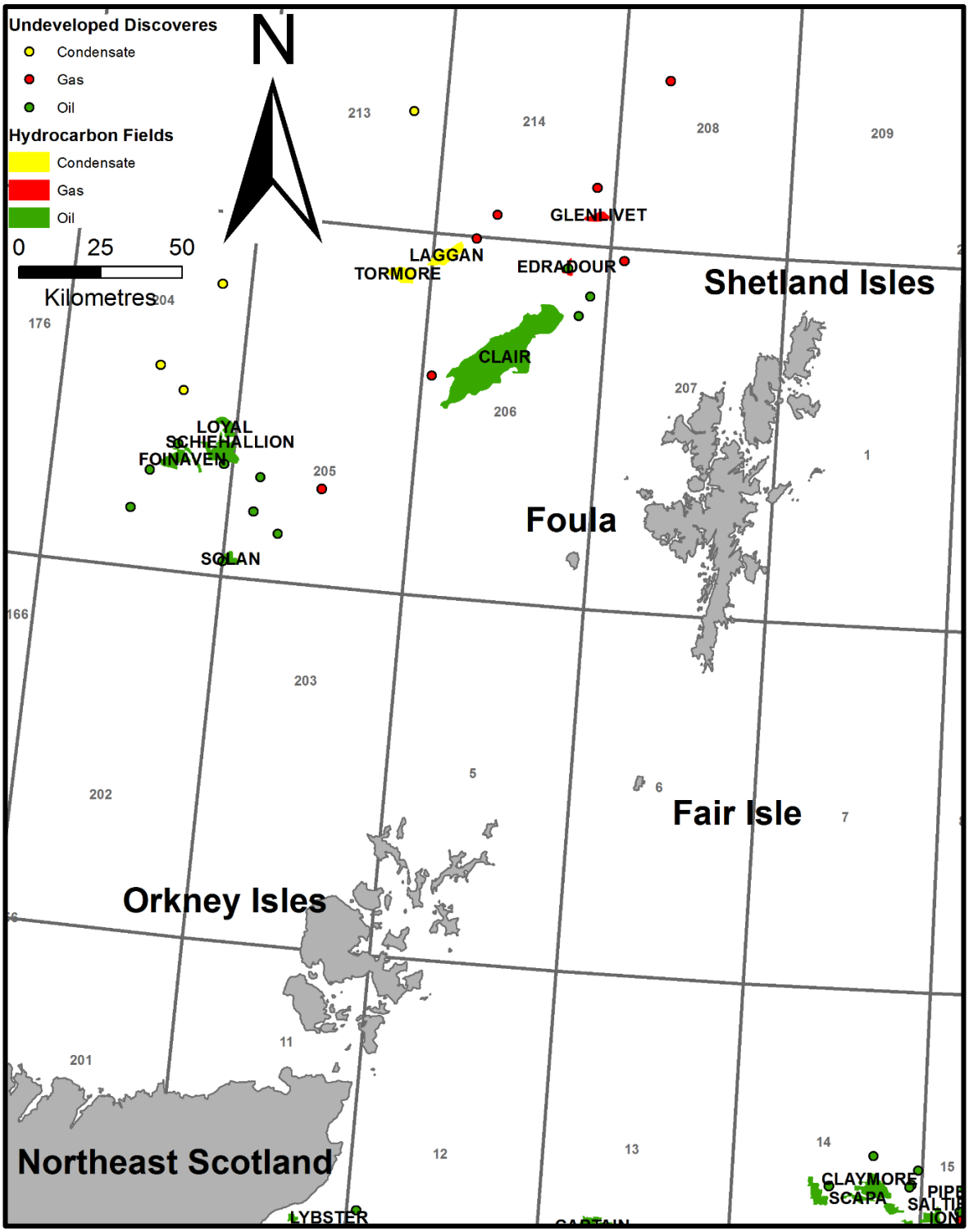

Figure 1.19: Map of hydrocarbon producing fields and undeveloped discoveries on the UKCS, West of Shetland. Shapefiles courtesy of the Oil and Gas Authority (2019).

The field is comprised of an elongate Northeast-Southwest trending ridge of fractured crystalline Lewisian basement known as the Rona Ridge and the overlying fractured

Devonian-Carboniferous clastic sedimentary rocks of the Clair Group (Figure 1.20). These are blanketed and sealed by a thick sequence of Cretaceous age shales (Allen and Mange-Rajetzky, 1992; Coney et al., 1993; Johnston et al., 1995; Ogilvie et al., 2015; Sircar, 2004) (Figure 20). A detailed summary of the exploration, development and production history of the Clair Field can be found in Appendix B.

The ongoing development Clair has led to further exploration West of Shetland. Clair is now just one of several developments and discoveries along and adjacent to, the Rona Ridge. These include the Foinaven, Schiehallion, Lancaster, Whirlwind, Halifax, and Typhoon fields. Several smaller undeveloped discoveries and oil and gas shows within both the basement and in Palaeozoic, Mesozoic and Cenozoic sediments adjacent to the Rona Ridge indicate that this province has great future potential.

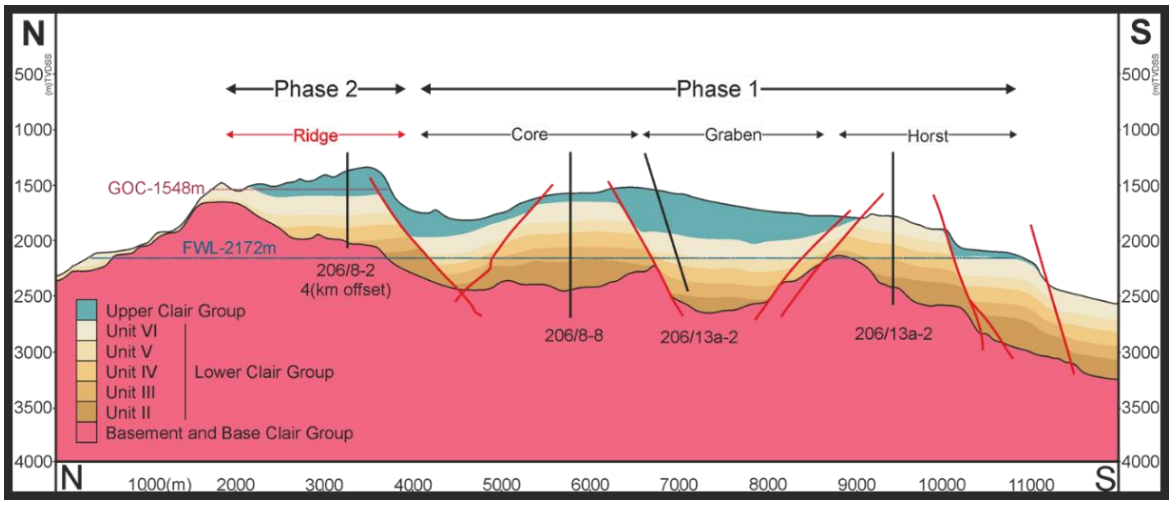

Figure 1.20: Cross section through the Clair Field. Modified after (Barr et al., 2007).

1.3.1. The Geology and Tectonic Evolution of the Clair Field and Clair Basin:

The tectonic evolution of the Clair Field can be traced as far back as the Archaean, through to the present day. This, together with its position on the margins of the North Atlantic, has resulted in a complex tectonic evolution (Duindam and van Hoorn, 1987).

The field is located on the eastern side of the extensional Faroe-Shetland Basin (FSB) which formed as the result of a series of rifting events from the Devonian (Figure 1.21) to the Palaeocene and comprises a several sub-basins which are separated by a series of NE-SW basement highs and horst blocks (Figure 1.22) (Stoker et al., 1993).

1.3.2. Precambrian Basement:

The basement rocks of the Rona Ridge are penetrated in numerous wells offshore and were originally attributed to the Lewisian foreland (Dean et al., 1999). The basement is predominantly granodioritic to granitic orthogneisses with subordinate granitoids, dioritic to mafic gneisses and amphibolites. Studies of basement cores by Holdsworth et al (2018) and Chambers et al., (2005) from the Rona Ridge and wider Faroe-Shetland Basin give a 2.7-2.8 Ga U-Pb zircon age for the gneisses offshore. Lu-Hf analysis of zircons suggest a wide variety of pre-crystallisation histories in the samples and also indicate involvement of a Paleo- to Mesoarchean crustal sources of 2.9Ga to 3.3Ga. This study also revealed a lack of evidence for Laxfordian events (1.7-1.8Ga), which are present in the Lewisian Gneiss Complex of Northwest Scotland. This suggests that a further terrane boundary should exist between the basement of Northern mainland Scotland and the basement of the offshore Faroe Shetland Basin and Shetland, see Figure 1.23.

The proposed Faroe Shetland Terrane would be the eastward continuation of the foreland (Rae Craton) to the Nagssugtoqidian orogeny, in the same way that the Hebridean Terrane (incorporating the Lewisian Complex) is the foreland to the younger Caledonian Orogen to the East of the Moine Thrust Zone. Thus the basement rocks that comprises the Rona Ridge are equivalent to Precambrian basement rocks that outcrop in Eastern Greenland and potentially similar to those exposed in Northern Shetland (Kinny et al., 2019) and are not part of the Lewisian Complex even if the protoliths are of a similar age.

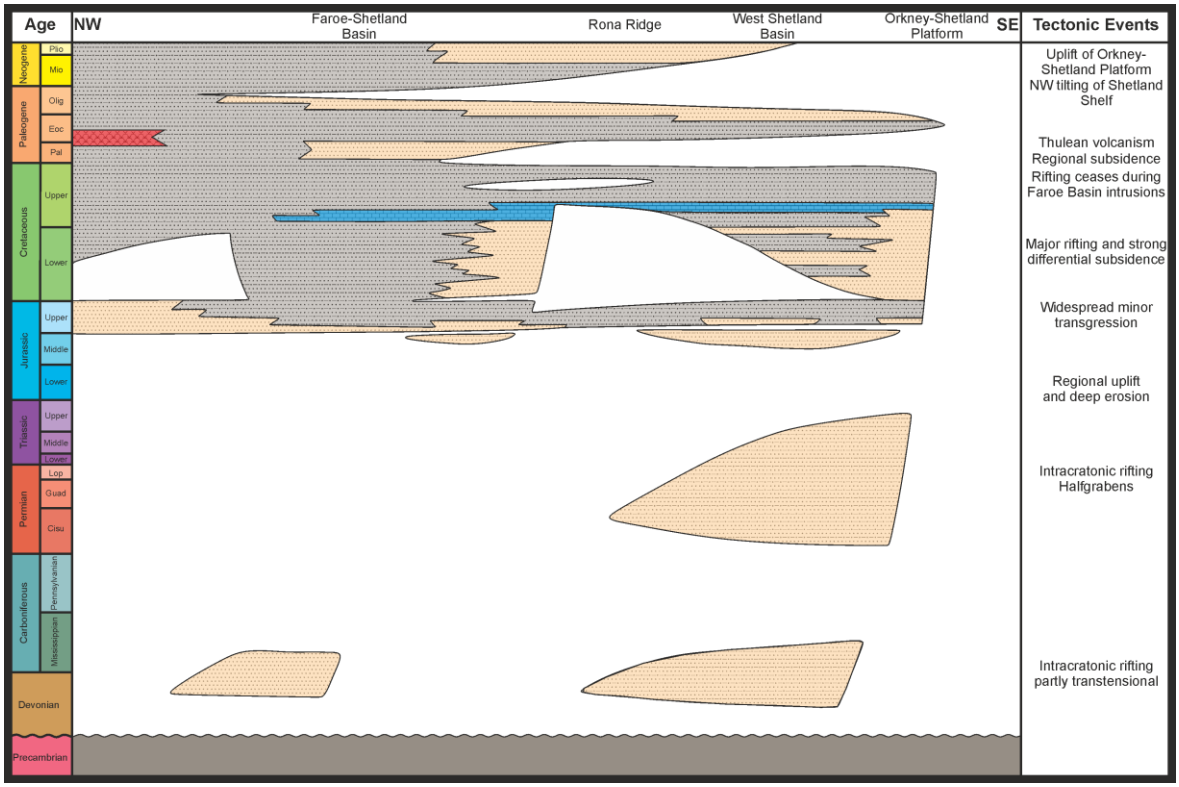

Figure 1.21: Chronostratigraphic chart for the UKCS, West of Shetland. Modified *after* Duindam and van Hoorn, (1987).

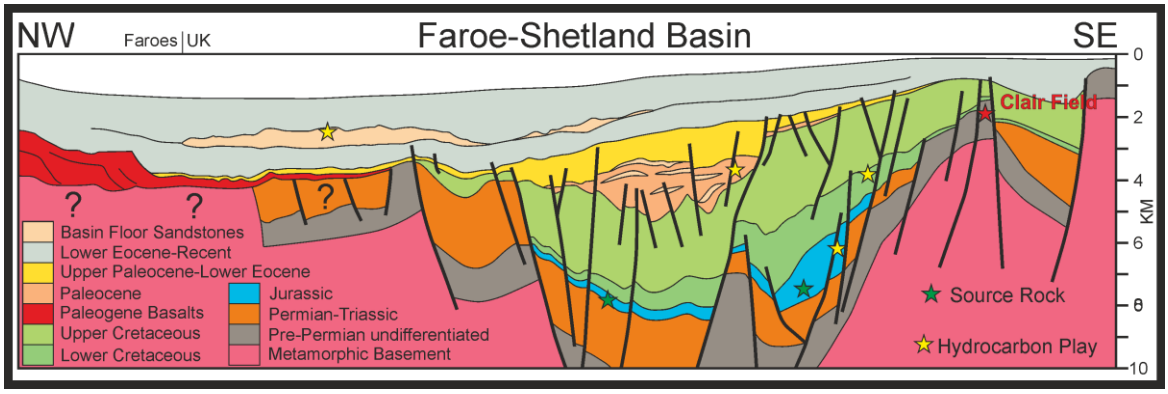

Figure 1.22: Cross section through the Faroe Shetland Basin. Modified *after* Stoker et al., (1993)

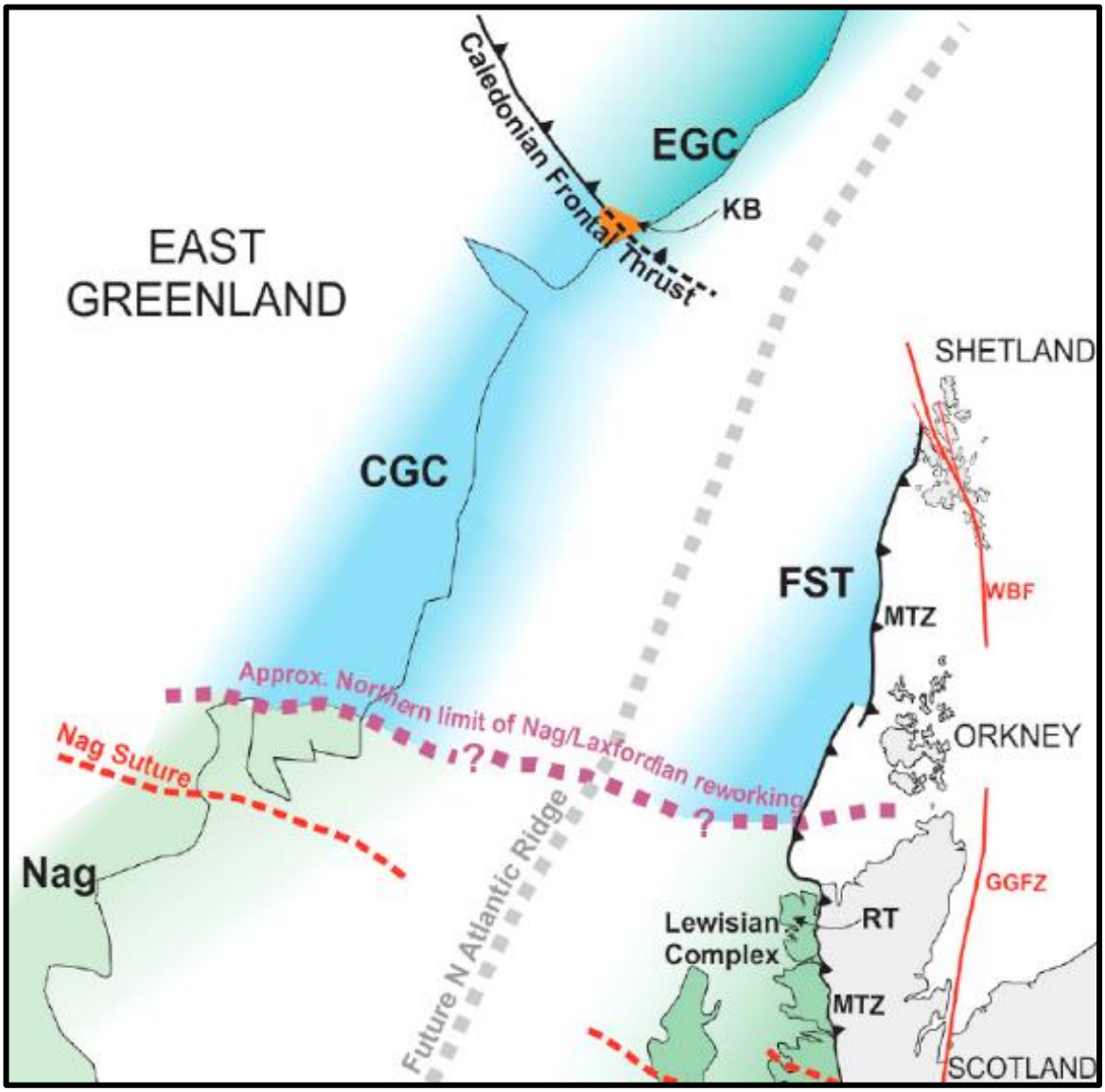

Figure 1.23: Simplified map showing the major age provinces of basement terranes in the British Isles. Abbreviations: MTZ = Moine Thrust Zone; WBF = Walls Boundary Fault; GGFZ = Great Glen Fault Zone; Nag = Nagssugtoqidian; CGC = Central Greenland Craton; KB = Kangerlussug Basin; EGC = East Greenland Caledonides; RT = Rhiconich Terrane of the Lewisian Gneiss Complex (Holdsworth et al. 2019).

1.3.3. Devonian-Carboniferous Clair Group:

Following the Caledonian Orogeny and formation of the ORS supercontinent as result of the closure of the Iapetus and Rheic oceans, the Caledonian mountain belt began to 'collapse' during the Devonian and into the Carboniferous and supposedly resulted in the extensional reactivation of pre-existing thrusts. This led to the formation of a series of small sedimentary basins , such as the Clair Basin, into which material shed from the Caledonian mountains was deposited, until eventually enough accommodation space was available to form the much larger Orcadian Basin (Bartholomew et al., 1993; Stoker et al., 1993).

The Clair Group was deposited in a Northeast-Southwest trending half graben as an inter-montane, arid continental rift basin. The Devonian age sedimentary rocks within the Clair Field were first described as the Clair Group by Blackbourn (1987) who grouped all Devonian age rocks between the metamorphic basement and regional Cretaceous age top seal as the Clair Group. It is predominantly comprised of fluvial, alluvial, aeolian and lacustrine sedimentary rocks with localised conglomerates (Figure 1.24).

Later, a field scale unconformity was recognised, and the Clair Group was subdivided into the Devonian age, Lower Clair Group, and the Carboniferous age, Upper Clair Group. In addition to the field scale unconformity a number of smaller intraformational unconformities, together with significant changes in provenance, were later identified by Allen and Mange-Rajetzky (1992) which led to a more detailed zonation of the Clair Group and a revision of its paleoenvironment (Figure 1.25). A more detailed stratigraphic framework was established by McKie and Garden, (1996) (Figure 1.26) who identified first, second and third order cycles related to tectonics and climate. A sequence stratigraphic approach identifying changes in the sedimentary system allowed for more detailed correlation and prediction of facies away from known data points.

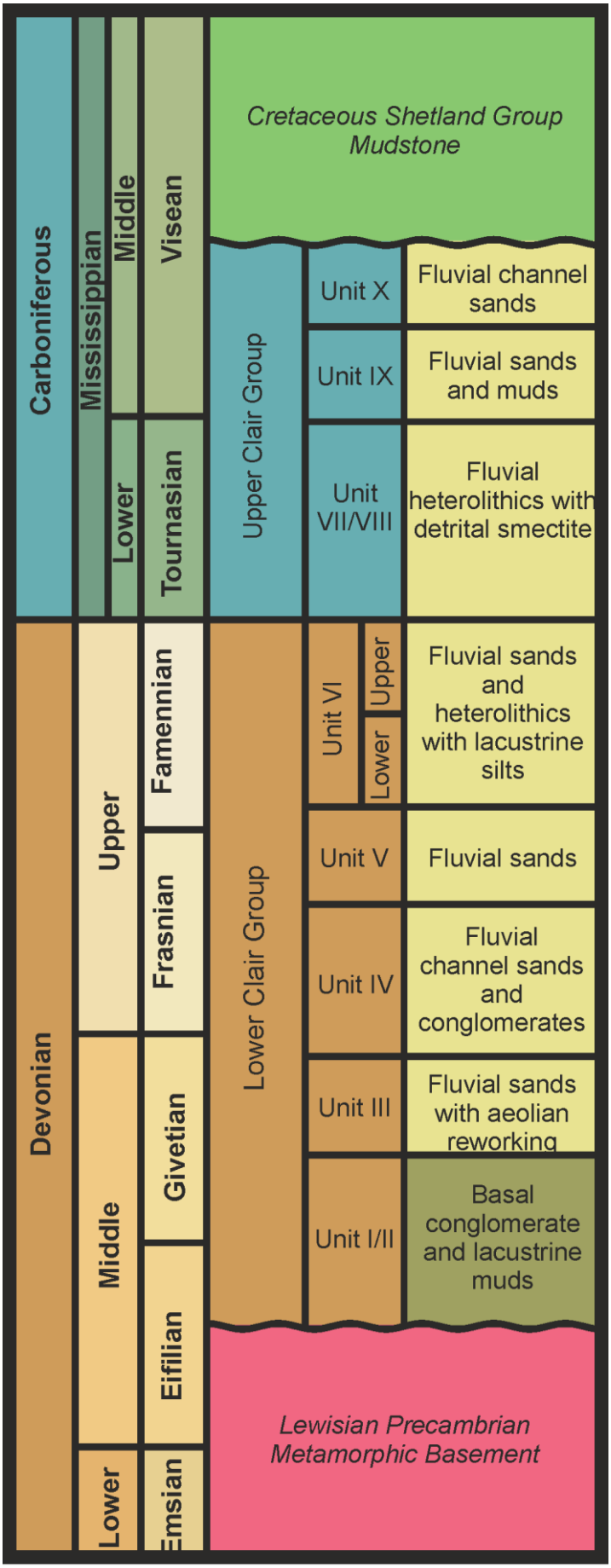

Figure 1.24: Stratigraphy of the Clair Field. Modified *after* Morton and Milne (2012).

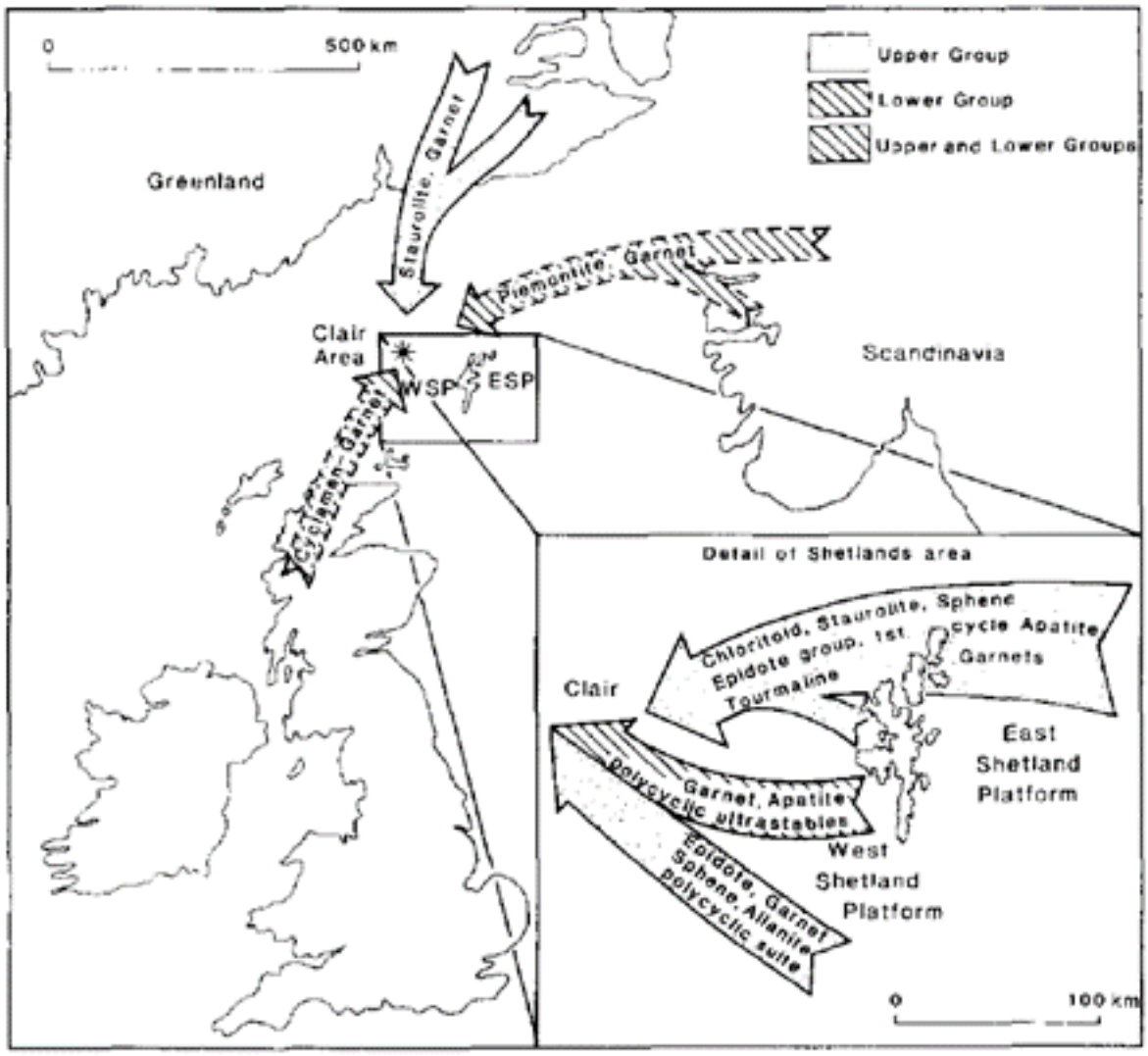

Figure 1.25: Provenance areas of heavy minerals in the Devonian-Carboniferous Clair Group (Allen and Mange-Rajetzky, 1992).

A conceptual basin model by Nichols (2005) combined the earlier work with facies analysis to build a more detailed model for the evolution of the Lower Clair Group and discussed the various controls on deposition; tectonics, base level, paleoclimate, and sediment supply. This was further revised through the use of heavy mineral provenance analysis due to the paucity of biostratigraphically datable material in the Clair Group (Morton and Milne, 2012; Morton, 2007; Schmidt et al., 2012). This analysis highlighted subtle variances in sedimentary provenance, backed up using zircon geochronology to date sediment source regions and correlate the Clair Group between wells (Figure 1.27).

To the West of Shetland, few wells have penetrated Devonian-Carboniferous sedimentary rocks, but many more wells have recorded reworked microfossils in younger host sediments (Dean et al., 1999; Hitchen and Ritchie, 1987). This evidence, together with

outcrop in Northern Scotland, Orkney and Shetland suggests that rocks of this age were far more widespread in the geological past.

The rocks that make up the offshore Clair Group may represent a transitional facies between the well-developed lacustrine facies of the Orcadian Basin further to the South and East and a montane environment that would have existed to the Northwest of the Clair Basin (Hitchen and Ritchie, 1987). The Devonian sequences West of Shetland have been correlated with the onshore Devonian age sedimentary basins in Northern Scotland, Eastern Greenland, Norway (Figure 1.14). This is based on distinct similarities in sedimentary facies, scarce palaeontological evidence and from palynology (Stoker et al., 1993). It is interpreted that the geology offshore represents a transitional environment (Hitchen and Ritchie, 1987) between the well-developed Devonian sequences seen in the Orcadian basin in Northern Scotland and the Orkneys, and an elevated area to the north and west which was supplying sediment to the Devonian basins.

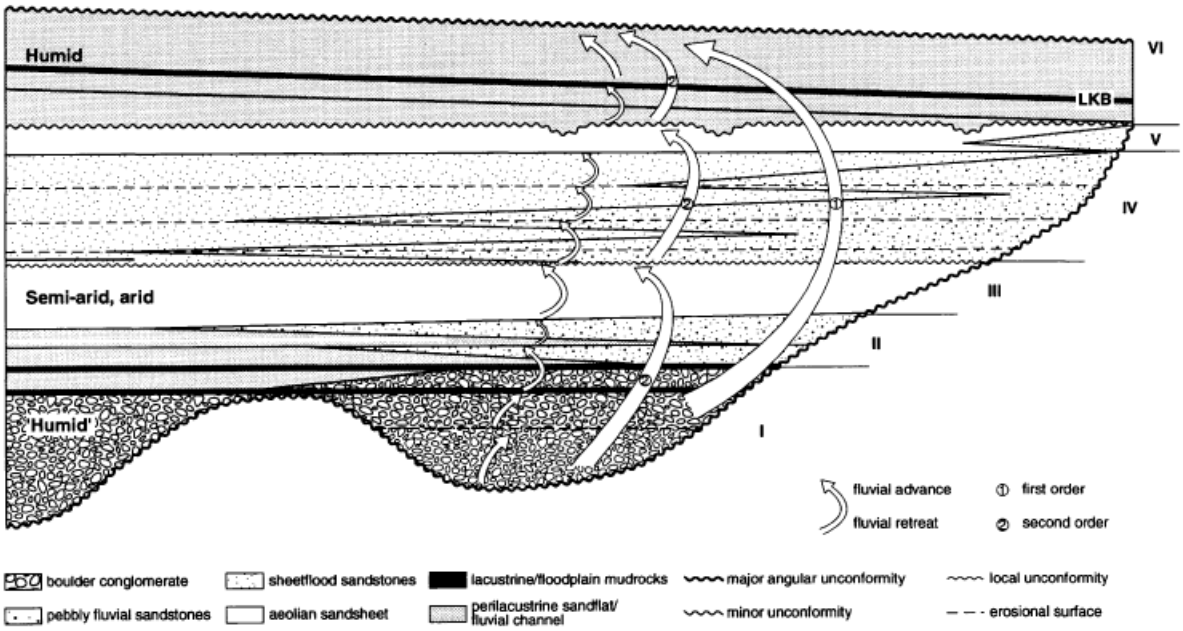

Figure 1.26: Synthesis of the hierarchical cycles identified in the Lower Clair Group, showing the progressive onlap onto the basement of the Rona Ridge and 1st, 2nd and 3rd order cycles that were identified in the Clair Group (McKie and Garden, 1996).

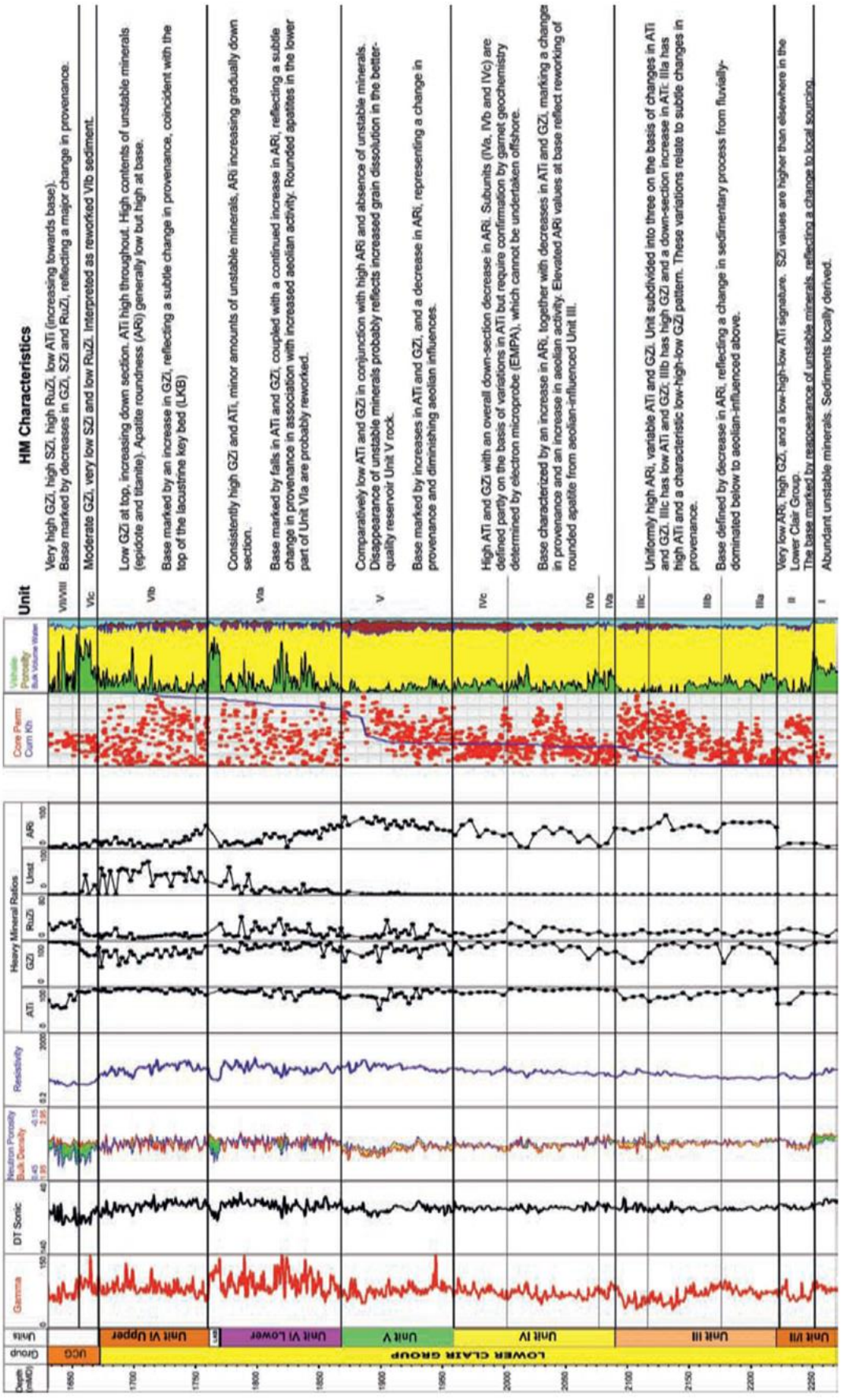

Figure 1.27: Heavy mineral stratigraphy of the Clair Group for the fully cored Core area template well 206/8-8 (Morton and Milne, 2012).

1.3.4. Post Devonian Geology:

The Clair area later experienced a series of rifting events with Northwest-Southeast and East-West extension through the Palaeozoic and Mesozoic forming new structures and repeatedly reactivating pre-existing ones (Bartholomew et al., 1993) during development of the Faroe-Shetland basin. The Clair Group sediments are truncated by the Base Cretaceous unconformity and overlain by a thick succession of shallow marine sands and mudstones of the Late Cretaceous Shetland Group. This transgressive unit provides 4 way dip closure not just to the Clair structure, but forms a regional seal and is the cap rock to many developments in the Faroe-Shetland Basin and wider UKCS (Barr et al., 2007). These are followed by Paleogene shallow water sandstones and mudstones and later by deep-water siltstones and mudstones into the Neogene as subsidence outpaced deposition(Stoker et al., 1993). Quaternary glaciations influenced sedimentation and the deposition of laterally extensive fluvio-deltaic to shallow marine sediments (Stoker et al., 1993). Following this series of pulsed extensional events, the Clair area experienced doming and uplift associated with seafloor spreading during the Palaeocene development of the North Atlantic Igneous Province (Eldholm and Grue, 1994) and opening of the North Atlantic. This involved the eruption of thick sequences of basaltic lava flows into the opening Faroe-Shetland Basin and the emplacement of suites of basaltic sills, some of which are present within the overburden in the southwest Clair area. This activity continued into the Eocene and was followed by post-rift subsidence and relaxation which was punctuated by several further localised pulses of uplift and compression, reactivating some faults, during the continued opening of the North Atlantic (Davies et al., 2004).

The presence of corrensite and Mg-rich chlorite suggests burial temperatures during these pulsed subsidence events approaching 150°c, which exceeds early estimates of 100°c (Pay et al., 2000). The Clair Field has thus been buried more deeply than previously assumed, or heat flow was higher in the past. The latter option is more likely given the areas complex thermal history due to its proximity to Paleogene age basalts associated with the North Atlantic Igneous Province, localised igneous activity associated with Caledonian plutons and syn-rift volcanism (Astin, 1990; Hillier and Marshall, 1992; Parnell et al., 2005).

The source of oil in the Clair Field has been geochemically matched to Late Jurassic, Kimmeridgian age shales, buried at much greater depth to the Northwest in the Faroe Shetland Basin (Finlay et al., 2011; Stoker et al., 1993), where high quality, oil prone source

rocks have been heated sufficiently to generate hydrocarbons and charge the present Clair Structure. More recent and detailed geochemical analysis of oils and fluid inclusions from the area, indicate multiple charge events (Blamey et al., 2009; Mark et al., 2008; Parnell et al., 2005) prior to the present day charge and several potential source rocks, with the dominant source being Kimmeridgian age shales. Through the use of Re/Os dating, Finlay et al. (2011; 2012) dated the age of charge to the Late Cretaceous (68 Ma ±13) and is associated with the opening of the North Atlantic, with migration from the source kitchen to the Northwest of the Clair Field through Jurassic age carrier beds up dip, into and through the fractured basement and Devonian sequences that overly the Rona Ridge.

Sediment filled fractures within the Rona Ridge and Clair Group, along with hydrothermal mineralisation which has been dated to the Late Cretaceous (Holdsworth et al., 2019), prove the presence of open fractures during the generation and migration of hydrocarbons and are likely to have played a key role in allowing hydrocarbons to charge not only the Clair structure, but many of the other fields along, and adjacent to the Rona Ridge.

1.3.5. The Clair Field as a fractured reservoir:

An early structural model for the Clair Field was developed classifying structures within fracture corridors into three types based on their spacing; 1) Regional fault zones with 1-1.5km spacing, 2) Intermediate fault zones with 100-200m spacing and 3) small scale faults with 30-35m spacing (Coney et al., 1993) This classification was based on fieldwork observations, cores and 3D seismic. Two main trends were identified in the basement with North-northeast–South-southwest faults truncating the ridge, and Northeast-Southwest to East-northeast-West-southwest normal fault segments with similar structures being identified within the Clair Group.

During appraisal and well tests, it was observed that better flow rates were achieved from zones of fractures and faulting (Coney et al., 1993; Falt et al., 1992). It was also observed that approximately a third of the effective permeability is attributed to the matrix, with the remainder to fractures (Barr et al., 2007). Almost all vertical permeability in the Clair Group comes from fractures, and thus horizontal wells are key to production. As a consequence of this, further wells were planned to penetrate the Devonian and basement at a low angle or horizontally and cross-cut the greatest number of faults and fractures. Ogilvie et al.,(2015) provides an overview of the significance of structural geology in the later

development of the Clair Field further highlighting four key issues: 1) judgment of distance to and geometry of faults in the Tertiary sections, 2) characterising polygonal faults in the Cretaceous sections, 3) the structural model for the Cretaceous section and an assessment of well bore stability and 4) fault seal in the reservoir section.

The Clair Group is classified as a Type 2 fractured reservoir as per the classification described by Nelson (2001); in that fractures provide the essential permeability and fluid pathways, with the rock matrix providing the porosity and storage of hydrocarbons (Nelson, 2001; Spence et al., 2014). This is not wholly the case in the second phase development, Clair Ridge, as oil is being produced from both the Clair Group and the fractured basement of the Rona Ridge. The latter reservoir would be classified as Type 1; in that the fractures provide the essential porosity and permeability within the reservoir (Nelson, 2001; Spence et al., 2014) as there is no inherent primary porosity within the metamorphic basement. Numerous analogue studies have attempted to lower the risk and reduce uncertainty, see Appendix B. These studies have assisted in fracture modelling and guiding well placement (Barr et al., 2007). Monitoring of reservoir performance during production will be key to testing how robust models are and minimising the chance of early water breakthrough during waterflooding (Clifford et al., 2005). Exploration well 206/7-1 produced oil from an open-hole test of fractured basement and further well tests in Clair have proven productive basement. With other nearby exploration successes by companies such as Hurricane, a fractured basement play is now developing, West of Shetland (Belaide et al., 2016; Belaidi et al., 2018, 2016; Bonter et al., 2018; Gutmanis et al., 2012; Hitchen and Ritchie, 1987; Spence et al., 2014).

Further full field fracture models have been developed at a series of smaller scales (subseismic fault models, systematic joint models) in order to capture the full range of potential reservoir performance models(Barr et al., 2007; Clifford et al., 2005). Advances in 3D modelling (Rawnsley and Wei, 2001) and the availability of production data since has meant more detailed models can now be built and tested. Reservoir monitoring has been key with advanced seismic imaging able to detect areas of fluid change and thus refine reservoir models and guide further drilling (Webster, 2018).

1.3.6. Clair Field Analogue Research:

Since the discovery of the Clair Field in the 1970's, a series of analogue studies have been carried out by both academia and by industry with much of the early work focusing on the sedimentology and stratigraphy of the onshore Orcadian Basin as an analogue for the offshore Clair Basin and attempted to better understand reservoir architectures and predict reservoir quality. In the late 1970's and 1980's projects examined the Devonian sequences of Caithness, Orkney and Shetland, largely with a focus on the sedimentology, reservoir quality and stratigraphic/structural framework of the Devonian Basins.

More recently a series of PhD projects, a number of which have been carried out at Durham University working in conjunction with the Clair Joint Venture Group, have since looked at the role of structures in reservoir development and appraisal, understanding the structural evolution and basin development history of the North Atlantic margins during the Palaeozoic and Mesozoic and also trying to better understand reservoir quality (Figure 1.28).

A paucity of offshore data together with the low number of wells penetrating Devonian sequences, means that the correlation of onshore and offshore data has been troublesome Focussed efforts such as the 21CXRM Palaeozoic Project by the BGS (Monaghan et al., 2016) aimed to better understand the petroleum systems that underlie the well explored Mesozoic sequences and better tie the onshore geology with the offshore data. These together with regional studies commissioned by the OGA are going some way to building a better understanding of the development of the ORS on the UKCS.A brief overview of the previous research in to Clair Field analogues and the key findings of each study can be found in Appendix B.

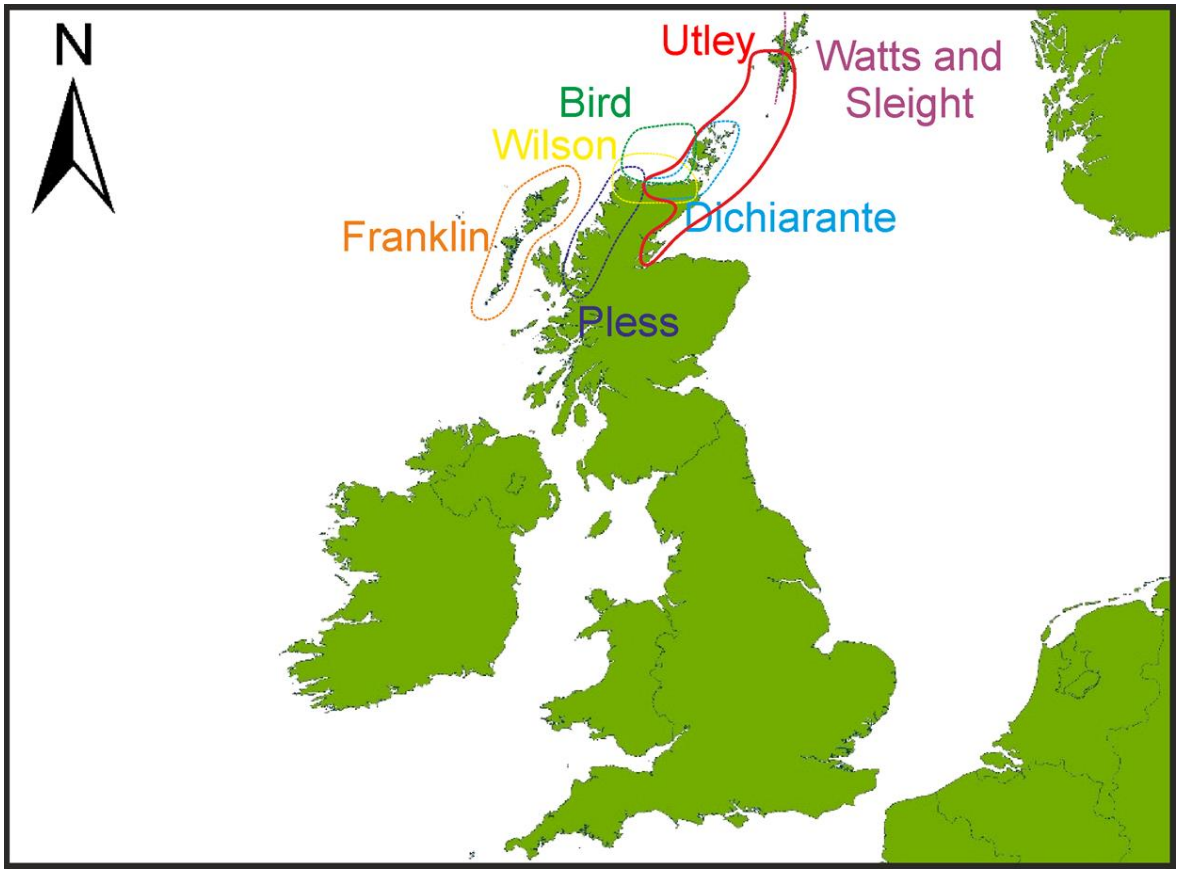

Figure 1.28: Map of previous study area locations. Shapefiles courtesy of the Oil and Gas Authority, (2019)

Chapter 2

Techniques and Methodology – a multiscale analysis:

Chapter 2 - Techniques and Methodology – a multiscale analysis:

This chapter describes the data sets that have been used in this study and explains in greater detail the different techniques and methodologies that have been used and developed during this research. It also covers the key definitions, terminology and geological concepts used or addressed during the course of this study.

The use of a range of different techniques that cover a range of scales has allowed for the greater integration of differing data types (Fig. 2.1.). It also captures observations at a scale missed by traditional analytical tools used in industry such as wireline logs and seismic (Figure 2.1 and 2.2).

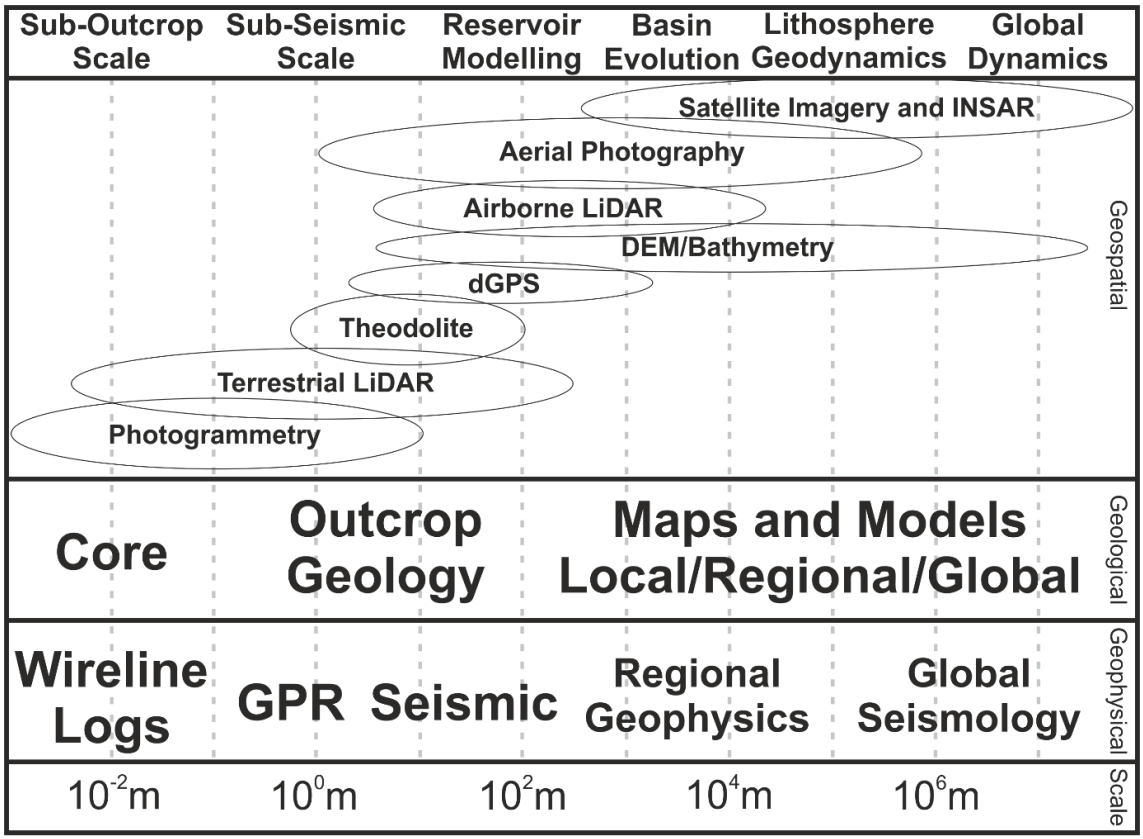

Figure 2.1: Range of data scales used within the geosciences. Modified *after* Jones et al., (2008)

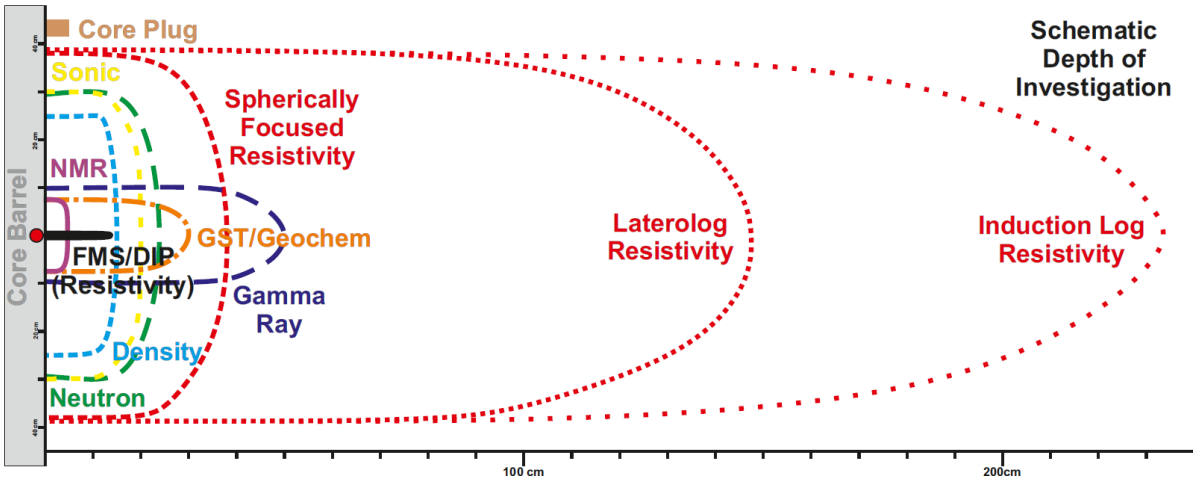

Figure 2.2: Schematic depth of investigation diagram for wireline logging tools.

2.1. Regional to sub-regional scale analysis – Remote Sensing, Desk Studies and GIS data collation:

2.1.1. Published maps and other datasets:

A variety of published maps and data sets were collated and geological data (e.g. bedding, foliation, lineations) were georeferenced, extracted and digitised in ArcGIS to produce maps, diagrams and carrying out further analysis. The data sets used here include:

- Oil and Gas Authority Maps and regional reports
    - 21 CXRM Palaeozoic Project courtesy of the BGS
    - 21 CXRM East Shetland Platform courtesy of Frogtech Geoscience
    - Lloyds Register and OGA regional reports
- UKCS relinquishment reports for offshore areas adjacent to study area (Oil and Gas Authority, 2019b).
- Ordnance Survey land and height data at 1:250,000, 1:50,000, 1:25,000, 1:10,000 and 1:1000 scale for the generation of backdrop mapping, field maps and figures.
- Published BGS/NERC geological maps and accompanying reports at the following scales:
    - 1:250,000 UTM series of onshore and UKCS (United Kingdom Continental Shelf)
    - Geological mapping fieldslips of Foula of W.Mykura and D.Flinn (viewed at the BGS, Edinburgh and in the Shetland Archives respectively).
    - Solid and drift geological maps at 1:50,000, 1:63360 and 1:100,000 scale.

- Archive oblique aerial imagery courtesy of BP (on behalf of the Clair Joint Venture Group) and Canmore, Historic Scotland. Images were used to produce virtual outcrop models and for making general observations e.g. Figure 2.3.

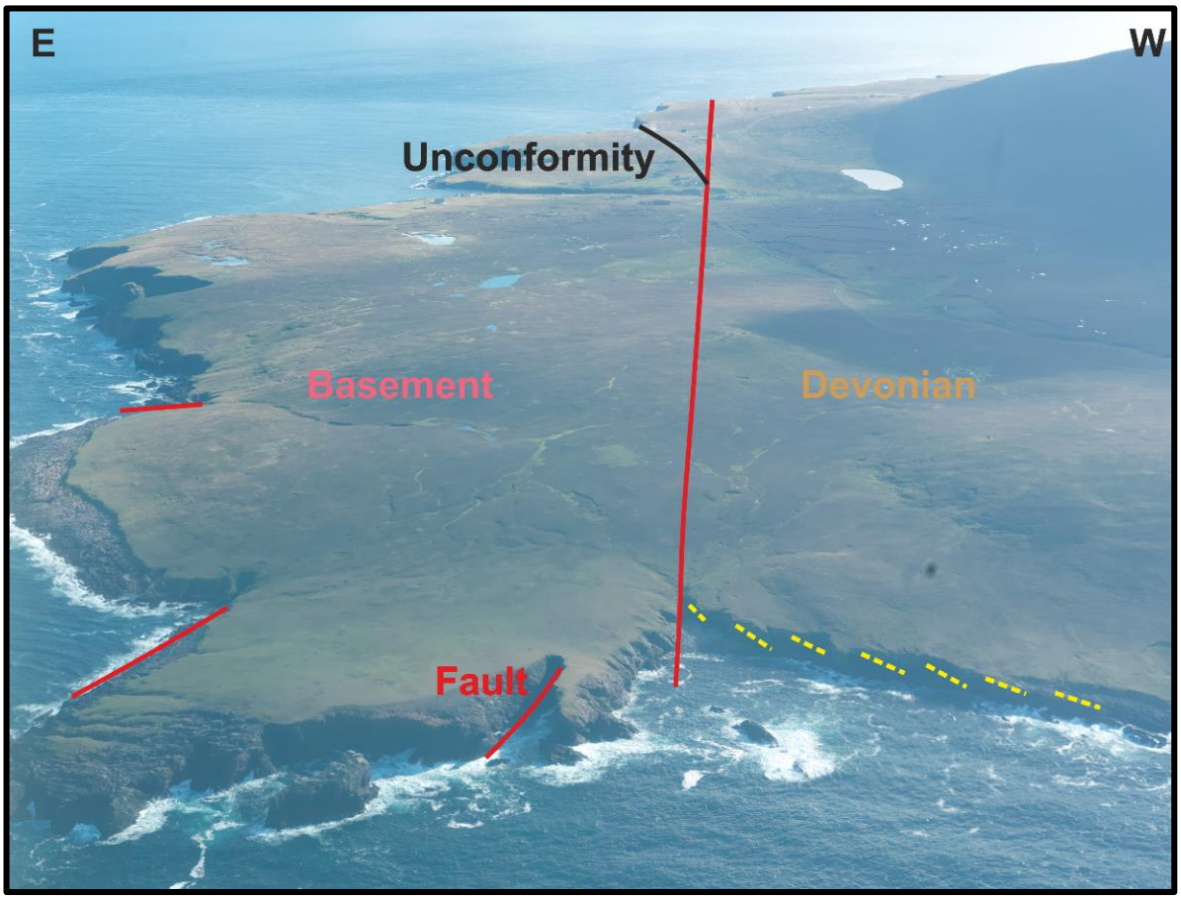

Figure 2.3: Oblique aerial image of island of Foula, Shetland. An example of an annotated aerial image as used in this study. Courtesy of Canmore, Historic Scotland.

2.1.2. Photogeology and Lineament Analysis - DEM/DTM (Digital Elevation Models/Digital Terrain Models) and Bathymetry:

A lineament is a linear or curvilinear geomorphic/topographic/bathymetric feature that can be identified and mapped from remotely sensed datasets such as aerial/satellite imagery. This analysis is a relatively easy way to gather a large, statistically significant dataset from which observations on the preferred orientation of surface features can be linked to the underlying geology. It can then be tied to observations made in the field, helping to identify any possible trends and scaling relationships, and can be directly compared to published data.

Lineament analysis was carried out on a combination of high-resolution aerial images, orthorectified UAV aerial imagery, DEM/DTM data and bathymetric data. Topological analysis was also carried out on selected datasets (see section 2.3). The initial data set used for this analysis was the OS MasterMap Imagery of mainland Scotland, the Orkney Isles, and Shetland Isles supplied by the Ordnance Survey via a Research Data Agreement. Data was supplied as 1km by 1km tiles at a resolution of up to 25cm in geoTIFF format. This data was processed in ArcGIS which enabled visualisation and manipulation of a variety of data types in real world space. Additional imagery was available from GetMapping PLC via the Edina Digimap portal, as some images in this dataset are taken at different times of day and/or tide level which allow for the better visualisation of certain features.

Lineaments from aerial images were picked at a scale of 1:500 as visible linear or curvilinear discontinuities on exposed bedrock surfaces or topographic features (Figure 2.5). Lineaments were picked in ArcGIS as polyline shape files using the digitise tools. Polylines that consist of multiple segments were split into segments using the *Split line at Vertices* ArcGIS tool. Using the *RunEasyCalculate* plugin for ArcGIS, the azimuth of all lines within the shapefile was generated and stored in a new field in the shapefile attribute table. Data was exported in ASCII format to excel for tabulation and further structural analysis. Lineaments were also digitised from DEM/DTM data sets in Globalmapper using the hillshade functions to highlight surface topographic features which may reflect underlying geological structures such as faults. A hillshade was applied with multiple light sources (8) being placed at principal cardinal points, at an azimuth of 45° above the horizon. These settings were used to highlight features, but without putting any strong emphasis on structures of a particular orientation. Lineaments were picked at 1:5000 and 1:10000 scale using a similar methodology to the aerial images. In addition to performing lineament analysis on DEM/DTM data, slope direction and slope angle attribute analysis of the data was carried out in order to independently verify remotely sensed data from Virtual Outcrop Models, e.g. bedding surfaces of offshore sea stacks.

Multibeam echosounder bathymetric data was sourced from the United Kingdom Hydrographic Office (UKHO) INSPIRE portal at a maximum pixel resolution of approximately 1m in either geoTIFF or ASCII format. Data was loaded into Globalmapper in ASCII format and was interpolated, specifying a ‘no data’ distance of 1m to form a smooth continuous

TIN (Triangulated Irregular Network) surface. Lineaments and other sea floor features were mapped at 1:5000 scale in order to produce maps of key geological and geomorphological features which include; subcrop, bedding traces, fold structures, faults/fault zones, areas covered by Quaternary sediments and anthropogenic features. Using the slope shader tools, maps of slope direction and angle were produced in order to collect submarine bedding readings (dip direction, and dip) which were added as attributes to a shapefile.

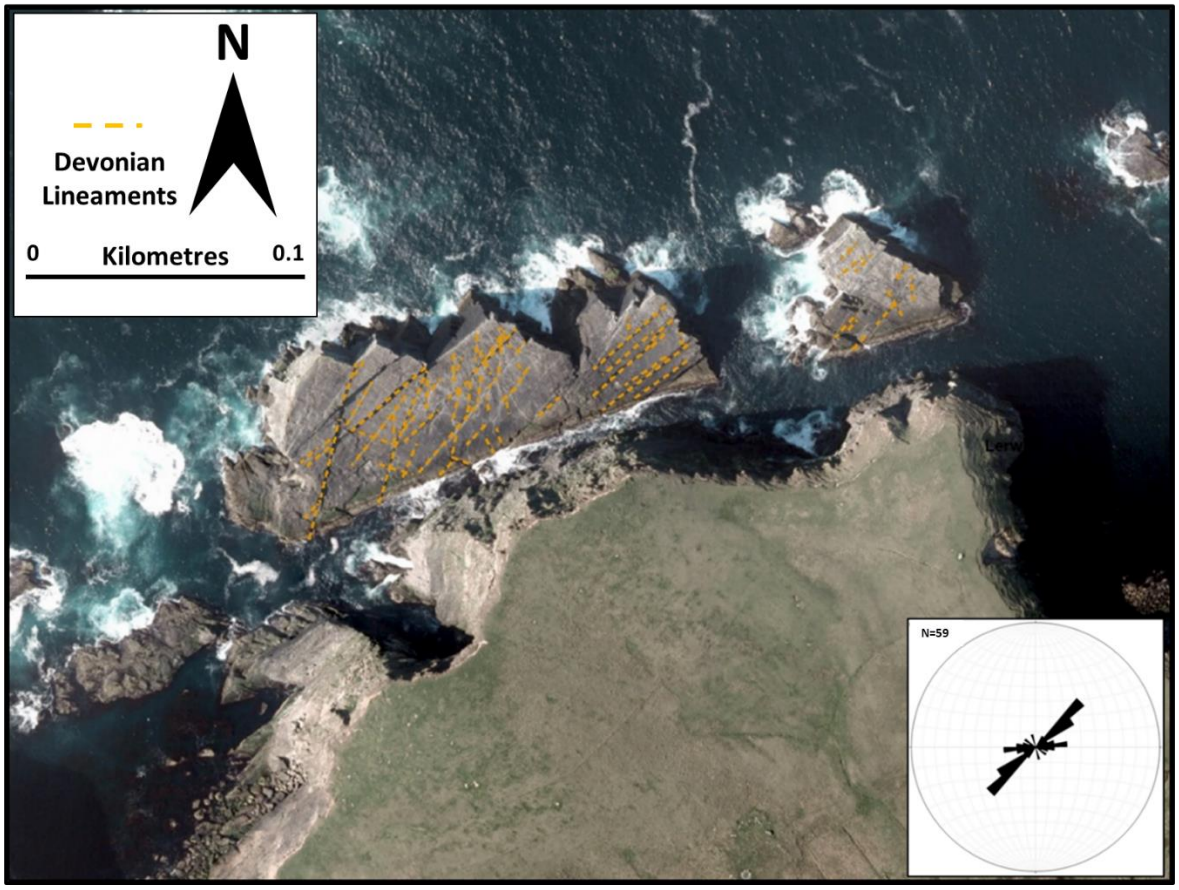

Figure 2.5: Example of lineament analysis used in this project. Aerial image of Da Stack O Da Logat, Foula, Shetland. Inset rose diagram of picked lineaments viewed in Stereonet.

2.1.3. Regional Scale Geophysics:

The geophysical datasets used in this project comprise newly acquired and reprocessed legacy 2D seismic, gravity and magnetic surveys, from the offshore UKCS that have been recently released courtesy of the Oil and Gas Authority (OGA). These data were used to help understand large scale basin structure and link field observations to larger, basin scale structures. Proprietary 2D seismic data courtesy of TGS and Shell were also provided. Onshore geophysical data used in the project includes 2D seismic courtesy of the UK Onshore Geophysical Library (UKOGL) and this was used to understand larger scale

structures that are poorly exposed onshore. Seismic interpretation of key horizons and faults was carried out in Petrel 2016 in two-way time (TWT). The quality of seismic data is diverse and reflects the date of acquisition and the acquisition and processing parameters used.

2.1.4. Structural Analysis:

Structural information that was extracted during regional scale desk studies and from outcrop scale field based studies (section 2.2) was analysed in Stereonet 9.5 (Allmendinger et al., 2011). Conventional structural analysis was performed and stereonets were produced using a lower hemisphere equal area projection with contouring of poles to planes of the data using 20 grid nodes, 2 intervals and to 1 significant figure. The axial plane finder function was used to calculate the orientation of fold structures for the construction of fold profiles.

2.1.5. Fold Profile Construction: Down Plunge Projection Method:

The down plunge method allows for the visualisation of geological structures in such a way as to avoid any distortion of a structures shape due to the influence of topography (Mackin, 1950; Ramsay and Huber, 1987). Thus, by viewing folds in the down dip direction, the true profile of the fold is seen. This method is best suited for cylindrical folds and uses orthographic construction to construct fold profiles (Ragan 2009) (Figure 2.6):

1) Folding lines FL1 and FL2 are constructed perpendicular to the trend of the plunging folds.
2) Scaled elevation lines are constructed at the same scale as the contour interval of the map and outcrop traces are projected through FL to the relevant elevation line.
3) Lines are projected to profile line OP using the plunge angle. Line OB is constructed to bisect the angle between POR and points are projected onto line OB.
4) Lines are then projected down parallel to line FL2 and the fold profile is constructed by joining the points.

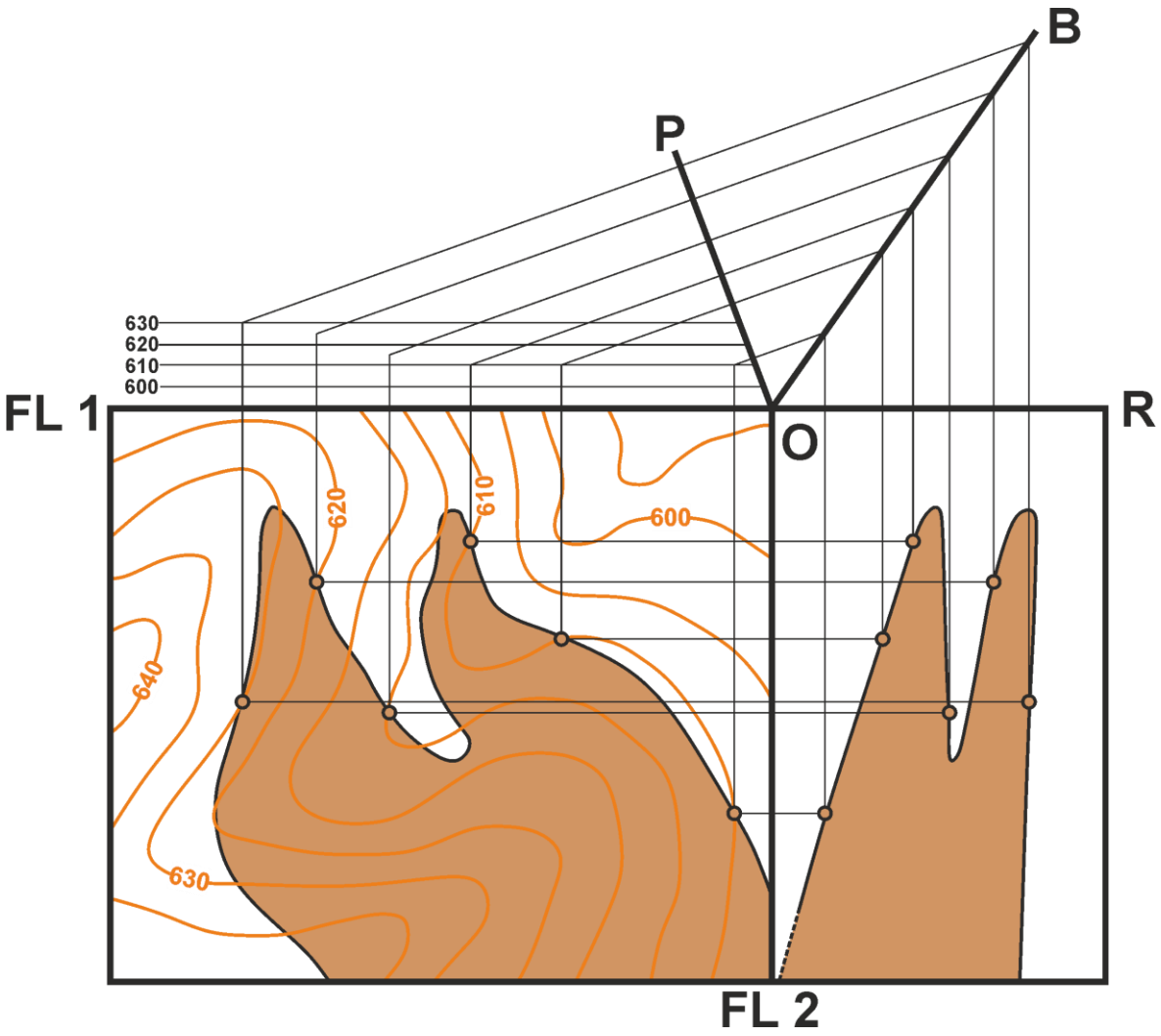

Figure 2.6: Down plunge fold profile construction method from an outcrop in an area of topographic relief. Modified *after* (Ragan, 2009).

2.2. Sub-regional to outcrop scale – Field Based Techniques:

2.2.1. Field mapping, structural data and sample collection:

Traditional geological field techniques were employed, which included, the collection of detailed primary field observations, structural information (bedding, fault information, kinematics, fold orientation, lineations) and photographs. Observations were recorded in a notebook or topographic maps along with the associated GPS location. Conventional fieldwork was supplemented using a drone to acquire imagery from inaccessible outcrops and some imagery was also captured from a boat, for areas and times when flying a drone was unsuitable. Analysis of structural data collected in the field was carried out as per the methodology outlined in section 2.1.4. Samples were also collected in the field for laboratory analysis, see section 2.3. Where necessary samples were collected orientated for microstructural analysis and strike and dip of surfaces on hand specimens were

recorded and marked on samples where appropriate. A total of 110 days was spent in the field, carrying out primary data and sample collection, familiarisation with techniques and the acquisition of images for the production of 3D Virtual Outcrop Models.

2.2.2. Virtual Outcrop Models:

The ability to visualise and capture information in three dimensions is a powerful tool for the analysis of geological problems due to the inherently three dimensional nature of geological structures (Jones et al., 2009) . The building of Virtual Outcrop Models (VOMs) (Figure 2.7) allows you to re-visit an outcrop and continue to analyse and interpret the geology even after you have left the field, bringing the geology into the office environment (Bemis et al., 2014; McCaffrey et al., 2010, 2005; Pringle et al., 2001; Westoby et al., 2012). They enhance conventional fieldwork and provide an alternative if areas are deemed unsafe, too expensive or inaccessible. Furthermore the ability to measure and record information from these models means you can derive new value from outcrops, increase the amount of data you are able to gather from the field, and acquire data from outcrops that are potentially inaccessible, e.g. cliffs, steep terrain, quarries, mines and coastal localities.

Recently the building of Virtual Outcrops has been done through the use of terrestrial laser scanning (TLS or LIDAR) (Brodu and Lague, 2012) and the generation of a 3D coloured point cloud, e.g. see Hodgetts (2013). More recently the use of photogrammetry (PG) has been developed as an alternative to generate the same 3D point cloud, but with much greater ease and lower cost using the more conventional and widely accessible imaging technique of digital photography (Bemis et al., 2014; Hodgetts, 2013). Familiarisation with both methodologies was undertaken and after an initial examination of field sites, it was decided that photogrammetric reconstruction was the preferred approach. This was primarily due to the inaccessible nature of many outcrops, and difficulties in setting up laser scanning equipment in coastal locations.

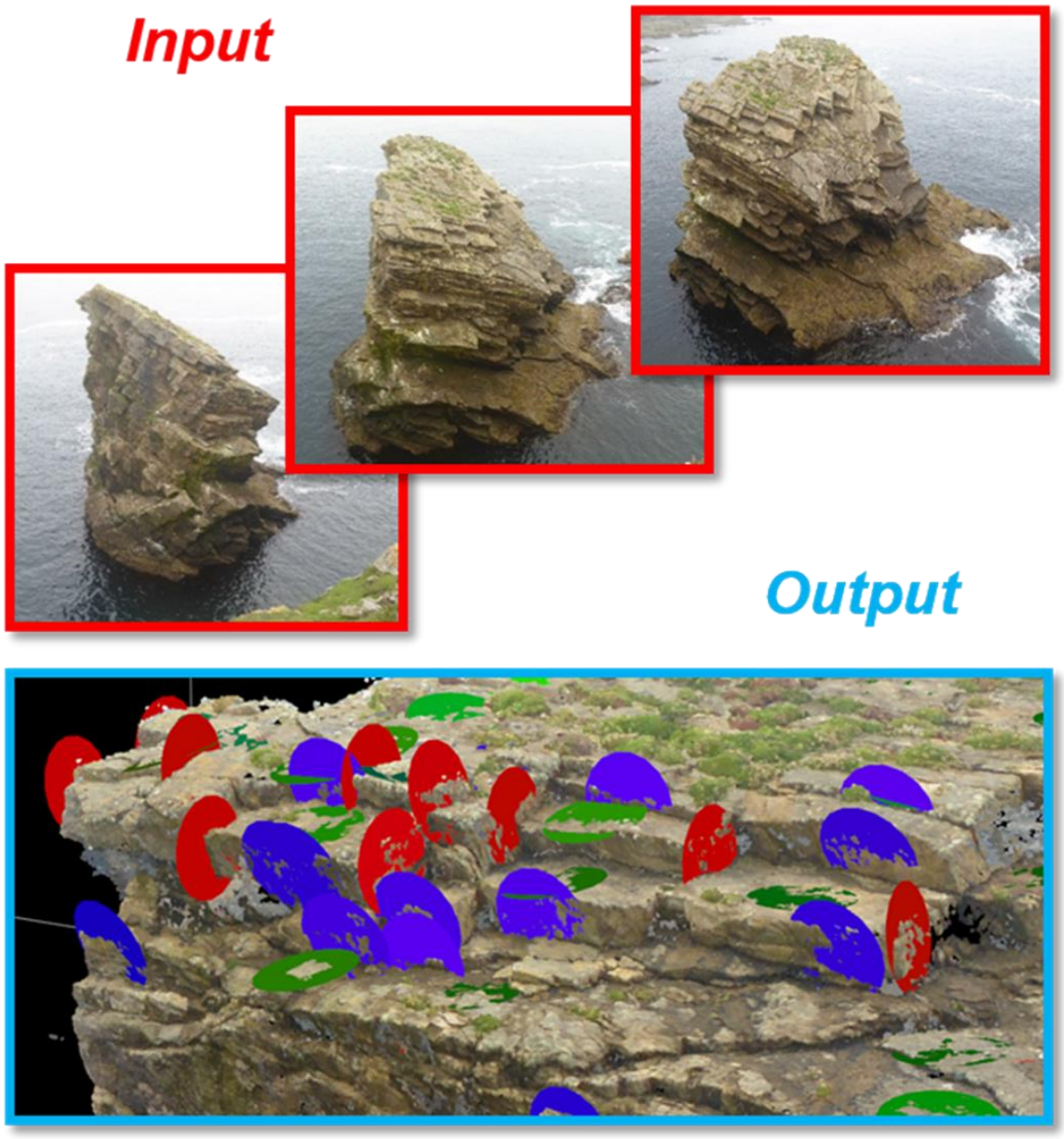

Figure 2.7: Example of inputs (images) and outputs (virtual outcrop with digitised structural measurements) from the Virtual Outcrop Model process.

2.2.2.1. Development of the Photogrammetric Workflow (PG):

2.2.2.1.1. Principles of Photogrammetry:

Photogrammetry can be used to estimate the size, shape and position of an object by analysing two or more images taken from multiple points of view. The main concept behind the technique of photogrammetric reconstruction is known as 'Structure from Motion' or SfM, which is the ability to calculate the three dimensional position of a point from overlapping two dimensional images when no three dimensional information is known (Ullman, 1979)(Figure 2.8). When combined with the computational power of modern

personal computers, along with modern GNSS/GPS, the ability to produce large 3D models is now possible even with quite modest equipment.

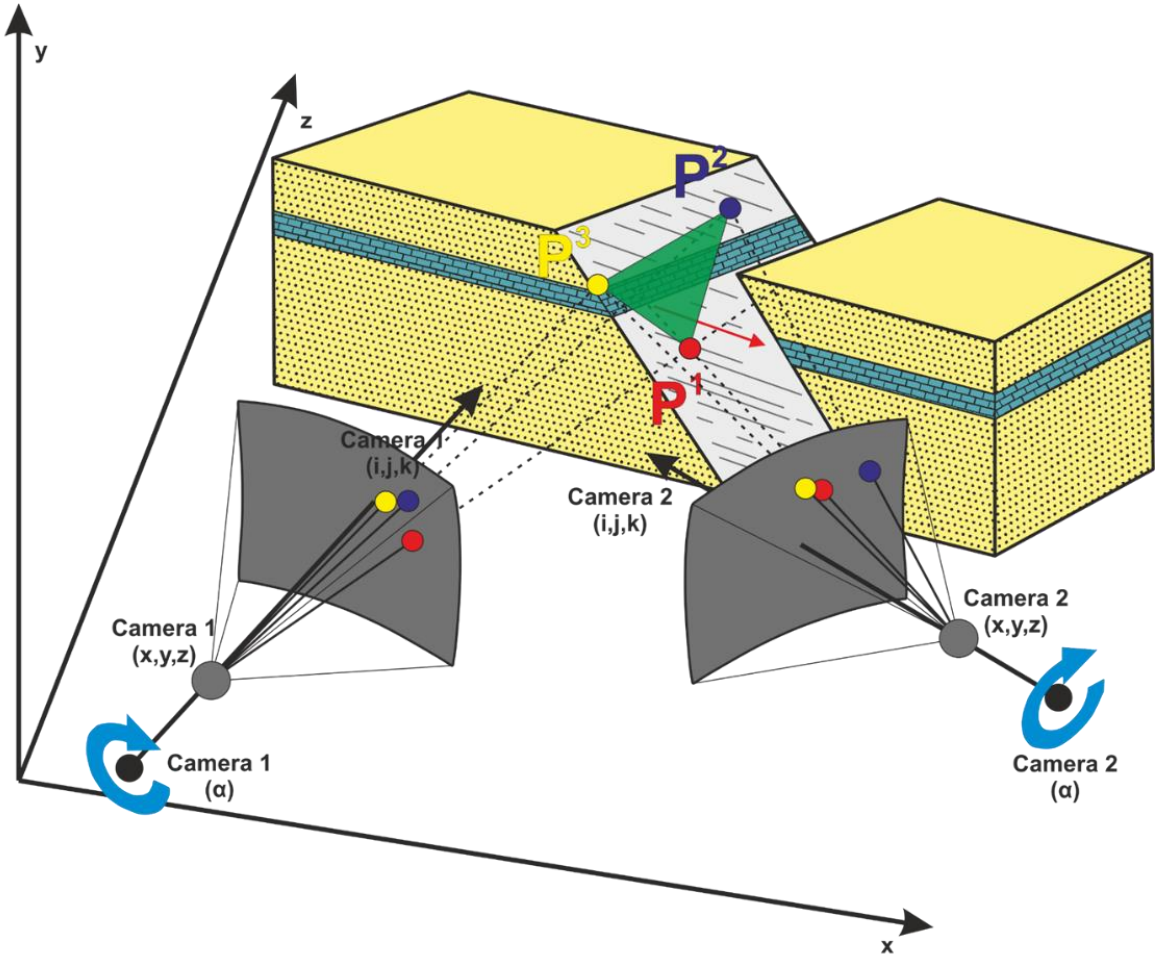

Figure 2.8: Idealised model of photogrammetric reconstructions using the SfM method. Points P1,P2,P3 are photographed from 2 positions (Camera 1 and Camera 2) and their positions in 3D space are calculated using the focal length of the cameras, and their orientation defined by the ijk versor and the amount of rotation about that axis. The three points can then be connected by defining a plane (green triangle) that runs through all three points. This planar surface can then be measured e.g. to define the dip/azimuth of a fault surface. Modified *after* Tavani et al., (2014).

2.2.2.1.2. Equipment and Software:

Experimentation with different photographic platforms was carried out to test the feasibility and capabilities of different cameras. The greatest success came from cameras with an inbuilt GPS. Images with location information speed up acquisition in the field, as less time is required to survey ground control points. It also helps with scaling models and also speeds up the process by which images are matched and points are detected during the model building process. The best results were achieved using a GPS enabled man-

portable folding quad-copter style unmanned aerial vehicle (UAV) (Figure 2.9) as it allowed for images to be taken from multiple positions and angles with ease and minimised the amount of equipment needed to be carried in the field.

Several authors (Bemis et al., 2014; Westoby et al., 2012) have compared the various software packages, both open source and commercial packages, that are available for the processing and building of three dimensional VOMs as well as detailing some best practices, e.g. Tavani et al., (2014). Over the course this study, several software packages were tested along with collection of several suites of images (Figure 2.12), in order to experiment and learn how to process and interpret 3D point clouds and VOMs. Several packages were also tested for the interpretation and measurement of data (Petrel, MOVE, AutoCAD) which has allowed me to develop a workflow by which image are acquired, processed then interpreted to analyse the geology of a virtual outcrop. Agisoft Photoscan (later Metashape) is one of the software packages most widely used which offers repeatable and reliable results. This package combined with the Virtual Reality Geological Studio (VRGS) and Cloud Compare have proven to be the most stable software packages to use for the processing and interpretation of VOMs (Figure 2.7 and 2.10).

Figure 2.9: Field equipment used from left to right: rucksack, protective case for drone, tablet and controller for UAV, standard field gear (hammer, notebook etc) and DJI Mavic Pro UAV. Inset, markers/targets and scale bars (1m folding ruler) used to georeference models.

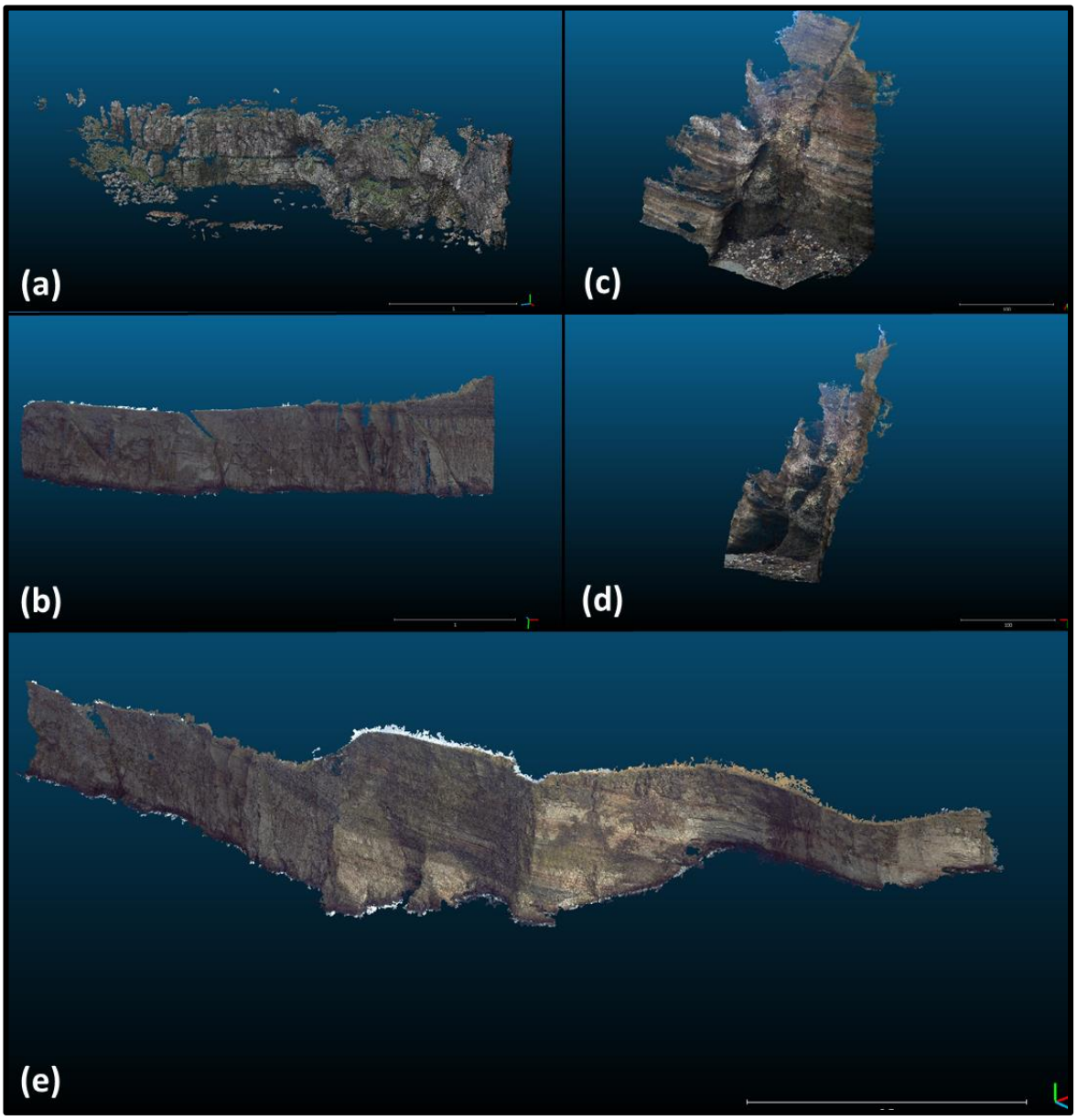

Figure 2.10: Examples of test models constructed using SfM software packages and visualised in CloudCompare. (a) Point cloud of Cullernose Point, Howick. An exposure of the Whin Sill into Carboniferous strata built using the open source software package of Visual SfM. (b) Photoscan derived point cloud of cliffs on Foula, Shetland Isles. (c) and (d) Photoscan derived point cloud of small fault in Devonian strata, Ham Harbour, Northern Scotland. Images collected using mobile phone to test feasibility and quality of using images from internal camera. (e) Photoscan derived point cloud of cliffs on Foula, Shetland Isles. Constructed using images collected in 1998 during a helicopter survey by BP. Trial conducted to test feasibility of using archive imagery and/or scanned images for photogrammetric reconstruction.

2.2.2.2. Virtual Outcrop Model Workflow:

Experimentation with a variety of cameras, and trialling of various methods of acquisition and processing was undertaken in order to develop a workflow for generating virtual

outcrop models. The acquisition of photos was achieved from a variety of platforms and even from multiple platforms and combined into one model. Figure 2.10 shows some examples of outcrops built from images taken to test different types of camera. Some success has even been achieved using archive imagery taken in the late 1990's (Figure 2.10e).

2.2.2.2.1. Acquisition:

Markers were laid or affixed to the outcrop for which a GPS location was recorded, along with 1m rulers from which the dip/azimuth was measured (see Figure 2.11). Structural data was also collected from key features such as faults, or bedding surfaces in order to verify and check the accuracy of models. Such information can also be later used to orientate the resulting 3D model with even greater accuracy.

Photographs were taken from multiple angles around the outcrop with ideally a 70-80% overlap (see Figure 2.12). An in-built GPS allows for approximate positioning of the camera locations relative to one another which allow for greater accuracy during the alignment stage of processing. Weather conditions and time of day must be taken into account, as bright conditions and/or the position of the sun being low in the sky, can lead to strong shadows which can cause problems during the model building process. Bright but cloudy conditions are ideal, as the diffuse light removes shadows. For optimum results, images must be well exposed, in focus and sharp. Ideally images should be collected using the largest aperture possible, a fast shutter speed and the lowest ISO possible in order to minimise camera shake and avoid poorly exposed and/or blurry images.

Images were collected with a variety of different cameras. Images were collected on foot using a handheld Panasonic TZ60 Lumix. This camera was chosen as it had a high sensitivity 18.1 MP camera, 30x optical zoom, high quality Leica lens and most importantly was GPS enabled. For outcrops inaccessible on foot, the use of a UAV (Unmanned Aerial Vehicle) or drone was employed. Images were collected using a DJI Mavic Pro, with a gyroscopically mounted 13.1 MP camera and footage was streamed via radio signal to the controller and viewed on a portable device (phone/tablet) during acquisition with images saved to internal 16GB MicroSD card.

Figure 2.11: Field photograph of an outcrop with 1m scale bars (folding rulers) and A3 size laminated targets ready for acquisition of images for photogrammetric reconstruction. Structural information is collected from surfaces adjacent to targets and scale bars and from the object itself. Location is a fracture zone in Precambrian metamorphic basement on Foula, Shetland.

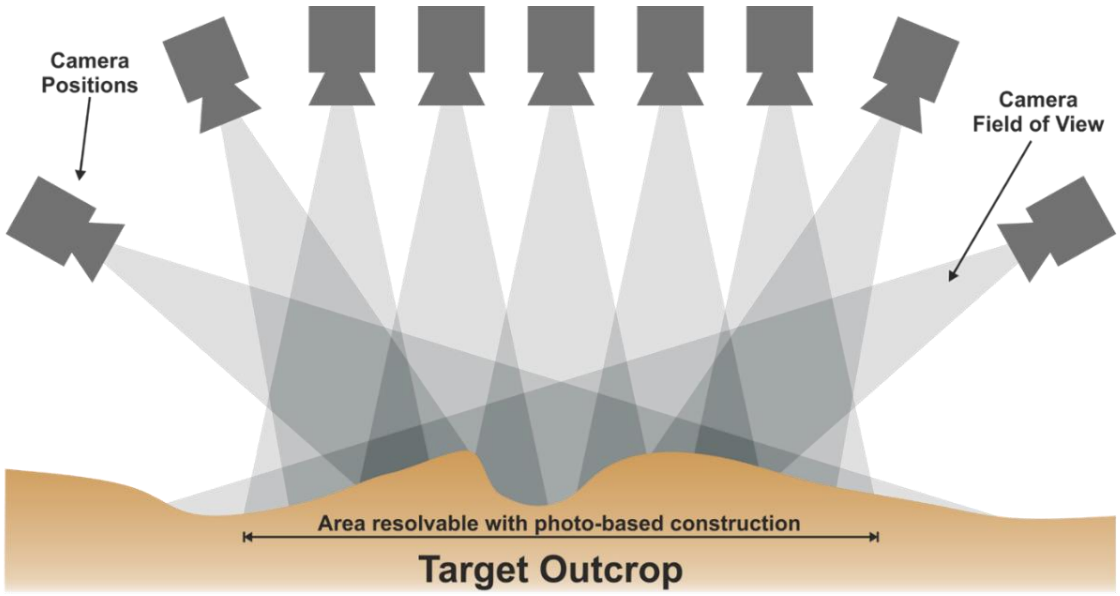

Figure 2.12: Schematic diagram showing optimal method for collecting images. Dark grey triangles represent areas with greatest amount of overlap with adjacent images. Lightest grey area not resolvable via photogrammetry. *After* (Bemis et al., 2014).

2.2.2.2.2. Processing:

Several software packages were explored for the generation of 3D models including Agisoft Photoscan (later updated to Agisoft Metashape), RealityCapture, Pix4D and VisualSFM, with Agisoft Photoscan being chosen as the preferred software package. It was chosen based on its reduced cost whilst still offering a reliable and easy to use package. VisualSFM

was tested as it is a free open source software package but was found to be unreliable and difficult to use during testing.

Before models are constructed, the images are visually checked, and only images that are in focus, well exposed and sharp are used in the modelling process. Images are then masked to cover areas of the image to not include in the model, e.g. sky, or features in the foreground (Figure 2.13). The masking process is time consuming but worthwhile as it reduces the amount of information that the software must process, saving time and computing power and ensures that the best quality model is produced.

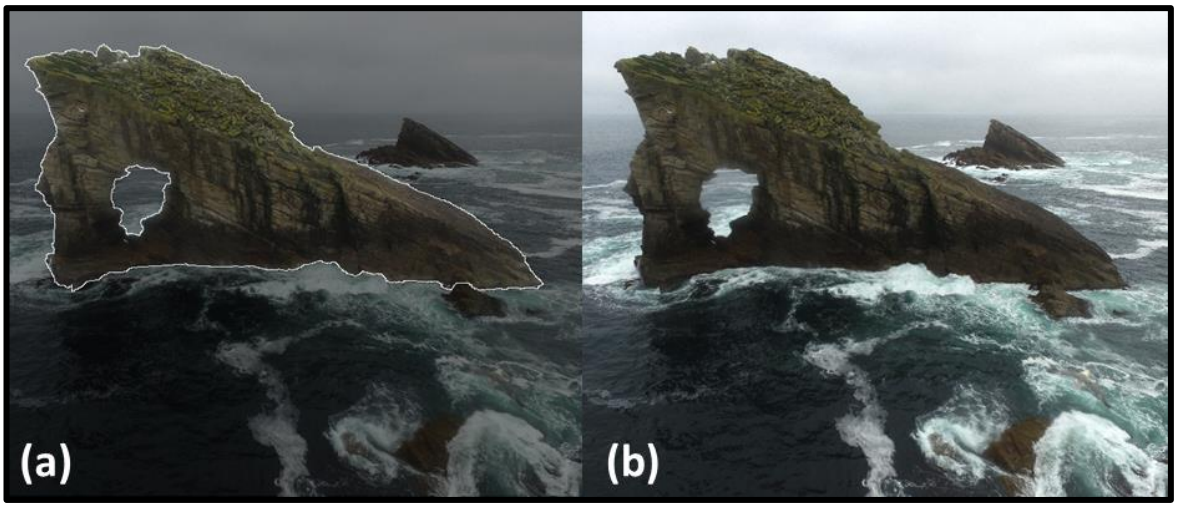

Figure 2.13: Example of a masked image in Agisoft Photoscan (a) masked (b) unmasked.

Ground control points laid out during acquisition or other markers can be positioned in images at this stage if no GPS information is available for the imagery. The 3D position and orientation of the model may be checked and refined further after model building using information collected in the field

The following is a guide to the production of VOMs and the values used at various stages in the modelling process derived through experimentation and guidance from the literature (Figure 2.14):

1. Photos are aligned, which involves the detection of features or points in multiple images and the reconstruction of the 3D position of the camera positions relative to one another. GPS information stored in the image metadata speeds this process up immensely. The result is a sparse cloud of data, which represents key points identified in several images (Fig 2.14). A key point limit of 100000 and tie point limit of 10000 were deemed suitable for most models.

2. The alignment of images is further optimised, and erroneous points are removed improving the accuracy of the sparse point cloud. The following optimisation values were used; Reconstruction uncertainty = ~1, Reprojection error = ~0.5 and Projection accuracy = ~1.
3. A dense cloud is generated using the sparse points as fixed points from which to calculate the position and geometry of a greater number of points. At this stage, the model will resemble the target outcrop in either greyscale or full colour. Depending on the density of points in the point cloud, geological interpretation can be done at this stage. Ultra-high/high quality point clouds were produced for structural analysis and medium quality point clouds were generated for general viewing and sharing online
4. To build a full 3D solid surface mode, or mesh, the points are joined by forming a series of triangular tiles or a TIN (Triangulated Irregular Network). The resultant model can be viewed as either a wireframe, solid or coloured mesh, using an average colour of the points they connect. Quality settings were partly dependent on settings used during previous stage but were generally built at high quality for geological analysis.
5. The final stages involve the draping over the original images over the 3D surface creating a textured mesh or tiled model. At this stage a fully photorealistic three-dimensional virtual outcrop model has been produced. Textures of 16384x1 were produced for general use. Larger outcrops produced with a greater number of textures were generated but were limited by computer memory.
6. The model is then exported for interpretation in a specialist software, as either a dense point cloud, tiled model or orthorectified image for further geological analysis.

Geological analysis may include the digitisation and measurement of geological features such as bedding, fractures or faults (see Figure 2.15), sedimentological interpretation, structural analysis and 3D model building. Orthorectified images in different orientations were produced dependent on the end use. Birdseye or z down images were produced for fracture mapping and topological analysis. Images perpendicular to outcrop/surface were produced for general use and for producing figures and diagrams.

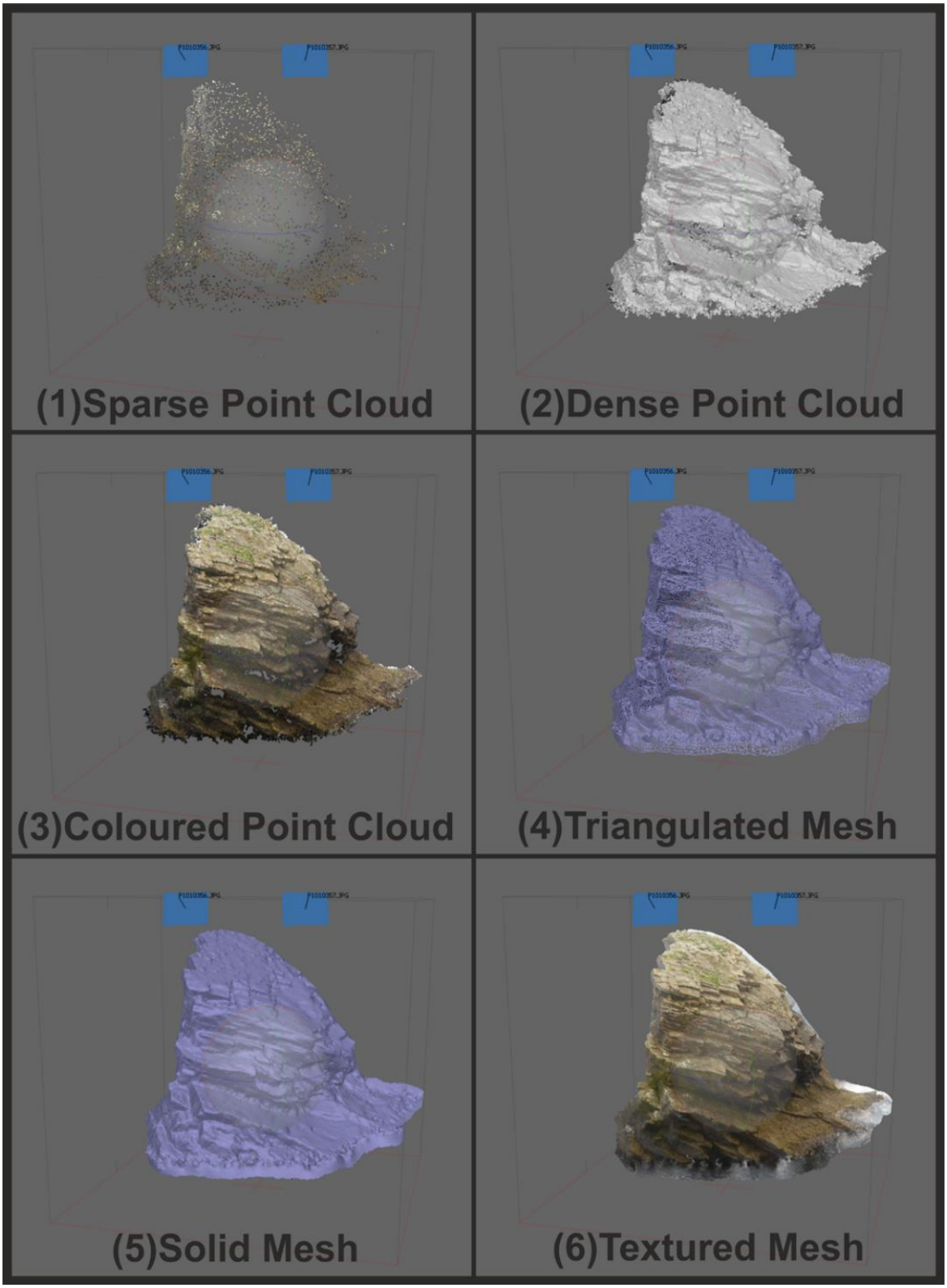

Figure 2.14: Stages of model building in Agisoft Photoscan. Da Rippack Stack, Foula, Shetland. (1) Sparse point cloud and photo alignment. Blue squares represent camera positions. (2) Dense point cloud. (3) Coloured dense point cloud. (4) Triangulated wireframe mesh (5) Solid Mesh (6) Textured Mesh.

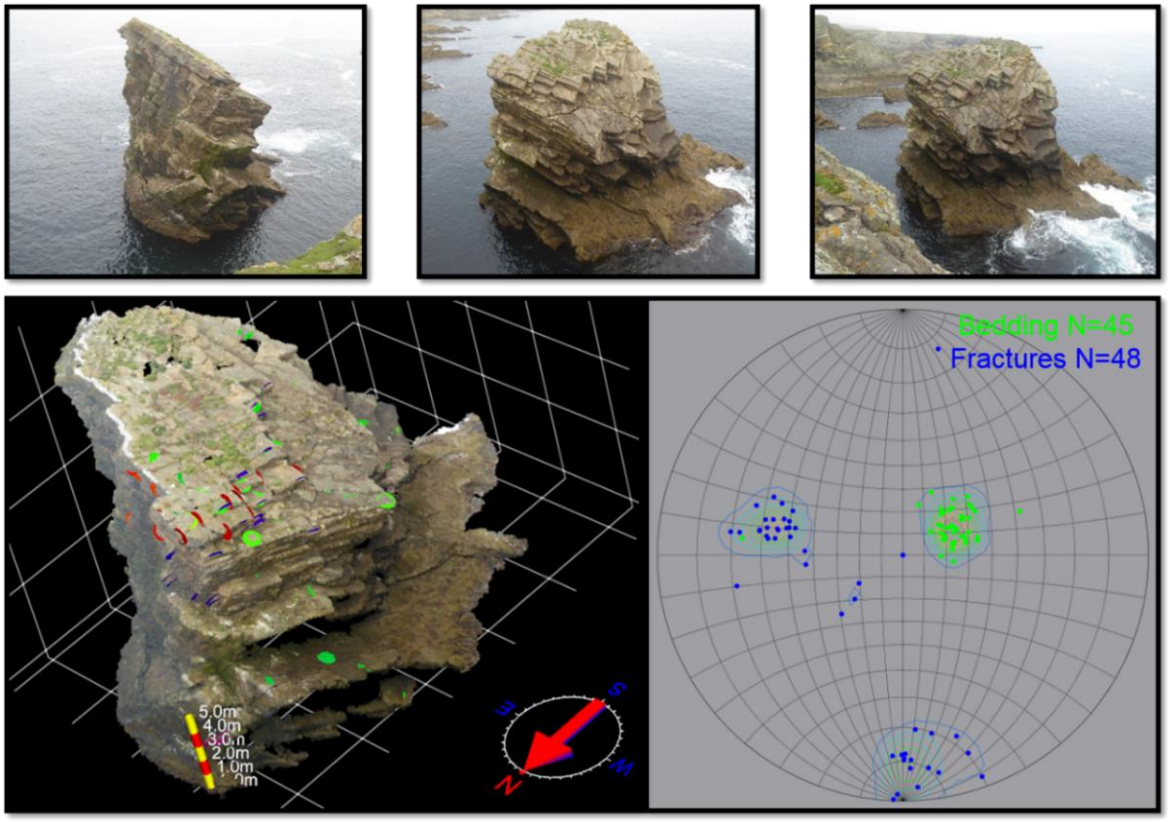

Figure 2.15: Point cloud of Da Rippack Stack showcasing the use of VRGS to interpret geology from a VOM with bedding (green discs), and fractures (red/blue) highlighted. *Inset*, stereonet of digitised bedding measurements.

2.2.2.3. Geological Analysis:

Several software packages are available for the interpretation and extraction of geological data from Virtual Outcrop Models. Table 2.1 is a comparison of the different packages available that were tested during this study. Experimentation with and testing of different packages was carried out in order to evaluate the suitability for the geological analysis of outcrop models. Features tested included, the ease of importing and exporting data, ease of interpretation and range of tools and functions available. Due to the availability of software licences and greater ease of interpretation offered by the Virtual Reality Geological Studio (VRGS), this software package was chosen as the principal Virtual Outcrop Model interpretation tool. A supplementary research project carrying out geological reconnaissance of remote Scottish Islands in and adjacent to this study area was carried out by a Miss Phoebe Sleath, whom I supervised and assisted. This supplementary study is provided in Appendix B and was presented as a poster at the Tectonic Studies Group Meeting, 2018.

Software Package	CoViz	Petrel	MOVE	LIME	VRGS	CloudCompare
Availability in academia	No.	Yes, and free to academics.	Yes, and free to academics.	Yes, and free to academics.	Yes, and free to academics. £5000 Annual Single User Licence	Open source and free.
Data Input/Output	3D Mesh Surface and Point Cloud.	3D Mesh Surface and Point Cloud.	3D Mesh Surface and Point Cloud.	3D Mesh Surface and Point Cloud.	3D Mesh Surface and Point Cloud.	3D Mesh Surface and Point Cloud.
Ease of 3D viewing	OK, but meshes require conversion.	Slow and not optimised for Digital Outcrop Model.	Fairly easy but some input errors can lead to poorly orientated models. Slow with large point clouds.	Very easy.	Very easy and VR ready.	Can load almost all data formats.
Ease of 3D interpretation	Has potential with further development	Very difficult. Tools not optimised for this purpose.	Fairly easy, but less intuitive. Struggles with large point clouds.	Intuitive but with basic tools.	Intuitive with lots of useful tools.	Fairly intuitive with Compass plugin.
Key Positives	Wider industrial applications and uses.	Wider industry use.	Advanced tools for structural analysis	Placement and overlay of supplementary materials and other data formats.	Processing and attribute analysis of meshes and point clouds.	Will import and export many data formats. Easy to use and free.
Key Negatives	Unusable on photorealistic models and lack of access.	Not optimised for Digital Outcrops and lacks tools.	Not bespoke package and prone to crash with large datasets	Lacks some useful tools available in VRGS.	Can be slow to load data and prone to crash.	Can only digitise on point cloud data.
Overall Verdict	Needs further development and lacks availability.	Lacks tools required.	Great for advanced structural analysis and integration with existing MOVE project	Potential alternative package.	Very powerful albeit expensive if outside academia	Useful alternative.

Table 2.1 (preceding page): Comparison of software packages available for the geological interpretation of VOMs

2.2.3. Paleostress Inversion Techniques:

In addition to carrying out conventional structural analysis of data collected in the field, paleostress inversion was carried out in order to quantify the orientation of principal stresses during faulting. Modern techniques typically calculate the stress tensor associated with a set of coeval kinematic indicators e.g. slickenlines, which are measured directly from fault surfaces and a variety of methods have been developed to compute these stresses. Dichiarante (2017) and Wilson (2006) both performed comprehensive reviews and tests of a variety of different stress inversion techniques and settled on using the MyFault software package, however this software package ceased being supported and was unobtainable. Instead the Midland Valley MOVE© and WinTensor software packages were used as suitable alternatives as they provided a quick and easy to use graphical method of analysing fault and fracture behaviour under 3D stress.

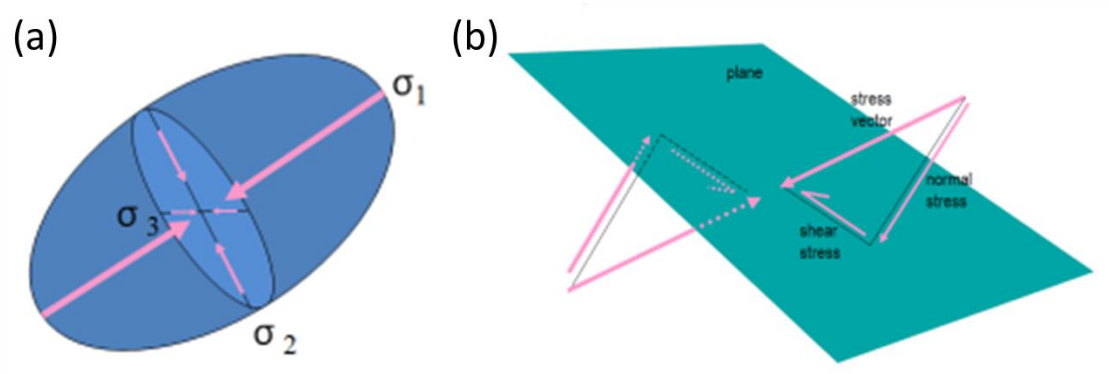

Figure 2.16: (a) Principal stress ellipsoid. σ (Sigma1,2,3) = Principal stress axes. Stresses in 3D are resolved for single point in 3D space. (b) Shear stress and normal stress acting on a plane from a single stress vector (Midland Valley, 2018).

For the purpose of this study, fault plane and fault-slip slickenline lineation measurements were collected *in situ* whilst in the field and conventional stress inversion (Angelier, 1984) was carried out using the Stress Analysis Tool in the Midland Valley MOVE© software package. Fault data is inverted for a common stress tensor using an algorithm based on the work of Angelier (1990) and is based on the following assumptions: 1) Andersonian rules of faulting (Anderson, 1905), 2) the measured lineations follow the Wallace-Bott (Bott, 1959; Wallace, 1951) hypothesis that the slip vector lies on the fault plane, and represents

the direction of maximum shear and 3) were formed by a single common stress tensor. This analysis produces a reduced stress tensor of the three principal axes (σ_1,σ_2 and σ_3) in addition to the shape ratio of the strain ellipsoid, $\delta = (\sigma_2 - \sigma_3)/(\sigma_1 - \sigma_3)$ (Figure 2.16). The angular misfit between the observed and predicted movement for a set of fault planes in different orientations that moved coevally is also calculated.

Later, the WinTensor software package was used (Delvaux and Sperner, 2003) which provided comparable results. This method reconstructs the four parameters of the reduced paleostress (orientation of the three principal stress axes and the shape ratio of the stress ellipsoid) using the refined Right Diherdron method and Rotational Optimisation procedure. (Delvaux and Sperner, 2003). This direct inversion method calculates a reduced stress tensor that simultaneously tries to minimise the angular misfit between a theoretical shear stress and the actual slip vector on the fault and also maintains a sufficiently large enough shear stress magnitude in order to overcome rock cohesion and/or friction.

The validity of paleostress inversion is questioned by some authors, and thus must not be used in isolation. Results must be compared to other data sets and other local or regional structures to validate and assess the correspondence of structures to regional stresses.

2.2.4. Fracture Network Analysis:

2D topological analysis of fracture systems as per the methodology of Sanderson and Nixon (2015) provides a measure of the connectivity of fractures by measuring nodes and branches. By using a combination of traditional fracture analysis together with topological methods a far greater understanding of the geometries and connectivity of fractures in three dimensions can be inferred which allows for improved modelling of how fractures will influence the flow of fluids in the sub-surface. It also provides a quantitative assessment of fracture connectivity and allows for comparison of datasets.

To understand the connectivity of fracture networks the method of Sanderson and Nixon (2015) (Figure 2.17) defines the number and type of nodes and branches of a network. Nodes are where a fracture terminates (I Node), where a fracture abuts against another fracture (Y Node) or cross cuts another fracture (X Node) with branches being the segments of a fracture between two nodes (Figure 2.17). Branches may be classified by their terminations with I-I type having two I nodes (isolated branches), I-C type having one I node and one X or Y node (singly connected) or as C-C type if it has an X or Y node at both termination (multiply connected). Networks with greater number of X and Y nodes and C-

C type branches will become progressively more connected and in the context of fluid flow would have a greater permeability.

Fracture and topological analysis was carried out on remotely sensed data such as field photographs, aerial images and other remotely sensed datasets (see section 2.12) and was carried out using the NetworkGT toolbox for ArcGIS (Nyberg et al., 2018).

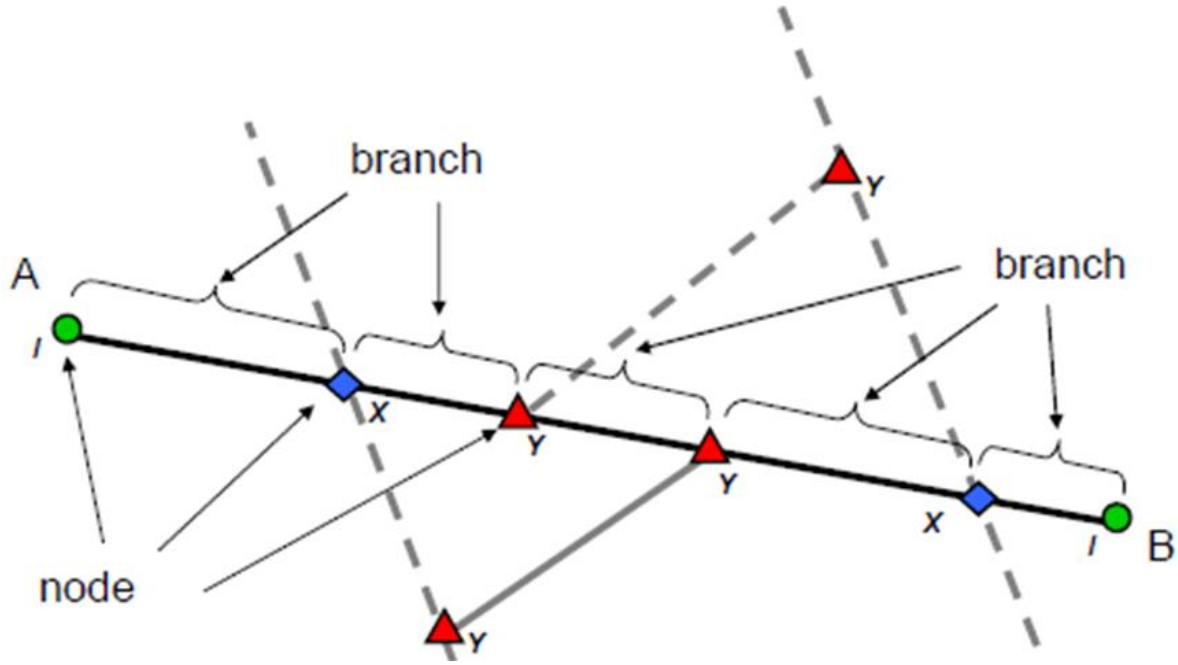

Figure 2.17: Classification of a fracture trace (A-B) with associated interesting fractures (dashed), nodes and branches: I nodes (circles), Y nodes (triangles) and X nodes (diamonds) (Sanderson and Nixon, 2015).

2.3. Macro to microscopic scale – laboratory studies:

2.3.1. Thin Section Analysis:

Optical analysis of thin sections, using transmitted light was carried out in order to characterise hand specimens and other samples in terms of their lithology, fault rock textures and microstructures and general mineralogy. Standard (30 micron) polished thin sections were made in the Department of Earth Sciences, Durham University, with selected samples impregnated with blue epoxy resin to highlight porosity. Sections were also scanned to produce digital images.

2.3.2. QEMSCAN Analysis:

Selected thin sections were sent to the Department of Earth, Ocean and Ecological Sciences, University of Liverpool, for FEI WellsiteQEMSCAN® (Quantitative Evaluation of Minerals by Scanning Election Microscopy – FEI Company, Hillsboro, OR, USA) analysis, operating at 15kv. This system comprises a Scanning Electron Microscope (SEM) and two Bruker Energy Dispersive X-ray (EDS) spectroscopy detectors (Bruker Corporation, Billerica, MA, USA). The system digitizes the thin section and undertakes chemical mapping with the resultant spectra compared to a library and assigned to a specific mineral (Armitage et al., 2010; Wooldridge et al., 2019). This process also produces a backscatter electron false colour image and digital map of the sample. This technique allows for the automated and quantitative analysis of samples deriving bulk mineralogy and chemical composition as well as textural information (grain size, grain shape, porosity, mineral associations etc.). Before analysis, samples were coated with a thin electrically conductive layer of carbon. A low-resolution scan of the whole sample was conducted with a spatial resolution of the approximately 20µm. Areas of specific interest or that required a greater level of detail were also analysed at a higher resolution of approximately 2µm.

2.3.3. Heavy Mineral Analysis:

Selected samples were sent to Palyno Services Limited, Aberdeen for standard Heavy Mineral separation. Crushing and disaggregation of samples to between 63-125 µm was carried out, before sieving and separation via gravity settling using 2.89 $kg.m^3$ density Bromoform fluid. Prepared samples were sent to Andrew Morton of HM Associates for analysis where separated grains were mounted on glass slides for identification upon which manual counting of grains was undertaken using an optical microscope.

2.3.4. Detrital Zircon Geochonrology:

Selected samples were sent for U-Pb detrital zircon dating using LA-ICPMS (Laser Ablation Inductively Coupled Mass Spectrometry) at the University of Hull. Zircon grains were manually picked from the heavy mineral separate before mounting in 25mm polished Perspex pucks for analysis.

The instrumentation comprised an Australian Scientific Instruments RESOlution-SE excimer 193nm laser ablation system with a Laurin Technic S155 2 volume sample cell, coupled to an Agilent Technologies 8800 Triple Quad ICPMS with an Argon carrier gas (0.85L/minute).

Zircon centres were ablated for 30 seconds with a 30µm spot size, a repetition rate of 10Hz, a fluence of 2.5 Jcm^2 and using a Helium (370ml/minute) and Nitrogen (1ml/minute) carrier gas. Data was continually logged and processed using the GeoStar and MassHunter 4.4 software packages with data reduction (calibration of downhole fractionation/background removal/calculation of isotopic ratio and preferred ages ages) performed in Iolite 3.4. Plesovice Zircon, 91500 Zircon and NIST 612 silicate glass standards were cyclically measured for standardisation and calibration.

Preferred ages were calculated using the uranium series isochrons; $^{206}Pb/^{238}U$ series for grains <1200Ma and the $^{207}Pb/^{206}Pb$ series for grains >1200Ma. Ages were plotted along a concordia line and data with greater than ±10% discordance were discarded. Data was analysed in IsoplotR and Provenace (an R package) and results displayed as KDE (Kernel Density Estimate), Wetherill, Tera-Wasserburg and MDS plots (Multi-Dimensional Scaling). The full uncertainties and results of this analysis can be found in Appendix C.

2.4. Key definitions and geological concepts:

2.4.1. Geological contacts and cross cutting relationships:

Contact relationships are important for establishing the chronology or relative ages of geological events. By understanding the nature of different structures, contact relationships and establishing cross cutting and/or abutting relationships the relative chronology of a series of geological events can be established (Figure 2.18). 4 main types of contact relationship can be identified in the field:

1. Conformable - conformable contacts are surfaces between layers of sedimentary rock that were deposited without a significant break in deposition. Layers are general parallel to sub-parallel to one another and it is assumed that in a sedimentary succession that is the 'right way up' it will conform to 'Steno's Laws'; 1) Law of superposition – younger layers sit atop older layers, 2) Law of original horizontality – layers of sedimentary rock are generally deposited flat, 3) Law of cross cutting relationships – structures that cut the rock layers must be younger than the rock it crosscuts, and 4) Law of lateral continuity – layers of rock are

continuous until they encounter other solid bodies that block their deposition or until they are acted upon by processes that occurred after deposition took place.

2. Unconformable - unconformable contacts or unconformities represent breaks in the stratigraphic record not marked by sediment deposition. A variety of unconformity types exist which include:
    a. A *Disconformity* exists between parallel layers of sedimentary rocks which represents a period of erosion or non-deposition.
    b. A *Nonconformity* exists when sedimentary rocks are deposited on eroded layers of pre-existing metamorphic or igneous rocks.
    c. An *Angular unconformity* exists when sedimentary rocks are deposited on tilted and eroded layers of sedimentary rock forming an angular discordance between layers.
    d. A *Paraconformity* is an unconformity in which strata are parallel but there is no apparent erosion and may resemble a simple bedding plane.
3. Tectonic - A contact formed where a fault plane juxtaposes two rock volumes that were not originally in contact, see section 2.4.5.
4. Intrusive - a contact formed from the intrusion of igneous and/or sedimentary material into a volume of rock, see section 2.4.10

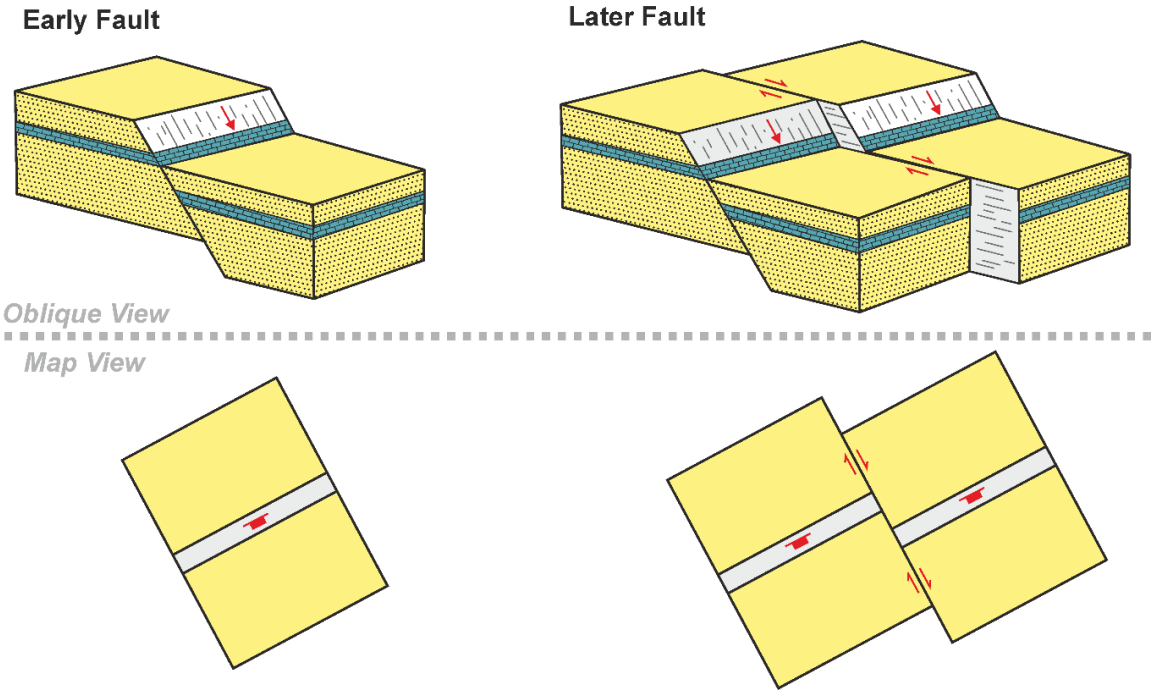

Figure 2.18: Oblique and map views of fault block diagrams showing crosscutting relation between two faults. An early normal extensional fault is cut by later strike-slip fault which crosscuts the normal fault with a dextral offset.

2.4.2. Foliations and Lineations:

A lineation is defined as any linear feature that occurs penetratively within a rock volume (O'leary et al., 1976; Twiss and Moores, 1992) and may subdivided into object (or penetrative) lineations that form due to the 'parallel alignment of distinct elongate parts with a measurable volume' (Piazolo and Passchier, 2002) and into trace lineations (or surficial) that 'represent lines of zero volume' and often form as result of in the intersection of two planes(Figure 2.19). This definition excludes lineations that are restricted to a single surface. Such features include slickenside lineations and slickenfibres found on fault planes which may be used to determine the direction of movement of a fault (see section 2.4.10).

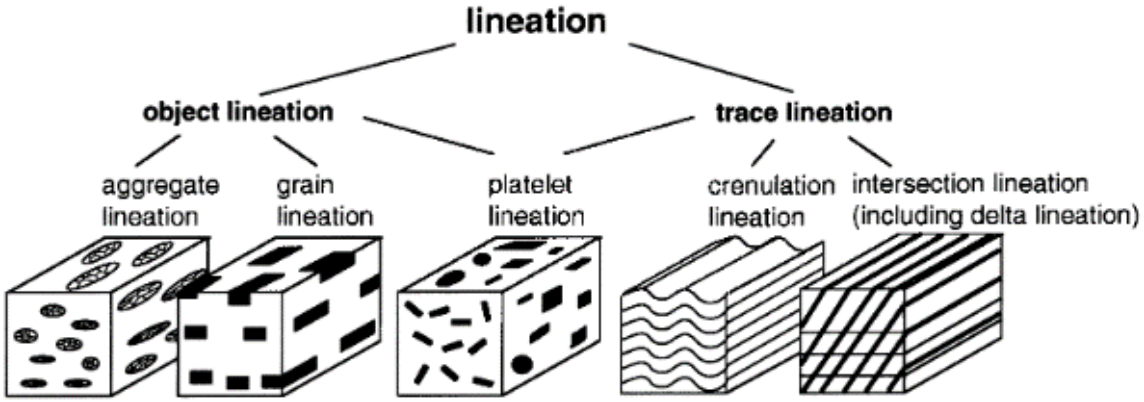

Figure 2.19: Terminology for the definitions of a lineation (Piazolo and Passchier, 2002)

A foliation is defined by Twiss & Moores (1992) as a 'planar structure in a rock that is homogeneously distributed throughout the volume'. This term covers a variety of kinds of planar structures and examples include bedding, parallel alignment of clasts and/or platy minerals, flattening of minerals and concentrations of particular minerals into layers. A detailed review of the types of foliations can be found in Passchier and Trouw, (1996), see Figure 2.20. The inferred origin of the structure must be ascertained as foliations and lineations are primary if they are as a result of sedimentary or igneous processes. They are secondary if they the result of metamorphism or deformation, in line with the definition of Park (2013) as 'a set of new planar surfaces produced in a rock as a result of deformation'.

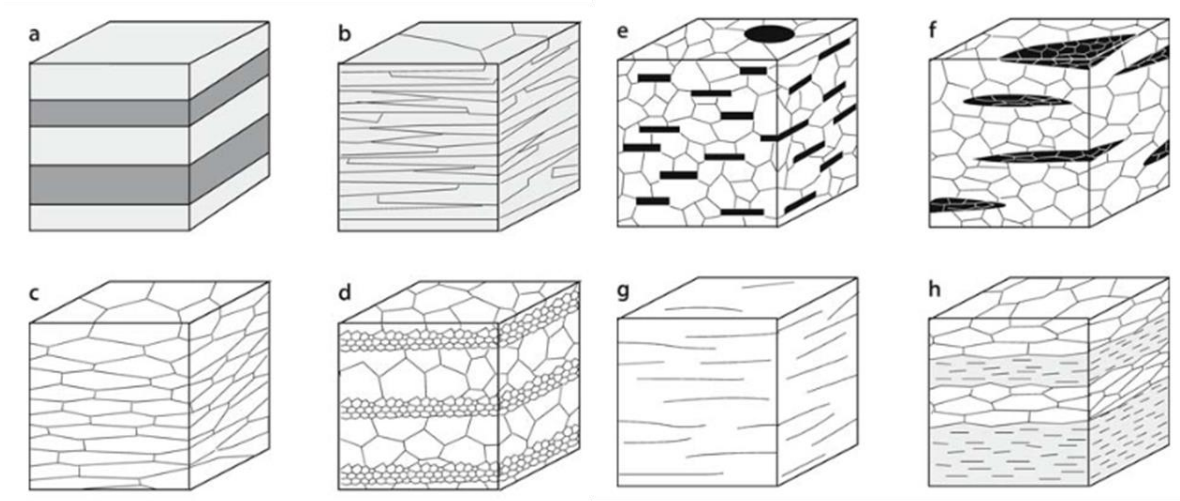

Figure 2.20: Schematic of various fabric elements that may define a foliation: (a) Compositional layering, (b) Preferred orientation of platy minerals (e.g. mica), (c) Preferred orientation of grain boundaries and shape of recrystallised grains (e.g. quartz, carbonate) in a grain shape preferred orientation (d) Grain-size variation, (e) Preferred orientation of platy minerals in a matrix without preferred orientation e.g. mica in micaceous quartzite or gneiss, (f) Preferred orientation of lenticular mineral aggregates. (g) Preferred orientation of fractures or micro-faults (e.g. in low-grade quartzites) and (h) Combination of fabric elements (a, b and c). Such combinations are common in metamorphic rocks. *After,* Passchier and Trouw, (1996).

2.4.3. Folds:

Geological folds are bent or curved layers of rock that occur as a result of the deformation of flat and/or planar surfaces e.g. bedding. They are an expression of continuous deformation with no breaks in the rock at the scale of observation. They generally result from the application of external compressional forces, shortening and ductile deformation. However, they may form in other tectonic settings such as transtension and transpression, and in conjunction with other brittle and ductile structures, e.g. faults, cleavages. A number of authors have developed ways of describing fold morphology (Fleuty, 1964; Fossen, 2016; Park, 2013; Ramsay, 1967; Ramsay and Huber, 1987) and classifying folds which include; orientation (dip/azimuth), dimensions, shape, geometry, layer thickness, dip isogons, wavelength, amplitude and cylindricity (Figure 2.21 and 2.22).

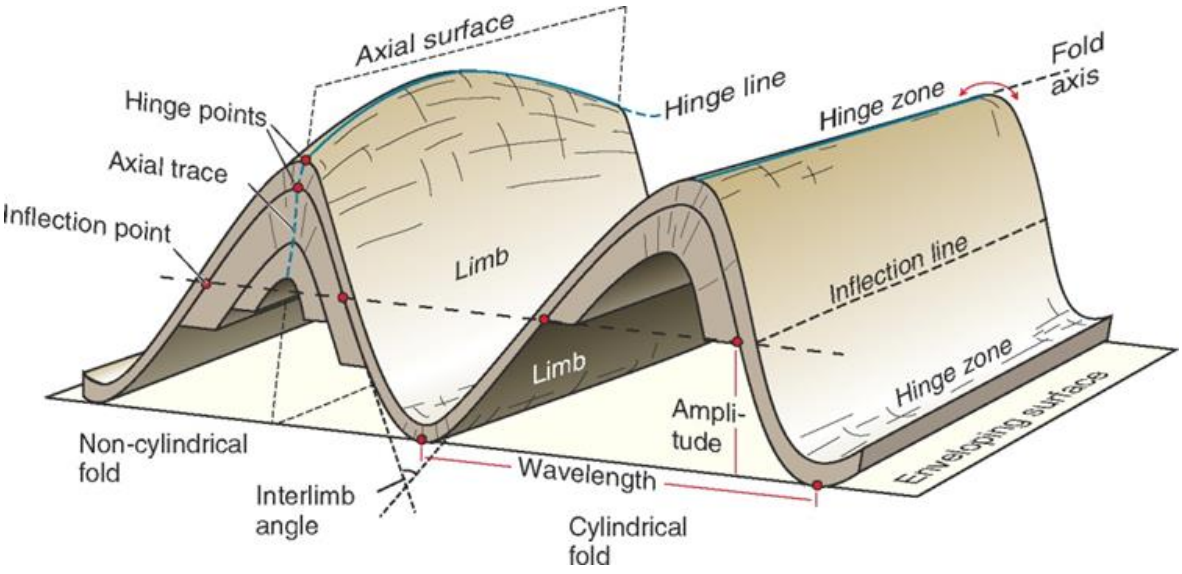

Figure 2.21: Nomenclature for describing fold structures (Fossen, 2016)

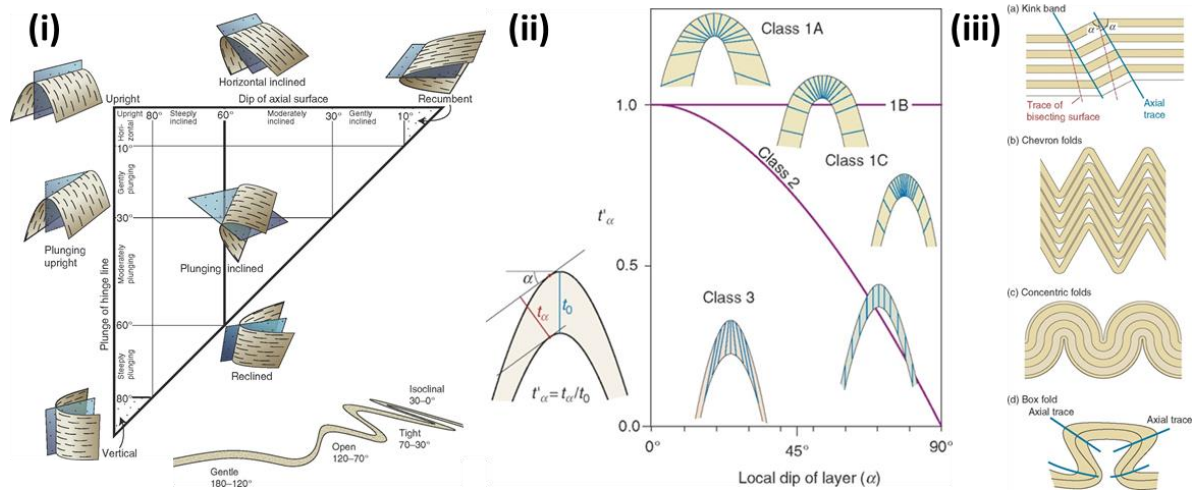

Figure 2.22: Classification of fold structures *after* (Fossen, 2016) (i) Fleuty Diagram and fold tightness (Fleuty, 1964) (ii) Ramsay classification (Ramsay, 1967), (iii) types of fold shape (Fossen, 2016).

2.4.4. Faults, fractures and joints:

Several different definitions of faults, fractures and joints are proposed in the literature. A useful definition is that of Park (2013) where *'Fractures are cracks across which the cohesion of the material is lost, and may be regarded as planes or surfaces of discontinuity'*. With this definition as a basis, joints and faults can be further defined. A fault is a discontinuity or fracture that has an 'observed or measurable displacement' that is generally parallel to the plane of the fracture. Thus, a fracture showing significant evidence of shear displacement is a fault. Faults are more complex structures and are defined as planar or zonal structures (metre to kilometre scale) and can be further classified based on

kinematics (see section 2.4.5). When displacement is too small to be measured, is difficult to distinguish or has an appreciable aperture the fracture may be referred to as joint.

A more dynamic description considers the direction the fracture propagates and direction of the displacement in order to differentiate between joints and faults. Two end members are defined, 1) Tensile (extension) fractures (Mode I opening or Mode IV closing) with displacement orthogonal to the fracture and 2) shear fractures where displacement is parallel to the fracture (Mode II sliding and Mode III tearing). A combination of both tensile and shear failure results in 'hybrid' fractures and fractures which open obliquely (Figure 2.23).

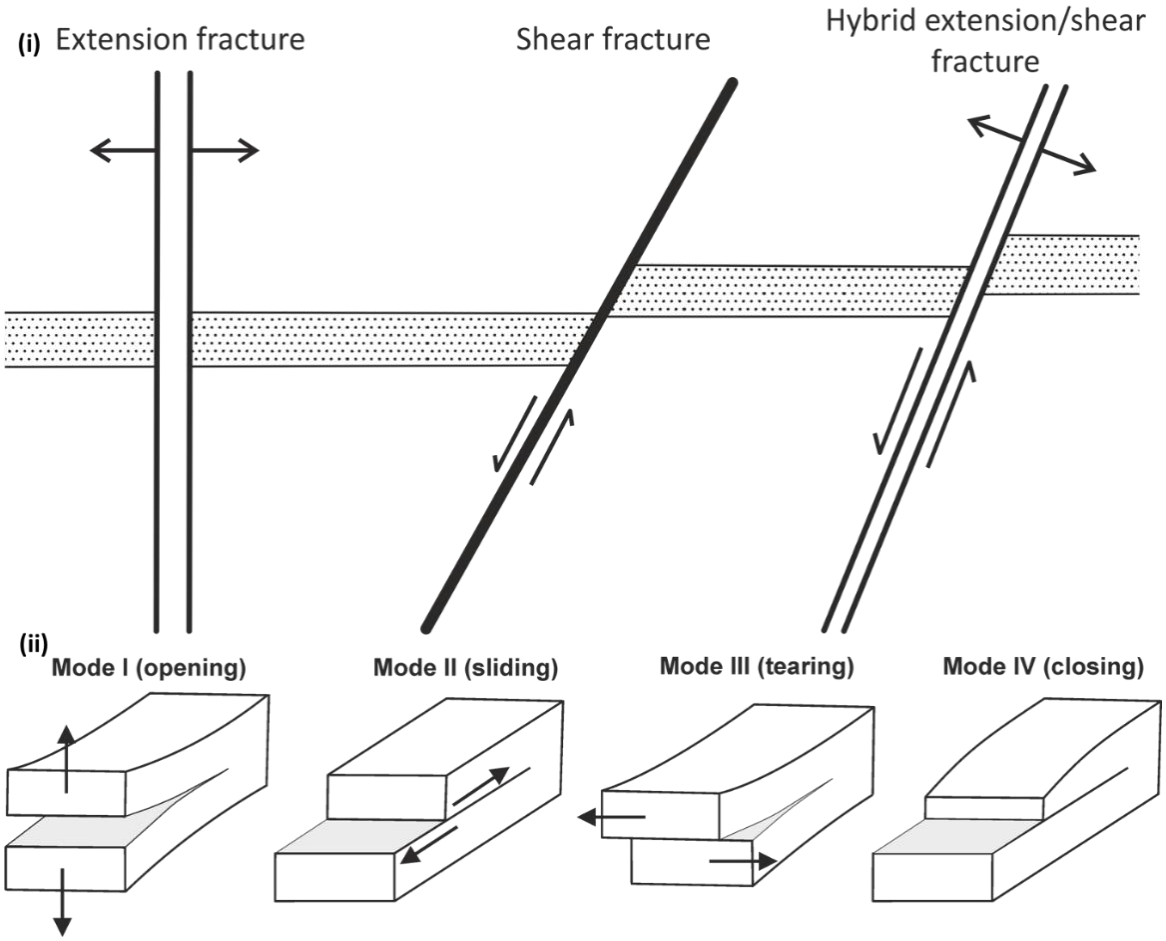

Figure 2.23: (i) The three principal types of fracture and (ii) four modes of fracture propagation.

The three principal orthogonal stresses involved in the deformation of rocks in the brittle crust and formation of fractures and faults are described as σ1, σ2 and σ3 or the maximum, intermediate and minimum principal stresses respectively. The stresses required for the brittle failure of a rock may be described on a Mohr circle diagram (Figure 2.24) which plots the shear stress (τ) against the normal stress (σn) and defines a failure envelope at which

point a rock will fail at a given orientation (θ) of a fracture plane. σ3 and σ1 are plotted to form a circle which will expand or shift due changes in these stresses bringing it closer to the failure envelope at which point the rock mass will deform and develop a fracture (Figure 2.24). Three principal types of fracture can be defined based on the point at which the Mohr circle touches the failure envelope:

1. Tensile fractures (Mode I) occur when the Mohr circle touches the failure envelope on the left where it intersects the horizontal axis. The plane that forms will have zero shear stress and an effective extensional normal stress.
2. Shear fractures (Mode II and Mode III) will occur when the Mohr circle touches the failure envelope to the right of the vertical axis. The plane that forms will have a net compressional normal stress and a non-zero shear stress forming shear fractures.
3. Obliquely opening fractures or hybrid fractures occur when the Mohr circle touches the failure envelope to the left of the vertical axis. The plane that forms will have a net extensional normal stress and non-zero shear stress forming hybrid fractures.

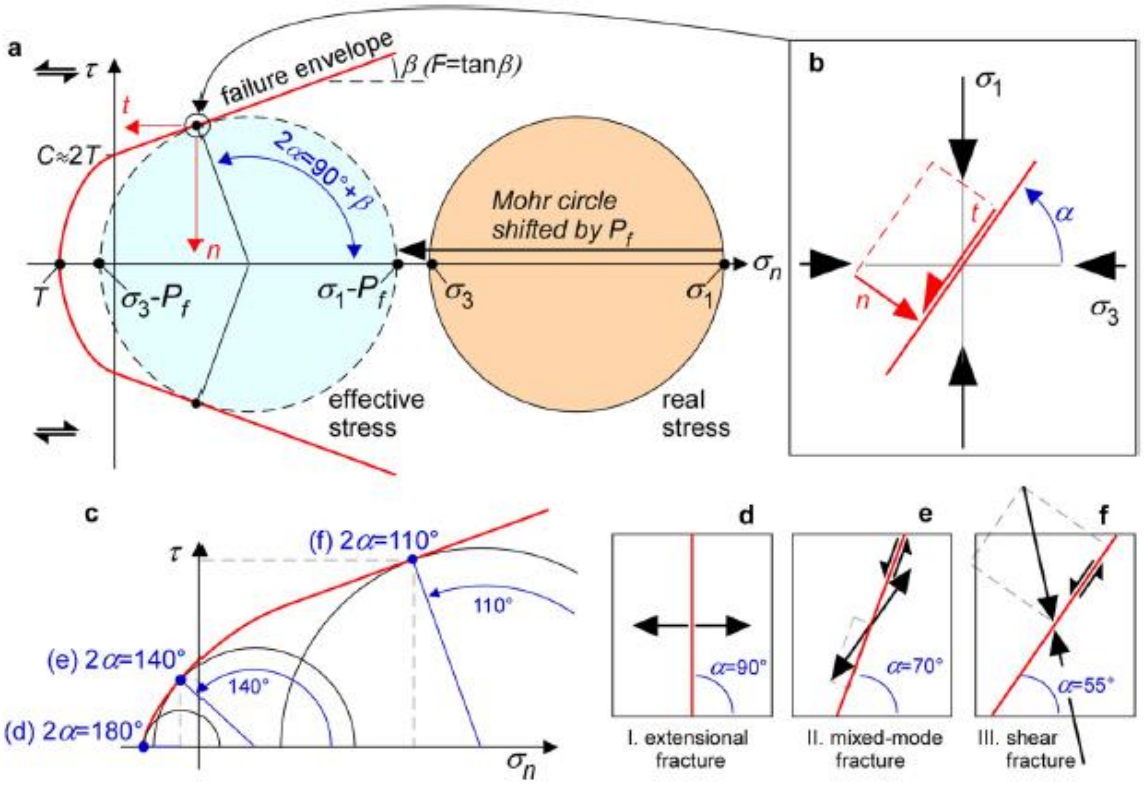

Figure 2.24: Mohr-Griffith-Coulomb failure. (a) Mohr circle diagram with shear stress (τ) versus normal stress (σ_n) for a plane with an angle *α* with the least compressive stress (σ3). All τ-σ_n combinations for a certain stress state (defined by σ1 and σ3) lie on a circle. As fluid pressure (P_f) counteracts imposed compression, effective stresses ($\sigma_n - P_f$) are used to determine whether a rock

will fail: this shifts the Mohr circle to the left by P_f. (b) Example of the normal (*n*) and shear stress (τ) on a plane at angle a to σ3, the magnitudes of which can be derived from the Mohr diagram (a). (c) Example of the position of the Mohr circle for three types of failure: (d) extensional failure with the extensional traction normal to the fracture, (e) mixed mode failure, with the traction having an extensional and shear component and (f) shear failure with the traction having a compressional and shear component (Bons et al., 2012).

2.4.5. Fault Classification:

Like fractures, faults can be classified based on their geometry and direction of displacement. A simple classification based upon the stress state responsible for faulting was developed by Anderson (1905) referring to faults as either: Normal (σ1 vertical), Wrench or Strike-slip (σ2 vertical) or as Reverse (σ3 vertical). Although this definition is sufficient, a better classification exists based on the sense of movement and direction of slip on the fault plane (Figure 2.25):

1. Normal Faults/Extension e.g. dip slip normal faults and extensional faults
2. Reverse Faults/Shortening/Compression e.g. dip slip reverse and thrust faults
3. Strike-slip faults e.g. wrench faults, transcurrent and transform faults
4. Oblique-slip faults e.g. a combination of both dip-slip and strike-slip motion
5. Rotational faults e.g. any combination of both dip-slip and strike-slip motion which results in rotation on the fault plane.
6. Bimodal, quadrimodal and polymodal faults where multiple fault sets form contemporaneously and frequently occur rocks with pre-existing fractures.

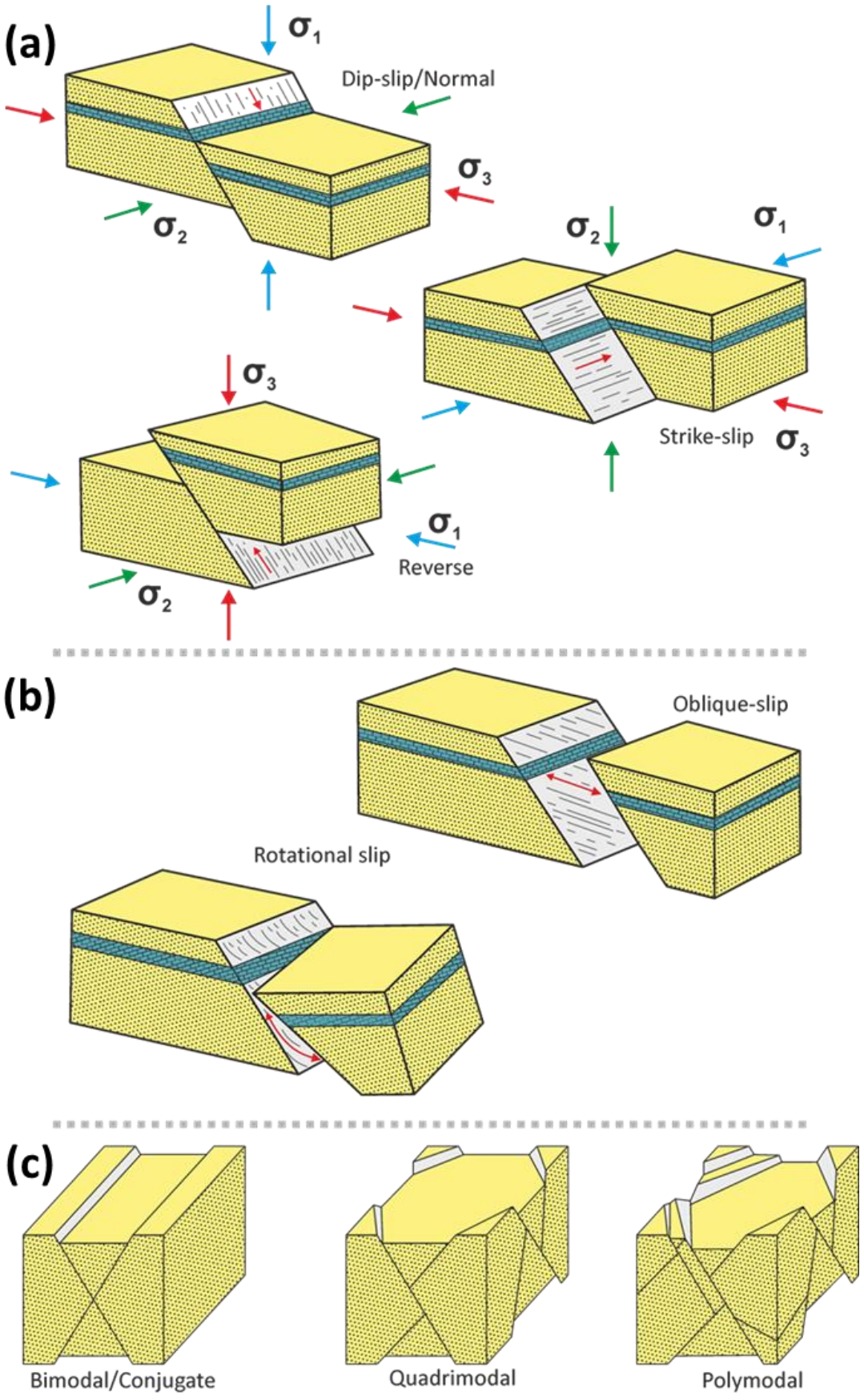

Figure 2.25: Block models and stereoplots of (a) the principal fault types as defined by (Anderson, 1905): Normal, Strike-slip and Reverse Faults, (b) those with elements of oblique motion or rotation and (c) bimodal, quadrimodal and polymodal faults.

2.4.6. Fault Zone Architecture and Genesis:

Faults are frequently simplified and visualised as simple 2D planes but are in fact complex 3D zonal structures or 'fault zones'. During progressive deformation small fractures will grow and coalesce forming larger structures and more complex fault zones. The physical properties of a fault zone change through time and the resultant fluid flow properties (porosity/permeability) will change with faults acting as both barriers, baffles and conduits to flow throughout their evolution, and may even during deformation be active conduits for flow (Caine et al., 1996) see Figure 2.26. Faulting may also juxtapose lithologies of different hydraulic properties which can generate fluid trapping geometries or cause fault zones to leak.

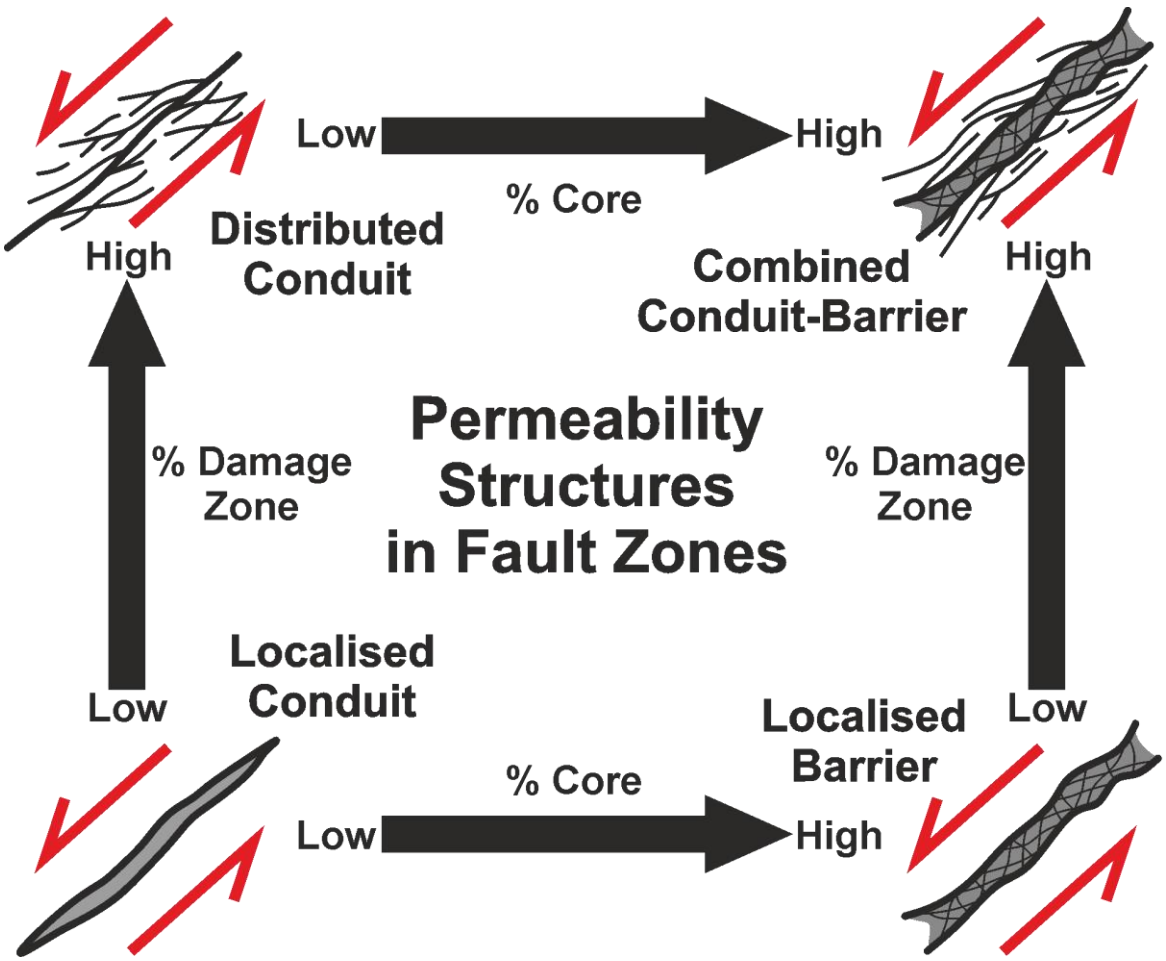

Figure 2.26: Schematic diagram showing relationship between fault core and damage zone size and relative fluid flow. Modified *after* Caine et al., (1996).

Fault zone architecture and genesis will also vary as the fault zone cuts different rock types in the protolith and more complex architectures develop. For example, in mixed clastic/carbonate sequences varying mechanical properties of the alternating units create

a ‘stepped geometry’ reflecting the mechanical stratigraphy of the wall rocks. This stepped geometry can also produce open voids and space into which mineral phases can be precipitated, fluids such as oil and water can flow or accumulate or where sediment may be deposited which can preserve the void spaces over geological timeframes (Figure 2.27).

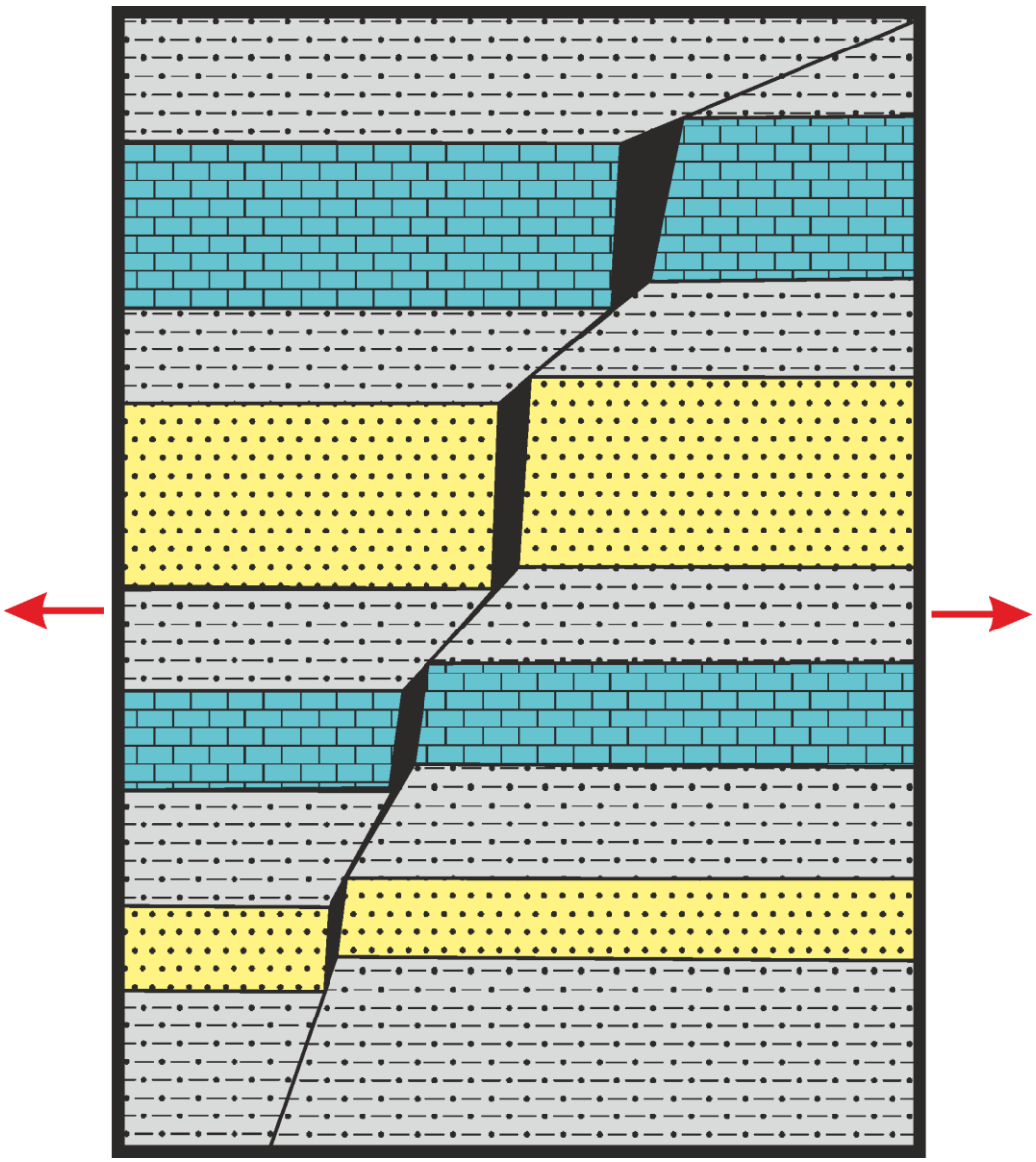

Figure 2.29: Schematic Diagram showing the effect of mechanical stratigraphy in a mixed clastic (yellow sandstones and grey shales) and carbonate (blue limestones) sequence.

Fault zones can be subdivided into three key components, see Figure 2.28 (Caine et al., 1996):

1) Fault Core - is defined as the structural, morphological and lithological portion of the fault zone where most displacement and deformation takes place. It may be comprised of a discrete single slip surface, unconsolidated clay rich gouges, geochemically altered

zones, breccias or highly indurated cataclasites/mylonites. Fluid flow properties of this zone can be highly variable both along strike and down dip due to thickness changes, different physical properties and different fault zone processes that have taken place. Grain size reduction and mineralisation will generally lower permeability, whereas fracturing will improve permeability.

2) Damage Zone – the network of subsidiary structures bounding the fault core that may enhance permeability relative to the core and the protolith. Common structures in this zone include small faults, veins, fractures, cleavage and folding. These structures cause heterogeneity and anisotropy within the damage zone and will alter the flow and physical properties of this zone. Wide damage zones can indicate multiple events overprinting successive deformation events.
3) Protolith – the relatively undeformed country rock where the physical properties of the rock reflect those of the unfaulted host rock. In this area, regional structures may be preserved and aid in understand pre-deformation conditions and evaluating potential for reactivation.

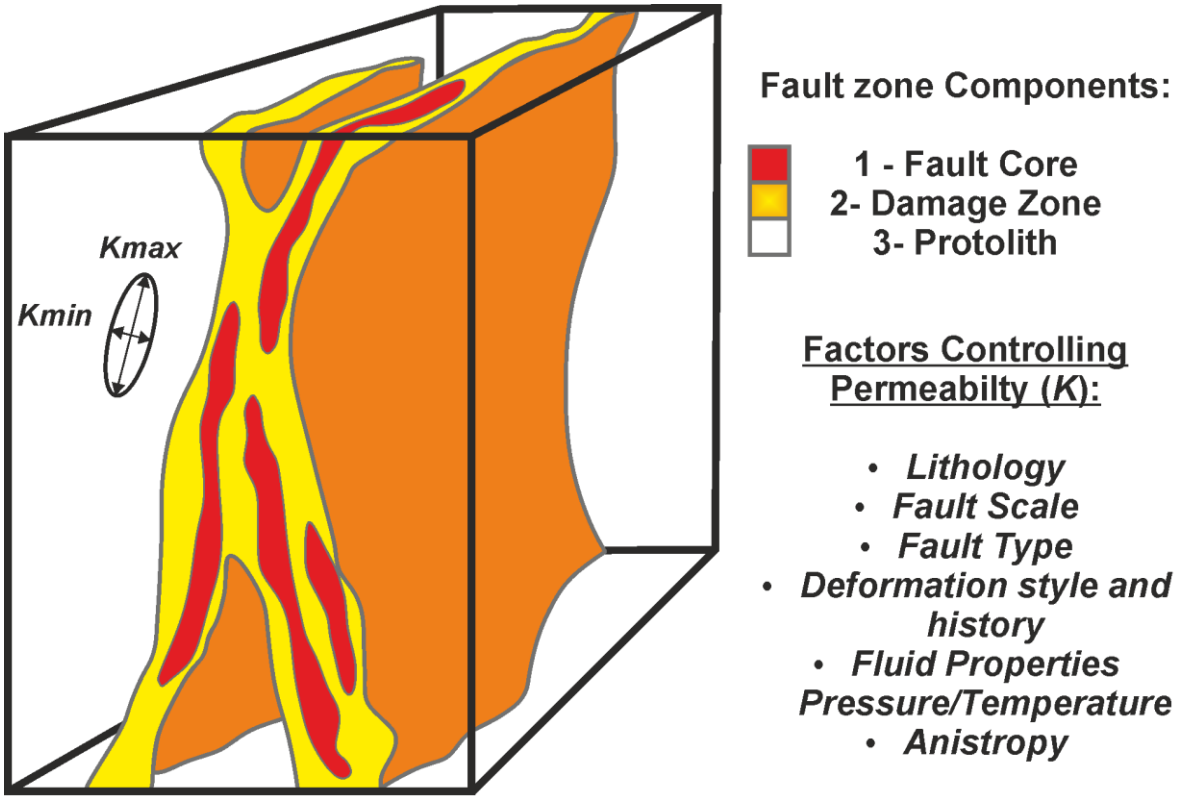

Figure 2.28: Conceptual model of fault zone with protolith removed. Ellipse represents relative magnitude and orientation of the bulk 2D permeability tensor (k) that might be associated with each distinct architectural component of a fault zone. Modified *after* Caine et al., (1996).

2.4.7. Fault Rocks:

A variety of different fault rocks are generated at different depths and in different deformation regimes (Figure 2.29). In the shallow crust (<10km) under low pressure/temperature conditions and generally fast strain rates, discrete, brittle faults and cataclastic fault rocks are generated. In deeper (>10km) settings and with increasing pressure/temperature conditions and slower strain rates more distributed fault zones and shear zones are developed with increasingly ductile structures being produced and the development of mylonitic fault rocks. In the shallow brittle crust, the fault rocks that are developed are primarily controlled by depth, fluid circulation, mineralogy and rheological conditions.

The classification of fault rock follows the definitions of Woodcock and Mort (2008) (Figure 2.30). Fault rocks are subdivided based on clast size and whether fault rocks are foliated or not. This classification builds on the conventional classification of Sibson, (1977) who classified fault rocks based on the cohesion at the time of faulting ,the matrix or cement in the fault rock and clast size. However, due to the difficulty in determining the degree of cohesion of faults in the field, the non-genetic classification of Woodcock and Mort (2008) is more suitable.

Fault breccias consist of angular clasts produced from friction in upper-crustal fault zones (Fossen, 2016; Woodcock and Mort, 2008) and are comprised of >30% large clasts >2mm in size. Cataclastic rocks such as breccias are characterised by sharp, angular fragments of rock, fractured grains and a large grain size range and show increasing amounts of grain size reduction, an increase in the volume of cataclastic material, greater grain rotation, dilatancy and grain boundary sliding through progressive deformation.

A lack of primary cohesion at the time of fault movement is characteristic of breccias and textural terms adopted from the cave-collapse literature have been adopted to define the proportion of large clasts; crackle, mosaic and chaotic breccias. A crackle breccia shows little rotation of clasts with minor quantities of matrix material or mineral cements. Mosaic and chaotic breccias show increasing amount of clast rotation, a higher proportion of interclast space, greater quantities of matrix material and/or mineral cements and an overall loss of geometric fit between adjacent clasts.

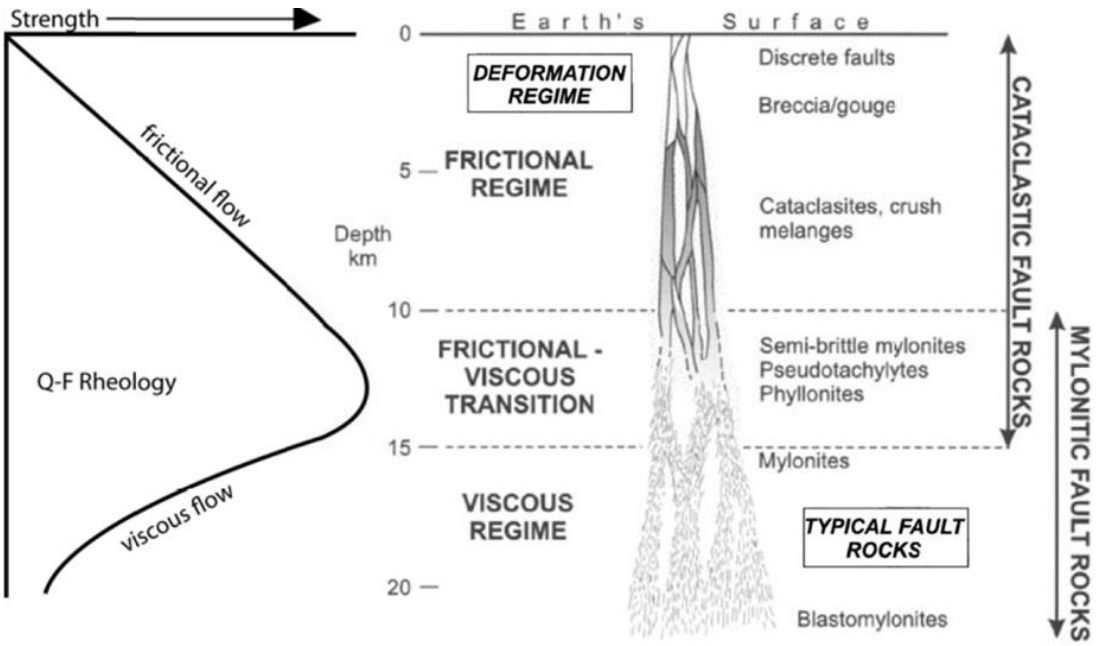

Figure 2.29: Schematic illustration of depth relationships in fault rocks, deformation processes and strength profile along a vertical orientated crustal scale fault zone. *After* Sibson (1977) Holdsworth et al. (2001) and Pless (2012).

An incohesive fault rock with <30% clasts >2mm is defined as a fault gouge. A fault gouge is comprised of fine grained highly crushed rocks and mineral fragments set in a clay (grainsize) rich matrix (Fossen, 2016) formed through the crushing and abrasion of wall rocks and subsequent entrainment into the fault zone (Figure 2.31). The development of a fault gouge can drastically change the hydraulic properties of a fault due to the fine grain size and high proportion of clay materials. Cohesive fault rocks with <30% clasts >2mm are defined as non-foliated cataclasites or as foliated mylonites and are given the prefix; proto, meso or ultra, depending on the proportion of matrix material. Cataclasites and mylonites are also distinguished based on the conditions they form under, with cataclasites occurring in more 'brittle' conditions and form from the breaking and crushing (cataclasis) of material whereas, mylonites form under more 'ductile' conditions and form from ductile processes such as recrystallisation or flow.

A cohesive fault rock with pronounced grain growth is termed a blastomylonite. Fault rocks without discernible grains composed of glass (or devitrified glass) are termed pseudotachylites which form from the frictional heating and melting of wall rocks during faulting.

			non-foliated	foliated
>30% large clasts >2 mm	75-100% large clasts (>2 mm)	fault breccia	crackle breccia	
	60-75% large clasts (>2 mm)		mosaic breccia	
	30-60% large clasts (>2 mm)		chaotic breccia	
<30% large clasts >2 mm	incohesive[1]		**fault gouge**	
	cohesive	glass or devitrified glass	**pseudotachylyte**	
		0-50% matrix (<0.1 mm)	**protocataclasite**	**protomylonite**
		50-90% matrix (<0.1 mm)	**(meso)cataclasite**	**(meso)mylonite**
		90-100% matrix (<0.1 mm)	**ultracataclasite**	**ultramylonite**
		pronounced grain growth		**blastomylonite[2]**

[1]incohesive at present outcrop

[2]some blastomylonites have >30% large porphyroclasts

(i)

(ii)

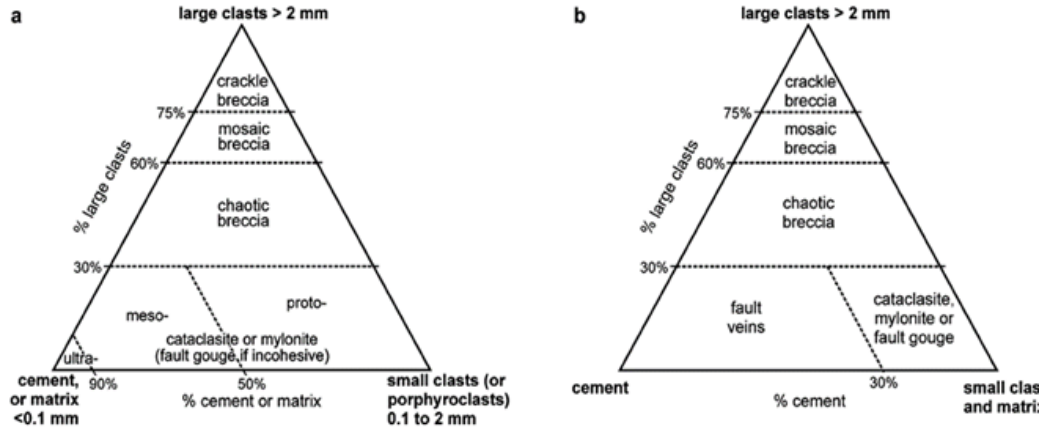

Figure 2.30: (i) Classification scheme for fault rocks and (ii) Ternary diagrams showing the two alternative graphical displays of the proposed fault rock classifications of Woodcock and Mort, (2008) (b) allows for the differentiation of cements from matrix which is not possible with (a). Modified *after* Woodcock and Mort (2008).

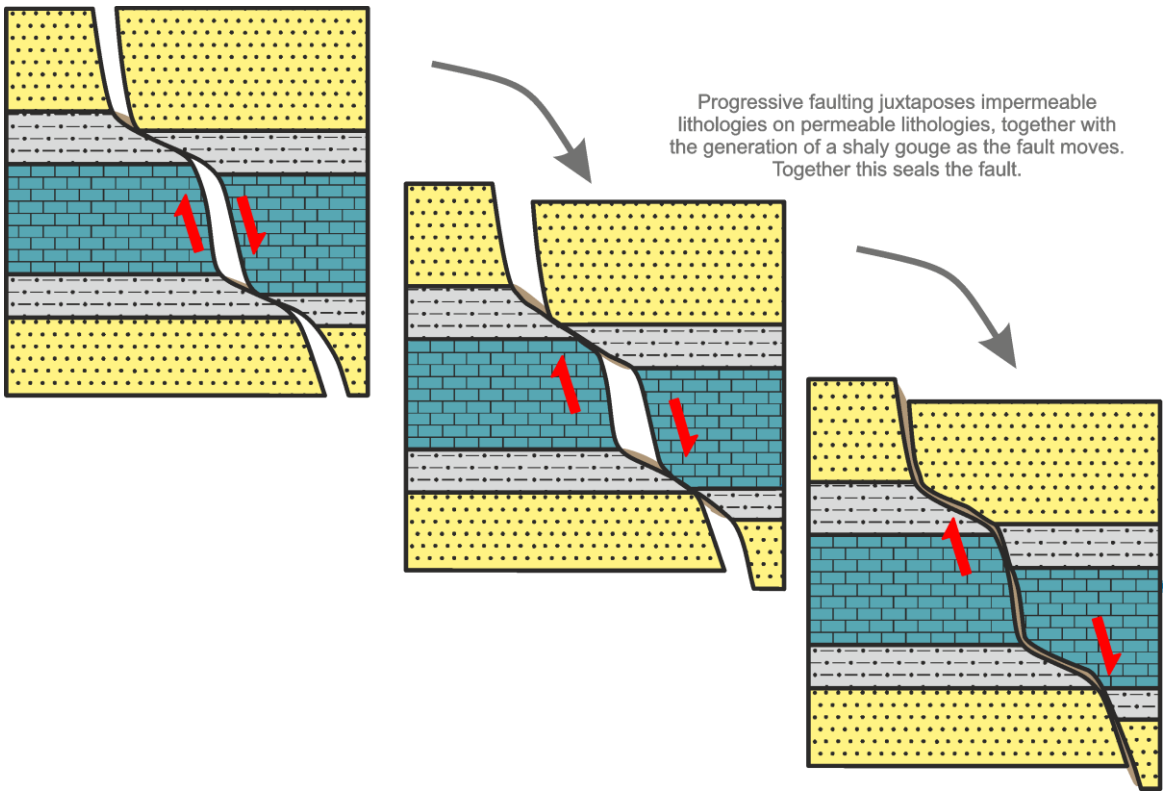

Figure 2.31: Generation of a fault gouge during progressive faulting. The juxtaposition of units of differing permeability can alter the transmissivity through and along a fault zone and will control whether it will act as a seal, baffle or conduit to fluid flow.

2.4.8. Deformation Bands:

Deformation bands refer to discrete, thin (mm-cm), tabular zones of shear strain that occur within porous rocks as result of strain localisation (Schultz and Fossen, 2008). In the literature they may also be termed 'shear bands', 'cataclastic slip bands' or 'granulation seams' (Figure 2.32). They are common structure in many upper-crustal tectonic and non-tectonic regimes. They form as a result of rotation and translation of grains causing friction and sliding along grain boundaries which can lead to cataclasis, compaction, phylosillicate smearing, dissolution and cementation. (Fossen et al., 2018, 2007).

Bands typically form sequentially, as individual bands, zones of bands or within fault zones associated with discrete slip surfaces. A discrete slip surface may not be formed, but they often form as a precursor to faults which may have a significant displacement and can represent a more mature stage of deformation band formation. Individual bands rarely have offsets more than a few centimetres, even if they are of a significant length (10s to 100s of metres).

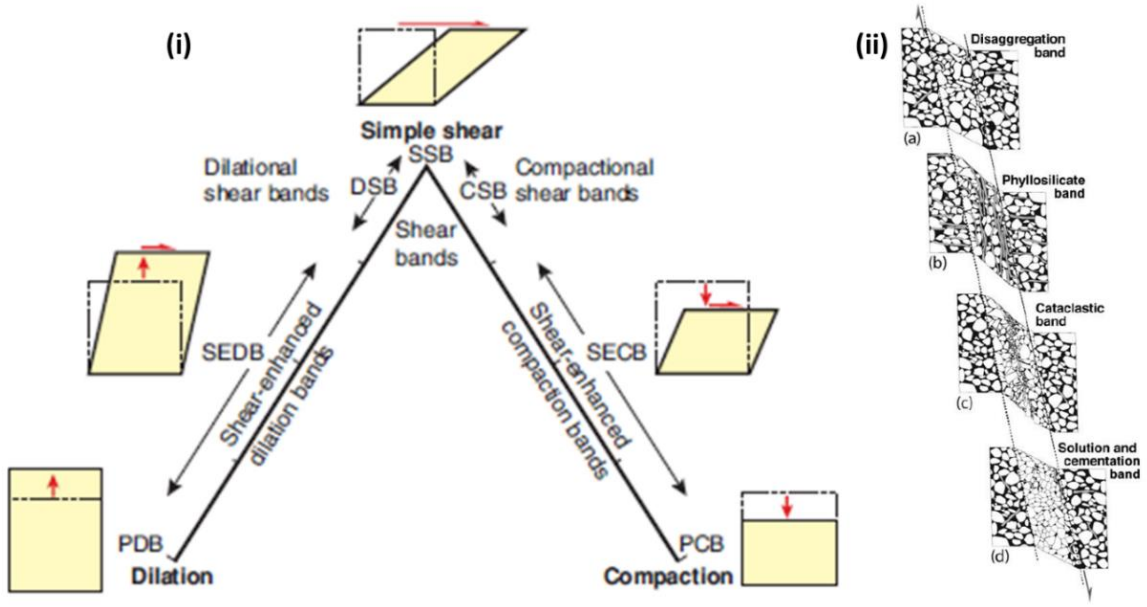

Figure 2.32: (i) Kinematic spectrum of deformation bands between the end member compaction, simple shear and dilation. PCB: pure compaction band; SECB: shear-enhanced compaction band; CSB: compactional shear band; SSB: simple shear band (or simply shear band); DSB: dilational shear band; SEDB: shear-enhanced dilation band; PDB: pure dilation band (Fossen et al., 2018). (ii) Principal types of deformation bands, based on deformation mechanism (Fossen et al., 2007).

2.4.9. Veins and Dykes:

A vein is defined as an extensional fracture that is filled with mineral deposits that precipitated from a solution under favourable conditions of temperature and pressure (Fossen, 2016; Park, 2013). The minerals deposit may be massive or show sequential growth which can aid in understanding the growth and kinematics of an opening vein (Figure 2.33). Mineral deposits may be massive or composed of fibrous crystals. The mineralogy and geochemistry of vein filling minerals a fluid inclusions can give valuable insight into the pressure/temperature conditions they formed in and the fluids they precipitated from (Bons et al., 2012). Geochronological analysis of vein forming minerals can help to determine the age of deformation. When a vein is filled with intrusive igneous or sedimentary material it is termed a dyke, which may form passively or forcefully with hydraulic failure driving fracturing and deformation.

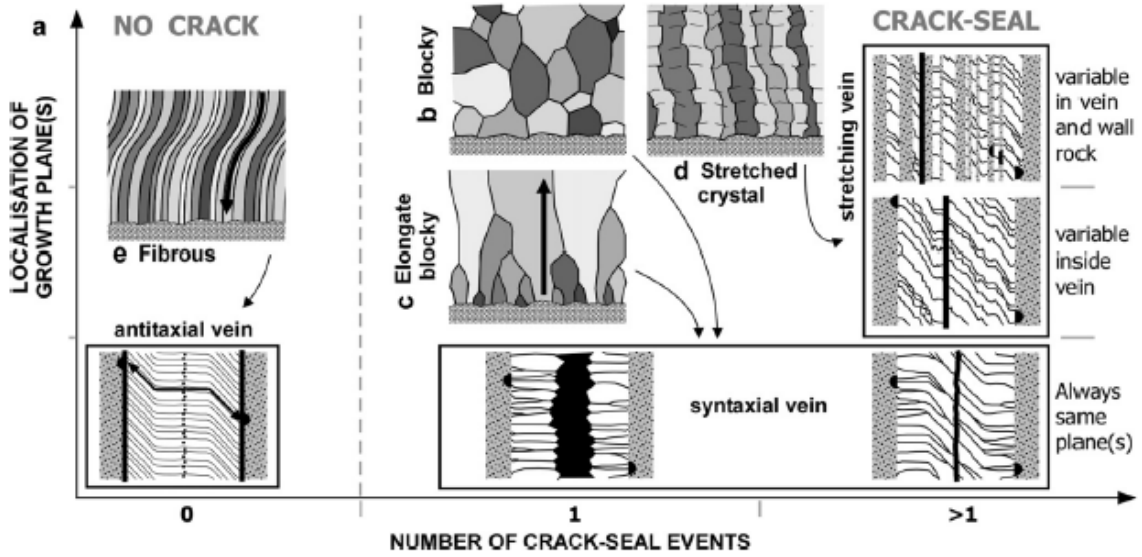

Figure 2.33: (a) Schematic linking vein types (antitaxial, syntaxial or stretching vein) and internal crystal morphology to localisation of the growth plane and number of crack seal events. Main vein crystal types: (b) blocky, (c) elongate blocky, (d) stretched crystals and (e) fibrous. (Bons et al., 2012)

2.4.10. Kinematic Indicators:

Kinematic indicators are key for the identification of the direction a fault or shear zone has moved and in determining past stress states. On brittle structures such as faults planes the most direct method of determining kinematics are from the analysis of linear features on a fault plane. These features are referred to as slickenlines and slickenfibres. The former are grooves produced when two surfaces pass over one another with the resistant or harder materials leaving scratch-like impressions on the fault plane. The latter are comprised of fibrous crystals which precipitate in the irregular gap between two fault surfaces. In either case the orientation of the resulting linear feature gives the direction but not the sense of shear. Other markings can be used to infer kinematics based on the following criteria of Doblas (1998)(Figure 2.34); 1) Crescentic markings, 2) Steps (or notches), 3) fractures, 4) trains of inclined planar structures, 5) trailed material, 6) asymmetric elevations, 7) deformed elements or 8) asymmetric plan-view features.

Figure 2.34 (overleaf): Classification of slickenside kinematic indicators. Legend: 1 = scale of occurrence of the indicators (a = microscopic; b = tens of millimetres; c = metric); 2 = three different types of arrows (pointing in the direction of movement of the missing block) indicate the degree of confidence in each one of the kinematic indicators (a = good; b = fair; c = poor); BD = block diagram; OMO = oblique mineralogical orientation; PPE = previous planar element; P = plane; S = section (Doblas, 1998).

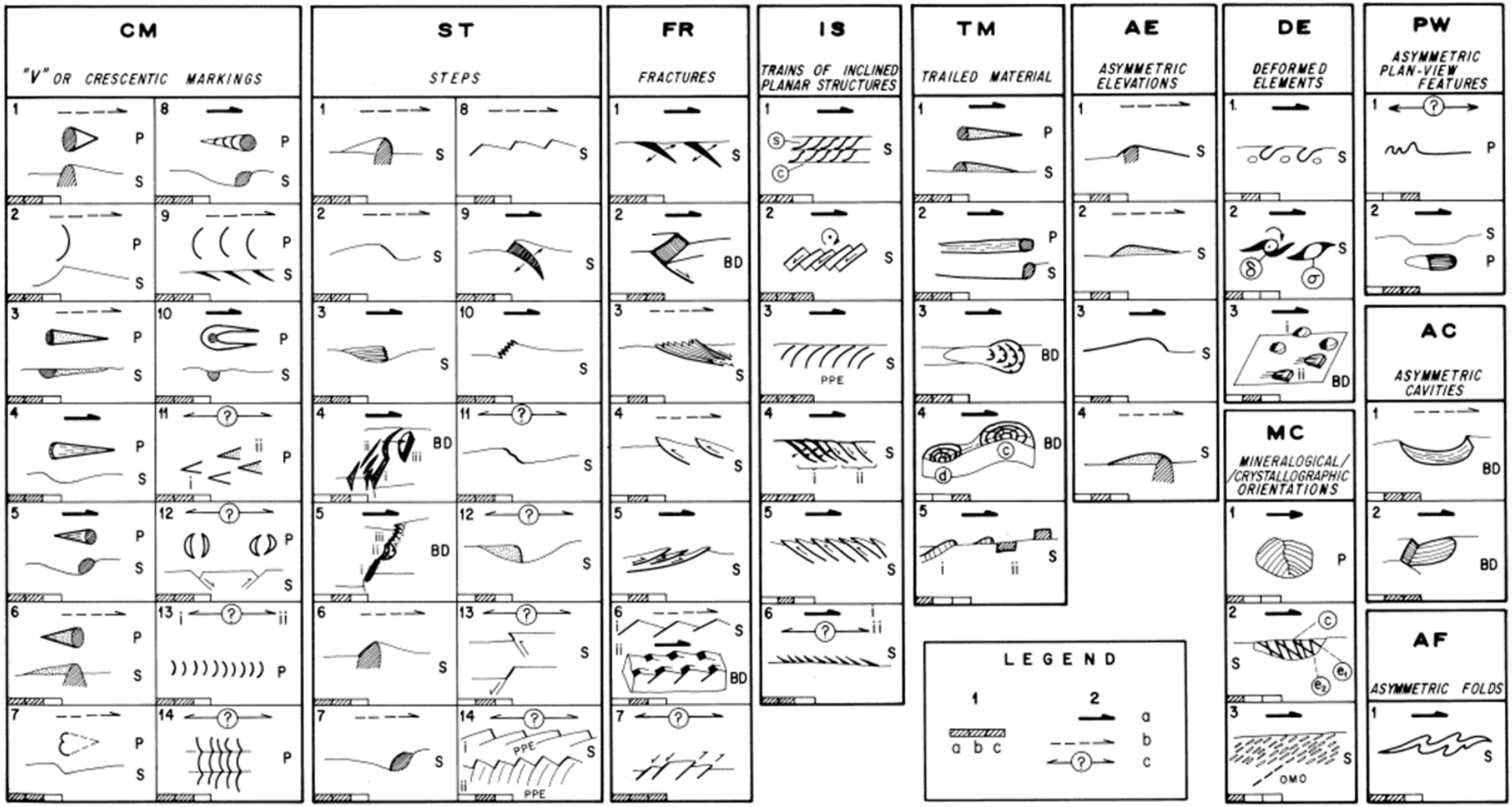
CM
"V" OR CRESCENTIC MARKINGS
ST
STEPS
FR
FRACTURES
IS
TRAINS OF INCLINED PLANAR STRUCTURES
TM
TRAILED MATERIAL
AE
ASYMMETRIC ELEVATIONS
DE
DEFORMED ELEMENTS
PW
ASYMMETRIC PLAN-VIEW FEATURES
AC
ASYMMETRIC CAVITIES
MC
MINERALOGICAL/ /CRYSTALLOGRAPHIC ORIENTATIONS
AF
ASYMMETRIC FOLDS
LEGEND
PPE
OMO
BD

Secondary or subsidiary fractures formed during faulting (e.g. Reidel shears and tensile fractures)in addition to internal fabrics preserved within fault rocks can indicate shear sense (Fossen, 2016; Twiss and Moores, 1992) (Figure 2.35). Reidel or R shears will form as synthetic fractures at 15° to the main fault with the same sense of shear. R' shears are antithetic to the main fault and are orientated 75-80° to the main fault with an opposed sense of shear. P shears will form approximately 10° from the main fault and tensile or T fractures will form at 30-90° to the major fault (Fossen, 2016; Twiss and Moores, 1992).

In the ductile regime the vergence of fold structures and the morphology and geometry of grains and porphyroclasts can assist in the assessment of kinematics within deformed rocks (Passchier and Simpson, 1986)(Figure 2.36).

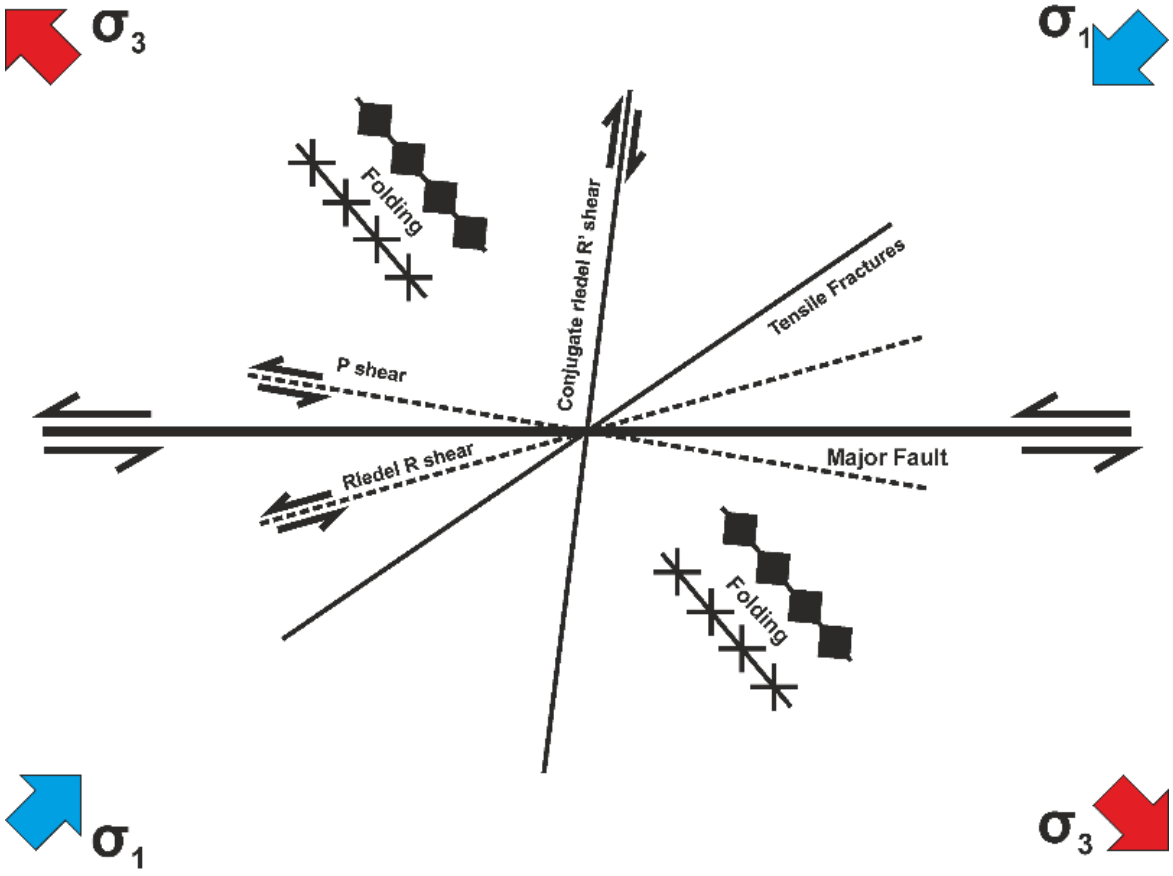

Figure 2.35: Schematic representation of a major sinistral fault with associated minor structures: Sinistral reidel r shear, conjugate dextral reidel R shear, sinistral P shear, tensile fractures, and orientation of associated fold structures.

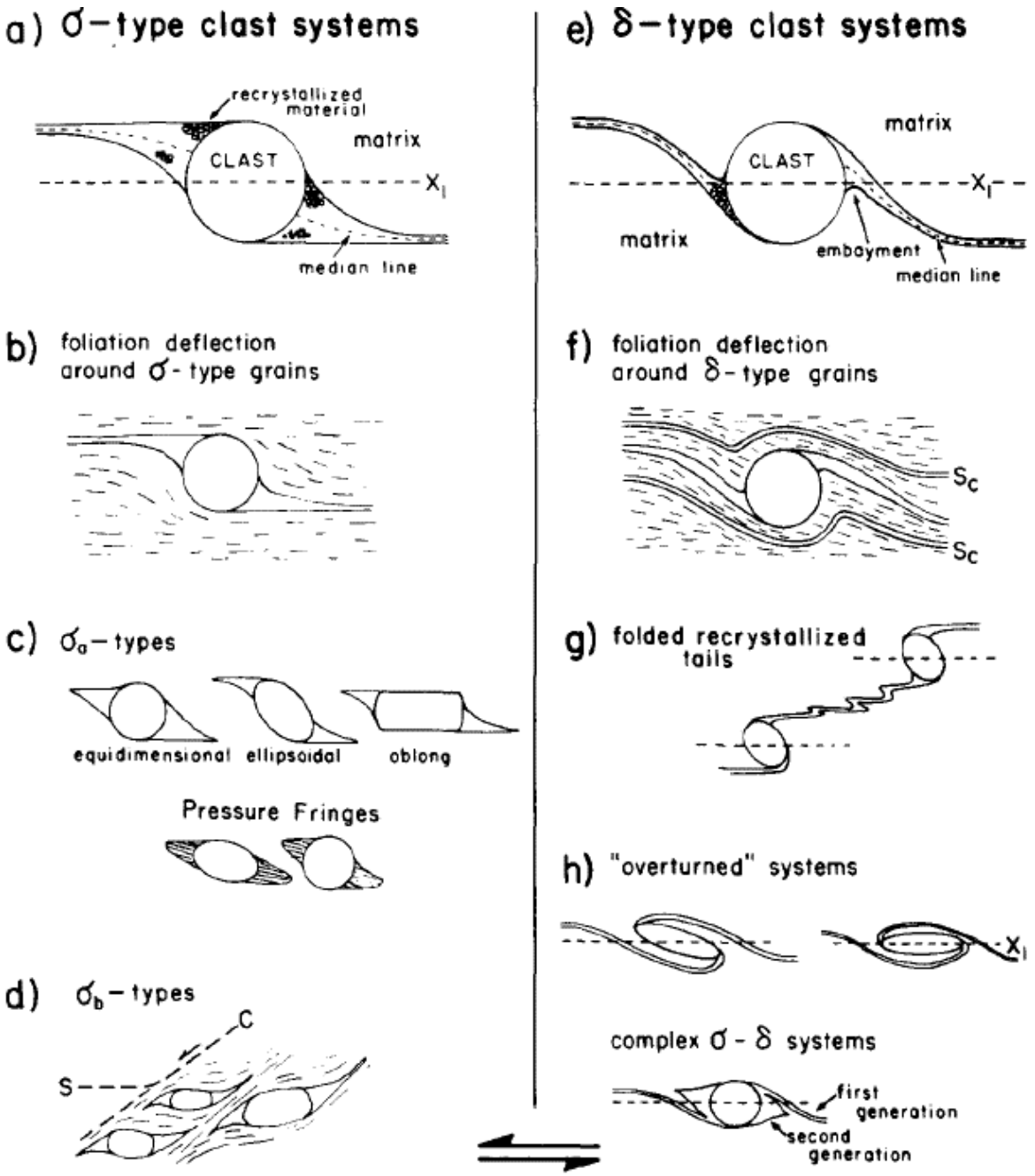

Figure 2.36: Classification of porphyroclast systems with sinistral sense of vorticity. (a) σ-Type system. (b) Foliation deflection around σ-type systems. (c) σ_a-Type (equidimensional, ellipsoidal, oblong); pressure fringes. (d) σ-Type in S-C mylonites. (e) & δ type system. (f) Foliation deflection around δ-type systems. S_c, compositional layering. (g) Folded recrystallized tails. (h) Complex and overturned δ-type systems. (Passchier and Simpson, 1986).

2.4.11. Structural Reactivation:

Reactivation of structures can be common due to the lower shear stress required to initiate faulting on a pre-existing surface compared to that required to nucleate a new fault. Reactivation may occur along any pre-existing discontinuity including, but not limited to:

faults, foliations, shear zones, fractures, compositional/rheological/mechanical boundaries (Beacom et al., 2001; Butler et al., 1997; Holdsworth et al., 1997) or any previously deformed or damaged rock including fold structures. The lower friction coefficient or cohesiveness of some fault rocks materials (e.g. talc, serpentine, various clays) may weaken fault zones and lead to reactivation and brittle failure of a rock at a lower shear stress. Two principal types of reactivation have been identified (Holdsworth et al., 1997)(Figure 2.37):

1. Geometric reactivation – occurs when reactivated structures display different senses of relative displacement for successive events.
2. Kinematic reactivation – occurs when reactivated structures display similar senses of relative displacement for successive events.

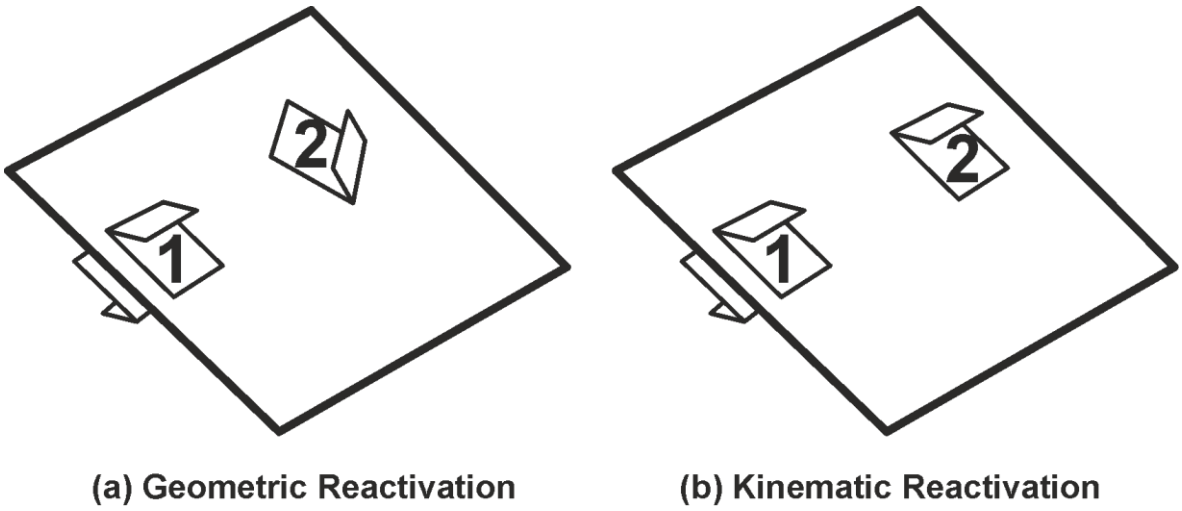

Figure 2.37: The two types of reactivation identified by Holdsworth et al., (1997) (a) geometric reactivation and (b) Kinematic reactivation. *After* Holdsworth et al., (1997).

Several stratigraphic, structural, geochronological and neotectonic criteria must be considered for the identification of reactivation (Figure 2.38) and ideally numerous criteria should be fulfilled to define it. Structures not optimally orientated in a given stress field may be reactivated due to the lower stresses required to reactivate an existing structure, and the orientation of structures alone is not sufficient for the conclusive identification of reactivation.

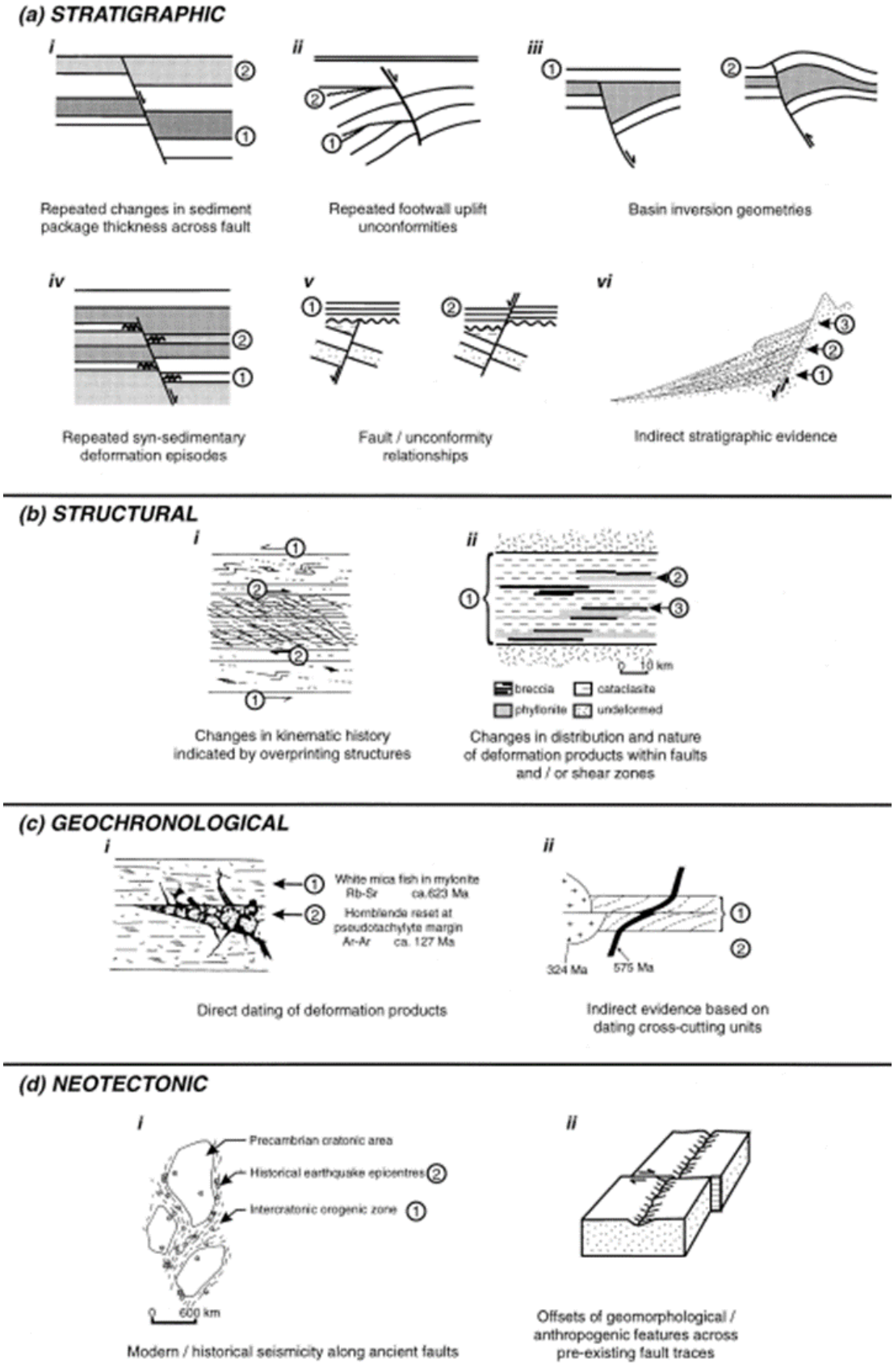

Figure 2.38: The four main criteria for the recognition of reactivation: (a) stratigraphic, (b) structural, (c) geochronological, (d) and neotectonic. Isotopic ages shown are illustrative (Holdsworth et al., 1997).

2.4.12. Transtension, Transpression and Oblique Tectonics:

Transtension and transpression, or oblique tectonics are the inevitable consequence of plate motion on a spherical surface (Dewey et al., 1998) and also because tectonic margins rarely form orthogonal to plate convergence/divergence, as they often form in areas of weakness and/or previous crustal strain. Harland, (1971) shows in a simple 2D plane plate diagram how different tectonic regimes can occur as a result of a different angles between the moving plate and the boundaries (Figure 2.39). This forms areas with orthogonal extension or compression and areas influenced by strike-slip or oblique motion generating transtension and transpression. Transtension (and transpression) can be qualitatively defined as the contemporaneous action of 'wrench' simple shear and 'extensional' (or compressional/shortening) pure shear, orthogonal to the deformation zone boundary (Dewey et al., 1998)(Figure 2.40).

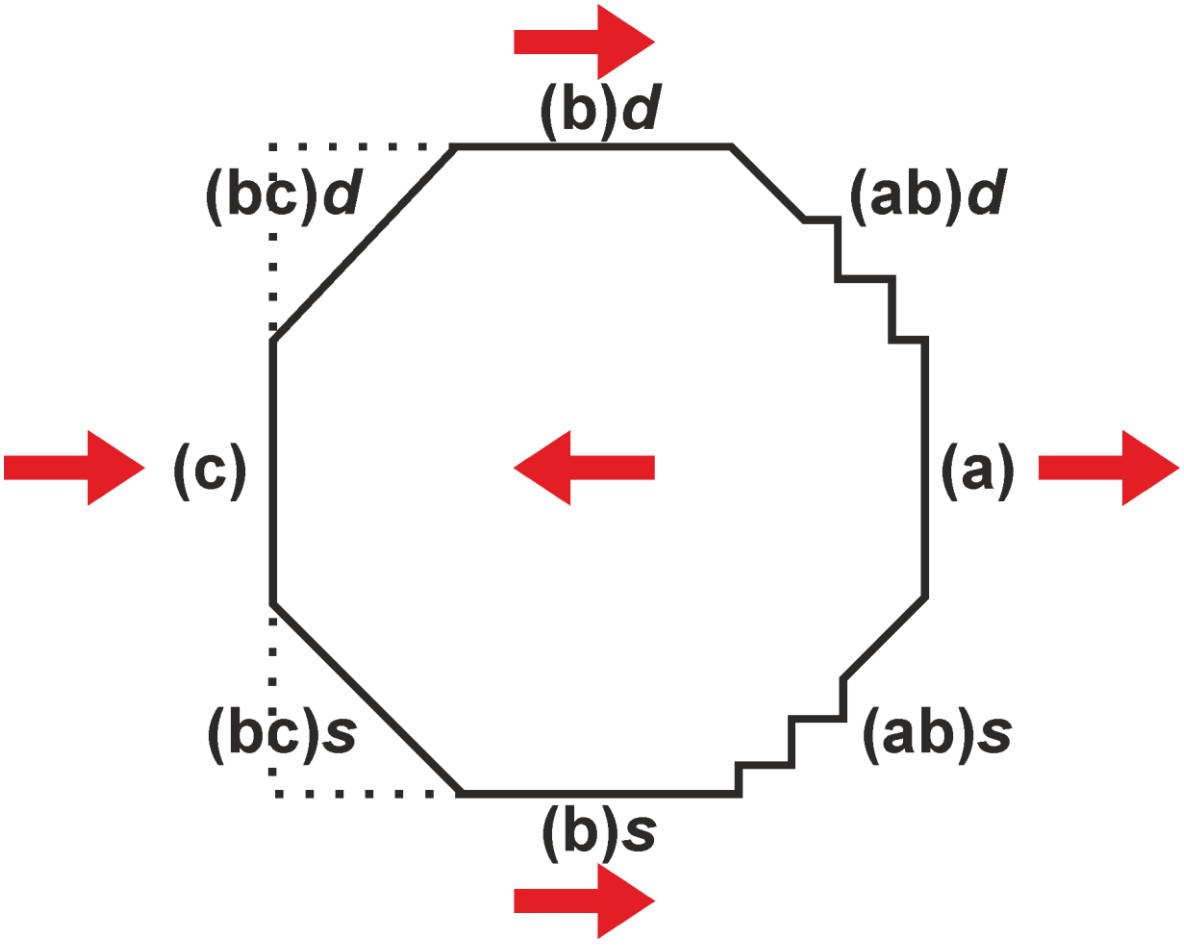

Figure 2.39: Schematic diagram of two plane plates generating different tectonic regimes at their margins by relative rectilinear motion (a) extension, (b) strike-slip *d=dextral and s=sinistral*, (c) compression, (ab) transtension and (bc) transpression (Harland, 1971).

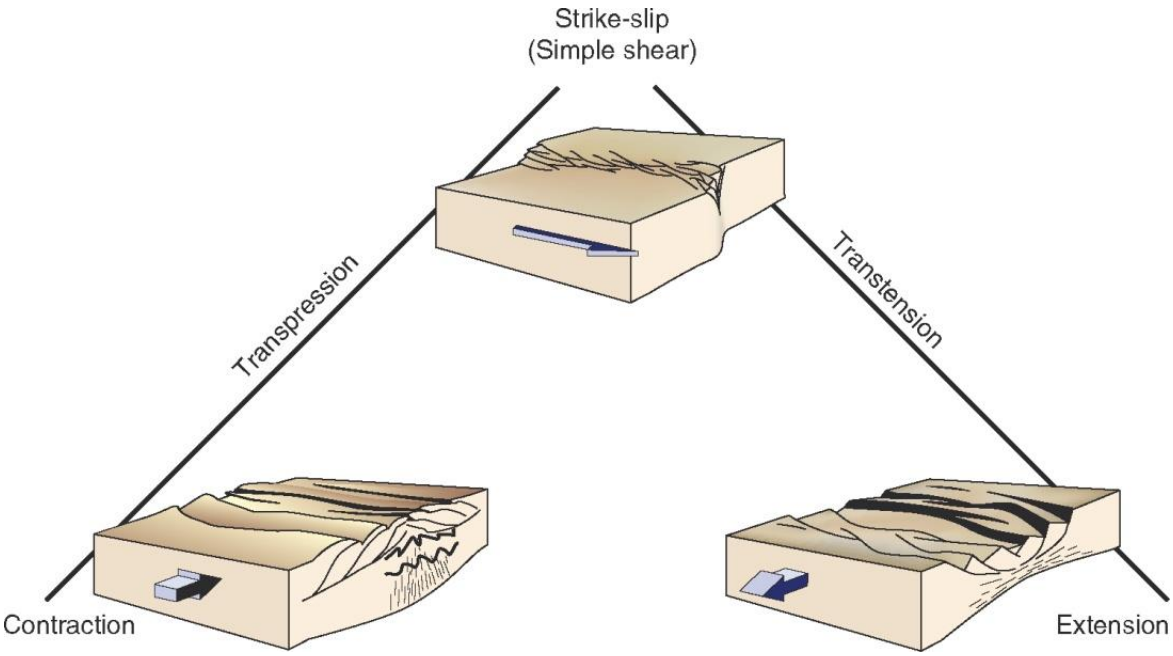

Figure 2.40: Simplified diagrammatic representation of the end member deformation regimes and associated structures developed in strike-slip simple shear and extension/contraction (compression) pure shear (Fossen, 2016).

In nature tectonic margins are rarely orthogonal to the direction of plate motion as they frequently represent inherited zones of weakness due to previous deformation e.g. shear zones (Dewey et al., 1998; Holdsworth et al., 1997) and therefore an element of obliquity is quite common in many tectonic settings. For example transtension will occur when the bulk displacement direction is at an oblique angle (α) to the angle of the deformation zone boundary faults (β_x) ($0°<\alpha<90°$). When the divergence angle α is perpindicular ($\alpha=90°$) or parallel ($\alpha=0°$) to the bouindary fault, pure shear coaxial extension and non-coaxial wrench simple shear will take place respectively (Figure 2.41).

A variety of structures can be produced during oblique deformation which will form across a broad range of scales (figure 2.42 and 2.43). Laboratory experiments conducting polyaxial or triaxial tests have identified that under 3D strain up to four sets of mutually cross-cutting faults and fractures are developed (Reches and Dieterich, 1983). Such multi-modal or polymodal fault patterns are interpreted to represent general triaxial strain as an alternative to bimodal patterns reflecting plane strain patterns (Figure 2.25).

Folds may be produced in both transtensional and transpression regimes but will differ in their orientation due to differences in the origin of motion. In transtension, folds are

formed wholly due the wrench component of motion, whereas in transpression they form as a result of wrench and compressive motion.

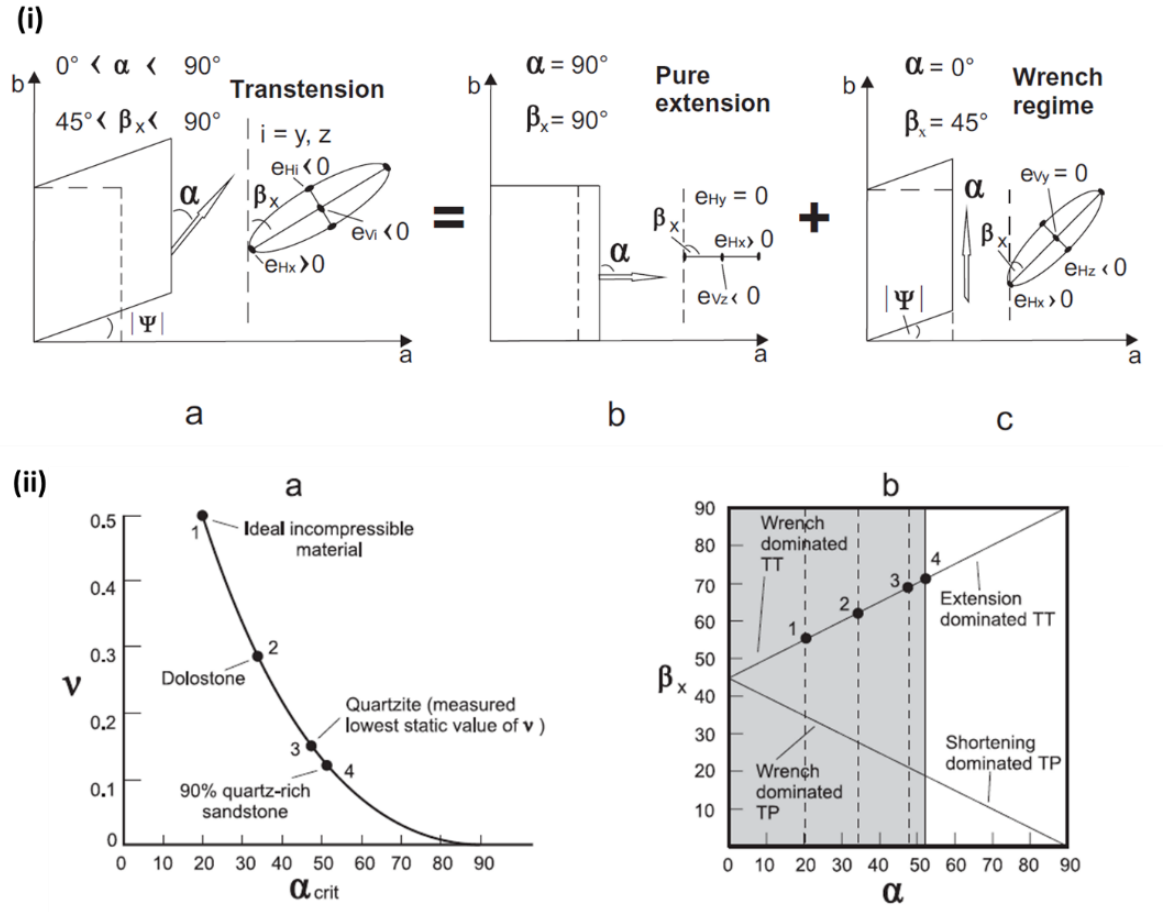

Figure 2.41: (i) Diagrams showing (a) transtension (b) pure extension and (c) wrench condtions during deformation. (ii.a)and (ii.b) α v. β_x diagram plotted with the fields of wrench (simple shear) and extension/shortening (pure shear). Modified *after* (De Paola et al., 2005; De Paola et al., 2005)

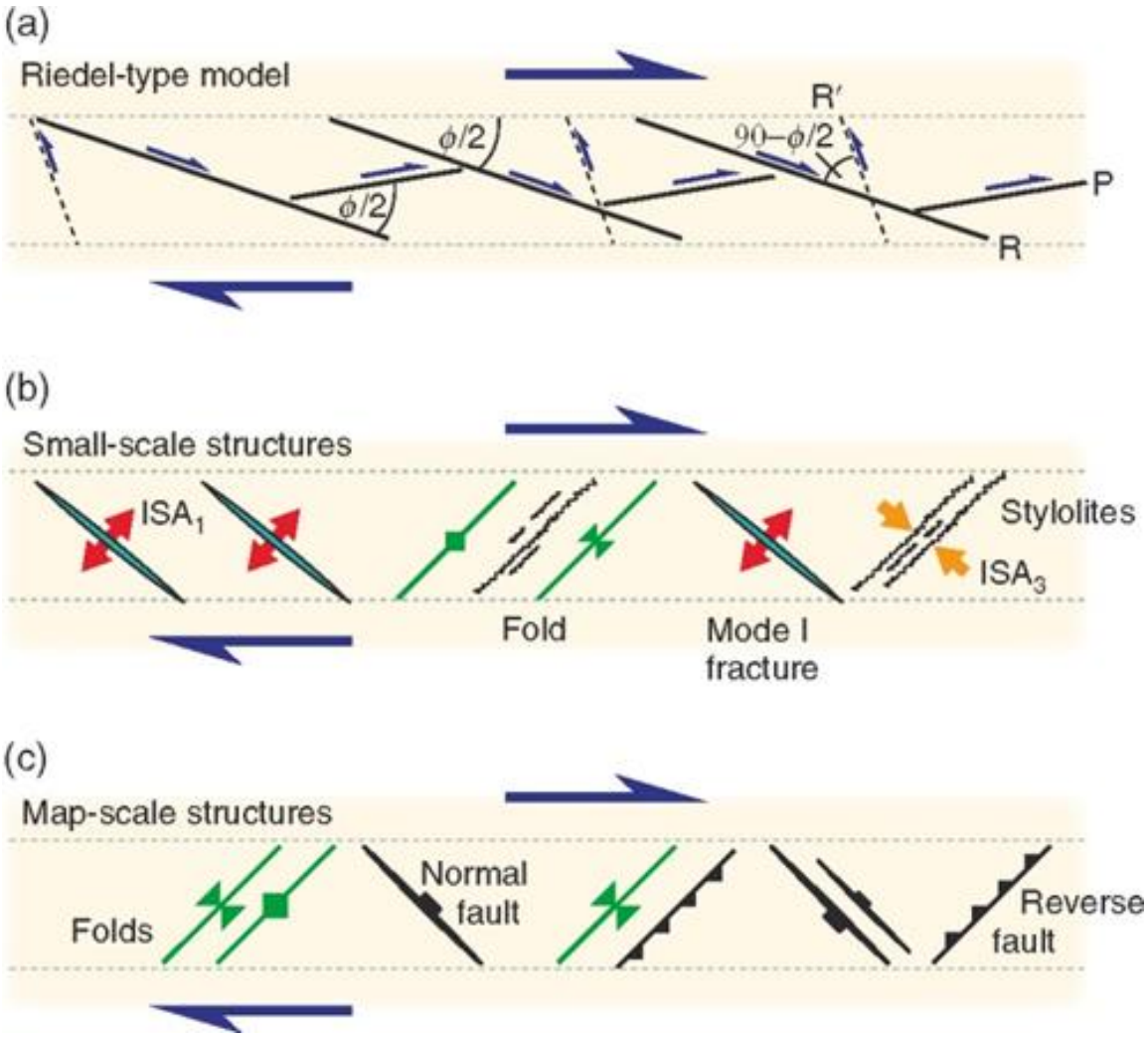

Figure 2.42: Types of structures developed during strike-slip deformation (a) reidel-type idealised model (b) micro to macro structures and (c) outcrop to map scale structures (Fossen, 2016).

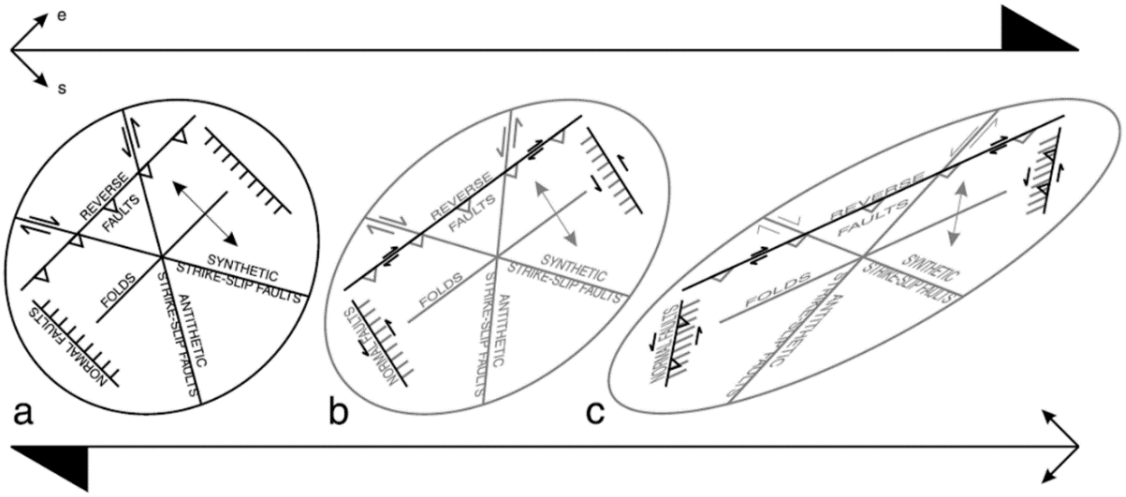

Figure 2.43: (a) Diagram illustrating incremental increasing strain in a simple shear strike slip zone leading to (b) which shows previous (grey) structures acquire oblique slip (black).Continued shearing leads to inversion (black) of early structures (grey) (Waldron, 2005).

Analogue modelling of transtensional deformation by Venkat-Ramani and Tikoff (2002) identified the generation of folds associated with the constrictional strain that develops during oblique extension with hinges that progressively rotate towards parallelism with the maximum horizontal finite stretching direction, which is consistent with a decreasing horizontal shortening component with increasingly oblique divergence (Figure 2.44). Thus during progressive deformation, the fold hinges will effectively rotate towards parallelism with the maximum extension direction. In transpression fold hinges will rotate towards parallelism with the fault boundary. In both cases, the fold hinges rotate with progressive deformation (Venkat-Ramani and Tikoff, 2002). The geometry of the resultant folds will vary, dependent on the deformation regime, with tighter folds being developed in wrench dominated transtension and broader more open folds developing in pure shear dominated transtension (Figure 2.45).

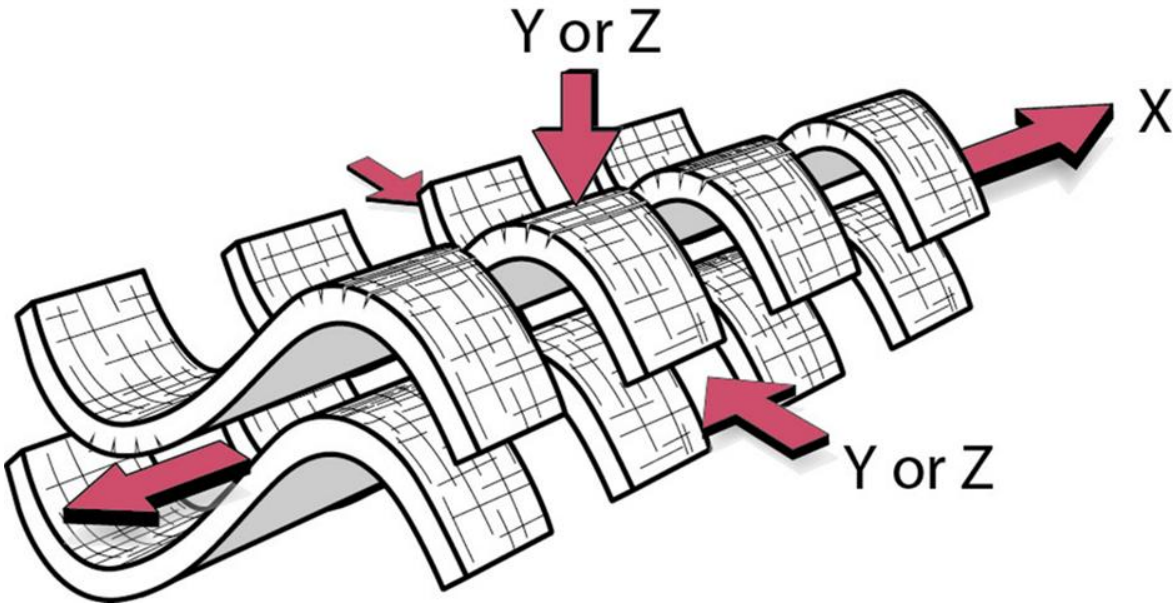

Figure 2.44: Schematic diagram of transtensional folds (Fossen, 2016).

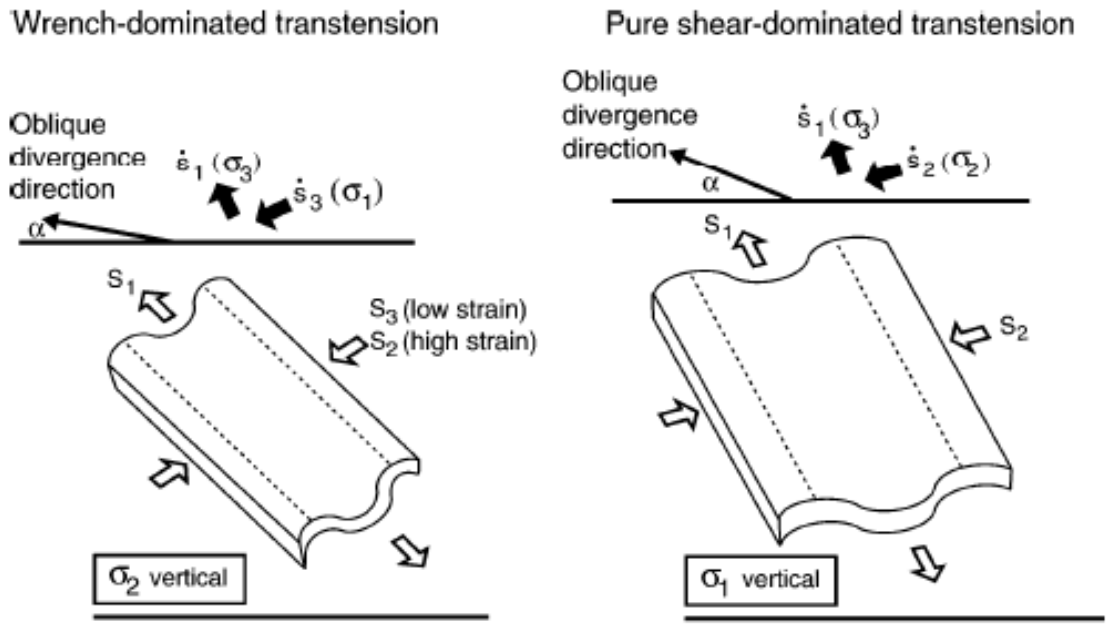

Figure 2.45: Fold shapes and orientations in wrench and pure shear dominated transtension (Venkat-Ramani and Tikoff, 2002)

2.4.13. The Recognition of Transtensional Basins:

The conclusive recognition of transtensional and strike slip influenced basins may be challenging due to a lack of exposure and difficulty in seeing the full 3D structure within subsurface or offshore datasets. In strike-slip basins, the rapid accumulation of sediments may occur, particularly in pull-apart basin settings and the rapid exhumation of deeply buried rocks during transtension can juxtapose high-grade metamorphic rocks against shallowly buried sedimentary rocks (Krabbendam and Dewey, 1998; Séguret et al., 1989). Further evidence for syn-depositional strike slip motion may include (Reading, 1980; Rodgers, 1980; M. Seranne, 1992; Steel and Gloppen, 1980):

1) Directly observable lateral motion and structural patterns directly indicative of strike-slip motion (Figure 2.37) together with significant vertical motions.
2) Onlap of units onto basement and the development of progressive unconformities
3) Syntectonic unconformities and internal angular unconformities
4) Development of new synsedimentary (growth) folds (Figure 2.46) together with changing hinge lines and interlimb angles
5) Asymmetric and spoon or scoop shaped basins.
6) Igneous activity.

7) Absence of regional metamorphism and if present likely due to earlier deformation or rapid exhumation of basement rocks.
8) Deep sedimentary basins that are elongate parallel to the orientation of the strike slip system with a dominance of longitudinal fill and migrating depocentres localised along the basin axis.
9) Rapid lateral facies changes with pebble mis-matches at the basin margins and fan bodies may be skewed indicating strike-slip motion.

Such features have been identified in numerous sedimentary basins globally. Identification of some these subtle indicators has led to reappraisal of many sedimentary basins worldwide and the correct identification of a series of these criteria can allow for the differentiation of early basin forming structures from later deformation (De Paola et al., 2005) and may provide an alternative model for a basins evolution. For example in the Orcadian Basin, Chauvet and Séranne (1994) identify Devonian age transtensional basins in Norway based on the above criteria with similar features having been identified in the conjugate Devonian Basins of Shetland and Northern Scotland contrary to the early purely extensional models, see Chapter 1.2.4.

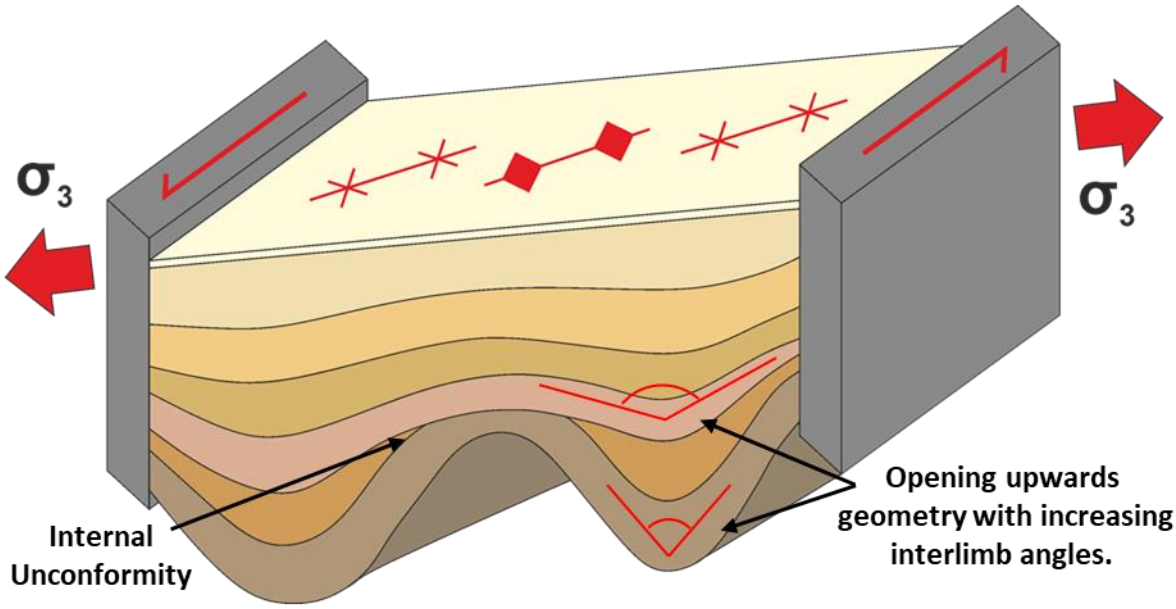

Figure 2.46: Schematic diagram of the development of transtensional growth folds with opening upwards geometry, internal unconformity and oblique hinge position.

Chapter 3

Sinistral transtension and the structural development of the Devonian Foula Sandstone Group, Shetland, Scotland: an onshore analogue for the Clair Oil Field.

Chapter 3- Sinistral transtension and the structural development of the Devonian Foula Sandstone Group, Shetland, Scotland: an onshore analogue for the Clair Oil Field.

Thomas A. G. Utley[1], Robert E. Holdsworth[1,5], Edward D. Dempsey[2], Rob A. Strachan[3], Ken J. W. McCaffrey[1,5], Andrew C. Morton[4], Anna F. Bird[2], Richard R. Jones[5,1] , Graham A. Blackbourn[6] and Alja Sassnowski [*]

[1]*Department of Earth Sciences, Durham University, Science Labs, Durham, DH1 3LE, UK*

[2] *School of Environmental Sciences, University of Hull, Hull, HU6 7RX*

[3]*School of Earth and Environmental Sciences, Burnaby Building, Burnaby Road, University of Portsmouth, PO1 3QL, UK*

[4]*HM Research Associates, Giddanmu, Musselwick Road, St Ishmaels, Pembrokeshire, SA62 3TJ*

[5]*Geospatial Research Limited, Office Suite 7, Harrison House, 1 Hawthorn Terrace, Durham, DH1 4EL, UK*

[6]*Blackbourn Geoconsulting, 26 East Pier Street, Bo'ness, West Lothian, EH51 9AB, UK*

Keywords:

Old Red Sandstone, Devonian, Basin Development, Transtension, West of Shetland, Clair Field, UKCS

Abstract:

The island of Foula located 25 km SW of Shetland preserves a gently folded, 1.6 km thick sequence of Middle Devonian sandstones that are spectacularly exposed in kilometre-long cliff sections up to 376m high. These rocks can be correlated with the nearby Lower Clair

[*] A version of this is in preparation for submission to the Journal of the Geological Society

Author and co-authors contributions: Thomas A.G.Utley conducted the fieldwork, analysed the data and wrote this chapter under the principal supervision of Robert E.Holdsworth who carried out principal edting and suggested the topic, adding valuable contributions during various discussions of the subject matter. Rob A.Strachan assisted in the field. Edward D. Dempsey and Anna F.Bird carried out geochronology and and provided valuable contributions during discussion of the data. Edward D.Dempsey also assisted with paleostress analysis. Ken J.W.McCaffrey and Richard R.Jones helped with the development of Virtual Outcrop Models and associated methodologies. Andrew C.Morton carried out HM analysis and assisted in interpretation of the data. Graham A.Blackbourn assisted with understanding aspects of the regional geology. Alja Sasnowski provided unpublished/published data for comparison with the geochronology data and aided in the discussion. All co-authors assisted with editing.

Group offshore. The Foula sequence unconformably overlies likely Precambrian-age amphibolite facies basement rocks, intruded by sheeted granites.

A new geological map has been created using new land and drone-based studies of basement-cover contacts and structures. Down-plunge section constructions show that growth faulting and folding on Foula were contemporaneous with sedimentation during basin filling. The large-scale structural geometries are consistent with regional constriction related to sinistral transtention along the Walls Boundary - Great Glen Fault Zone system during the Middle Devonian. Detrital zircon provenance studies indicate that the Devonian sequences of Foula (and nearby Melby in Western Shetland) show similarities with the Clair Group and Orkney successions. Our findings suggest that the development of transtensional folds contemporaneous with subsidence may be more widespread than has previously been realised in the Devonian Orcadian basins. Folds previously interpreted to be related to Permo-Carboniferous inversion may have initiated much earlier in the basin history than has previously been recognised.

3.1 Introduction – The Clair Oil Field:

The Clair Oil Field, situated 75km W of the Shetland Isles, is the largest known hydrocarbon resource on the UKCS, with a closure of ~250 km^2 and an estimated 7-8 billion barrels of oil equivalent (BOE) in place (Figure 3.1a) (Ogilvie et al., 2015; Webster, 2018; Witt et al., 2010). It comprises naturally fractured Devonian-Carboniferous sandstones, designated the Clair Group, which overlie an up-faulted ridge of fractured Precambrian metamorphic basement (Coney *et al.*, 1993; Holdsworth *et al.* 2019) (Figure 3.1b).

The supposedly extensional Orcadian Basin has long been used as the classic analogue for the Clair Field, however other alternatives do exist in Shetland, which are thought to be transtensional (Dewey and Strachan, 2003; Fossen, 2010; Seranne, 1992). Furthermore, the recognition of transtensional folding in the Devonian basins of Norway has revolutionised our understanding of these basins (Fossen et al., 2017; Séguret et al., 1989; Seranne and Seguret, 1987; Tikoff and Fossen, 1999), and a similar tectonic setting could be considered as an alternative model for the development of Clair.

This paper aims to appraise the structure, stratigraphy and tectonic evolution of an onshore analogue to the Clair Basin on Foula. This little studied island represents the closest land to

the Clair Oil Field and has poorly constrained geology relative to the Clair Field itself and the more distal analogues in the Orcadian Basin.

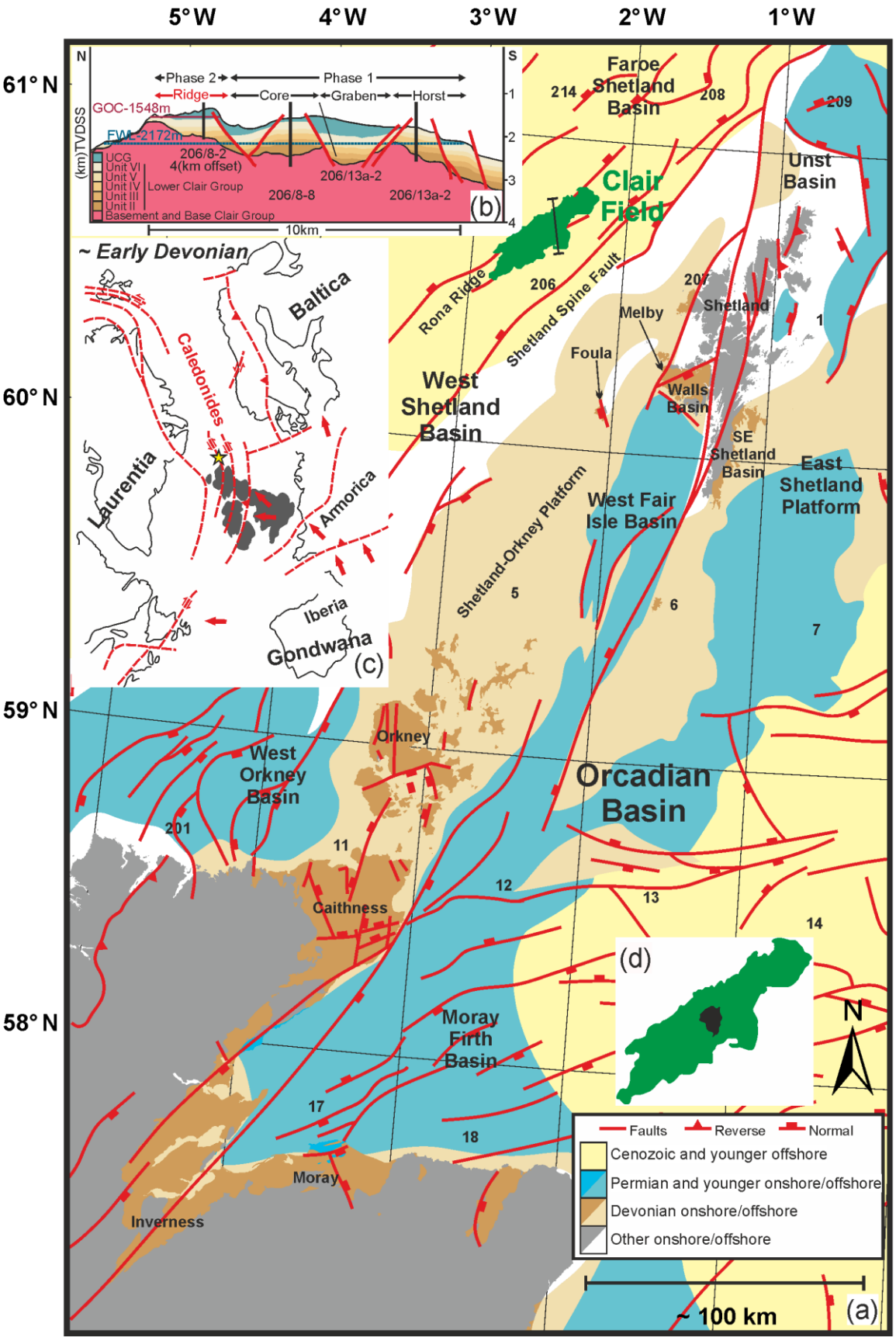

Figure 3.1 (preceding page): (a) Regional map of the Orcadian Basin study area with Clair oilfield highlighted. Modified *after* Dichiarante et al., (2016; and Oil and Gas Authority, (2019) Clair Field Map and Cross Section modified *after* Barr et al., (2007) and Ogilvie et al., (2015) (c) Devonian paleogeography and simplified reconstruction of the North Atlantic Modified *after* Dewey and Strachan (2003). (d) Enlarged size comparison of the Clair field (green) and Foula (black) drawn to the same scale.

3.2 Regional Framework:

3.2.1 The Orcadian Basin in Shetland:

The Clair and Orcadian basins are just two of a number of Devonian continental sedimentary basins that formed in the North Atlantic region (Friend, 1981; Friend et al., 2000) following the collision of Laurentia, Baltica and Avalonia, and subsequent formation of the Caledonian mountain belt (Figure 3.1c). Thick sequences (several km) of siliciclastic sediments and lesser volumes of volcanic rocks were deposited in a series of sedimentary pull-apart and rift basins from the Silurian to the Carboniferous in Eastern Greenland, Northern Scotland and Western Norway(Friend et al., 2000) (Figure 3.2).

The Orcadian Basin occurs onshore and offshore in the Shetland, Orkney, Caithness and the Moray Firth regions of Northeast Scotland. The N-S oriented Shetland Isles, part of the extensive Shetland Platform (Figures 3.3 and 3.4a), comprise highly deformed and metamorphosed Precambrian rocks (Mykura et al., 1976a). These were intruded by a suite of igneous rocks during the Caledonian orogeny, and later flanked and overlain by three separate Devonian sedimentary basins (Mykura et al., 1976a) and subsequently by later Mesozoic basins which now mostly lie offshore (Figure 3.4b). The Shetland Platform forms a regional basement high which now separates the Northern North Sea rift in the East from the Faroe-Shetland Basin to the Northwest. The Shetland archipelago is cut by up to three major strike-slip faults; the Walls Boundary Fault, the proposed northward continuation of the Great Glen Fault (Flinn, 1992, 1979; McBride, 1994; McGeary, 1989; Ritchie and Hitchen, 1993; Watts, 2001; Watts et al., 2007), the Melby Fault and the Nesting Fault (Mykura, 1976, Flinn and May, 1976).

Figure 3.2 (overleaf): Regional Devonian stratigraphic correlation chart and stratigraphy of the Clair Field. *After* Allen and Mange-Rajetzky, (1992); Barclay et al., (2005); Barr et al., 2007; Gautier et al., (2011); House, (2000); Marshall et al., (2003); Ogilvie et al., (2015); Trewin and Thirlwall, (2002).

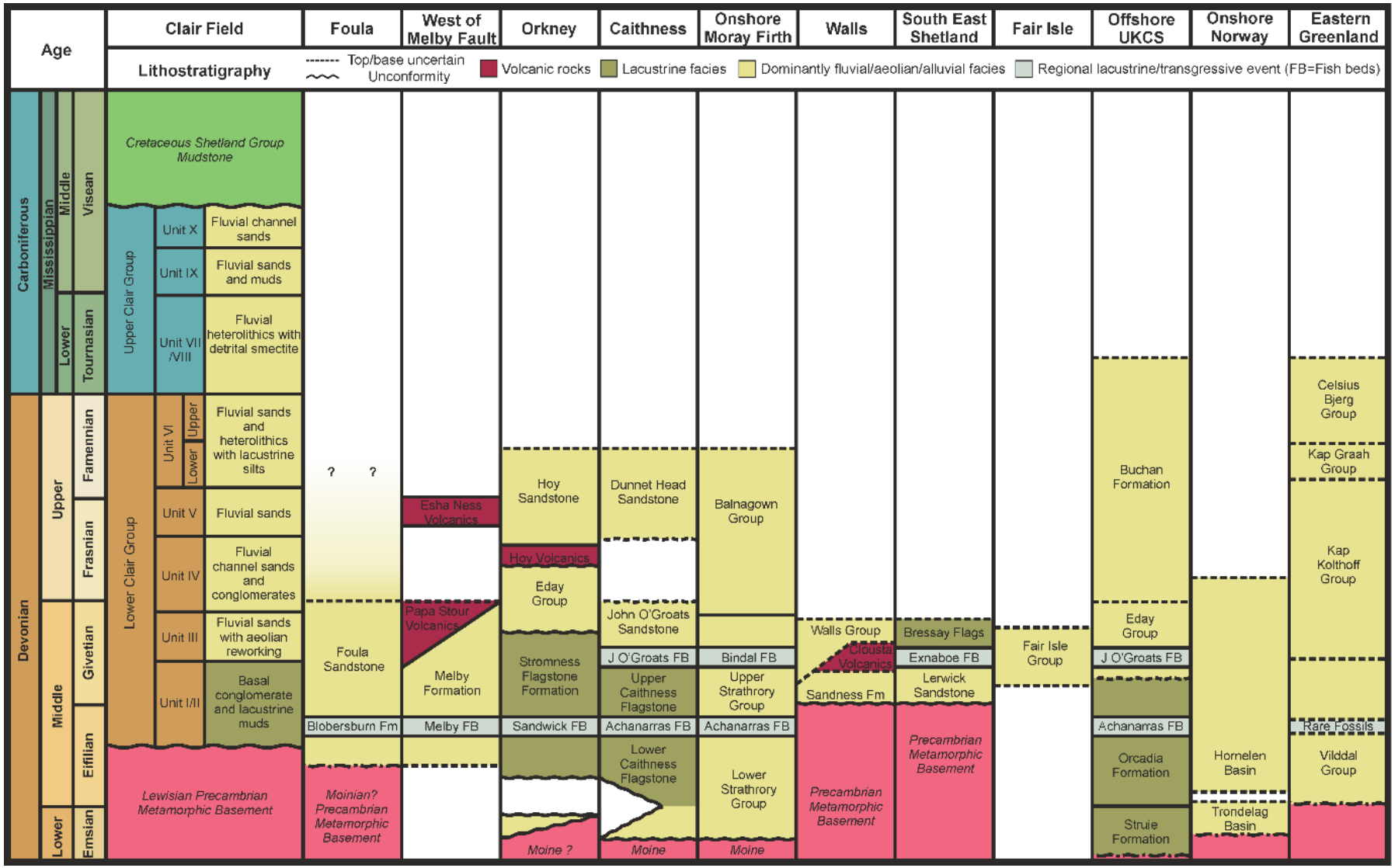
Age
Clair Field
Foula
West of Melby Fault
Orkney
Caithness
Onshore Moray Firth
Walls
South East Shetland
Fair Isle
Offshore UKCS
Onshore Norway
Eastern Greenland
Lithostratigraphy
Top/base uncertain
Unconformity
Volcanic rocks
Lacustrine facies
Dominantly fluvial/aeolian/alluvial facies
Regional lacustrine/transgressive event (FB=Fish beds)
Carboniferous
Devonian
Mississippian
Upper
Middle
Lower
Visean
Tournasian
Famennian
Frasnian
Givetian
Eifilian
Emsian
Cretaceous Shetland Group Mudstone
Upper Clair Group
Lower Clair Group
Unit X
Unit IX
Unit VII /VIII
Unit VI
Upper
Lower
Unit V
Unit IV
Unit III
Unit I/II
Fluvial channel sands
Fluvial sands and muds
Fluvial heterolithics with detrital smectite
Fluvial sands and heterolithics with lacustrine silts
Fluvial sands
Fluvial channel sands and conglomerates
Fluvial sands with aeolian reworking
Basal conglomerate and lacustrine muds
Lewisian Precambrian Metamorphic Basement
Foula Sandstone
Blobersburn Fm
Moinian? Precambrian Metamorphic Basement
Esha Ness Volcanics
Papa Stour Volcanics
Melby Formation
Melby FB
Hoy Sandstone
Hoy Volcanics
Eday Group
Stromness Flagstone Formation
Sandwick FB
Moine ?
Dunnet Head Sandstone
John O'Groats Sandstone
J O'Groats FB
Upper Caithness Flagstone
Achanarras FB
Lower Caithness Flagstone
Moine
Balnagown Group
Bindal FB
Upper Strathrory Group
Achanarras FB
Lower Strathrory Group
Moine
Walls Group
Clousta Volcanics
Sandness Fm
Precambrian Metamorphic Basement
Bressay Flags
Exnaboe FB
Lerwick Sandstone
Precambrian Metamorphic Basement
Fair Isle Group
Buchan Formation
Eday Group
J O'Groats FB
Achanarras FB
Orcadia Formation
Struie Formation
Hornelen Basin
Trondelag Basin
Celsius Bjerg Group
Kap Graah Group
Kap Kolthoff Group
Rare Fossils
Vilddal Group

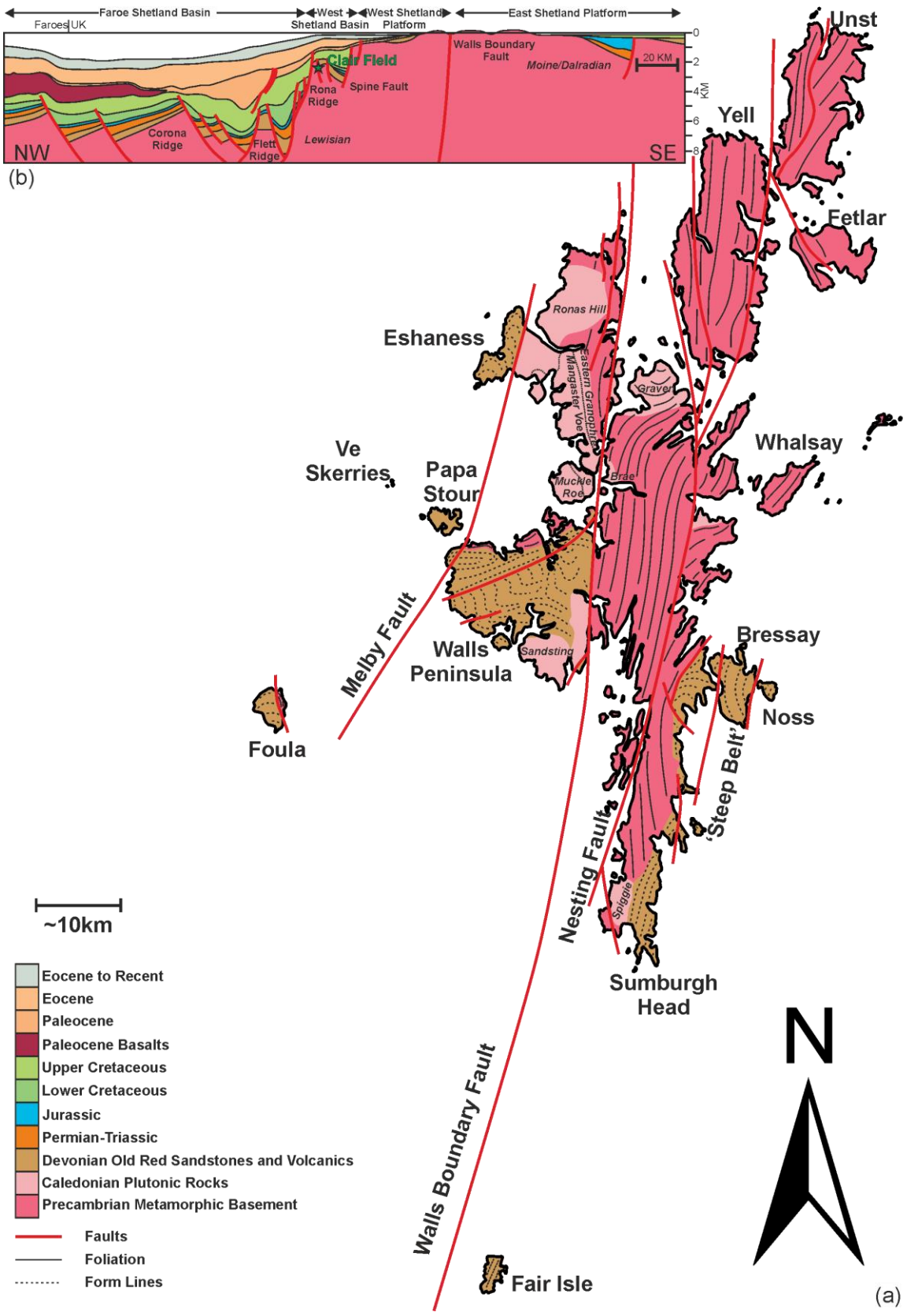

Figure 3.3: (a) Simplified geological map of Shetland with key structures *after* Mykura et al., (1976) and BGS (2019). (b) Regional section line through Faroe Shetland Basin and Shetland (see Figure 3.4 for location of line of section labelled A-A'). Modified *after* Stoker et al., (1993).

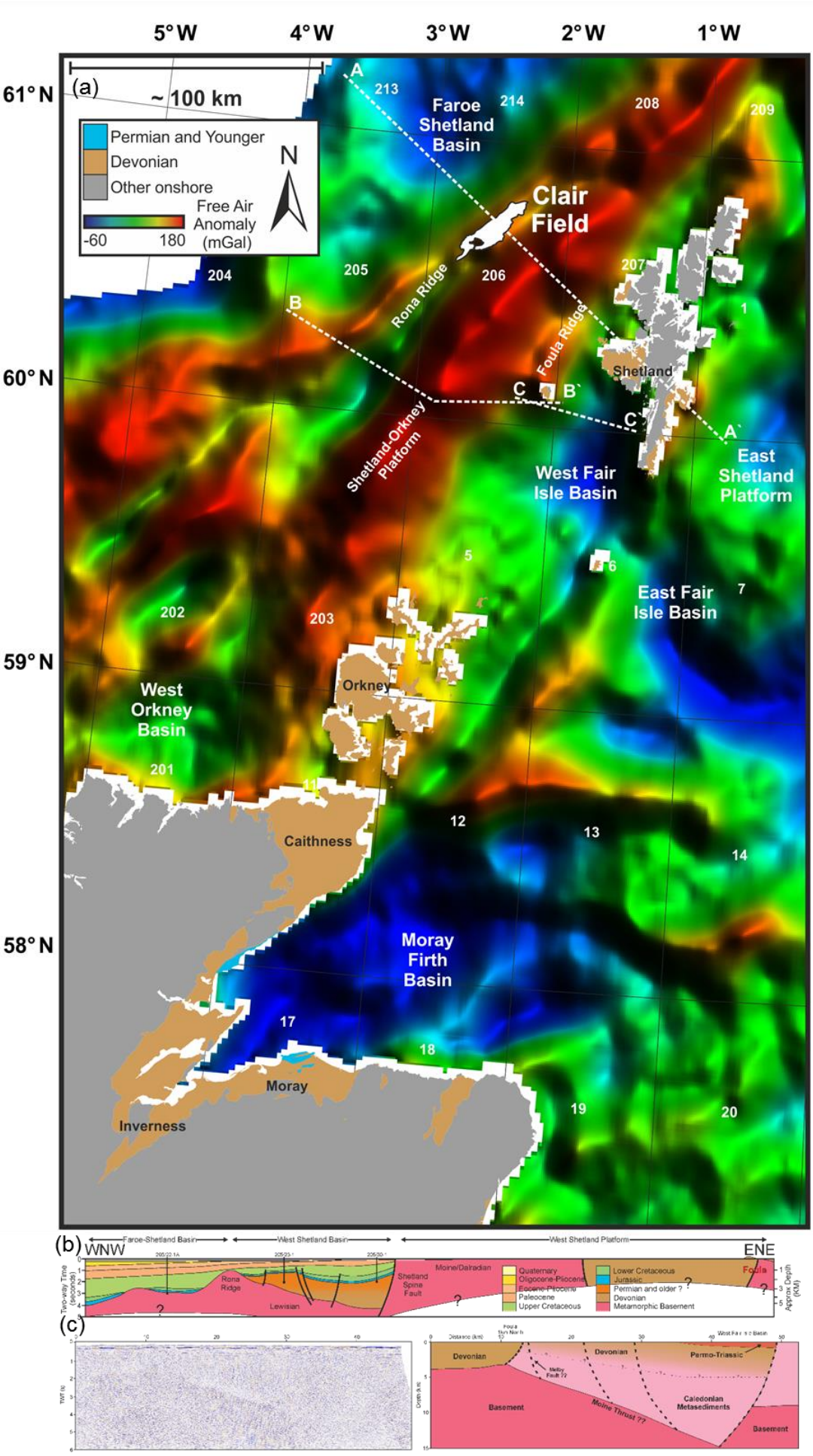
5° W
4° W
3° W
2° W
1° W
61° N
60° N
59° N
58° N
(a)
~ 100 km
Permian and Younger
Devonian
Other onshore
Free Air Anomaly (mGal)
-60
180
N
Faroe Shetland Basin
Clair Field
Rona Ridge
Foula Ridge
Shetland
Shetland-Orkney Platform
West Fair Isle Basin
East Shetland Platform
East Fair Isle Basin
West Orkney Basin
Orkney
Caithness
Moray Firth Basin
Moray
Inverness
A
A`
B
B`
C
C`
201
202
203
204
205
206
207
208
209
213
214
(b)
WNW
ENE
Faroe-Shetland Basin
West Shetland Basin
West Shetland Platform
Two-way Time (seconds)
Approx Depth (Km)
Rona Ridge
Lewisian
Shetland Spine Fault
Moine/Dalradian
Foula
Quaternary
Oligocene-Pliocene
Eocene-Pliocene
Paleocene
Upper Cretaceous
Lower Cretaceous
Jurassic
Permian and older ?
Devonian
Metamorphic Basement
(c)
Devonian
Devonian
Permo-Triassic
Basement
Caledonian Metasediments
Basement
Moine Thrust ??

Figure 3.4 (preceding page): (a) Free Air Gravitational Anomaly for the study region (Getech Multisat Gravity Data, 2017). (b) Regional cross section Faroe-Shetland Basin, West Shetland Basin and Foula. Modified *after* British Geological Survey (1988). (c) 2D Seismic line SWS82-628- offshore Foula. Section Line A-A` refers to Figure 3.3b.

The current configuration of the Devonian basins is thought to reflect subsequent post Devonian transcurrent motion along the Nesting, Walls Boundary and Melby faults (Mykura et al., 1976a; M. Seranne, 1992). The exact amount of strike-slip motion along the Walls Boundary fault has been a topic of debate but is generally accepted as being in the region of several tens or hundreds of kilometres of sinistral motion during the Silurian-Devonian, followed by subsequent dextral motions of 20-30km during the Carboniferous and Permian, and a further 15km in the Mesozoic (Watts et al., 2007 and references therein). To the west of the Melby Fault, sedimentary and volcanic rocks are exposed at Melby, Eshaness and on the islands of Foula and Papa Stour (Figure 3.3). They are juxtaposed against the thermally mature and more deeply buried and folded, sedimentary and volcanic rocks that comprise the majority of the Walls Peninsula (Melvin, 1985), into which granites are emplaced and are bound to the east by the Walls Boundary Fault (Figure 3.3). E of the Nesting Fault, in eastern and southern Shetland, sedimentary rocks are exposed in a strip along the eastern coast from Lerwick to Sumburgh Head, and on the islands of Bressay, Noss, Mousa and Fair Isle (Figure 3.3).

3.2.2 The Clair Basin:

The Clair Basin lies on the eastern margin of the mainly extensional Faroe-Shetland Basin (FSB) (Figure 3.1a), which is composed of a series of NE–SW orientated sub-basins, separated by basement highs and horst blocks, that formed through a series of rifting and subsidence events from the Devonian to the Palaeocene (Ellis and Stoker, 2014; Stoker et al., 2016, 1993). It is generally believed that the Clair Basin represents a transitional area between the well-developed Devonian sequences of the Orcadian basin and an elevated area to the NW that was supplying sediment to the Devonian basins of NE Scotland and Shetland (Hitchen and Ritchie, 1987; McKie and Garden, 1996).

Blackbourn (1987) interpreted the Clair Basin, using core and log data from the first six wells drilled on the field and early seismic lines, as one of a series of NE-SW trending half-grabens formed in response to transtensional stresses associated with regional sinistral movements which were accommodated by oblique and dip-slip movements along

reactivated Caledonian faults. The Basin, whose SE margin is defined by the Shetland Spine Fault which separates it from the Shetland Platform, developed during the Middle Devonian to Early Carboniferous, and is bounded in the NW by the Rona Ridge (Figure 1a), a NE–SW orientated, regional structural high (Figure 3.4a) composed of Precambrian metamorphic basement. Blackbourn (1987) designated the Devonian-Carboniferous basin-fill the Clair Group, divided into lower and upper units filled with up to around 1 km of continental fluvial, alluvial, minor aeolian and lacustrine deposits, unconformably overlying Lewisian basement and overlain by Cretaceous marine mudstones of the Shetland Group, which form a regional seal (Figure 3.2). The dominant sediment source-area was interpreted as uplands to the northwest. The sedimentary fill recorded a general upward increase in sediment maturity from basal alluvial fans, through mainly braided streams in the Lower Clair Group (mainly Upper Devonian) which may have flowed along the basin axis from the northeast, and with subordinate aeolian deposits. The Upper Clair Group (Lower Carboniferous) was interpreted as dominated by higher-sinuosity rivers and lakes, and was capped by a carbonaceous unit associated with an increase in sediment-transport distances, increasing humidity and a rise in sea level, with deposition in an environment interpreted as comparable to that of parts of the fluvio-deltaic Oil-Shale Group (now the Strathclyde Group) of the Midland Valley of Scotland.

Following further drilling (Coney et al., 1993), Allen and Mange-Rajetzky (1992) undertook a more detailed study of the Clair Group, including heavy mineral studies. They refined the stratigraphy, dividing the Lower Clair Group into six separate units (Figure 3.2), and suggested that inter-fan lakes recognised by Blackbourn in the basal unit were arms of a single basin-wide rift lake. They interpreted the boundary between the Lower and Upper Clair groups as an erosional unconformity, and divided the Upper Clair Group into four units, interpreting parts of the uppermost “carbonaceous” unit as marginal-marine deposits in the form of interdistributary bays. Provenance studies based on heavy mineral suites were interpreted in terms of varying sediment source-areas including the Shetland Platform, Greenland, the Scottish mainland and Norway.

Further refinements to the sedimentary systems and stratigraphy of the Clair Group have been reported by McKie and Garden (1996), Nichols (2005), Schmidt et al. (2012) and others, although no substantial revisions were proposed to the general depositional model

established earlier. Further detailed work on the heavy-mineral stratigraphy was published by Morton and Milne (2012), who established a detailed field-wide correlation on this basis.

Evidence for the precise age of the deposits remains sparse and has been summarised by Schmidt et al. (2012). Ritchie et al. (1996) recorded the presence of Eifelian-Givetian spores in Unit III of the Lower Clair Group, indicating that the lower part of the succession is as old as the Middle Devonian. Allen and Mange-Rajetzky (1992) reported the presence of reworked late Eifelian to early Givetian sporomorphs within the Kimmeridgian of well 206/5-1 to the north of Clair, but this is the only possible indication that deposition may have begun in the earlier part of the Middle Devonian. It is perhaps significant that aeolian intervals are present low down in the Lower Clair Group (Unit III; Allen and Mange-Rajetzky, 1992). Elsewhere in Northern Scotland, aeolian intervals are uncommon in the Devonian until the upper part of the Givetian and into the Upper Devonian, and are found within the Eday Group and Hoy Sandstone of Orkney (Astin, 1985; McAlpine, 1978) and the Southeast Shetland Basin (Allen and Marshall, 1981) (Figure. 3.2). This is consistent, therefore, with Unit III of the Lower Clair Group correlating with the upper Givetian.

3.3 The Geology of Foula:

3.3.1 Introduction and Methodologies:

Foula, a 13km^2 island (Figure 3.5a) situated 25km SW of Shetland lies approximately 70km SE of the Clair field (Figure 3.1a). 1.6 km of gently folded and fractured Middle Devonian continental clastic deposits unconformably overlie, and are faulted against, fractured metamorphic basement and granite, which are exposed on the E side of the island (Mykura et al., 1976a, 1976b) (Figures 3.5b and 3.5c).

Foula lies at the southern end of the Foula Ridge, one of several NE–SW (Figure 3.4a) trending basement structural highs in this region, one of which is also exposed at Ve Skerries, ~ 27km to the north-northeast. This ridge is seen on regional geophysical surveys as a positive gravitational anomaly, and a positive topographic feature on bathymetric surveys, and in regional 2D seismic surveys (Figure 3.4a). The Ridge marks the NW limit of the West Fair Isle and Melby Basins, and the eastern margin of the Orkney-Shetland Platform and Foula Basin (Figure 3.4b). The ridge is bound to the west by the Foula Fault, which may potentially truncate or link to the Moine Thrust at depth (Figure 3.4c). Andrews (1985) postulated that the northward continuation of the Moine Thrust Zone subcrops to

the west of Foula (Figure 3.4c) and continues N, passing to the E of Ve Skerries, where Lewisian type basement is supposedly exposed, and lies offshore to the W of North Roe. To the E of Foula, the Melby Fault can also be seen as a relatively steep structure with little vertical displacement of reflectors within the West Fair Isle Basin, which is bounded to the east by the Walls Boundary Fault (Figure 3.4c).

Mykura et al., (1976b) correlated the sedimentary rocks of Foula with the Old Red Sandstone (Devonian) successions observed on mainland Shetland, principally those exposed at Melby and near Lerwick (Figure 3.2). Significant differences with the Devonian sedimentary rocks of the Walls Peninsula were noted, for which it was proposed that the present day juxtaposition of the ORS basins of Shetland arose due to strike-slip faulting, and was not representative of their position during the Devonian. Blackbourn and Marshall (1985) showed that the sandstones on Foula were a suitable analogue to those of the Clair Group and grouped the sequence exposed on the island as the Foula Sandstone Group. This was based on the similarity in depositional environments, predominantly fluvial and alluvial sediments, as opposed to the thick lacustrine sediments exposed onshore in Caithness and Orkney. Analysis of spores from Foula has allowed further correlation with the basal Clair Group, the Melby Fish beds and Achanarras Horizon in Caithness, all of which are thought to be Middle Devonian (Donovan et al., 1978). Despite this work, no comprehensive account of the structural, sedimentological or stratigraphic evolution of Foula has yet been published.

Figure 3.5a presents a new geological map of the island of Foula, which integrates the mapping of Blackbourn and Marshall (1985) and Mykura et al. (1976b), together with primary observations and analysis from recent fieldwork carried out by the authors. Due to poor inland outcrops and the inaccessible coastal nature of many of the exposed cliff sections, some of which are up to 376m high, fieldwork was supplemented by the use of aerial and drone based imagery and photogrammetric 3D models interpreted in VRGS (Virtual Reality Geological Studio) to extract geological information and structural measurements (Hodgetts et al., 2007). Lineament analysis of air photos (Figure 3.5d) was carried out at a scale of 1:500 in ArcGIS. Lineament and structural data were analysed using Stereonet 9.5 (Allmendinger et al., 2011). Sampling was undertaken for thin section, microstructural and QEMSCAN analysis, heavy mineral provenance analysis and detrital zircon geochronology.

Detailed methodologies for the aforementioned techniques and full results of analysis can be found in Chapter 2 and Appendix C respectively.

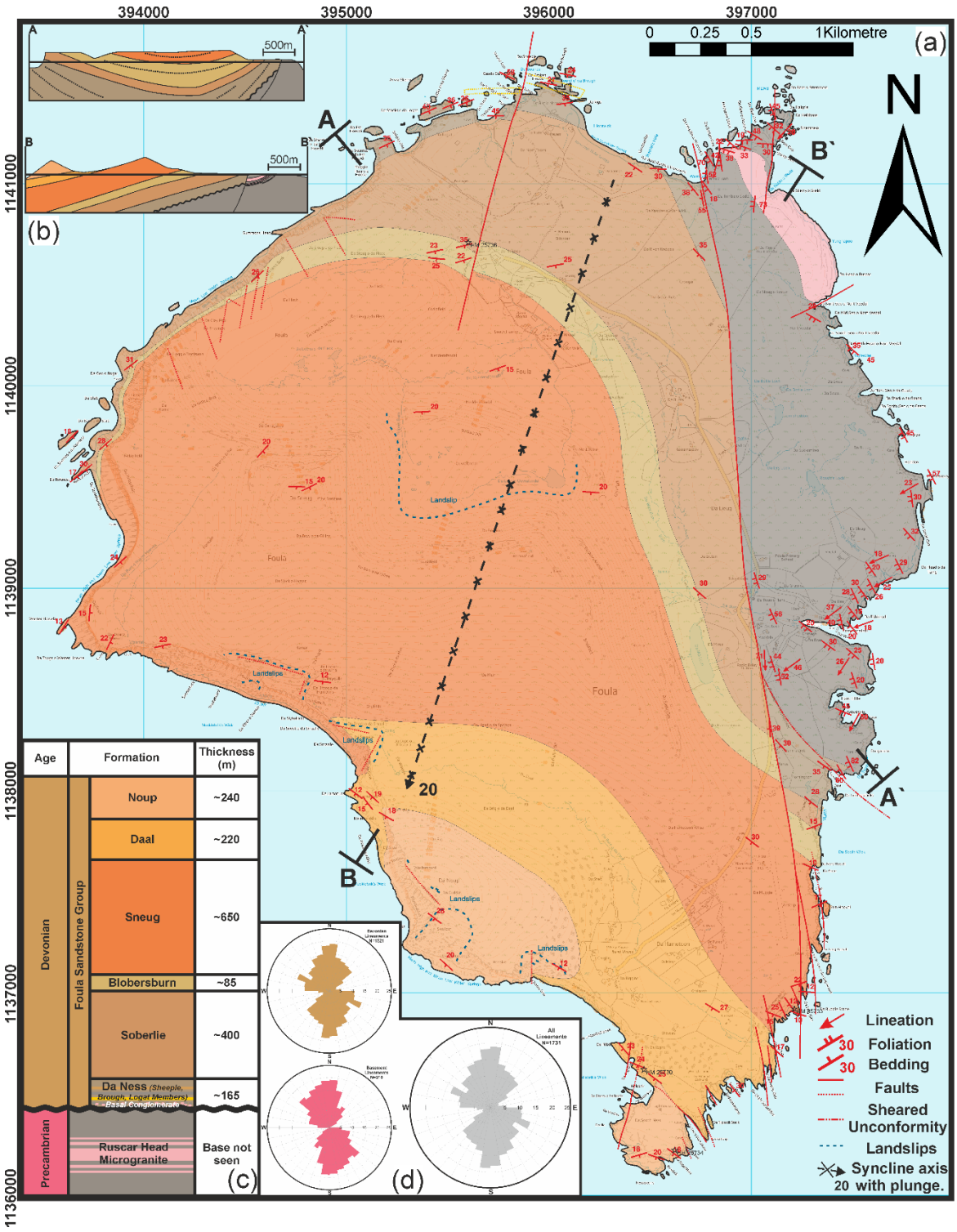

Figure 3.5: (a) Updated geological map of Foula compiled from primary field observations, remote sensing and existing maps (Blackbourn and Marshall, 1985). Base map courtesy of the Ordnance Survey. Grid references are prefixed by OS National Grid Reference HT. Contour interval = 10m. Structural data shown was collected in the field. (b) Schematic cross sections. (c) Stratigraphic

Column for the Foula Sandstone Group and (d) Rose diagrams of interpreted lineaments from aerial Ordnance Survey aerial images for Foula Basement and Foula Sandstone Group.

3.3.2 Metamorphic Basement and Minor Intrusions:

Probable Precambrian metamorphic basement forms a ~ 1km wide strip along the eastern side of the island (Figure 3.5a), comprising (Figures 3.6a and 3.6b) metasediments, and a suite of microgranite sills and dykes (Figure 3.6c) (Mykura, Phemister, et al. 1976a,b).

The basement is dominated by interbanded psammitic psammites and semi-pelitic paragneisses, with subordinate amphibolites and hornblende schists and possible felsic orthogneiss (Figure 3.7a). Several bands of crystalline limestone are also reported (Mykura et al., 1976b) which supposedly bear a resemblance to similarly altered limestones on the Walls Peninsula (Mykura et al., 1976b). Epidotised layers and lenses are concentrated around major N–S faults and may represent highly altered and reactivated basic to ultra-basic sills and dykes. Garnet porphyroblasts up to 5-6mm in size indicate peak metamorphism to at least garnet grade.

The basement was initially thought to have some similarities to the Neeans Group of the Walls Peninsula, Western Shetland (Mykura et al., 1976b, 1976a; Wilson and Knox, 1936). However, a precise age for the basement has yet to be determined, but it is lithologically most comparable to the early Neoproterozoic Yell Sound Group on mainland Shetland (Jahn et al. 2017). Flinn *et al.,* (1979) reported K-Ar ages of 443±14 Ma to 426±20 Ma in hornblende and biotite respectively, from amphibolites on Foula, suggesting that the basement here was metamorphosed during the Caledonian orogeny. At Ve Skerries, basement samples have yielded whole rock K-Ar and hornblende dates of 1350±40 Ma to 1142±30 Ma respectively. This older age of the basement rocks may be due to uncertainty in the location of the Caledonian frontal thrusts in this region and the islands may represent a Lewisianoid inlier within the Caledonian nappe or the basement rocks of the Caledonian foreland (Flinn et al., 1979). This may be accounted for by the proposed northward continuation of the Moine Thrust zone (McBride and England, 1994; Ritchie et al., 1987a; Snyder, 1990), which is interpreted as the prominent dipping structure beneath and to the West of Foula, imaged on regional seismic reflection data (Figure 3.4c).

In NE Foula, a pink microgranite (Ruscar Head Microgranite) forms part of a sheeted complex of sills and feeder dykes (Figure 3.6d) [HT 397167 1140733]. The main intrusion is

granitic to granodioritic in composition, with fine-grained plagioclase phenocrysts set in a groundmass of quartz and orthoclase, with minor patches of muscovite and biotite (Figure 3.7b). The intrusion was emplaced as a series of sills that amalgamated to form a single large, laccolith-like intrusion (Figure 3.7c), with contacts sub-parallel to the foliation within the basement. South of Ruscar Head, on the coast E of Da Swaa [HT 397486 1140048], a second thick sill (10-15m) is exposed within inaccessible cliff sections. A suite of paler granite and aplite veins and pegmatites cut both the granites and basement, interpreted to represent the final phases of melt emplacement associated with the microgranite. Neither the Ruscar Head Microgranite or later intrusions are particularly deformed, however, some are locally foliated and boudinaged.

An age for the Ruscar Head Microgranite is undetermined but is highly likely to be pre-Middle Devonian in age, as identical granite clasts are preserved in sedimentary breccias in the Foula Sandstone Group, overlying the basement.

Figure 3.6 (overleaf): Field photographs of examples of the Foula Basement and Foula Sandstone Group; (a)(b) Southerly dipping well foliated and fractured basement cut by granite veins at Stremness, rucksack and notebook for scale [HT 397013 1141160] and *inset* close up of garnetiferous basement. (c) Polyphase brittle deformation and granite emplacement at Nort Veedal [HT 393340 1140383]. (d) Contact of the Ruscar Head Microgranite [HT 396868 1141157] and *inset*, enlargement of the Muntavie Stack [HT 396904 1141244] showing the complex geometry and cross-cutting relationships of the pink granite sheets, sills and dykes. (e) Oblique aerial image showing the gently plunging syncline of the Foula Sandstone Group, courtesy of Canmore, Historic Scotland. (f) Cliffs at Wester Hoevda [HT 393746 1138832] expose the organic rich Blobersburn formation and highly fractured sandstones of the Sneug and Soberlie formations, photo courtesy of Jim Henderson. (g) Soft sediment deformation and fluid escape structures and (h) syneresis cracks in the Da Ness formation, compass for scale. *Inset* of granitic pebble. (i) Cross bedded sandstones in the Daal Formation with occasional pebbles, hammer for scale [HT 395047 1137999]. Pebbly bands are widespread throughout the Foula Sandstone Group and found within thick cross bedded and trough cross bedded sandstone units, and commonly form pebbly channel lags. *Inset* Granitic pebble within a coarse-grained sandstone in the Daal formation, hand for scale. (j) Well developed symmetric ripples in the Sneug Sandstone at Da Doon Banks [HT 397153 1136918], notebook for scale.

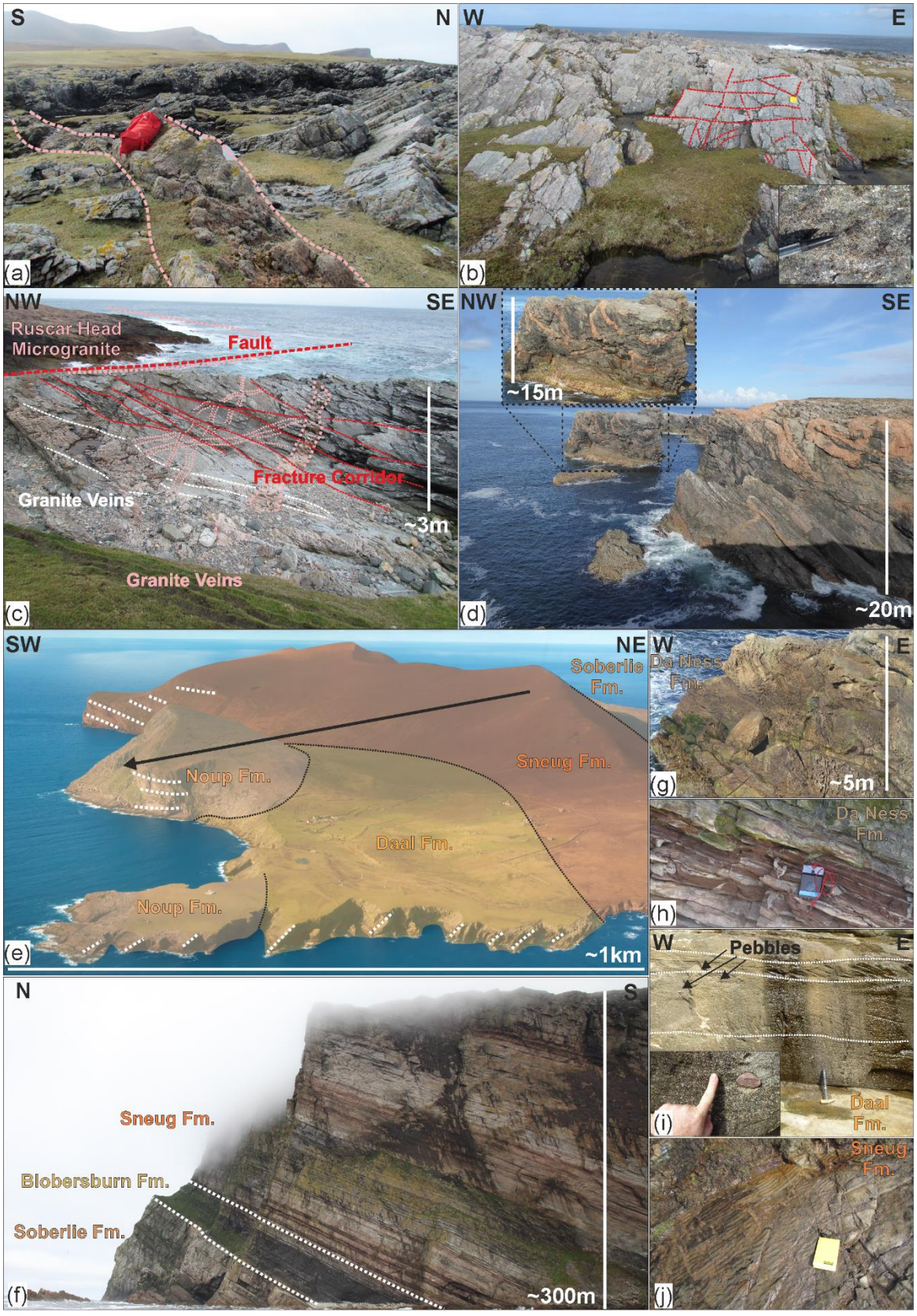
S
N
(a)
W
E
(b)
NW
SE
Ruscar Head Microgranite
Fault
Fracture Corridor
Granite Veins
~3m
Granite Veins
(c)
NW
SE
~15m
~20m
(d)
SW
NE
Soberlie Fm.
Sneug Fm.
Noup Fm.
Daal Fm.
Noup Fm.
~1km
(e)
W
E
Da Ness Fm.
~5m
(g)
Da Ness Fm.
(h)
W
Pebbles
E
(i)
Daal Fm.
Sneug Fm.
(j)
N
S
Sneug Fm.
Blobersburn Fm.
Soberlie Fm.
~300m
(f)

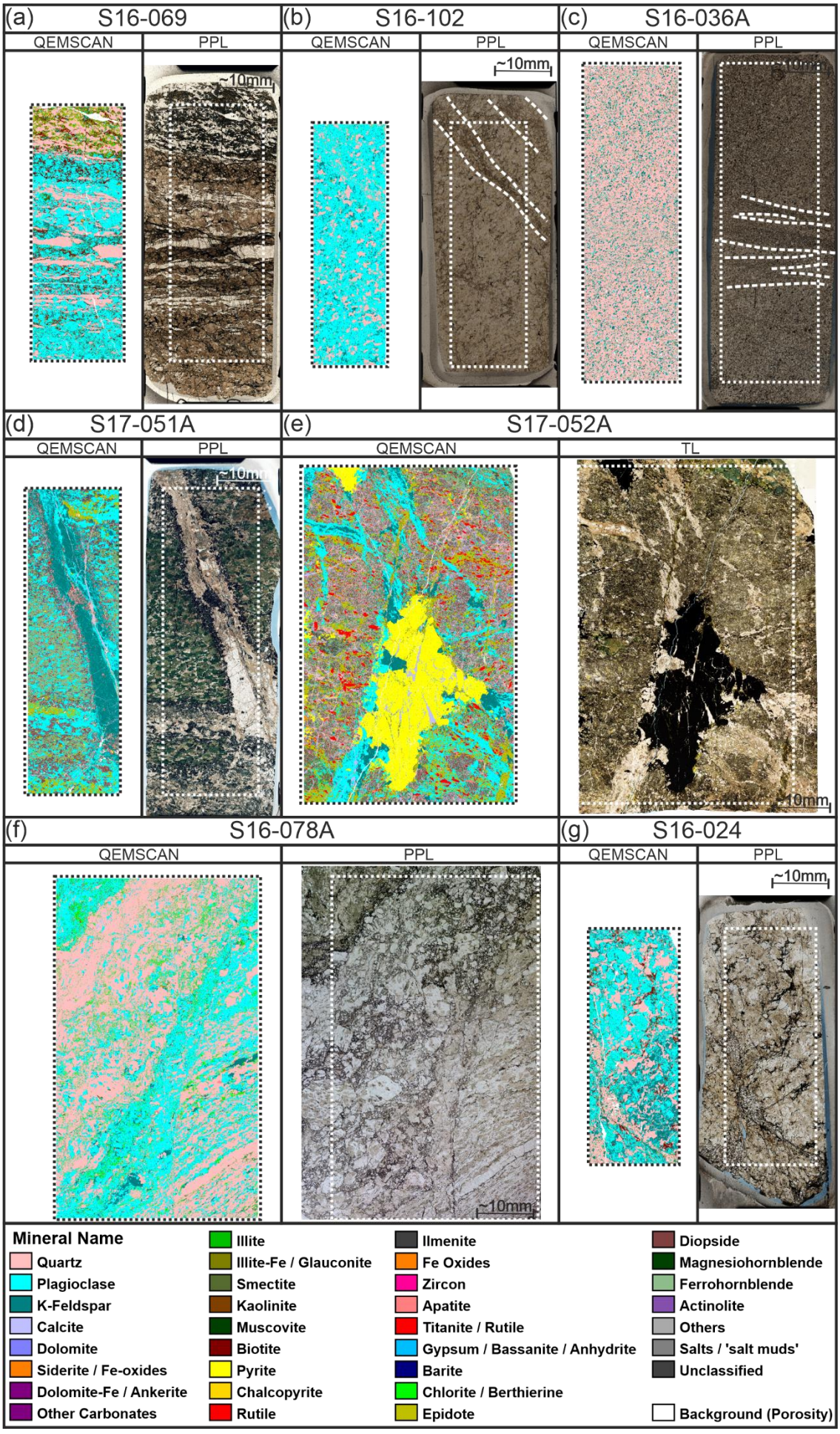
(a) S16-069
QEMSCAN
PPL
~10mm
(b) S16-102
QEMSCAN
PPL
~10mm
(c) S16-036A
QEMSCAN
PPL
(d) S17-051A
QEMSCAN
PPL
(e) S17-052A
QEMSCAN
TL
10mm
(f) S16-078A
QEMSCAN
PPL
~10mm
(g) S16-024
QEMSCAN
PPL
~10mm
Mineral Name
Quartz
Plagioclase
K-Feldspar
Calcite
Dolomite
Siderite / Fe-oxides
Dolomite-Fe / Ankerite
Other Carbonates
Illite
Illite-Fe / Glauconite
Smectite
Kaolinite
Muscovite
Biotite
Pyrite
Chalcopyrite
Rutile
Ilmenite
Fe Oxides
Zircon
Apatite
Titanite / Rutile
Gypsum / Bassanite / Anhydrite
Barite
Chlorite / Berthierine
Epidote
Diopside
Magnesiohornblende
Ferrohornblende
Actinolite
Others
Salts / 'salt muds'
Unclassified
Background (Porosity)

Figure 3.7: QEMSCAN and thin section images of key samples and fault rocks from Foula (a) Sample S16-069 Foliated Basement from Ham Little [HT 397802, 1138556]. (b) Sample S16-102 - Granodiorite with fine grained breccia from Ruscar Head [HT 397334, 1140664], (c) Sample S16-036A - Deformation bands in sandstone of the Daal formation from Da Dog Geo [HT 396468 1136618]. (d) Sample S17-051B - Fault rock from basement fault zone at Da Head o Da Taing [HT 397802 1139275] showing feldspar mineralisation. (e) Sample S17-052A - Fault rock from basement fault zone at Da Head o Da Taing [HT 397802 1139275] showing pyrite mineralisation. (f) Sample S16-078A - Fault breccia from the Foula fault at Wurrwick [HT 396749 1140994] and (g) Sample S16-024 - Sedimentary breccia from Shoabul [HT 397390 1138110] showing clasts of granitic basement within a matrix of well cemented sand.

3.3.3 Foula Sandstone Group:

The Foula Sandstone Group (Figure 3.6e) is subdivided into six formations, comprising three major subarkosic sandstone units, separated by more mixed, shale-dominated units (Blackbourn and Marshall, 1985) (Figure 3.6f). The stratigraphic succession is approximately 1.6 km thick and comprises alluvial, fluvial and lacustrine sedimentary rocks. The subdivision, description and interpretation of the depositional environments of the Foula Sandstone Group follows and builds upon that of Blackbourn and Marshall, (1985).

3.3.3.1 Da Ness Formation:

The Da Ness Formation is 165 m thick and subdivided into three members with a 3-5m localised basal breccia which is best exposed on the coast at Shoabill (Figure 3.5) [HT 397390 1138110] and rests unconformably on an irregular basement surface. Overlying the basal breccia is the Sheepie Member which is exposed in an inaccessible cliff section. It is approximately 50 m thick and comprises massive yellow sandstones with rare, thin (cm to dm), finer-grained beds. Above this, the Brough Member comprises c. 15m of grey mudstones and sandstones.

In contrast to the remainder of the sedimentary rocks on Foula, the Da Ness Formation is both calcareous and mica rich. Sand bodies are up to 3m thick and are composed fine- to medium-grained sand with cross-lamination, and planar and trough cross-bedding. Scoured hollows up to 1m deep and 6m wide are draped by sandstones and mudstones, and the thick sandstones are enclosed in a sequence of grey, green, and red siltstones and laminated fine- to very-fine grained sandstones. Soft-sediment deformation is common with concentric laminated slump balls and convolute bedding (Figure 3.6g) and sand-filled

desiccation cracks are well developed in the mudstones (Figure 3.6h). The depositional environment of the Da Ness Formation is predominantly fluvial, with sandstones being deposited in sandy rivers, with finer-grained material being deposited as fluvial overbank and floodplain deposits (Blackbourn and Marshall, 1985). The compositional immaturity, particularly within the micaceous sandstones of the Brough Member, suggests a local source of sediment, with a generally eastward paleocurrent direction. The presence of abundant planar bedding in addition to large well-developed dunes suggest high flow rates and a well-developed flow regime.

3.3.3.2 Soberlie Formation:

In the N of Foula, the Soberlie Formation forms a 400m thick uniform succession of buff to yellow, medium- to fine-grained sandstones with occasional scattered pebbles. The pebbles are up to 7cm in size, but most are 1-2cm, well-rounded, and are quartz, quartzite, pink granite, and granite gneiss in composition (Figure 3.6i). There is a consistent south-eastward paleocurrent direction and the dominant sedimentary structures are trough cross- and convolute-bedding. Towards the top of the sequence, tabular beds up to 15-20cm thick, with pebbly lags, are more common. In the SE and centre of Foula, the Formation is poorly exposed and thinner, at approximately 35m. Here, it comprises fine- to coarse-grained sandstones with rare pebbles and intraclasts of siltstone and mudstone. Rare cross-bedding foresets indicate a general southwest-directed palaeocurrent. The depositional environment of the Soberlie Formation is similar to that of the underlying Da Ness Formation but is distinguished by the presence of thicker sandstones and by less frequent and thinner floodplain and fluvial overbank facies.

The marked southward thinning of the Formation could occur for several reasons: 1) deposition on a steep slope, such as an alluvial fan, 2) asymmetric basin subsidence and syn-sedimentary faulting, or 3) subsequent uplift and erosion. The lack of evidence of erosion, and the lack of significant thinning in the overlying Blobersburn Formation, seems to preclude the first and third hypotheses. Thus, deposition and accumulation in a developing basin is the most likely option, with the main river systems flowing down the axis of the developing basin. This is supported by the presence of soft-sediment deformation structures, indicating rapid deposition and/or burial.

3.3.3.3 Blobersburn Formation:

The Blobersburn Formation is an approximately 85m thick lacustrine unit that is easily distinguished from the underlying Soberlie sandstone due to its distinctive darker colouration and fragility making it more susceptible to erosion, forming a prominent break in slope and a small gully, known locally as the Blobersburn. In the cliffs on the W of the island (Figure 3.6f) it is well-exposed but inaccessible, while it is accessible yet poorly exposed in the stream bed at Blobersburn [HT 395540 1140636]. Here it is composed of interbedded, fine-grained sandstones, dark-grey micaceous siltstones and thin calcareous siltstones. It provides a key marker horizon due to its relatively uniform thickness and lack of lithological variation. Blackbourn & Marshall (1985) highlighted similarities with facies reported in the lacustrine successions of southeast Shetland (Allen, 1982, 1979; P.A. Allen, 1981; Allen and Marshall, 1981) with three main facies identified on Foula.

The first facies comprise fine-grained sandstones with horizontal bedding, low-angle planar cross bedding, ripple cross-lamination and convolute bedding with slump and load structures. These are interpreted as being shoreline sands subject to wave action, with recumbent slump folds, indicating some downslope movement. The second facies comprise ripple cross-laminated and horizontally laminated siltstones with rare plant remains, some convolute lamination and syneresis cracks. Irregular, indistinct and questionable crawling trails and shallow parallel grooves can be found. These facies may have been deposited in a lake floor which was subject to continuous wave action forming continuous sheets, with partially submerged vegetation being dragged across the sediment surface. Water depth is estimated to have been between 3-10m. The third facies comprise fine-grained calcareous siltstones and ankeritic siltstones. They lack sedimentary structures and are therefore thought to represent the most distal offshore lacustrine deposits. TOC values are generally below 0.5%, but they represent the most organic-rich unit on the island and the only unit to contain amorphous organic matter within the kerogens (Marshall et al., 1985). The presence of this form of organic material, derived from algal matter, indicates that anoxic conditions prevailed for a time, but they did not become established for long periods as in the fish-bearing units of Caithness and Shetland (Marshall et al., 1985). A single probable *Asmussia (Estheria)*, a small freshwater brachiopod which is common in the Middle Devonian of the Orcadian Basin in Caithness and Orkney, has been discovered in the Blobersburn Formation on Foula (Donovan et al., 1978).

The Blobersburn Formation is interpreted as a shallow freshwater lake (Blackbourn and Marshall, 1985) that occupied the whole Foula area. It is believed to have had a variable water depth, potentially and probably no greater than 10m. Well-developed sedimentary cyclicity, as seen in Caithness (Andrews et al., 2016), is not obvious, but on the whole it is remarkably similar in character to other lacustrine units in the Orcadian Basin such as the Achnarras Horizon in Caithness and Orkney, and the Melby Formation and Exnaboe Fish beds in Shetland.

3.3.3.4 Sneug Formation:

The Sneug Formation has a maximum thickness of c. 650m and forms the greater part of the cliffs in the W of the island. It comprises red- to buff-coloured, pebbly, fine- to coarse-grained sandstones which thin considerably from 650m in the W to 220m in the E. This thinning, much like that seen in the Soberlie Formation, can be attributed to deposition into a developing half graben. Sedimentary structures present include a variety of cross bedding, with trough cross bedding being dominant (sets averaging ~ 50cm) and symmetric ripples (Figure 3.6j) with a predominant south-southwest directed paleocurrent. Floodplain and fluvial overbank deposits are preserved as thin red mudstone beds, which contain some convolute bedding and sand-filled desiccation cracks. This unit is interpreted as being like the Soberlie Formation, representing an alluvial to fluvial system with axial flow through the basin. There is evidence towards its base of infrequent flooding, leading to more lacustrine condition.

3.3.3.5 Daal Formation:

The Daal Formation is c. 220m thick and is largely composed of medium-grained sandstones with scattered pebbles (Figure 3.6i), and laterally extensive interbeds of buff-yellow dolomitic siltstones and grey-green mudstones. The relative softness of this unit compared to the rocks above and below have led to the formation of a broad valley known as the Daal in the southern part of the island where this unit outcrops. Sedimentary structures include well-defined planar beds, with some less-common trough cross bedding. The interbeds are usually only a few centimetres in thickness, although some reach 0.5m and include horizontal and ripple cross lamination, with some soft-sediment deformation structures. Plant material is also common. This unit is interpreted as representing wide alluvial fans and fluvial channels with fine-grained overbank and crevasse-splay deposits. The lack of

any notable thickness change in this formation, as well as the wider alluvial fan and unconfined fluvial systems, indicate that differential subsidence had stopped or slowed and that sedimentary systems were less structurally confined at this stage. However, the coarser grain size indicates that sediment input into the basin remained steady.

3.3.3.6 Noup Formation:

The Noup Formation is the youngest formation outcropping on Foula. It has a maximum thickness of 240m, with the top unseen. The lithology and sedimentary structures are like those of the underlying Soberlie and Sneug formations, especially the latter, which together with a dominant southward paleocurrent direction suggests a similar tectonic and sedimentary setting, with fluvial systems being channelled along the basin axis. Some discontinuous overbank silts and muds occur which yield occasional plant remains.

3.3.4 Structural Geology:

The island is cut by a regional-scale N-S to NNW–SSE orientated W dipping normal fault; the Foula Fault, that splays into a series of fault zones which can be observed in the numerous steep sided, narrow geos (gullies) (Hansom, 2007) along the coastline to the south (Figure 3.5). Near Da Sooth Wick [HT 397297 1137958], numerous, closely spaced faults which splay from the Foula Fault have weakened the rocks in this area leading to landslips.

The underlying geology and structure have a strong control on the present-day topography, with the metamorphic basement forming low-lying boggy land in the east of the island, and the Devonian sedimentary rocks forming cliffs up to 376m high in the W. Landslips and subsidence/sinkholes pick out both N-S and E–W orientated faults and fracture zones, such as at Da Sneck o Da Smaalie [HT 395044 1138286]. Here, a relatively recent landslip on a seaward-dipping bedding plane has opened a chasm, almost down to sea level. Recent glaciation and landslips have also thought to have taken advantage of these pre-existing weakness, to generate geomorphological features such as the corries at Ouvrandal, Flect and Netherfandal (Figure 3.5a) (Finlay et al., 1926; Flinn, 1977; Mykura, 1976; Mykura et al., 1976b).

3.3.4.1 Structures in Basement Rocks:

The basement on Foula is strongly foliated and records multiple phases of brittle and ductile deformation. The gneissic to schistose foliation in the basement is subtly folded into a large-scale open fold, dipping approximately to the W through to the SW (Figure 3.8a and 3.8i). Mineral lineation (quartz and feldspar rodding) within the basement plunges predominantly towards the SW (Figure 3.8i). The basement is highly fractured, and is dominated by major N-S orientated, E dipping normal faults and lesser N-S orientated fracture zones and brittle shear zones (Figure 3.5b and 3.5d). In addition to these major structures are three well defined joint/fracture sets which trend (Figure 3.8i); 1) NNE–SSW to NE–SW 2) E–W to ENE–WSW and 3) NNW–SSE to N–S. The dominant North–South trend of these structures in the basement is reflected in the results of lineament analysis from aerial images (Figure 3.5d).

The major normal faults mainly dip between 30° and 40° to the E and have measurable throws of between a few tens of centimetres and several metres. They are associated with epidote alteration (Figure 3.8d), quartz/feldspar (Figure 3.7d and 3.8e) and Fe/Cu sulphide mineralisation (Figure 3.7e and 3.8f) and are significantly iron stained as a result of intense weathering. This alteration/mineralisation is restricted to the foliated basement lithologies, and thus appears to pre-date the emplacement of the Ruscar Head Microgranite and deposition of the Foula Sandstone Group. Some faults have normal to sinistral normal slickenlines preserved and mineralised en-echelon tension-gash arrays with a sinistral sense of shear. Some NE–SW conjugate faults exhibit faint slickenlines, with dextral kinematics acting as dextral reidal shears to the major N–S faults.

N–S orientated vertical to sub-vertical fracture zones form discrete corridors of deformation, and are largely barren of mineralisation, with some exhibiting dextral kinematics and rare slickenlines. However, many also show fracturing consistent with an opposite sinistral sense of shear (Figure 3.8g). In addition, subordinates sets of NE–SW and E-W fractures are present. Abundant fractures perpendicular to the granite contact with the host lithology, likely represent cooling joints. Fractures and faults within the granite are largely barren of mineralisation, although a small proportion are associated with a faint green fault breccia and gouge, the colour being attributed to diffuse chlorite and kaolinite alteration due to breakdown of the feldspar and mica within the granite (Figure 3.7b).

Rare, low angle detachments and thrusts are exposed on the coastline, and are orientated approximately N–S to NNW–SSE and E–W to ENE–WSW, with top to the N dextral shear fabrics(Figure 3.8h and 3.8i)). The low angle faults are, in places, close to horizontal, but in general, are sub parallel to the dipping foliation. These low angle structures are generally localised to more mica rich areas, particularly in the schists, which may act as a preferential slip horizon. The age of these structures is uncertain, but the presence of thin veins of granite, some of which have been folded, with hinges plunging to the S–SSW suggest that these structures are either younger than the granites, or are much older and have been reactivated.

Figure 3.8 (overleaf): Representative images of key basement structures; (a) oblique aerial image of Northeast Foula, showing subtle folding of the foliation and major fault, courtesy of Canmore, Historic Scotland. (b) Aerial image showing major North/South fracture corridors, courtesy of the Ordnance Survey. (c) Major mineralised and highly altered normal faults within the basement at Da Head o Da Taing, rucksack for scale [HT 397802 1139275]. (d) Detailed image of tensile fractures mineralised with quartz, feldspar and pyrite [HT 3978061139277]. (e) Vuggy cavity adjacent to altered fault zone partially infilled with quartz and feldspar. (f) Mineralised fracture infilled with pyrite. (g) Fracture corridor within the Ruscar Head Granite [HT 397331 1140687]. (h) Low angle thrust fault/ dextral shear zone with folded granite veins, showing top to the North sense of shear [HT 397326 1140366]. (i) Stereonets of basement foliation and lineation, major faults and slickenlines and systematic fracture sets. Plotted as contoured poles to planes with best fit great circle.

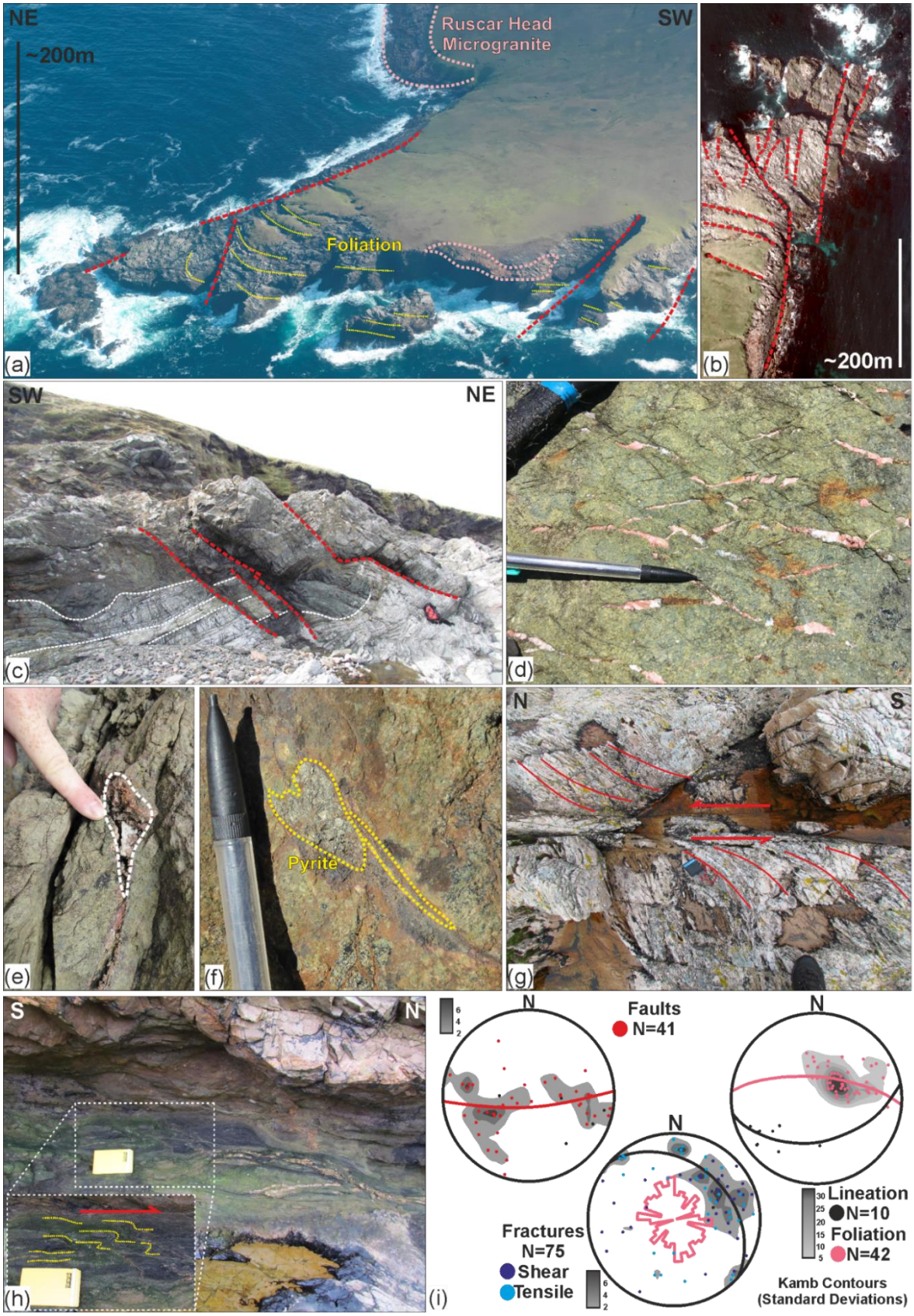

3.3.4.2 Basement/Cover Relationships:

The Foula Fault is exposed on the coastline at the N end of the island, in Rotten Geo, as a W dipping normal fault and associated fault zone (Figure 3.9a and 3.9i). Foliated basement

with abundant granite sheets in the footwall are juxtaposed against interbedded sandstones and siltstones of the Da Ness Formation, with approximately 100m throw (Figure 3.9b)(Blackbourn and Marshall, 1985). On the principal slip surface, a thin (few mm thick) layer of bluey/grey clay-rich fault gouge is developed and beneath this is 20-30cm of mullioned, chaotic microbreccia (Figure 3.7f) that has been folded and dragged into the fault with S to SSW plunging fold hinges (Figure 3.9c). In the hangingwall, the Da Ness formation is folded and cut by sub-parallel conjugate curviplanar faults and fracture corridors (Figure 3.9d). Some shale rich units are also folded into tight chevron folds (Figure 3.9f). Further to the W are several shallow, sub-horizontal, approximately bedding parallel faults which likely acted as slip zones to accommodate differential displacement between units and subordinate fracture corridors and faults (Figure 3.9g). The beta axes of the folded bedding, foliation and curviplanar faults are also all sub parallel to one another (Figure 3.9h).

To the S at Shoabill, a 3-5m zone of sheared basal conglomerate is in contact with an SW dipping undulating, erosional basement unconformity surface, above which the bedding of the Da Ness formation is sub-parallel (Figure 3.10a, 3.10b and 3.10h). This sedimentary breccia infills an irregular unconformity surface (Figure 3.10c). In the zone of shearing, the long axis of the clasts are orientated parallel to the SW dipping fabric, and exhibit well-developed asymmetric boudinage with a sinistral sense of shear (Figure 3.10e). The clasts comprise basement material set in a matrix of coarse to medium grained sand (Figure 3.7g). Minor syn-sedimentary NE dipping normal faults can be seen cutting through this zone, and can be traced into the basement units below (Figure 3.10d and 3.10f), which indicate top to the SW/SSW extension coeval with slip along this unconformity surface. Open, brittle fractures of unknown age can be observed in the basement, particularly within more granitic and pegmatite rich material which trend NW–SW and N–S.

Small-scale mm- to cm-scale sediment-filled fractures are present and are particularly prevalent within more brittle or crystalline units, such as the Ruscar Head microgranite. These fractures are filled with fine- to medium-grained sand- and clay-rich silt. These sediment-filled fractures, at or close to the unconformity surface, indicate the presence of open fractures at or near to the surface during the Devonian.

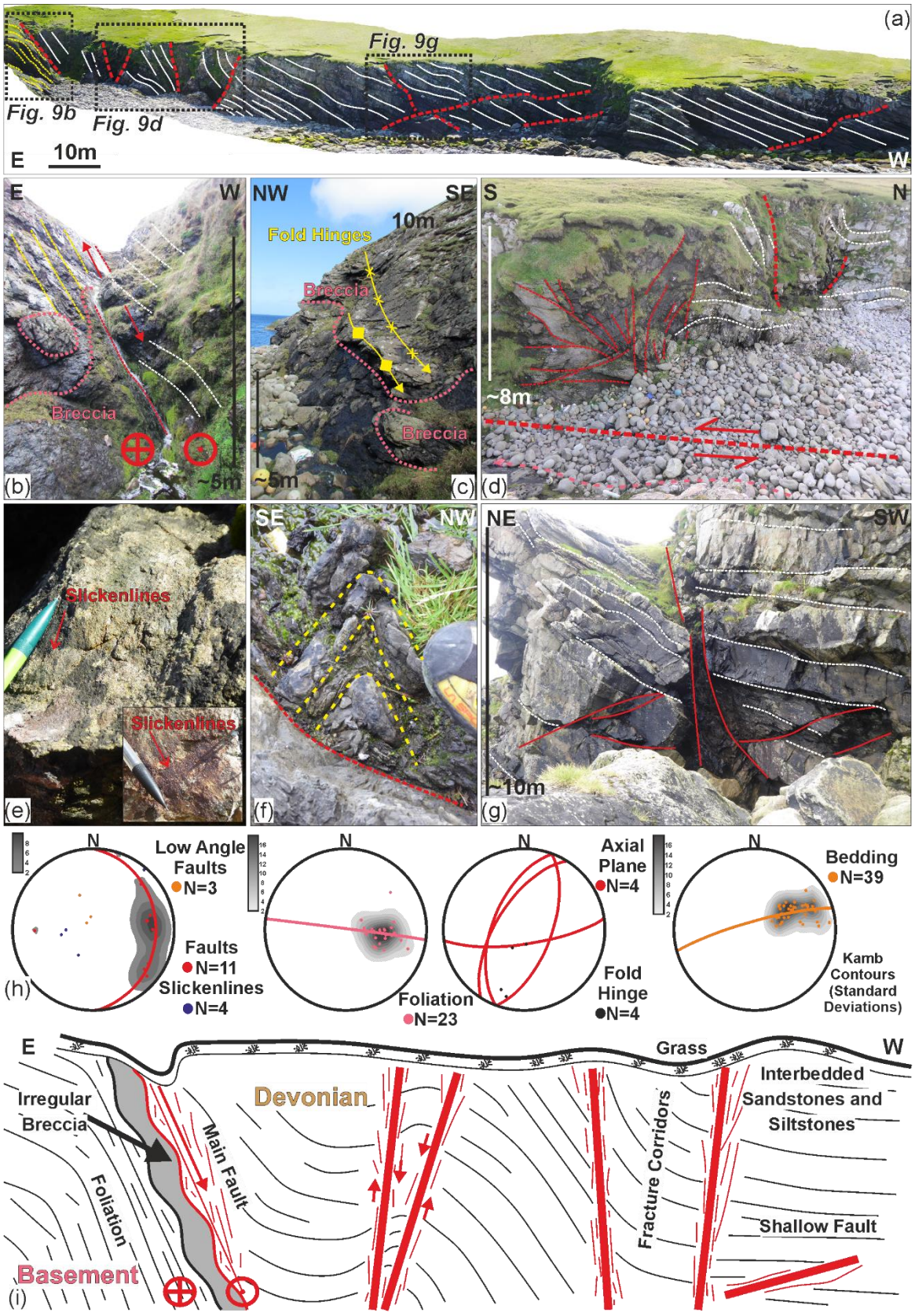
(a)
Fig. 9g
Fig. 9b
Fig. 9d
E
10m
W
E
W
Breccia
~5m
(b)
NW
SE
10m
Fold Hinges
Breccia
Breccia
~5m
(c)
S
N
~8m
(d)
Slickenlines
Slickenlines
(e)
SE
NW
(f)
NE
SW
~10m
(g)
N
Low Angle Faults
N=3
Faults
N=11
Slickenlines
N=4
(h)
N
Foliation
N=23
N
Axial Plane
N=4
Fold Hinge
N=4
N
Bedding
N=39
Kamb Contours (Standard Deviations)
E
Grass
W
Irregular Breccia
Foliation
Main Fault
Devonian
Basement
(i)
Fracture Corridors
Interbedded Sandstones and Siltstones
Shallow Fault

Figure 3.9 (preceding page): Images showing the basement/cover relationships at Wurrwick [HT 396749 1140994]; (a) Annotated Virtual Outcrop Model of cliffs at Da Wast Banks o Wurrwick. (b) Principal slip surface of the Foula Fault. (c) Plunging folds in the footwall fault breccia. (d) Folding and fracturing in the hangingwall. (e) Close up of hangingwall fault breccia showing sinistral oblique slickenlines. (f) Minor small-scale folding within siltstones/mudstones in the hangingwall. Folds plunge steeply towards the Southwest. (g) Fault zone in the hangingwall showing complex geometries and interaction of steeply dipping faults/fracture corridors and shallow bed parallel faults. (h) Stereonets of major faults, foliation, fold axial planes and hinges and bedding. Plotted as contoured poles to planes and best fit great circle. (i) Schematic diagram of the fault zone at Wurrwick.

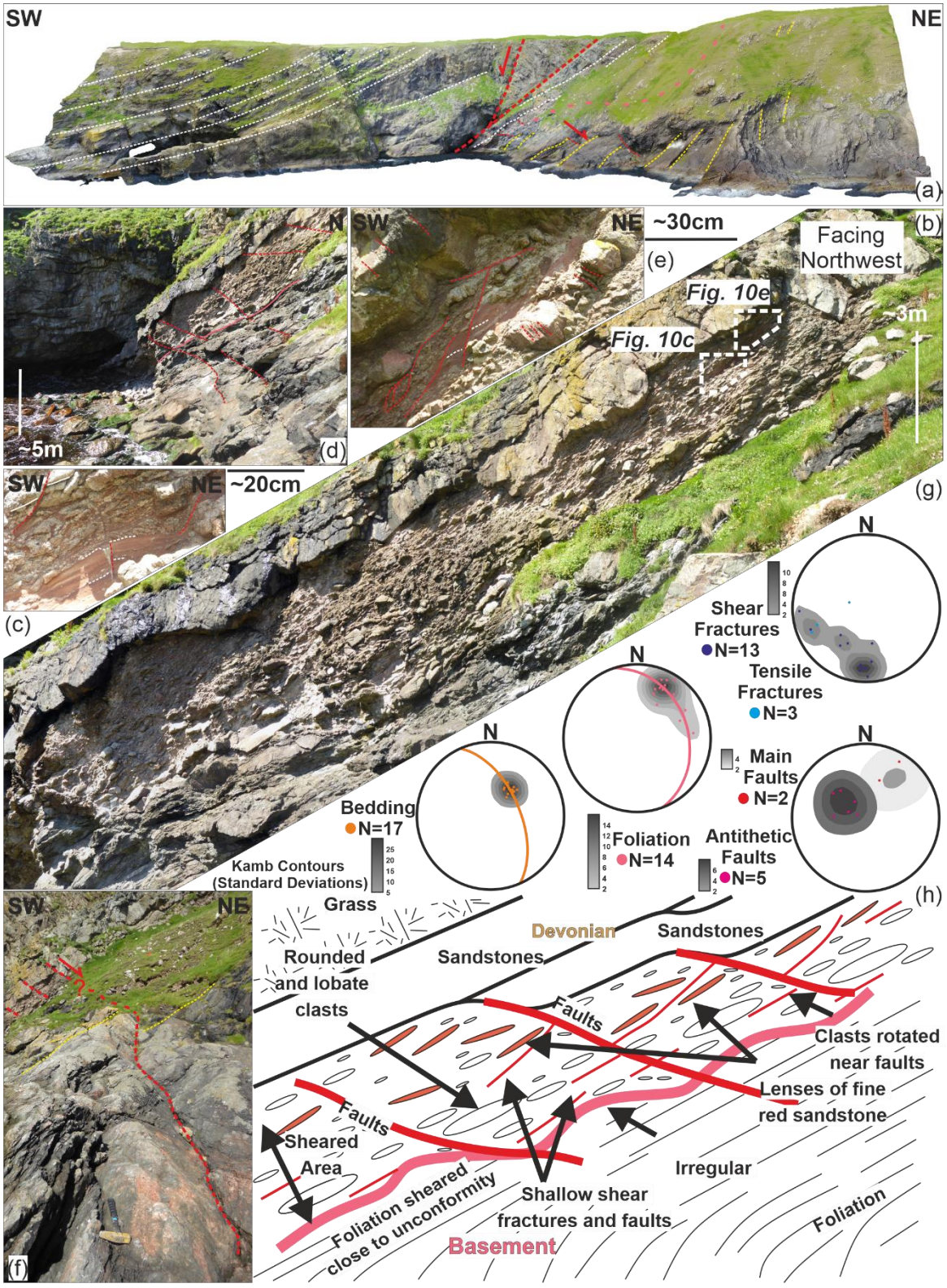

Figure 3.10: Images showing basement/cover Relationships at Shoabill [HT 397390 1138110]; (a) Interpreted orthorectified image of a Virtual Outcrop Model of the cliffs at Shoabul. (b) Panoramic image of sheared basal breccia. (c) Detailed image of sheared breccia showing lenses of finer grained red matrix being cut by small synsedimentary faults displaying several cm offsets. (d) Synsedimentary faults cut through breccia and can be seen to pass into the basement. (e) Detailed image showing boudinage and shearing of basal breccia and fracturing of clasts. (f) Several small

faults can be seen within the basement showing tens of cm's of displacement which can be traced upwards into the overlying Foula Sandstone Group. Hammer and red rucksack for scale. (g) Stereonets of bedding, foliation, and faults. Plotted as contoured poles to planes and best fit great circle. (h) Schematic diagram of the fault zone at Shoabill.

3.3.4.3 Structures in Devonian Rocks:

3.3.4.3.1 Faulting and Fracturing:

The earliest structures in the Devonian strata are NE/SW to N/S orientated deformation bands (granulation seams) and fractures (Figure 3.7c, 3.11a, and 3.11j) with rare quartz cement fills. These structures increase in number with proximity to major faults and are the likely pre-cursor structures to the major N/S orientated normal to sinistral oblique normal faults, which cut these structures and which also increase in number with proximity to the major basement bounding fault to the E of the island.

The most dominant structures are N/S orientated normal faults (Figure 3.11j), such as the Foula Fault which, as in the basement, are eroded to form distinct 'geos' (Hansom, 2007) (Figure 3.11b). In the footwalls of these faults, there is minor brecciation and the development of small (<5mm) vuggy fractures. Unlike in the basement, these major N/S faults do not contain mineralisation and form 'clean breaks', which preserve rare sinistral oblique to sinistral strike-slip slickenlines and dextral oblique slickenlines on antithetic Reidel shears. Sub-vertical, en-echelon N/S and E/W discrete fracture corridors (Figure 3.11c and 3.11d) with limited normal offsets are common and decrease in frequency away from the Foula Fault. Fracture corridors are particularly well developed in both thicker and coarser grained units showing a clear relationship to the mechanical properties of the host lithology. These left stepping en-echelon arrays in cross section resemble negative flower structures.

In a small quarry near to Hamnabrek, a ~15m wide fault zone is exposed which juxtaposes the sandstones and siltstones of the Soberlie Formation against the sandstones of the Da Ness Formation (Figure 3.11e). It is comprised of a series of steeply W dipping N/S orientated faults and antithetic E dipping shear fractures with abundant tensile fractures, sigmoidal tension gashes with a sinistral sense of shear and small open tensile fractures with some rare quartz fills (Figure 3.11f). Shale-rich units close to faults have a well-developed cleavage and their brittle deformation has contributed to the development of

1-2cm thick clay rich fault gouge in the main fault. In the hangingwall, a crackle/crush breccia is developed with clasts of ~0.5mm (Figure 3.11e). The main fault is stained red by leaching of iron rich groundwater flowing down the fault from the overlying Quaternary peat and acid rich soil horizons, indicating that these faults and fracture zones are likely highly permeable at the present day.

Away from larger faults, the Devonian sequences are heavily fractured and have an overall polymodal fracture pattern with a dominant N/S trend (Figure 3.11j) with distributed small normal to strike-slip offsets (Figure 3.11h) with mutually cross cutting and abutting relationships (Figure 3.11i). Many of the smaller faults have a 'piano-key' style of offset, with faults tipping out over short distances. The fractures are broadly open, although with small apertures (<2mm) with no fracture fills or mineralisation. Some faults preserve minor quantities of fine angular fault breccia <2mm thick which is partially cemented with quartz and rare dextral slickenlines are preserved on some N/S faults.

Figure 3.11 (overleaf): Representative field images of key Devonian structures; (a) Deformation bands. (b) Major normal fault in Da Dog Geo [HT 396407 1136427]. (c) Cross sectional view through a fracture corridor at Da Klettgeo [HT 395957 1141452]. (d) Plan view of fracture corridor showing en echelon arrangement of fractures at Da South Ness [HT 396499 1136199]. (e) Exposure of the major North/South fault that bisects the island in small quarry near Hamnabrek , *inset* stereonet of plane of major fault and poles to planes of cleavage and shear fractures (f) Open tension gashes developed in the hangingwall of the major fault in the quarry near Hamnabrek, *inset* stereonet of tensile fractures. (g) Minor folding at Da Est Hoevdi [HT 395188 1141176] forming a natural sea arch. These minor folds have variable hinges that plunge gently towards the South or Southwest. (h) Normal offset distributed over numerous fractures and minor faults. Fracturing also picks out a clear mechanical stratigraphy with through going faults in thicker coarse-grained units, and smaller fractures in more fissile and layered units. (i) Complex fracturing in Da Stacks o Da Logat [HT 395436 1141366] and (j) Stereonets of Devonian deformation bands, faults, and fractures. Plotted as contoured poles to planes and best fit great circle.

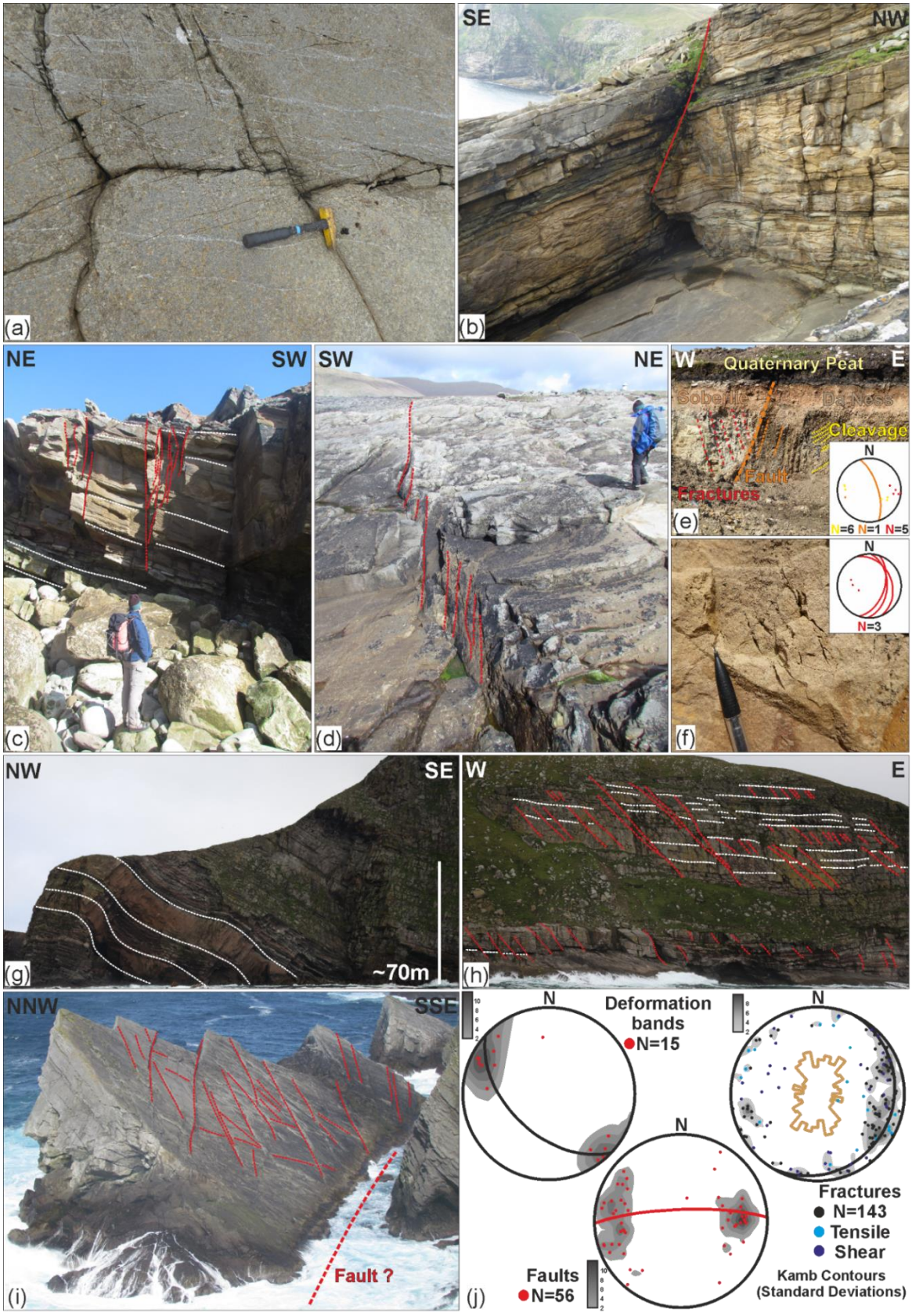

3.3.4.3.2 Folding:

The entire Devonian sequence on the island of Foula is folded into a broad open syncline that gently plunges ~20° to the SSW (Figure 3.12b). Field data (Figure 3.12b-i) was

supplemented with data derived from virtual outcrop models (Figure 3.12b-ii) and remote sensing in order to collect data from the western limb of the fold due to the inaccessible nature of outcrops in the of the island (Figure 3.12a). Analysis of the basement foliation shows that it is also folded in a similar manner and hence it was incorporated into the analysis (Figure 3.12c-iii). This modification of the basement foliation may account for the relatively shallow dip of some of the normal faults (30-40°) in the basement which have been tilted towards the W from a potentially more upright position(~60°).

A down-plunge projection of the Foula syncline reveals an opening upward syncline with interlimb angles increasing upwards from 129° to 168° (Figure 3.12c). Major thickness changes are apparent within the Soberlie and Sneug sandstones, consistent with the mapped thickness changes in these units over the Foula Fault. Smaller-scale, more localised folding (Figure 3.11g) is observed which also have S to SSW orientated fold hinges, as well as later, minor and much smaller-scale fault-related drag folds. The Foula syncline is therefore likely to be the above sea-level equivalent of dipping reflectors that are visible to the SW of the island on 2D seismic (Figure 3.4c).

Figure 3.12 (overleaf): (a) Virtual Outcrop Model of Da Kame, Foula. Model built in Agisoft Photoscan from archive helicopter-based imagery (*inset*) courtesy of BP. Model analysed in the Virtual Reality Geological Studio (VRGS) courtesy of David Hodgetts, University of Manchester. *Inset* Stereonet of data shown on the model with mean pole and plane of the digitised data and examples of the oblique aerial images the model was built from. Remotely sensed data from Virtual Outcrop Models was used to supplement the data collected in the field and enhance structural analysis. (b) Stereonets showing contoured poles to planes of (i) Bedding collected in the field (ii) Field data and remotely sensed data (iii) Bedding data and foliation. (c) Down plunge projection with interlimb angles for Foula Sandstone Group formation tops. Note the subtle changes in hinge location and the opening upwards geometry as indicated by the increasing interlimb angle up stratigraphy. Horizontal scale = vertical scale.

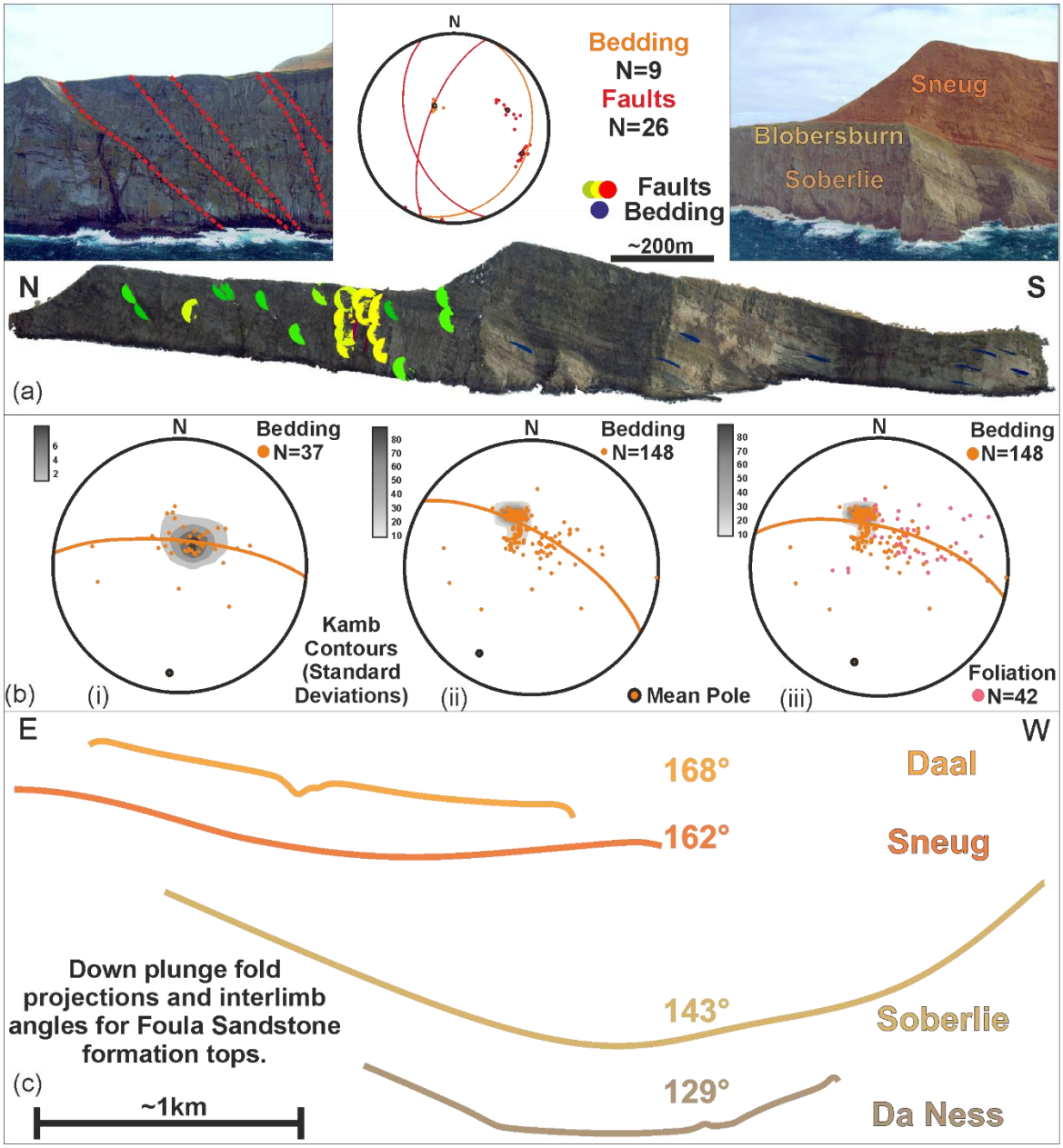

3.4 Geological evolution of the Foula Sandstone Group:

3.4.1 Basin initiation and evolution:

Figure 3.13 is a schematic basin development model for the Foula Sandstone Group, which illustrates a suggested scheme of interaction between differing depositional systems and changes in paleocurrent, in response to changes in tectonics and possible climatic changes driving changes in lake level in the Orcadian Basin.

It is suggested that the basin may have initiated as a half graben, with sediments being shed off from regional highs to the N and W and from more localised features, such as the Foula Ridge (Figure 3.14a) to the NE. With progressive subsidence and periods of active faulting, the basin began to fill. During Orcadian Lake high stands, a broad alluvial plain was flooded,

forming units such as the Blobersburn Formation and other more minor lacustrine intervals within the Foula Sandstone Group. Widespread soft-sediment deformation structures and water-escape structures in the lower units of the Foula Sandstone Group are indicative of high sedimentation rates, rapid burial (Leeder, 1987) and the expulsion of high-pressure pore fluids. These structures, in conjunction with major thickness changes across the Foula Fault, indicate an active tectonic environment in which rapid burial and deposition could induce such behaviour.

Spore colours are mid- to dark-brown with a vitrinite reflectance between 1.2% to 1.8% (Hillier and Marshall, 1992), considerably lower than values from the Walls Group, Eastern Shetland and Fair Isle. Values on Foula are closer to those obtained from, Melby, Orkney and Caithness (Hillier and Marshall, 1992; Marshall et al., 1985), although they are higher than at Melby, which has VR values of 0.8-1.0% (Hillier and Marshall, 1992), suggesting slightly deeper burial. Thus, the burial history of the Foula succession is more likely to be closer to that of the main Orcadian Basin, as suggested by Astin (1985) and Bird (2014) who both propose rapid burial during the Devonian, reaching a maximum depth during the Carboniferous before exhumation during the Permo-Carboniferous. Permian deposits sub-cropping in the West Fair Isle Basin(BGS, 1988) immediately to the East suggest that Foula may have been partially buried again during the Mesozoic, but these deposits were subsequently eroded in onshore areas.

3.4.2 Paleostress analysis:

Despite the paucity of kinematic indicators from faults on Foula, due to the barren 'clean break' nature of the faults, a total of 10 faults with slickenlines were recorded (Figure 3.14b). Fault-slip slickenline data measurements were collected *in situ* and conventional stress inversion (see chapter 2) was performed). The results of this analysis (Figure 3.14c) show that minimum principal stress (σ_3) was orientated NE/SW (09/240). The shape ratio (ø=0.4) (Figure 3.14d and 3.14e) indicates that local faulting was extension dominated, however regionally the faults are in extension dominated transtension (Figure 3.14f) (approx. half way between wrench and extension dominated transtension). This analysis shows that the faults on Foula were developing under a regional sinistral transtension regime relative to the major basin bounding structures/shear zone. Figure 3.14g is a summary schematic box diagram which shows the development of transtensional growth folds in the Foula Basin during regional NE/SW to ENE/WSW orientated transtension.

These observations and analysis are consistent with a model of regional scale sinistral transtension along the Great Glen-Walls Boundary Fault Zone during the Mid-Devonian, complimenting the analysis done by Donovan *et al.*, (1976); Seranne (1992); Fossen (2010); Dichiarante *et al.*, (2016); Dichiarante (2017) and models of partitioned transtension (De Paola et al., 2005).

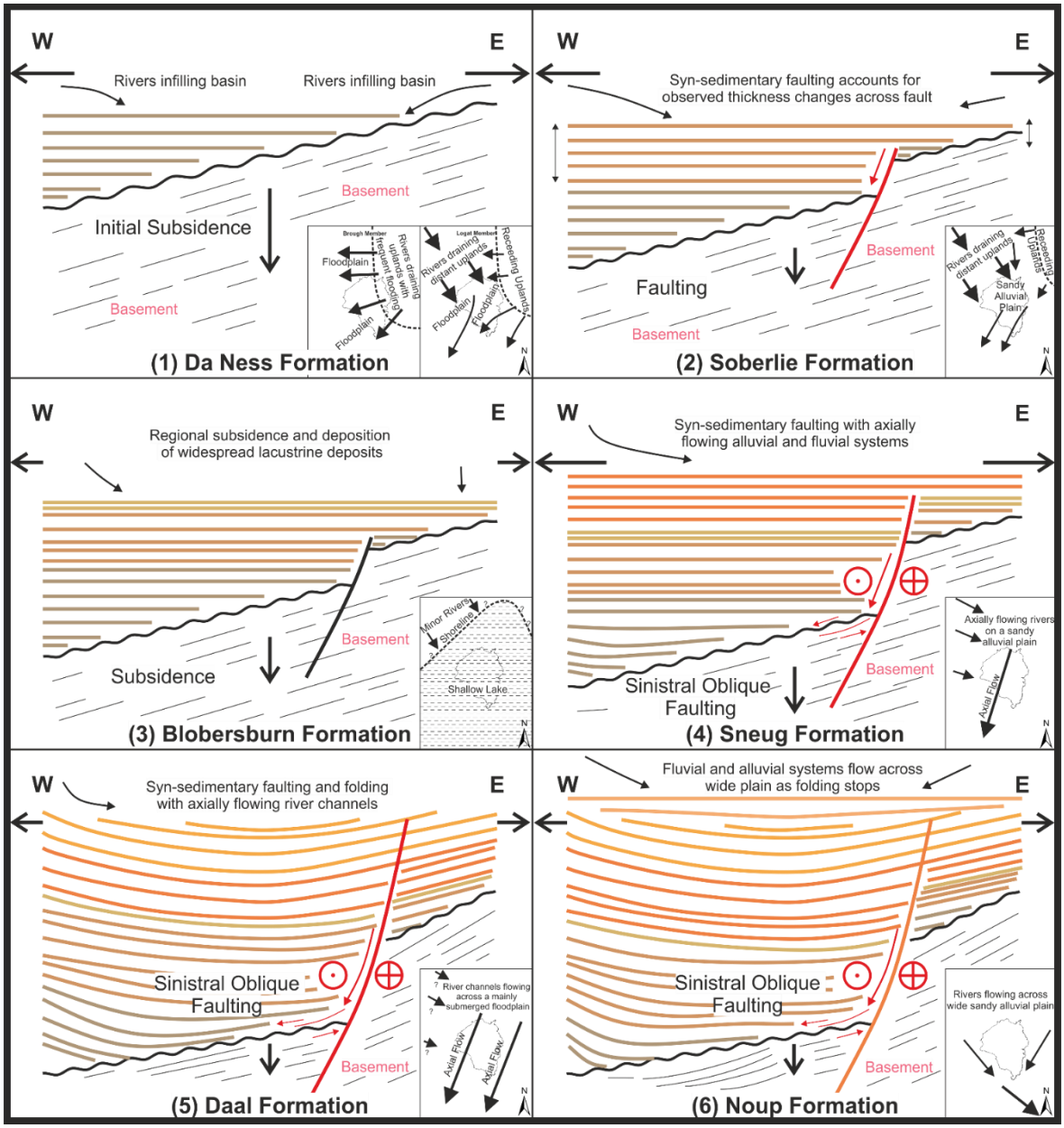

Figure 3.13: Integrated Basin Development Model for island of Foula with *inset* maps of paleocurrent split by formation, modified *after* (Blackbourn and Marshall, 1985).

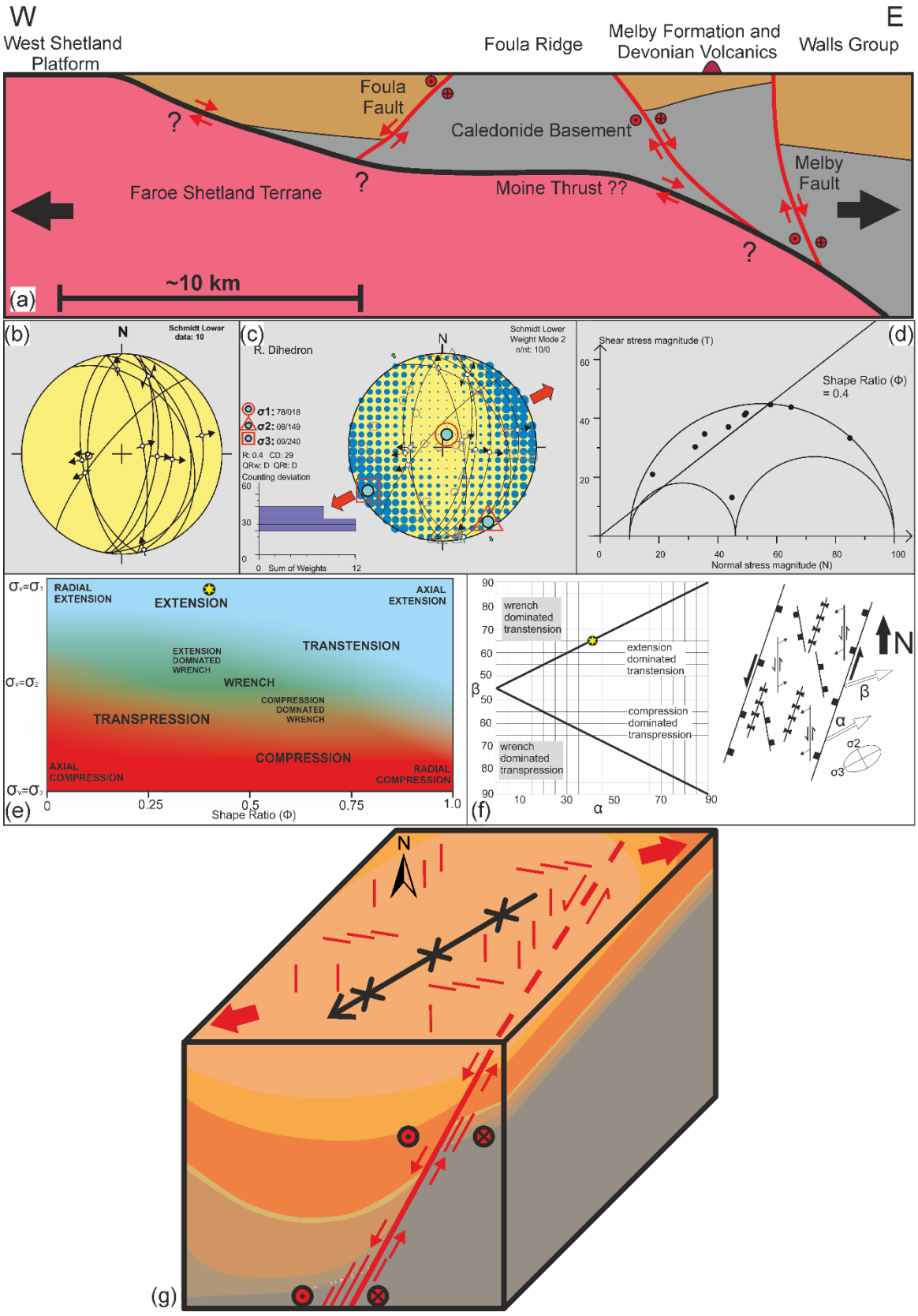

Figure 3.14: (a) Schematic Structural Section through Foula during the Devonian. Horizontal scale = vertical scale. (b) Lower hemisphere equal angle stereonet plot of analysed faults and slickenlines with fault kinematics. (c) r-dihedron stress inversion. (d) Mohr circle diagram (e) Stress regime diagram. (f) α vs. β diagram and plan view of structural style and geometries of associated structures

for the proposed tectonic setting. β and α are the angle between the boundary fault and infinitesimal maximum extension axis and the transport direction, respectively. (g) 3D box diagram for the structural evolution of Foula.

3.4.3 The age, provenance and detrital zircon geochronology of the Foula Sandstone Group:

Despite a lack of conclusive fossil evidence, the Foula Sandstone Group has long been considered to be of Old Red Sandstone (Devonian) age (Mykura et al., 1976b). Palynological samples collected from throughout the sequence (Donovan et al., 1978; Fletcher, 1977; Lundmark et al., 2011) suggest a Middle Devonian, late Eifelian to early Givetian age. The Blobersburn Formation has therefore been correlated with the Achanarras Horizon, and the Sandwick (Figure 3.2). It is also time-equivalent with the lacustrine facies of the basal Clair Group (Figure 3.2). The Foula Sandstone Group is also deemed to be equivalent to the Melby Sandstone (the Melby Fish Beds) and Eshaness Volcanics, which are exposed in the footwall of the Melby Fault on the Walls Peninsula, on the islands of Papa Stour and the Eshaness Peninsula (Mykura, 1976; Mykura et al., 1976b).

Palaeocurrents in the Foula Sandstone Group (Figure. 3.13) show a progressive change through time, with material initially being shed from paleo highs to the immediate North and East, and evolving to more potentially more distally derived material being transported from the NW as the basin began to fill. As these fluvial systems developed, they passed through the Foula area and towards the centre of the Orcadian Basin.

Heavy mineral analysis and detrital zircon geochronology of sandstones was undertaken, (see Appendix C) in order to discern the provenance of the Foula Sandstone Group and Melby Formation. Variations in the quantity and ratios (Mange and Morton, 2007; Morton, 1991; Morton and Hallsworth, 1994, 1999) of key heavy minerals is known to reflect changes in paleocurrent and source provenance (Figure 3.15a). RuZi (Rutile to Zircon ratio) is generally higher in samples from Melby than those on Foula, although there are variations that likely reflect subtle differences in provenance between the two areas. GZi (Garnet to Zircon ratio) is highly variable within samples from Foula and may reflect diagenesis due to garnet dissolution (Morton et al., 2002). A higher GZi ratio is apparent in samples from Melby and may indicate a shallower burial. This is supported by lower vitrinite reflectance values intially reported by Hillier and Marshall (1992) for the Melby

Formation (0.8-1.0) and Foula (1.0-1.8). The higher proportion of garnet in the Melby Formation and in the Soberlie Formation may also reflect proximity to basement rocks. Sample S16-040 has a low ATi (Apatite to Tourmaline ratio), due to modern weathering at outcrop as indicated by the low number of grains and etching of the apatite grains. Figure 3.15b is a plot of heavy mineral data from the Orcadian and Clair Basins which shows that samples from Foula overlap with those from Clair and the Orcadian Basin of Caithness and Orkney. This suggests that the sandstones in the Foula Sandstone and Lower Clair Group were sourced from similar geographic/geological areas (Figure 3.15b).

Samples were sent for U-Pb LA-ICPMS detrital zircon geochronology at the University of Hull, to determine the age and provenance of sediment source regions to enable comparison against published data on the provenance of the Clair Group and other Devonian sequences of the Orcadian Basin. LA-ICPMS detrital zircon age dating was carried out on 5 samples from the westernmost Devonian basins in Shetland, four from Foula and one from Melby. Results are displayed as KDE (Kernel Density Estimation) and MDS (Multi-Dimensional Scaling) plots. A total of 476 grains were considered reliable, with zircon ages falling in the range of 366.1± 3.7 Ma and 3483± 6.7 Ma, with zircons with ± 10% discordance being discarded.

The distribution of zircons in the Foula Sandstone Group and Melby formation reflect a diversity of sediment sources with zircon ages falling into three main groups: Phanerozoic, Proterozoic and Archaean (Figure 3.16a). Within these groups, discrete sub-populations can be identified. Neoproterozoic zircons are distinct from a cluster of Meso-Paleoproterozoic zircons from which a series of major tectonic events (Schmidt et al., 2012; Strachan et al., 2013; Jahn et al., 2017; Lancaster et al., 2017; Kinny et al., 2019 and references therein) potentially be identified which may include the formation of the Lewisian Complex (2.7-3.0 Ga), Inverian and Badcallian metamorphism (2.4-2.5 Ga), emplacement of the Scourie Dykes (2.4-2.0 Ga), Laxfordian deformation (1.7Ga), the Grenvillian orogeny (1.3-0.95 Ga), and other tectonic events and/or orogenic plutonism which may associated with the Valhalla orogen along the margins of Rodinia (ca. 1.0Ga, 0.95-0.87 Ga, 0.8-0.7 Ga) (Cawood et al., 2010). Within the Phanerozoic, the youngest Devonian age zircons are distinct from Silurian to Ordovician zircons that are likely associated with the series of tectonic events that occurred during the Caledonian orogeny (Dewey and Strachan, 2003).

This diversity of zircons reflect derivation from a mixed source, in a similar manner to the Clair Group with Archaean zircons, likely derived from the Faroe Shetland Terrane (Holdsworth et al., 2019), Proterozoic zircons from Moinian- and Dalradian- like basement from within the Caledonides of Scotland and Shetland (Strachan et al., 2013; Jahn et al., 2017; Lancaster et al., 2017; Kinny et al., 2019 and references therein) or perhaps as far away as Eastern Greenland (Sasnowski, 2015; A. S. Schmidt et al., 2012), in addition to some younger Paleozoic zircons likely derived from more local metamorphic basement and Caledonian igneous rocks (Lancaster et al., 2017 and references therein). These broad similarities in the distribution of zircons suggests that Foula not only has a similar provenance to the Clair Group, but also to the Upper Devonian sequences of Caithness and Orkney (Figures 3.16c and 3.16d) and represents the broadly geographic and sedimentological midpoint between the more proximal Clair Basin, and the more distal, Shetland part of the Orcadian Basin.

An average of three youngest zircons which overlap in age at 2σ, give a maximum depositional age (Dickinson and Gehrels, 2009) for the Foula Sandstone Group of ~386 Ma seemingly confirming a Middle Devonian Givetian age comparable to previous suggestions. In the Melby Formation, the youngest detrital zircon yields a Middle Devonian Givetian to Upper Devonian Frasnian age of 382.2±7.7 Ma, a result similar to dates yielded from palynological analysis (Donovan et al., 1978).

However, in the Sneug Sandstone, the youngest detrital zircon yields an Upper Devonian Fammenian age of 366.1±3.7 Ma, despite being one of the lower stratigraphic units, and immediately overlying the palynological constrained, Middle Devvonian Blobersburn Formation. This may suggest that the Foula Sandstone Group spans a longer period of time that has been previously thought, possibly expanding the age range from the Middle to the Upper Devonian. However, owing to the limited number of grains, this should not be taken as conclusive.

Close similarities in the distribution of zircons from the Sneug Sandstone and Melby Formation (Figure 3.16b), together with both formations yielding the youngest zircons, suggest a period of tectonic, sedimentological and/or volcanological rejuvenation when the two areas were better connected, perhaps as one basin. This is supported by the presence of the regionally correlated horizons of the Blobersburn Formation, and Melby Fish beds, which they overlie respectively (Figure 3.2).

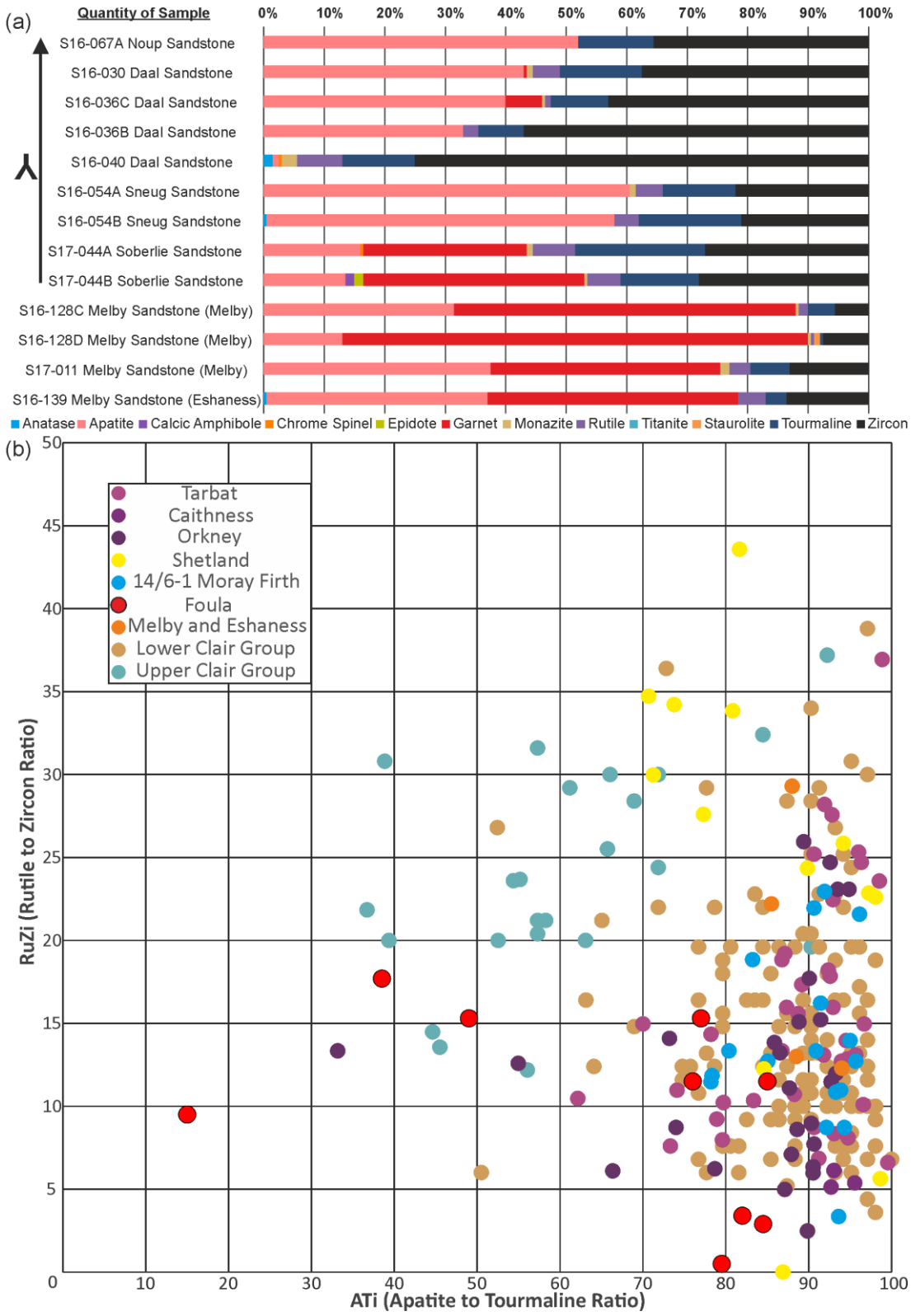

Figure 3.15: (a) Heavy Mineral Data for Foula Sandstone Group and Melby Formation. Samples from basal part of Foula Sandstone Group and Melby show greater similarities in provenance and a greater contribution of locally derived basement grains e.g. garnet. (b) Compilation of data from the Orcadian Basin for the key heavy mineral indices of RuZi (rutile to zircon ratio) and ATi (apatite to tourmaline ratio). Samples from Foula show closer similarities to samples from Clair and Orkney.

Samples from Shetland are distinct from samples from mainland Scotland, Orkney and the Moray Firth. Data compiled from Morton and Milne (2012), Morton(2007) and Sasnowski (2015).

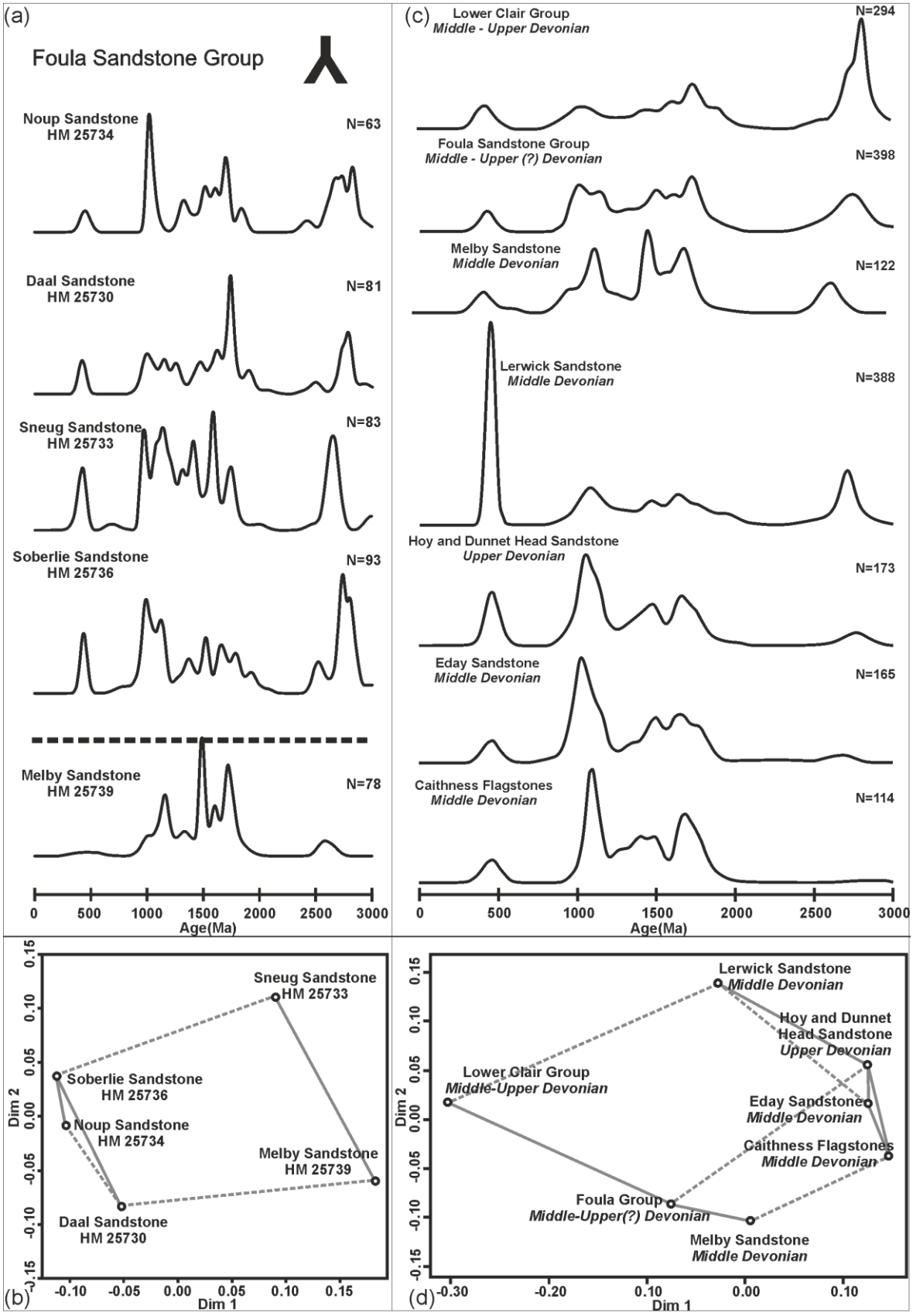

Figure 3.16 (preceding page): (a) KDE plots of analysed samples sent for detrital zircon geochronology. N equals concordant data between -10% and 10% discordance of all data. (b) MDS plot of samples showing degree of similarity between analysed samples. Solid and dashed lines link the two most similar samples and next most similar samples, respectively. Comparison of KDE plots (c) and MDS plot (d) for Foula Sandstone Group against existing published detrital zircon data for the Lower Clair Group, Middle and Upper Devonian of Caithness and Orkney, Middle Devonian Melby Formation, and Middle Devonian Lerwick Sandstone of Eastern Shetland (Modified *after* Sasnowski, 2015; Schmidt et al., 2012). Data grouped by area and age. N equals the number of concordant data between -10% and 10% discordance of all data. Note the close similarity in zircon distributions between the Lower Clair Group and the Foula Sandstone Group.

3.5 Discussion:

3.5.1 Regional tectonics and paleogeography:

The pre-Devonian geological history is poorly constrained on Foula, with the basement preserving both brittle and ductile deformation up to amphibolite facies metamorphic grade, and the emplacement of granites. On Orkney, similar basement rocks crop out on Graemsay, near Stromness and at Yesnaby in a roughly N/S trend (Strachan, 2003). These metasedimentary gneisses are dated to between 900-1300Ma, and are intruded by granites emplaced ca. 431-430 Ma (Bjerga, 2017). These rocks are overlain by extrusive volcanics, dated to 390 Ma and intercalated with conglomerates and sandstones which helps to constrain the approximate age of basin formation in Orkney to the Middle Devonian. Despite the lack of volcanics on Foula, a variety of extrusive rocks and intercalated sedimentary rocks are exposed on the nearby island of Papa Stour, at Melby to the Northeast and on the Eshaness Peninsula in a manner similar to those on Orkney. Analysis of spores from these successions yields an Eifelian to Givetian age, close to the inferred age of the Achanarras horizon, Melby Fish Beds and Blobersburn Formation on Foula.

The metamorphic basement exposed on Foula and Orkney may represent parts of poorly exposed metamorphic core complexes that have been rapidly exhumed from great depths from within the Caledonian orogenic belt, like in the Hornelen Basin and associated basement in Western Norway (Krabbendam and Dewey, 1998; Osmundsen and Andersen, 2001; Séguret et al., 1989; Seranne et al., 1991; Seranne and Seguret, 1987; Templeton, 2015). The emplacement of granitic material may have also played a role in the subsequent

structural development, due to the buoyancy of hot material, preventing further burial. The Foula Fault may also represent a complete de-coupling of the basement and overlying Devonian sedimentary rocks, as evident by the intense deformation observed at Shaobull which would help to accommodate differential burial between the more buoyant and rigid basement blocks and the sedimentary basins adjacent to them.

The Foula Sandstone Group records a dynamic and active depositional environment that was responding to both tectonic and climatic changes. Similarly dynamic sequences, with active basin margin faulting, diverse basement/cover relationships, as well as folding are reported across the region, in the Walls Basin (Astin, 1982; Melvin, 1985; Seranne, 1992), in Eastern Shetland (Allen, 1981) near Yesnaby and Stromness in Orkney (Astin, 1985; Hippler, 1989), and around the margins of the Inner Moray Firth (Clarke and Parnell, 1999; Dec, 1992)(Chapter 4). Along the North Coast of Caithness and Sutherland, similar sequences are also exposed, at Kirtomy, Strathy, Red Point, Balligill, Portskerra, Dirlot and on the Roan Islands (Blackbourn, 1981a, 1981b; Donovan, 1975, 1973). Similar growth structures and possible transtensional folds are also potentially present offshore, on the East Shetland platform (Patruno et al., 2018). Like on Foula, alluvial deposits are piled up against synsedimentary faults, which are intercalated with fluvial, aeolian and lacustrine deposits, in a series of small sub-basins along the margins of the Orcadian Basin. These represent the derivation of sediment from upland source areas to the W and NW being transported into the Orcadian Basin. Astin (1985) interprets the Eday Sandstone Group on Orkney as representing a fluvial system that was feeding the Orcadian lake from this W margin. Comparison of heavy mineral and detrital zircon data from Foula and Melby to published data from the Clair Field (Morton, 2007; Schmidt et al., 2012; Morton and Milne, 2012) and studies from the Orcadian Basin (Sasnowski, 2015) indicate that the sequences on Foula and at Melby are more similar to those in Caithness and Orkney (Figure 3.16c and 3.16d). It seems reasonable to suggest that they were located on the North to Eastern margin of the Orcadian Basin, separate from the Walls and East Shetland Basins that were somewhat further N, and that they were located somewhere intermediate between the Clair Basin and centre of the Orcadian Basin in Caithness and Orkney.

Thus, we propose that the Foula Sandstone Group is coeval with the Eday Group/Upper Stromness Flagstones/Hoy Sandstone/Dunnet Head Sandstone and represents a similar fluvial/alluvial system on the margins of the Orcadian basin. We also suggest that it may

have been part of a system that was feeding an intra montane lake further to the S and E from upland areas in the N and W, and is the along-strike equivalent of similar deposits in Caithness and Sutherland. We also propose that Foula is of closer affinity to both the basement and cover sequences exposed onshore in Caithness and Orkney, and may have a similar sequence of exhumation as proposed by Bjerga (2017) for Orkney.

The opening upward geometry of the Foula Syncline, the growth strata thickening in some parts of the Foula Sandstone Group, paleostress analysis, in addition to the presence of numerous strike-slip faults and fracture corridors, orientated sub-parallel and perpendicular to the hinge of the Foula Syncline, are consistent with syndepositional folding related to sinistral transtension (Fossen et al., 2013) during the Devonian and the development of the Orcadian Basin. This is contrary to early models of Devonian basin development attributed to extensional collapse (Coward, 1993, 1990; Coward et al., 1989; Enfield and Coward, 1987; Friend, 1981; Friend et al., 2000; McClay et al., 1986; Norton et al., 1987). Figure 3.17 is a paleogeographic map of the Orcadian Basin, which integrates these observations together with data from other provenance and paleogeographic studies. This possible configuration of the Orcadian Basin places the island of Foula and the Clair Basin in closer proximity to Orkney and mainland Scotland, as suggested by the provenance data.

An affinity between the Devonian of Foula and that of Orkney and Caithness suggest that it may have a similar burial history to that of the West Orkney Basin (Bird, 2014) and Orkney (Astin, 1985) on the basis of vitrinite-reflectance data. Foula is situated close to the W margin of the West Fair Isle Basin, which is filled with both Devonian and Permian sediments. However, the Foula area was not subject to any later rifting during the Mesozoic, perhaps owing to its location on the relatively stable Shetland-Orkney Platform. This suggests that Foula underwent rapid burial during the Devonian and early Carboniferous before uplift during the latter part of the Carboniferous and into the Permian and may have acted as an uplifted footwall block during the Permian development of the West Fair Isle Basin. Devonian and Permian outcrop is also thought to have been more extensive across the Scottish Highlands (Flinn, 1977; Thomson et al., 1999; Wilkinson, 2017), with several kilometres of sediment having been eroded since burial and following uplift since the Cretaceous.

Thus, Foula may represent the basal section of a much thicker Devonian sequence that once covered more of Shetland, but subsequent erosion and uplift, or buoyancy the Orkney-Shetland Platform, has led to a greater proportion of the metamorphic basement being exposed.

3.5.2 Implications for ORS Basin Development:

The Devonian structures of Foula are equivalent to the Group 1 structures as described by Dichiarante (2017), Dichiarante et al., (2016) and Monaghan et al., 2016). These earliest Devonian age structures are poorly exposed in the Caithness/Orkney region, and as a result, are poorly understood and under-represented in the early works attempting to understand the development of the Devonian basins of NE Scotland. The folding on Foula is indicative of the low amplitude, long wavelength fold structures that are common throughout the offshore Devonian sequences as imaged in seismic that have long been attributed to Carboniferous inversion or possibly later Permian reactivation.

Yet, on Foula, a significant part of the deformation is clearly Devonian in age based on the evidence of growth folding, and is in agreement with observations made by Seranne (1992) from Shetland and in the Devonian basins of Norway (Fossen, 2010; Séguret et al., 1989; Seranne and Seguret, 1987). Thus, not all fold structures in the Orcadian Basin are necessarily solely inversion related, compressional structures. It is also possible that some early transtensional folds may have been reactivated and tightened, forming some of the more substantial fold structures that are mapped in the Orcadian Basin for example the Eday Syncline in Orkney (Mykura et al., 1976a).

The orientation of fold hinges in relation to the bounding faults on Foula are consistent with sinistral transtension and regional NE/SW extension, as reported in Shetland and Norway, assuming that the N/S to NE/SW orientated Walls Boundary-Great Glen Fault Zone is the dominant and controlling regional structure. This is counter to the original theory, attributing the development of the Devonian basins to E/W extension and later inversion, as proposed by earlier workers (Coward et al., 1989; Enfield and Coward, 1987; Friend et al., 2000; McClay et al., 1986; Norton et al., 1987).

Folds generated during oblique extension are not uncommon, and have been shown in laboratory experiments by (Venkat-Ramani and Tikoff, 2002). They show that fold hinges rotate in parallelism with the bulk extension direction. Furthermore, the results of

palaeostress analysis are complimentary to those of Dichiarante (2017), who has proposed that the earliest faults in the Orcadian Basin formed under transtension related to the NE-SW Great Glen Fault, and not extension. Wu *et al.* (2009) have also shown in laboratory experiments that the geometry of strike-slip influenced extensional and pull apart basins are consistent with models of transtension and the formation of the Orcadian basin within a large scale dilational jog located between the More-Trøndelag/Walls Boundary/Great Glen Fault zones and the Harder Fjord/Highland Boundary Fault zones, as is proposed by Fossen (2010).

Figure 3.17 (overleaf): Paleogeographic map of the Orcadian Basin showing major structures, sediment sources and major paleocurrents. Major sinistral transcurrent faults, separate the different Devonian sub-basins, partitioning deformation and the associated structures which are controlling basin development. This reconstruction places Foula and Melby (precise lateral position of three Devonian basin of Shetland along strike of the major strike-slip faults is unknown and is meant to be diagrammatic) in a position between Clair and Orkney, reflecting the new provenance data and integrating them with the observations of Allen and Mange-Rajetzky, (1992); Blackbourn, (1981); Donovan et al., (1976); Duindam and van Hoorn, (1987); Mykura et al., (1976); Schmidt et al., (2012); and Smalley, (2011).

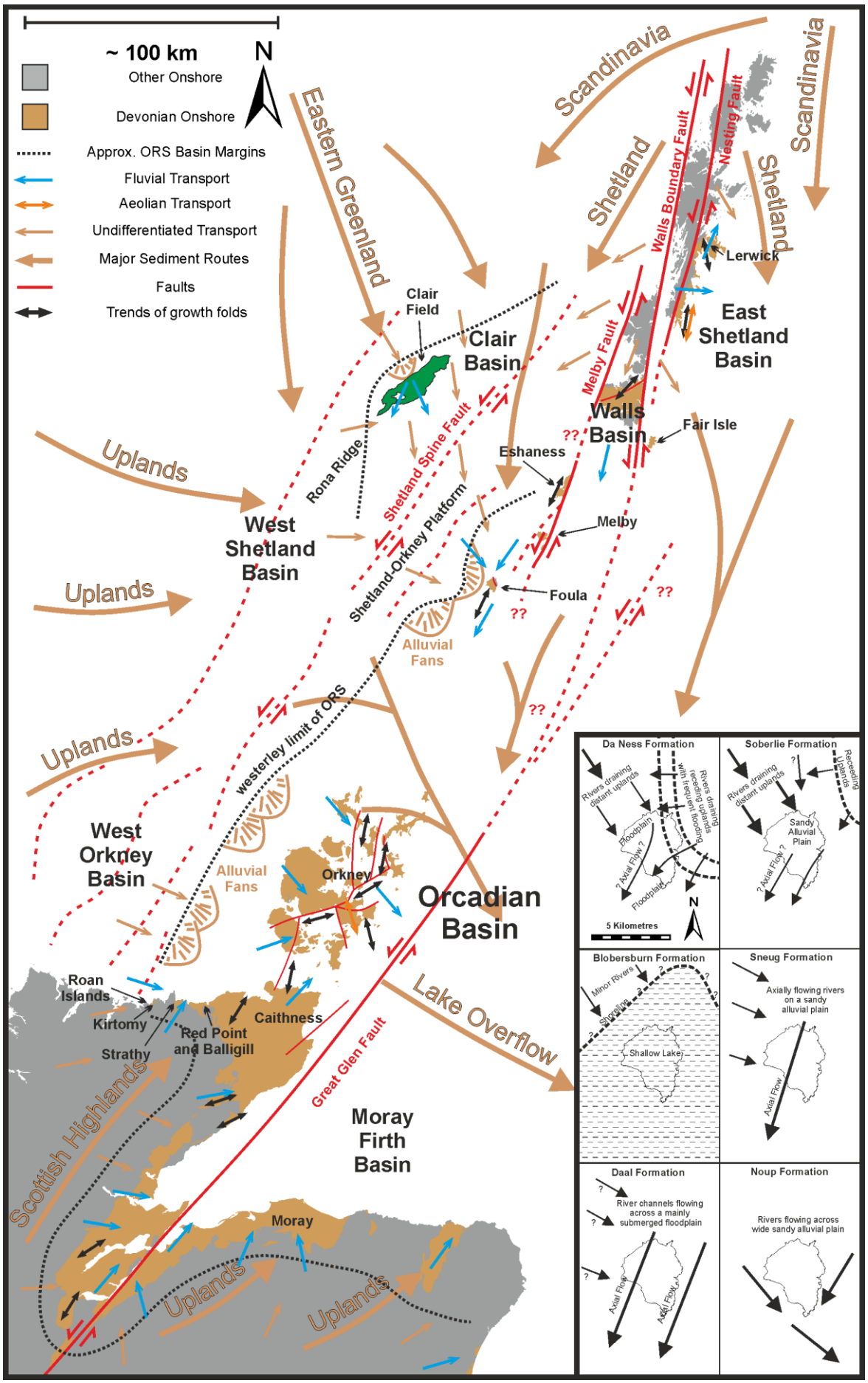
~ 100 km
N
Other Onshore
Devonian Onshore
Approx. ORS Basin Margins
Fluvial Transport
Aeolian Transport
Undifferentiated Transport
Major Sediment Routes
Faults
Trends of growth folds
Scandinavia
Eastern Greenland
Shetland
Walls Boundary Fault
Nesting Fault
Lerwick
East Shetland Basin
Clair Field
Clair Basin
Melby Fault
Walls Basin
Fair Isle
Eshaness
Melby
Foula
Rona Ridge
Shetland Spine Fault
Shetland-Orkney Platform
Uplands
West Shetland Basin
Alluvial Fans
Westerley limit of ORS
West Orkney Basin
Orkney
Orcadian Basin
Lake Overflow
Great Glen Fault
Moray Firth Basin
Roan Islands
Kirtomy
Strathy
Red Point and Balligill
Caithness
Scottish Highlands
Moray
Da Ness Formation
Soberlie Formation
Blobersburn Formation
Sneug Formation
Daal Formation
Noup Formation
5 Kilometres
Rivers draining distant uplands
Floodplain
Axial Flow ?
Rivers draining receding uplands with frequent flooding
Receding Uplands
Sandy Alluvial Plain
Minor Rivers
Shoreline
Shallow Lake
Axially flowing rivers on a sandy alluvial plain
Axial Flow
River channels flowing across a mainly submerged floodplain
Rivers flowing across wide sandy alluvial plain

3.5.3 Implications for the Clair Basin and Clair Oil Field:

The large-scale structural setting of Foula is like that of the Clair Field, with both comprising Devonian sandstones that overlie a NE/SW orientated up-faulted ridge of metamorphic basement. The stratigraphy of Foula bears a stronger similarity to the stratigraphy of the Clair Group than too many parts of the Middle Devonian in Caithness and Orkney, due to the presence of thick sequences of fluvial and alluvial sediments. In Clair, Units I-VI are largely continental fluvial/alluvial facies with unit VI bearing the closest similarity to the lacustrine, Caithness flagstone group of the onshore Orcadian basin. At the base of the Clair Group and onshore, a variety of basement/cover relationships are evident with rapid lateral and vertical facies changes and a variety of structures developed. The physical size of Foula is comparable in scale to the Clair Field itself (Figure 3.1d), so that the magnitude and number of structures observed on Foula may be representative of those at or below seismic resolution. For example, the Foula Fault may be analogous to the major Clair Ridge Fault (Figure 3.5c) which, as on Foula, may exhibit a wide range of deformation styles and juxtaposition relationships, and thus prove troublesome for reservoir modelling.

However, on Foula, the absence of definitive post-Devonian deformation contrasts with the Clair Field, where most of the important structures are Permian or younger (Robertson et al., 2020). This lack of later deformation limits the effectiveness of Foula as a fractured-reservoir analogue. Despite this, the style of deformation and types of structure on Foula are like those reported in the Clair Field, and both have similar structural trends. Deformation styles within the Orcadian basin are also similar to those in Clair (Coney et al., 1993; Ogilvie et al., 2015; Robertson et al., 2020) and therefore a greater understanding of the early structures in the Clair Basin may have important implications for understanding later deformation events. The presence of deformation bands in the Foula Sandstone Group, even close to relatively minor faults and fracture zones, is therefore important to consider owing to their lower permeability, and they may act as significant baffles or barriers to flow. Adjacent to these low-permeability zones are higher-permeability open fractures and faults which, in combination, may act as highly-permeable fluid-flow corridors which could act as ‘thief zones’ even away from the major fault zones, and are likely to be poorly resolved or overlooked in seismic datasets.

3.5.4 Implications for wider resource development:

Folds and trapping geometries which developed early in the Devonian basins, and not during later reactivation and/or inversion, could have important implications for modelling the petroleum systems of the Moray Firth, West Orkney Basin and East Shetland Platform. For example, an early charge of Devonian-sourced oil into a Devonian trap with a Devonian reservoir could have preceded the better-documented Mesozoic oil-charge. Such a scenario has been recorded onshore in Caithness by Baba *et al.* (2018) and parts of Scandinavia (Rønningen, 2015). Offshore (Figure 3.18)., Devonian lacustrine source rocks are known to contribute to the Beatrice , Oseberg, Judy and Embla oil fields (Stevens, 1991) and have been encountered in wells on the Norwegian Continental Shelf.

The significant thickness of highly fractured coarse-grained clastic rocks in the Orcadian Basin, together with an active Devonian source kitchen, may also represent an under-explored petroleum play on the UKCS. This is despite several fields producing from Devonian age reservoirs (Clair, Buchan, Argyll, Stirling, Embla, Ardmore), reasonable reservoir quality sandstones being discovered offshore, and numerous oil shows being reported in relinquishment reports and during drilling operations. Discoveries near to the Clair Field e.g. Freya, Fulla, North Uist, Boulmer, and Eriboll (Oil and Gas Authority, 2019b) remain undeveloped due in part to their small size, but compounded further by their low-API oil. With a greater understanding of fractures and fluid flow in the Clair Group, together with proven deliverability, these smaller peripheral fields may become economically viable as tie-backs to new infrastructure being developed and planned West of Shetland.

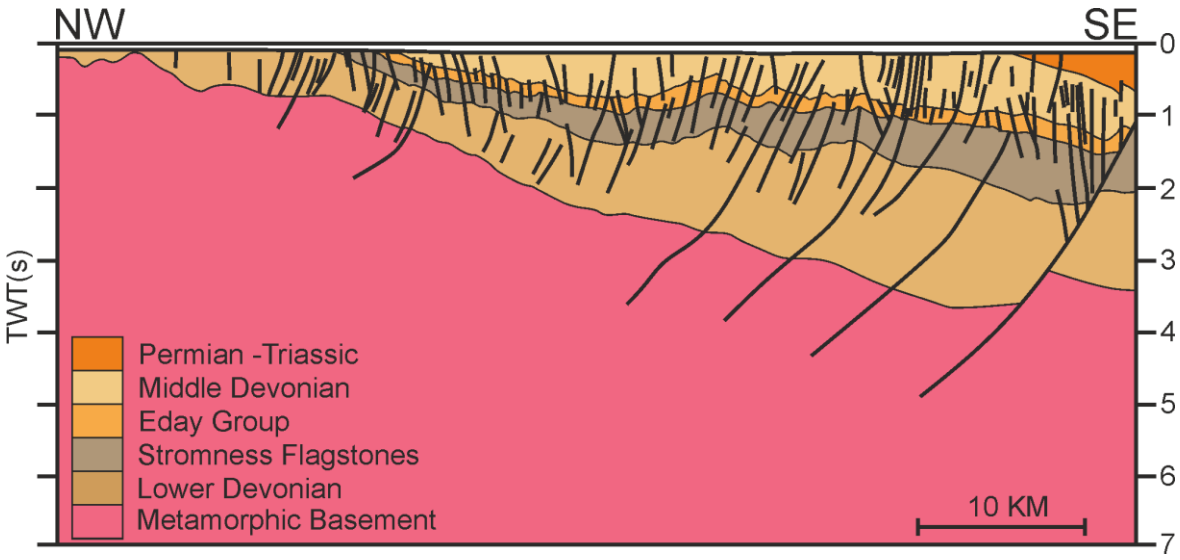

Figure 3.18 (preceding page): Interpretation of seismic line though Orkney Shetland platform. Foula is located approximately 40 km to the North. Survey collected as part of Frontier Licence P1884. Modified *after* Oil and Gas Authority, (2019b).

3.6 Conclusions:

We propose that the Devonian rocks of Foula (and nearby Melby) are geologically more similar to mainland Scotland and Orkney than Shetland. They also show sedimentological characteristics that are intermediate between those of the Clair Basin and the larger Orcadian Basin. They therefore preserve insights into the early structural and stratigraphic evolution of the Devonian basins of Northeast Scotland that are relatively poorly exposed elsewhere onshore, and help to understand the early evolution of the Clair Basin

The basin fill on Foula shows synformal growth folding, which is consistent with constrictional extension during regional sinistral transtensional Devonian basin development, related to the Walls Boundary Fault. These observations are complementary to the findings of Seranne (1992) in Shetland, where the geometry and orientation of structures and basin-fills indicate oblique extension during the opening and development of the Old Red Sandstone basins. They are also similar to structures observed in Orkney/Caithness, the Inner Moray Firth (Clarke and Parnell, 1999), Greenland (Hartz, 2000), the East Shetland Platform (Patruno and Reid, 2017) and the Devonian Basins of Norway (Krabbendam and Dewey, 1998; Séguret et al., 1989; Seranne and Seguret, 1987) where the evidence for transtension and the role of strike-slip faulting is now widely accepted as an alternative to the orthogonal 'extensional collapse hypothesis' as favoured by many early workers and now accepted as an alternative by Dewey and Strachan, (2003), Fossen (2010) and Dewey *et al.,* (2015). These authors instead attribute the development of the ORS basins of Northeast Scotland, Shetland, Western Norway, Eastern Greenland and possibly Svalbard, in part to sinistral oblique transtension following the collision of Laurentia and Baltica. This is supported by the recognition that folding does not necessarily signify crustal shortening, but can also be generated during oblique extension (Fossen et al., 2013). This has been further demonstrated by laboratory experiments (Venkat-Ramani and Tikoff, 2002; Wu et al., 2009) and through numerical modelling (Fossen et al., 1994; Fossen and Tikoff, 1998).

The presence of folds that formed during early basin development, synchronous with basin filling and not due to later reactivation, is also important for the assessment of the UKCS

petroleum systems. Potential hydrocarbon-trapping geometries may have developed much earlier than often thought, during basin formation and in proximity to potential Devonian lacustrine source rocks, which in the Orcadian Basin were mature during the Carboniferous (Astin, 1990, 1985; Hillier and Marshall, 1992; Marshall et al., 1985; Parnell et al., 1998). Such traps may have formed before Permo-Carboniferous basin inversion and exhumation, to which these folds have previously been attributed. Furthermore, these trapping geometries would have remained available for later reactivation and/or charge.

Finally, the possibility that the Clair Basin was also transtensional during its early development must be considered. If correct, is there evidence for growth folding within the Lower Clair Group? Are Palaeozoic source rocks a potentially overlooked element of the petroleum system? With the wealth of legacy data now available, in addition to new and reprocessed seismic data, there may be prospective Devonian basins that have been overlooked, which are now ready for reappraisal and further exploration.

Chapter 4

A reappraisal of Devonian Basin Evolution and Basement Cover Relationships in NE Scotland and Shetland: Analogues for the offshore Clair Oil Field, West of Shetland, UK.

Chapter 4 - A reappraisal of Devonian Basin Evolution and Basement Cover Relationships in NE Scotland and Shetland: Analogues for the offshore Clair Oil Field, West of Shetland, UK.

Thomas A. G. Utley[1], Robert E. Holdsworth[1], Ken J. W. McCaffrey[1], Rob A. Strachan[2], and Edward D. Dempsey[3].[†]

[1]*Department of Earth Sciences, Durham University, Science Labs, Durham, DH1 3LE, UK*

[2]*School of Earth and Environmental Sciences, Burnaby Building, Burnaby Road, University of Portsmouth, PO1 3QL, UK*

[3] *School of Environmental Sciences, University of Hull, Hull, HU6 7RX*

Keywords:

Devonian, ORS, Old Red Sandstone, Orcadian Basin, Basin Development, Clair Field, Clair Basin, Unconformity, West of Shetland, UKCS

Abstract:

The evolution of sedimentary basins can be highly dynamic, but much of the geological detail and variation in them is at the limit of/below the resolution of traditional offshore/subsurface data acquisition methods (e.g seismic, core etc.). The use of suitable surface analogues onshore helps to understand these details and thus reduces uncertainty and subsequently lowers risk.

The Clair Field, west of Shetland, represents one of the largest hydrocarbon resources in the UKCS. It comprises fractured Devonian-Carboniferous sandstones, the Clair Group which overly a fault bounded ridge of fractured Precambrian metamorphic basement. With the continuing development of the field, an improved understanding of the structural and stratigraphic evolution of the Clair Group and its relationship with the basement is now required. We present here a reappraisal of the stratigraphy, structure and tectonic evolution of onshore analogues for the Devonian-Carboniferous Clair Basin that focusses

[†] A version of this chapter is in preparation for submission to the journal Petroleum Geoscience.
Author and co-authors contributions: Thomas A.G. Utley conducted the fieldwork, analysed the data and wrote this chapter under the principal supervision of Robert E. Holdsworth who carried out principal editing, suggested the topic, and added valuable contributions during interpretation of the data/observations and various discussions of the subject matter. Ken J. W. McCaffrey and Edward D. Dempsey assisted with the development of techniques and interpretation/discussion of the data. Rob A. Strachan aided in the field and with the wider discussion of the data/observations.

on a detailed study of basement/cover contacts, and structure of the overlying Devonian sequences. This is achieved through a mixture of desk-based studies, conventional fieldwork, structural analysis, and the production of Virtual Outcrop Models derived from aerial (drone) images.

This synthesis covers a wide region of the Orcadian Basin, extending through Shetland, Orkney and Caithness. It reveals widespread developments of synsedimentary faulting with synformal growth folding throughout the Lower to Middle Devonian and a diverse range of basement/cover relationships in all areas. This diversity along with varied basin geometries and architectures apparent throughout the Orcadian Basin could lead to difficulties in exploration and development in the Devonian basins offshore. This improved understanding should aid in the future appraisal of resources on the UKCS.

4.1. Introduction:

The Clair Oil Field, situated 75km W of the Shetland Isles, is the largest hydrocarbon resource on the UKCS, with a closure of 250 km^2 and an estimated 6-7 Billion BOE in place (Coney et al., 1993; Robertson et al., 2020; Webster, 2018; Witt et al., 2010) (Figure 4.1a). It is comprised of naturally fractured Devonian-Carboniferous sandstones, the Clair Group, that overlie an up-faulted ridge of fractured Precambrian metamorphic basement (Coney *et al.*, 1993; Holdsworth et al. 2019) (Figure 4.1b).

The field was discovered 1977 (Coney et al., 1993; Johnston et al., 1995) and after a lengthy appraisal programme, production finally started in 2005 via a phased development plan, and is estimated to continue until 2050. The 1st phase of development targeted the 'Core, Graben and Horst' areas of the field, producing oil from the Lower Clair Group. However, with the continued development of the field, the 2nd phase of development is targeting the 'ridge' area which will produce oil from a thinner sequence of Clair Group sedimentary rocks which unconformably overlie the fractured, oil bearing metamorphic basement of the Rona Ridge. Therefore, an enhanced understanding of the structure of the Clair Group and its unconformity with the basement is now required in order to produce effectively and efficiently.

The supposedly extensional Orcadian Basin in mainland Scotland has long been used as the classic analogue for the Clair Field. However, alternative Devonian analogues exist in Shetland which are thought to be transtensional (Dewey and Strachan, 2003; Fossen, 2010;

Seranne, 1992). The recognition of transtensional folding in the Devonian basins of Norway has revolutionised our understanding of these basins (Fossen et al., 2017; Séguret et al., 1989; Seranne and Seguret, 1987; Tikoff and Fossen, 1999) and the proximity of similar folded basin fills in the Shetland mainland (Seranne, 1992) with those in Clair suggests that this tectonic setting also needs to be considered as an alternative. Furthermore, due to the location of the Clair Field on the margin of the N Atlantic, an underexplored and frontier region of the UKCS, the structural geometry and Devonian structural and stratigraphic evolution of the Clair Basin is still relatively poorly understood relative to the more well understood and explored parts of the North Sea.

As with any subsurface development much of the geological details are in between the resolution scales of conventional data acquisition methods such as seismic and well information i.e. core and wireline. However, outcrop geology and analogue studies can help to span this data gap. Therefore, this paper aims to reappraise the structure, stratigraphy and tectonic evolution of onshore analogues to the Clair Basin in Shetland, Orkney and NE Scotland (Figure 4.1a) in order to better understand, describe and compare the range of basement/cover relationships that are present throughout the Orcadian Basin and improve our understanding of Devonian basin development more regionally. These observations are set in the context of the ongoing development of the Clair Oil Field and could help to reduce uncertainty, leading to improved business making decisions and safety during development offshore of not only the Clair Field but other assets in areas such as the North Sea with Devonian age reservoirs.

Figure 4.1 (overleaf): (a) Regional map of the Orcadian Basin (study areas outlined in green) with Clair Oil Field highlighted. Modified *after* Dichiarante et al., (2016; and Oil and Gas Authority, (2019). (b) Clair Field cross section. Modified *after* Barr et al., (2007) and Ogilvie et al., (2015). (c) Devonian Paleogeography and simplified reconstruction of the North Atlantic Modified *after* Dewey and Strachan (2003).

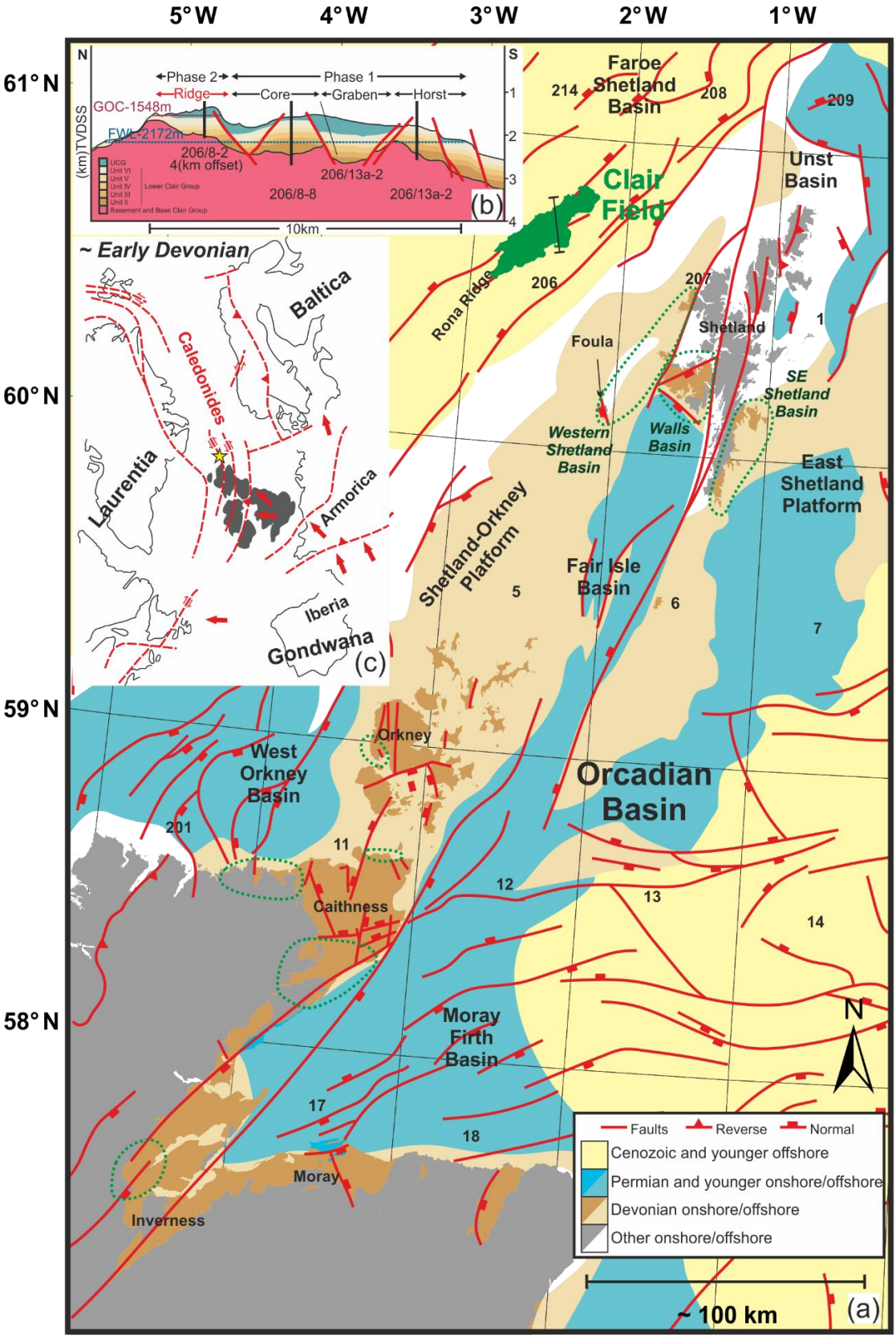

4.2. Regional Framework:

4.2.1. The Orcadian Basin:

The margins of the North Atlantic preserve a series of Palaeozoic sedimentary basins that developed following the sinistral oblique continental collision of Laurentia, Baltica and

Avalonia (Marshall et al., 2003; Ziegler, 1988) as a result of the closure of the Iapetus Ocean (Figure 4.1c). During closure, a series of orogenic events occurred that are collectively referred to as the Caledonian Orogeny, leading to the formation of the 'Old Red Sandstone' (or ORS) continent during the Silurian and Early Devonian (Woodcock & Strachan 2012 and references therein). Following regional-scale gravitational collapse of the orogenic belt, coupled with significant left-lateral displacement along major strike-slip faults, a series of arid to semi-arid marginal marine and intra-continental sedimentary basins (e.g. Orcadian Basin) developed, into which the material being shed from the eroding mountain belt was deposited (Fossen 2010).

The Orcadian Basin is a thick development of Devonian age ORS continental facies, which are predominantly composed of alluvial, fluvial, lacustrine and aeolian deposits (Marshall et al., 2003; Trewin and Thirlwall, 2002). These sediments were deposited in a series of smaller, linked, sub-basins which eventually coalesced to form the considerably larger Orcadian basin. The ORS in the Orcadian Basin is subdivided into the Lower, Middle and Upper ORS which largely equate to the Lower, Middle and Upper Devonian, which are partially separated by local unconformities. The basin extended some 600km from Northeast Scotland to the Western coast of Norway and as far as Eastern Greenland, and was strongly influenced by several major strike-slips faults (the Great Glen Fault Zone, Walls Boundary Fault Zone, and More-Trøndelag Fault Zone) which together accommodated many tens if not hundreds of kilometres of sinistral displacement during the development of this basin(Dewey and Strachan, 2003; Fossen, 2010) . Following the deposition of the Orcadian Basin, a series of pulsed rifting events took place during the Paleozoic, Mesozoic and Cenozoic which would ultimately lead to the development of the North Sea Basin and Atlantic Ocean (Woodcock & Strachan 2012).

The Devonian fills of the Orcadian Basin are exposed onshore in the UK, in Northern Scotland, around the margins of the Inner Moray Firth, and on the island archipelagos of Orkney and Shetland (Figure 4.1a and Figure 4.2). Deposits of the Orcadian Basin also occur onshore in Western Norway (Fossen, 2010), in Eastern Greenland (Hartz, 2000) and are encountered offshore on the UK and Norwegian continental shelves where they underlie much of the more prospective Mesozoic sedimentary basins of the North Sea (Marshall et al., 2003), and also form the reservoir for a number of oil and gas fields, most notably Clair.

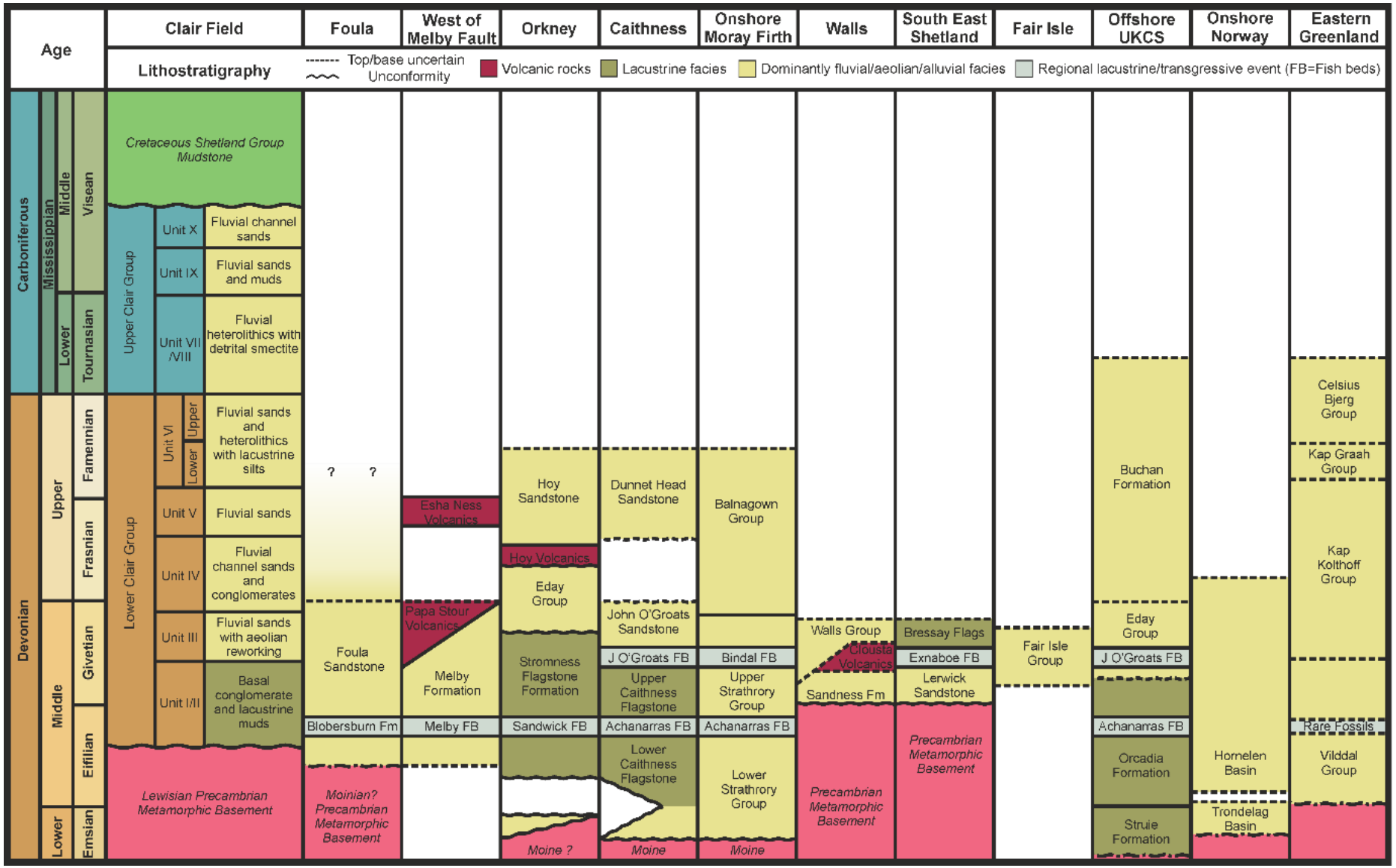
Age
Clair Field
Foula
West of Melby Fault
Orkney
Caithness
Onshore Moray Firth
Walls
South East Shetland
Fair Isle
Offshore UKCS
Onshore Norway
Eastern Greenland
Lithostratigraphy
Top/base uncertain
Unconformity
Volcanic rocks
Lacustrine facies
Dominantly fluvial/aeolian/alluvial facies
Regional lacustrine/transgressive event (FB=Fish beds)
Carboniferous
Mississippian
Middle
Lower
Visean
Tournasian
Devonian
Upper
Middle
Lower
Famennian
Frasnian
Givetian
Eifilian
Emsian
Cretaceous Shetland Group Mudstone
Upper Clair Group
Unit X
Fluvial channel sands
Unit IX
Fluvial sands and muds
Unit VII /VIII
Fluvial heterolithics with detrital smectite
Lower Clair Group
Unit VI
Upper
Lower
Fluvial sands and heterolithics with lacustrine silts
Unit V
Fluvial sands
Unit IV
Fluvial channel sands and conglomerates
Unit III
Fluvial sands with aeolian reworking
Unit I/II
Basal conglomerate and lacustrine muds
Lewisian Precambrian Metamorphic Basement
? ?
Foula Sandstone
Blobersburn Fm
Moinian? Precambrian Metamorphic Basement
Esha Ness Volcanics
Papa Stour Volcanics
Melby Formation
Melby FB
Hoy Sandstone
Hoy Volcanics
Eday Group
Stromness Flagstone Formation
Sandwick FB
Moine ?
Dunnet Head Sandstone
John O'Groats Sandstone
J O'Groats FB
Upper Caithness Flagstone
Achanarras FB
Lower Caithness Flagstone
Moine
Balnagown Group
Bindal FB
Upper Strathrory Group
Achanarras FB
Lower Strathrory Group
Moine
Walls Group
Clousta Volcanics
Sandness Fm
Precambrian Metamorphic Basement
Bressay Flags
Exnaboe FB
Lerwick Sandstone
Precambrian Metamorphic Basement
Fair Isle Group
Buchan Formation
Eday Group
J O'Groats FB
Achanarras FB
Orcadia Formation
Struie Formation
Hornelen Basin
Trondelag Basin
Celsius Bjerg Group
Kap Graah Group
Kap Kolthoff Group
Rare Fossils
Vilddal Group

Figure 4.2 (preceding page): Regional Devonian stratigraphic correlation chart and stratigraphy of the Clair Field. *After* Allen and Mange-Rajetzky, (1992); Barclay et al., (2005); Barr et al., 2007; Gautier et al., (2011); House, (2000); Marshall et al., (2003); Ogilvie et al., (2015); Trewin and Thirlwall, (2002).

Recent work (Dichiarante, 2017; Dichiarante et al., 2016; Wilson, 2006; Wilson et al., 2010) has reappraised the structural evolution of the area, as an analogue to better understand the detailed geology and development of the offshore basins. This work identified three three main phases of deformation with associated structures, based on their orientation, kinematics and fabric/fill that were developed during regional deformation and phases of movement and reactivation of the Great Glen and Walls Boundary Fault Zones (GG/WBFZs.).

The first group of structures are Devonian in age (Dichiarante et al., 2016) and include NW/SE to N/S trending sinistral-normal dip slip and strike slip faults related to the opening and development of the Orcadian Basin during regional ENE/WSW sinistral transtension associated with sinistral strike-slip motion along the GG/WBFZs (Dichiarante et al., 2016; Wilson et al., 2010). These structures are largely clean break faults, with minor quantities of fault gouge, little to no mineralisation, and often show significant thicknesses of growth strata in the hangingwalls.

The second group of structures are Late Carboniferous to Early Permian in age and include km-scale N/S trending folds and thrust faults (Dichiarante et al., 2016), attributed to regional E/W shortening, inversion and reactivation of pre-existing faults during regional dextral reactivation of the GG/WBFZs (Dichiarante et al., 2016; M. Seranne, 1992). The structures are also associated with little or no mineralisation.

The third group of structures include dextral oblique NE/SW to NNE/SSE trending faults and sinistral E/W-ENE-WSW trending faults (Dichiarante et al., 2016) associated with abundant carbonate mineralisation, base metal sulphides (pyrite), and bitumen. Re/Os dating of vein hosted pyrite mineralisation yielded Permian ages (ca. 267Ma; Dichiarante et al., 2016) for this event. These structures together with a lamprophyric dyke swarm (Chapman, 1975; Baxter and Mitchell, 1984; Brown, 1975) are thought to be related to regional NW/SE extension and rifting and the development of the Permo-Triassic sedimentary basins offshore, most notably the nearby West Orkney Basin (Bird et al., 2015; Dichiarante et al., 2016).

4.2.2. The Clair Basin:

The Clair Basin lies on the E margin of the mainly extensional Faroe-Shetland Basin (FSB) (Figure 4.1a), which is composed of a series of NE/SW orientated sub-basins, separated by basement highs and horst blocks, that formed through a series of rifting and subsidence events from the Devonian to the Paleocene (Ellis and Stoker, 2014; Stoker et al., 2016, 1993).

The Clair Basin developed during Middle Devonian to Early Carboniferous times as an elongate, NE/SW orientated (Blackbourn, 1987b), supposedly extensional half graben. The margins of the basin are broadly defined by the Shetland Spine Fault and West Shetland Platform to the SE and bound by the Rona Ridge to the NW (Figure 4.1a), a NE/SW orientated, regional scale, structural high (Figure 4.1b) comprised of Precambrian metamorphic basement.

The Clair Basin is filled with up to 1 km of continental fluvial, alluvial, minor lacustrine and marginal marine deposits of the Clair Group (Allen and Mange-Rajetzky, 1992; Coney et al., 1993), which are unconformably overlain by Cretaceous age marine mudstones of the Shetland Group, forming a regional seal.

The Clair Group is subdivided into the Middle to Upper Devonian age Lower Clair Group and Lower to Middle Carboniferous, Upper Clair Group. It is generally believed that the Clair Basin represents a transitional area between the well-developed Devonian sequences of the Orcadian basin and an elevated and potentially more isolated area to the NW that may have at times been connected with the larger Orcadian Basin and was supplying sediment to the Devonian basins of NE Scotland and Shetland (Allen and Mange-Rajetzky, 1992; Hitchen and Ritchie, 1987; McKie and Garden, 1996).

4.3. Methodologies:

Locations throughout the Orcadian Basin, particularly in areas around the basin margins were visited in order to understand the variety of outcrop scale basement/cover relationships, together with the distribution and types of structures and sedimentary architectures developed. This study was carried out using a combination of traditional fieldwork techniques and conventional structural analysis, supplemented by the digitisation and analysis of data from published geological maps and other analogue datasets. Structural data were analysed using Stereonet 9.5 (Allmendinger et al., 2011) and

folds were studied though the production of form line maps and down plunge fold projections, following the method of Ragan (2009) and using the GMDE (GeolMapDataExtractor) (Allmendinger and Judge, 2013).

Due to the generally poor inland outcrop and the inaccessible nature of many of the exposed coastal cliff sections, fieldwork was supplemented by aerial imagery, and drone-based photogrammetry using 3D S*f*M (Structure *from* Motion). This enabled geological reconnaissance whilst in the field and for the collection of observations and images from difficult to access or inaccessible outcrops. 3D photogrammetric models of key outcrops were then generated in Agisoft Photoscan and the resultant models analysed and interpreted using the VRGS (Virtual Reality Geological Studio) (Hodgetts, 2019) in order to extract geological information and structural data (Hodgetts et al., 2007).

This combination of methods was a time efficient and safer approach, enabling targeted fieldwork to key locations, the collation of a greater quantity of data and avoiding the unnecessary duplication of datasets. Further, detailed methodologies and the background to the aforementioned techniques can be found in Chapter 2.

4.4. Basement/Cover relationships in the Orcadian Basin:

A wide variety of basement/cover relationships are present in the Orcadian Basin, which are described in the following section, sub-divided into the three principal geographic areas onshore; Shetland, Orkney and NE Scotland (Caithness-Sutherland).

4.4.1. Shetland:

The N/S oriented Shetland Isles and offshore Shetland Platform (Figure 4.3 and 4.4) comprise highly deformed and metamorphosed Precambrian rocks, intruded by a suite of igneous rocks during the Caledonian orogeny, flanked and overlain by Devonian age sedimentary basins (Mykura et al., 1976a) and offshore by later Mesozoic sedimentary basins on the East and West Shetland Platforms (Figure 4.3). This regional basement high separates the Northern North Sea rift in the East, from the Faroe-Shetland Basin and N Atlantic to the NW.

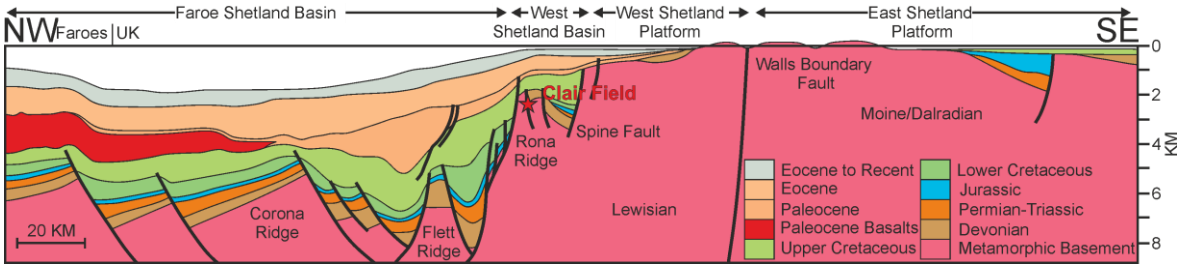

Figure 4.3: Regional cross section through the Faroe Shetland Basin and Shetland Isles showing the prominent ridge of basement, flanked by Paleozoic to Mesozoic sedimentary basins Modified *after* Stoker et al., (1993).

The archipelago is cut by three major strike-slip faults; the Walls Boundary Fault, the proposed northward continuation of the Great Glen Fault (Watts et al., 2007 and references therein), the Melby Fault and the Nesting Fault (Mykura, 1976, Flinn and May, 1976) (Figure 4.4), which separate three distinct Devonian basins in Shetland (Figure 4.2).

To the W of the Melby Fault, sedimentary and volcanic rocks exposed at Melby, Eshaness and on the islands of Foula and Papa Stour comprise the Western Shetland Basin. They are juxtaposed against the more deeply buried and intensely folded, sedimentary and volcanic rocks of the Walls Basin that comprise the majority of the Walls Peninsula (Melvin, 1985), into which granites are emplaced (Mykura et al., 1976a). This basin is bound to E by the Walls Boundary Fault and a ridge of metamorphic basement that forms the spine of the Shetland Isles.

To the E of this ridge and E of the Nesting Fault, the SE Shetland Basin comprises gently folded Devonian sedimentary rocks which are exposed in a narrow strip along the Eastern coast from Lerwick to Sumburgh Head, and on the islands of Bressay, Noss, Mousa and Fair Isle (Figure 4.4). This basin is also cut by a major N-S orientated zone of deformation, the 'steep belt', which is associated with reverse faulting, folding and mineralisation (Mykura et al., 1976a).

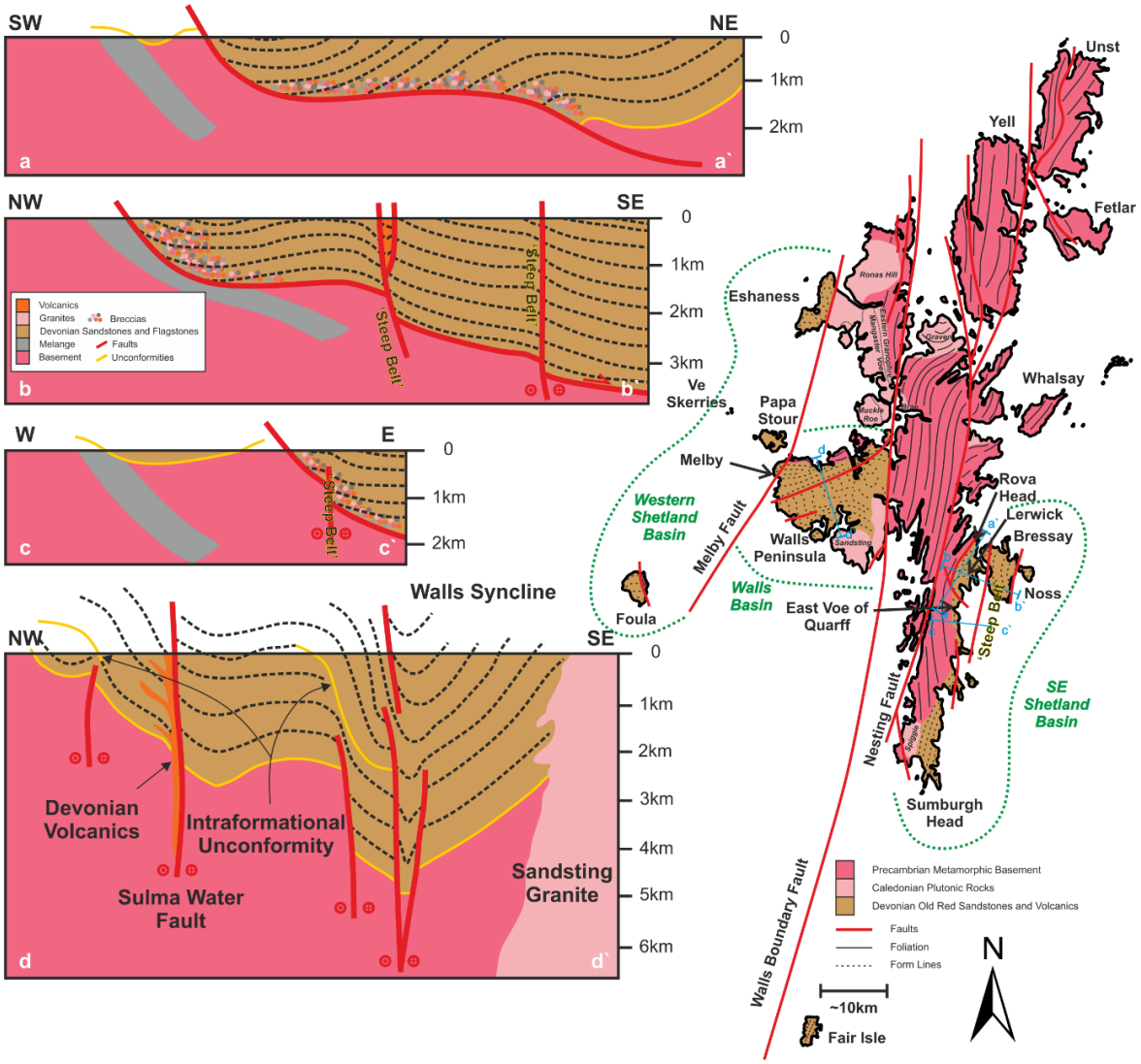

Figure 4.4: Simplified geological map of Shetland. Form lines show generalised structure (foliation and bedding) of the rocks that comprise Shetland. Form lines derived from the extraction of structural data from published maps and modified *after* BGS (1971, 1978a, 1978b, 1994, 2005a, 2005b). Cross sections modified *after* Seranne (1992).

4.4.1.1. Western Shetland Basin:

At the western-most tip of the Walls Peninsula, the rocks exposed at Melby, Papa Stour, the Holm of Melby, the Eshaness Peninsula and Foula form the exposed part of the Western Shetland Basin (Mykura, 1976). The rocks of the Walls Group and Walls Metamorphic Series that comprise the majority of the Walls Peninsula are juxtaposed against the Devonian sediments of the Melby Formation by the NNE/SSW trending Melby Fault which is traced to the N through St Magnus Bay to the Eshaness Peninsula (Marshall, 2000; Mykura et al., 1976b, 1976a). The unconformity with the basement that underlies the Melby Formation is not exposed, but the structural evolution of the Melby Formation has been studied. A

detailed description of the onshore basement/cover relationships and geology of Foula together with a discussion of the implications in Shetland and the wider Orcadian Basin can be found in Chapter 3.

4.4.1.1.1. Melby and Papa Stour:

Rocks of the Middle Devonian aged St. Magnus Bay Group (BGS, 2005a, 1971) (Figure 4.2) are exposed along the coastlines around the village of Melby at the W end of the Walls Peninsula, and on the islands of Papa Stour and the Holm of Melby. This group comprises the predominantly coarse, clastic sedimentary rocks of the Melby Formation and the volcanic and volcaniclastic rocks of the Papa Stour Volcanic Formation (BGS, 1971; Mykura et al., 1976a). Likely Precambrian aged granitic gneisses, foliated granites, hornblende schists and undeformed basic dykes of uncertain age outcrop (Mykura et al., 1976b) on the small rocky low lying islands at Ve Skerries, ~5km to the NW of Papa Stour (Fig. 4.4) which may be similar to the basement rocks that underlie other parts of this basin. The rocks exposed on Ve Skerries are however dissimilar to those exposed on Foula and possibly those on the Walls Peninsula and were initially correlated on lithological grounds to those exposed at North Roe (Mykura et al., 1976a and references therein) and attributed to the Lewisian. Up to date geochronological studies are now hoping to answer this question (Strachan*, pers comms*. 2019). Together, these rocks mark the E limit of exposure of the Western Shetland Basin, which is bound to the E by the NNE/SSW trending Melby Fault (Figure 4.5a).

In the S, on the Walls Peninsula, the contact between the rocks of the adjacent Walls Basin and the Melby Formation is poorly exposed and NE of the village of Melby is interpreted to pass out through the beach at The Crook (Figure 4.5b) [HU 419218 1157806], past the Neap of Norby and out into St. Magnus Bay towards Eshaness (McKay, 1974). Inland it is inferred based on the presence of a distinct break in slope and is traced towards the SW before being exposed, although largely inaccessible in Hesti Geo (Figure 4.5c) [HU 417051 1155460], NW of the Bay of Deepdale. Here, the rocks of the Melby Formation and Walls Group are intensely folded (Mykura et al., 1976b) and cut by numerous faults.

The Melby Formation generally dips 20-40° towards the SE (Figure 4.5d) and comprises red to buff, predominantly pebbly sandstones and sandy siltstones of fluvial-alluvial origin with cross bedding, indicating paleo flow from the W-WNW (Mykura et al., 1976a, 1976b). Towards the base of the unit, several carbonate-rich siltstones and thin limestones of

lacustrine origin, known as the 'Melby Fish Beds' are exposed along the coastline near to Matta Taing [HU 416582 1156126] and Pobie Skeo [Hu 416582 1156788]. They contain examples of sedimentary structures including ripples, convolute bedding, water escape structures and early diagenetic nodules (Hall and Donovan, 1978) (Figure 4.6a i-iii). Also contained in these units are fish (Figure 4.6a iv) and plant remains which, together with spores collected on Papa Stour, give a Middle Devonian Eifelian to Givetian age (Marshall, 1988; Mykura et al., 1976a). This age allows for correlation with the Sandwick Fish Bed, Achnarras Horizon and Blobersburn Formation in Caithness, Orkney and Foula and indicate that these deposits are the equivalent basin marginal deposits of the main Orcadian Basin in Scotland – a conclusion supported by the findings on Foula set out in Chapter 3.

Towards the top of the unit are several thick beds of feldspathic sandstones containing abundant plant material and clasts of rhyolite and basalt, and bioturbated sandy siltstones (Mykura et al., 1976b, 1976a). These are overlain by several thick flows of silicified rhyolite or ignimbrites (Mykura et al., 1976a). These units are deemed the distal equivalent of the Papa Stour Volcanic Formation, which outcrops on Papa Stour (Mykura et al., 1976a). Here the sequences comprises basalt lava flows and intercalated sandstones, rhyolite lava flows, rhyolitic tuffs and agglomerates and tuffaceous sandstones (Figure 4.5a; Mykura et al., 1976a, 1976b; Marshall, 1988).

2 main sets of structures are observed in the Melby Formation. The first phase include N/S to NNE/SSW-NE/SW synsedimentary normal faults with rare sinistral oblique to normal slickenlines (Figure 4.6b *inset*). Cm to dm scale normal offsets on these structures, distributed over many small faults are observed as well as the development of small graben structures (Figure 4.6b). In places these normal faults dip quite shallowly and steeply towards the NW and SE, respectively, due to the tilting of the Melby Formation towards the SE, and are likely Devonian in age, consistent with observations made on Foula (Chapter 3) which indicate ENE/WSW orientated principal extension.

Cutting the normal faults and in some places reactivating them, are SE dipping (Figure 4.6c and 4.6d) thrust faults relating to a second phase of deformation. Good exposures of these structures are found in Pund Geo [HU 416582 1156106] (Figure 4.6d). Smaller thrusts are particularly well developed in the siltstones and limestones of the Melby Formation, in particular, the organic/clay rich Melby Fish Beds which act as preferential slip horizons and detachments (Figure 4.6c). Frequently these thrusts sole out onto bedding planes and

often, can only be traced for several metres along strike. Associated with the thrusts are 2 sets of curvilinear folds (Figure 4.6e) with hinges sub-parallel and perpendicular to the strike of the thrusts, which predominantly verge towards the NW (Figure 4.7f). As such, bedding in these units is far more chaotic and uneven. Bedding-parallel slickenlines are observed which plunge towards the SE and are particularly well defined on the surface of blackened, organic rich layers (Figure 4.6g). Sub-parallel to the thrusts and low angle faults are tensile fractures infilled with fibrous calcite which shallow to become parallel to bedding (Figure 4.6h). These tensile fractures developed in association with mostly compressional features suggest high fluid pressures which are likely aiding in the development of the thrusts

Associated with the earlier faults and cut by the thrusts are abundant deformation bands (Figure 4.6i) which are particularly well developed in some of the more coarse and sandier units. These deformation bands in places are sub-parallel to the cross bedding within some of the thicker bedded units and appear to nucleate on and/or reactivate individual foresets (Figure 4.6j).

At Matta Taing [HU 416621 1156216], a NE/SW orientated shear zone (Figure 4.6k) is developed with E/W conjugate shear fractures and NW/SE tensile fractures. Within some NE/SW fractures there is brecciation and the development of a mosaic/crackle breccia with <2mm fragments. These are consistent with dextral shear and NW/SE compression, and are likely related to inversion of the Melby Fault. In addition to the reactivation of early normal faults, these structures in places cut early deformation bands and faults. Paleostress inversion of fault lineation data associated with these thrusts (Figure 4.6l) indicates NW/SE compression together with minor dextral strike-slip.

These observations made at Melby are in agreement with those made by Seranne (1992 and references therein) for regional dextral oblique inversion, likely during the late Carboniferous following the rapid subsidence and burial of the Devonian sequences during sinistral transtension.

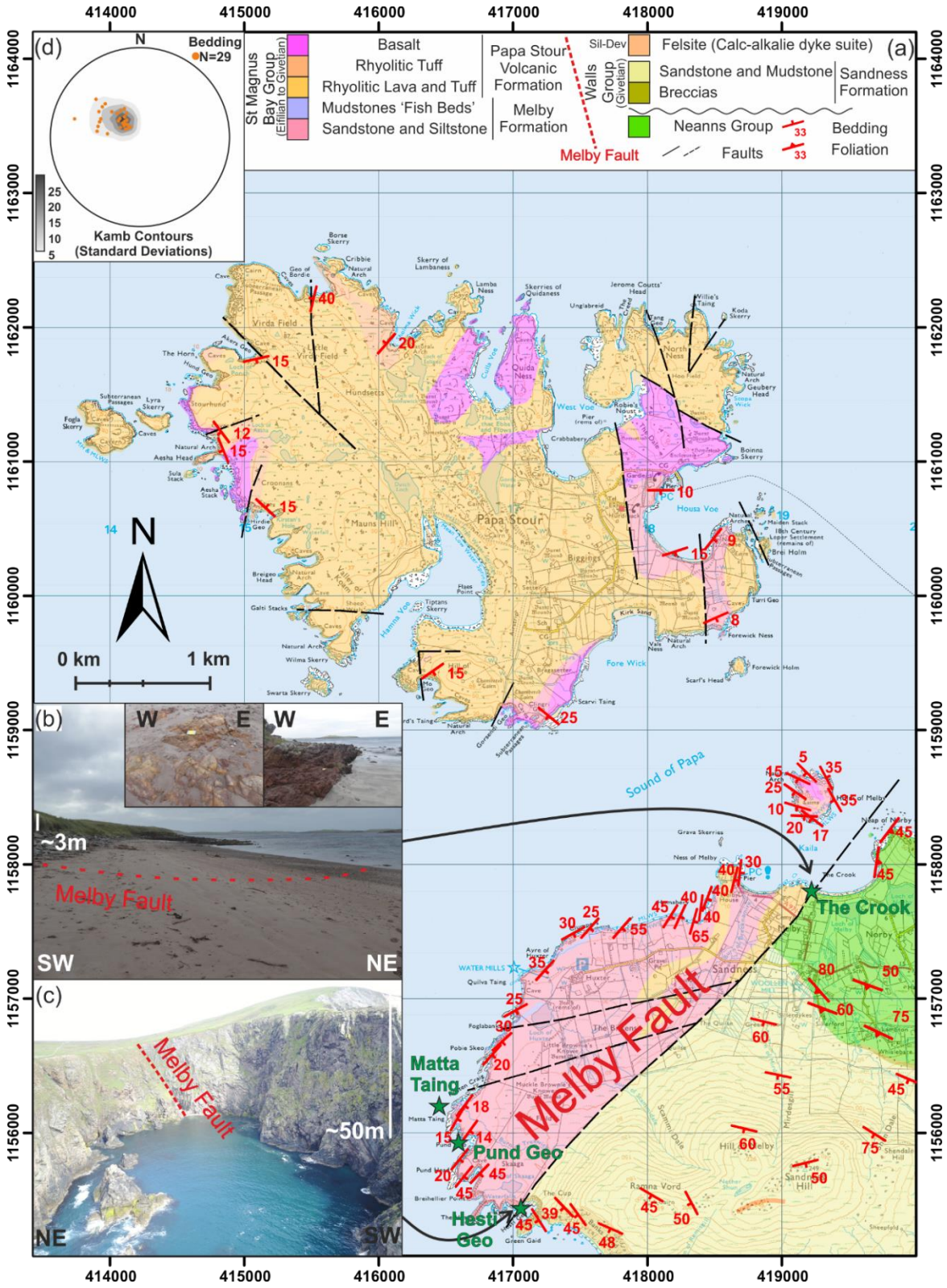

Figure 4.5: (a) Geological map of Melby and Papa Stour area. Modified *after* BGS (1971) (b) Trace of the Melby Fault on the beach N of Melby. *Inset* nearest outcrops of Melby Formation at W end of the beach. (c) Outcrop of the Melby Fault in Hesti Geo. (d) Stereonet showing poles to plane for bedding for the Melby Formation on mainland Shetland.

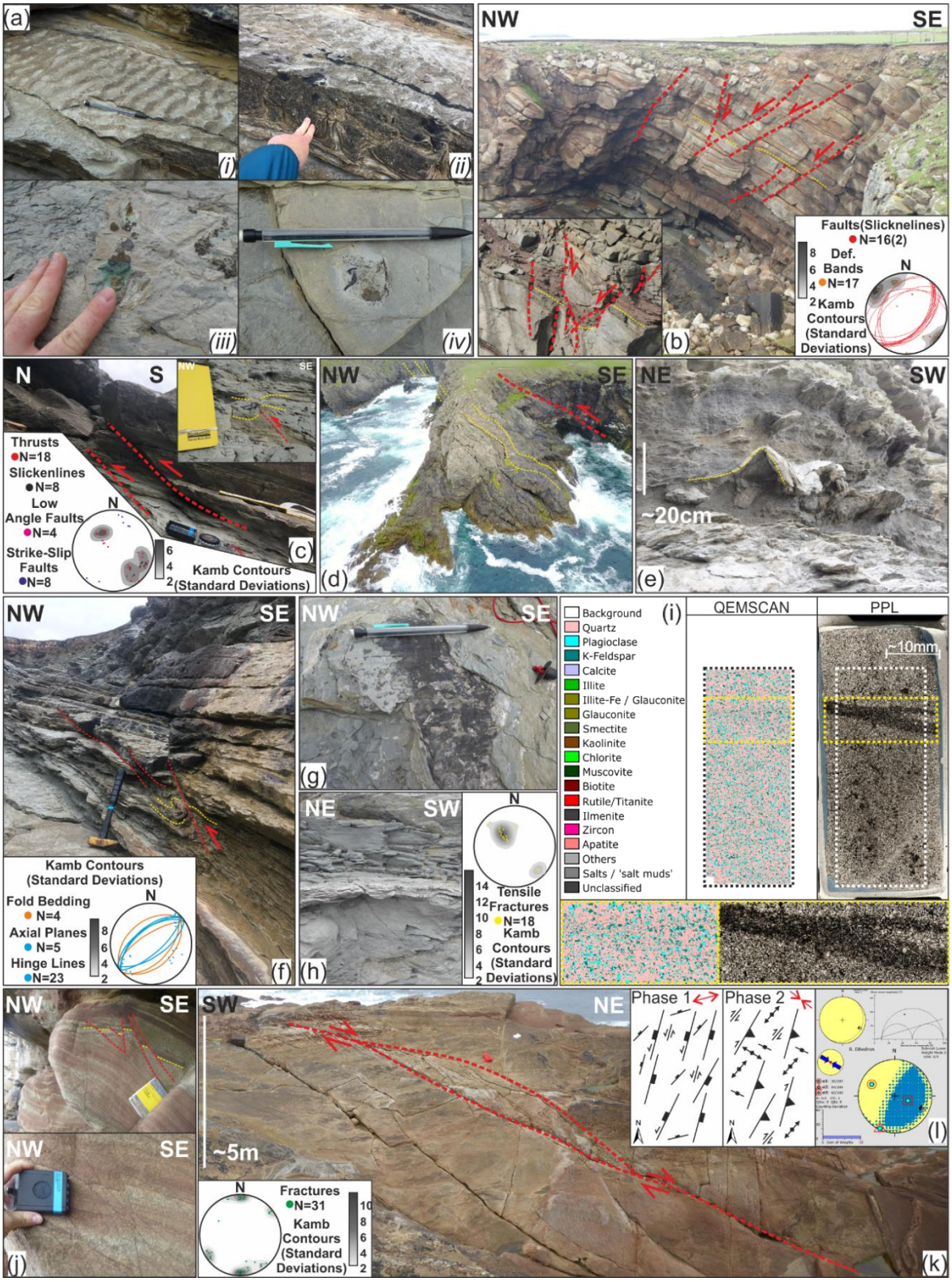

Figure 4.6: Field images and *inset* lower hemisphere, equal area stereonet of associated structural data from the Melby area; (a) Sedimentary structures in the Melby Formation. (i) ripples, (ii) convolute bedding and water escape structures, (iii) nodules, (iv) fragments of fish fossil; (b) normal faults and graben structures; (c)small scale thrusts faults developed in the Melby Fish Beds In Pund Geo [HU 416582 1156106] and larger thrusts and folded strata at Beihellier Point [HU 416713 1155542](d); (e) tight folds in the Melby Fish Beds; (f) fold and thrust relationships; (g) bed parallel

slickenlines on organic rich bedding surface; (h) fibrous calcite filled tensile fracture with *inset* lower hemisphere equal area projection stereonet of associated data; (i) Qemscan and PPL image of deformation band in sandstones of the Melby Formation; (j) deformation bands at Matta Taing; (k) dextral shear zone at Matta Taing and (l) schematic summary diagram showing the main phases of deformation observed at Melby and paleostress inversion for phase 2 thrusts faults, indicating NW/SE compression.

4.4.1.1.2. Eshaness Peninsula:

In the NW of Shetland, on the Eshaness Peninsula the Northward continuation of the Melby Fault is exposed (Fig 4.4). The peninsula comprises andesitic to rhyolitic lavas, tuffs, ignimbrites, some basalts and minor micaceous/tuffaceous sandstones of the Esha Ness Volcanic Formation (BGS, 2005a; Mykura et al., 1976a) (Figure 4.7a). This sequence is correlated with the volcanic rocks to the S on Papa Stour (Marshall, 1988), which are dated to the Late Eifelian based on palynology and are therefore, time equivalent to the Upper Stromness Flagstones (Marshall, 1988), providing further evidence that the westernmost Devonian Basin is of a closer affinity to Orkney and Caithness. The sequence is subtly folded into a NE trending, doubly plunging syncline (Figure 4.7b) which plunges towards the NE in the north, and towards the SW in the south. The age and origin of this structure is unclear, but faint growth and an opening upwards geometry observed on the down plunge projection of this structure which may suggest a Devonian origin for this structure (Figure 4.7b).

Inland outcrop is poor, but on the S coast, at the W end of the beach at Braewick [HU 424506 1178583] volcanic and sedimentary rocks of the Esha Ness Volcanic Formation are exposed, which dip steeply to E that are cut by tensile fractures filled with quartz. These rocks are juxtaposed against the Ronas Hill Granite, a red leucocratic granophyre (Mykura et al., 1976a)(Figure 4.7a) whose intrusion is dated at 427.5± 5.1 Ma(U-Pb zircon); Lancaster et al., 2017) which is exposed at the Eastern end of the beach. The Melby Fault itself which runs through the centre of the beach is not exposed, however a string of small lakes and boggy ground elucidates to the position of the fault going inland and towards the North. To the north the Melby Fault is exposed on the Northern coast of the Eshaness Peninsula in Ronas Voe near to Sumra [HU 426260 1183762]. Here, the Ronas Hill Granite lies in the hangingwall and is juxtaposed against andesitic to rhyolitic lavas, tuffs, and ignimbrites of the Esha Ness Volcanic Formation (Mykura et al., 1976a) (Figure 4.7a). A

prominent gully is developed along the line of the fault which is filled with unconsolidated sediments subject to recent landslips and collapse (Figure 4.8a).

The fault plane dips ~50° towards the SE and preserves rare dextral reverse slickenlines (Figure 4.8c). The fault plane is fairly planar and produces a pronounced cliff face. A highly angular crackle breccia can be found in patches on the fault plane as well as smaller regions of chaotic breccia, finer breccias, and cataclasites. These patches seem to correspond with pockmarks, hollows and other asperities on the fault plane (Figure 4.8b). In the footwall the andesite is highly fractured with a well-developed steeply dipping rectilinear fracture pattern which trends NW/SE, NE/SW and E/W (Figure 4.8c).

In the hangingwall, the granite is intensely brecciated and fragmented, and as result is highly altered due to weathering. Further from the fault the granite has a strong fracture cleavage which trends N/S and dips steeply (70-80°) towards the E/SE (Figure 4.8c). The fault zone itself comprises slices and lenses of interleaved, granite and andesitic material which have a well-developed NE/SW trending foliation and sinistral shear fabric which dips steeply (70-90°) towards the SE(Figure 4.8c). The fault zone is cut by several antithetic shear fractures and is intensely veined with quartz (Figure 4.8d and 4.8c). The foliation is locally folded into steeply plunging NE to N verging S-folds (Figure 4.8e and 4.8c) and veined with quartz.

The structures observed at Sumra are consistent with both reverse faulting, and elements of dextral shear. The well-developed foliation and cleavage suggest elements of shear which in conjunction with the mineralised shear fabrics with dextral shear indicators and N-verging folds suggest dextral motion in the fault zone. This is confirmed by the dextral oblique, reverse slickenlines on the fault plane. These observations, together with the juxtaposition of extrusive volcanics rocks, against deeply buried plutonic rocks indicate the likely dextral oblique reactivation and inversion of the Melby Fault.

4.4.1.1.3. Western Shetland Basin Summary:

The sporadic outcrop of the Western Shetland basin precludes a detailed picture of the evolution of the basin; however several distinct phases have been identified. The first phase of deformation is well recorded on the island of Foula (Chapter 3) where the following key

features have been identified (Figure 4.9a); sinistral oblique normal faulting and transtensional growth folding, a diverse suite of basement/cover relationships, and a strong structural control on the development of sedimentary systems as well as a closer affinity to the Middle Devonian sequences of Orkney.

The sequences at Eshaness and Papa Stour, indicate a volcanologically active basin, which is not indicated from the sequences on Foula, however may further indicate elements of sinistral strike-slip tectonics and development of pull-apart structures which could act as a conduits for volcanism (Lundmark et al., 2018). Observations at Melby further confirm broadly E/W extension with an element of sinistral obliquity.

Soft sediment deformation features throughout the Middle Devonian sequences of this basin suggest rapid deposition, burial and subsidence of the basin, broadly in line with burial models for the Orcadian Basin in Orkney and Caithness (Bird, 2014). This was followed by a period of uplift and dextral oblique reverse motion along the Melby Fault with NW/SE orientated compression (Figure 4.6l), which inverts the basin and moves it in an opposed direction along the Melby Fault, and towards its present structural configuration.

Figure 4.7 (overleaf): (a) Geological map of the Eshaness Peninsula. Modified *after* BGS (2005) (b) Down plunge fold projection and lower hemisphere equal area stereonet of bedding data for the Eshaness Peninsula. Lines coloured according to the geology key. Green stars denote locations discussed in the text.

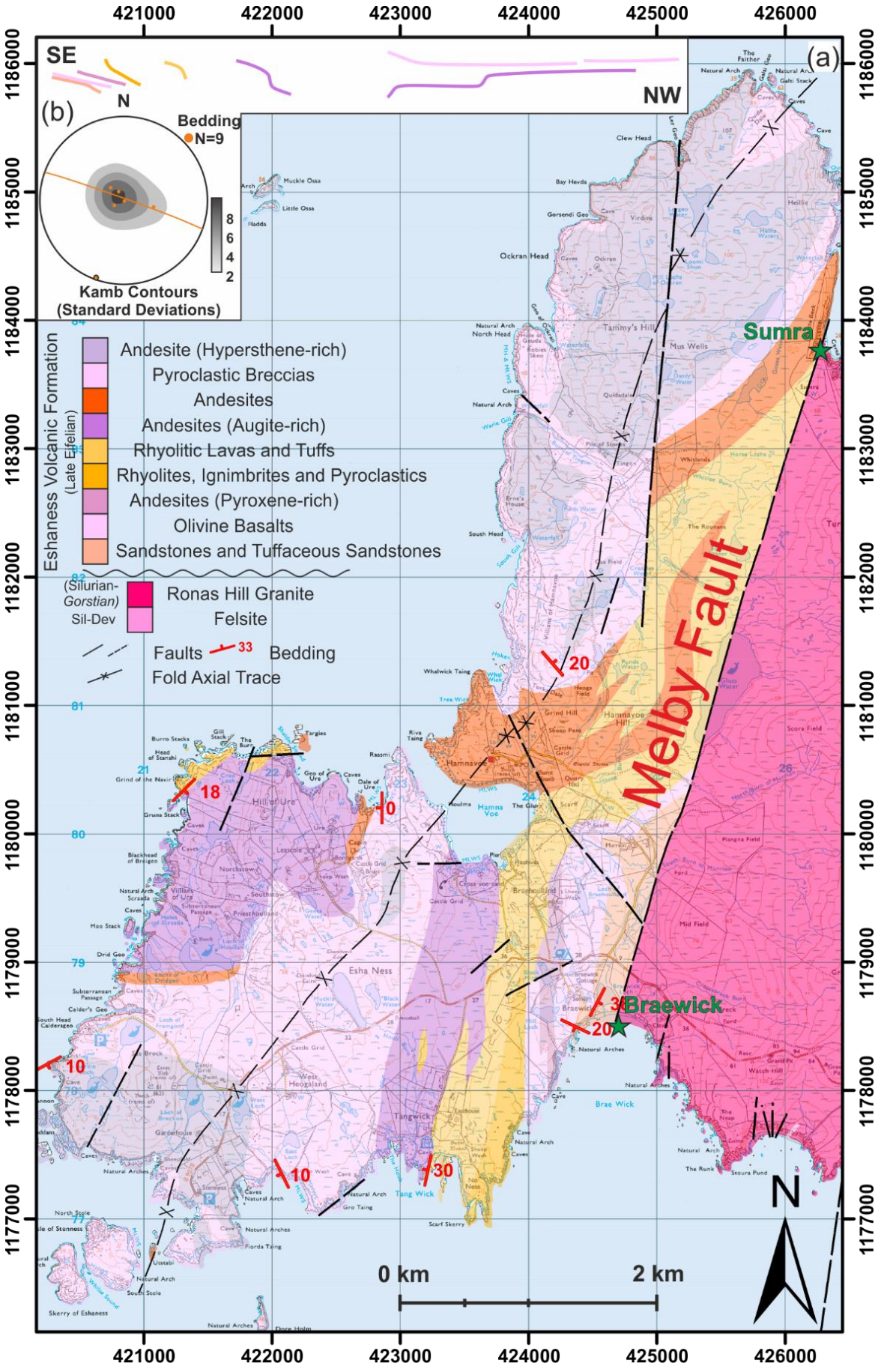
421000
422000
423000
424000
425000
426000
1186000
1185000
1184000
1183000
1182000
1181000
1180000
1179000
1178000
1177000
SE
NW
(a)
(b)
N
Bedding
N=9
8
6
4
2
Kamb Contours
(Standard Deviations)
Eshaness Volcanic Formation
(Late Eifelian)
Andesite (Hypersthene-rich)
Pyroclastic Breccias
Andesites
Andesites (Augite-rich)
Rhyolitic Lavas and Tuffs
Rhyolites, Ignimbrites and Pyroclastics
Andesites (Pyroxene-rich)
Olivine Basalts
Sandstones and Tuffaceous Sandstones
(Silurian-Gorstian)
Sil-Dev
Ronas Hill Granite
Felsite
Faults
33
Bedding
Fold Axial Trace
Melby Fault
Sumra
Braewick
Esha Ness
Hillswick
Hamnavoe
Tangwick
Ockran Head
Clew Head
Tammy's Hill
Hill of Ure
Grind Hill
Hamnavoe Hill
Mus Wells
Quildadale
Whalwick Taing
Hoogs Field
Sheep Pens
Castle Grid
Northstow
Leasdale
Priesthoulland
Braehoulland
Cross-voe-sand
Mid Field
Plangea Field
Scora Field
Natural Arches
Brae Wick
Tang Wick
Scarf Skerry
Skerry of Eshaness
Muckle Ossa
Little Ossa
Hadda
Gorsendi Geo
Virdins
Bay Hevda
Heillis
Natural Arch North Head
Whistlands
Horse Lochs
The Roosens
South Head
Hamna Voe
Scarf
Murrion
Ford
Watch Hill
Stoura Pund
The Runk
Natural Arch
Cave
Caves
Gro Taing
Florda Taing
Dore Holm
Burro Stacks
Head of Stanhi
Gruna Stack
Grind of the Navir
Gill Stack
Targies
Rassmi
Dale of Ure
Gep of Ure
Blackhead of Bridgen
Natural Arch Scraafta
Villians of Ure
Moo Stack
Drid Geo
Subterranean Passage
Calder's Geo
South Head Caldersgeo
Loch of Framgord
Loch of Dridgeo
Garderhouse
West Heogaland
Natural Arch North Stole
South Stole
Weisdale Sound
Skerry of Eshaness
The Father
Natural Arch
Galti Stack
Gorsendi Geo
Ockran
Waterfall
Natural Arch
Warie Gill
Pile of Stone
Tingon
Brae Field
Brae Burn
Whiteness Burn
Brae Burn
Ford
Mid Burn of Murrion
Scora Burn
Clarence Burn
Grand Pit
Natural Arch
Natural Arches
Cave
Caves
Natural Arch
Natural Arches
Natural Arch
Natural Arches
Natural Arches
Natural Arch
Natural Arches
Natural Arches
Natural Arches

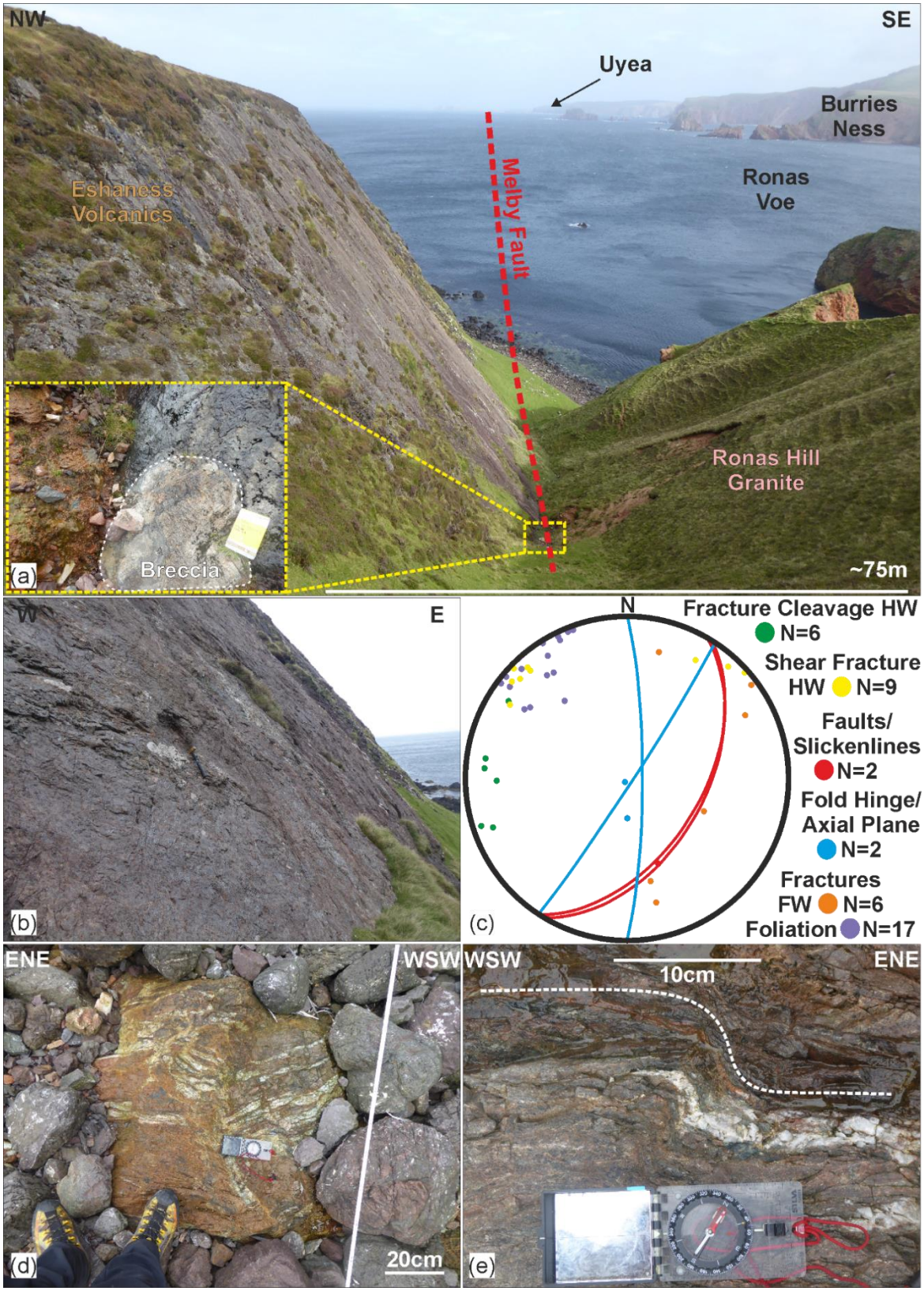

Figure 4.8: (a) overview of the Melby Fault at Eshaness. *Inset* detail view of fault plane showing patch of breccia. (b) Image of fault plane showing hollows and asperities on fault plane. (c) lower hemisphere equal area stereonet of principal structures developed in the fault zone. FW=Footwall, HW=Hangingwall. (d) Detailed image of mineral veins and (e) quartz veins showing top to NE dextral shear.

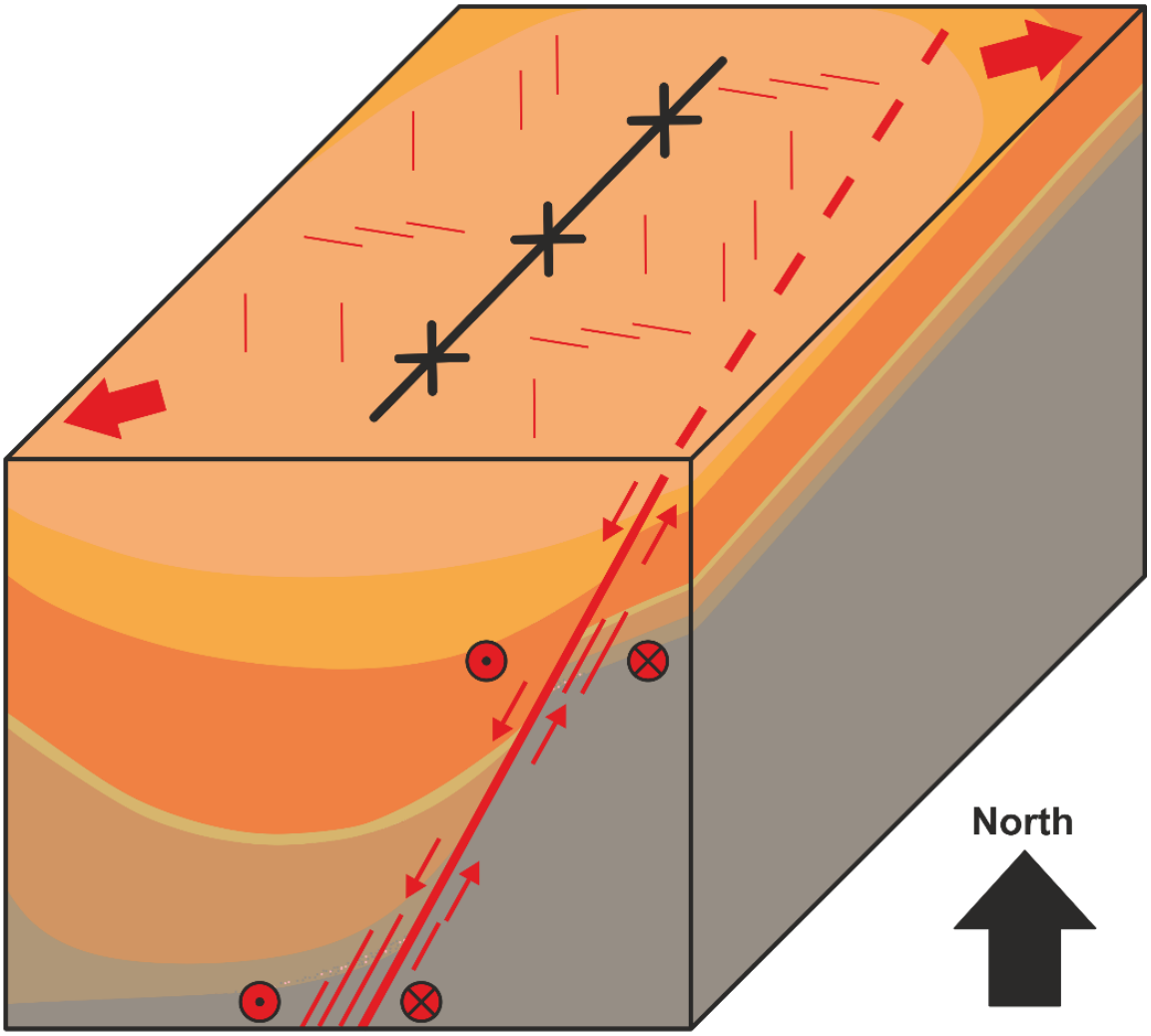

Figure 4.9: Schematic box diagram showing the structural development of Foula with sinistral oblique faulting and transtensional growth folds.

4.4.1.2. Walls Basin:

The central Devonian basin of Shetland, the Walls Basin, comprises the remainder of the Walls Peninsula (Figure 4.10a) and is the partial onshore expression of the Devonian-Permian West Fair Isle Basin (BGS, 1984). Along the north of the Walls Peninsula, the contact between the Walls Metamorphic Series basement and the Walls Group is generally poorly exposed. In the E, this contact is predominantly faulted, but towards the W, near to the Voe of Snarraness, it becomes an undulating unconformity, which is cut by smaller faults. In many places the contact is at or close to sea-level, precluding detailed observation and inland is often only indicated by a faint break in slope (Mykura et al., 1976b).

The Walls Metamorphic Series outcrops along the N side of the Walls Peninsula as a roughly ENE/WSW trending elongate strip. It comprises mica, hornblende and calc schists, and highly altered limestones (Mykura et al., 1976b). These units are cut by veins of granite and

pegmatites which are likely associated with the emplacement of the nearby Sandsting Complex to the S (Mykura et al., 1976b). The basement has a well-defined foliation which dips towards the S (Figure 4.10b) and is gently folded into S plunging open folds (Figure 4.10a). Lineations in the basement (mineral alignment, minor folds, crinkles, rodding, moulin, boudins) plunge gently towards the S-SSW (Figure 4.10b). The age of the Walls Metamorphic Series is uncertain, although the protolith has been speculatively assigned an Archaean age (Lancaster et al., 2017).

Overlying these rocks are the Devonian sediments of the Walls Group, subdivided into the Walls and Sandness Formations (Mykura et al., 1976b) (Figure 4.2 and 4.10a), separated by the ENE/WSW trending Sulma Water Fault. This fault is interpreted to have been an active normal to sinistral oblique strike slip fault during the development of the basin (M. Seranne, 1992) interpreted as being active during the Devonian (Melvin, 1985, Serrane 1992) and that the two formations are thought to represent the distal and proximal equivalents of the same depositional system (Melvin, 1985, 1977). Both formations are highly deformed and are folded into predominantly ENE/WSW and N/S trending folds (Figure 4.10b and 4.10c).

The Sandness formation lies unconformably on the metamorphic basement of the Walls Metamorphic Series and comprises coarser grained fluvial-alluvial sandstones and conglomerates in the lower part. They become increasingly intercalated with basaltic to andesitic lava flows, ignimbrites, tuffs and acid agglomerates of the Clousta Volcanic series (4.11a) in the upper part of the formation along with finer grained lacustrine and more distal fluvial deposits (Mykura et al., 1976b, 1976a). The Walls Formation comprises mainly finer grained fluvial sandstones, siltstones, shales and rocks that were deposited by braided fluvial systems on a more distal alluvial plain into a rapidly subsiding basin (Melvin, 1985).

The Walls Group is interpreted to have been developed in a small, active, strike-slip influenced intermontane basin with material being shed off mountainous areas to the N and W (Astin, 1982). Sedimentation rates were high as evidenced by the development of widespread load structures, convolute bedding pseudonodules, crevasse splay deposits and flood deposits (Astin, 1982), particularly within the Walls Formation (Melvin, 1985).

In the S of the Walls Peninsula, granites, diorites and minor ultramafic rocks of the Sandsting Complex are intruded into the Walls Group which are dated to between 390-360Ma based on U-Pb in zircon (Lancaster et al., 2017). These ages, together with a Givetian

age derived from palynological studies in the Walls Group (Marshall, 2000) suggest a Mid to Late Middle Devonian age for the Walls Basin, equivalent in age to the South East Shetland Group and John O'Groats Sandstone Group, and therefore younger than the Melby Formation and Foula Sandstone Group.

4.4.1.2.1. Folding:

The rocks of the Walls Group are openly to tightly folded into predominantly W to SW plunging folds and more localised N/S trending folds (Mykura et al., 1976b). In places the bedding is extremely steep (≤90°) (Figure 4.11a), and has been attributed to Devonian age growth folding in the Walls Group (Figure 4.4), (Seranne, 1992) and likely modified by the later intrusion of the Sandsting Complex (Mykura et al., 1976b) and deformation related to subsequent movement along the Walls Boundary Fault (Mykura et al., 1976a). The folds of the Walls Group are cut by the Sandsting Granite complex (Figure 4.11b and 4.11c), which lacks both the folds and pervasive cleavage that is developed in the strata of the Walls Group (Mykura et al., 1976b). Associated minor intrusions also cut the rocks of the Walls Group, however no systematic cutting of these structures by later features is apparent (Mykura et al., 1976b), apart from in the region surrounding the Walls Boundary Fault Zone in the E (Watts et al., 2007).

Associated with the folding, is the development of a strong cleavage (Figure 4.11f), which is particularly well developed in the area around The Hamar and to the SW of Mid Walls. In this area the strata of the Walls Group are locally folded into a series of shorter wavelength (100-200m) folds with localised areas of complexity and detachments (Mykura et al., 1976b) (Figure 4.11g and 4.11h).

Structural data was extracted from published maps in order to understand the geometry and orientation of these folds. The E and S limit of this analysis was Brindister Voe and Vaila Sound respectively in order to avoid the potential influence of the WBF and Sandsting Granite. The Djuba Water Syncline plunges moderately steeply towards the SE (35°→232°) (Figure 4.10) however towards the W this fold dies out and the strata of the Walls Group are tilted even more steeply towards the S, as observed in the Bay of Deepdale (Figure 4.11d and 4.11e). Analysis of both bedding and foliation in the Djuba Water (Figure 4.10c) area has also identified folding of the basement foliation beneath the unconformity in a manner like that of the overlying bedding in the Walls Group. This similarity in fold orientation suggests that the orientation of the foliation prior to deposition of the Walls

Group may have been sub-parallel to the depositional slope and during subsequent folding was incorporated into the fold structure.

To the S of the Sulma Water Fault the Stourbrough Hill Syncline and Watsness Anticline plunge moderately towards the SSW (30°→257° and 34°→242° respectively) (Figure 4.10c), and in the area of The Hamar-Mid Walls-Walls bedding dips are highly variable and more tightly folded. To the S and E, the Walls Syncline plunges moderately towards the E (34°→242°) (Figure 4.10c).

Down plunge projections of these folds (Figure 4.10c) reveal an opening upwards geometry to the folds with increasing interlimb angles as you go up stratigraphy (Figure 4.10c). This geometry together with the internal unconformities identified by Seranne (1992) and the Middle Devonian age of the Sandsting Granite (Lancaster et al., 2017) suggest these fold structures are Devonian in age and were formed during filling and development of the basin, further indicating a tectonically active basin, and in agreement with observations made in the Walls Group by Melvin (1985). It is also suggested that the generation of folds and cleavage occurred whist the rocks were relatively poorly lithified, perhaps whilst still waterlogged as indicated by the presence of fairly convolute bedding in places, attributed to the escape of over-pressured pore fluids and which continued to be modified during early burial (Mykura et al., 1976b) and subsequent deformation.

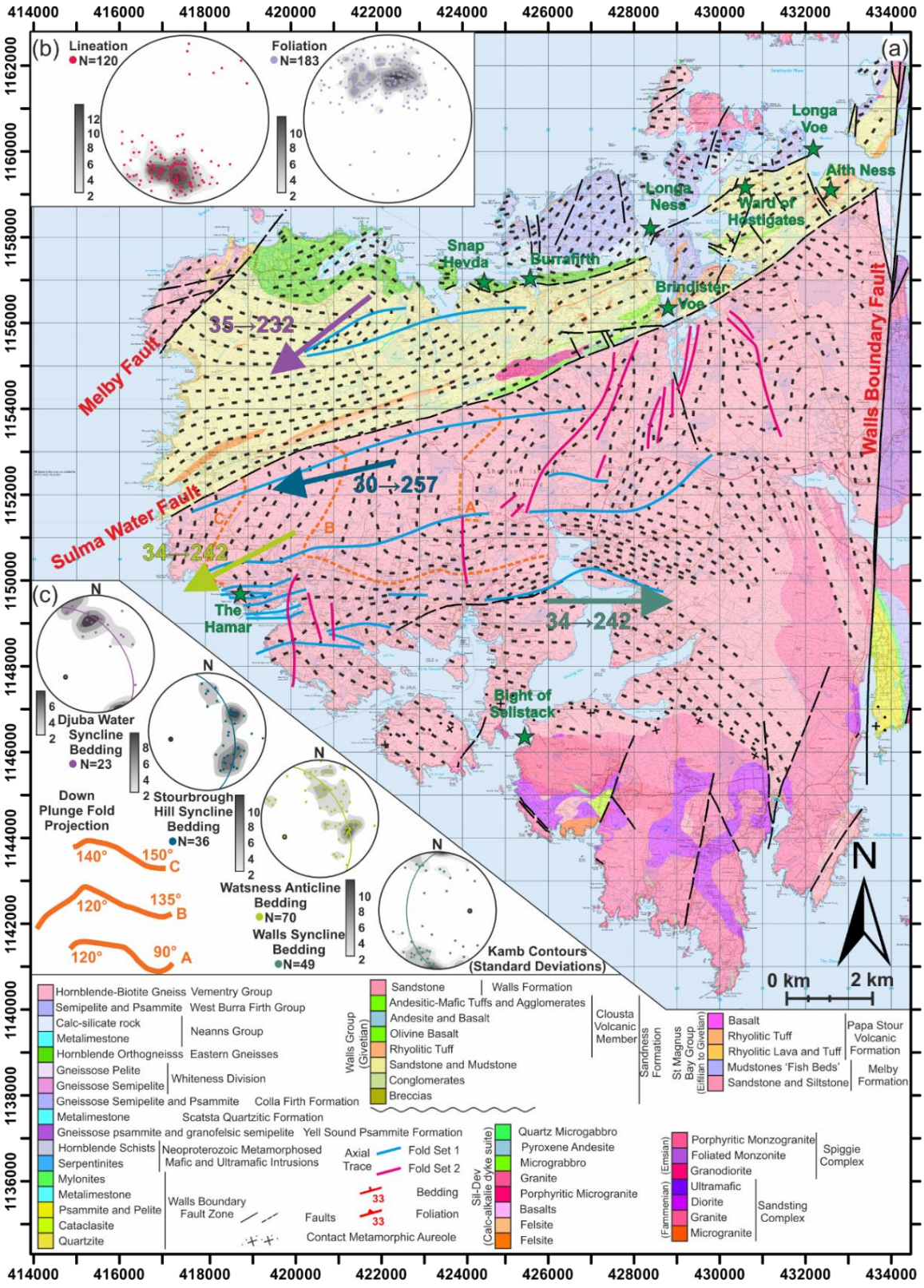

Figure 4.10: Geological map of the Walls Peninsula, Shetland. Modified *after* (BGS, 1971). Coloured arrows denote principal folds structures. Form lines modified *after* (Mykura et al., 1976b, 1976a; Seranne, 1992) (b) Principal structural data for the Walls Metamorphic Series showing predominant S dip of foliation and plunge of the lineations.(c) Stereonets of folds in the Walls Group and down plunge fold projection of the Stourbrough Hill Syncline and Watness Anticline fold pair with approximate interlimb angles. Data coloured according to coloured arrows on the map.

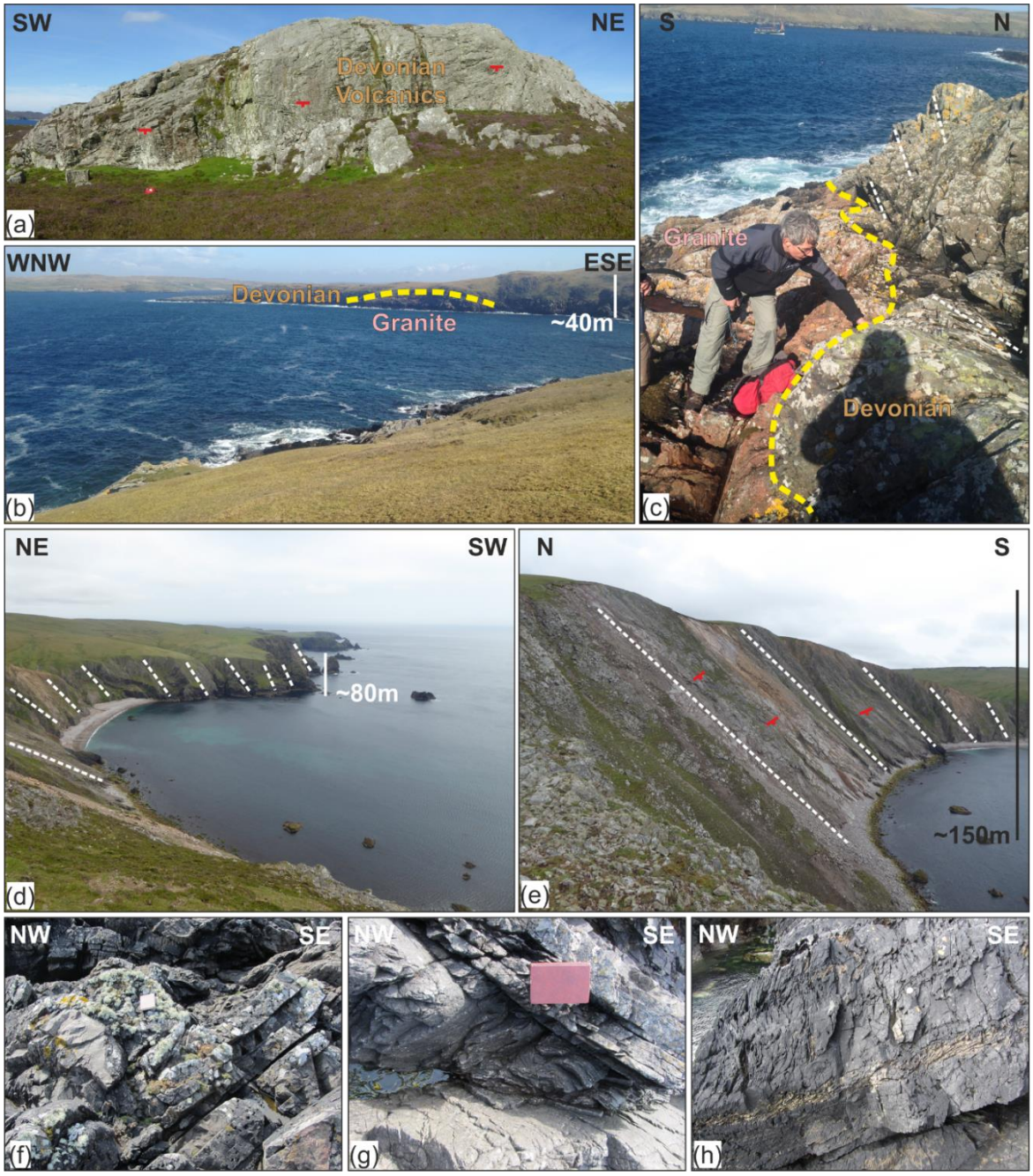

Figure 4.11: Field photographs of structure in the Walls Group; (a) steeply dipping rhyolites of the Clousta Volcanic Member at Aith Ness. (b) and (c) Contact between the Sandsting Granite and strata of the Walls Group near the Bight of Selistack. (d) and (e) Steeply dipping strata of the Sandness Formation in the Bay of Deepdale. The bedding steepens towards the S in proximity to the Sulma Water Fault. (f) and (g) localised folding and detachments in the Walls Formation and (h) well developed cleavage in the area around The Hamar. Photos (f), (g) and (h) courtesy of Bob Holdsworth.

4.4.1.2.2. West Burra Firth and Snarra Ness:

To the NW of Snap Hevda [424174 1156887] on the N coast of the Walls Peninsula near to Snarraness the basement comprises foliated felsic gneisses, psammitic mica schists, granite

sheets and pegmatites. Along the unconformity and faulted against the basement are well sorted, very fine grained to silty sandstones with shaley intercalations which dip steeply towards the S-SW (Figure 4.12a-i). Two predominant fault sets are developed along the unconformity; N/S trending sinistral oblique normal faults which dip steeply towards both the E and W and E/W trending normal faults which systematically drop to the S (Figure 4.10b). A 20cm thick crackle breccia is developed on one larger fault containing angular fragments of sandstone, but also more rounded clasts of granite and quartzite (Figure 4.12a-ii). On NE/SW trending faults and fractures, shallowly dipping fibrous quartz filled tensile fractures are form perpendicular to the fault plane (Figure 4.12a). In some places these are offset along small dextral oblique normal faults (Figure 4.12a-iii). Sigmoidal tension gash arrays are also found adjacent to some of these faults (Figure 4.12a-iv). The degree of fracturing and damage increases in proximity to the unconformity and away from the major faults, a thin veneer of quartz is found to partially infill NW/SE trending tensile fractures within the sandstones and between the foliation planes in the basement.

In the footwall away from the immediate unconformity, the SW dipping foliated basement is subtly folded into S verging open folds (Figure 4.12b) and is cut by three principal sets of faults (Figure 4.12c). The first and predominant set are NNW/SSE to N/S trending sinistral oblique and sinistral strike-slip faults/fault zones which are weathered into deep gullies or 'geos' (Figure 4.12c and 4.12d). Shallow dipping quartz mineralised tensile fractures are developed adjacent to the fault zone. The second set are steeply dipping NE/SW to ENE/WSW dextral oblique faults (Figure 4.12e) which in places are associated with abundant epidote and quartz mineralisation/alteration of sub-vertical amphibolite bodies. A conjugate set of E/W to NW/SE trending S to SE dipping normal faults (Figure 4.12f) which downthrow to the S are associated with a foliated, soft, green tinged fault gouge. Granite sheets in the basement are particularly well fractured with NW/SE trending tensile fractures and NNE/SSW trending shear fractures (Figure 4.12g) and in places appear brecciated or crushed and likely reflects the lack of a pre-existing fabric (i.e. foliation) along which to deform. This mechanical anisotropy is reflected in the foliated basement where well foliated schists deflect faults and preferentially form shear fracture sand are folded in S verging folds (Figure 4.12b), compared to the gneisses and granite sheets which form more brittle tensile fractures or are more brecciated and crushed.

Further inland away from the unconformity, the siltstones and sandstones coarsen into coarse immature sandstones and conglomerates (Figure 4.12h) which outcrop on the hillside S of Snap Hevda [HU 424314 1156764]. The clasts up to cobble/pebble in size, are set in a coarse, angular, immature arkosic matrix and mostly comprise fine grained quartzites granites and coarse pegmatites. They are cut by two sets of faults/fractures which trend NNE/SSW and NW/SE. NNE/SSW structures dip steeply towards the W and have small sinistral oblique normal offsets. Conjugate to these are predominantly NE dipping NW/SE trending, open, tensile fractures.

Normal displacements along E/W orientated faults and sinistral oblique movements along NE/SW and N/S orientated structures would broadly suggest NE/SW to ENE/WSW orientated extension which is partially reactivating a pre-existing basement fabric, observations that are consistent with those made by Seranne (1992), suggesting regional sinistral transtension and reactivation and protracted deformation along the unconformity, accommodating differential movement between the basement and overlying Devonian cover sequences.

Figure 4.12 (overleaf): Field photographs and lower hemisphere equal area stereonets of structural data from the Snap Hevda area [424174 1156887]: (a)(i) overview of the faulted unconformity, (ii) detailed image of the fault breccia, (iii)slickenlines on small dextral oblique normal fault, (iv) sigmoidal tension gash array; (b) detailed image of principal fault zone/unconformity; (c) N/S trending fault zone in the basement which preferentially weather into distinct, deep 'geos'; (d). ;(e) NE/SW faults with dextral offsets; (f) subordinate E/W trending fault zones in the basement; (g) fractured granite with predominantly brittle fractures; (h) coarse sandstones and conglomerates in the Sandness Formation.

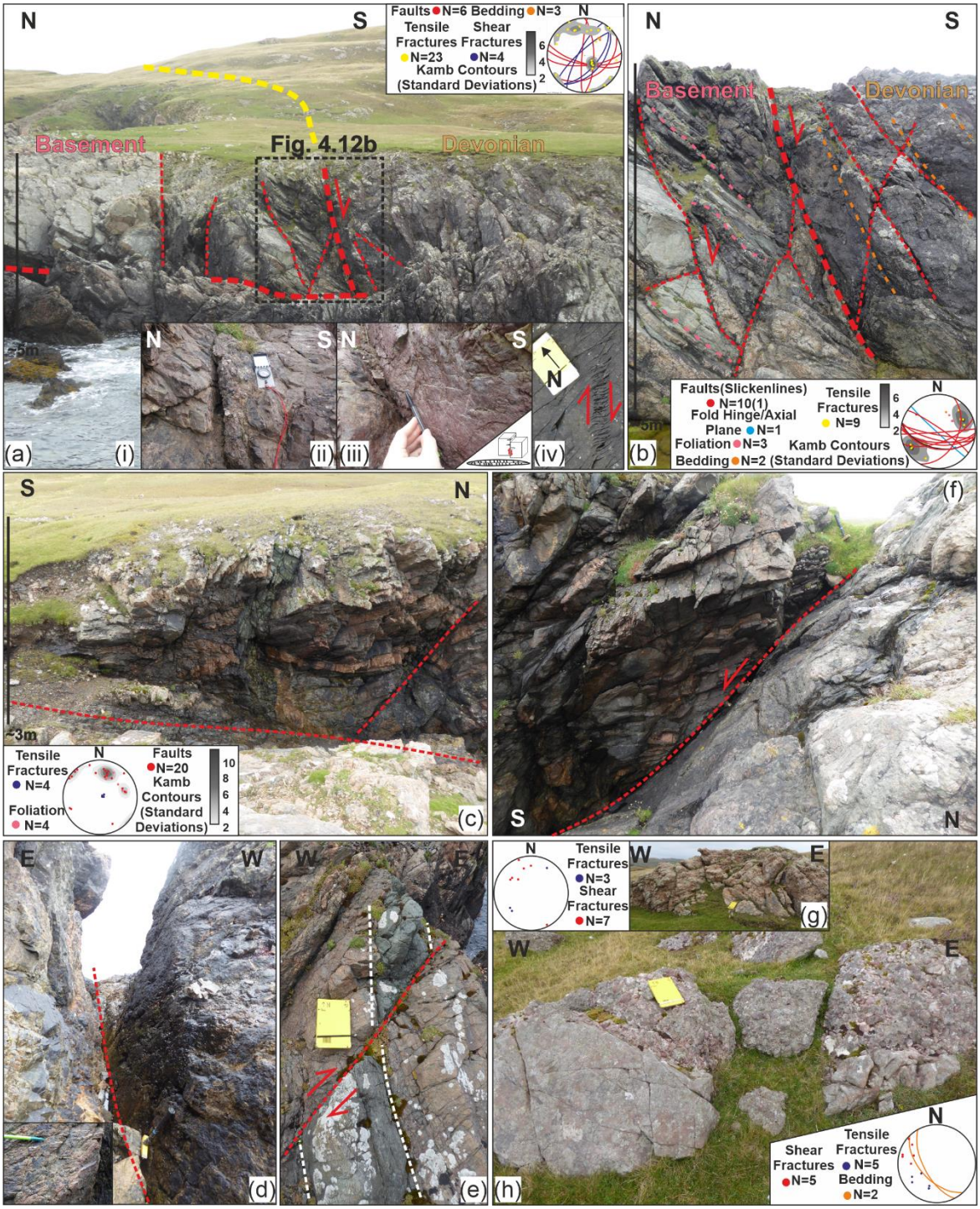

Along strike at Burraview [HU 25050 56910] the basement comprises E/W trending, well foliated felsic orthogneisses, garnet bearing, mafic gneisses with garnetiferous veins, foliated amphibolites with epidote rich layers and granitic/pegmatic sheets up ~10cm thick (Figure 4.13a) which dip towards the SW (Figure 4.13f). The Devonian sedimentary rocks comprise massive, well cemented, fine grained, arkosic sandstones. Adjacent to the Jetty near West Burrafirth [HU 25410 56915] the contact is faulted along two S dipping faults. The first is largely obscured beneath grass (249/80/SE) (Figure 4.13b) and the second (270/81/N) is only observed in the basement where it has ~2cm of soft reddish fault gouge

and fault breccia. These faults offset the unconformity by about 40-50 cm and in the footwall the foliation steepens and has been is dragged into the fault zone. The bounding fault is traced through the harbour onto the opposite shoreline [HU 25739 56921] where it steepens to vertical (257/90/SSE) and has thicker 6-7cm of foliated red fault gouge (Figure 4.13c). The basement is cut by numerous N/S to NE/SW trending fractures and faults with small cm scale sinistral offsets (Figure 4.13e). In places, smaller faults splay off and shallow away from the larger faults to join the dipping foliation (Figure 4.13d) which in places is brecciated where the foliation planes have slid past one another and vuggy quartz lined cavities are developed (Figure 4.13e).

These observations suggest NE/SW orientated extension, with normal displacements along E/W orientated faults and sinistral oblique movements along NE/SW and N/S orientated structures.

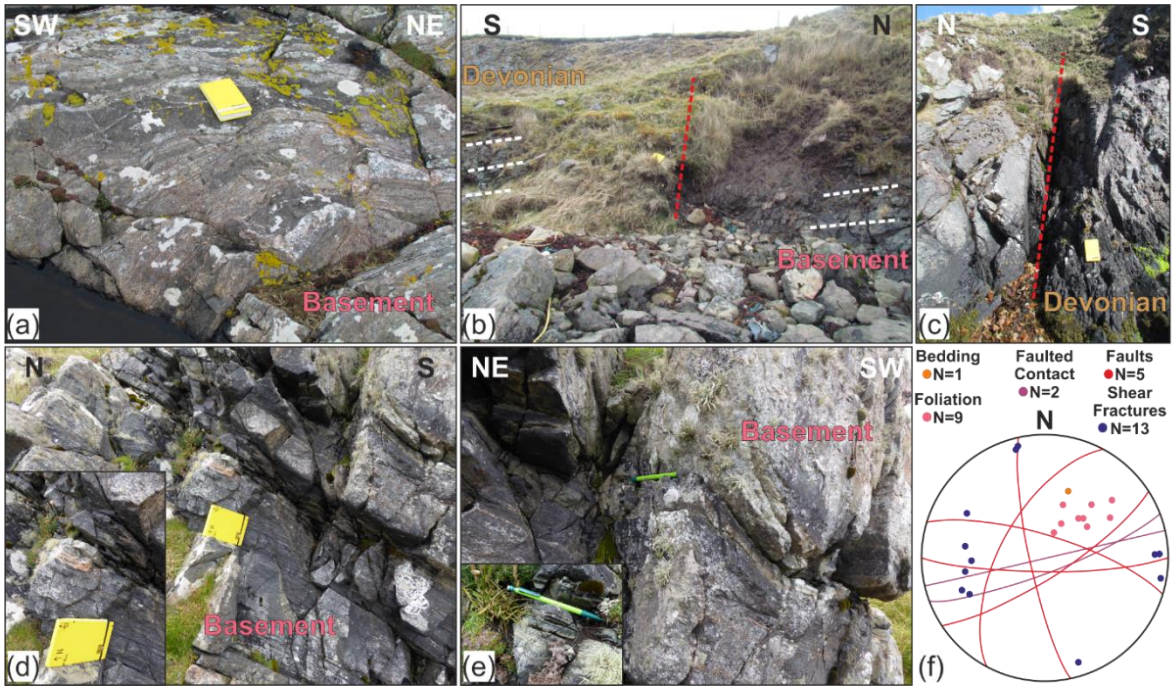

Figure 4.13: Field photographs from the Burrafirth area; (a) foliated basement; (b) faulted contact N of the West Burrafurth Jetty; (c) faulted contact opposite the harbour; (d) dipping foliation with granite sheets and veins; (e) folded foliation around smaller faults with *inset* vuggy cavity from weathered epidote rich layers; (f) lower hemisphere equal area stereonet of structural data from the Burrafirth area.

4.4.1.2.3. Brindister Voe to the Ward of Hostigates:

In the area around Brindister Voe, the trend of the unconformity changes from E/W to NE/SW. At Longa Ness [HU 428397 1157919] a steeply dipping NE/SW (219/75/SW)

trending fault juxtaposes rubbly and highly brecciated sandstones against foliated basement similar to that in the Burrafirth area (Figure 4.14a). On the fault plane, a thin (several mm) smear of red cataclasites/fault gouge and fine fault breccia is developed with slickenlines indicating normal displacement. In the footwall, several subordinate fault zones (Figure 4.12b) are developed in the foliated schistose basement rocks and is highly fractured particularly in areas where it is more granitic or gneissose (Figure 4.14c). Along strike, in the area around the Ward of Hostigates the unconformity trends NE/SW from Sonso Ness [HU 429660 1158700] towards Longa Voe [431967 1159874] and is poorly exposed along the shoreline around Cribba Sound. Inland a break in slope (Figure 4.14d), provides some indication of its location and in outcrops above the unconformity, bedding in arkosic sandstones dips steeply towards the S (239/60/SSE) and is cut by numerous sub vertical (Figure 4.14e) and bed parallel tensile quartz veins (Figure 4.14f). S of Longa Voe the contact appears to be faulted although largely inaccessible (Figure 4.14g).

Poor outcrop and increasing proximity to the Walls Boundary Fault Zone precludes a detailed summary of the Devonian structural evolution in this area, however the steep dip of bedding, the bedding parallel tensile veins in the Sandness Formation and development of fault breccias and gouges in this area are consistent with being associated to Devonian basin development.

Figure 4.14 (overleaf): Field photographs from the unconformity on the Walls Peninsula; (a) steeply dipping fault zone with reddish fault gouge at Longa Ness [HU 428397 1157919]; (b) subordinate fault zones with further red fault gouges and red staining; (c) highly fractured granitic basement; (d) break in slope along trace of the unconformity looking towards Vementry at Sonso Ness [HU 429768 1158778]; (e) quartz veining in massive Devonian sandstones; (f) tensile quartz veins along bedding planes of thinly bedded sandstones (g) trace of fault S of Longa Voe [431967 1159874].

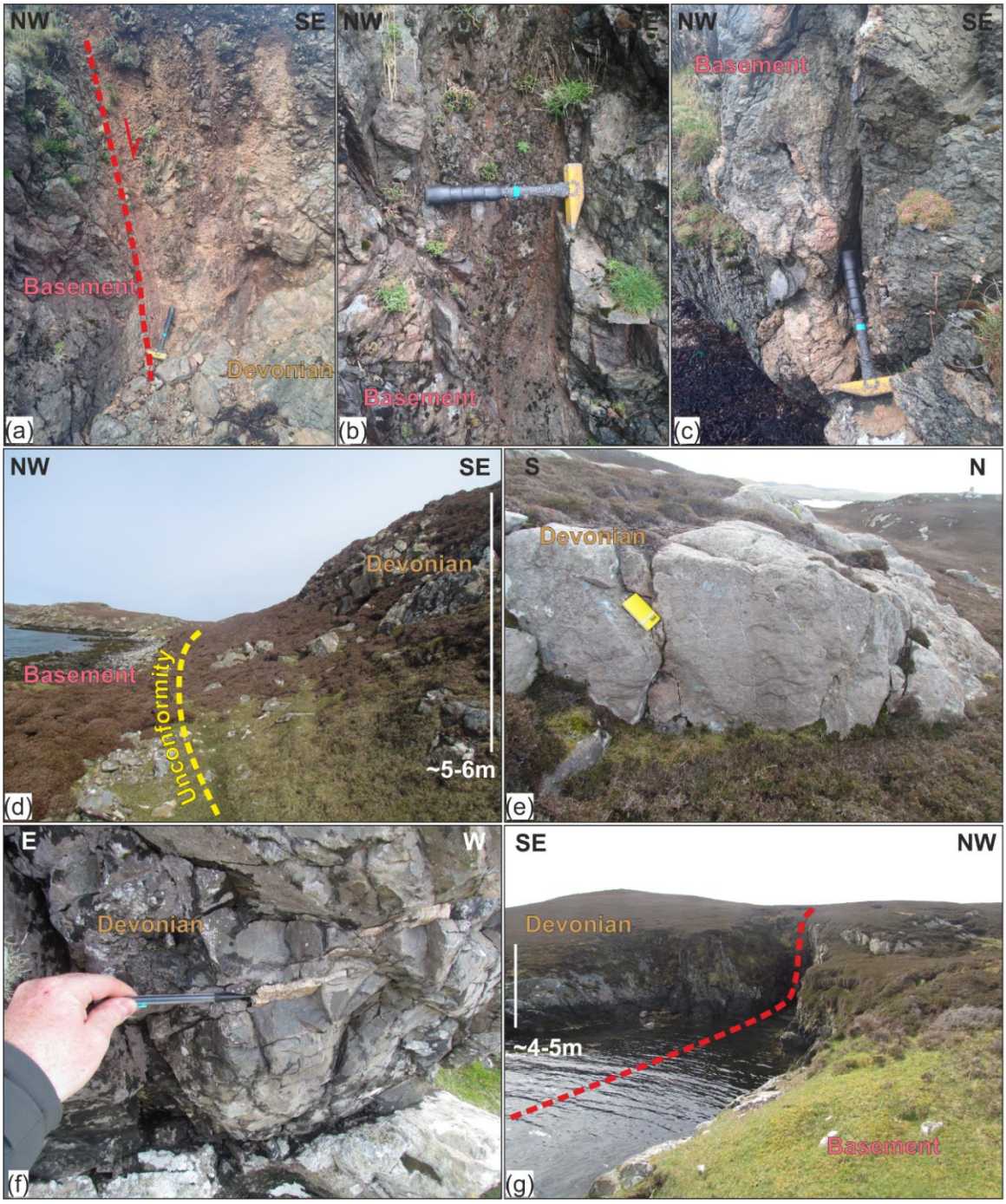

4.4.1.2.4. Walls Basin Summary:

Observations from the Walls Basin suggest a highly dynamic and tectonically active basin. The orientation and kinematics of structures in the Walls Basin suggest broadly NE/SW to ENE/WSW orientated extension. This is also suggested by (Seranne, 1992) who proposed sinistral shearing along ENE/WSW orientated basement faults, which act as transfer faults to ENE/WSW orientated extension. The orientation of growth folds oblique to the major basin bounding fault (the N/S orientated Walls Boundary Fault) are consistent with models of regional sinistral transtension where folds hinges rotate into parallelism with the principal extension direction (Fossen et al., 2013). These observations together suggest a

strongly strike-slip influenced, perhaps pull-apart basin during its development in the Devonian and may help to explain the significant extrusive and intrusive volcanism in the Walls Basin.

Later deformation in the Walls Basin is less certain, however Seranne (1992) identifies some dextral strike-slip indicators on faults cutting the Sandsting Granite, indicating a later E/W to NE/SW orientated compressive event. These observations are also complimentary to those made at Melby (see chapter 4.4.1.1) where evidence for NW/SE to E/W compression is observed, together with dextral strike-slip related to the juxtaposition of the two basins during inversion. The orientation of thrusts at Melby may indicate NW/SE compression, counter to the suggestion of broadly E/W orientated compression in the Walls Basin, however this can be explained by dip of the Melby Formation towards the SE, providing a pre-existing weakness that can be reactivated and thus not forming structures in an ideal orientation. These observations however, do not preclude a model of E/W compression related to regional Carboniferous inversion (Dichiarante, 2017; Seranne, 1992).

4.4.1.3. South-Eastern Shetland Basin:

The easternmost Devonian basin of Shetland extends from Rova Head, N of Lerwick to Sumburgh Head at the S end of Shetland and may extend much further to include the island of Fair Isle (Mykura, 1972a), some 35km S of Sumburgh Head (Figures 4.4, 4.15 and 4.16). The unconformity and basin margin outcrops in several places along the coastline at Rova Head, in the Lerwick and Quarff areas, the Bay of Okraquoy, Aith, in the Sandwick area, near Levenwick and around the Bay of Quendale. Inland outcrops of the unconformity and contact are poorly exposed.

The basin fill typically comprises localised basal breccias which are overlain by more widespread conglomerates and pebbly sandstones that are interdigitated with lacustrine flagstones. Together this sequence comprises the Sumburgh (or South East Shetland) Group and is dated biostratigraphically to the Middle Devonian Givetian (Newman and Den Blaauwen, 2018) and correlated with the Eday sequences in Orkney (Figure 4.2). However the faunal assemblage in these rocks indicates that the basin remained largely isolated from the main Orcadian Basin except during lake highstands, which are believed to have provided connectivity between otherwise isolated sub-basins (Newman and Den Blaauwen, 2018).

The SE Shetland Basin is sub-divided into two smaller sub-basins, separated by a localised basement high in the Quarff-Cunningsburgh area (Mykura et al., 1976a). The Devonian sequences of the basin generally dip gently offshore towards the E and ESE, dipping more steeply in the Sumburgh area. To the N of the basement high, in the Lerwick area (Figure 4.15), the strata are folded into a series of shallowly plunging open E to SE trending folds (Serrane, 1992). To the S of the basement high, the strata are folded into S trending, more steeply plunging folds (Figure 4.16; Serrane, 1992).

The SE Shetland basin is cut by two N/S orientated 'steep belts' which are associated with locally inverted and steeply inclined Devonian strata, irregular masses of sediment-breccia, volcanic vents and dykes of tuffsitic breccias, hydrothermal carbonate mineralisation and minor deposits of base metal sulphides (Fe, Cu). These steep belts correspond to near vertical limbs of monoclinal structures developed overlying likely N/S trending fault/fractures zones in the basement (Mykura et al., 1976a). The age of this deformation and mineralisation has been assigned a Permian-Carboniferous age and is deemed to be equivalent to similar mineralisation observed on Fair Isle (Mykura and Harrison, 1972) and may also be equivalent in age to monchiquite vents and dykes and the associated mineralisation that can be observed in Orkney and Caithness (Baxter and Mitchell, 1984; Mykura, 1972b; Rock, 1983) and dated to the Permian (267.5±3.4Ma) (Dichiarante et al., 2016).

4.4.1.3.1. Folding:

To the N of the basement high, the basin is folded into four open fold structures (Figure 4.15). Furthest N and E are the Noss Syncline which plunges shallowly to the ESE (7°→116°) and the Bressay Syncline which plunges more steeply towards the ENE (17°→084°). These two structures may actually be one larger fold structure, however, have been modified and cut in two by faults associated with the N/S orientated 'steep belt'. In the N, around Rova Head and Lerwick is a poorly defined, SE orientated, shallowly plunging anticline which is truncated by the 'Steep Belt'. In the Gulberwick and Voe of Sound area, the strata are folded into almost horizontally plunging syncline which also trends towards the SE (3°→136°).

To the S of the basement high, the sub-basin appears to be one larger synclinal structure (Figure 4.16), which plunges shallowly to moderately towards the SSE (18°→169°). The fold seems to shallow towards the S, plunging most steeply in the area around Mousa and

Sandwick (24°→179°), shallowing slightly in the Levenwick area, which is roughly in the hinge zone of the fold (18°→196°) before flattening in the Sumburgh area (7°→185°).

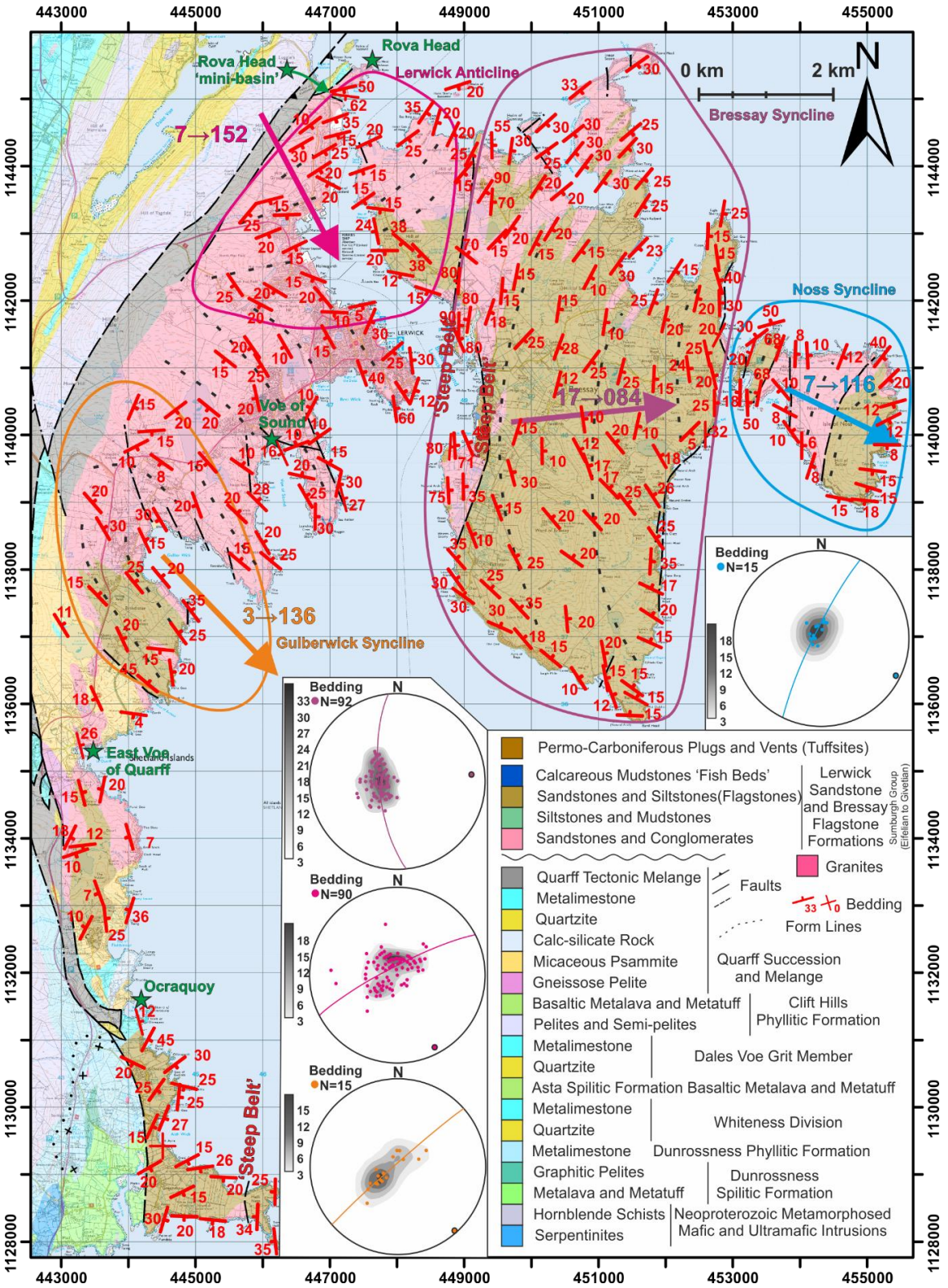

Figure 4.15: Geological map of the Lerwick area showing major fold structures. *Inset* lower hemisphere equal area stereonets of major folds. Map modified *after* (BGS, 1978a, 1978b). Coloured arrows indicate the orientation of principal fold structures.

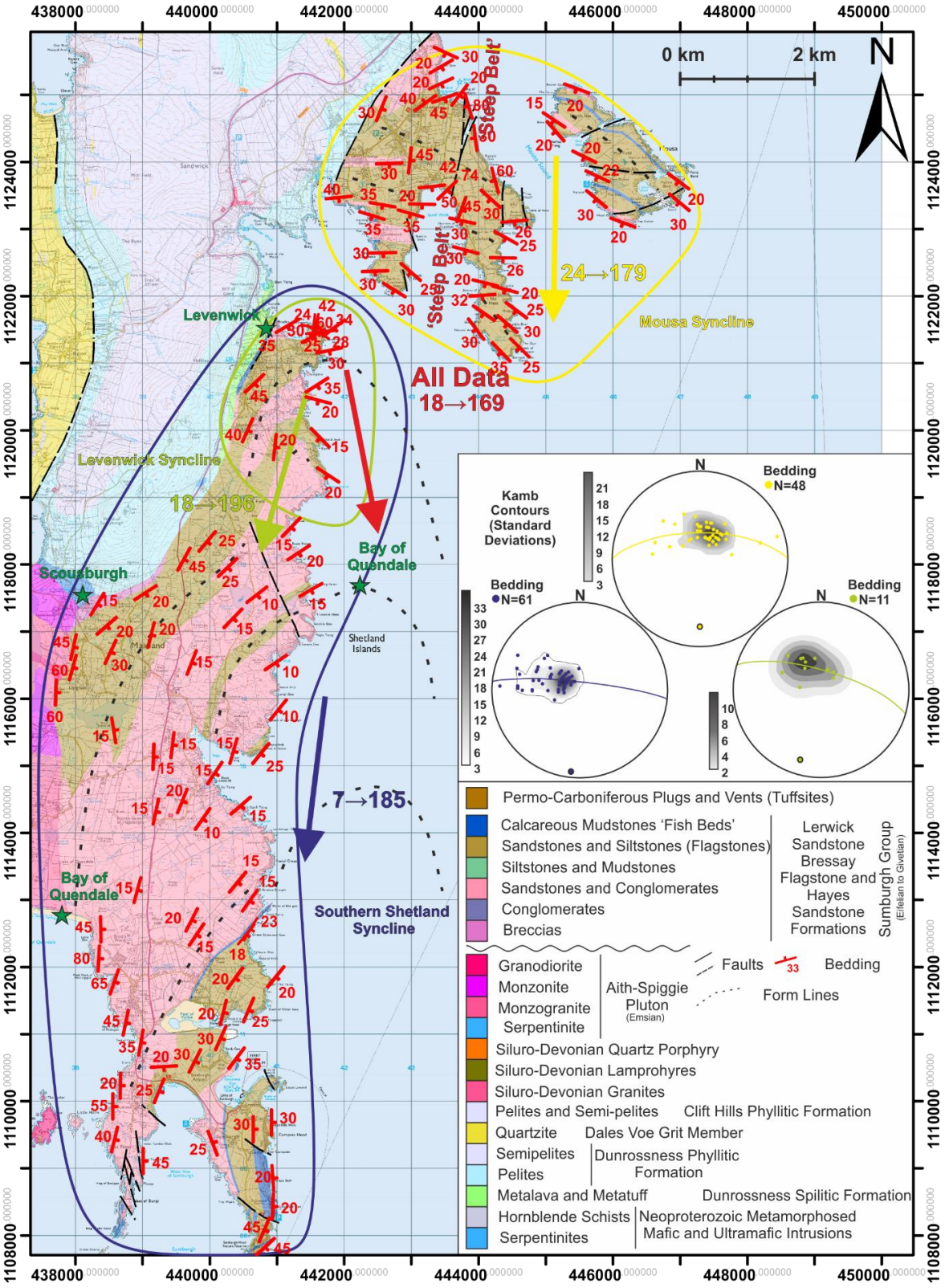

Figure 4.16: Geological map of the Sumburgh area showing major fold structures. *Inset* lower hemisphere equal area stereonets of major folds. Map modified *after* (BGS, 1978a, 1978b). Coloured arrows indicate the orientation of principal fold structures.

4.4.1.3.2. Rova Head and Lerwick:

In the area surrounding the lighthouse at Rova Head [HU 447616 1145473], which is approximately within the hinge of the Rova Head anticline, highly deformed Middle Devonian breccias, conglomerates, sandstones, siltstones and shales of the Lerwick Sandstone Formation (Mykura et al., 1976a) are juxtaposed against and partially overly and onlap an erosional and faulted unconformity which is intermittently exposed along the shoreline(and described in detail by Seranne, (1992)). The basement comprises highly sheared and deformed limestones, quartzites, pelitic schists and phyllites of the Quarff succession and tectonic melange which trend N/S and are intensely deformed (Mykura et al., 1976a; Seranne, 1992). Overlying breccias and conglomerates are composed of pink granitic material, local metamorphic basement and clasts of previously cemented angular fragments that have been reworked and partially rounded, indicating extensive transport and reworking.

Sheets of faintly imbricated, clast supported conglomerates of the Lerwick Sandstone Formation onlap onto basement around the area of Rova Head, which are well exposed in road sections [HU 46830 44397] and around the coastline where they are less intensely deformed (Figure 4.17a). The sheets of conglomerate are separated by more matrix supported conglomerates, immature sandstones with pebble-cobble lags and siltstones and dip gently (~20) towards the SE. These sheets fine and spread out away from the unconformity towards the town of Lerwick, becoming sandier towards the S and E where they feather into pebbly sandstones and siltstones. Lenses of finer grained material in these units show faint cross lamination, which increase in size with an increase in grain size forming reasonably well-defined cross bedding. The clasts, up to 20cm in size are predominantly composed of quartzite and granite, are very well rounded, and moderately spherical. The clasts are set in a matrix of angular, very coarse to coarse, poorly sorted, arkosic sand. Rare, E/W trending dextral, steeply dipping shear fractures form en-echelon fracture corridors in these units. Fractures in the corridors tend to wrap around clasts, reflecting a mechanical anisotropy between the matrix and the clasts. Where clasts are cut by brittle fractures, they largely remain open, however some are mineralised with a small quantity of quartz (Figure 4.17b).

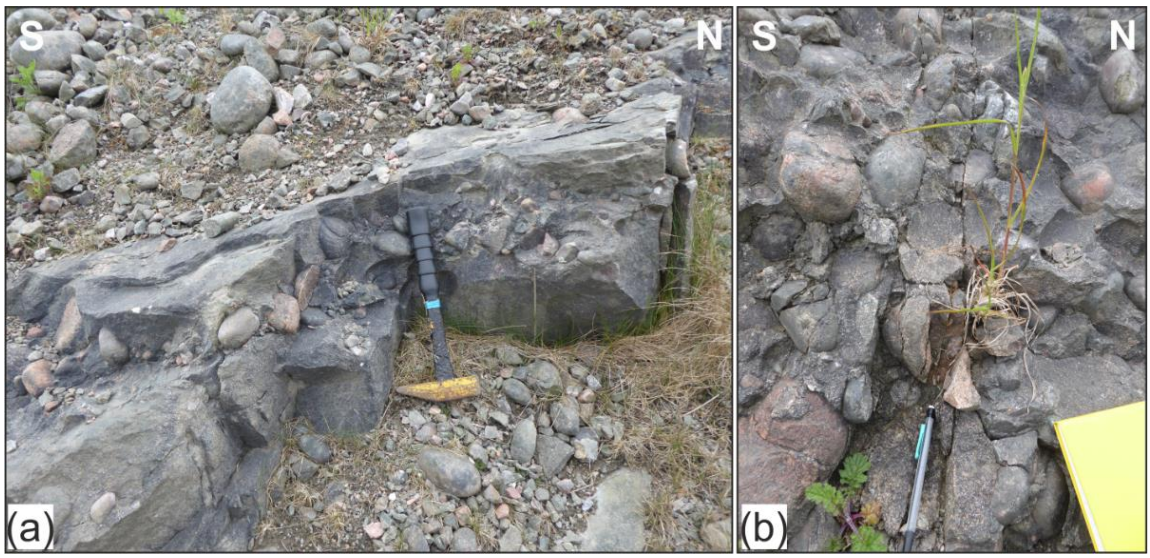

Figure 4.17: Field photographs of (a) matrix supported conglomerates and sandstones cut by (b) E/W trending fracture corridors.

To the S of the lighthouse at Rova Head [447128 1145001], a small fault bound half graben or 'mini-basin' (Figure 4.18a) orientated ESE/WNW to NW/SE is tightly folded into a shallowly plunging, roughly E/W trending syncline (Figure 4.18b). The bounding fault trends ESE/WNW (4.18c), dipping towards the N with two set of slickenlines. One set shows strike-slip motion and are horizontal, however the second set show dextral oblique motion complimenting open, tension gashes that are developed on the fault surface which trend NW/SE (Figure 4.16c). Adjacent conglomerates overstep and erode down into this mini-basin (Figure 4.18d).

In the hangingwall, the half graben is infilled with laminated siltstones and fine-grained sandstones that fine into the centre of the half-graben and conformably overly conglomerates. Locally these sediments are folded into tight NW/SE trending folds which generally plunge towards the NW with a dextral vergence (4.18e).

In the footwall, bedding dips ~30° towards the NW (Figure 4.18a), steepening towards the N and in proximity to the bounding fault. Here sheets of breccias-conglomerates and coarse-grained sandstones (4.18f) are cut by a series of N/S trending faults and fracture corridors. Sinistral oblique slickenlines are found on some N/S faults, with dextral oblique slickenlines on conjugate NW/SE trending faults (4.18g). Associated with these structures are N/S orientated shear fractures and deformation bands which are cemented with quartz (Figure 4.18h and 4.18i).

In the area immediately to the W of the Rova Head Lighthouse N/S trending brittle faults dip steeply to the W, together with discrete fracture corridors and NE/SW trending shear zones which increase in frequency towards the contact with the basement. In places the conglomerates are highly deformed, with brecciation of the conglomerates, variable bedding dips and in places clasts appear to have been torn apart by the generation of numerous tensile fractures. Offset of broken cobbles indicate predominantly W down normal motion on these structures however rare sinistral normal slickenlines may be found indicating some degree of obliquity. Fractures in this area are highly irregular and in places bend around cobbles in the conglomerates forming a strong cleavage. Many fractures are also associated with rare calcite veining potentially related to dissolution and re-precipitation of local carbonaceous material in the Quarff melange.

Seranne, (1992) summarises the deformation in this area as being related to extension with a significant component of left-lateral slip that was active during sedimentation. The 'mini basin' developed in this location indicates an early phase of faulting in which fine grained sediments were deposited, perhaps due to the development of a localised 'hollow' causing ponding of water and deposition of fine grained sediments, in an otherwise coarse clastic setting. These observations indicates an early, localised phase of faulting and syndepositional growth folding which are likely related to NE/SW to E/W sinistral oblique extension along the basin margin in the Rova head area in agreement with observations made by Seranne, (1992).

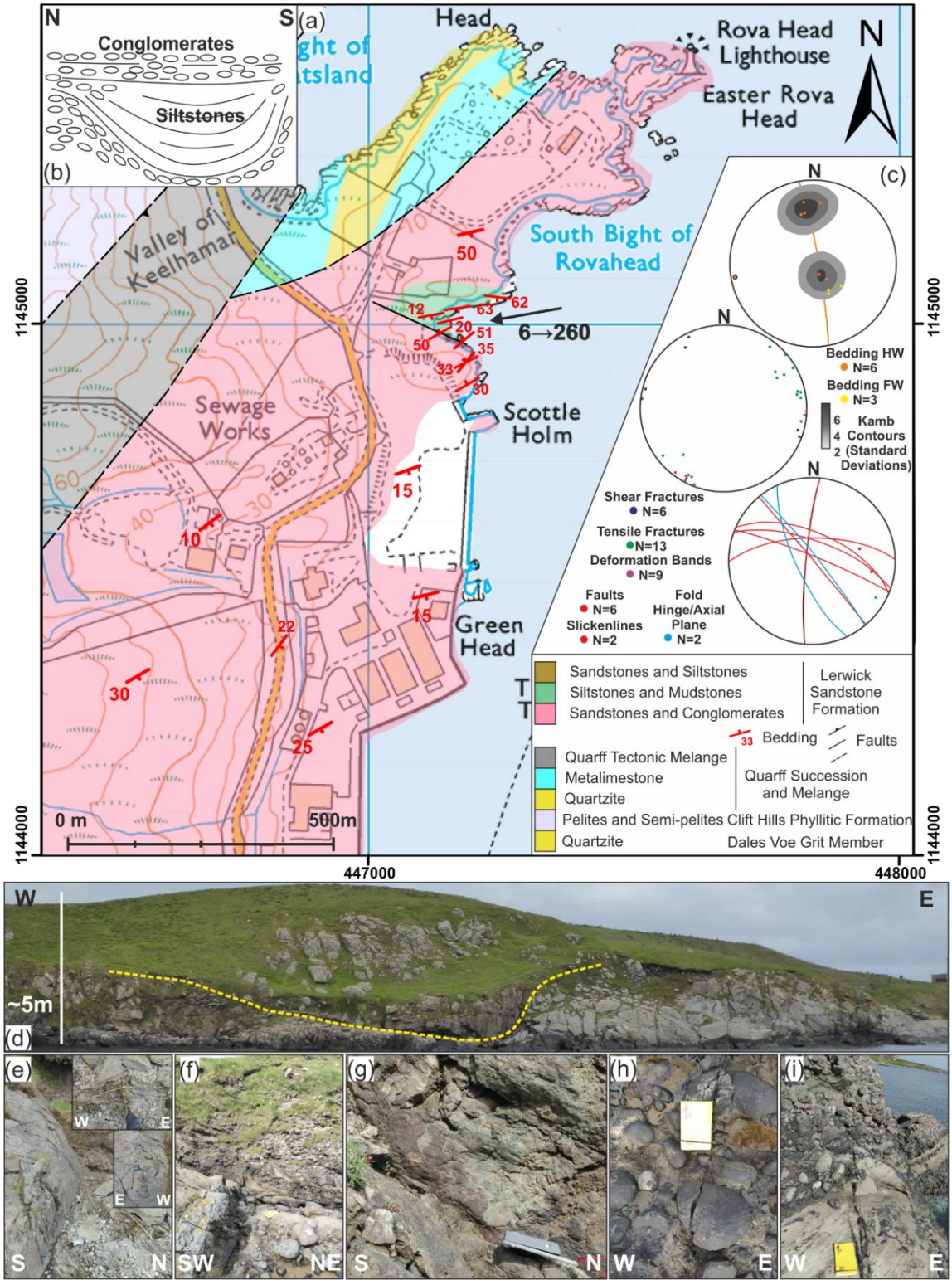

Figure 4.18: (a) Geological map of the Rova Head area. Map modified *after* (BGS, 1978a, 1978b). (b) Sketch cross section through half graben. (c) Structural data from the Rova Head 'mini-basin'. Lower hemisphere equal area projection. (d) Overview image of localised unconformity and downcutting conglomerates. Detailed field photographs of (e) basin margin fault plane showing *inset* localised folding and tensile fractures, (f) Interbedded conglomerates and sandstones cut by N/S trending faults with sinistral oblique slickenlines (g), (h) and (i) shear fractures cutting through the conglomerates.

4.4.1.3.3. Voe Of Sound:

In the Lerwick area at the N end of the Voe of Sound [HU 446314 1139783], on a limb of the Gulberwick syncline, W dipping conglomerates are locally developed around a fault that is ~2km from the basin margin unconformity (Figure 4.19a) with the Quarff Melange near the Hill of Dale [HU 444161 1141373] to the NW. The conglomerates comprise well-rounded clasts up to 30cm in size which in places are faintly imbricated. They are interbedded with angular, pebbly, cross bedded sandstones and thin sheet sandstones. Where coarsest, the conglomerates are clast supported, but most are supported by a matrix of poorly sorted, very coarse to granular sand.

The main structures in this area are N/S to NNW/SSE, E dipping normal faults (Figure 4.19b) and discrete fracture corridors (Figure 4.19c and 4.19d). Offset on these faults is generally small with most having cm to dm offsets which is picked out by thin sandstones (Figure 4.19e). Conjugate to these structures are NE/SW, predominantly NW dipping dextral oblique normal faults and shear fractures. Both sets of structures are un-mineralised, with fractures generally forming clean breaks through clasts (Figure 4.19f and 4.19g). However, towards the tips of smaller faults, fractures tend not to break clasts but instead wrap around the larger clasts. The lack of clear cross-cutting relationships observed, suggests these structures are coeval.

The orientation and clean-break nature of these structures are consistent with being developed during the Devonian during regional sinistral oblique transtension and with small offsets developed on numerous small faults leading to the development of thicker localised deposits, which in this case are coarse conglomerates.

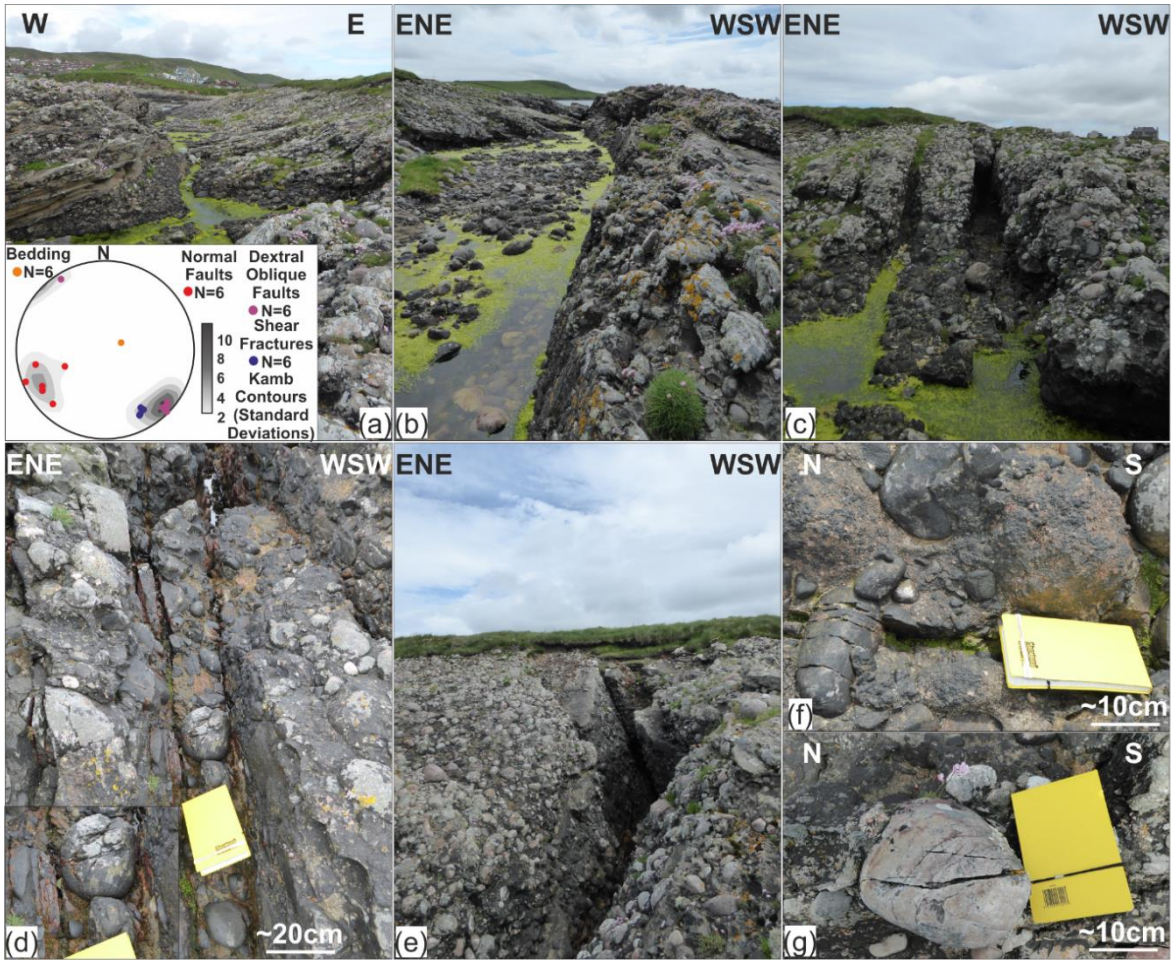

Figure 4.19: Field photographs from the Voe of Sound [HU 446314 1139783]; (a) W dipping conglomerates and sheet sandstones and *inset* stereonet of data showing key structures; (b) N/S trending normal fault; (c) fracture corridor; (d) fracture corridor margins corresponding to large cobble size clast; (e) dm scale offsets picked out by thin sandstones and; (f),(g) clean break shear fractures through clasts.

4.4.1.3.4. East Voe of Quarff:

Along on the coastline near to the East Voe of Quarff [HU 43262 35375] a highly erosional unconformity exists between the Middle Devonian age breccias of the Lerwick Sandstone Formation and metamorphic basement comprising foliated micaceous psammites and granites/pegmatites of the Quarff Succession and melange. Here the basement is well foliated and dips shallowly (~10°S) towards the south and contains thin granites and quartz/feldspar/mica rich pegmatites with crystals up to 1cm in size. The basement is cut by a fine grained, mafic, igneous grey-green dyke containing amphibole, hornblende, and olivine (Figure 4.20a and 4.20b).

The basement is overlain by crudely and faintly bedded sheets of breccia-conglomerates which dip shallowly offshore (~26°E) (Figure 4.20c). The unconformity is highly irregular (Figure 4.20b), with several metres of topography, reflecting a highly eroded Pre-Devonian land surface. At the base of steeper sections of the unconformity, slumping and shearing is evident which indicates down slope motion and/or differential compaction (4.20b).

The breccia-conglomerates are comprised of clasts 30-40cm up to boulders in size and generally matrix supported. Many clasts are more oblong in shape, due to the foliation within the basement clasts, and close to the unconformity are smaller and more angular (Figure 4.20d). However, many are more rounded, particularly the smaller pebble to cobble sized clasts which indicate longer transport distances, and/or more extensive reworking. The matrix is composed of red-brown, poor to moderately sorted coarse to fine grained sand which is quartz/feldspar dominated but is mica rich reflecting derivation from the local mica rich basement. Lenses of fine grained red/brown sand with grading, planar tops and an uneven base indicate settling out of water (Figure 4.20e). Brittle fractures in the basement, cleaved open foliation planes and abundant brittle fractures in the basic dyke in the basement are infilled with this same fine-grained sedimentary matrix (Figure 4.20f, 4.20g and 4.20h) and also mineralised with small quantity of iron-rich minerals.

Cutting the conglomerates are numerous, small N/S trending normal faults, which dip 60-70° towards the E and W (Figure 4.20g). Faults in places have a minor quantity of faint reddish, fine grained fault gouge, but lack visible slickenlines and are generally clean, through-going breaks, as observed by the sheared clast, see Figure 4.20j. Smaller fractures trend N/S with subordinate E/W fractures and joints acts as transfer structures for the main N/S trending faults.

In summary the area around the East Voe of Quarff preserves a relatively quiescent location, away from the influence of major faults and major folds, with deposition being principally controlled by regional, far-field tectonics, principally subsidence. The substantial topography of the unconformity surface likely had a strong control on deposition, which likely happened rapidly during flash-flood events, as indicated by the large size of breccias clasts but also from the presence of fine grained interstitial material and fracture fills in the basement. Indistinct faults with normal displacements in the conglomerates indicate roughly E/W orientated extension and slumping suggests down slope movement driven by the topography of the unconformity.

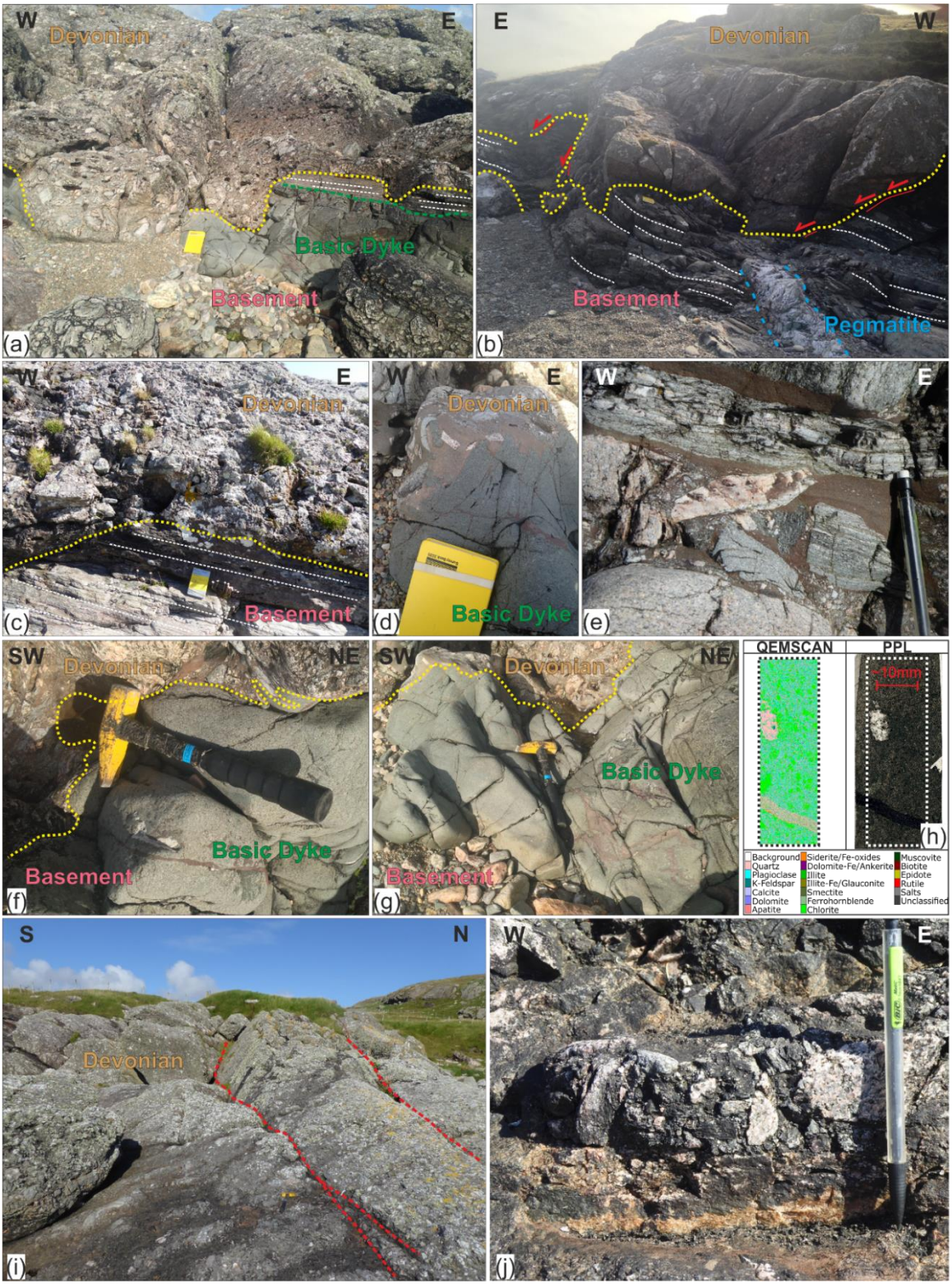

Figure 4.20: Field photographs from in and around Foula Geo [HU 443269 1135385], East Voe of Quarff, Shetland; (a) and(b) undulating, m-scale topography of the unconformity; (c) clast supported conglomerates; (d) mafic dyke in basement with sediment filled fractures showing fragments of basement floating in brown sandy matrix; (e) grading in sediment fills and matrix of the basal breccia; (f) and (g) sediment filled fractures in the dyke; (h) thin section and Qemscan image of sediment filled fracture. Fracture infilled with very fine grained to silt size quartz, feldspars

and clays minerals; (i) small normal faults cutting basal breccia/conglomerate and (j) detail image of fault surface showing clean breaks through clasts.

4.4.1.3.5. Ocraquoy

In the Ocraquoy area [HU 444164 1131311], an undulating unconformity comprising series of small basement highs, preserve a Pre-Devonian topography separates isolated areas of Devonian sedimentary rocks which is bound to the W by the Quarff melange and its associated faults. This area corresponds to the larger basement high that separates the two sub-basins that comprise the SE Shetland Basin and appears to be unaffected by the larger scale folding observed to the N and the S.

However, due to the presence of a large quantity of landslip material and much of the unconformity being close to sea-level detailed examination is difficult. Here, the basement comprises foliated hornblende schists and crystalline limestones which dip shallowly towards the E (Figure 4.21a). These are unconformably overlain by basal breccias, sandstones and minor siltstones which also dip shallowly towards the E (Figure 4.21b).

Locally, there is much alteration of the basement and Devonian cover sequences by later 'steep belt' mineralisation and many N/S trending vertical fractures up to 10cm in width, infilled with tuffsite breccias and carbonate minerals (Figure 4.21c and 4.21d). Small, dm scale, W dipping, low angle, E verging thrusts are also well-developed in the basement, likely due to the presence of more ductile minerals such as mica.

Little of the original Devonian structure is apparent in this locality other than the shallow dip of the strata towards the E. The majority of deformation structures in this area are associated with the development of the 'Steep Belt'(Mykura et al., 1976a) as indicated by the pervasive development of mineralised breccias.

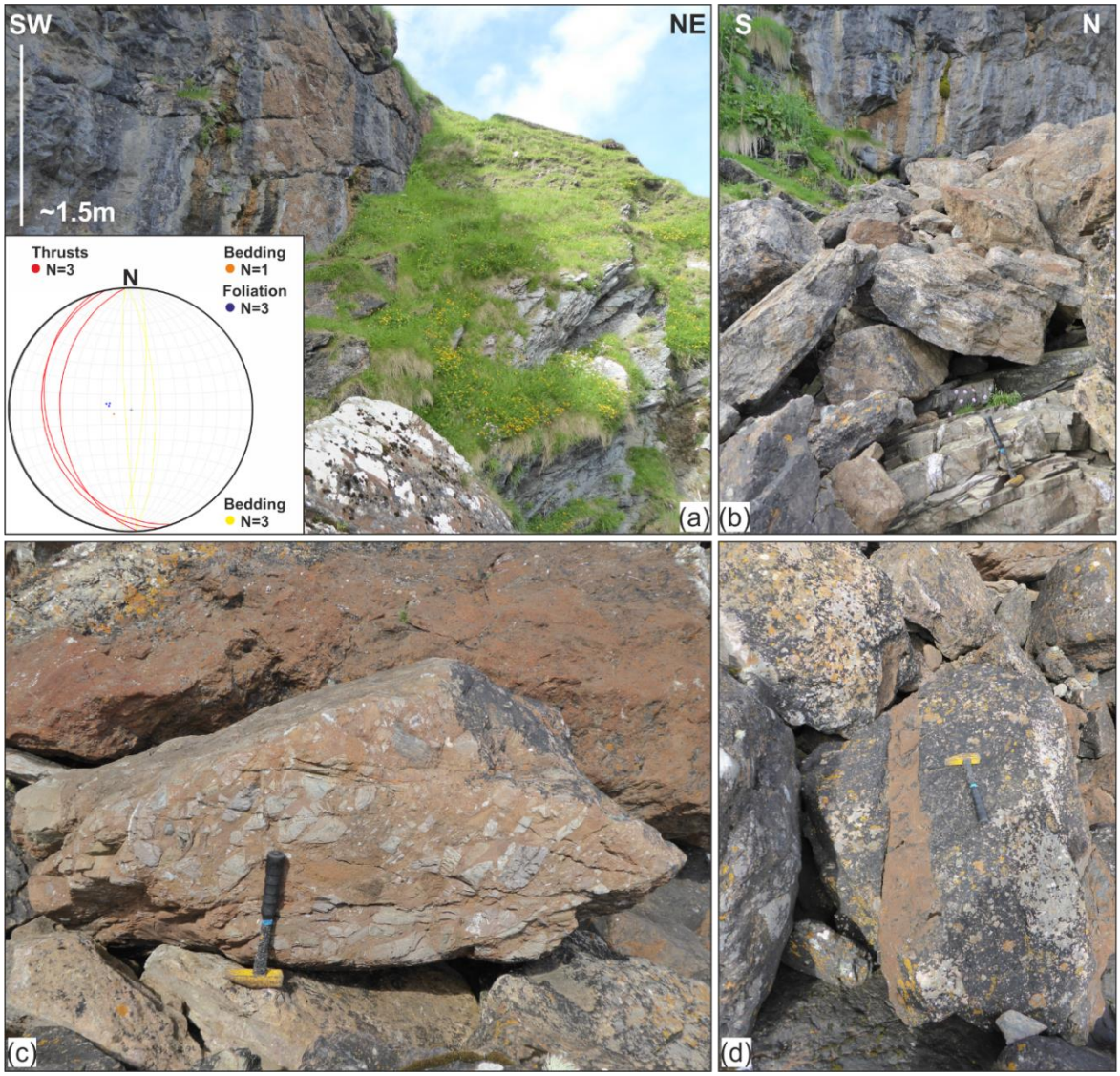

Figure 4.21 (overleaf): Field images from Bay of Okraquoy [HU 444164 1131311]: (a) Alteration of crystalline limestones in cliff face, and foliated basement beneath grassy bank. *Inset* stereonet of structural data from the locality; (b) thinly bedded flagstones beneath boulders and rubble; (c) tuffsite breccia and (d) ~10cm thick fracture infilled with tuffsite breccia and carbonate mineralisation.

4.4.1.3.6. Southern Shetland:

To the S of the basement high in the Quarff-Cunningsburgh area, the unconformity between the basement and Devonian strata is affected by mineralisation and pervasive deformation associated with the 'Steep-Belt' as seen in the Bay of Okraquoy. This deformation obscures much of the original structure which is compounded by poor outcrop in many coastal sections and a lack of inland outcrop. Inland, small outcrops of the Hayes Sandstone Formation, an angular basal breccia comprising local metamorphic and igneous rocks is developed in the Spiggie-South Scousburgh area, however for the most part

sandstones are deposited directly onto basement (Mykura et al., 1976a). From Levenwick [HU 440961 1121619] towards Sumburgh Head, the unconformity is very poorly exposed and largely does not outcrop inland. It is mapped out through the centre of the Bay of Quendale [HU 437810 1112865] where it is not exposed.

4.4.1.3.7. South Eastern Shetland Basin Summary:

Basement/cover relationships in the SE Shetland Basin may be split into two main types. The first are tectonically, relatively inactive, e.g. at Quarff and the Voe of Sound and reflect predominantly regional tectonics and subsidence. However, elsewhere the influence of the basement and pre-existing structures in the basement have had a strong influence on the development of the basement which suggests a much more dynamic basin. The folds in SE Shetland Basin are described as 'forced folds' by Seranne (1992), related to plastic deformation and folding of the sedimentary sequences over rigid basement blocks leading to the development of a scoop shaped basin during regional sinistral oblique extension. This motion being accommodated by sinistral shearing along the basin margins (e.g. Rova Head) and along major basement faults. These basement faults likely correspond to the position of the 'Steep Belt' which was later reactivated and is sub-parallel to many other basement structures (e.g. Quarff Melange and overall trend of the basement along the spine of Shetland). The orientation of the folds could however be partially related to oblique extension and the development of transtensional folds, with the hinges forming oblique to basin margins and rotating with progressive deformation in a manner similar to what has been observed on the Walls Peninsula, and on Foula.

4.4.2. Orkney:

The Orkney Isles are predominantly comprised of sedimentary and volcanic rocks of Middle to Upper Devonian age, along with a suite of Permian-Carboniferous basic dykes and vent agglomerates (BGS, 1999; Mykura et al., 1976a) (Figure 4.22). In Orkney, exposure of the unconformity with the basement is limited to small inliers exposed in the W part of Mainland Orkney and on the island of Graemsay (Mykura et al., 1976a).

The basement has been studied in detail by Strachan (2003) who subdivided it into 3 units of decreasing age: paragneiss and amphibolites; foliated meta-granites; and late, undeformed granitic-aplitic veins. The basement is interpreted to have formed a roughly N/S orientated line of hills that were inundated and buried during the development of the

Orcadian Basin (Brown et al., 2019) which are onlapped by breccias and sandstones of the Lower Devonian Yesnaby Sandstone Group (BGS, 1999).

Much of the remainder of Orkney is comprised of the predominantly lacustrine Upper and Lower Stromness Flagstone Formations, which are overlain by the Eday Group (Mykura et al., 1976a). This sequence of deposits shows a transition from mixed lacustrine and marginal fluvial/alluvial deposits to predominantly fluvial deposits. The Eday Group, like in Caithness, is faulted against the Upper Devonian, Hoy Sandstone, which is confined to the island of Hoy where a ~1km thick sequence of fluvial and aeolian sandstones and marls are partly unconformable on lavas and tuffs of the Middle Devonian Eday Group, known as the Hoy Volcanics.

The rocks of Orkney are folded into a series of broad, open, N trending, gently dipping folds (Figure 4.22), although locally they are intensely folded, damaged and associated with mineralised breccias. These zones of more intense damage generally form monoclinal structures sub-parallel to major faults (Mykura et al., 1976a). Minor folding in the Yesnaby Sandstone Group gives rise to an angular unconformity of ~10° with the overlying Stromness Flagstones and reflects syndepositional tectonics (Mykura et al., 1976a). Three major fault trends are identified (Mykura et al., 1976a); ENE to NE, NNW to NNE and NW and like much of the ORS elsewhere is relatively highly fractured. These structures are attributed to three principal phases of deformation (Dichiarante, 2017; Dichiarante et al., 2016), which are outlined in section 4.2.1.

Due to this relative lack of basement exposed on Orkney, only two locations are covered in detail in the following section. This lack of basement is however not unexpected given the position of Orkney, more centrally within the Orcadian Basin.

Figure 4.22 (overleaf): Simplified geological map of Orkney. Form lines show generalised structure of the rocks that comprise Orkney. Modified *after* (BGS, 1999). Green stars denote areas discussed in the text.

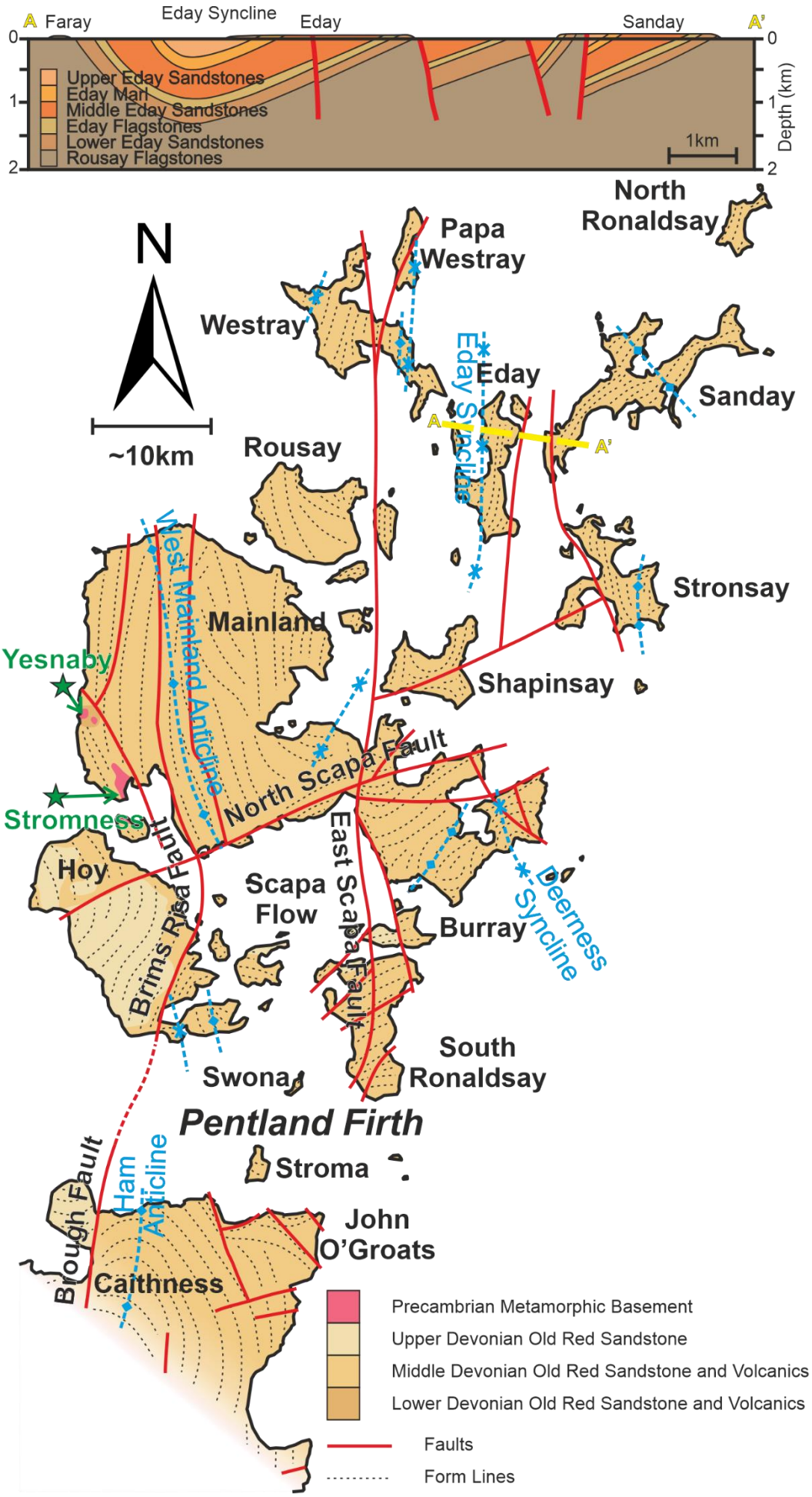
A
Faray
Eday Syncline
Eday
Sanday
A'
0
1
2
Upper Eday Sandstones
Eday Marl
Middle Eday Sandstones
Eday Flagstones
Lower Eday Sandstones
Rousay Flagstones
1km
Depth (km)
North Ronaldsay
N
Papa Westray
Westray
Eday
Sanday
~10km
Rousay
Eday Syncline
Stronsay
West Mainland Anticline
Mainland
Yesnaby
Shapinsay
North Scapa Fault
Stromness
Hoy
Brims Ness Fault
Scapa Flow
East Scapa Fault
Deerness Syncline
Burray
South Ronaldsay
Swona
Pentland Firth
Stroma
Brough Fault
Ham Anticline
John O'Groats
Caithness
Precambrian Metamorphic Basement
Upper Devonian Old Red Sandstone
Middle Devonian Old Red Sandstone and Volcanics
Lower Devonian Old Red Sandstone and Volcanics
Faults
Form Lines

4.4.2.1. Stromness:

Small outcrops of basement may be found around the coastline, the harbour, and further inland around the town of Stromness (Figure 4.23a). In the area to the S of the harbour around the Point of Ness [HY 328820 1010161], the basement is comprised of granitic gneisses with pegmatites and granitic veins. In places it is very well foliated, dipping towards the south (20-30°) (Figure 4.23b). Locally, however, over short distances (several metres) the foliation becomes very indistinct or is completely missing. The basement is bound to E by a N/S trending fault which juxtaposes the basement against the Lower Stromness Flagstone formation; this contact is poorly exposed. In the footwall fine to medium grained fining upwards sandstones, and thinly bedded siltstones/laminates with mud cracks and ripples are well jointed/fractured (Figure 4.23c and 4.23d) but are not strongly deformed.

Along the coastline, W of the Skerry of Ness in the footwall to this fault, a gradual transition from the basement through coarse angular breccias, more rounded conglomerates and into bedded sandstones and siltstones of the Lower Stromness Flagstone Formation is observed (Figure 4.23e). Here, the unconformity surface is deeply weathered and has distinct patches of breccia plastered onto the unconformity surface (Figure 4.23f and 4.23g). Bedding in the overlying breccia-conglomerates is highly irregular in places, but in general dips gently towards the W becoming more distinct and more well bedded up stratigraphy. The clasts are comprised of local foliated gneissic material (Figure 4.23h) and quartz rich pegmatites contained within a yellow to orange coarse grained, quartz- and feldspar-rich arkosic matrix. Clast size varies from 20-30cm in size down to pebbles. Clast size and rounding decreases up stratigraphy, and faint imbrication of clasts is visible, particularly clasts which contain a foliation and have a well-defined long axis as a result. More exotic clasts appear higher up in the sequence and in places some sheets of breccias are particularly angular and poorly sorted (Figure 4.23i). Passing upwards the breccias and conglomerates become interbedded with very coarse to coarse grained, immature sandstones with granular lags, pebbly lenses faint cross bedding and the occasional pebble/cobble (Figure 4.23j). The total thickness of breccia-conglomerate is in the region of 10-20m, thickening where it infills the pre-existing topography.

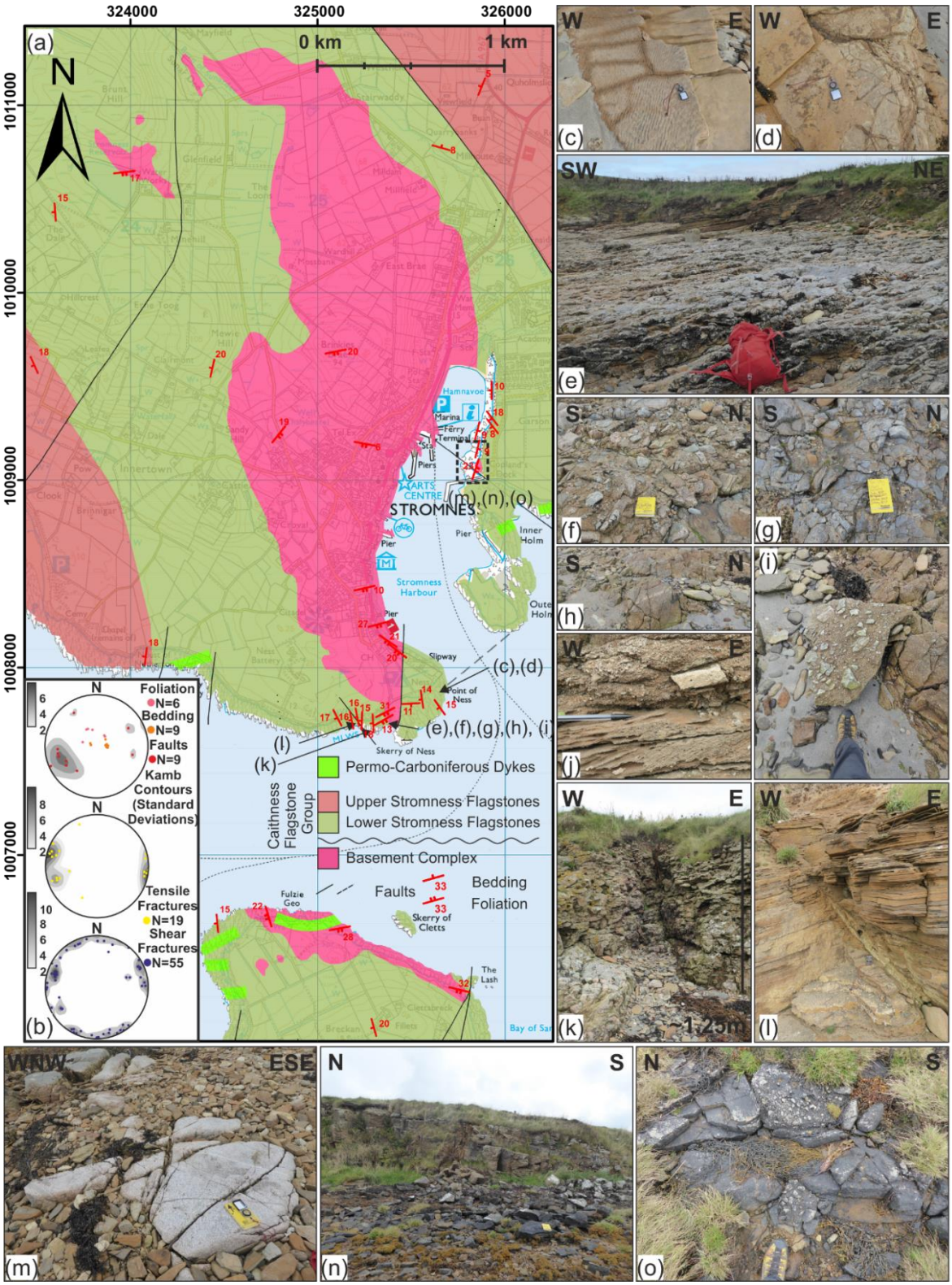

Figure 4.23: (a) Geological map of the Stromness area and (b) Stereonets of structural data collected in the field. Map modified *after* (BGS, 1999). Field data supplemented with data digitised from British Geological Survey (1999) and Strachan (2003). Lower hemisphere, equal area projection. Field photographs from the Stromness area; Mud cracks (c) and ripples (d) developed in the Lower Stromness Flagstones; (e) weathered unconformity showing transition into more well bedded units; (f) and (g) breccia-conglomerate plastered onto the unconformity surface; (h) gneissic

basement being reworked and incorporated into the breccias.; (i) highly angular breccias; (i) Immature sandstones with pebbles showing cross stratification; (k) fault zone within conglomerates; (l) N/S fault with carbonate mineralisation; (m) sea washed coarse grained granitic gneisses; (n) thinly bedded sandstones overlying the basal breccias and unconformity; (o) highly angular breccias comprised of clasts of local basement.

Cutting these sequences are several NNW/SSE to N/S and NE/SW trending normal to dextral oblique normal fault zones which drop down generally to E (Figure 4.23b and 4.23k). These faults juxtapose conglomerates against more mature sandstones from higher in the sequence. N/S faults tend to cut NE/SW faults and along some of the larger faults, a small smear of fine-grained fault breccia is developed. 4 major trends in fractures are also observed; N/S, NW/SE, E/W and NE/SW (Figure 4.23b). N/S trending tensile fractures and faults are preferentially mineralised with fibrous carbonate minerals and minor quantities of pyrite (Figure 4.23k). Dextral offsets on some N/S fractures and sinistral offsets on some E/W fractures are consistent with NW/SE extension (cf. Group 3 structures of Dichiarante 2017).

Fractures pass up and down through the unconformity with no dislocation and where sandstones are coarser grained, they are particularly well fractured. Smaller faults become very indistinct within the breccia-conglomerates and tensile fractures seem more well developed within the conglomerates as opposed to better developed shear fractures within the sandstones and siltstones, reflecting a lithological control on the mode of fracturing.

On the shoreline opposite the harbour, in the area around Coplands Dock [HY 325773 1009948], patchy outcrops of breccia-conglomerate close to sea-level exhibit crude bedding which dips gently towards the E. The breccia-conglomerates overly and onlap a flat, sub-horizontal unconformity with the basement which comprises weakly foliated coarse-grained granite gneiss with felsic veins and pegmatites (Figure 4.23m). The breccia-conglomerates fine upwards and are interbedded with wavy, thinly bedded, very coarse to angular, immature, sandstones (5-10cm) which exhibit faint ripples and flaser bedding (Figure 4.23n). The breccias are largely matrix supported however the proportion of matrix increases upwards. Clasts are highly angular, 4-5cm size clasts and composed of locally derived granitic gneiss (Figure 4.23o). Both the basement and overlying Devonian strata are fairly fractured with three predominant trends; E/W, NNE/SSW to NE/SW and NW/SE.

Up stratigraphy, and overlying the conglomerates and sandstones are thinly bedded flagstones and sandstones of the Lower Stromness Flagstones. Further towards the E, in the area around Quoyelsh promontory, horizontal, flow banded felsites are intercalated with sandstones and breccias which have been dated to the Eifelian/Givetian (390.35±0.39Ma U/Pb zircon) (Bjerga, 2017). Erosion of this material and its incorporation into the breccias suggests that these volcanic deposits were erupted prior to deposition of the remainder of the Middle Devonian stratigraphy and helps to constrain the age of basin subsistence (Bjerga, 2017). This date also suggests a Middle Devonian age for some of the basal breccias and conglomerates of the Lower Stromness Flagstone Formation deposited in the Stromness area, and therefore older than the basal deposits in the Yesnaby area (see below). However, this does not preclude an older Lower Devonian age for some of the basal deposits in this region.

On the S side of Hoy Sound, similar basement rocks to those seen around Stromness, outcrop in a narrow strip along the N coastline of Graemsay from The Lash to the lighthouse at the Point of Oxan (Fig 4.23a; Strachan, 2003). On Graemsay it is reported that some clasts are coated within a thin layer of dolomite and siltstone interpreted to represent stromatolites (Mykura et al., 1976a and references therein).

In summary these observations suggest that the Stromness area was tectonically relatively inactive with the major controls on deposition being related to far-field tectonics, principally regional subsidence. Differences in thickness of the basal deposits are largely related to the pre-existing topography of the unconformity surface. The predominance of N/S tensile fractures and E/W trending shear fractures and small N/S faults could be related to Devonian transtension, however the presence of carbonate mineralisation does suggest a Permian age for some of these structures.

4.4.2.2. Yesnaby:

Around the area of Yesnaby, on the W coast of the mainland (Fig. 4.24) Middle Devonian rocks of the Stromness Flagstones Formation onlap and overstep localised deposits of Lower Devonian aged Yesnaby Sandstone Group with an angular discordance of 6-10° (Mykura et al., 1976a). The Yesnaby Sandstone Group is deposited on and around an eroded hill of granitic gneiss (Brown et al., 2019; Mykura et al., 1976a) (Figure 4.24a and 4.24b) and minor pelites/psammites, cut by granitic veins and pegmatites (Strachan, 2003) which at the time of deposition, may have had several hundreds of metres of topographic

relief (Brown et al., 2019). Cutting both the basement and the Devonian sedimentary rocks are younger, Permo-Carboniferous aged lamprophyric dykes (Figure 4.24c).

The basal deposits, known as the Yesnaby Sandstone Group are subdivided into the lower Harra Ebb Formation and upper Qui Ayre or Yesnaby Formation (BGS, 1999). The Harra Ebb formation comprises breccias, conglomerates and interbedded siltstones and muddy sandstones. These sediments are plastered onto the unconformity and towards the top of the 'hill' are thinly bedded siltstones which dip steeply away down slope from the top of the paleo hill (Figure 4.24d). These sedimentary rocks drape the pre-existing topography of the unconformity with varying dips related differential compaction. Towards the base of hill, lobes/tongues of breccia and conglomerate extend down slope and paleocurrent indicators indicate that current was down slope and likely originated as local alluvial fans (Mykura et al., 1976a).

The Yesnaby formation consists of 200m of aeolian sandstones which gradually transition into reworked fluvial sandstones and marginal lacustrine flagstones. Large-scale dune cross bedding can be seen in coastal sections and in offshore stacks (Figure 4.24e). Towards the top of the unit the beds become more massive and contain ripples, localised trough cross bedding and bioturbation (Mykura et al., 1976a). The localised distribution of this unit is interpreted as a result of wind-blown sands being trapped against the base of the basement hill (Brown et al., 2019).

Along the N margin of the 'buried hill' an NE/SW to ENE/WSW trending, 1.5-2.0m thick lamprophyric dyke is observed which seems to have been emplaced along a pre-existing fault and/or along the mechanical contrast between the basement and Devonian sedimentary rocks. Smaller dykes of similar composition are observed intruding the Devonian sedimentary rocks to the N, in addition to several smaller sub-parallel dykes. The dyke dips steeply towards the N and has a distinctly vesicular centre (Figure 4.24g) with dyke margin perpendicular fractures which are likely cooling joints. In the basement wall rocks, shear fractures indicate dextral motion along the dyke margins. Subparallel E/W and NE/SW trending fracture corridors cut the foliated basement (Figure 4.24h) and locally the surroundings rocks are intensely veined with Fe-rich carbonate minerals, and in places are highly brecciated (Figure 4.24i).

Several further dykes of similar composition are found throughout Orkney and Caithness, associated with normal faulting, base metal sulphide and carbonate mineralisation (Figure 4.24j) and bitumen, which are dated to 267.5 ± 3.4Ma (Dichiarante et al., 2016). Solid bitumen within pore spaces of the aeolian Yesnaby Formation (15-25% porosity) (Brown et al., 2019) also indicates a previous oil charge from nearby Middle Devonian lacustrine source rocks that entered the early oil window during burial, providing evidence for a working petroleum system in the Orcadian Basin with Devonian age source rocks, reservoirs, sealing units and traps.

Like at Stromness these observations suggest that the Yesnaby area was also tectonically relatively inactive with the major controls on and deposition being related to far-field tectonics, principally regional subsidence. However here, significant thickness differences in the basal deposits reflect a highly irregular pre-existing topography of the unconformity surface. In contrast however to Stromness, are the presence of Permian age dykes and associated carbonate mineralisation are consistent with the structures developed during Group 3 deformation.

4.4.2.3. Regional Summary of Basement/Cover in Orkney:

In summary, the locations around Stromness and Yesnaby suggest a largely quiescent tectonic setting, with the major controls on structure and deposition being related to far-field tectonics, principally regional subsidence. Differences in thickness of the basal deposits are primarily related to the pre-existing topography of the unconformity surface which in some places is in the order to many tens of metres.

Some small normal faults are likely related to later deformation, based on carbonate mineral fills, kinematics, and emplacement of dykes which suggests a Permian age, related to Group 3 deformation and regional transtension. However this does not preclude an earlier Devonian age for some N/S faults which have been subjected later reactivation, given that greater thicknesses of Devonian sediments are found in the footwalls of some N/S faults in Orkney(Brown et al., 2019).

Figure 4.24 (overleaf): (a) Oblique aerial image of the Yesnaby area, cross section and key. Cross section modified *after* (Brown et al., 2019). (b) Geological map of the Yesnaby area. Modified *after* (BGS, 1999) (c) oblique aerial image of Garthna Geo. Field photographs of; (d) thinly bedded siltstones draped and plastered onto the basement, (e) sea stack showing a cross section through the stratigraphy of the area and transition from a more marginal lacustrine and aeolian setting to

a fluvial and lacustrine setting; (f) small dykes as offshoots off of the major dyke; (g) vesicular centre to the dyke and stereonet showing data for faults; dyke margins and mineralised tensile fractures (h) subsidiary fracture corridor; (i) pervasive fracturing and carbonate mineralisation and (j) base metal sulphide and carbonate mineralisation. Field data supplemented with data digitised from the BGS (1999) and Strachan (2003).

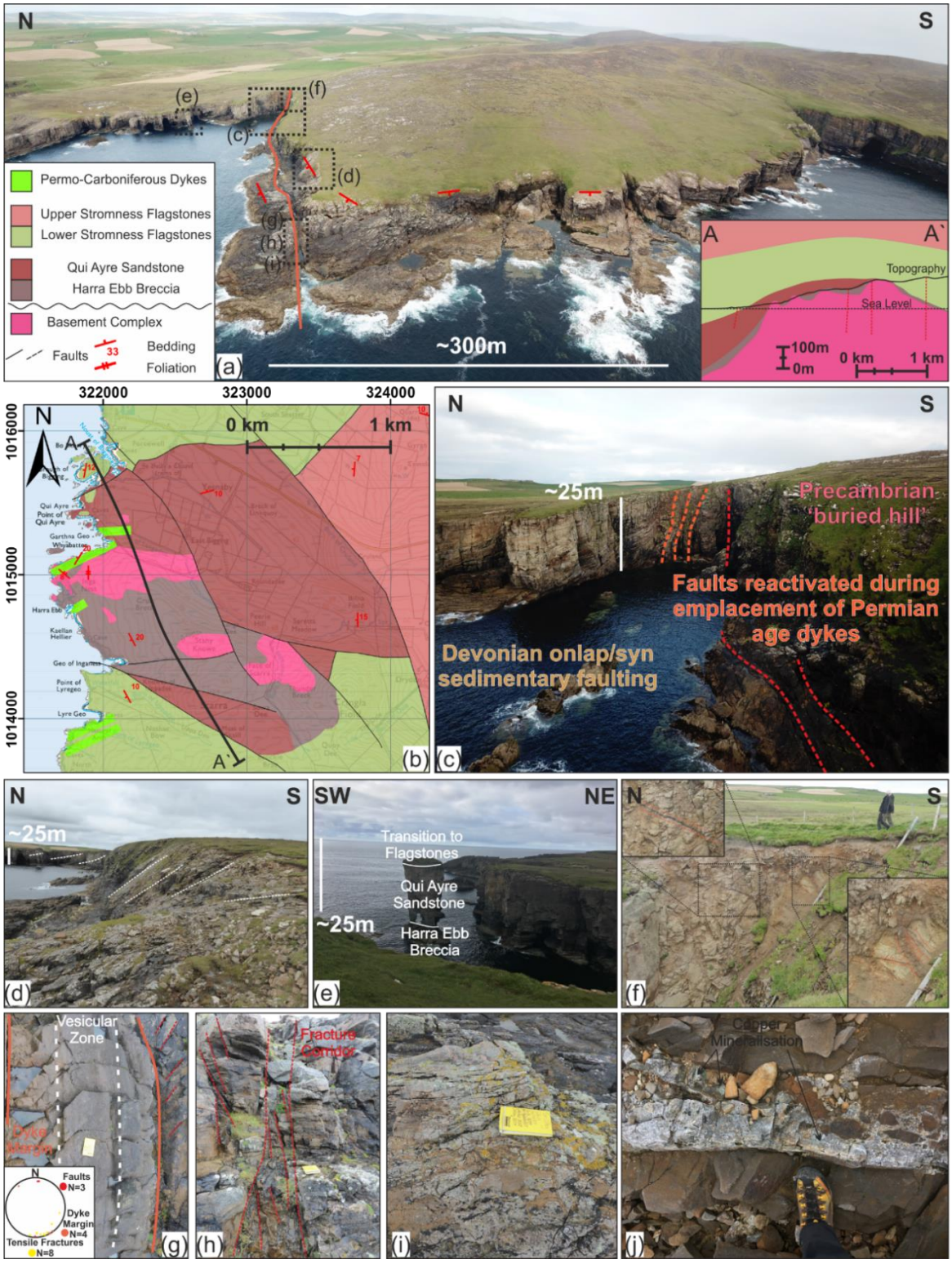

4.4.3. NE Scotland:

In NE Scotland, the Orcadian Basin fills are found along the North Coast in Caithness, and Sutherland and around the margins of the Inner Moray Firth (Figure 4.25). The Devonian sequences of NE Scotland are generally folded into broad, open, N to NE trending gently dipping folds and cut by predominantly N to NE and E/W trending faults and faults zones which are attributed to three principal phases of deformation (Dichiarante, 2017; Dichiarante et al., 2016), which were outlined in section 4.2.1.

Lower Devonian sedimentary rocks outcrop around the margins of the Orcadian Basin and were deposited in more isolated basins, prior to the development of the main Orcadian Basin (Johnstone and Mykura, 1989). Such deposits are well developed in the Dingwall-Strathpeffer area and are also found elsewhere in a number of small isolated basins and outliers (see below in Section 4.45). These sequences predominatly comprise fluvial-alluvial sedeimantary rocks, although locally, lacustrine sediments were deposited in isolated lakes, prior to the development the larger Orcadian Lake.

Middle Devonian rocks are particularly well developed in Caithness, where the geology predominantly comprises the sedimentary rocks of the Caithness Flagstone Group, subdivided into the Lybster Flagstone, Spital Flagstone and Mey flagstone formations (Johnstone and Mykura, 1989). These formations are predominantly fluvial and lacustrine and contain several fossil rich horizons or 'fish beds'. Overlying the Caithness Flagstone Group are predominantly fluvial sedimentary rocks of the John O'Groats Sandstone Group (Johnstone and Mykura, 1989).

Faulted against the Middle Devonian strata are the Upper Devonian aged fluvial and aeolian sedimentary rocks of the Dunnet Head Sandstone Formation which are restricted to the headland of Dunnet Head (Johnstone and Mykura, 1989). Similar, Upper Devonian sedimentary rocks of the Balnagown Group are exposed on and around the Black Isle and Dornoch Firth. In the Nairn-Elgin area, the Middle Devonian Inverness Group and Upper Devonian-Tournasian (Lower Mississippian) Forres Sandstone Group comprise coarse clastic, predominantly fluvial and alluvial sediments which were deposited in lacustrine marginal areas (BGS, 2012, 1990, 1969). Around the margins of the Moray Firth region, the rocks of the Old Red Sandstone are overlain by Permian and younger strata, which obscure much of the Devonian strata offshore.

The following section provides an overview of the field locations that were studied around the margins of the basin, where Lower and Middle Devonian strata immediately overlie basement. This starts at Kirtomy in the W, at the margin of the Orcadian Basin, and moves further E and S towards the centre of the basin and closer to the influence of the Great Glen Fault Zone. This is followed by a summary of Devonian outliers in NE Scotland and other previously published examples in order to provide context and enable a regional summary.

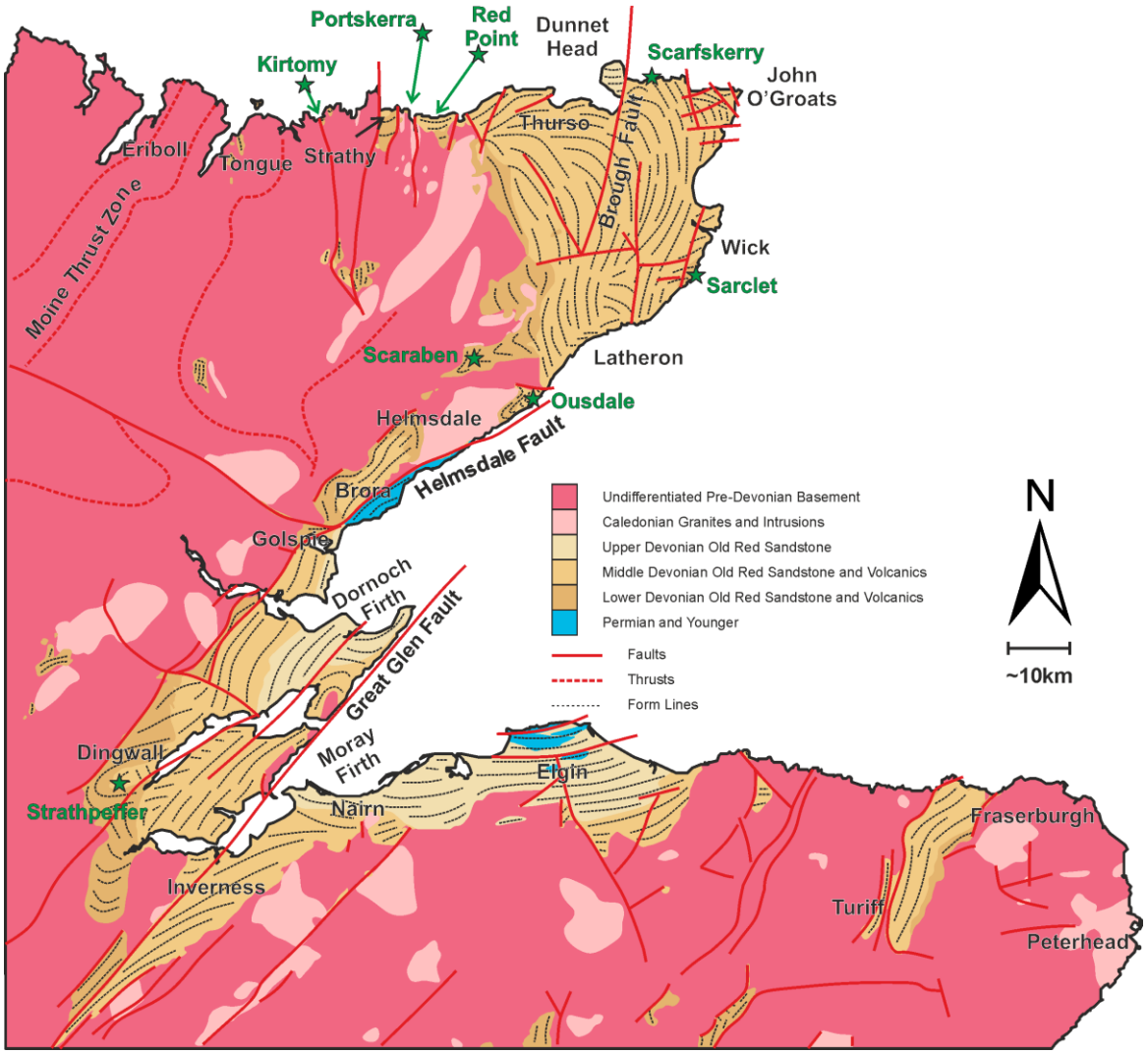

Figure 4.25: Simplified geological map of NE Scotland and the Inner Moray Firth. Form lines show the generalised structure of the Devonian strata and reveal the large-scale fold geometries in the ORS of the region. Locations described are labelled with a green star. Modified *after* (BGS, 2012, 2004b, 1990, 1986, 1985c, 1985a, 1985b, 1973, 1969, 2004a, 2003a, 2002, 2001, 1998, 1997, 1996, 1995). Green stars denote areas discussed in the text.

4.4.3.1. Kirtomy Bay:

At the western most margin of the Orcadian Basin near Kirtomy Bay are several outliers of likely Lower to Middle Devonian sedimentary rocks (Johnstone and Mykura, 1989). The largest outlier corresponds to a small 'mini' basin in Kirtomy Bay and is described in detail by Wilson (2006), Wilson et al. (2010) and Dichiarante (2017)(Figure 4.26a-i). The overall geometry of the basin is an isolated half graben approximately the width of the valley (Figure 4.26a-ii). Infilling the basin are conglomerates and sandstones of Lower Devonian which grade and fine towards the centre of basin. The basin fills dip inwards into the centre of the basin and progressively onlap the existing basement topography around the margins. The basement around the margins comprises steeply dipping Moinian migmatitic, pelitic and semi-pelitic gneisses (Strachan et al., 2010).

On the hills to the E of main 'mini-basin' are two further outliers (Figure 4.26a-iii) of Devonian rocks overlying Moine basement in the cliffs of exposed in the cliffs at Geod'h Ghamhainn and in the banks of streams near Allt Lagain Biere and the Allt a'Phuill-aonaich (Blackbourn, 1981b). These deposits, like those at Kirtomy are thought to have been deposited in N/S trending valleys and reflect the existing Pre-Devonian topographic surface into which coarse, locally derived sediments were being deposited.

The Kirtomy basin is bound to the W by a N/S to NNW trending steep fault (Figure 4.26d) (Wilson, 2006), which in places cross-cuts, but is often parallel to the well-developed basement foliation which contains brittle faults and cataclastic shear bands which are reactivating ductile blastomylonite fabrics within the basement. Smaller ENE/WSW faults accommodate along strike variation in throw along this basin bounding fault.

This basin controlling fault is interpreted to have initiated as normal fault, but was later reactivated forming a steeper dip-slip to dextral oblique strike-slip fault zone with ENE/WSW faults being reactivated in a sinistral sense (Wilson et al. 2010; Dichiarante, 2017). Cutting both sedimentary rocks and the basement are later brittle faults, attributed to the dextral reactivation of major basin bounding faults during the development of the Permian basins offshore and the development of the North Coast Transfer Zone (Wilson et al., 2010; Dichiarante et al. 2016).

Reconnaissance with a drone along the eastern side of the basin has identified a further large synsedimentary fault which cuts the basement (Figure 4.24b) and offsets the basal

unconformity by 20-25m. This fault trends towards the NNW dipping towards the WSW (330/66/WSW). Towards the top of the cliff, the bedding becomes continuous and may be traced over the fault indicating clear growth on this structure, with bedding in the footwall dipping more steeply than in the hangingwall (Figure 4.24b). This fault dips steeply towards the SW (Figure 4.26c) and can be traced into the basement where it becomes sub-parallel to the foliation, and like on the W margin of the basin, is likely reactivating the steeply dipping pre-existing fabric. The presence of these faults suggest that the basin formed not as a half graben but may have in fact developed as one larger graben structure bound by basement horst blocks to the E and W during which it was actively subsiding and accumulating sediment (Figure 4.26c). Once full, the sediments infilling the basin then flowed over the bounding faults and onlapped onto the surrounding basement hills. Lower down in the outcrop are several smaller NW to NNW trending faults that pass from the basement through the unconformity but are discontinuous in the Devonian strata (Figure 4.26b).

This locality preserves not only evidence for NW/SE extension and dextral reactivation of basin margin faults related to the development of Permian basins offshore (Dichiarante, 2017), but also an earlier phase of deformation related to development of the basin which predates this event. This deformation is associated with ENE/WSW orientated extension, reactivation of a NNW//SSE trending basement fabric and development of a Devonian age graben structure that was infilled with locally derived coarse clastic sediments.

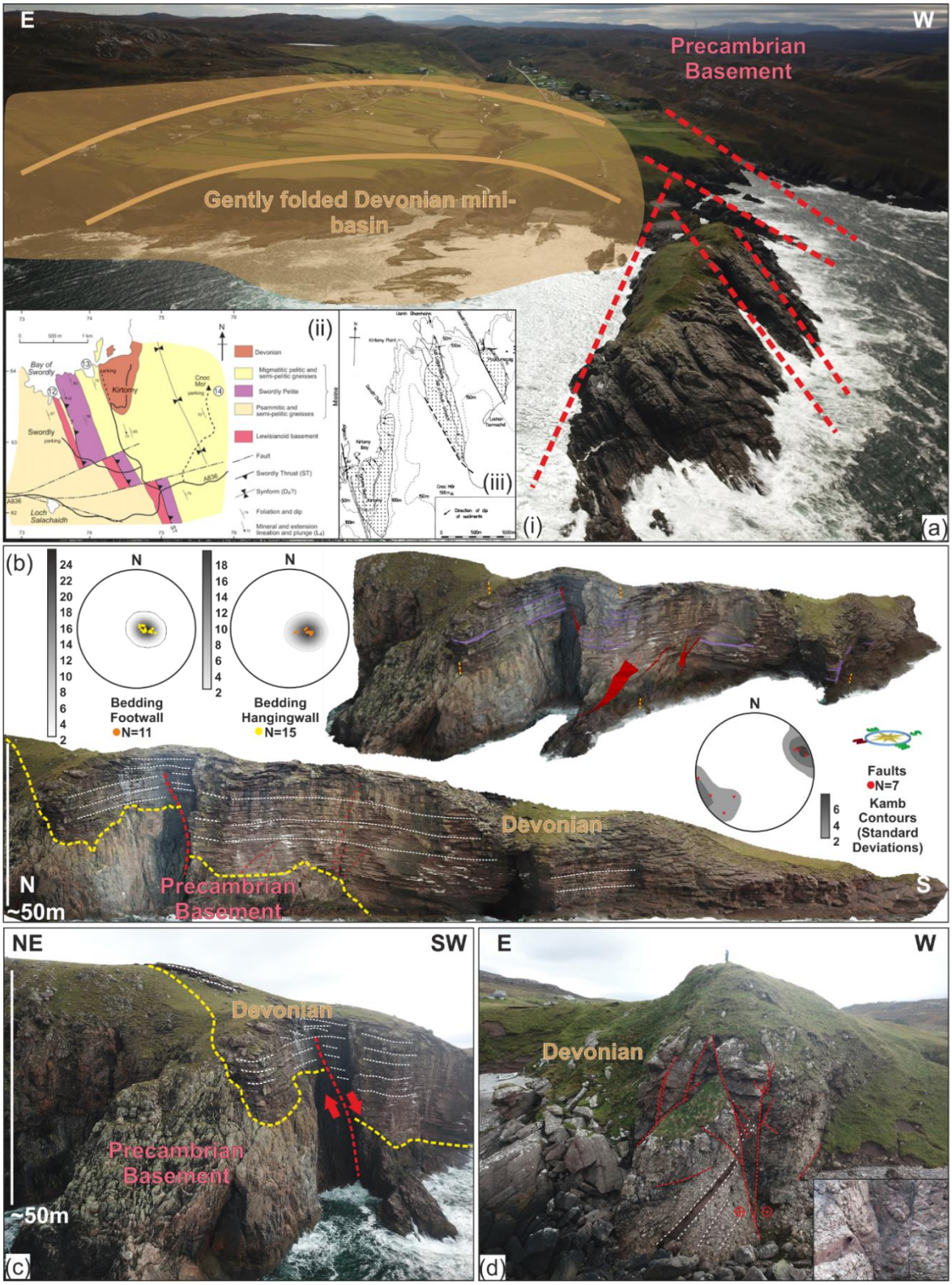

Figure 4.26: (a)(i) Oblique aerial image of the Kirtomy mini-basin. *Inset* (ii) Geological map of the Swordly-Kirtomy area (Burns, 1994; Strachan et al., 2010) and (iii) sketch map of outliers near Kirtomy(Blackbourn, 1981b); (b) oblique orthorectified aerial image of the E margin of the basin, showing syn-sedimentary growth faults and interpreted Virtual Outcrop Model with stereonets of structural data; (c) oblique aerial photograph of the basin margin fault on the E side and (d) oblique aerial image of basin margin fault on the W side.

4.4.3.2. Portskerra:

Portskerra lies close to the western margin of the main Orcadian basin, in the immediate footwall to the N-S trending, regional scale Strath Halladale Fault (Figure 4.27). At Portskerra harbour, an irregular basal unconformity is overlain by well bedded, breccia-conglomerates and sandstones of Middle Devonian age.

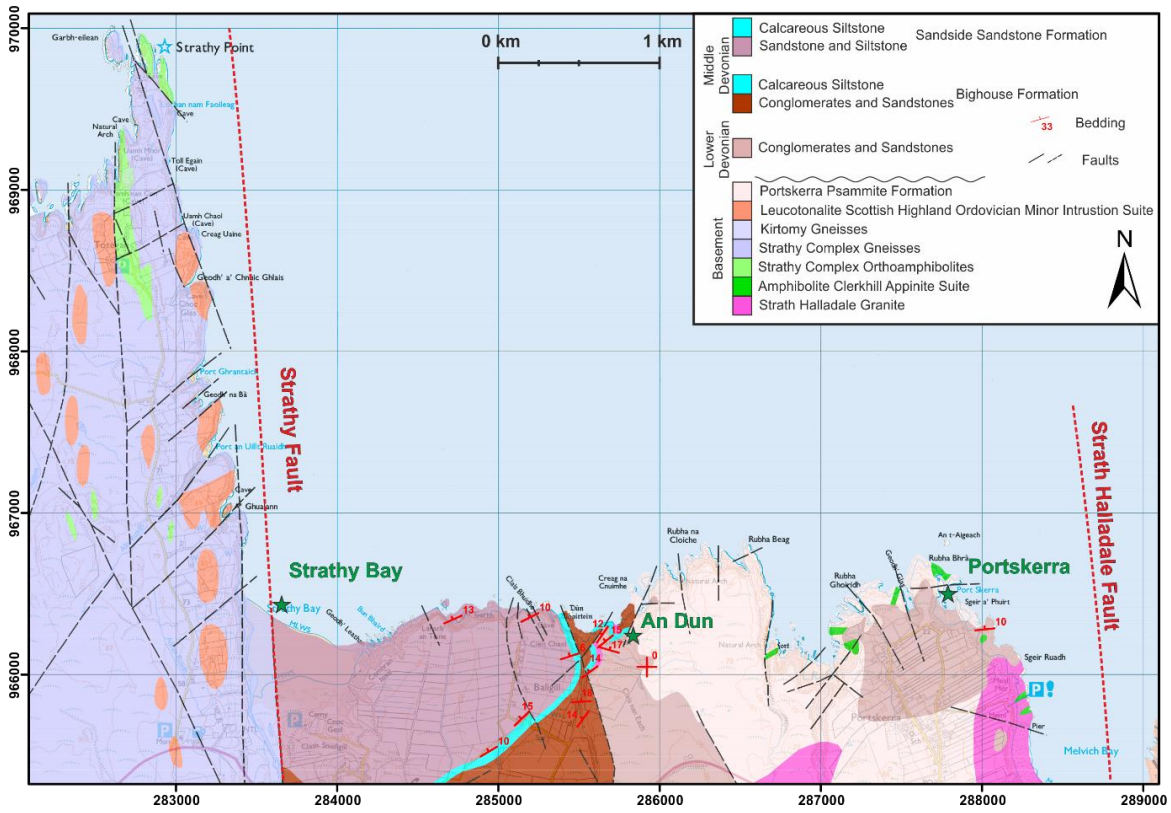

Figure 4.27: Geological map of the Strathy to Portskerra area. Modified *after* (BGS, 2003b, 1996). Green stars denote locations of interest.

The basal breccias and lenses of graded breccias/sandstones drape an irregular unconformity surface (Figure 4.28a) of Moinian basement with abundant granite sheets, with no more than a few metres total relief (5-10m) (Figure 4.28a,b). The basement mound seen in Figure 4.28b may be traced through the headland as a NW/SE orientated ridge, bound by small faults which outcrops in the adjacent inlet as seen on the virtual outcrop model (Figure 4.28c). Bedding dips are somewhat variable over the basement highs and reflect differential compaction and localised syn-sedimentary folding and faulting.

Despite the Devonian rocks being highly fractured, the degree of fracturing is much lower than in the basement which indicates that at least some of the fractures predate deposition of the cover sequences. Evidence for this may be found in the form of fissures and vuggy

cavities of variable orientation that are infilled with Devonian sediment proving the existence of open fractures prior to and during deposition (Figure 4.28d and 4.28e).

Faults and fractures predominantly trend NE/SW and ENE/WSW to E/W (Figure 4.28c) and no clear distinction is apparent between the orientation of faults and fractures in the Moine basement and those developed the overlying Devonian sedimentary rocks (Dichiarante 2017), however numerous E/W trending faults can be seen to propagate upwards from the basement with normal displacements of several tens of centimetres (e.g. 255/62/S, slickenlines 65→180) which are partially cemented with quartz.

Some possible later reactivation of fault zones is evident by minor carbonate mineral fills of NE/SW trending tensile fractures and faults which are likely Permian in age (Dichiarante et al., 2016). Some shearing along the unconformity, particularly where steeper and compactional features associated with small normal faults which terminate at the unconformity are also observed (Figure 4.28f).

At this locality, evidence for Devonian syn-sedimentary faulting and compactional folding over an irregular basement topography reflects its location in a relatively tectonically inactive part of the basin during its development, which may be in part due to its location in the footwall to major fault. Sediment filled fissures together with the high relief on the unconformity indicate a highly weathered land surface prior to deposition of the Devonian strata. Later deformation is preserved in carbonate minerals fills on predominantly NE/SW trending faults. Similar geological features are also reported in and around the locality of An Dun (Figure 4.27) by Donovan (1975) some 2km further west.

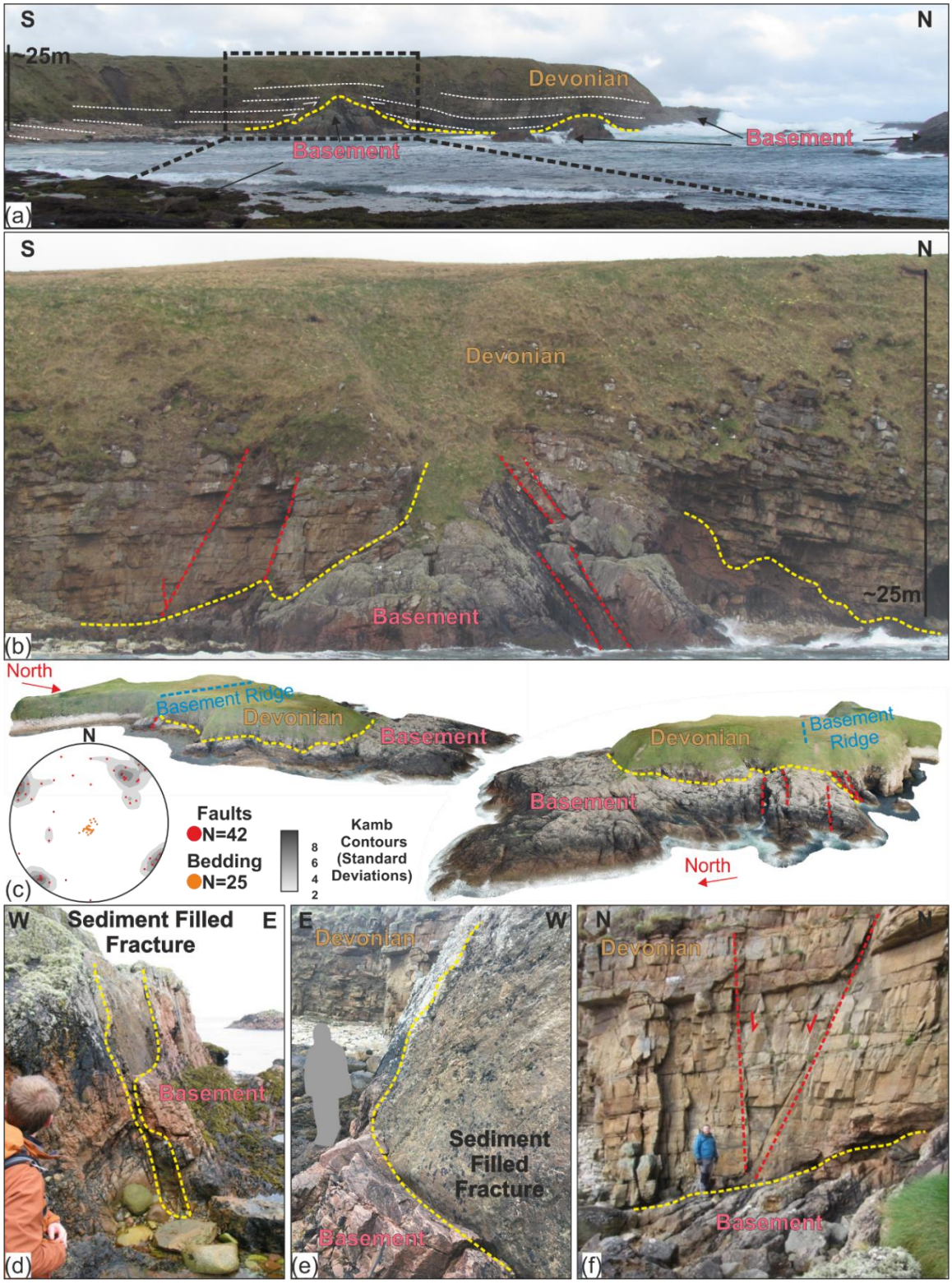

Figure 4.28: (a) overview field photograph of Portskerra Harbour; (b) detail field photograph of basement knoll showing onlap of Devonian sandstones; (c) oblique view of virtual outcrop model showing the undulating basal unconformity and stereonets of structural data derived from models; (d) field photograph sediment filled fissure in basement; (e) close up field photograph showing angular clasts contained within a finer grained matrix; (f) field photograph of small faults which terminate against the basement. Photo (d) and (f) courtesy of Bob Holdsworth.

4.4.3.3. Sarclet:

At Sarclet and Riera Geo [ND 35357 43640] (Figure 4.29) spectacularly folds within the Sarclet Group are well exposed, although largely inaccessible in the cliffs surrounding the harbour (Figure 4.30a). The Sarclet Group forms the core of domal anticlinal structure and comprises the Sarclet Conglomerate, Sarclet Sandstone, Ulbster/Riera Geo Mudstone and Ulbster/Ires Geo Sandstone formations which are all Lower Devonian in age (Figure 4.29).

These sediments represent some of the earliest basin fills into the Orcadian Basin and are interpreted to show a transition from deposition by braided streams in an alluvial fan environment to a more distal fluvial system/playa lake (Donovan, 2002). Clasts in the conglomerates are sub-rounded, poorly sorted and comprised of granite, schist, quartzites, basalt and andesite, which may indicate contemporaneous igneous activity (Trewin and Hurst, 2009). The pebbly sandstones and sandstones are medium grained, show cross bedding and parallel lamination with four fining upwards cycles identified (Donovan, 2002).

Within these largely well bedded units are contorted, disturbed and folded beds with small faults and detachments (Figure 4.30 a), which are highly fractured and veined with quartz. Overlying this sequence and further inland the units become well bedded again and dip less steeply (Figure 4.30b). The lower contact between this two units is brecciated and shot through with calcite and can be traced around the outcrop, where it is observed down-cutting into the bedded sandstones beneath (Figure 4.30c). It is interpreted as detachment that dips shallowly towards the SE, which has allowed differential motion and sliding of the strata above it. In the footwall, beneath the detachment the bedding consistently dips gently towards the NW (Figure 4.30e) whereas, in the hangingwall, above the main detachment, bedding is contorted into tight, recumbent folds which trend towards the NE (Figure 4.30e) and verge towards the NW and SE. Smaller detachments are also observed which steepen back from the main detachment, akin to an imbricate thrust sheet. Further examples of similar folds are exposed in the cliffs surrounding the harbour (Figure 4.30f).

The whole sequence is cut by 3-5m wide sub-vertical, steeply dipping fracture corridors, which trend NW/SE to WNW/ESE and NE/SW to ENE/WSW. The fracture corridors are finely brecciated at the boundaries, showing an increase in angular fragments and sub-parallel fractures towards the centre of the corridors. These zones are cut by a further set of later carbonate/pyrite cemented fractures which are likely Permian in age. These numerous

fractures are potentially due in part to the localities proximity to several major faults, the Wick, Helmsdale and Great Glen Faults which lie immediately offshore.

These folds are interpreted to have formed prior to full lithification as gravity driven soft sediment deformational features, and are related to the sorts of structures developed widely associated with MTCs (Mass Transport Complexes) laid down in tectonically active settings (Alsop et al., 2019). Smaller detachments inclined at steeper angles to the main one appear to be small back-thrusts which likely originated as a result of the mass of sediment slowing or stopping and causing compression. The numerous fractures and fracture corridors that cut the sequence are likely related to deformation along the Great Glen and Helmsdale Fault Zones, principally the NE/SW trending fracture corridors which are-parallel to the coastline and the trend of these major fault zones (BGS, 1998; Roberts et al., 1990).

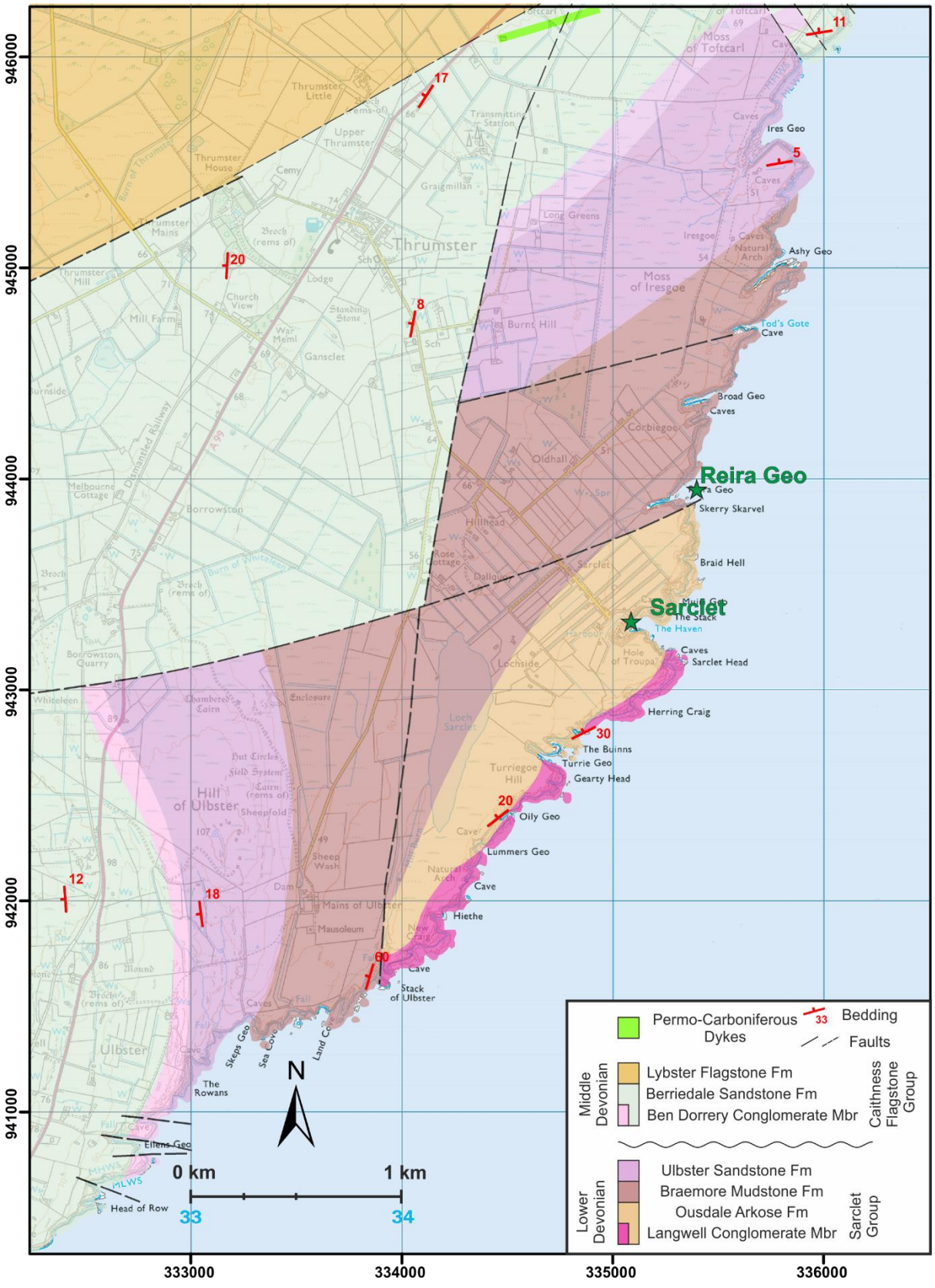

Figure 4.29: Geological map of the Sarclet area. Modified *after* (BGS, 1986, 1985c). Green stars denote locations of interest.

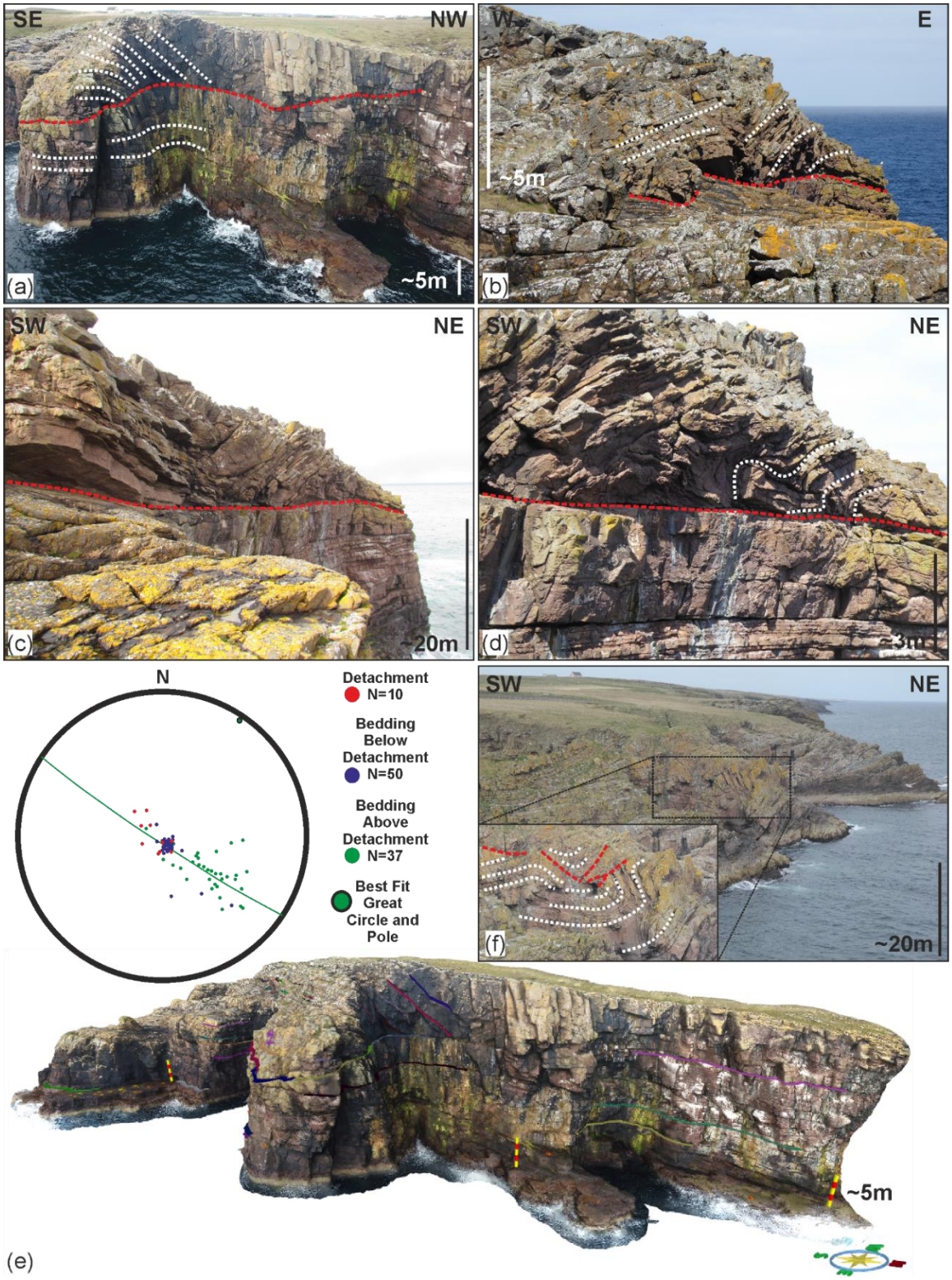

Figure 4.30: (a) Oblique aerial image of the folds at Sarclet. Field photographs of the lower detachment showing the bedding steepening towards the E and down cutting the bedded units below (b); tight, recumbent folds developed in the disturbed unit (c) and (d). (e) Interpreted virtual outcrop model of the cliffs at Sarclet. (f) Oblique field photograph of folds in the cliffs surrounding the harbour at Sarclet.

4.4.3.4. Braemore-Scaraben and Berriedale-Ousdale Synclines:

On the SW margin of the Orcadian Basin close to the border between Caithness and Sutherland, a series of folded Lower Devonian rocks outcrop along the margins of the main Orcadian Basin in NE Scotland (Figure 4.31a). These are overlain by Middle Devonian rocks of the Caithness Flagstone Group which overstep and onlap onto the basement. The published section through this area shows folded Devonian stratigraphy with internal unconformities and possible growth (Figure 4.31b). To explore this further, extraction of bedding from these two areas from published maps was carried out in order to understand the geometry of these structures which reveals two, gently plunging, NE-ENE trending synclines. A down plunge projection of both fold structures in these sub-areas (Figure 4.31c and 4.31d) reveals synchronous growth folding and sedimentation with a decreasing interlimb angle up stratigraphy, which indicates that sediments were being deposited during folding.

Inland, in the area around Braemore-Scaraben-Morven Lower Devonian strata are folded into an ENE trending syncline, which plunges very shallowly towards the ENE (4°→072°) (Figure 4.31c). The down plunge projection through this structure reveals a slightly asymmetric syncline that open upwards and is capped by unfolded Middle Devonian strata of the Berriedale Sandstone Formation.

To the S, the Berriedale outlier near to Ousdale is dated, based on palynology to the Lower Devonian Emsian (Wellman, 2014). This outlier is separated from the remainder of the Orcadian Basin by a localised high which is bound by the ESE/WSW trending Berriedale Fault. A down plunge projection of this structure also reveals a more tightly folded, shallowly plunging, NE trending syncline (17°→045°) with an opening upwards geometry (Figure 4.31d). It is capped by the Badbea Conglomerate and Berriedale Sandstone Formation which are relatively undeformed, and folded less tightly, indicating that folding had occurred prior to deposition (Donovan, 1993) and continued into the Middle Devonian.

In summary these two fold structures are clear evidence for an early phase of syn-sedimentary growth folding during the Early-Middle Devonian, and are not related compression/transpression related to the Acadian Event (Wellman, 2014 and references therein) and that the Early Devonian basins were instead developing in smaller more isolated, strike-slip influenced transtensional basins.

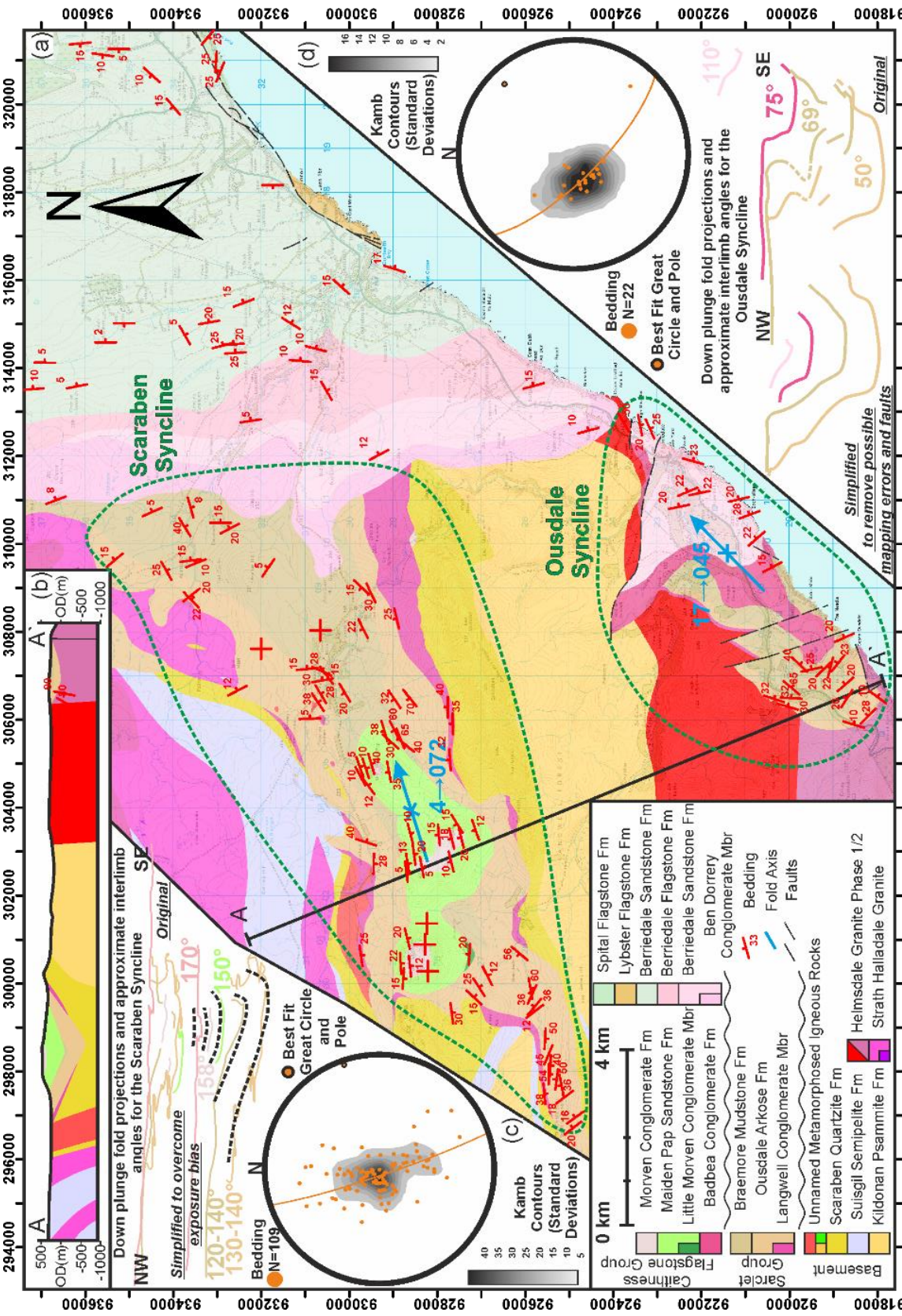

Figure 4.31: (a) Geological map of the Braemore-Scraben-Berridale-Ousdale area. Modified *after* (BGS, 2003a, 1998, 1986). Areas of growth folds outlined in green. (b) Published regional section showing faint growth folds in Lower Devonian strata. Modified *after* (BGS, 2003a). (c) Down plunge

fold projection and structural data for the Scaraben Syncline. (d) Down plunge fold projection and structural data for the Ousdale Syncline. Lower hemisphere equal area projections used for stereonets.

4.4.3.5. Strathpeffer Syncline:

The Strathpeffer Basin to the N of Inverness (Fig. 4.25) is a small half-graben which thickens into the Helmsdale–Polinturk Fault (Clarke and Parnell, 1999), a splay off the major strike-slip Great Glen Fault Zone (Figure 4.32a), which contains stratigraphy of Lower Devonian to Middle Devonian age (Figure 4.32a).

Facies analysis by Clarke and Parnell (1999) allowed for the distinction of facies associations which represent alluvial fan, perennial lake and playa mudflat–ephemeral stream environments. Fault motion and/or climatic fluctuations are thought to have caused significant interdigitation of the facies (Clarke and Parnell, 1999). The lacustrine facies are fringed by alluvial facies, and are thickest closer to the basin margin, but at times of high-water level, the lacustrine margin extended out right to the active basin margin. Sedimentary structures and pseudomorphs after gypsum suggest an arid to semi-arid environment in which the alluvial fan, stream and floodplain sedimentation was largely ephemeral. During arid periods, the basin-centre lake environment was constricted, and the surrounding mudflats experienced intense evaporation, while after flooding episodes the lake increased in size. Syn-sedimentary faulting at the margin was identified as the major control on alluvial fan sedimentation and Clarke and Parnell (1999) interpret the development of this basin as a back-tilted basin, attributing the folding that is observed to later inversion (Figure 4.32b).

This fold plunges very shallowly towards the ENE (Figure 4.32b) and a down plunge projection reveals some elements of growth in this structure, as noted by Clarke and Parnell (1999) (Figure 4.28c). Measurement of the approximate interlimb angles highlights some variation from unit to unit, however definite evidence of growth folding is inconclusive (Figure 4.28c) and may be being obscured by the effects of later fold tightening due to inversion caused by its proximity to several significant faults including the Helmsdale-Polinturk, Strath Glass Fault and Great Glen Faults (Clarke and Parnell, 1999; Mendum and Noble, 2010; Underhill and Brodie, 1993). It is compounded by the SE limbs being truncated against the Strath Glass Fault and obscuring the geometry of the whole fold structure.

The Strathpeffer Syncline is a useful analogue, as it provides plentiful evidence for the interaction of tectonics and climatic variations on the control of deposition. Clear evidence for syn-sedimentary faulting can be found, and it is likely that some degree of tilting and folding of the strata is Devonian in age. However, its proximity to several major faults obscures the evidence, if any, for syn-sedimentary growth folding, but given its similarity to other basin fills elsewhere is likely to have been folded during deposition.

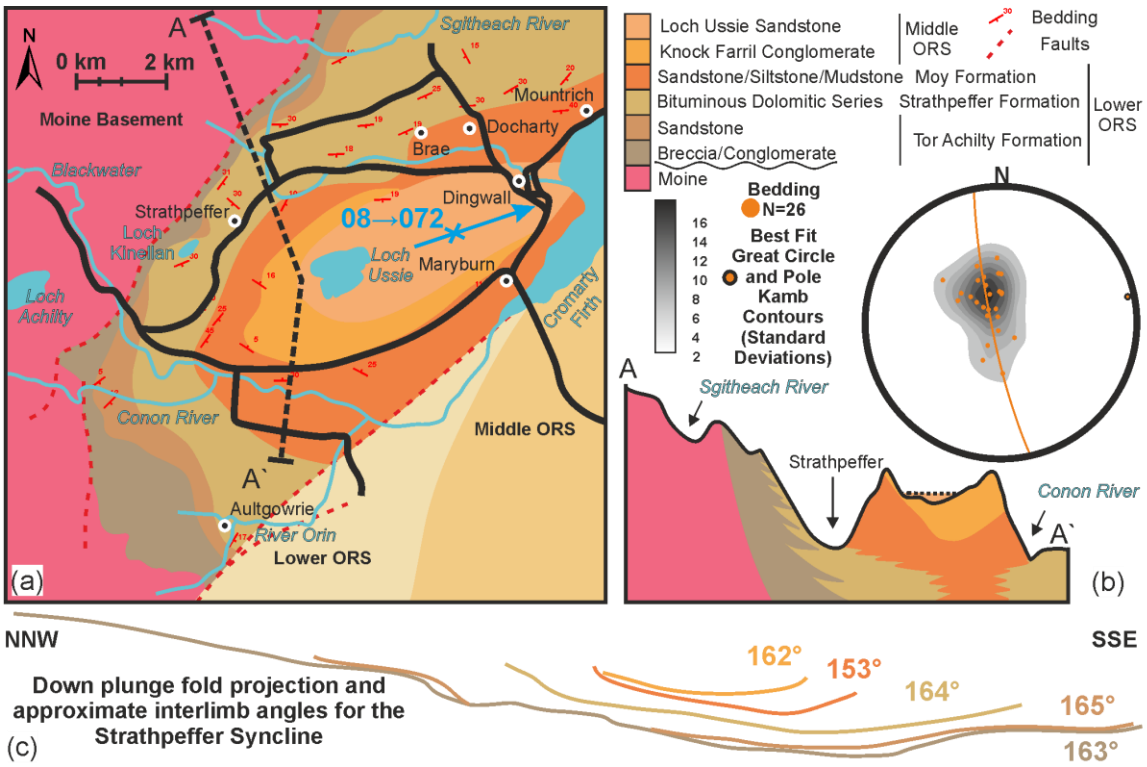

Figure 4.32: (a) Simplified geological map of the Strathpeffer Basin. Modified *after* Clarke and Parnell, (1999); (b) Key and lower hemisphere equal area stereonet of bedding data with best fit great circle and pole and schematic cross section through the Strathpeffer Syncline modified *after* Clarke and Parnell (1999). Data extracted from published geological maps (BGS, 1990; Clarke and Parnell, 1999) (c) Down plunge fold projection through the Strathpeffer syncline with approximate interlimb angles.

4.4.3.6. Scarfskerry:

Previously unreported small scale (<15-20cm thick) examples of sandstone injectites were identified in the field at Scarfskerry Harbour [ND 326036 974464] (Figure 4.33a-4.33g). These injectites increase in number and thickness with proximity to the NW-SE trending Scarkskerry Harbour Fault, which runs through the centre of the harbour parallel and just to the northeast of the slipway NW/SE. The fault zone cuts the flaggy interbedded sandstones and siltstones of the Spital Flagstone Formation of the Upper Caithness

Flagstones and lies an area of intense NW/SE orientated dextral shearing close to a major fault, interpreted to run through the harbour however is not exposed (Dichiarante *et al.,* 2016). The fault zone is intensely folded on a cm to m scale and is highly sheared with indications of bed parallel slip and a consistent dextral shear criteria seen as dextral offsets of tensile carbonate veins that cut the shear zone. Asymmetric fold hinges plunge steeply and show a consistent dextral vergence. Areas adjacent to shear zone are highly fractured and veined with carbonate with both dextral and sinistral offsets, orientated perpendicular to bedding.

Incorporated into this zone are units of pale, sandy, fine to medium grained and poorly sorted material which contains angular clasts of sandstone and laminated siltstone/mudstone (Figure 4.33f and 4.33g) locally cemented with a small amount of carbonate and pyrite (Figure 4.33j). In outcrops immediately to the west, the same sandy material is observed crosscutting highly irregular units (Figure 4.33a and 4.33b). These can be traced downwards into a largely concordant 20-30cm thick pale grey sandstone (Figure 4.33c) which is 20-30cm interleaved with the host strata. Locally it contains fragments or lenses of host rock material, which are partially or fully enclosed within it (Figure 4.33c and 4.33d). Smaller cross-cutting units of pale sandstone are common in the immediately adjacent host rocks and are often ptygmatically folded (Figure 4,33e).

These features are interpreted to be sandstone intrusions or injectites of Middle to Upper Devonian age, formed prior to full lithification of the sediment and predating later shearing, as evident by their folding and incorporation into the shear zone. Their localisation in the region of the Skarfskerry Harbour Fault suggests a link between early movements along this fault in the Devonian, presumably during the initial development of the Orcadian Basin. Similar structures are reported by Andrews and Hartley (2015) in similar facies from Devonian Strata near Easter Ross who propose the early cementation of overlying laminated sediment leading to overpressure in the underlying sediments, which is released in the form of these injectites.

Soft sediment deformation features are also widespread in the Devonian Caithness outcrops and include, fluid escape/dewatering structures, convolute bedding, ball and flame structures and slump structures (Figure 4.33h and 4.33i). These features have mostly been related to near surface sedimentation processes during the Devonian, however it is

also possible that some were induced by active faulting and seismicity. Similar structures are reported in Foula (Chapter 3) and on the Walls Peninsula (see chapter 4.4.1.2).

The presence of these structures in the field may provide evidence for earlier, Devonian age fault movements when other evidence is lacking, proves inconclusive or is obscured due to reactivation. Thus, in areas where Devonian movements have been postulated, effort should be made to identify and classify these where possible, as it provides an independent means by which to identify early fault movement.

Figure 4.33: Field evidence for soft sediment deformation in the Orcadian Basin associated with Group 1 basin forming structures. Field images from Skarfskerry Harbour Fault Zone [ND 326020 974492 showing (a) irregular and angular injectite margin which has been modified by later faulting; (b) and (c) discordant injectite margin which thins and cuts through layers above; (d) detail of

feathered edge of injectite with angular fragments of host rock; (e) ptygmatically folded injectite; (f) and (g) thicker injectite with fragments of host lithology. Field photographs of (h) Dish and saucer shaper shaped fluid escape structures in otherwise undeformed thin bedded sandstones of the John O'Groats Sandstone Formation at Gills Bay [ND 332848 972824 and (i) Fluid escape structures in thin bedded sandstones and siltstones of the John O'Groats Sandstone Formation to the East of the Ness of Duncansby [ND 339314 973732]. (j) Thin section images and QEMSCAN analysis of samples collected from injectites within the Skarfskerry Harbour Fault Zone. Fragments of finer grained laminated sediments are contained as clasts within a coarser grained and much cleaner sandstone which is partially cemented with carbonate and pyrite.

4.4.4. Devonian outliers and other examples of basement-cover in the Orcadian Basin:

Outliers of probable Lower to Middle Devonian age show similar relationships to those seen in the Orcadian Basin at Tongue, Roan Islands, Strathy, Ben Griams, Crask, and Strath Rannoch are discussed by Blackbourn (1981a) (Figure 4.34a) who identified four key depositional units. Unit 1 consists of conglomerates, breccias and arkoses which are locally deposited by alluvial fans on an eroded unconformity of metamorphic basement which transition into Unit 2 which comprises sandstones and flagstones deposited by fluvial-lacustrine systems. Units 1 and 2 are generally deemed to be Lower Devonian and are capped by laterally extensive fluvially derived conglomerates, pebbly sandstones and breccias of Unit 3 and by great thicknesses of fluvial-lacustrine sandstones and flagstones of Unit 4. These latter units are deemed Middle Devonian in age and represent the establishment of the laterally extensive Orcadian Lake and the connection of previously more isolated sub-basins. Note that some of the units included in this regional correlation (e.g. Tongue, Roan Islands) are now viewed as being Permo-Triassic based on apatite fission track data and other geological factors (see Wilson et al., (2010) for discussion).

At Foyers (Figure 4.34b), Stephenson (1972) describes a highly irregular unconformity surface with deep infilled channels that overlain widespread breccias, conglomerates and coarse sandstones deposited by alluvial fans on the edge of an arid intramontane basin (Stephenson, 1972). The great thickness of deposits at Foyers is attributed to its location adjacent to the Great Glen Fault, which likely developed a distinct fault scarp and steep slopes down which coarse grained, immature sediments were being transported into a deep basin which eventually merged with the Orcadian Basin in the Moray Firth (Stephenson, 1972).

To the SW of Fort William, a small outlier of supposedly Lower to Middle Devonian age rocks outcrop alongside Loch Linnhe at Rubha na h-Earba which are described by Stoker, (1982) (Figure 4.34c). This outlier adjacent to the Great Glen Fault Zone records syndepositional intrabasinal fault activity, reflecting a strong tectonic control on sedimentation (Stoker, 1982). The basin is interpreted to have been subsequently inverted and folded during later movement on the Great Glen Fault (Stoker, 1982) and is cut by a NE-SW trending steeply dipping thrust fault along its E margin.

In the area surrounding Dirlot Castle, breccias of Middle Devonian age overly an inlier of Moine basement (Trewin and Hurst, 2009) (Figure 4.35a). The breccias contain clast of pebble to boulder size, some coated with algal stromatolites (Donovan, 1973) and fissures in the basement are lined with tufa. These are overlain by fine grained sandstones, siltstones and laminated shales with parallel and ripple lamination, desiccation and syneresis cracks and loading features (Trewin and Hurst, 2009). The environment observed at Dirlot Castle is inferred as marginal lacustrine environment with the basement rocks exposed here potentially forming a small island within the Orcadian Lake which was progressively buried and inundated by lacustrine and fluvial sediments which terminated the stromatolite supporting environment (Donovan, 1973).

At Balligill and An Dun, a complex unconformity is poorly exposed which is described by Donovan (1975) (Figure 4.35b). Here, a highly eroded surface of granite is draped by breccias, limestones and interbedded siltstones and mudstones which dip steeply down paleoslope. In places these earliest sediments have developed recumbent soft sediment folds indicating down slope movement away from the basement high and contain sediment-filled fissures and fractures (Donovan, 1975). These are overlain and overstepped by relatively flat lying coarse grained sandstones generating an angular unconformity between the two sets of deposits that is likely unrelated to tectonics, but instead to deposition of sediments on a slope, and subsequent differential compaction (Donovan, 1975) of the basement topography.

At Red Point [NC 293055 966007], on the N coast NW of Reay, a complex unconformity (Figure 4.36a) exists which is described in detail by Donovan (1975) (Figure 4.36b) who notes the significant differences in facies that occur over small distances, the highly irregular and pronounced relief of the unconformity surface (Figure 4.36c) and the highly

variable dip of the sedimentary rocks (Figure 4.36d). In many places the relief of basement is in the order of 5-10m however locally this relief is in excess of 15m.

Calcite cemented basal breccias (4.36e and 4.36f) drape the basement and imbricate away or are plastered onto localised highs (4.36c) which progressively onlap the eroded basement fining upwards and interdigitate outwards into finer breccias and calcareous sandstones, massive sandstones and finally into fine grained shales and siltstones (flagstones) (Figures 4.36g, and 4.36h). Localised massive limestones are formed on basement highs and sediments locally dip quite steeply down paleoslope reflecting differential compaction over the basement knolls and hills. Recumbent folds in the sediments reflect down slope movement of unlithified sediment (Donovan, 1975).

Sediment filled fractures with stratification can be found in the basement (Figure 4.36i) and overlying sedimentary rocks which reflect active faulting and differential movement of the basement. This is reflected further by the presence of syndepositional normal faults which trend E/W which show evidence of growth and the development of small graben structures which are infilled with greater thickness of Devonian sediment (Figures 4.36j and 4.36k). Calcite mineralisation and reactivation of these E/W trending fault zones in the basement and overlying Devonian sedimentary sequences may be related to later Permian movements based on the presence of calcite mineralisation (Dichiarante, 2017). Orientation and slickenline data from these E/W trending fault zones are also consistent with Permian transtension which indicate sinistral oblique movement on these structures. A strong contrast in fracture intensity between basement and the cover should also be noted (Donovan, 1975) suggesting a mechanical control on fracture distribution.

These examples from outliers throughout NE Scotland and from other examples within the Orcadian Basin are helpful, as they preserve many of the same basement/cover relationships as those seen elsewhere in the Orcadian Basin providing a more complete picture of Devonian basin development. Many preserve great thicknesses of coarse-grained sediments in the hangingwalls of major active faults during the Devonian and suggest the localised deposition of Lower Devonian sediments, before regional subsidence and widespread deposition of the Middle Devonian sediments. Many of the localities also preserve complex unconformities and highly variable sedimentary cover over relatively small distances. More widely, they all record a complex interplay of tectonics and climate on the deposition of Devonian strata.

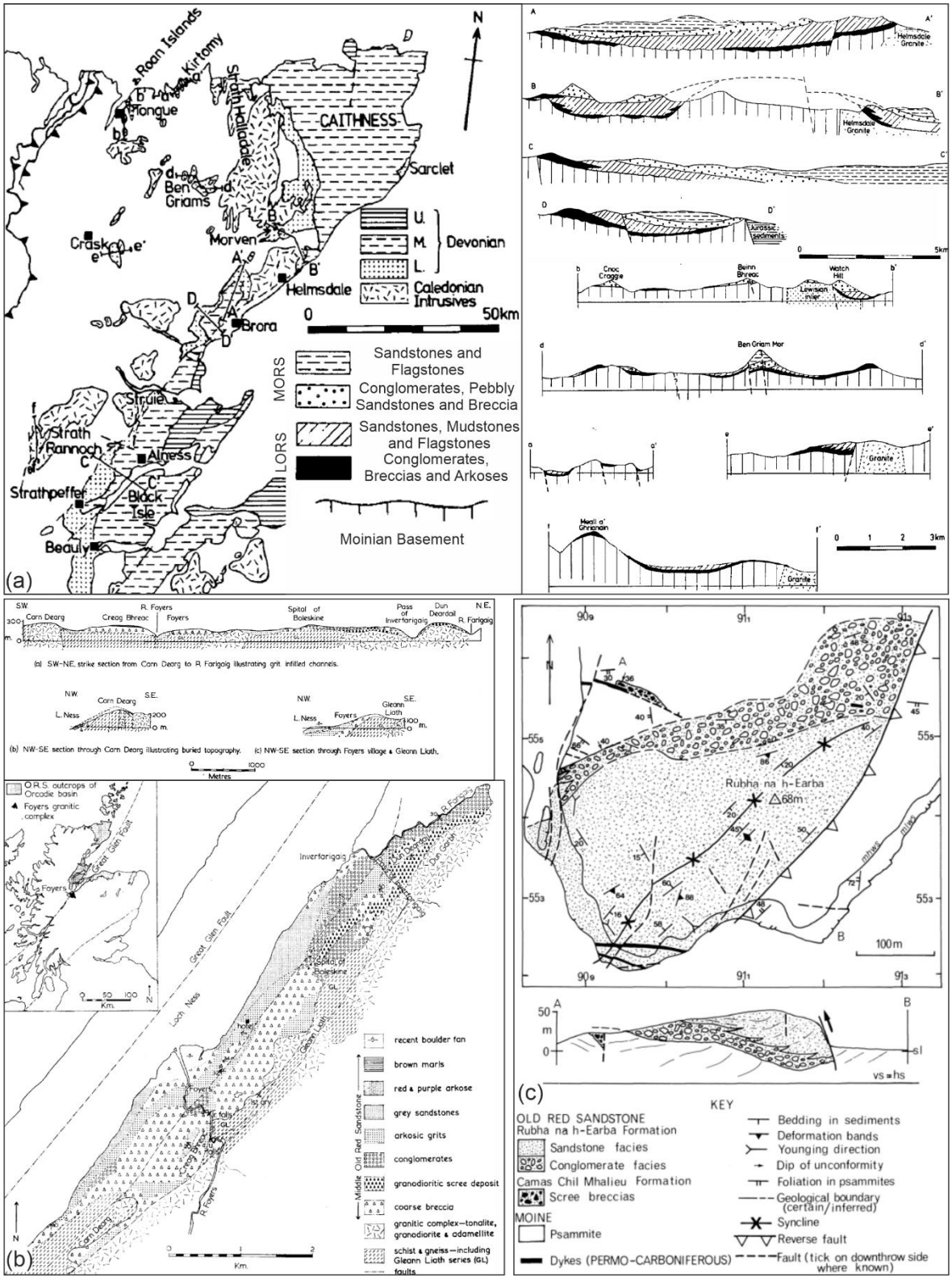

Figure 4.34: (a) ORS outliers in NE Scotland (Modified *after* Blackbourn, 1981b) and other published examples; (b) adjacent to the Great Glen Fault Zone at Foyers (Stephenson, 1972), and (c) near Loch Linnhe (Stoker, 1982).

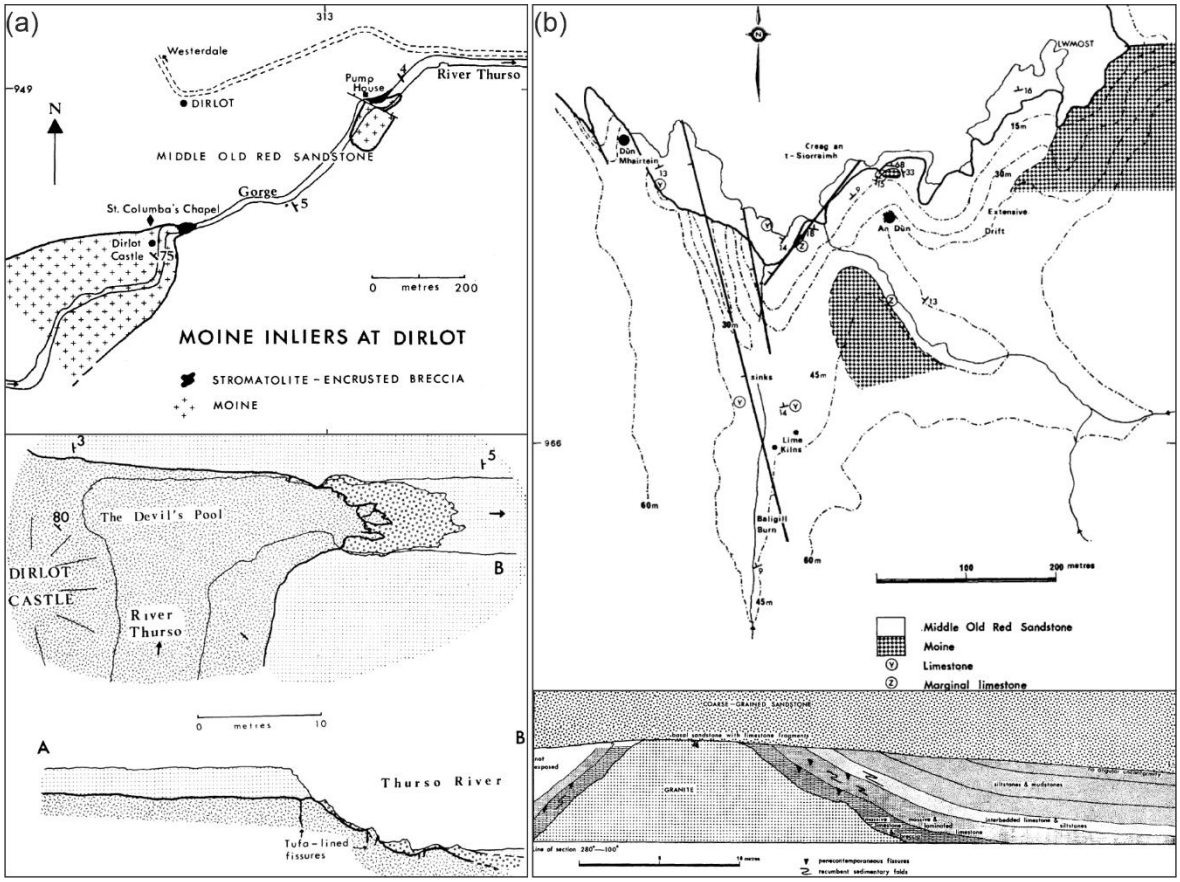

Figure 4.35: ORS outliers within the Orcadian basin at Dirlot (a) and towards the margins of the Orcadian Basin (b) at An Dun and Balligill (Donovan, 1975).

Figure 4.36 (overleaf): (a) Orthorectified oblique aerial image of Red Point. (b) Map and cross section of Red Point (Donovan, 1975). Field photographs of Red Point; (c) steep sided basement hill in the with patches of breccia plastered onto it, (d) differential dip of the basal sediments over the unconformity, (e) erosional unconformity with breccias overlying granodioritic basement (f) wedging basin margin breccias and (g) schematic diagram (Donovan, 1975), (i) sediment filled fractures which show stratification, (j) and (k) reactivated E/W trending basement fault zones with *inset* lower hemisphere equal area stereonet of data from these faults.

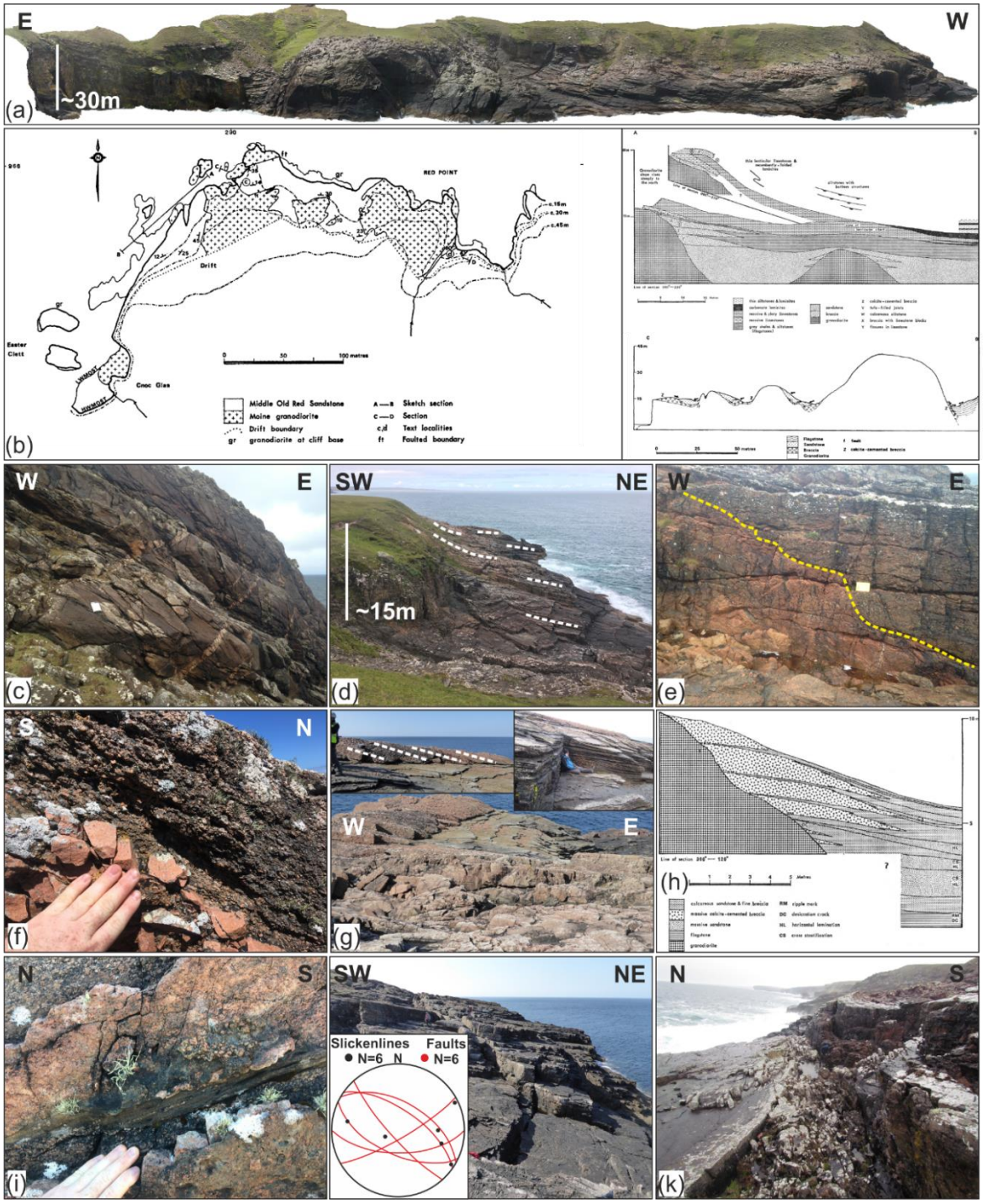

4.5. Discussion:

4.5.1. Devonian Basin Evolution:

4.5.1.1. Shetland:

In Shetland, the Devonian Basins formed in similar but distinctly different basins. The Western Shetland Basin is interpreted to have developed in a basin undergoing regional sinistral transtension, as observed on Foula (Chapter 3) with the development of transtensional growth folds (Figure 4.37). Being the more distal equivalents to units that

outcrop on Foula and in the major Orcadian Basin to the S (Mykura et al., 1976a), the structures observed in the Melby Formation are likely consistent with this tectonic setting. Thus, the Melby Fault is thought to have initiated as a normal to sinistral oblique fault which accommodated growth of the Melby Formation during the Devonian in a fashion like the Foula Fault (see Chapter 3).

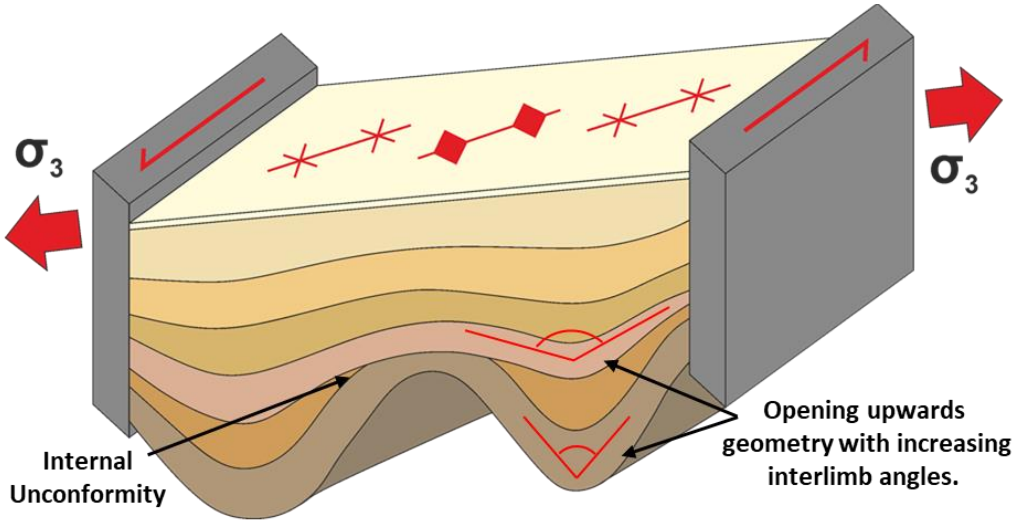

Figure 4.37: Schematic diagram of transtensional growth folds. Hinges rotate towards parallelism with the principal extension direction

The sediments of the Walls Basin were deposited in a tectonically active basin which were deeply buried, as evident by its substantial thickness, and high thermal maturity of organic matter (Marshall, 2000). This, in combination with the thermal metamorphism associated with the emplacement of the Sandsting Complex into the Walls Group (mineral assemblages associated with hornblende/hornfels facies) (Mykura et al., 1976b, 1976a) suggests a rapidly subsiding and tectonically active basin in agreement with Melvin (1985) who postulates that the basin likely formed in a strike-slip influenced setting. Thus, it is likely that it was undergoing regional NE/SW to E/W orientated sinistral transtension (Seranne, 1992) as indicated by the orientation of transtensional growth folds (Figure 4.36) forming oblique to the major basin bounding fault (Walls Boundary Fault).

In Southeast Shetland, the basin was overall less tectonically active with basin fills being controlled predominantly by changes in lake level forcing sedimentary systems to retreat and advance. However the localised development of distinct facies in addition to the E to SE plunging folds, and ‘scooped geometry’ (Seranne, 1992) of the basin which have been attributed to regional sinistral transtension and the movement of basement blocks leading

to the development of forced folds during the Devonian (Seranne, 1992) suggests a basin that was still strongly influenced by transtensional tectonics. The orientation of fold hinges, oblique to the major N/S trending basin margin faults, like in the Walls Basin, suggests regional sinistral transtension.

The present-day configuration of the three Devonian basins in Shetland reflects transcurrent motions along the Nesting, Walls Boundary and Melby Faults. The exact amount of strike-slip motion along these faults has been a topic of great debate but is generally accepted as being in the region of several tens or hundreds of kilometres of sinistral motion during the Silurian-Devonian, followed by subsequent dextral motions of 20-30km during the Carboniferous and Permian, and a further 15km in the Mesozoic (Watts *et al.,* 2007 and references therein). In order to juxtapose the deeply buried sediments of the Walls Group against the more shallowly buried sediments of the Melby Formation (Hillier and Marshall, 1992) it would require subsequent dextral oblique motion, which is consistent with the observations made at Melby and at Eshaness and by Seranne, (1992) on the Walls Peninsula.

The exact amount of reverse and strike-slip motion along the Melby Fault is unknown but may in the region of tens of kilometre dextrally. However the reverse motion and dextral strike-slip motion could have occurred as two distinct and separate events, as suggested by Marshall (2000).

4.5.1.2. Orkney:

In Orkney, the relative simplicity of unconformities suggests a more passive position within the basin that was tectonically, relatively quiescent. Active faulting occurred on predominantly N/S trending faults during the Middle Devonian (Figure 4.38a) together with the accumulation of sediments in the hangingwalls of these faults e.g. North Scapa Fault (Figure 4.38b) and has been identified within the Eday Group, which thickens towards the E (Astin, 1990, 1985; Brown et al., 2019; Hippler, 1993, 1989). Astin (1985) also suggests that some folds adjacent to these faults may have initiated during the Devonian as growth folds. The location of the basement inliers in the footwall to the North Scapa fault may explain the relative lack of tectonic influence on the development of the unconformity in this area.

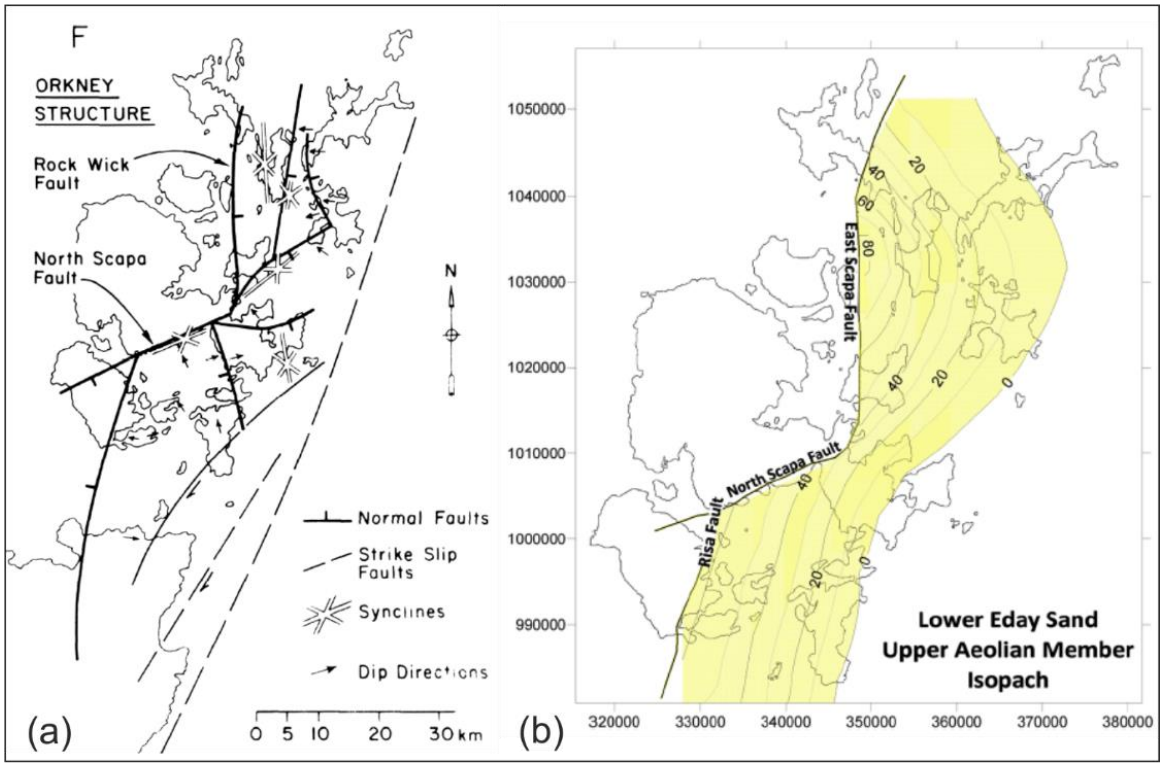

Figure 4.38 (a) Structure of Orkney during the Devonian (Astin, 1985) and (b) isopach map of the Lower Eday Sandstone (Brown et al., 2019).

4.5.1.3. NE Scotland:

In mainland Scotland the Orcadian basin evolved rather more uniformly, particularly during the Middle-Upper Devonian with predominantly N/S trending normal faults accommodating growth and deposition of sediments. However, where local complexities exist, they are driven by local tectonics or by the strong influence of a pre-existing basement topography which exerts a strong control on the deposition of different facies. This is particularly apparent in the Lower Devonian of NE Scotland, where deposits of this age are restricted to the margins of the basin, usually in fault and/or topographically controlled mini-basins. With increasing proximity to the Great Glen, transtensional growth folding and tectonically driven depositional systems and soft sediment deformation become more common, along with a greater diversity in basement-cover relationships.

4.5.1.4. Regional Synthesis:

Widespread and hitherto generally unrecognised Devonian age growth folding has been identified, which is counter to much of the previous work which has traditionally attributed the development of folds to regional inversion during the Permo-Carboniferous (Coward et al., 1989; Enfield and Coward, 1987; Norton et al., 1987) or interpreted to be related to the

Acadian event (Wellman, 2014), . Thus, some – or maybe many - folds in the Orcadian Basin may have already been present prior to inversion and have been subsequently modified and potentially tightened during later phases of deformation to form the more significant fold structures such as the Ham Anticline or Eday Syncline.

Further, post-Devonian deformation in the Orcadian Basin is well accounted for and better understood in mainland Scotland and Orkney (Dichiarante et al., 2016). However, it is relatively poorly understood and documented in Shetland. Evidence for later deformation in the Walls and West Shetland Basins is unfortunately, largely inconclusive due to a lack of clear cross-cutting relationships and/or diagnostic fault/fracture fills. Seranne (1992) suggests that the 'Steep Belt' in Shetland developed during the Permo- Carboniferous and is related to reactivation of a pre-existing basement structure. Mineralisation and deformation in the steep belt are consistent with that found in Scotland and Orkney, and adjacent to the GGFZ throughout mainland Scotland, but requires the use of modern geochronology and geochemistry to confirm this.

4.5.2. Diversity of Basement/Cover Relationships:

The variety of basement/cover relationships observed in the Orcadian Basin, indicate a highly dynamic and varied basin geology and associated unconformities which can be broadly subdivided into 2 types:

- Type 1 unconformities are dominated by local to regional tectonics which drive sedimentary processes and depositional systems. Growth faulting and folding are widespread in these settings which is reflected in the development of depositional systems which are strongly structurally confined or controlled. Type 1 unconformities likely have pre-existing structures which are reactivated in order to provide accommodation space and may be laterally extensive. These structures localise later deformation and are frequently reactivated, by both faulting, mineralization and igneous events, e.g. dyke emplacement.

- Type 2 unconformities are dominated by sedimentary processes driven largely by fluctuations in lake level either due to far-field regional/basin scale tectonics or climate cyclicity and generally form further away from the influence of major basin structures. However, these unconformities may form close to major structures

during periods of tectonic inactivity. Localised unconformities may also form due to differential compaction and transgression/regression of the sedimentary systems.

Figure 4.39 is a schematic diagram that summarises the variety of basement/cover relationships and the structural and stratigraphic architectures and basin settings that are evident in the Devonian sequences which have been observed onshore and are described in greater detail in section 4.4. However, these variations occur not only spatially but also temporally.

Figure 4.39 attempts to preserve a snapshot in basin development that would be equally applicable to any period during the Devonian at across a range of scales. For example, in Orkney, similar basal deposits of breccias and conglomerates are deposited during both the Lower and Middle Devonian and similar deposits are found developed in localised mini basins or in more widespread dm to km scale sheets. Localised deposits of highly varying type are developed adjacent to the basement which in conjunction with varying tectonics through could lead to facies dislocation and unpredictable facies mapping. Further examples of this complexity include; aeolian deposits being reworked by fluvial processes (Tang et al., 2017), which could lead to misidentification of facies. Coarse conglomerates of differing provenance near the basement may have highly variable rock properties and subsequent reservoir quality differences. Differential subsidence could lead to ponding of water, or the development of localised lacustrine conditions and/or carbonates in an otherwise predominantly clastic-rich deposits which are deposited directly onto basement. Localised deposits of carbonates could impact local reservoir quality, providing a source of carbonate for diagenetic pore filling cements.

However, some broad depositional/tectonic settings can be attributed to the Lower, Middle and Upper Devonian. The Lower Devonian of the Orcadian Basin is dominated by tectonic processes with the development of isolated ‘mini’ basins in filled with coarse clastic material delivered by alluvial and fluvial processes. Blackbourn (1981) summarised the origin of the earliest basin fills as being due to differential movements of small basement blocks leading to localised deposition of Lower Devonian sediments. Growth folding is also widespread throughout the Orcadian Basin at this time.

The Middle Devonian is dominated by sedimentary processes, but locally some Middle Devonian basins are similar to the Lower Devonian Basins, particularly where Middle

Devonian sediments are unconformable and faulted against basement or were being deposited in depocentres close to major basin scale structures allowing for the development of growth strata.

Despite no unconformity being directly observed between the Upper Devonian and the basement it is likely that by this time the Orcadian Basin was one larger, intramontane basin. However, deposition in places of the basin was still likely in part controlled by regional or sub-regional structures despite the major control on depositional systems being controlled by far-field tectonics, regional subsidence and/or changes in lake-level.

Figure 4.39 (overleaf): Summary schematic box diagram of Devonian basin development. Horizontal and vertical scale of the diagram is in the order of dm to km but is purposely unscaled as the variation observed is applicable across the whole scale range.

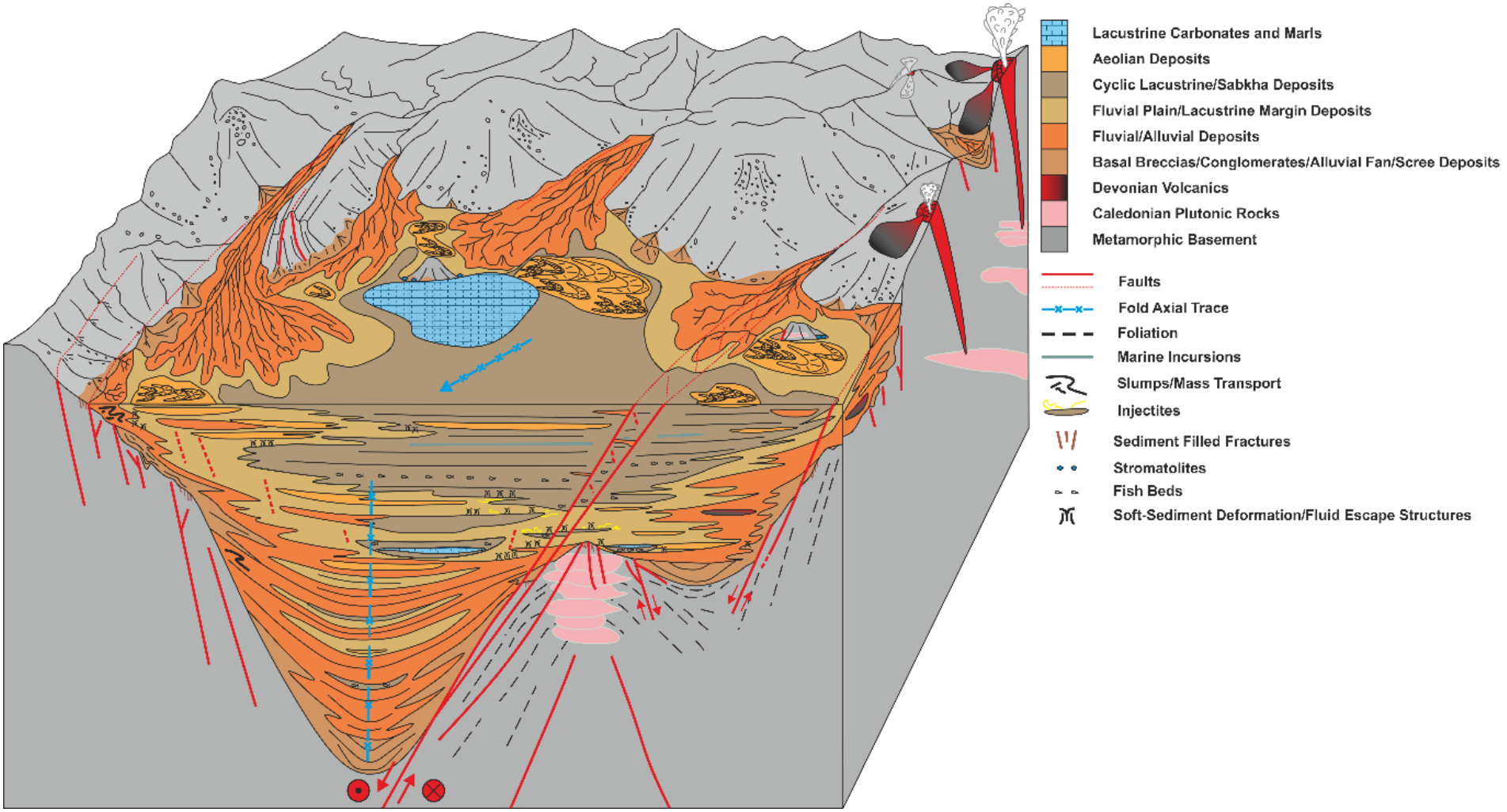
Lacustrine Carbonates and Marls
Aeolian Deposits
Cyclic Lacustrine/Sabkha Deposits
Fluvial Plain/Lacustrine Margin Deposits
Fluvial/Alluvial Deposits
Basal Breccias/Conglomerates/Alluvial Fan/Scree Deposits
Devonian Volcanics
Caledonian Plutonic Rocks
Metamorphic Basement
Faults
Fold Axial Trace
Foliation
Marine Incursions
Slumps/Mass Transport
Injectites
Sediment Filled Fractures
Stromatolites
Fish Beds
Soft-Sediment Deformation/Fluid Escape Structures

4.5.3. Implications for Resource Development and the Clair Oil Field:

In general, an improved understanding of unconformities and basement/cover relationships could help to improve seismic imaging and processing due to the greater understanding of the lateral distribution of key facies and structures. An improvement in seismic imaging and processing has knock on impacts for all subsequent reservoir development phases, improving as the accurate imaging and prediction of facies away from the wellbore is key to optimal future well placement, safer drilling, and ultimately improved production. This improvement in seismic processing can be achieved via the integration of observations made in the field, e.g. the geometry, scale and distribution of facies or fault zone architecture into the seismic processing workflow via the production of synthetic seismic sections of outcrop analogues (Magee et al., 2015; Rabbel et al., 2018; Townsend et al., 1998).

For example, the presence of coarse-grained conglomerates which compositionally, may be very similar to the basement they immediately overly will have similar rock properties and thus similar seismic response. This similarity could lead to the misidentification of 'top basement' on seismic and could be critical in mapping horizons, in volumetric calculations and for guiding drilling. Fault zones in the Orcadian Basin also show various levels of complexity across a range of scales many of which are below the resolution of most reservoir models. This is exemplified in faults and zones in conglomerates which are poorly defined often due to the lack of distinct bedding. The lack of distinct acoustic impedance properties together would further lead to difficulties in seismic imaging. The accurate prediction or imaging of faults and faults zones is key to prevention of the loss of drilling fluid into highly permeable zones which could act as thief zones during production (Feng et al., 2010).

Evidence for a working petroleum system in the Orcadian Basin has been found onshore, at Houton Head and Yesnaby in Orkney (Brown et al., 2019), in addition to small quantities of bitumen, infilling veins and pore spaces in many of the higher reservoir quality sandstones in Caithness (Dichiarante et al. 2016; Baba et al., 2018). The presence of bitumen filled fractures associated with the emplacement of Permian age dykes (Dichiarante et al., 2016) is widely reported in the Orcadian Basin (Parnell, 1985)and oil has also been found in fractured Moinian basement near Castle Leod, Ross-shire and in the Helmsdale Granite (Parnell, 1996; Parnell et al., 2017; Parnell and Bowden, 2017). Offshore,

Devonian lacustrine source rocks are known to contribute to the Beatrice , Oseberg, Judy and Embla oil fields (Stevens, 1991) and have been encountered in wells on the Norwegian Continental Shelf and in metamorphic basement in various parts of Scandinavia (Rønningen, 2015).

The presence of folds that formed during early basin development, synchronous with basin filling and not due to later reactivation, is also important for the assessment of the UKCS petroleum systems. This is primarily due to the formation of potential hydrocarbon trapping geometries much earlier, during basin formation and in proximity to potential Devonian lacustrine source rocks which in the Orcadian Basin were mature during the Carboniferous (Astin, 1990, 1985; Hillier and Marshall, 1992; Marshall et al., 1985; Parnell et al., 1998). Such traps may have formed prior to basin inversion and exhumation in the Permo-Carboniferous, the event to which folds in the Orcadian Basin have been typically attributed to. Furthermore, these trapping geometries would be present for later reactivation and/or filling in other potential petroleum play scenarios elsewhere.

Together, the significant thickness of highly fractured coarse grained clastic rocks in the Orcadian Basin, an active Devonian source rock kitchen with an early charge of Devonian sourced oil (preceding the better documented charge of oil during the Mesozoic) into the folds and trapping geometries that developed early in the development of the Devonian basins and not during later reactivation and/or inversion could represent an underexplored petroleum play on the UKCS and have important implications for the modelling of the petroleum systems in the Moray Firth, West Orkney Basin and East Shetland Platform.

The presence of metre-scale coarse grained sand injectites close to major faults and below conventional seismic resolution could present problems with fault seal integrity and provide relatively permeable conduits for fluid flow in an otherwise fine-grained and relatively impermeable material (Grippa *et al.,* 2019). These structures indicate an early fault zone history that may be overprinted and/or obscured by later deformation, as in the case of the Skarfskerry Harbour Fault.

The presence of soft-sediment deformation structures are also often overlooked in offshore datasets (Dodd *et al.,* 2018) and are particularly overlooked in geological settings they are not expected to form in e.g. shallow water lacustrine settings as opposed to settings such as the deep-water, where turbidites and debris flows are more expected.

Therefore, detailed analysis of core materials, wireline and outcrop with a knowledge and understanding of soft-sediment deformation structures may aid in the understanding of sub-surface fluid flow to help better understand sub-surface data and build more realistic fault zone and reservoir models.

4.6. Conclusions:

The onshore Orcadian Basin preserves insights into the development of the Devonian Basins which is uncomplicated by overprinting due to later deformation seen offshore associated with the development of the North Sea Rift and North Atlantic. Through the study of the structural and stratigraphic evolution of a broad range of analogues throughout the Orcadian Basin, several key conclusions can be drawn:

- Devonian basin development was highly dynamic both spatially and temporally.
- Growth folding and faulting widespread in the Orcadian Basin during the early stages of basin development, particularly during the Lower Devonian, although it continues into the Middle Devonian in Shetland where it is related to oblique sinistral transtension.
- There is evidence for widespread soft sediment deformation and mass transport during the early development of the basin.
- A diversity of basement/cover relationships, together with the distribution, type, and size of structures apparent in the Orcadian Basin could lead to difficulties in exploration and appraisal of resources offshore.
- Folding in the Orcadian Basin not exclusively related to Carboniferous inversion and is prevalent throughout its history, and across a range of scales.
- The Western Shetland Basin is juxtaposed against the more deeply buried transtensional Walls Basin by oblique dextral reverse movement along the Melby Fault
- The findings may have wider implications for not only the Clair Basin and Clair Oil Field but other Devonian reservoirs offshore, and analogues from other parts of the Orcadian Basin may be suitable alternatives going forward.

Finally, due to a lack of information pertaining to the structural development of the Clair Basin during the Devonian, we propose that the established models for Devonian basin development used offshore may require revision and should consider the role of strike-slip tectonics and transtension as an alternative.

Chapter 5

An onshore-offshore interpretation of structures in the Devonian rocks of the Caithness/Orkney region of North-East Scotland, UK: Insights from the seabed geomorphology and onshore exposures of the Pentland Firth.

Chapter 5- An onshore-offshore interpretation of structures in the Devonian rocks of the Caithness/Orkney region of North-East Scotland, UK: Insights from the seabed geomorphology and onshore exposures of the Pentland Firth.

Thomas A. G. Utley[1]*, Robert E. Holdsworth[1], Edward D. Dempsey[2], Ken J. W. McCaffrey[1,] Anna Dichiarante[3], and Thomas J. Jones[1].

[1]*Department of Earth Sciences, Durham University, Science Labs, Durham, DH1 3LE, UK*

[2] *School of Environmental Sciences, University of Hull, Hull, HU6 7RX*

[3]*NORSAR, Gunnar Randers Vei 15, N-2007 Kjeller, Norway*

**Corresponding author (e-mail: thomas.a.utley@durham.ac.uk)*

Keywords:

Bathymetry, Faulting, Folding, Old Red Sandstone, ORS, Devonian, Orkney, Caithness, Basin Development, West of Shetland, Clair Field, UKCS

Abstract:

In this paper we present a geological analysis and reappraisal of the structure, stratigraphy and tectonic evolution of the Devonian strata of North-East Scotland, Orkney Isles and surrounding offshore areas using a 220km² high resolution bathymetric dataset from the Pentland Firth, used in conjunction with aerial imagery, field observations, and photogrammetric 3D Virtual Outcrop Models from onshore coastal outcrops. This has been carried out in order to better understand the scale and distribution of structures within the Orcadian Basin, to better understand the type of structures developed at sub-seismic to reservoir scales and explore the implications for the Orcadian Basin as an analogue to the offshore Clair Oil Field.

Strong tidal currents in the Pentland Firth have stripped the seafloor of recent sediment revealing in unprecedented detail the geological structure in parts of the Orcadian Basin which is obscured or poorly exposed onshore. This has enabled the mapping of a major basin scale fault as a single structure which has partitioned deformation in the Orcadian Basin, acting as a buttress to E/W orientated inversion during the Carboniferous.

Widespread N/S orientated folds and thrusts have been identified across range of scales, in addition to an extensive fault/fracture system dominated by ENE/WSW and subordinate WSW/ESE trending faults and fracture systems developed during Permian transtension.

5.1 Introduction:

The Orcadian Basin outcrops in Caithness have long been used as an analogue for the Devonian-Carboniferous rocks forming the offshore Clair Oil Field, situated 75km W of the Shetland Isles. The Clair Oil Field is the largest known hydrocarbon resource on the UKCS, with a closure of 250 km^2 and an estimated 6-7 Billion BOE in place (Figure 5.1a) (Ogilvie et al., 2015; Webster, 2018; Witt et al., 2010). It is comprised of naturally fractured Clair Group sandstones, that overlie an up-faulted ridge of fractured Precambrian metamorphic basement (Coney et al., 1993)). A significant proportion of the hydrocarbons are stored within fractures, which combined with a viscous heavy oil (API gravity of 23-25°), means that a greater understanding of fracture systems and the structural evolution of Clair and other Devonian basins is required to produce effectively and efficiently from this challenging reservoir.

The Pentland Firth is a narrow sea corridor (~ 16km) that connects the North Atlantic Ocean to the North Sea. It is located between the island archipelago of the Orkney Isles and North-eastern Caithness, mainland Scotland (Figure 5.1a and 5.1b). A two hour difference in tidal phase on either side of the Pentland Firth (Easton *et al.,* 2012) drives tidal currents in the North Atlantic through this narrow channel, around the islands, and into the North Sea, generating some of the strongest tidal currents not only in the UK, but also globally, with peak velocities of 5-6 m/s (Draper et al., 2014 and references therein). As a result of the strong currents generated in the Pentland Firth, a number of wave and tidal energy projects are planned or have been put in place to take advantage of this resource (Easton et al., 2012; Shields et al., 2009). High resolution bathymetry has been collected as part of feasibility and pilot studies, which spectacularly reveals the structure of the underlying bedrock, which in many places has been scoured free of modern sediment by the strong tidal currents, providing an unparalleled insight into the geological structure of the region which is poorly exposed onshore.

In this paper we use recently acquired bathymetric data covering a region comparable in size to the Clair Field (Figure 5.1c) to produce a new geological map of the Pentland Firth,

between mainland Scotland and the Orkney Islands. Analysis of these data provides new insights into the structures developed within the Devonian stratigraphy of the Orcadian Basin, which are poorly exposed in onshore sections away from the coast. New folds have been mapped and the onshore geology has been tied to the offshore subcrop, giving a more complete insight into the size, scale, and type of structures within the Orcadian Basin. Field observations and desk studies have been supplemented using virtual outcrop models to interrogate and understand the geology of inaccessible coastal successions around the Pentland Firth.

The principal aim of this study is to gain an improved knowledge of the scale and distribution of structures in the Orcadian Basin, improve understanding of Devonian basin development and strengthen the link between onshore and offshore geology across a range of scales, particularly at the sub-seismic to seismic scale, in order to help reduce uncertainties during offshore developments. The impacts for petroleum systems are explored in the context of continued development on the Clair Field and its surrounding areas, and the renewed interest in the Paleozoic basins of the Northern North Sea and Moray Firth Basins.

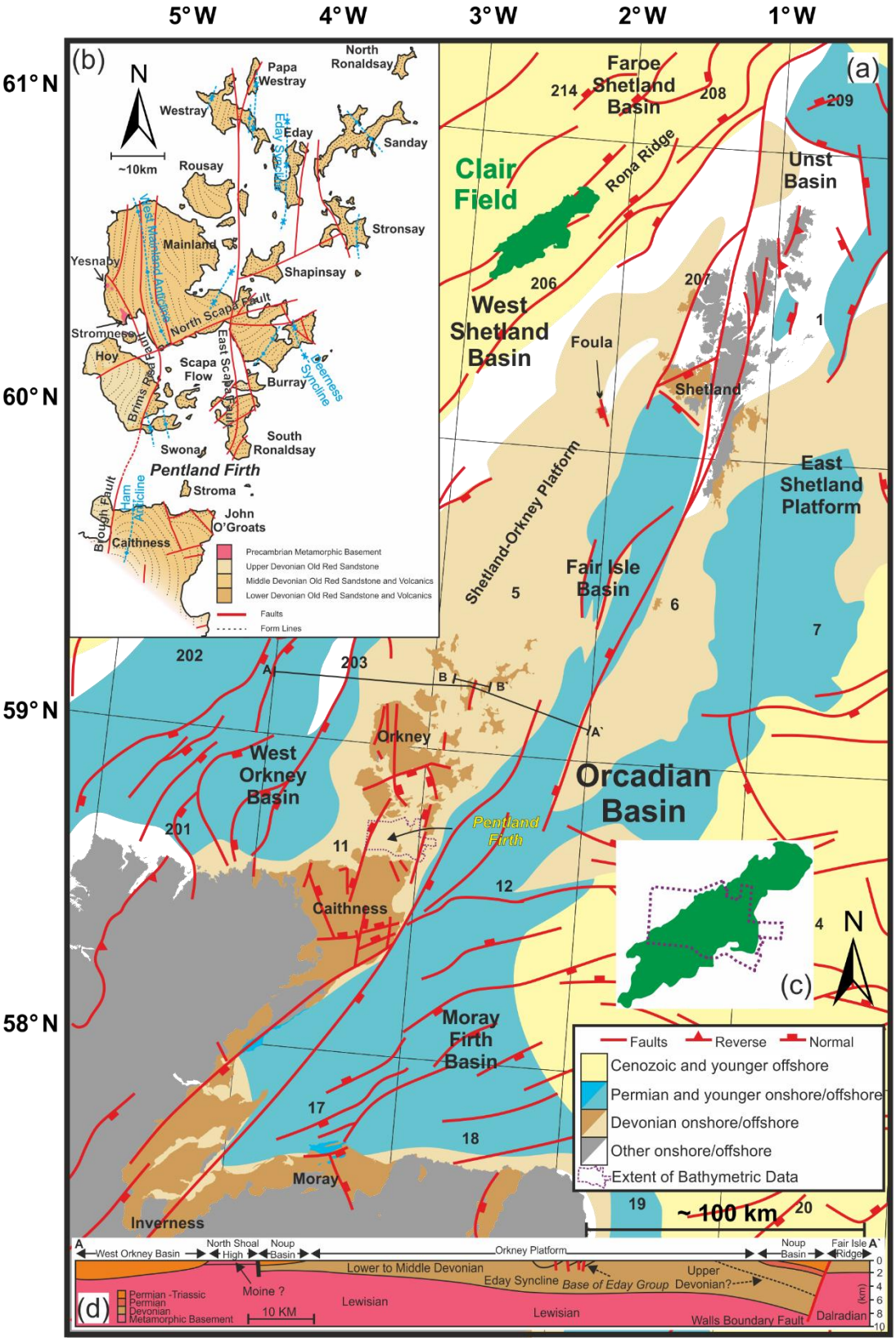

Figure 5.1: (a) Regional map of the Orcadian Basin with Clair Oil Field highlighted. Modified *after* Dichiarante et al., (2016) and Oil and Gas Authority, (2019) (b) Simplified geological map of Orkney and Northeast Caithness with principal structures. Modified *after* (Astin, 1990, 1985; BGS, 1985d, 1982; Brown et al., 2019; Mykura et al., 1976a). (c) Size comparison of Clair Field to area of bathymetric survey. (d) Regional cross section through the Orkney-Shetland Platform showing the

regional basement high which is flanked and overlain by Paleozoic sedimentary basins. Modified *after* (BGS, 1985d).

5.2 Regional Framework:

The margins of the North Atlantic, adjacent to Northern Scotland preserve a series of Paleozoic sedimentary basins that developed following the sinistral oblique continental collision of Laurentia, Baltica and Avalonia (Marshall et al., 2003; Ziegler, 1988) during the closure of the Iapetus Ocean.

During closure, a series of orogenic events occurred which generated the Caledonian orogen and led to the formation of Laurussia (or the 'Old Red Sandstone' (ORS) continent) during the Silurian and Early Devonian (Dewey and Strachan, 2003) (Woodcock & Strachan 2012). Following the gravitational collapse of the orogenic belt, coupled with significant left-lateral displacement along major strike-slip faults, a series of arid to semi-arid marginal marine and intra-continental sedimentary basins developed, into which material shed from the eroding mountain belt was deposited.

The Orcadian Basin is a thick development of Devonian age continental facies, which are predominantly composed of alluvial, fluvial, lacustrine and aeolian deposits. These sediments were deposited in a series of smaller linked sub-basins which eventually coalesced to form the much larger regional-scale feature. It extended some 600km from modern day NE Scotland to the Western coast of Norway and as far as Eastern Greenland, and was strongly influenced by several major strike-slip faults (e.g. Great Glen Fault Zone, Walls Boundary Fault Zone, and More-Trøndelag Fault Zone) which together accommodated many tens if not hundreds of kilometres of sinistral displacement prior to and during the development of this basin.

The Devonian-age fills of the Orcadian Basin are preserved onshore in the UK in Northern Scotland, along the north coast, around the margins of the Inner Moray Firth, and on the island archipelagos of Orkney and Shetland (Figure 5.1a). They are associated with a long-lived NE/SW trending basement high known as the Shetland-Orkney Platform (Figure 5.1d), which is flanked and partially overlain by younger late Paleozoic to Cenozoic sedimentary basins. Deposits of the Orcadian Basin also occur onshore in Western Norway, in Eastern Greenland and are encountered offshore on the UK and Norwegian continental shelves where they form the reservoir for several oil and gas fields.

The Lower, Middle and Upper Devonian sequences of the Orcadian Basin show significant lateral variations in regional stratigraphy and are in places separated by local unconformities (Figure 5.2). In the coastal regions of Caithness and Orkney, the onshore geology predominantly comprises sedimentary and volcanic rocks of Middle to Upper Devonian age, along with a suite of Permian-Carboniferous basic dykes and vent agglomerates (Figure 5.1b). Older, Lower Devonian strata are largely restricted to inland areas and the margins of the Inner Moray Firth Basin where they onlap metamorphic basement. In Orkney, breccias and sandstones that immediately overly small inliers of metamorphic basement that outcrop near Yesnaby, Stromness and the island of Graemsay (Mykura et al., 1976a) are also of Lower Devonian age.

Recent work (Dichiarante, 2017; Dichiarante *et al.,* 2016) has reappraised the structural evolution of the Devonian sedimentary sequences in Caithness and Orkney. Three main phases of deformation have been recognized based on orientation, kinematics and associated fault rocks/vein fills:

- Group 1 structures are thought to be Devonian in age and include NW/SE to N/S trending sinistral oblique to dip slip normal faults related to the opening and early development of the Orcadian Basin. In Caithness, this deformation is best preserved in the older parts of the sequence preserved closer the margins of the basin, where syn-sedimentary faults and growth folds record the early basin development. Initially smaller isolated Lower to Middle Devonian basins coalesced to form the larger Orcadian Basin during the Middle and Upper Devonian. Major through going faults such as the Brough, Brims-Risa and North Scapa Faults (Astin, 1990, 1985; Hippler, 1993, 1989) record this subsequent development accumulating greater thicknesses of sediment in their hangingwalls. Stress inversion analyses of slickenline lineations along faults suggested that this deformation occurred during regional ENE/WSW sinistral transtension associated with sinistral strike-slip motion along the GG/WBFZs (Dichiarante *et al.,* 2016; Wilson *et al.,* 2010).
- Group 2 structures are Late Carboniferous to Early Permian in age and include km-scale N/S trending folds and thrust faults, attributed to regional E/W shortening (Dichiarante et al., 2016; Seranne, 1992). Regional-scale structures developed include the shallowly plunging N/S trending open folds such as the Ham Anticline in Caithness and Eday Syncline in Orkney(Mykura et al., 1976a) (Figure 5.3 and 5.1b).

Smaller, cm to dm scale folds and thrusts are locally developed and pre-existing N/S trending faults such as the Brough and Brims-Risa Fault systems show evidence of compressional reactivation and inversion. The effects of E-W compression are more widely developed in the eastern parts of the Caithness & Orkney outcrops and are attributed to regional dextral reactivation along the Great Glen – Walls Boundary Fault Zone at this time (Seranne 1992; Watts et al. 2007; Wilson et al. 2010; Dichiarante 2017).

- Group 3 structures include dextral oblique NE/SW to NNE/SSE trending faults and sinistral E/W trending faults associated with abundant carbonate, base metal sulphide (pyrite), and hydrocarbon mineralization within faults and in associated fractures/veins. Re/Os dating of vein hosted pyrite mineralisation yields Permian ages ca. 267Ma (Dichiarante *et al.,* 2016). Synchronous with this deformation was the emplacement of a regional ENE/WSW trending lamprophyric dyke swarm, and the development of small basic tuffaceous volcanic vents (Chapman, 1975; Baxter and Mitchell, 1984; Brown, 1975) of Permian age. This deformation is interpreted to be related to regional NW/SE extension and rifting, and the development of the Permo-Triassic sedimentary basins offshore; e.g. the West Orkney Basin (Bird *et al.,* 2015; Dichiarante *et al.,* 2016). In places, the oblique reactivation of existing Group 1 and Group 2 structures has led to complex zones of transtensional and transpressional folding and faulting; e.g. Brough Harbour (Dichiarante, 2017). At outcrop scale, Group 3 structures are dominant in the Devonian rocks along the North Coast of Scotland and are interpreted to have formed in a regional transtensional transfer zone (the North Coast Transfer Zone) which relayed deformation from the West Orkney Basin westwards into the Minch Basin (Dichiarante *et al.,* 2016)

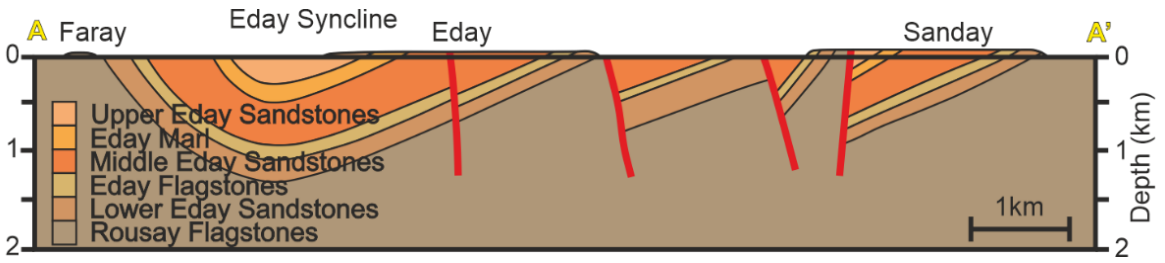

Figure 5.2: Cross section through the Eday Syncline. Modified *after* (BGS, 1985d, 1982; Mykura et al., 1976a). For location of cross section see Figure 5.1. No vertical exaggeration.

5.3 Bathymetric data and methods:

Mapping of the seafloor geology and geomorphology of the Pentland Firth was carried out using bathymetric data (Figure 5.3i) (Survey: 2009 2011-147366 Isle of Stroma Pentland-Firth) sourced from the United Kingdom Hydrographic Office via the ADMIRALTY Marine Data Portal. The data was collected for Marine Scotland between the 18th July 2009 and 5th August 2009 by the *MRV Scotia* using a Teledyne Reson Seabat7125 400 kHz Multi-Beam Echosounder. Survey lines were spaced to ensure a >50% overlap and tidal gauges were deployed during the survey to enable tidal corrections to chart datum. Georeferencing of the data during collection was provided by Applanix POS MV and Fugro STARFIX dGPS. The data was delivered in geoTIFF format (WGS 1984 UTM 30N) with a max vertical and horizontal resolution of 6mm and 2m respectively. Data coverage begins between 500-700m from the shoreline and covers an area of approximately 220km^2 with large gaps (18-20 km^2) in the data surrounding the islands of Swona and Stroma.

Bathymetric data was loaded into Globalmapper v17.0 for the production of hillshade, slope direction (Figure 5.3ii) and slope angle(Figure 5.3iii) maps and collection of orientation data before export into ArcGIS 10.5 for mapping, geological interpretation and lineament analysis at a scale of 1:5000. 2D topological analysis of bathymetry and aerial imagery was undertaken using the NetworkGT toolbox for ArcGIS (Nyberg *et al.,* 2018). This was carried out in order to provide a quantitative assessment of fracture (lineament) connectivity using dimensionless intensity (2D fracture intensity x average branch length), a scale invariant measure of fracture intensity which takes into account sampling bias (Nyberg et al., 2018; Sanderson and Nixon, 2015).

Fieldwork was carried out to ground truth interpretations and investigate the outcrop scale expression of structures observed on bathymetric data in coastal sections adjacent to the offshore study area. The use of a drone allowed images to be collected from several inaccessible coastal locations that were used to create 3D Structure *from* Motion (S*f*M) Virtual Outcrop Models at several locations. Models were generated in Agisoft Photoscan and were analysed and interpreted within the VRGS software package (Hodgetts, 2019) to extract geological orientation data. Structural analysis was carried out in Stereonet 9.5 and the study was supplemented by pre-existing datasets including onshore seismic, high resolution aerial imagery courtesy of the Ordnance Survey and published onshore and

offshore geological maps courtesy of the BGS. Further detailed methodologies for the aforementioned techniques can be found in Chapter 2.

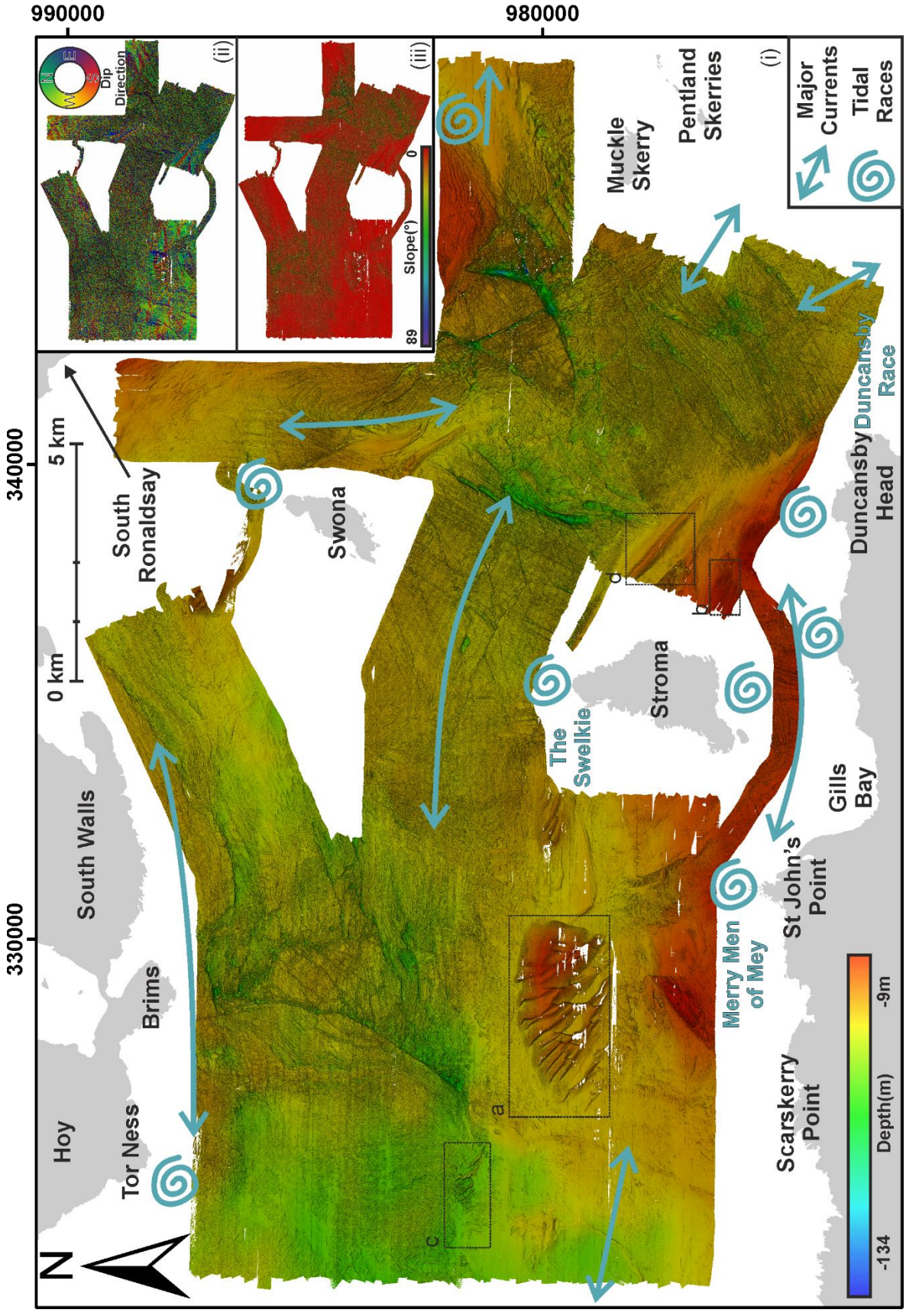

Figure 5.3 (preceding page): (i) Uninterpreted bathymetric map of the Pentland Firth showing direction of principal ocean currents and named tidal races (UKHO, 2019) and main geographic features/locations. *Inset* (ii) bathymetry coloured by slope direction and (iii) by slope angle. Dashed boxes refer to features of interest shown in Figure 5.4 and Figure 5.10.

5.4 The Geology and Submarine Geomorphology of the Pentland Firth:

5.4.1 Description of Seabed Morphology:

Water depth ranges from -9 to -135m with the seafloor dominated by rocky sea floor and exposed swept bedrock, classified as "Atlantic and Mediterranean high energy infralittoral rock" (EUNSIS 2007-11 Scheme) (Martin-Short et al., 2015; Shields et al., 2009). These areas of swept bedrock clearly reveal the underlying geological structure of the Pentland Firth accentuated by the differential erosion of weaker geological structures and stratigraphic units e.g. faults and associated damage zones, some of which have been eroded many tens of metres deeper than the surrounding sea floor, into distinct gullies and chasms.

However, local areas of modern marine sediment are also observed proximal to islands in the Pentland Firth such as Stroma and Swona. The islands alter flow patterns through the channel, causing eddies and the generation of extremely strong currents or 'tidal races' (Figure 5.3i). In areas of lower current velocity, deposition and accumulation of sediment has occurred or has prevented the erosion of existing material by the strong currents. Bottom sampling shows that the unconsolidated sediments are predominantly composed of poorly to well sorted coarse sands, fine gravels and gravel sized, benthic bioclasts (BGS, 2019).

A series of intriguing geomorphological and marine sedimentary features have been identified (Figure 5.3i), the most obvious and easily discernible being dm-hm scale subaqueous dunes and megaripples that have formed in the lee of the islands of Swona and Stroma.

To the west of Stroma a large dune field (4x3km) has developed (Figure 5.4a). It rises ca.15m above the surrounding sea floor which has superimposed smaller dunes-megaripples. Inclination of lee and stoss slopes suggest W to E migration of these dunes. To the E of Stroma a km scale field of smaller metre size dunes-mega ripples rises ca.20-25m above the swept bedrock (Figure 5.4b). These dunes are largely orientated NNW/SSE and are developed there due to water being driven to the S around the island of Stroma.

Further to the W of the study area, smaller dm-hm scale arcuate barchan dunes are developed (Figure 5.4c), which reflect westward going currents through the Pentland Firth.

To the E of Swona and Stroma, SE orientated linear, 10-20m high longitudinal dunes have formed due to the convergence of currents around the islands (Figure 5.4d). Adjacent to the linear dunes formed in the lee of Stroma, 10-15m deep dunes/scours have been formed in this embankment of sand.

Figure 5.4 (overleaf): Geomorphological features of interest with cross sections; (a) Large dune forms with smaller superimposed dunes, (b) smaller scale dunes, (c) barchan dunes with *inset* oblique 3D view, (d) linear dune and scour in sand flat. Cross sections have 5x vertical exaggeration. For location of features see Figure 5.3

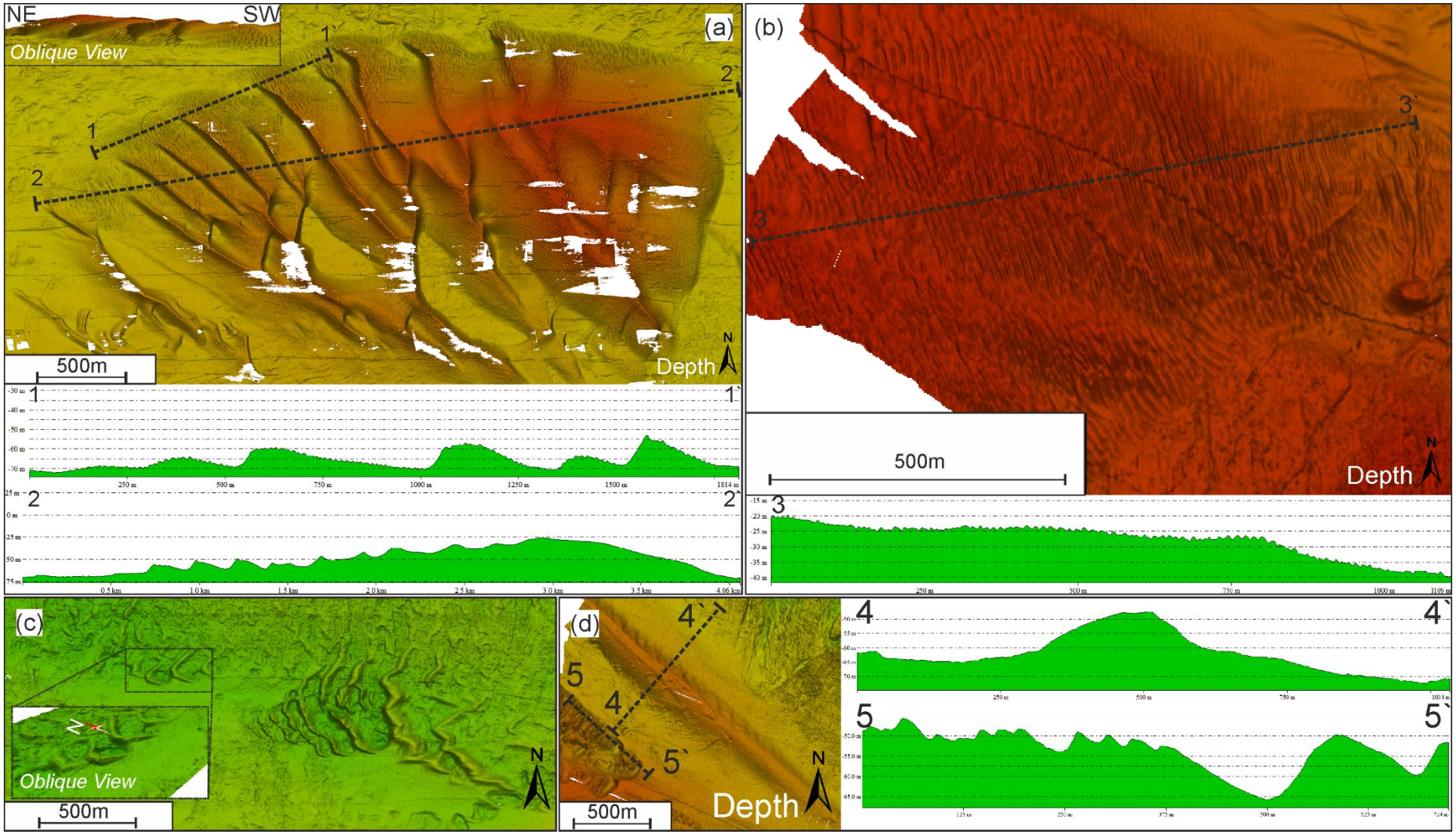
NE
SW
Oblique View
(a)
1`
2`
1
2
500m
Depth
N
(b)
3`
3
500m
Depth
N
1
1`
2
2`
3
(c)
Oblique View
500m
N
(d)
4`
5
4
5`
500m
Depth
N
4
4`
5
5`

5.4.2 Stratigraphy:

5.4.2.1 Onshore:

The southern shoreline in Caithness is dominated by Middle Devonian sedimentary rocks of the Caithness Flagstone Group (Figure 5.5), which is subdivided into the Lybster Flagstone, Spital Flagstone and Mey Flagstone formations (BGS, 1986, 1985a). These formations are predominantly fluvial and lacustrine in origin and contain several fossil rich horizons or 'fish beds' (Johnstone and Mykura, 1989). They are overlain by the predominantly fluvial sedimentary rocks of the John O'Groats Sandstone Group. Upper Devonian fluvial and aeolian sedimentary rocks of the Dunnet Head Sandstone Formation are restricted to the headland of Dunnet Head and are faulted against older rocks to the east by the Brough Fault (Figure. 5.5) (Johnstone and Mykura, 1989).

On the shorelines of the Orkney Isles, Middle to Upper Devonian sedimentary rocks and minor volcanics dominate which are the lateral equivalents to the Caithness Flagstone Group (Figure 5.5) (Mykura et al., 1976a). Much of Orkney comprises the lacustrine Upper and Lower Stromness Flagstone Formations (BGS, 1999), which are overlain by the rocks of the Eday Group, which preserve a transition from mixed lacustrine and marginal fluvial/alluvial deposits to predominantly fluvial deposits. The Upper Devonian Hoy Sandstone on the island of Hoy is formed by a ~1km thick sequence of fluvial and aeolian sandstones and marls that unconformably overlie lavas and tuffs of the Middle Devonian Eday Group, and termed the Hoy Volcanics (BGS, 1999; Mykura et al., 1976a). They are a faulted against other parts of the Eday Group by the Brims-Risa Fault which is thought to link southwards to the Brough Fault in Caithness (Figure. 5.5) (Coward et al., 1989; Mykura et al., 1976a; Seranne, 1992).

5.4.2.2 Offshore:

Based on the adjacent onshore geology, it seems likely that the seafloor to the W of the Brough-Brims-Risa Fault comprises Upper and Middle Devonian units equivalent to the Eday Group and younger strata (Figure 5.5). To the E of the fault, it is likely that the sea floor comprises Middle Devonian units from the Caithness-Stromness Flagstones and overlying units. Further detailed stratigraphic assignment is challenging, although it may be possible in the future to attempt to differentiate and contrast units that are more sand rich

and massive (e.g. aeolian/fluvial deposits), from those that are more heterogeneously layered, and likely represent more interbedded/stratified units (e.g. lacustrine deposits).

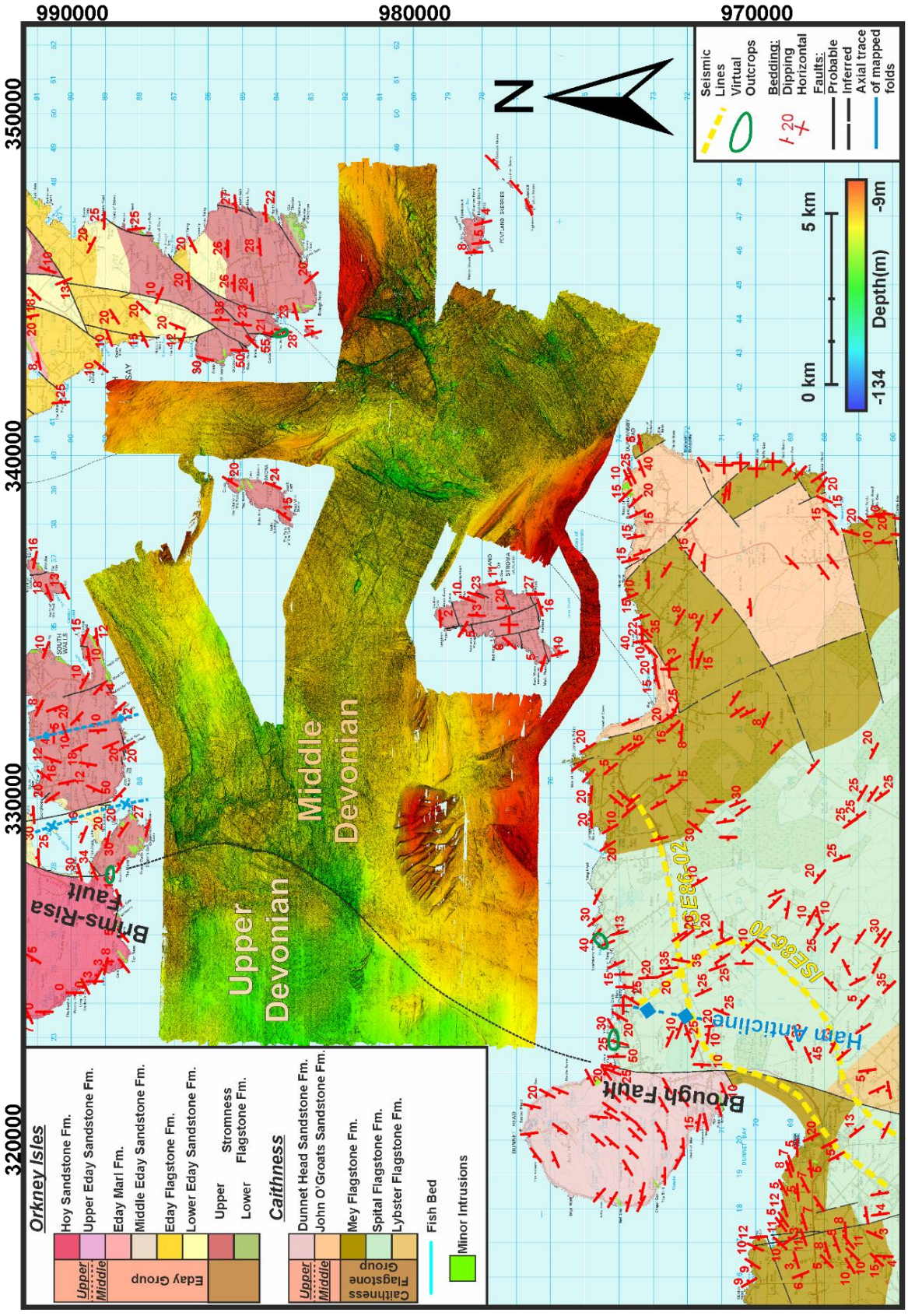

Figure 5.5 (preceding page): (a) Map of the Pentland Firth showing uninterpreted bathymetry, onshore geology, and major mapped structures. Seismic lines and virtual outcrop locations are highlighted. 1:50,000 base map courtesy of the Ordnance Survey. Geology courtesy of the BGS.

5.4.3 Structural Geology:

Various styles of faulting and folding are observed in the study area, and it is generally possible to link structures mapped onshore with those exposed extending offshore, providing an almost continuous structural map of the Pentland Firth and surrounding area. Bedding lineaments were differentiated from fault lineaments based partially on the dip of the adjacent sea floor but also from the morphology of the lineament, with more deeply eroded lineaments more likely to correspond to structural lineaments as opposed to the more regular and often more asymmetric lineaments when viewed in cross section . The kinematics of faults are inferred from the apparent offset of bedding traces (pixel resolution ca.2m) where visible, although vertical throws are difficult to assess. Further constraints come from known senses of offset and displacement for faults with particular trends seen in the adjacent onshore areas (Dichiarante, 2017) (See section 5.2).

Two structural domains are apparent which are separated by the generally NNE-SSW Brough-Brims-Risa Fault Zone (Figure 5.5). The region to the west is less deformed, with bedding, which gently dips towards the W/NW together with a lower number, density and diversity of lineaments (Figure 5.5 and 5.6). This is due in part to occlusion by modern marine sediments, however in places free of sediment, fewer lineaments are observed. This is also consistent with these rocks being Upper Devonian in age, as onshore, they are also much less effected by deformation compared to the Middle Devonian. Most lineaments in this region trend ENE/WSW through to NE/SW. These lineaments are frequently isolated or terminate within the Brough-Brims-Risa fault zone and many are crosscut by shorter, uncommon WNW/ESE to NW/SE trending lineaments.

The region to the east of the Brough-Brims-Risa Fault Zone is generally more deformed (Figure 5.5 and 5.6, with more variable bedding and a higher concentration of lineaments. This variation is due in part to the presence of several km-scale N/S orientated fold structures (see section 5.4.3.1) in addition to localised zones of complexity and folding related to major fault zones (see section 5.5.4.2). Further E, in the region between John O'Groats and South Ronaldsay, bedding dips are highly variable which may reflect the differential movement of fault blocks. In this region ENE/WSW to NE/SW lineaments are

the most numerous, however several regions of N/S trending lineaments are observed to the North of Stroma and immediately NE of John O'Groats. In the region between Stroma and Swona, there is a distinct clustering and concentration of ENE/WSW and NW/SE to WNW/ESE trending lineaments, which produce a very distinctive rectilinear pattern which is a relatively pattern elsewhere in the dataset.

5.4.3.1 Folding:

The bathymetry data reveal the presence of several large, km-scale, upright to gently plunging open fold structures. These folds trend NNW to NE and can be traced as continuous features for several kilometres. Between the islands of Swona and South Ronaldsay, a large N/S trending plunging syncline can be traced across the full width (~18km in length) of the dataset. A down plunge projection of this fold reveals a slightly asymmetrical open synform which plunges extremely shallowly towards the S (0.5°→189°) (Figure 5.7a) with gentle (120-180°) interlimb angles, and a slight westward vergence. The oblique cut through this structure makes it appear far more extreme than it is but is in fact an incredibly open and gentle structure.

To the west of this fold structure a smaller N/S trending anticline is observed, with the hinge trending southwards towards the island of Stroma (Figure 5.6). Fault-related drag folding associated with several N/S major faults and fault zones (see section 5.4.4.2) is also observed and the W limb of the smaller fold N of Stroma is truncated by one such structure. These more complex and variably orientated fold structures may be related to transtensional reactivation of these fault zones, as is observed onshore (Dichiarante, 2017).

Further fold structures with more variable trends (NW-NE) are also observed, in addition to similar, but considerably smaller N/S trending folds (Figure 5.6 and 5.7b). To the W of the Brough-Brims-Risa Fault, bedding is quite variable, which may reflect the development of numerous smaller fold structures and the differential movement of fault blocks in the hangingwall to this basin wide structure.

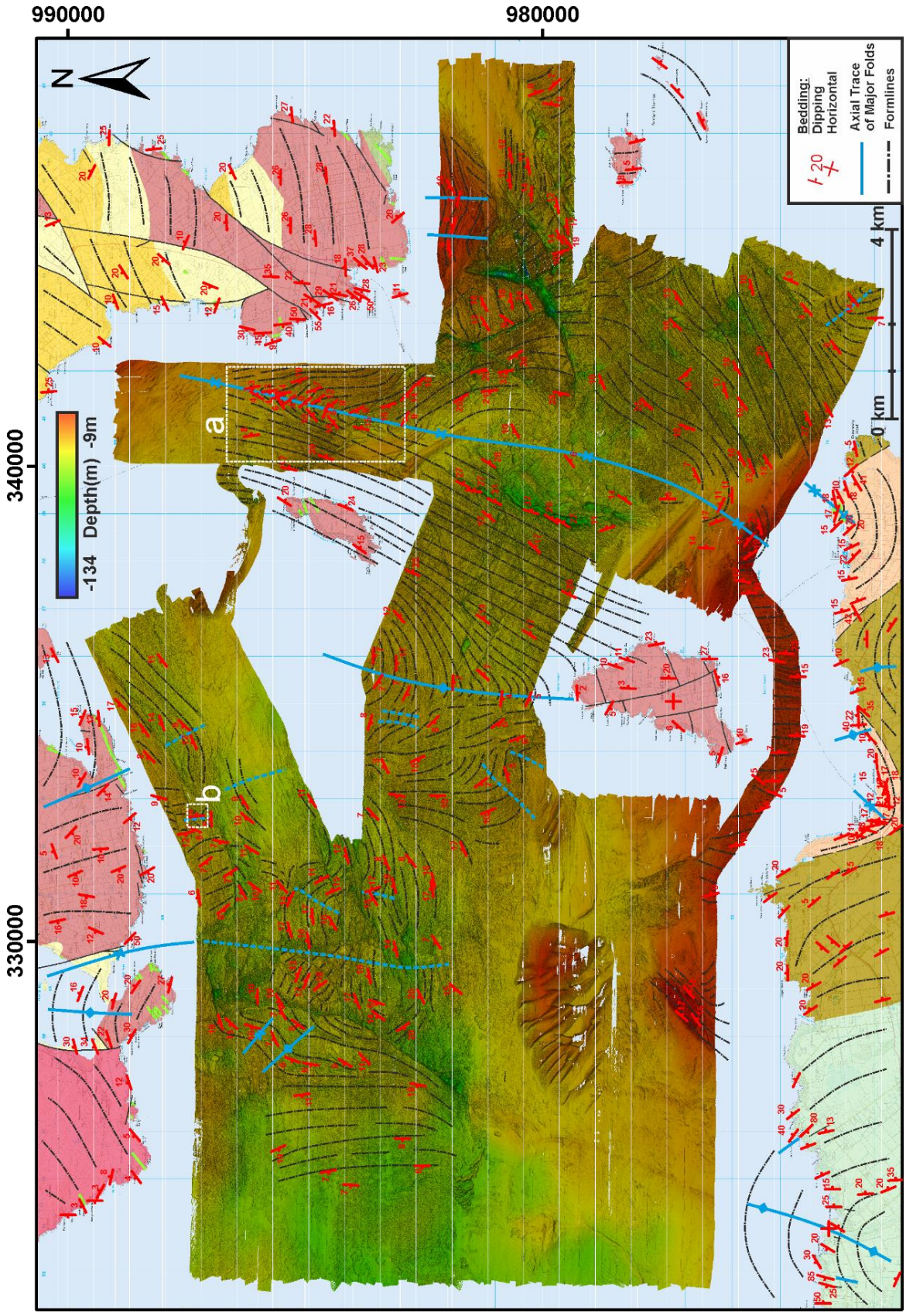

Figure 5.6: Form map of the onshore and offshore Pentland Firth showing the major fold structures. Lettered boxers refer to features of interest shown in Figure 5.7. Geology courtesy of the BGS, for key see Figure 5.5. 1:25,000 base map courtesy of the Ordnance Survey.

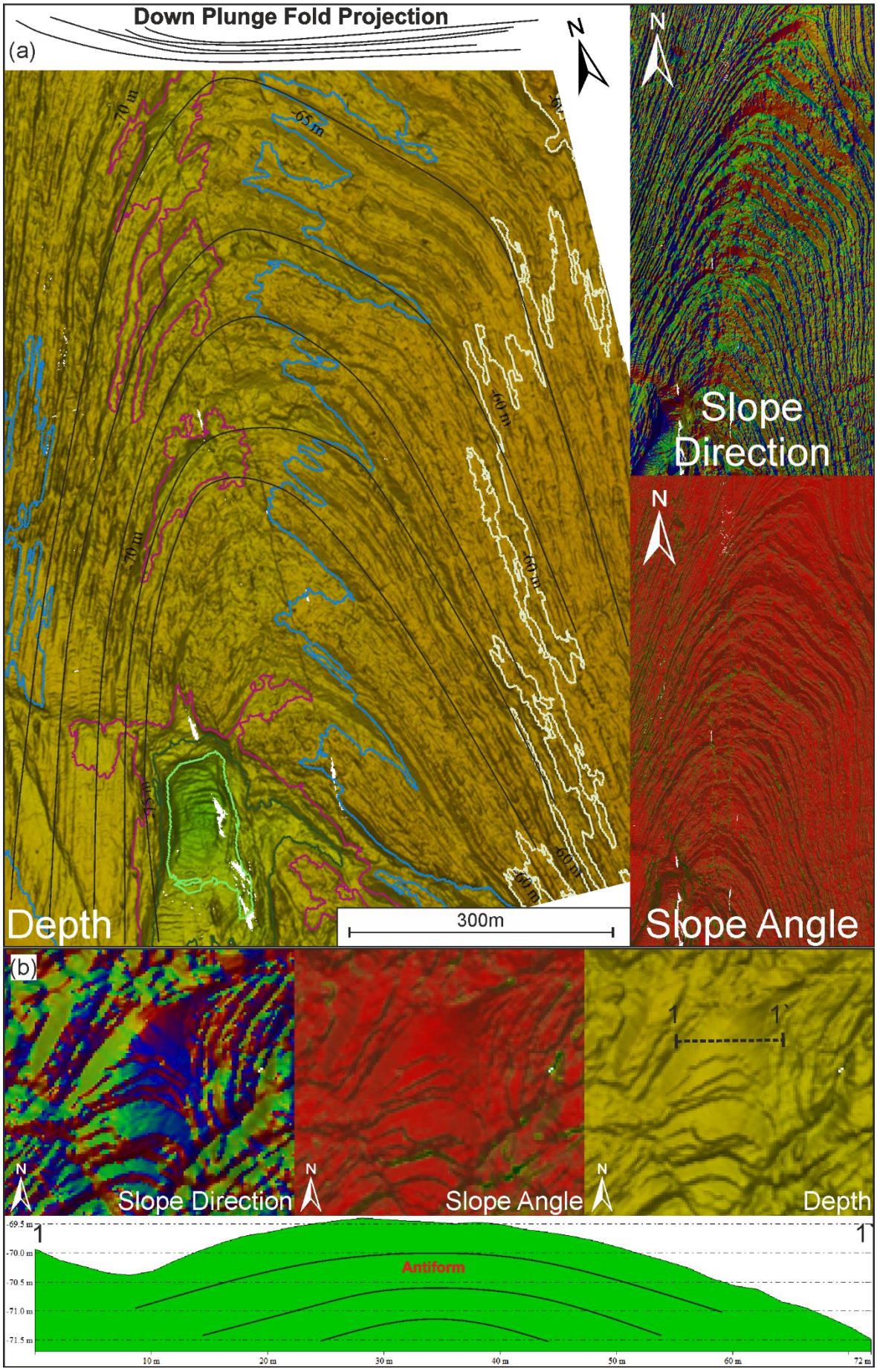
Down Plunge Fold Projection
(a)
N
-70 m
-65 m
-60 m
-70 m
-60 m
-60 m
-60 m
-60 m
Depth
300m
Slope Direction
Slope Angle
(b)
Slope Direction
Slope Angle
Depth
1
1'
Antiform
-69.5 m
-70.0 m
-70.5 m
-71.0 m
-71.5 m
10 m
20 m
30 m
40 m
50 m
60 m
72 m

Figure 5.7 (preceding page): Detailed images of examples of fold structures in the Pentland Firth; (a) major synform between South Ronaldsay and Swona southerly plunging km scale synform with down plunge projection showing roughly cylindrical fold geometry; (b) smaller dm scale northerly plunging anticline. For locations, see Figure 5.6.

5.4.3.2 Faulting and Fracturing:

A total of 3178 offshore lineaments were mapped from the bathymetry (Figures 5.8 and 5.9a), with a trace length of <1500km, a mean length of 247.96m and a range of 3717.55m (Table 5.1). Mapped lineaments are interpreted to correspond to faults, fault zones and large scale fracture systems with 4 predominant trends identified (Figure 5.9b); ENE-WSW (n=1607), NE-SW (n=443), WNW-ESE to NW/SE (n=740) and N/S (n=388). Figure 5.9c shows lineament length against orientation and shows that the longest lineaments are orientated N/S to NE/SW and ENE/WSW.

Sample Area	Onshore	Offshore
Area (m^2)	60889.22	1005053316.79
No. Lineaments	8077	3178
Mean Lineament Length (m)	3.05	247.96
Max Lineament Length (m)	45.13	3717.55
StDev Lineament Length (m)	3.53	257.28
Mean Lineament Orientation (°)	82.49	74.16
StDev Lineament Orientation (°)	42.48	46.12
No. Edge Nodes (E)	215.00	39.00
No. I Nodes (I)	2358.00	2479.00
No. X Nodes (X)	669.00	246.00
No. Y Nodes (Y)	3623.00	953.00
No. Unknown Nodes (U)	0.00	0.00
No. Nodes	6650.00	3678.00
No. Branches	7951.50	3161.00
No. Lines	2990.50	1716.00
No. Connections	4292.00	1199.00
Average Connect/Line	2.87	1.40
Average Line Length (m)	8.21	1010.25
Average Branch Length (m)	3.09	607.06
Average Connect/Branch	1.70	1.22
2D Intensity	0.40313	0.00174
Dimensionless Intensity	1.24449	0.83033

No. Branches (minus unknown branches	7939.50	3153.50
No. C – C (doubly connected branches)	5737.00	1281.00
No. C – I (singly connected branches)	1864.00	1258.00
No. C – U (singly connected branches)	92.50	8.00
No. I – I (isolated branches)	234.00	595.00
No. I – U (singly connected branches)	12.00	11.50
No. U – U (unknown/edge branches)	0.00	0.00
Total Length C – C (m)	15517.42	513847.72
Total Length C – I (m)	6442.53	626695.92
Total Length C - U(m)	1118.40	10792.43
Total Length I - I(m)	1200.65	348663.71
Total Length I - U(m)	200.16	7070.10
Total Length U - U(m)	67.40	0.00
Total Trace Length (m)	24546.57	1507069.88

Table 5.1: Comparison of fracture data from the onshore and offshore Pentland Firth.

The two structural domains (see section 5.4.3) are separated by the longest mapped lineament, which comprises several segments up to 3-4km long length trending NNW/SSE to NE/SW (Figure 5.10a), with a total length of ~12 km.

We interpret this feature to be the offshore continuation of the Brough-Brims-Risa Fault Zone. On bathymetry, this structure forms a deeply eroded 10-15m deep gully feature with several NNE to NE trending splays developed on the E side of the structure (Figure 5.10a). These structures are concentrated in the area where the fault swings from a NE to NNW trend, and may have formed due to strain localisation adjacent to a restraining and/or releasing bend during movement on the fault. In the immediate area surrounding the fault zone, particularly in the hangingwall, bedding is difficult to identify, and this region may correspond to the faults damage zone, with numerous subordinate faults and folds (Figure 5.8).

Several other N/S lineaments (NNW to NNE) up to ~1 km long show significant deformation, such as localised kink folding, e.g. North of Stroma (Figure 5.10b) which are likely related to reactivation of these N/S structures in an oblique manner. Deeply eroded gullies developed along these features immediately to the S of South Ronaldsay are likely the offshore expression of the major mapped faults onshore on South Ronaldsay (Figure 5.5). Seemingly related to these lineaments are a series of NE-SW trending features which frequently connect with or curve round into N/S orientated structures.

Regionally, the most numerous, laterally extensive and deeply eroded lineament set trends ENE-WSW (Figure 5.10c). Many of these features show clear apparent sinistral offsets, particularly where they bisect and offset the trend of dipping beds (Figure 5.10c). A subordinate set of WNW/ESE to NW/SE trending lineaments appear form the conjugate set to the ENE/WSW trending lineaments and show some apparent dextral offsets. These structures are generally some of the shortest and frequently terminate against ENE/WSW and NE/SW trending lineaments. Swarms of these structures produce a pronounced rectilinear pattern occur in the area between Stroma and Swona (Figure 5.10d). NE of Duncansby Head and immediately to the SW of South Ronaldsay, a ~2.5km long lineament bisects a large fold with an apparent dextral offset of the bedding.

A deep roughly rectilinear hollow of unknown origin ca.25m deep (Figure 5.10e) is observed in the centre of the data, which is ca.400m in length and ca.100-125m in width. It is bound by ENE/WSW and NW/SE trending fractures/faults zones. This feature appears to be partially filled with modern sediment, with faint dunes-mega ripples being visible in its base. We interpret this feature as some sort of pull-apart mini-basin and/or volcanic feature, similar in origin to those observed onshore (Baxter and Mitchell, 1984; Chapman, 1975; Kellock, 1969; Lundmark et al., 2011; Macintyre et al., 1981; Parnell, 1983), which has been over-deepened by marine and/or glacial erosion.

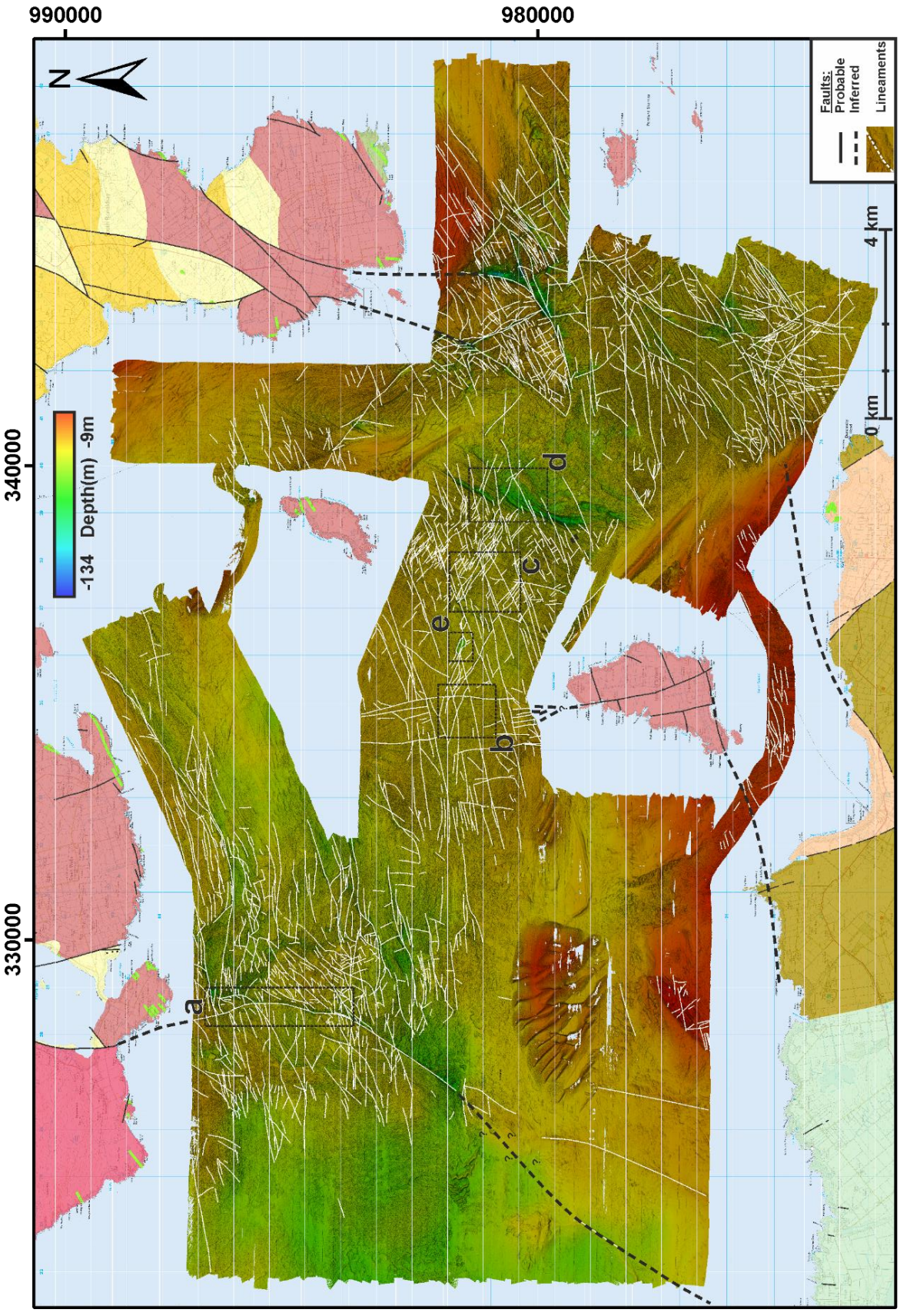

Figure 5.8: Lineament map of the onshore and offshore Pentland Firth showing the mapped faults and fracture systems. Geology courtesy of the BGS, for key see Figure 5.5. 1:25,000 base map courtesy of the Ordnance Survey.

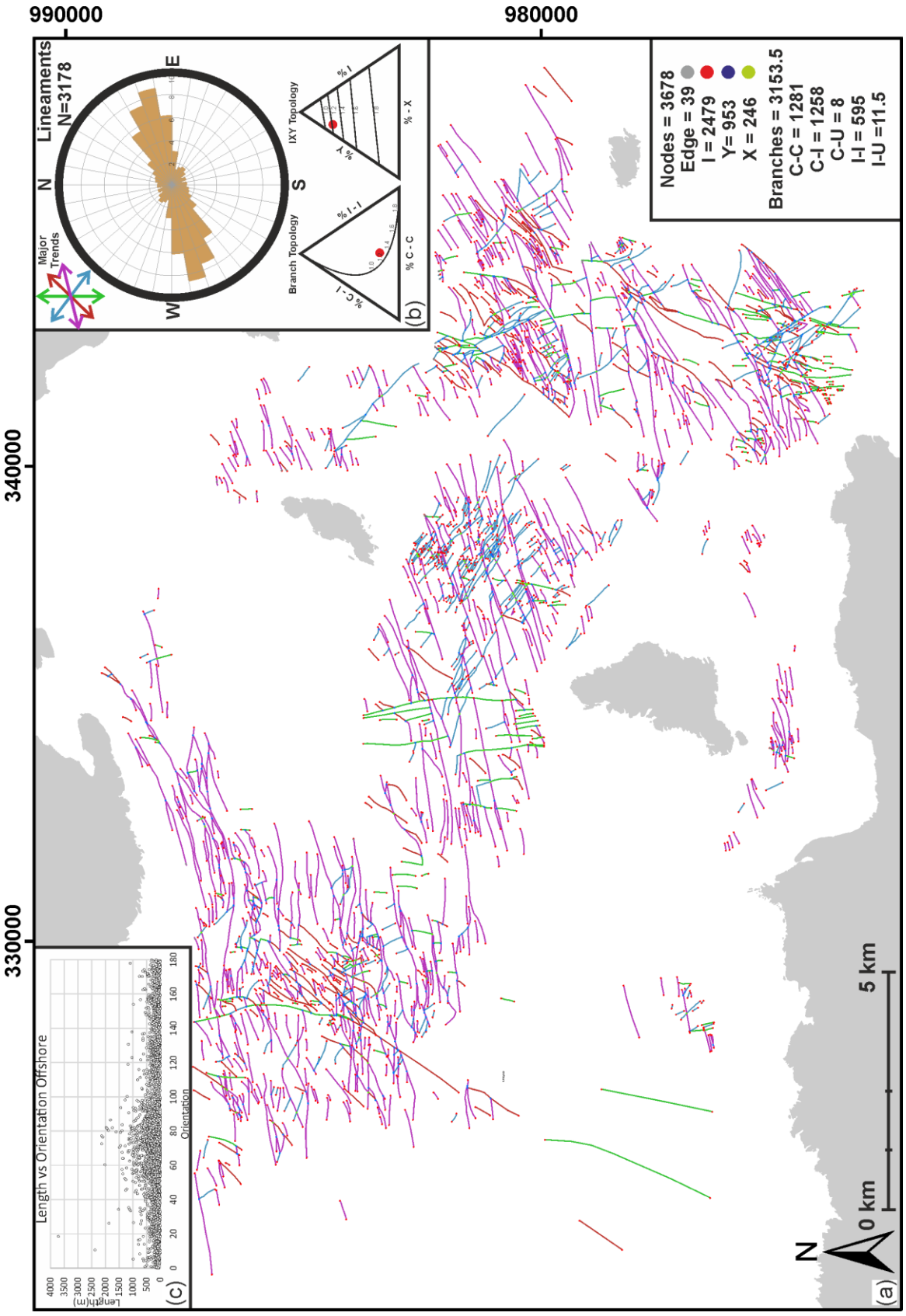

Figure 5.9: (a) Topological analysis of mapped lineaments. Orientation of lineaments subdivided by set and nodes coloured by node type. (b) Length weighted rose diagram of mapped lineaments showing 4 major trends; N-S, ENE-WSW, NE-SW and NW-SE. Ternary diagrams showing branch and node topology for mapped lineaments. (c) Length vs orientation plot for mapped lineaments.

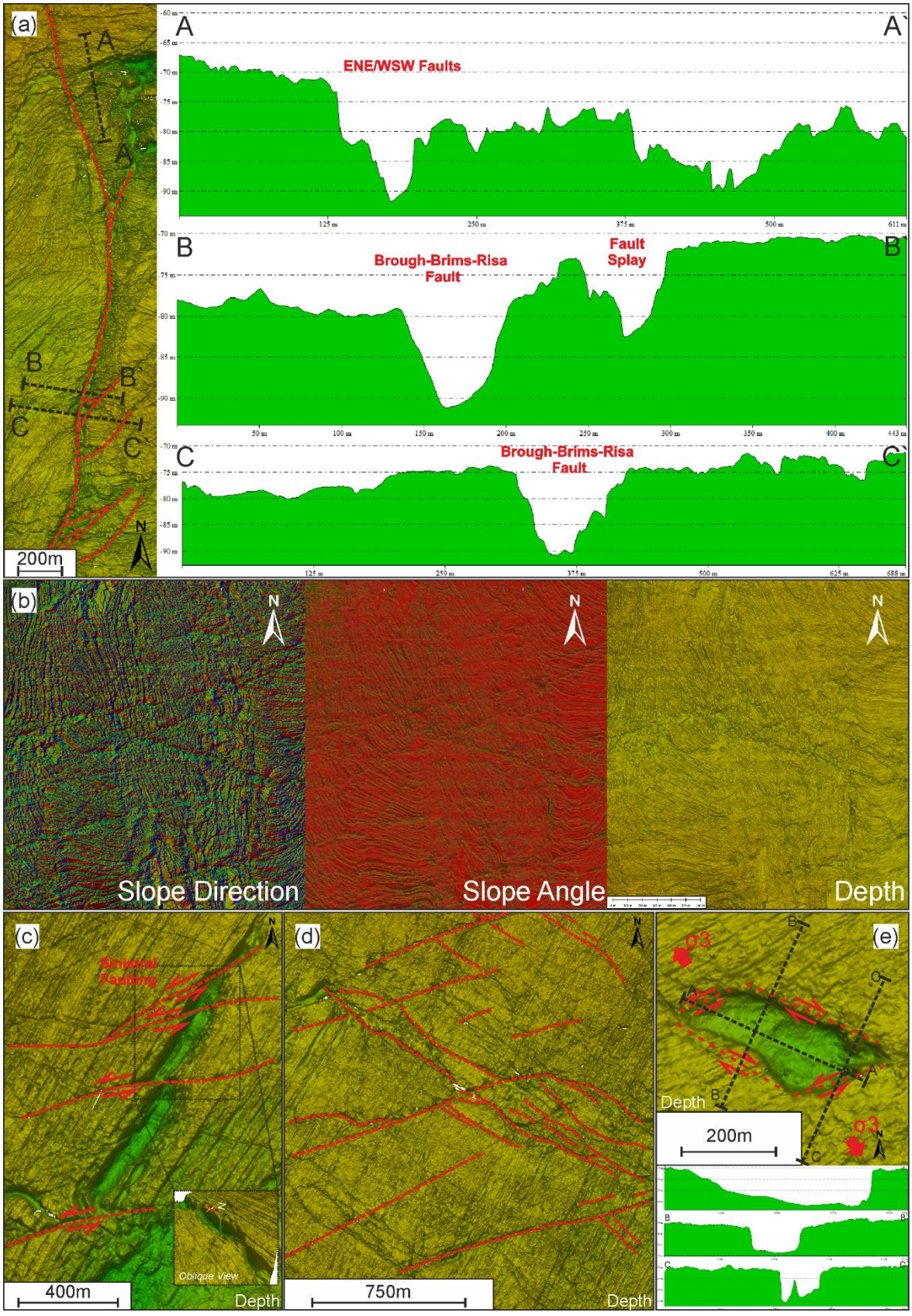

Figure 5.10: Detailed images of examples of faults/fracture systems in the Pentland Firth; (a) Deeply eroded Brough-Brims-Risa Fault and subordinate fault zones; (b) faulting generating more diverse fold patterns and highly variable bedding orientation; (c) apparent sinistral offset of submarine bedding planes. Inset oblique view; (d) rectilinear pattern of lineaments in the area between Stroma

and Swona; (e) deeply eroded rectangular hollow/scour identified on bathymetry. Steep sides of the hollow suggest a tectonic origin in order to produce such a pronounced feature. Annotations show possible structural interpretation as pull-apart structure produced during NW/SE extension. For location of features see Figure 5.8. Cross sections have 5x vertical exaggeration.

5.4.3.3 Topology:

Nodal analysis of mapped lineaments (Figure 5.9) shows a low overall connectivity in the Pentland Firth with a predominance of I nodes as seen on the IXY topology plot (Figure 5.9b). However, locally connectivity is much higher (Figure 5.11) in particular, around major N/S to NE/SW structures. Connectivity is highest in the central part of the study area, in the area between Stroma and Swona and in the hangingwall to the Brough-Brims-Risa Fault due to a higher number of Y and X as a result of conjugate sets of ENE/WSW and WNW/ESE lineaments. Connectivity also appears to increase towards the E, partly due to an increase in lineament density, but may also be due to the greater area of exposed bedrock in this area, where the Pentland Firth narrows, and stronger currents have stripped more of the seafloor sediment away.

Branch topology is dominated by C-C and C-I branches (Figure 5.9b) indicating moderate connectivity in areas close to major faults and fault zones where clustering of lineaments occurs (Figure 5.11).This clustering can be seen on Figure 5.11 where it occurs around some of the longer N/S to NE/SW trending lineaments, in particular in areas where the dominant trend changes from N/S to NE/SW. This clustering around areas where faults change orientation may be as result of stress and/or strain localisation.

Overall connectivity in the Pentland Firth may be higher, however is likely limited by the resolution of the data and distribution of marine sediments.

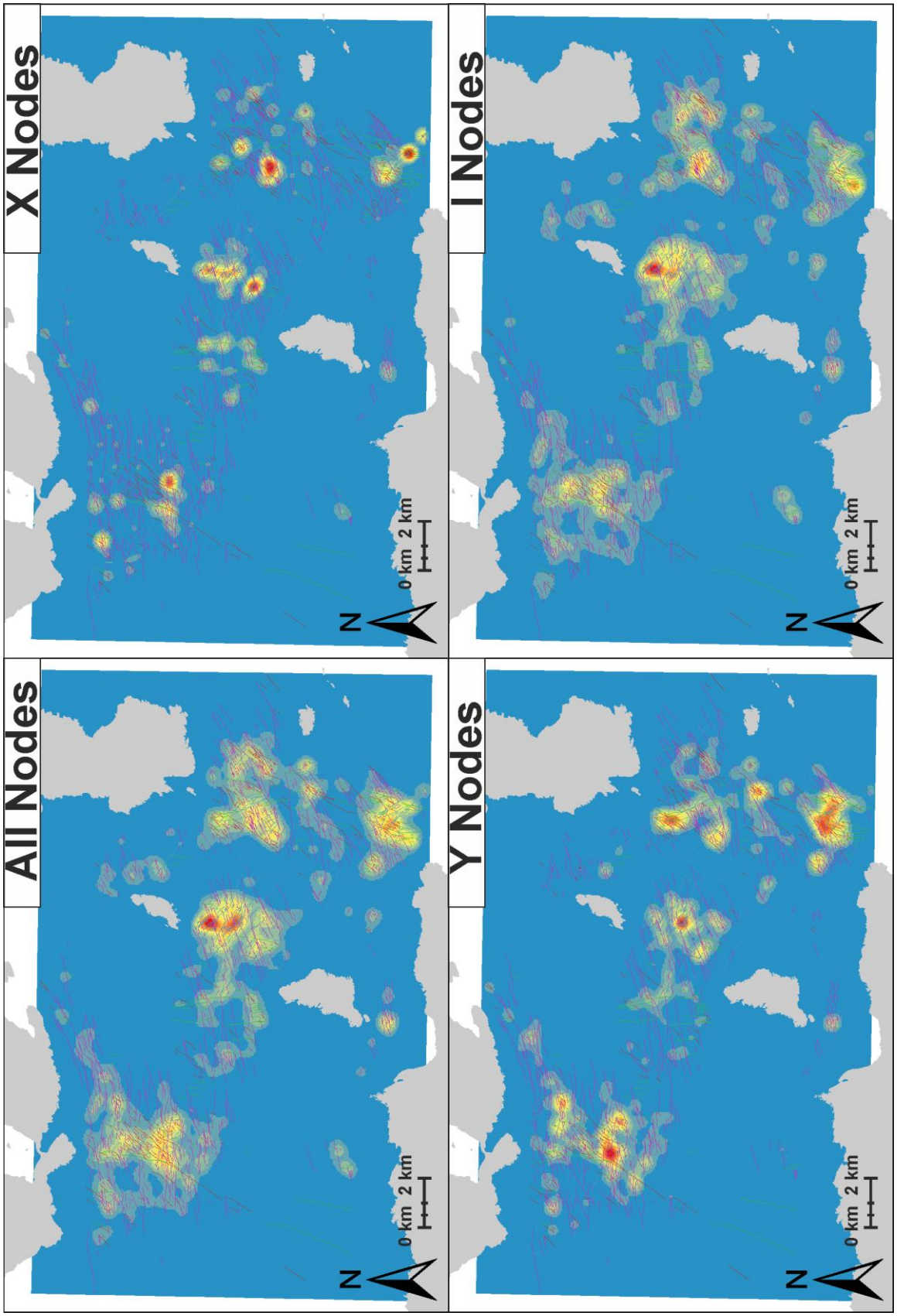

Figure 5.11: Heat maps of Nodal Density. Red = High, Blue = Low. Lineaments coloured by trend, as per Figure 5.9.

5.5 Fieldwork:

The offshore data used provides good spatial coverage, but at a lower resolution. Whereas onshore studies provide a good level of detail but are limited by the spatial coverage. Therefore, the key aims of this fieldwork were to understand the manifestation of equivalent folds and faults observed offshore and understand there spatial distribution, kinematics and structural continuity of structures in the Orcadian Basin. The examination of equivalent structures onshore allowed for a greater understanding of the heterogeneity of structures below the resolution of the bathymetry and to understand those structures across a range of scales.

The onshore structural geology of the Pentland Firth was studied through targeted fieldwork, supplemented by the use of a drone to capture the geology of inaccessible coastal locations and for the production of Virtual Outcrop Models. Areas of structural complexity identified during desk studies were visited in order to ground truth bathymetry observations, collect data and understand the onshore expression of the features observed offshore.

5.5.1 Brough-Brims-Risa Fault Zone:

The Brough-Brims-Risa Fault zone is a N/S to NNE/SSW orientated fault zone, which can be traced ca 12 km along-strike offshore which connects the Brough Fault in Caithness to the Brims Risa Fault in Orkney and confirms the hypotheses that they are in fact one linked structure (Coward et al., 1989; Seranne, 1992) (Figure 5.5). This structure has been interpreted as both a W dipping normal fault (BGS, 1985a) which developed in the Devonian and as an E dipping reverse fault (Coward et al., 1989; Seranne, 1992) which developed during the Permo-Carboniferous. The former seems unlikely given its later history, and is most likely an E dipping normal fault which underwent reactivation and inversion during Group 2 deformation (Dichiarante, 2017). It was reactivated a second time as a Group 3 dextral strike-slip fault, which formed a series of m-scale steeply plunging Z folds which are associated with a small Permian age volcanic vent. It is seen in the footwall on the foreshore near Brough (Dichiarante, 2017).

On the S coast of the island Hoy this structure juxtaposes Upper Devonian rocks of the Hoy Sandstone Formation against the Upper Stromness Flagstone and Lower Eday Sandstone Formations (Figure 5.12a). On the S coast, the Brims-Risa Fault is exposed yet inaccessible

near The Witter [ND 327783 988866]. Here the fault dips ~50° towards the NE (150/50/NE) and juxtaposes grey thinly bedded flaggy sandstones of the Upper Stromness Flagstones against the thicker, red-orange sandstones of the Lang Geo Sandstone Member (Figure 5.12a). In the footwall, the beds of the latter unit dip gently to the west (Figure 5.12b) and contain relatively few faults, although they become more highly fractured in proximity (<50m) to several N/S to NE/SW trending fracture corridors, 150m further to the W. In the hangingwall, the Upper Stromness Flagstones dip steeply to the N (Figure 5.12b) and are highly fractured and faulted throughout. The dominant fault trends (Figure 5.12b) are ENE/WSW, NE/SW and N/S with normal to oblique offsets. Inland, at the Witter Quarry [ND 327945 989146], N dipping flagstones are cut by several equivalent NE/SW trending normal faults and NE/SW to E/W trending steeply dipping tensile fractures, which are partially mineralised with calcite. The fault and fracture trends observed both on the coast and inland are like those observed on bathymetry, which suggests that the structures observed offshore are likely similar in nature to those observed onshore.

On the North Coast of Caithness, the Brough Fault passes through the harbour North of the village of the Brough [ND 322097 973978]. Here, Upper Devonian rocks of the Dunnet Head Sandstone Formation are juxtaposed against the Middle Devonian Spital Flagstone Formation. The fault itself is not exposed, and is interpreted to pass out through the harbour close to the offshore stack of the Clett, a tight overturned synform (Dichiarante, 2017). Deformation in the hangingwall to the E, is intense and pervasive with the development of tight folds, numerous fracture corridors and sub-ordinate fault zones. Such structures are particularly well developed some 800 m to the east at Langypo [ND 322880 974189]. Here a shallowly N plunging, westerly-verging open fold is exposed (Figure 5.13d), which is cut by two associated thrust faults, bisecting the hinge and steepest limb of the fold. The thrusts dip ~20° towards the ENE (Figure 5.13e). This structure is likely similar to some of the smaller folds (Figure 5.7b) identified in the offshore data and is a good example of a Group 2 structure developed during inversion in association with minor thrusts. In the footwall to W the Upper Devonian fluvial and aeolian sandstones are relatively undeformed, except for discrete fracture corridors and normal faults with small amounts of normal offset (Dichiarante 2017).

We suggest that given the field evidence and observations made offshore, the Brough Fault and Brims-Risa Fault systems are in fact on linked fault system that likely initiated as an E

dipping normal fault, which was subsequently inverted and acted as buttress to deformation in the basin. This buttressing has led to the preferential development of fold and thrust structures in its hangingwall to the W. The observations made onshore also help to understand the heterogeneity observed in the offshore data, where the highly variable bedding is likely the offshore manifestation of the sub-ordinate fold structures and fault zones observed onshore.

Figure 5.12 (overleaf): Onshore exposure of the Brough-Brims Risa Fault Zone at The Witter, Hoy [ND 327783 988866] (a) Aerial image of the Brims Fault near The Witter. (b) Stereonets of structural data derived from 3D photogrammetric model of the coastline at The Witter, Hoy. (c) Aerial image of ENE/WSW trending faults/fault zones (d) Aerial image of folding in the hangingwall. (e) Oblique aerial overview image of Brough Harbour showing the onshore exposure of the Brough-Brims-Risa Fault Zone in Brough Harbour, Caithness [ND 322105 974007]. Main fault passes close to the position of the jetty (f) Oblique field photograph of deformation in the hangingwall. Tight Z folds such as these likely developed during oblique reactivation of the Brough fault during the Permian transtension. *Inset* detailed imaged of deformation.

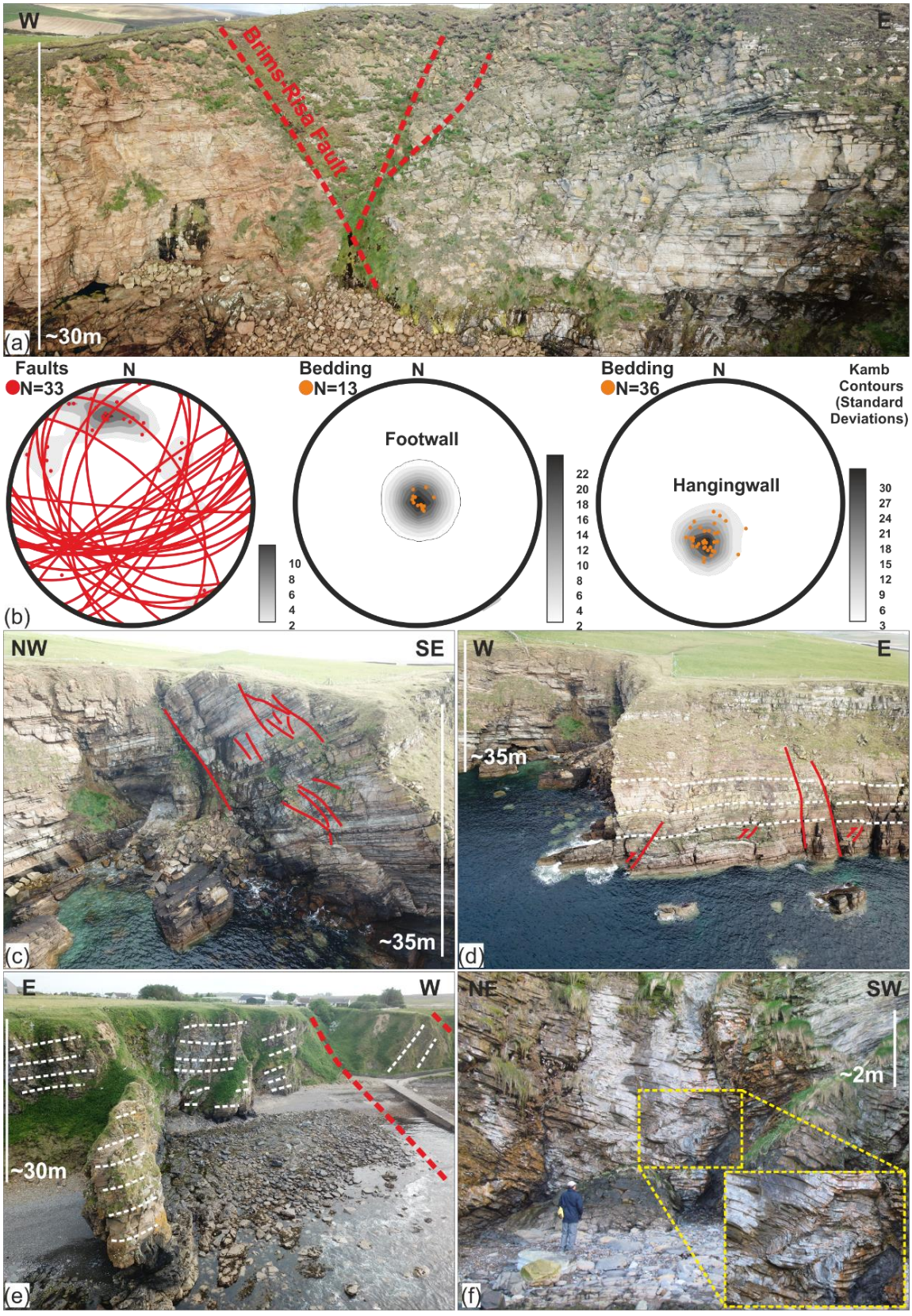

5.5.2 Faulting and Folding:

In Caithness and Orkney, the Ham Anticline and Eday Syncline (Figure 5.1b) are the principal regionally recognised folds. These folds are generally accepted as being related to Group 2 deformation associated with regional inversion during the Carboniferous and are visible on

regional onshore 2D seismic (Figure 5.13) and offshore bathymetry. They are N-S trending, low amplitude, gently plunging, long wavelength structures. Smaller scale folds from localised cm to dm scale fault related structures, through to large, km scale folds are also recognised right across Caithness and Orkney (Coward et al., 1989; Dichiarante, 2017; Enfield and Coward, 1987) and seem to be most widely developed east of the Brough-Brims Risa Fault which are associated not only with Group deformation, but have likely been modified during later Group 3 Deformation

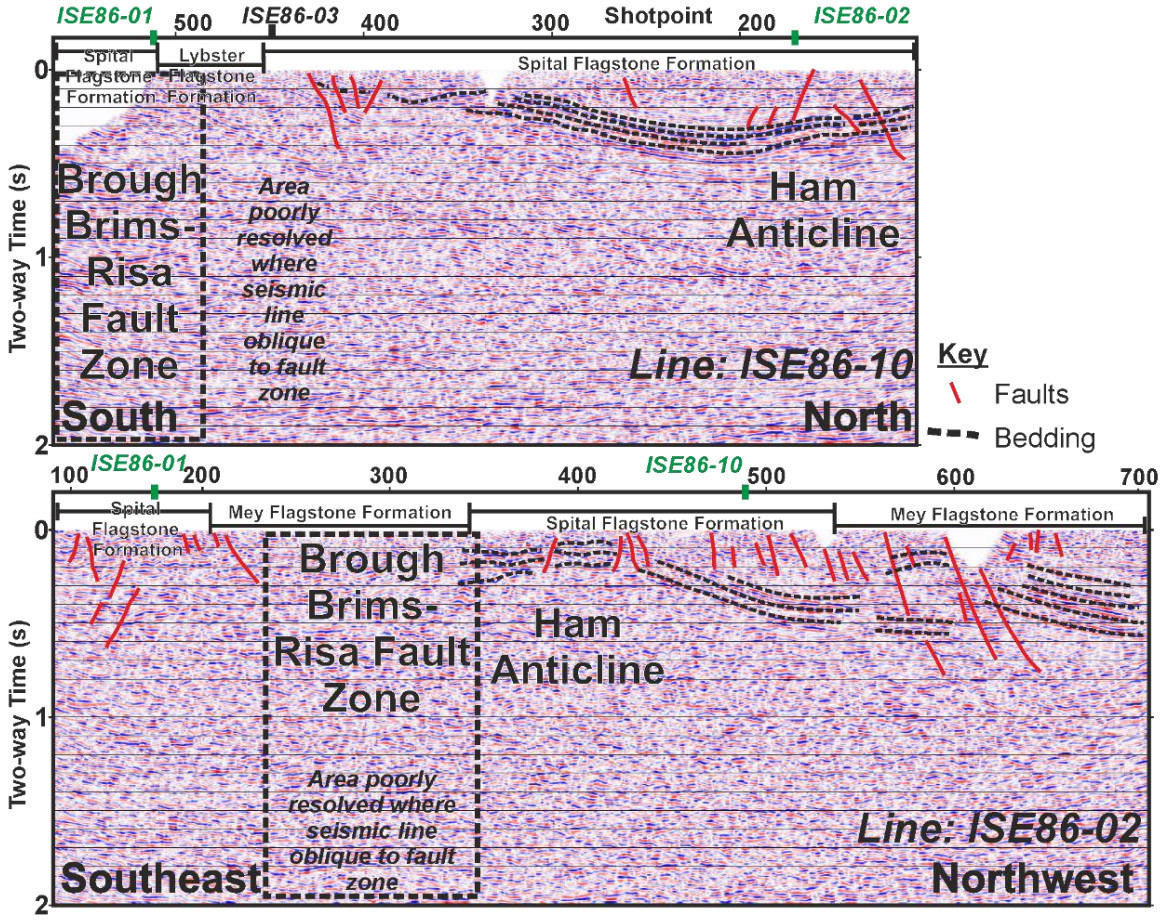

Figure 5.13: Interpreted onshore seismic sections. Despite poor data quality reflecting the highly fractured nature of the ORS, large folds are visible in addition to small closely spaced faults. Poorly resolved area corresponds to the damage zone around the Brough Fault. The poor data quality seen in this data is presumably due to the highly fractured nature of the bedrock as seen at outcrop and on bathymetry. See Figure 5.4 for location of seismic lines. Seismic lines courtesy of UKOGL.

A series of N-plunging folds (Figure 5.14a) are recognised along the N coast from Dunnet Head towards John O'Groats which can be traced offshore, using the bathymetry (Figure 5.4). In Gills Bay [ND 332848 972824] sedimentary rocks], sediments of the John O'Groats Sandstone Formation are folded into an open NE trending gently plunging syncline (Figure

5.14b). Near Duncansby Ness, sediments of the same unit are folded into a similar an open NE trending, gently plunging syncline (Figure 5.14c). Close to the hinge of this fold, a small, Permian aged, volcanic vent outcrops which comprises monchiquites and tuffs (Chapman, 1975) dated using K-Ar to 270Ma (Macintyre *et al.,* 1981). Separating these synclines is a N trending, anticlinal structure, which is obscured by faulting and a lack of outcrop.

We interpret these structures as the onshore equivalent of the large km-scale folds that are observed offshore (Figure 5.5 and Figure 5.6) and on seismic (Figure 5.13), and suggest that folding associated with Group 2 deformation in the Orcadian Basin is actually more widespread than previously thought. Direct correlation of folds is challenging due to the presence of ENE/WSW trending fault zones which run parallel to the shoreline e.g. St Johns Point, which may have offset the position of the folds relative to one another (Dichiarante, 2017; Dichiarante et al., 2016). It is also compounded by the lack of data along the shoreline and occlusion in places by marine sediment. However, the trend, and morphology of these structures is quite similar, and it is therefore highly likely that these are onshore continuation of these structures or are at least equivalent in size, shape and origin.

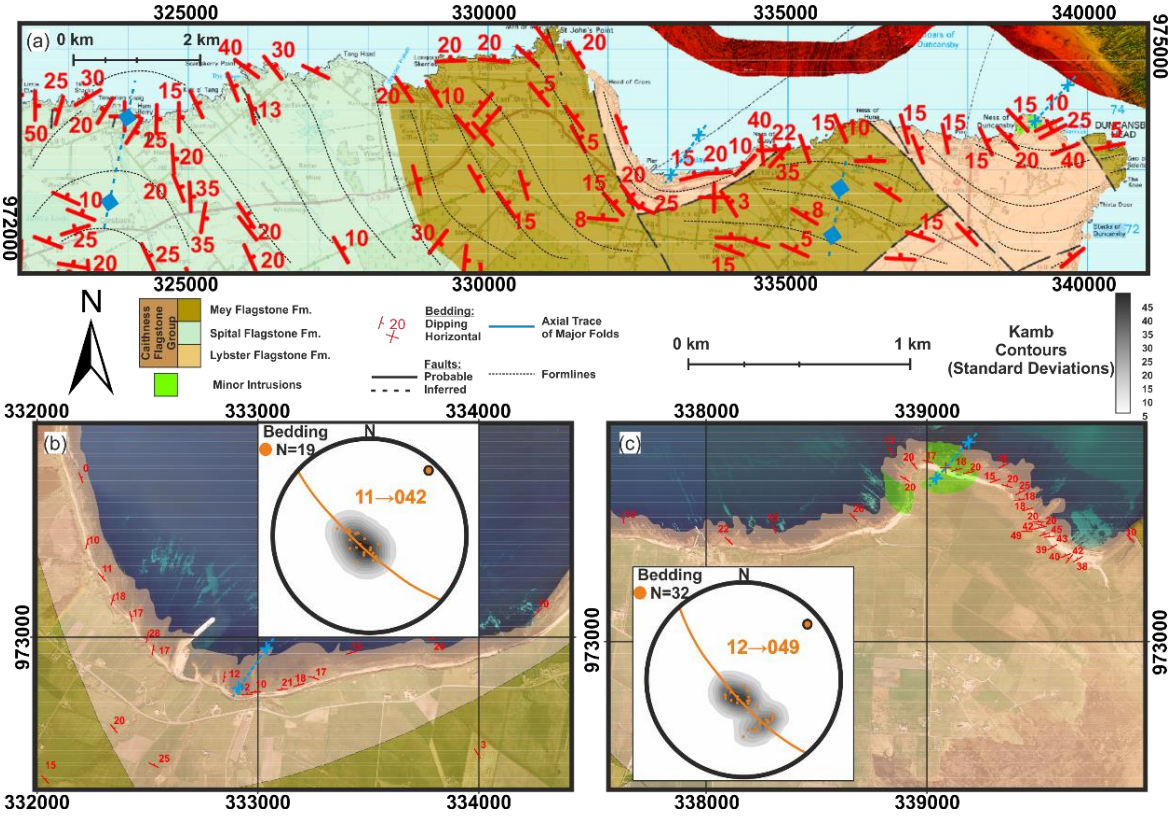

Figure 5.14: Mapping of regional scale fold structures around the margins of the Pentland Firth. (a) Geological map of coastline from Brough to John O'Groats showing long wavelength fold structures and bedding. (b) Stereonet for Ham Anticline. (c) Aerial image and stereonet of Gills Bay Syncline.

(d) Aerial image and stereonet of Gills Bay Syncline. Bedding data sourced from the BGS and supplemented with additional field data. Stereonets show best fit great circle and plunge/trend of fold axis. Lower hemisphere equal area projection for stereonet. Aerial images courtesy of the Ordnance Survey

In addition to these regional-scale (km size) structures, numerous smaller (cm-dm) scale folds, localised dm-scale fold/thrust structures and complex fault zone architectures are developed which are well exposed but, however often difficult to access, around the coastlines of the Pentland Firth.

Examples of these complex fault zones occur along the SW coast of South Ronaldsay, where several N to NE trending fault zones mapped offshore on bathymetry may be traced onshore. Bedding here generally dips offshore towards the W but is locally strongly affected by folding and faulting.

In Horse Geo [ND 343140 984995] a deeply eroded gully corresponding to an ENE/WSW trending fault zone exposes complex N/S orientated, polyphase deformation with unclear and inconsistent cross-cutting relationships. This complexity can be seen in Figure 5.14a, which shows bedding parallel thrusts, back thrusts, fault propagation folds, shallow and over-turned normal faults, and reactivated normal faults. In the geo immediately to the N, the nature of this fault zone changes further (Figure 5.14b) and tracing of discrete structures from one location to the next is challenging. Further to the North at Tainga [ND 342703 986012], (Figure 5.14c) closely spaced (0.5-1m) top to the west thrusts and fault propagation folds locally steepen the bedding with small, distributed reverse offsets and elsewhere, discrete thrusts are developed in otherwise relatively undeformed strata (Figure 5.14d). Pervasive N/S orientated fractures are commonly filled with calcite, which frequently crosscut NE/SW, NW/SE and E/W orientated shear fractures.

To the south at The Wing [ND 343599 983915], a large E dipping thrust fault (Figure 5.15a) is exposed which locally steepens the bedding in the footwall (Figure 5.15c). This thrust bifurcates into several smaller E dipping thrusts which are truncated against a N/S orientated steeply dipping fault zone/fracture corridor (Figure 5.15b) further to the W which appears to act as a buttress to the further propagation of these faults. Such distributed and highly variable deformation is thus likely to be analogous to the level of complexity in similar structures offshore but is generally below the resolution of the bathymetric data.

In summary, Figures 5.15 and 5.16 help to highlight the immense along strike variation and the diversity of fault zones associated with Group 2 and later Group 3 deformation and reactivation. Variation is observed across several orders of magnitude (cm-km), and at a level of detail that cannot be attained in the offshore data.

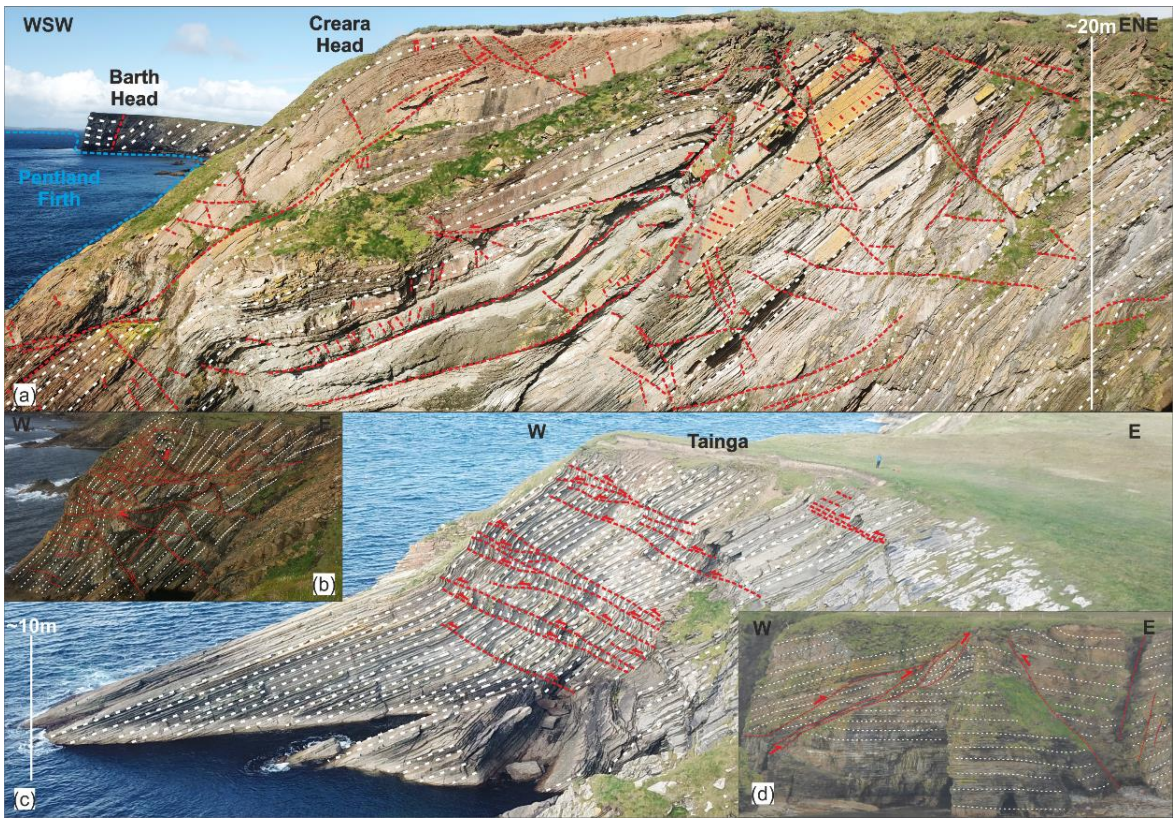

Figure 5.15: Aerial images of complex polyphase structures related to repeated oblique reactivation that are developed along the coastline of South Ronaldsay, Orkney Isles. (a) Polyphase deformation exposed in the cliffs on the Northern side of Horse Geo [ND 343140 984995], which is itself an eroded East-Northeast trending fault zone. The headland of Barth Head [ND 342655 985574] can be seen in the background which is cut by a significant North/South trending steeply dipping sub-vertical fault, which may be the onshore continuation of significant and deeply eroded lineaments observed on bathymetric data. (b) Along strike variation in complex fault zones along coastline N of Horse Geo [ND 343058 985082]. (c) Distributed fault propagation folds and thrusts exposed at Tainga, South Ronaldsay, Orkney Isles [ND 342703 986012]. These examples show the mechanical controls on the structures that develop, in addition to recording the complex structural evolution of the basin with later, Group 2 and 3 structures cross cutting and reactivating early normal faults. Geometries of faults further complicated due to tilting. (d) Smaller discrete thrust faults in largely undeformed strata exposed in cliffs NW of Burwick [ND 343539 984638].

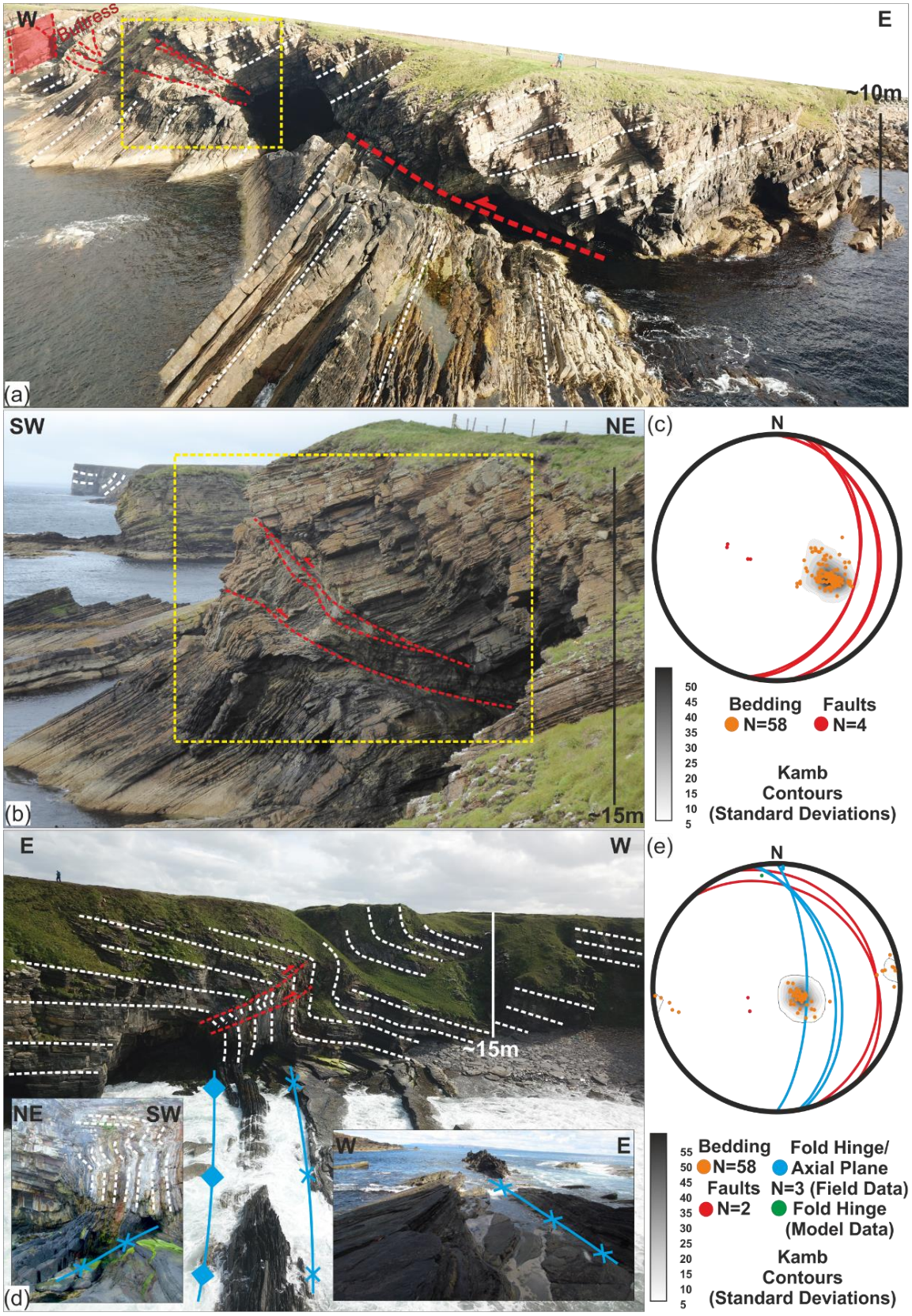

Figure 5.16: Examples of deformation commonly associated with Group 2 structures and inversion during the Carboniferous. (a) Aerial image of thrust fault exposed at The Wing, near Burwick, South Ronaldsay, Orkney Isles [ND 343599 983915]. (b) Detail of fault zone showing distorted and contorted bedding in a zone bound by two top the west thrusts. (c) Stereonet of structural data

derived from 3D photogrammetric model (d) Annotated aerial image and 3D outcrop model of intense folding and localised deformation in the Spital Flagstone Formation at Langypo [ND 322880 974189]. *Inset* - Detailed images of thrust faults in core of fold structure and fold hinges. (e) Stereonet of structural data collected in the field, supplemented by data derived from 3D photogrammetric model.

5.5.3 Onshore Fracture Networks and Topology:

Topological analysis of fracture networks was carried out for comparison to the offshore data, and to other published examples in the Orcadian Basin. Figure 5.17a is an orthorectified aerial image of the coastline, west of Ham Harbour, where the hinge of the Ham Anticline is exposed [ND 323912 973928]. Lineament and topological analyses were carried out on high resolution (2.87cm/pixel) orthorectified aerial imagery acquired with a drone.

A total of 8077 lineaments were mapped from the aerial imagery with a trace length of ~24.5km, a mean length of 3.05m and range of 45.13m (Table 1 and Figure 5.17a). Mapped lineaments correspond to faults, fracture corridors and fractures, with three principal trends identified (Figure 5.17a); ENE/WSW to E/W (n=3216), NE/SW to N/S (n=3417) and NW/SE (n=1444).

NE/SW to N/S lineaments are concentrated into discrete corridors which are linked by numerous closely spaced ENE/WSW to E/W trending lineaments that commonly terminate against these N/S trending fractures/faults forming Y nodes. ENE/WSW to E/W trending lineaments are the most numerous and spatially extensive across the rock platform and form discrete corridors of fractures (Figure 5.17b). NW/SE lineaments are the least numerous, are generally the shortest, frequently crosscut other fractures and have a relatively high proportion of X nodes. Figure 5.17c plots length against orientation, which shows distinct clusters of long lineaments orientated NE/SW, ENE/WSW and NW/SE which correspond to the three main trends that are observed.

Topological analysis of the data shows a moderate level of connectivity, with Y nodes being dominant (Figure 5.17b). Branch topology shows a high degree of connectivity with C-C (doubly connected) branches being the most numerous (Figure 5.17b). A high number of I nodes and lower proportion of X nodes suggest that many fractures do not crosscut or remain isolated. Overall connectivity may be higher, however is likely limited by the

resolution of the data. Due to erosion and the tide, the N/S orientated faults/fault zones and associated structures are also likely under-represented, with connectivity in these areas likely higher than estimated. This is reflected in the areas adjacent to these zones, where X and Y node density are high (Figure 5.17d), suggesting that fracturing is more intense around these N/S structures.

Topological analysis carried out by Dichiarante, (2017) identifies the same three fracture sets and same predominance of N/S to NE/SW fractures. However, in this study, I nodes are the most dominant (n=916) with roughly equal proportions of X and Y nodes (n=202 and n=240). This predominance of I nodes is likely partly due to the small sample size but mainly due to the small area of study and higher resolution which is able to identify very small fractures.

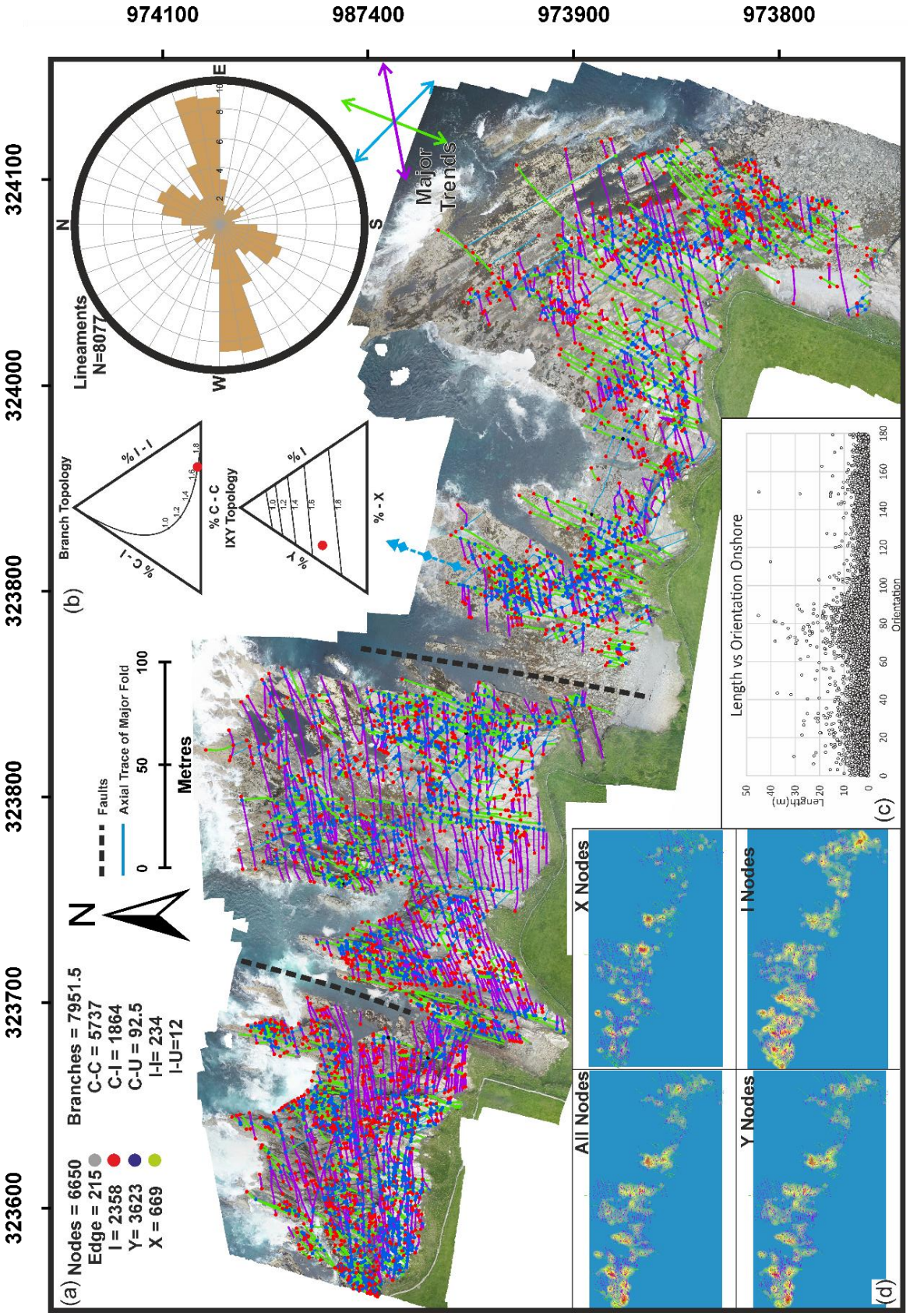

Figure 5.17: (a) Orthorectified aerial image of Ham Anticline with interpreted lineaments with three principal trends identified; ENE-WSW, N-S to NE-SW and NW-SE. (b) length weighted rose diagram of mapped lineaments and ternary diagrams showing branch and node topology. (c) Plot of

lineament length vs orientation. (d) Heat maps of Nodal Density. Red = High, Blue = Low. Lineaments coloured by trend.

5.6 Discussion:

5.6.1 Structural Evolution:

Discerning the kinematics of faults is challenging using the offshore data and many of the low angle or bedding parallel structures seen onshore (Figures 5.15 and 5.16) are likely to be hard to confidently identify on bathymetry and are likely under-represented here. However, the general trends in structure seen onshore are also seen offshore – as are the folds. In summary this allows the observations made onshore to be used to help to constrain the kinematics offshore and help to understand what processes and structures are formed at or below the resolution of the bathymetric data.

In the study area structures representing all three phases of deformation are likely present. However it is difficult to identify unambiguously Group 1 structures as these are likely obscured by later deformation and reactivation (Dichiarante, 2017) and/or remain buried at a greater depth in the centre of the Orcadian Basin. Such structures likely include the Brough-Brims-Risa Fault, in addition to many of the other NNW to NE trending faults. Group 2 structures include the widespread N/S trending folds that have been mapped onshore and offshore. Associated with many of these fold structures are discrete N/S trending thrusts and localised fault- related folds which show predominantly vergence towards the W.

Group 3 structures likely include reactivated existing structures e.g. N/S faults, as well as sinistral ENE/WSW and dextral WNW/ESE trending structures which are consistent with NW/SE extension, associated with regional transtension during the Permian (Dichiarante *et al.,* 2016). Onshore, some of these ENE/WSW trending structures correspond to faults and/or Permian age dykes, such as those mapped onshore in Caithness (Dichiarante *et al.,* 2016) and as such it is likely that similar material may be found along these structures.

Deformation in the footwall of the Brough-Brims-Risa Fault is less intense, both onshore and offshore, with fewer large-scale folds like those observed in the hangingwall. We interpreted the relative lack of deformation seen west of the Brough-Brims-Risa Fault zone as being due to this fault system acting as a buttress, preventing deformation from propagating further west, and partitioning most of the Group 2 E-W shortening-related

formation into the E and SE parts of the Orcadian Basin close to the Great Glen Fault Zone. This seems also to be consistent with the link proposed between dextral reactivation of this fault and the E-W compression and inversion (Coward et al., 1989; M. Seranne, 1992).

Burial history models (Figure 5.18) for the area consistently show a relatively rapid exhumation of at least 1.5-2k before burial in the Permo-Triassic (Evans, 1997; Fame et al., 2018; Hall and Bishop, 2002; Holford et al., 2010; Thomson et al., 1999; Wilkinson, 2017), suggesting a link to inversion associated with the development of the Group 2 structures regionally . This may also explain the relative lack of Upper Devonian strata onshore in the Orcadian Basin particularly to the East of the Brough-Brims Risa Fault.

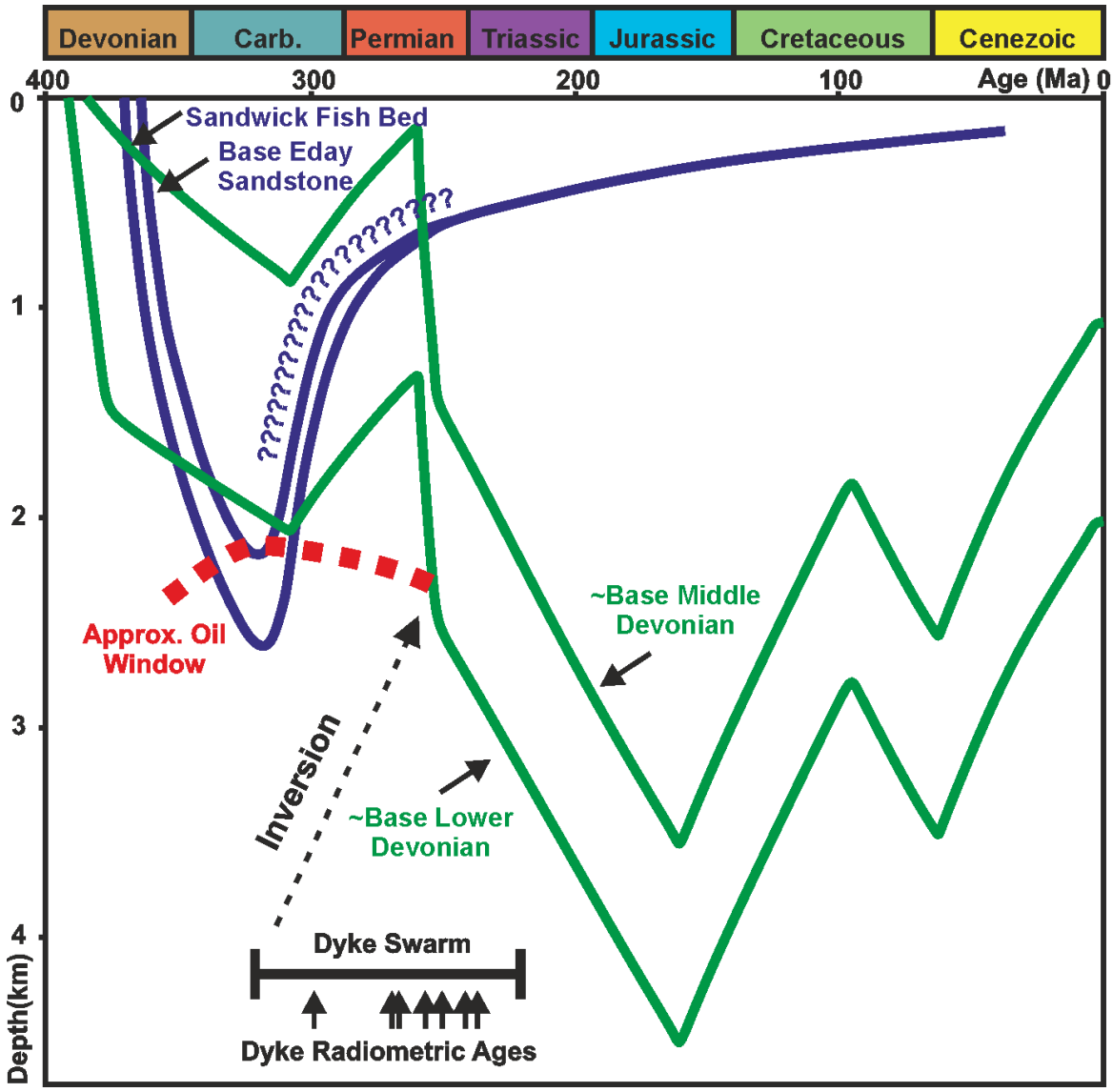

Figure 5.18: Burial History for the Devonian Rocks of Orkney (blue lines) and West Orkney Basin (green lines). Modified *after* Astin (1990) and Bird (2014) respectively. Despite differences in the exact point at which the basins are inverted, both show maximum burial in the late Carboniferous

and exhumation during the Permo-Carboniferous. Note the lack of post Permian burial history for the Orkney area compared to the offshore basins.

The orientation and plunge of fold structures may have influenced the Quaternary to recent development of the Pentland Firth, as the islands of Stroma and Swona appear to correspond with localised highs, developed on or adjacent to the hinges of major anticlines (Figure 5.19a). Correspondingly, some of the deepest parts of the bathymetry align with the hinges of major synclines (Figure 5.19a).

5.6.2 Comparison of Fracture Networks:

Fracture systems in the offshore study area (Figure 5.19a) are broadly similar to those onshore (Figure 5.19b) and those mapped elsewhere in the Orcadian Basin, in agreement with observations made by Dichiarante (2017) and Dichiarante *et al.,* (2016) with the same key trends identified both onshore and offshore (Figure 5.19b). However, there are some distinct differences. Both data sets have similar dominant trends that are dominated by numerous smaller fractures and infrequent, longer fractures. Onshore, the spread of lineament orientations is greater (Figure 5.19b), with less distinct and well defined sets of trends, perhaps reflecting the polygonal nature of fracturing, particularly away from the major N/S faults and fracture corridors and being to being able to identify more of the smaller connecting structures.

In a smaller offshore dataset Dichiarante (2017) maps a comparable network of lineaments which also has a predominance of I nodes with increasing connectivity in proximity to longer N/S trending structures and 'fracture corridors'(Figure 5.19c), and in an onshore dataset (Dichiarante et al., 2016) notes an increase in connectivity with increasing resolution provided by the window sampling method (Figure 5.19c). In this study the onshore data also shows greater connectivity than offshore (Figure 5.19b), in agreement with Dichiarante (2017) and Dichiarante *et al.,* (2016), who note that overall connectivity increases close to larger structures.

This increase in connectivity is due to clustering of fractures. This clustering increases the possibility that fractures intersect, in turn reducing the number of I nodes, resulting in fewer unconnected branches and higher levels of sub-vertical connectivity within these clustered 'fracture corridors'. Lower values for 2D intensity, average connections per line, average connections per branch and in particular especially dimensionless intensity (Table

5.1), further support this statement, with the higher connectivity in the onshore dataset being attributed to the several large faults that dissect the area of study increasing the degree of deformation together with the censoring of the data by marine sediments.

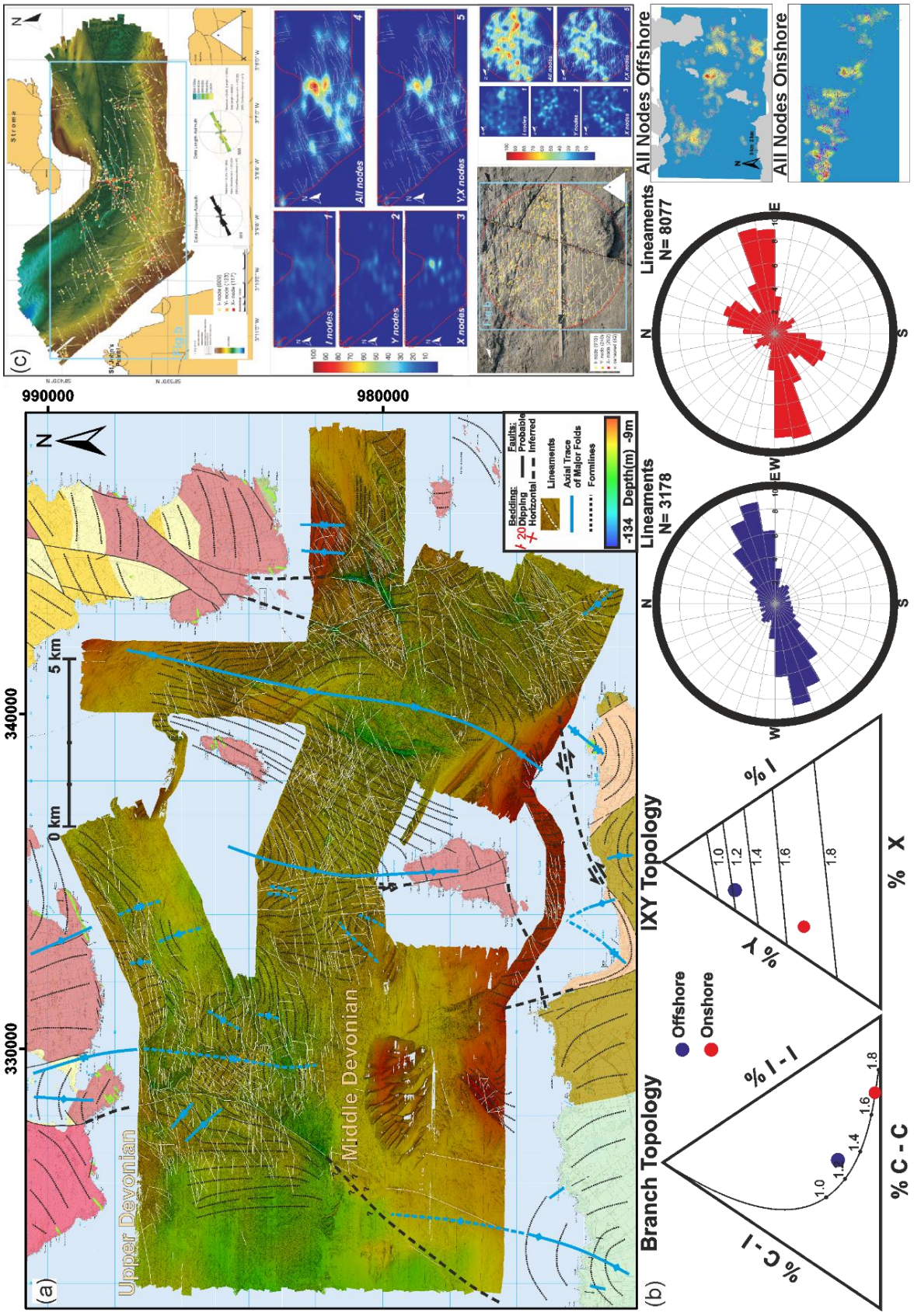

Figure 5.19 (preceding page): Summary interpretation of the onshore and offshore geological structure of the Pentland Firth. (b) Comparison of fracture topology, orientation and node density for onshore and offshore datasets. (c) Examples from other studies in the Orcadian Basin (Dichiarante, 2017) which show similar orientations of lineaments and clustering patterns.

5.6.3 Resource Implications:

The bathymetric data used in this study could be equivalent in terms of spatial coverage and resolution to a Z (horizontal) slice from a 3D seismic volume. With this in mind, the fault zones in the Orcadian Basin show various levels of complexity across a range of scales, with much of the observed complexity, at or below the resolution of the bathymetry and by proxy not seismically resolvable.

If the Orcadian Basin is viewed as a potential analogue to fractured reservoirs offshore, it appears that deformation is concentrated around major N/S trending structures. However, these structures do not connect a large volume of rock and it is the cross cutting structures that trend NE/SW, NW/SE, ENE/WSW and WNW/ESE that provide a majority of the connectivity to the larger rock volume. It is therefore important to not only characterise the major sub-seismic scale structures, but also those which are smaller and more widely distributed, which may deliver a significant proportion of fluids to a wellbore.

The presence of large km scale fold structures as seen in this study may be analogous to many trapping geometries in geometry and size, to those seen in offshore data which host hydrocarbon accumulations. Offshore, many of the Devonian sequences are buried beneath significant thicknesses of Mesozoic and Cenozoic fine grained lithologies and evaporates, which prevent detailed imaging of these structures which underlie potential seals to hydrocarbon accumulations sourced from Devonian and Carboniferous source rocks in a potentially under-explored petroleum play, or could provide structures for long term geological storage of carbon dioxide.

Offshore, younger Mesozoic and Cenozoic sedimentary rocks overlie equivalent Devonian rocks in the Moray Firth, on the East and West Shetland Platforms (Patruno *et al.,* 2018; Patruno and Reid, 2017; Monaghan *et al.,* 2016), and Faroe Shetland Basin (Schöpfer and Hinsch, 2019). With a significant number of exploration wells on the UKCS/NCS failing due to issues with trap and/or seal (Myers *et al.,* 2019), any advances in the understanding of

Paleozoic basin development together with improvements in the understanding of the development and distribution of structures offshore is of merit.

Modern deposits of dm thick coarse-grained sands such as those observed would make ideal reservoirs within shallow marine tidal deposits particularly in otherwise finer grained deposits. Furthermore, with paralic reservoirs being a significant contributor to the production of hydrocarbons (Reynolds, 2017), modern sedimentary features in the near offshore may prove useful analogues. Such current driven deposits may also be analogous in size and geometry to clastic deposits formed by contourites in deeper marine settings (Lague et al., 2013; Rebesco et al., 2014; Stow et al., 2002; Viana et al., 2007).

5.7 Conclusions:

Recently acquired offshore multibeam bathymetry in combination with aerial imagery, photogrammetric 3D virtual outcrop models and fieldwork to ground truth observations, provides new insights into the size, shape, continuity, distribution and complexity of the structures within the Orcadian Basin across a range of scales. Analysis of a 220 km^2 survey of the Pentland Firth has produced a new geological map of the Pentland Firth (Figure 5.19a) and revealed aspects of the structure and geology of the region that are poorly exposed onshore:

- The dominant feature is a 12km long roughly N/S trending curvilinear lineament which is interpreted as the offshore continuation of the Brough and Brims-Risa Faults, likely one linked structure. This key basin wide structure seems to partition later deformation and inversion by acting as a buttress to reactivation, with well-developed long (km scale) wavelength folds and complex fault/fold relationships well developed only to the East of the structure and relatively undeformed strata to the West.
- North-South trending open folds are more widespread than previously identified, particularly in the footwall of the Brough-Brims-Risa Fault. Locally, much smaller and tighter dm scale folds are developed near faults developed during inversion and/or during oblique reactivation of existing structures.
- Numerous faults and fractures have been mapped offshore and fracture network analysis has identified 4 predominant trends; ENE-WSW, NE-SW, WNW-ESE to NW/SE and N/S, which are consistent with trends identified during studies onshore

(e.g. Dichiarante et al. 2016). Major N/S fault zones are connected with a wider rock mass by orthogonally crosscutting and connecting fracture systems. Fault/fracture networks become better connected at higher resolutions as numerous smaller features can be identified.

- A rectangular pull-apart feature has been identified that is likely related to oblique NW/SE is rifting during the Permian.
- Due to lack of inland outcrop in Caithness and Orkney, the length, continuity and spatial distribution of many structures has likely been underestimated with widespread faulting and folding being identified offshore.
- Modern sedimentary features are also beautifully imaged giving an insight into the current driven sedimentary processes that occur in shallow tidal environments and may prove useful analogues to paralic reservoirs in the subsurface.

These findings may have impacts for hydrocarbon exploration and development, and future operations in the under explored and more poorly understood Paleozoic basins of the Moray Firth, East Shetland Platform, East Orkney Basin, West Orkney Basin, East Fair Isle Basin, West Fair Isle Basin and West of Shetland in the Faroe Shetland Basin. Findings have implications not only the Clair Basin and Clair Oil Field but other Devonian reservoirs offshore e.g. Buchan Formation.

Lastly, this study highlights the spatial and temporal variations in structure present within the Orcadian Basin that are poorly exposed, due to the limited onshore outcrop. This emphasises the importance and value of fieldwork and analogue studies working in conjunction with desk studies and remote sensing methods, to collect data across a range of scales, and to directly link onshore and offshore geology where possible. The use of underutilised data, such as bathymetry, to supplement traditional field techniques is a useful tool for the structural geologist and can be used to great effect to help link onshore-offshore data more effectively, as well as providing a helpful way of scaling up and down observations.

Chapter 6

Discussion, Conclusions and Future Work

Chapter 6- Discussion, Conclusions and Future Work:

In this chapter, the key themes of the project explored in the preceding chapters (3-5) are discussed in the context of the four principal project aims that were outlined in Chapter 1:

1. To reappraise the development of the Devonian sedimentary basins in mainland Scotland and Shetland with a focus on the region closest to the Clair Oil Field, i.e. Foula-Shetland. Sampling will be undertaken to determine the provenance and age of the Devonian sequences of Foula and Western Shetland.
2. Undertake detailed field studies of exposed basement-cover contacts and the structure of the overlying sandstone-dominated sequences exposed in large coastal sections throughout the Orcadian Basin in NE Scotland, Orkney and Shetland, in order to better predict the nature of these contacts in the subsurface.
3. Understand the type, scale and distribution of structures in the Orcadian Basin and improve the understanding of sub-seismic and field scale structures.
4. Further develop the structural model proposed by Dichiarante (2017) in other parts of the Orcadian Basin in particular, the evaluation of the role of strike-slip tectonics during Devonian basin development.

To address these four aims the discussion is subdivided into the following four sub-sections:

- The first section will explore and discuss the implications for the sedimentological and structural models of Devonian basin development, the role of transtension in controlling the basins evolution and the diversity of basement-cover relationships evident in the basin.
- The second section will discuss the suitability of the Orcadian Basin as an analogue for the Clair Basin, in particular the island of Foula, as an analogue to Clair Ridge
- The third section will discuss more general implications for the ongoing development of the Clair Oil Field and other offshore resources that has been gained from an improved understanding of sub-seismic to field scale structures.
- The fourth section outlines the applications to and implications for other sedimentary basins and geological settings both modern and ancient.

The discussion is followed by a conclusion, which summarises the key project findings, in addition to making some suggestions for avenues of future research.

6.1. Discussion:

6.1.1. Implications for Devonian Basin Development:

This study has highlighted several implications for the understanding of Devonian Basin development, in particular the role of transtension during basin development (Chapter 3), the wide range of basement/cover relationships that developed during the course of the basins evolution (Chapter 4) and a greater understanding of the distribution and continuity of structures in the Orcadian Basin (Chapter 5).

Transtension as an alternative for the development of the Orcadian Basin was proposed by Seranne (1992) who first studied structures in the Devonian Basins of Shetland in detail. Their proposed hypothesis was contrary to many early and current workers (Brown *et al.,* 2019; Marshall *et al.,* 2003; Rogers *et al.,* 1989) who state that there is no evidence for transtension or significant strike slip motion during deposition of the Devonian in Scotland, and that any late Caledonian sinistral strike slip motion had ceased by the late Emsian (Rogers *et al.,* 1989).

However, it is now becoming increasingly acknowledged that regionally, the Orcadian Basin was likely acting as one larger strike-slip influenced transtensional basin (Fossen, 2010) (Figure 6.1 and 6.2). Evidence for regional transtension during the development of the Devonian Basins has been reported more widely in Scandinavia, Eastern Greenland and in Shetland (Dewey and Strachan, 2003; Hartz, 2000; M. Seranne, 1992; Seranne and Seguret, 1987) (Figure 6.2).

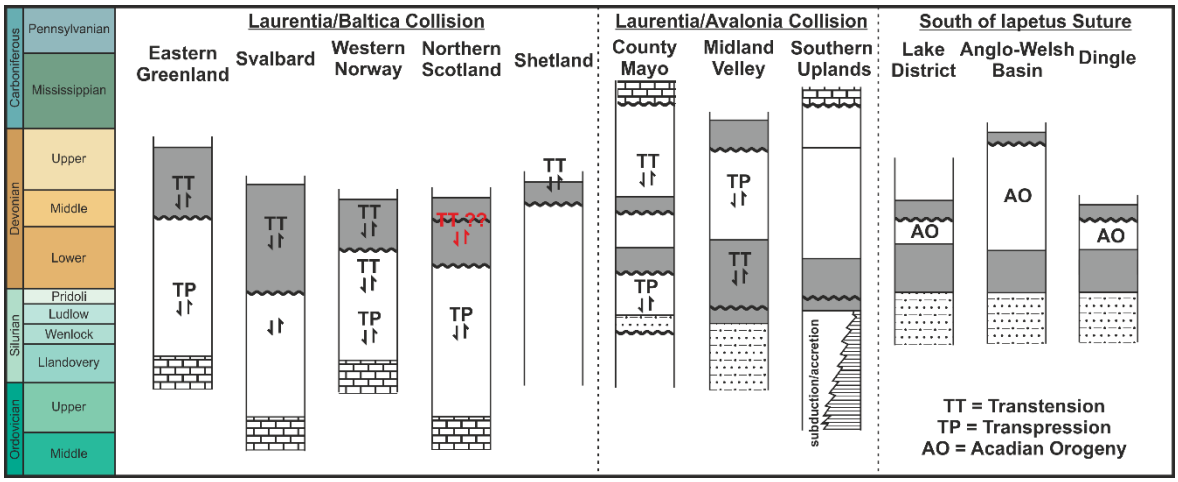

Figure 6.1 Structural time chart for the Caledonian Orogeny showing the change in structural regime during the Caledonian orogeny. Modified *after* Dewey and Strachan (2003).

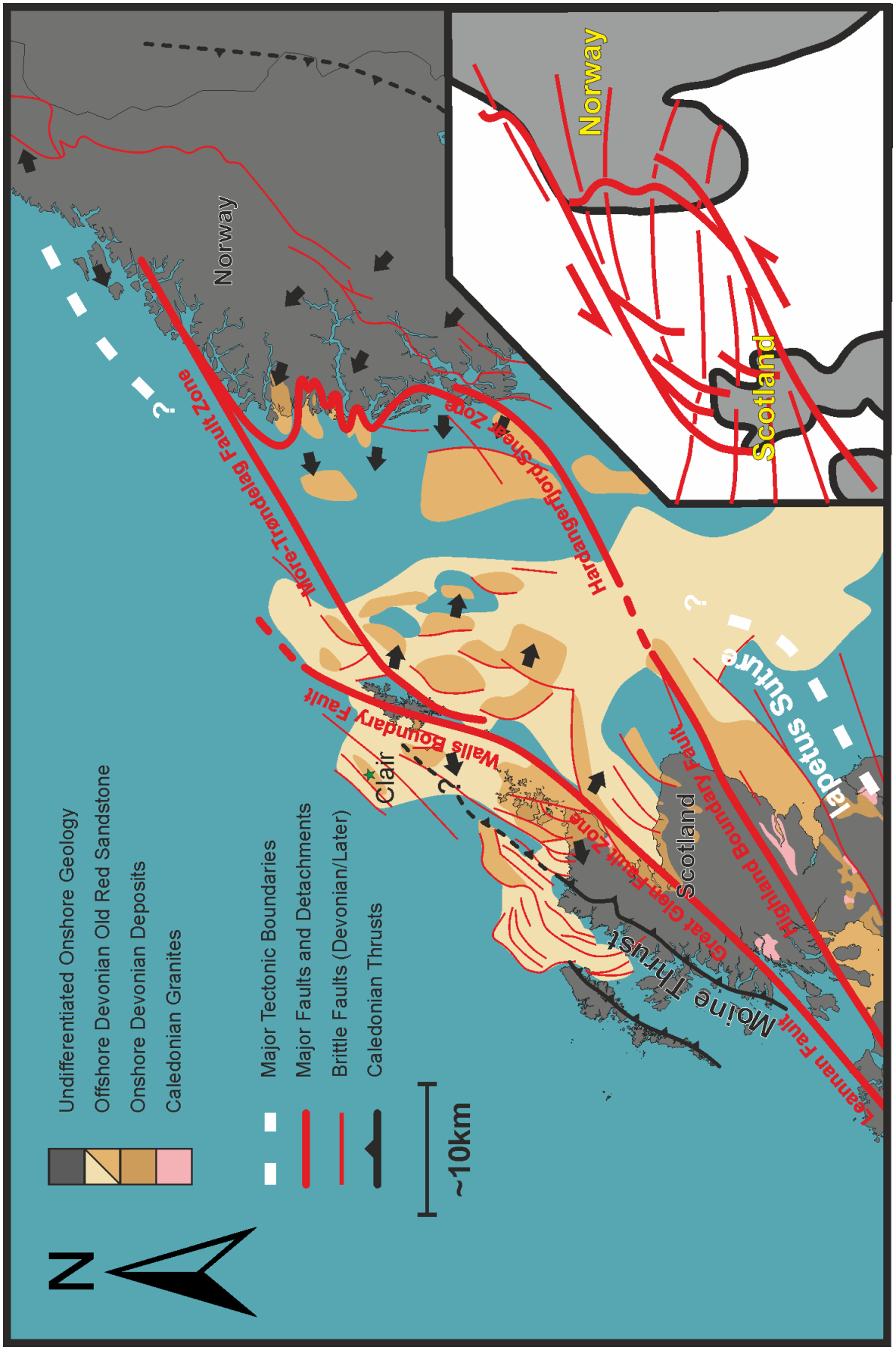

Figure 6.2: Regional transtensional model for the development of the Orcadian Basin. Modified *after* Fossen (2010).

It has now been recognised that folding does not only have to signify crustal shortening, but can also be generated during oblique extension (Figure 6.3) (Fossen *et al.,* 2013), as demonstrated by laboratory experiments (Figure 6.4) (Venkat-Ramani and Tikoff, 2002; Wu *et al.,* 2009) and numerical modelling (Fossen *et al.*, 1994; Fossen and Tikoff, 1998).

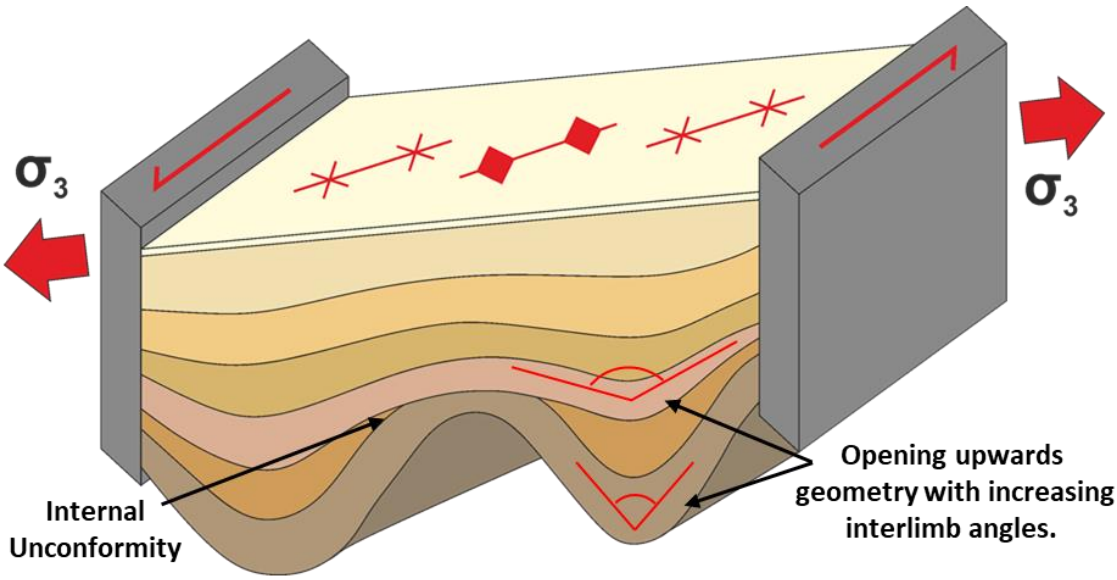

Figure 6.3 Schematic diagram for the development of transtensional fold with hinges oblique to bounding shear zones, internal unconformity and opening upwards geometry.

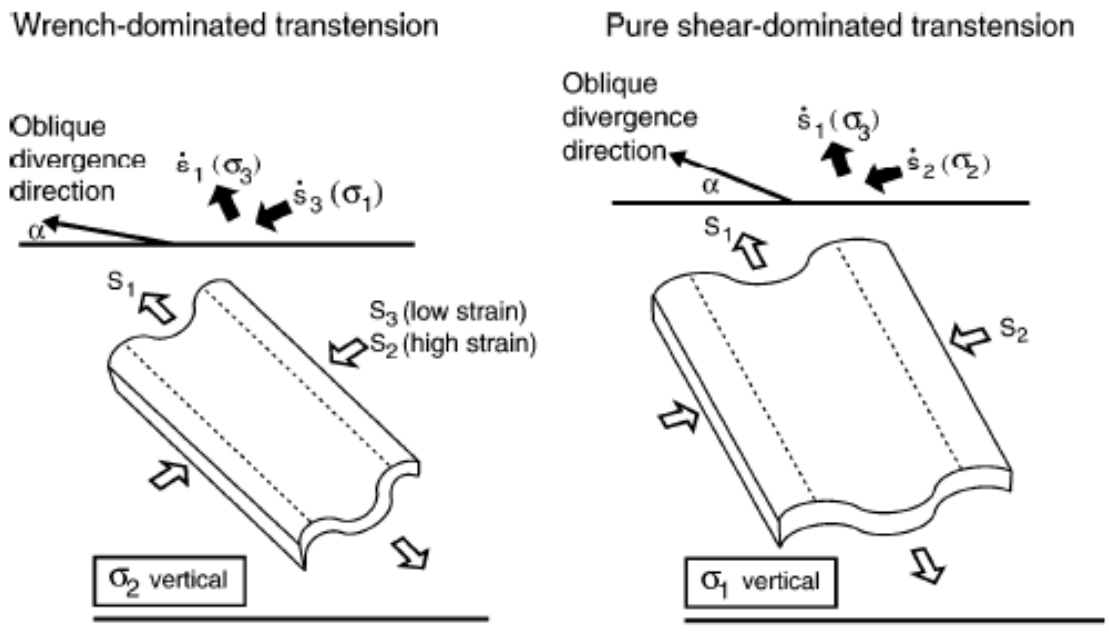

Figure 6.4: Fold shapes and orientations in wrench and pure shear dominated transtension (Venkat-Ramani and Tikoff, 2002)

Thus, the assumption that folding equals inversion may contradict the notion that folding in the Orcadian Basin is primarily related to Permo-Carboniferous reactivation as previously

suggested (Coward, 1993; Coward *et al.,* 1989; Enfield and Coward, 1987; Norton *et al.,* 1987). For example, the local unconformities between Lower and Middle Devonian strata observed in parts of the Orcadian Basin could instead be due, in part, to transtensional folding, and not uplift, transpression and deformation associated with the Mid Devonian Acadian Event as suggested by Mendum and Noble (2010). The significant variations in thickness between LORS deposits can also be explained by the localised development of pull-apart style basins, which are known to rapidly accommodate significant thicknesses of sediments (Reading, 1980) as proposed for the Walls Basin (Melvin, 1985).

Our observations from across the Orcadian Basin are complimentary to those made by Seranne, (1992) and others, which indicates regional sinistral transtension, in particular the development of growth folds with an opening upward geometry. This similarity in fold geometry, and the generation of folds with hinges oblique to the major basin bounding structures in the Orcadian Basin, suggests that growth folding was widespread, and in Shetland was associated with sinistral transtension along the Walls Boundary Fault Zone. Similar growth folds in mainland Scotland may also in fact be associated with transtension and related to sinistral transtension along the Great Glen Fault Zone.

A number of other criteria can be used to indicate transtension which have been previously observed in the Orcadian Basin (Reading, 1980; Rodgers, 1980; Steel and Gloppen, 1980). These include and are not limited to: opening upwards folds; intra/inter formational unconformities; paleovalleys, changing hinge positions and rapidly changing sedimentary fills (facies dislocation).

Thus, we suggest that despite some evidence which can indicate extensional tectonics in parts of the Orcadian Basin, much of this does not preclude a regional sinistral transtensional setting, with strain partitioning leading to some areas developing predominantly extensional structures, and others being more strongly influenced by regional strike-slip tectonics which together are influencing the distribution of sediments in the basin (Figure 6.5) as discussed in Chapter 3.

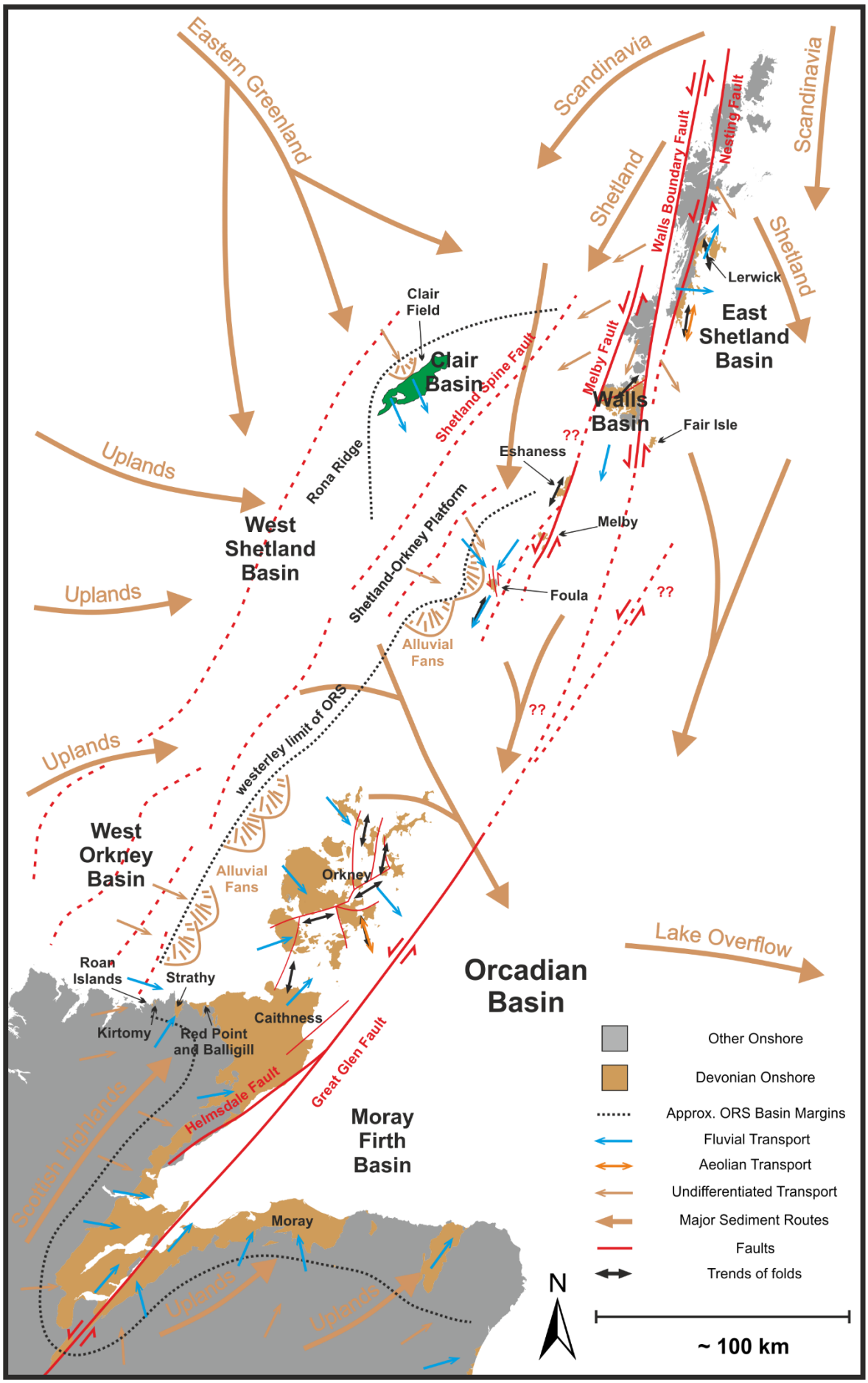
Eastern Greenland
Scandinavia
Scandinavia
Shetland
Shetland
Walls Boundary Fault
Nesting Fault
Lerwick
East Shetland Basin
Clair Field
Clair Basin
Shetland Spine Fault
Melby Fault
Walls Basin
Fair Isle
Eshaness
??
Uplands
Rona Ridge
West Shetland Basin
Shetland-Orkney Platform
Melby
Foula
??
Uplands
Alluvial Fans
??
Uplands
westerley limit of ORS
West Orkney Basin
Alluvial Fans
Orkney
Lake Overflow
Roan Islands
Strathy
Caithness
Kirtomy
Red Point and Balligill
Orcadian Basin
Great Glen Fault
Helmsdale Fault
Scottish Highlands
Moray Firth Basin
Moray
Uplands
Uplands
Other Onshore
Devonian Onshore
Approx. ORS Basin Margins
Fluvial Transport
Aeolian Transport
Undifferentiated Transport
Major Sediment Routes
Faults
Trends of folds
N
~ 100 km

Figure 6.5 (preceding page): Paleogeographic map of the Orcadian Basin showing major structures, sediment sources and major paleocurrents. Major sinistral transcurrent faults, separate the different Devonian sub-basins, partitioning deformation and the associated structures which are controlling basin development. This reconstruction places Foula and Melby (precise lateral position of three Devonian basin of Shetland along strike of the major strike-slip faults is unknown and is meant to be diagrammatic) in a position between Clair and Orkney, reflecting the new provenance data and integrating them with the observations of Allen and Mange-Rajetzky, (1992); Blackbourn, (1981); Donovan et al., (1976); Duindam and van Hoorn, (1987); Mykura et al., (1976); Schmidt et al., (2012); and Smalley, (2011).

A diverse range of basement cover relationships have also been identified which reflect the dynamic environment that existed during the deposition of the Orcadian Basin. The model proposed by (Dichiarante, 2017) for Devonian basin development has been updated and expanded upon (Chapter 4)(Figure 6.6) in order to reflect the observations made during this study and adequately represent the diversity observed which include:

- The complex interplay of tectonics and climate leading to diverse range of sedimentary architectures and facies.
- The greater variety in basin geometry and shape.
- The role of transtension and strike-slip tectonics and the strong structural control on sedimentary systems with development of isolated mini-basins.
- Early syn-sedimentary growth folds and transtensional growth folds.
- Widespread evidence of soft-sediment deformation.

In addition to these principal implications, this study has also highlighted:

- A range of fold types:
    - Early transtension and growth folds (Chapter 3 and Chapter 4) related to the development of the basin during the Devonian.
    - Larger, km-scale, low amplitude, long wavelength inversion folds with localised folds related to discrete thrusts and reactivated fault zones (Chapter 4).
    - Smaller, mm-hm scale folds related to oblique transtension/transpressional reactivation of pre-existing structures (Chapter 5) which are often localised around reactivated faults.

- Differing structural style in parts of the basin, related to partitioning and relative proximity to major structures e.g. pre-existing basement structures and earlier basin forming or basin bounding structures, an insight gained from the interpretation of bathymetric data (Chapter 5).
- Differences to the model proposed by (Dichiarante, 2017), which include the relative lack of definitive later deformation and reactivation, lack of mineralisation and associated features, which are particular evident in the Shetland region.

Figure 6.6 (overleaf): Summary schematic box diagram of Devonian basin development showing the variety of basement cover relationships, structural elements and gross stratigraphic architectures. Numbers refer to locations described in Chapters 4 and 5.

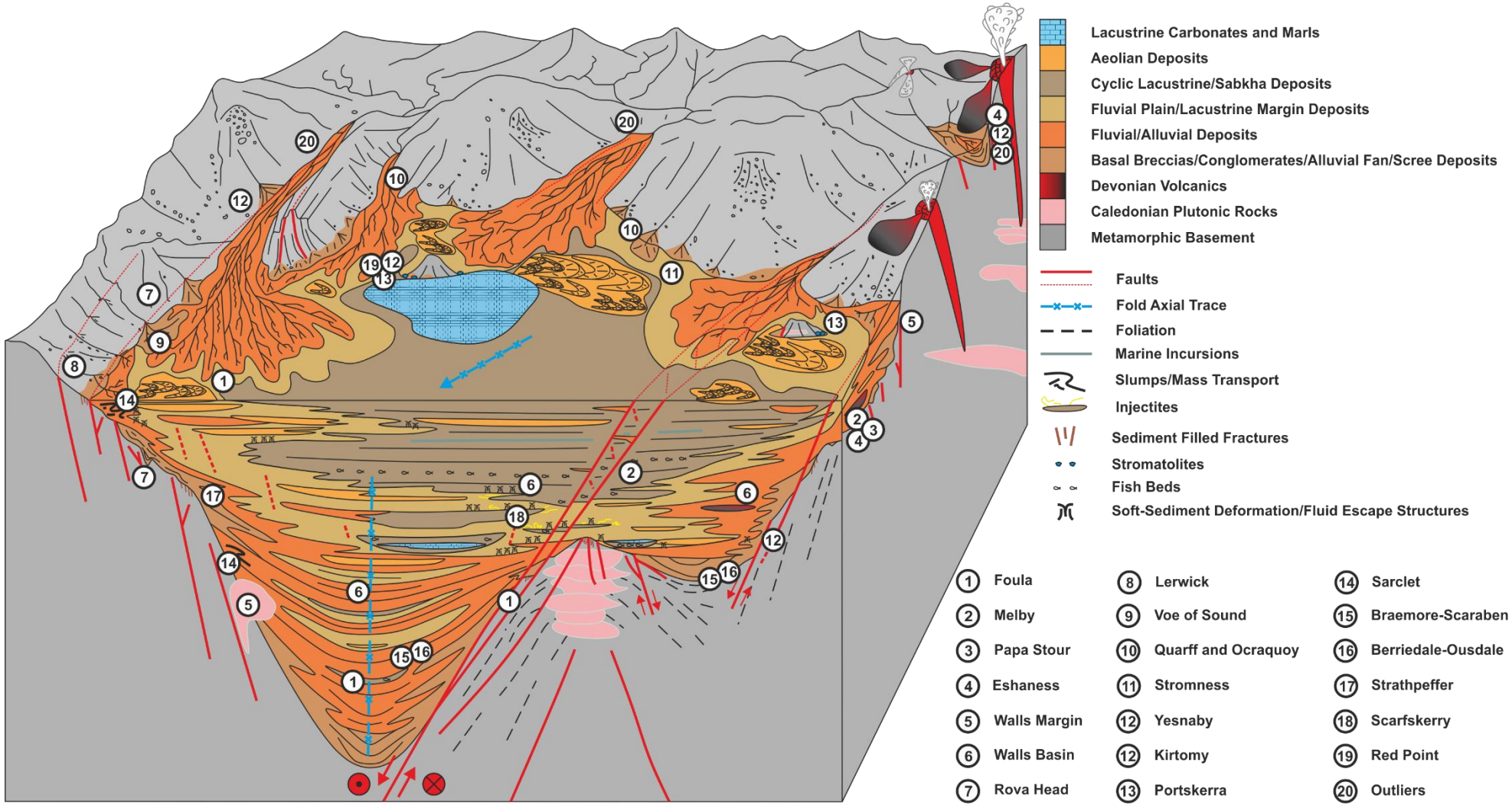
Lacustrine Carbonates and Marls
Aeolian Deposits
Cyclic Lacustrine/Sabkha Deposits
Fluvial Plain/Lacustrine Margin Deposits
Fluvial/Alluvial Deposits
Basal Breccias/Conglomerates/Alluvial Fan/Scree Deposits
Devonian Volcanics
Caledonian Plutonic Rocks
Metamorphic Basement
Faults
Fold Axial Trace
Foliation
Marine Incursions
Slumps/Mass Transport
Injectites
Sediment Filled Fractures
Stromatolites
Fish Beds
Soft-Sediment Deformation/Fluid Escape Structures
1 Foula
2 Melby
3 Papa Stour
4 Eshaness
5 Walls Margin
6 Walls Basin
7 Rova Head
8 Lerwick
9 Voe of Sound
10 Quarff and Ocraquoy
11 Stromness
12 Yesnaby
12 Kirtomy
13 Portskerra
14 Sarclet
15 Braemore-Scaraben
16 Berriedale-Ousdale
17 Strathpeffer
18 Scarfskerry
19 Red Point
20 Outliers

6.1.2. Suitability of the Orcadian Basin as an analogue to the Clair Basin:

This section is a summary of the key similarities and differences in the geology and geological history of the Orcadian Basin as an analogue to the offshore Clair Basin:

- Both the Clair and Orcadian Basins are Devonian age, continental clastic basins which were infilled to varying degrees with alluvial, fluvial, aeolian and lacustrine sedimentary rocks which overlie metamorphic basement rocks and developed following the Caledonian orogeny.
- The Clair Basin was smaller and more isolated (Blackbourn, 1987b) and did not develop the extensive and thick lacustrine deposits compared to the Orcadian Basin (Nichols, 2005). Analogues in Shetland i.e. Foula (Chapter 3) and around the margins of the Orcadian Basin (Chapter 4) may be more suitable than the predominantly lacustrine Middle Devonian outcrops in central Caithness and Orkney.
- Source rocks in the two basins differ in origin and age. In the Clair Basin (and elsewhere, West of Shetland), Late Jurassic, Kimmeridgian source rocks, buried more deeply in the Faroe-Shetland Basin, provided charge which has been dated to the Cretaceous (Robertson et al., 2020). In the Orcadian Basin, local Devonian source rocks are known to have provided minor quantities of hydrocarbons during the Carboniferous.
- Both the Clair and Orcadian Basins overlie fractured metamorphic rocks. In Clair the basement is similar to the Lewisian Complex (Holdsworth *et al.,* 2019; Kinny *et al.,* 2019), whereas the Orcadian Basin overlies more variable Moinian/Lewisian like basement which was deformed during the Caledonian orogeny (Dewey *et al.,* 2015).
- Both the Clair and Orcadian Basins have polyphase fracture systems which are similar in structural style and in fracture fills (Dichiarante, 2017).
- However due to the locations of the Clair Basin on the margins of the North Atlantic rift, the Clair Basin has been subjected to a greater degree of Mesozoic and Cenozoic deformation which is more poorly understood onshore. The extensive period of uplift in the Orcadian basin has likely affected the diagenetic and fluid flow properties of onshore analogues.
- Despite the highly fractured nature of the Devonian sequences throughout the Orcadian Basin, fracturing appears to be focused into discrete 'fracture corridors' which has also been noted by previous workers in all other parts of the Orcadian

Basin (Dichiarante, 2017) and is reported in the Clair Field (Coney *et al.,* 1993). These structures are likely key conduits for fluid flow in the sub-surface, however it is the connection of these structures to the wider pervasive fracture systems that is likely the key to adequate production (Chapter 5).

- Away from major basin bounding and basement structures, the Clair Group is far less fractured, and analogues such as Foula may be better analogues for these less fractured, predominantly fluvial/alluvial reservoir units e.g. Clair South (Robertson *et al.,* 2020)
- The Orcadian and Clair Basins may have formed in different tectonic settings and the role of strike-slip tectonics and transtension should be considered as an alternative (Chapter 3 and 4).
- The main hydrocarbon bearing fracture systems are of different ages. In Clair they are Cretaceous in age (Robertson *et al.,* 2020) as opposed to Permian in the Orcadian Basin (Dichiarante *et al.,* 2016).
- The Devonian rocks of the island Foula (and nearby Melby) are geologically more similar to mainland Scotland and Orkney than Shetland. They also show sedimentological characteristics that are intermediate between those of the Clair Basin and the larger Orcadian Basin.

6.1.3. Implications for the Clair Oil Field and wider resource development:

The key implications for the Clair Oil Field and for wider resource development derived from this study include:

- A greater understanding of the diversity of basement-cover relationships that may exist in the Clair Basin. This spatial and temporal diversity may have implications on the processing and interpretation of seismic data, due to the highly variable sedimentary facies and structural configurations that exist over relatively small distances (dm-km). This sub-seismic diversity may have knock-on implications for reservoir modelling, reservoir management, fluid flow and waterflood modelling, drilling and well placement

- The possibility that the Clair Basin is transtensional - and as result the Clair Group may have a geometry and contain structures that differ from the existing models used offshore.
- Deformation is concentrated not only around major, seismically resolvable structures, but also in complex zones away from these areas, which are likely below the resolution of conventional methods and may have a strong influence on the fluid flow properties of fractured reservoirs offshore.
- Fault zone architectures are highly complex in the Orcadian Basin. For example, adjacent to Devonian age faults and fracture zones are abundant deformation bands, which may act as baffles/barriers to fluid flow adjacent to highly permeable fluid flow corridors. A greater understanding of the diversity of sub-seismic fault zone architecture can be used to direct drilling and water-flood operations in the Clair Field.
- The recognition of soft sediment deformation features such as those observed in the Orcadian Basin may aid in the identification of early syn-sedimentary tectonic activity (Novak and Egenhoff, 2019), particular in the absence of larger more obvious structures and geometries, e.g. growth structures.
- The recognition of folds and trapping geometries developed early in the development of the Devonian basins and not during later reactivation and/or inversion could have important implications for modelling the petroleum systems of the Moray Firth, West Orkney Basin and East Shetland Platform. For example, an early charge of Devonian sourced oil into a Devonian trap developed in Devonian reservoir rocks could occur, which would precede the better documented charge of oil during the Mesozoic. Such a scenario has been recorded onshore in Caithness by Baba *et al.* (2018),in Orkney by Brown *et al.,* (2019) and various parts of Scandinavia (Rønningen, 2015). Offshore, Devonian lacustrine source rocks are also known to contribute to the Beatrice, Oseberg, Judy and Embla oil fields (Stevens, 1991) and have been encountered in wells on the Norwegian Continental Shelf.
- The significant thicknesses of highly fractured coarse-grained clastic rocks in the Orcadian Basin, together with an active Devonian source rock kitchen, may also represent an underexplored petroleum play on the UKCS or provide an alternative for future Carbon Capture and Storage operations.

- A greater understanding of the structural and stratigraphic evolution of analogues to the Clair Group, together with a proven deliverability of low API hydrocarbons to the wellbore exhibited by Clair, may make smaller peripheral fields economically viable as tie-backs to new infrastructure being developed and planned West of Shetland. These include prospects/discoveries that contain oil in Devonian age reservoirs near to the Clair Field but remain undeveloped due in part to their small size, but compounded further by the heavy oil present (Oil and Gas Authority, 2019b):
    - Marmaduke, Ginger and Paddy are undrilled prospects adjacent to and overlying the Rona Ridge to the SW of Clair owned by Spark Energy.
    - Boulmer Prospect, to the SW of Clair but relinquished by CNOOC.
    - Freya Discovery drilled by Mobil (206/10a-1) to the NE of Clair.
    - Fulla Discovery drilled by Faroe Petroleum (206/5a-3) to the NE of Clair.
    - North Uist Discovery drilled by Nexen (213/25c-1v) to the NW of Clair overlying the Corona Ridge.
    - Eriboll Discovery drilled by Mobil (213/23-1) but now owned by Apache.

  Together, these also suggest that the Clair Basin may have been part of a much larger basin that underlies a greater area of the Faroe-Shetland Basin (Foula and Flett sub-basins), at least as far as the Corona Ridge to NW of Clair.
- The growing and improved understanding of the Devonian Basins more regionally onshore may also help to reduce uncertainty in some of the more peripheral areas of the UKCS that have been targeted and licenced in the past e.g. West Fair Isle Basin (Figure 6.5) and West Orkney Basin and others that are now the focus of ongoing exploration and appraisal for example on the East Shetland Platform.

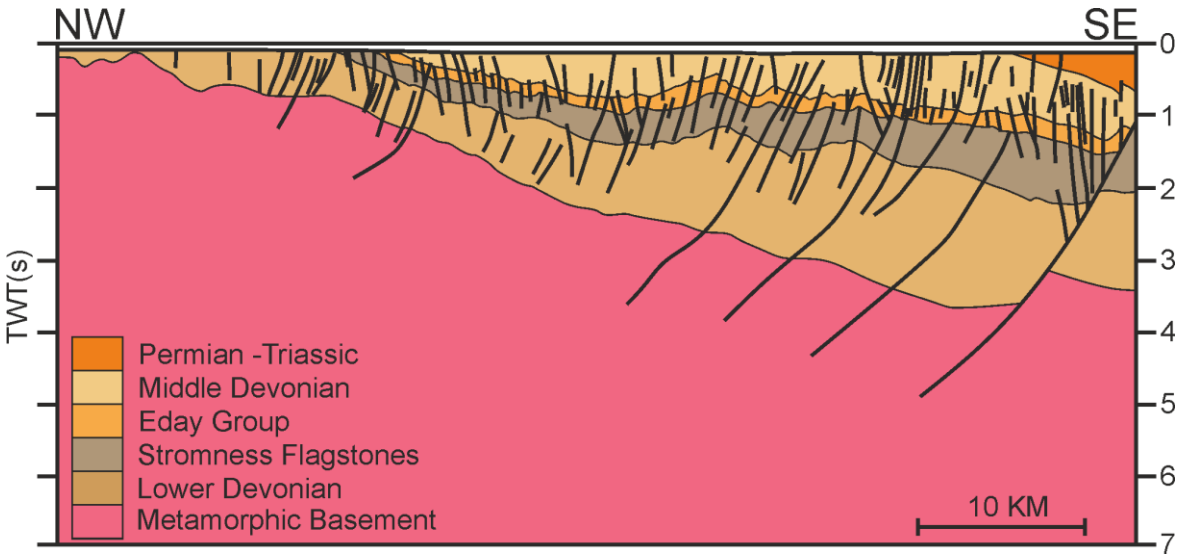

Figure 6.5: Interpretation of seismic line though Orkney Shetland platform and part of the West Fair Isle Basin. Foula is located approximately 40 km to the North. Survey collected as part of Frontier Licence P1884. Modified *after* Oil and Gas Authority, (2019b).

6.1.4. Implications for other basins and geological settings

The observations and understandings developed from this study may have application to other sedimentary basins both modern and ancient, and other geological settings, which include and are not limited to:

- The Dead Sea Transform - a strike slip pull apart basin (Girdler, 1990) which may be analogous to areas of the Orcadian Basin that were strongly influenced by strike-slip motion e.g. the Walls Basin. In such a strongly strike-slip influenced basin, such as the Dead Sea you would expect rapid subsidence and sedimentation, and abundant soft sediment deformation, as observed in parts of the Orcadian Basin which could be seen as analogous.
- The Great Basin, North America – e.g. Lake Bonneville, an endorheic, arid, lacustrine intra-montane basin which may be analogous to the general climate and geographic setting of the Orcadian Basin (Dickinson, 2006). Studies of this modern environment may provide further insight into the sedimentary processes that were ongoing during the deposition of the rocks in the Orcadian Basin.
- The Salton Sea, North America – an endorheic, arid, lacustrine, intra-montane basin that developed astride a major, continental scale transform fault. The geological setting of this location is directly analogous to the Great Glen Fault Zone (Brothers

et al., 2009) and may provide an ideal opportunity to understand the sorts of sedimentological and structural processes that may have been underway during the evolution of the Orcadian Basin.

- Lake Balkhash, Kazakhstan – an endorheic, arid, intra-montane basin, which unlike the Orcadian Basin, formed as foreland basin during the Alpine Orogeny, however is filled with similar sediments and is influenced by both climate and tectonics (Petr, 1992).
- The Caspian and Black Sea are two further basins that developed during the Alpine orogeny, however, are thought to be the remnants of the Tethys Ocean and back arc basins developed during the subduction of the Tethys Ocean.
- Tien Shan, Central Asia – e.g. Issyk Kul, an arid, endorheic, intra-montane, lacustrine basin, bound by large strike-slip faults (Buslov *et al.,* 2007) in a similar tectonic setting to the Orcadian Basin.
- Tarim Basin and Taklamakan Desert, China- an arid, intra-montane basin that developed in the immediate vicinity of a major orogenic belt (Wang *et al.,* 1992), and is directly analogous to the Orcadian Basin, particularly during times when the basin was drier and influenced more by fluvial and aeolian processes i.e. Upper Devonian times.

The Orcadian Basin would also be an appropriate analogue to other arid and/or intra-montane, alluvial – fluvial - lacustrine depositional systems such as the Permian basins of the North Sea and Western Europe (Marshall *et al.,* 2003) or the Eocene, Green River Formation of Wyoming, North America (Surdam and Wolfbaeur, 1975).

6.2. Conclusions

The main aim of this project was to carry out a reappraisal of Devonian basin development using the Devonian rocks of Shetland and NE Scotland, evaluate and understand the geology of the Orcadian basin as an analogue to the offshore Devonian Basins e.g. Clair Basin, West of Shetland, and aid in the ongoing development of the Clair Oil Field.

The main conclusions from this research study are as follows:

- The western most of the three Devonian basins of Shetland (Foula-Melby) is of a closer geological affinity to the Devonian sequences of Orkney and Caithness and is

likely the Northernmost and most proximal expression of the Eday Group and Stromness Flagstone Group of Orkney. This region likely also represents a transitional region between the Clair and Orcadian Basins.

- The structural model proposed by (Dichiarante, 2017; Dichiarante *et al.,* 2016) is largely applicable to the Devonian rocks of Shetland with some local differences, principally the lack of Permian age deformation.
- However, the model has been updated to reflect new observations made on the Devonian development of the region, principally the existence of more widespread transtensional basin development, growth folding coeval with sedimentation, a diverse range of unconformity and basement/cover relationships and widespread evidence of soft-sediment deformation.
- The development of the Devonian Basins was dynamic, with a complex interplay of tectonics and climate, with active folds and faults controlling sediment routing and influencing sedimentary processes.
- Unconformities in the Orcadian Basin may be sub-divided into two main types; type 1 unconformities dominated by local to regional tectonics, and type 2 unconformities dominated by sedimentary processes and fair field to regional scale tectonics.
- Although possible to sub-divide unconformities into two broad types, a highly diverse range of basement/cover relationships are evident throughout the Orcadian Basin which span several orders of magnitude, leading to complex sedimentological and structural configurations and juxtapositions both spatially and temporally even within the sub-divisions.
- Such levels of diversity may lead to difficulty in the ongoing development of the Clair Oil Field, where production is focused on a thinner sequence of Devonian strata that overlie metamorphic basement.
- A diverse range of fold types are found in the Orcadian Basin, at a wide range of scales, which reflect the polyphase history of the basin which include; localised growth folds related to transtension during basin development; km to cm scale folds related to inversion, thrusting and regional transpression; complex dm to cm scale transtensional folds and the repeated reactivation of existing folds.

- Deformation in the Orcadian Basin is partitioned by predominantly N/S trending structures which control both the types of structures being developed but also the spatial distribution and temporal evolution.
- Structures observed offshore are comparable to those onshore and the analysis of offshore and near shore datasets has allowed for a greater understanding of the range, style and size of structures developed within the Orcadian Basin and allows for greater comparison between onshore analogues and traditional datasets used in hydrocarbon exploration e.g. seismic.
- The combination of new digital technologies in conjunction with traditional field techniques and remote sensing studies is a powerful means for the collection of field data.

6.3. Future Work

Potential future work or elements of the research that went beyond the scope or remit of this study and may provide the logical continuation of this research could include:

- An in-depth study of deformation and mineralisation associated with the development of the East Shetland 'Steep Belt'. Geochronology of samples collected using Re/Os of pyrite or U/Pb in calcite would be of merit and was initially planned but went beyond the scope and budget of the project. Re abundancy tests were performed on samples (Appendix C) but yielded marginal quantities of Re for reliable analysis, however further crushing and sample preparation may improve this. Due to the abundance of calcite and dolomite cements in the samples, U/Pb dating may prove a viable alternative and help to elucidate the age and origin of these structures and associated mineral deposits.
- A detailed study of the Devonian rocks on Fair Isle, building on earlier work (Mykura, 1972a; Mykura and Harrison, 1972) to better understand the tectonic and stratigraphic evolution of the island and the age and genesis of mineralisation, in order to ascertain a link, if any, to deformation and mineralisation seen elsewhere in the Orcadian Basin. Its proximity to the offshore continuation of the WBF and GGF will aid in understanding the tectonic evolution of these structures and regional structural evolution during the Paleozoic and Mesozoic.

- Further detailed analysis of structures onshore in the Orkney Isles, particularly on the smaller islands in the North and those that are less accessible, together with further analysis of inshore bathymetry, to build on this study and the work of Dichiarante (2017).
- Geochronology of basement samples from Western Shetland, notably, the Walls Peninsula, samples collected from Foula during this study and other outliers including the islands of Ve Skerries.
- Examination of outliers of supposedly Devonian rocks North of Shetland on the island of Gruney and the coastline Northeast of North Roe near to Lokati Kame [HU 438000 1192000](BGS, 2005a). The use of a drone to remotely capture the geology of these remote exposures would be advantageous in addition to ground-based sampling for heavy mineral, detrital zircon and palynological analysis.
- Geophysical analysis of offshore 2D seismic and gravity data would help to understand the sedimentary basins immediately to the North of Shetland and adjacent to the offshore continuation of the Walls Boundary Fault. E.g. Sandwick Basin, where BGS borehole 78/10 recovered friable red sandstone of presumed Devonian age (Stoker *et al.,* 1993).
- Provenance and geochronological analysis of samples recovered from the sea floor and from the islands offshore in this area would enable the offshore geology to be better linked to that onshore and more regionally.
- Geophysical analysis of offshore 2D seismic and gravity data from the West Fair Isle Basin would help to better understand the Devonian sedimentary basins between Shetland and Orkney.
- Further examination of bathymetric day from the offshore regions of the study area would allow for further mapping of the distribution of structures in the Orcadian Basin.
- Re-examination of all earlier work done on Clair analogues, and the extraction of data from previous studies, to build a dedicated Clair analogue database integrating all geophysical, petrophysical, geochemical and geological data for ongoing reservoir modelling. This work could also extend to include other elements of the petroleum system for potential Paleozoic and Mesozoic plays overlying and adjacent to the Rona Ridge, and could form the basis of a dedicated West of Shetland petroleum system analogue database.

- Extraction of geometric data pertinent to sedimentary facies and architectures from the Virtual Outcrop Models produced in this study which could be used an input into reservoir models.
- The compilation and statistical analysis of fault/fracture attributes and scaling relationships from Devonian and basement analogues in Shetland, Orkney and other offshore datasets in order to provide a comparative database for fractured reservoirs on the UK and Norwegian Continental Shelf.

References

Allen, P.A., 1982. Cyclicity of Devonian fluvial sedimentation, Cunningsburgh Peninsula, SE Shetland. J. Geol. Soc. London. 139, 49 LP – 58.

Allen, P.A., 1981. Devonian lake margin environments and processes, SE Shetland, Scotland. J. Geol. Soc. London. 138, 1–14. doi:10.1144/gsjgs.138.1.0001

Allen, Philip A, 1981. Sediments and processes on a small stream-flow dominated, devonian alluvial fan, Shetland Islands. Sediment. Geol. 29, 31–66. doi:http://dx.doi.org/10.1016/0037-0738(81)90056-7

Allen, P.A., 1979. Sedimentological aspects of the devonian strata of SE Shetland. PhD Thesis, Cambridge University.

Allen, P.A., Mange-Rajetzky, M.A., 1992. Devonian-Carboniferous sedimentary evolution of the Clair area, offshore north-western UK: impact of changing provenance. Mar. Pet. Geol. 9, 29–52. doi:10.1016/0264-8172(92)90003-W

Allen, P.A., Marshall, J.E.A., 1981. Depositional Environments and Palynology of the Devonian South-east Shetland Basin. Scottish J. Geol. 17, 257–273. doi:10.1144/sjg17040257

Allmendinger, R.W., Cardozo, N., Fisher, D.M., 2011. Structural geology algorithms: Vectors and tensors. Cambridge University Press.

Allmendinger, R.W., Judge, P., 2013. Stratigraphic uncertainty and errors in shortening from balanced sections in the North American Cordillera. Bulletin 125, 1569–1579.

Alsop, G.I., Weinberger, R., Marco, S., Levi, T., 2019. Identifying soft-sediment deformation in rocks. J. Struct. Geol. 125, 248–255. doi:https://doi.org/10.1016/j.jsg.2017.09.001

Anderson, E.M., 1905. The dynamics of faulting. Trans. Edinburgh Geol. Soc. 8, 387 LP – 402.

Andrews, I., 1985. The Deep Structure of the Moine Thrust-Short Communication. Scottish J. Geol. 21, 213–217. doi:10.1515/cclm.1993.31.5.329

Andrews, S.D., Cornwell, D.G., Trewin, N.H., Hartley, A.J., Archer, S.G., 2016. A 2.3 million year lacustrine record of orbital forcing from the Devonian of northern Scotland. J. Geol. Soc. 173, 474–488. doi:10.1144/jgs2015-128

Andrews, S.D., Hartley, A.J., 2015. The response of lake margin sedimentary systems to climatically driven lake level fluctuations: Middle Devonian, Orcadian Basin, Scotland. Sedimentology 62, 1693–1716.

Angelier, J., 1990. Inversion of field data in fault tectonics to obtain the regional stress—III. A new rapid direct inversion method by analytical means. Geophys. J. Int. 103, 363–376.

Angelier, J., 1984. Tectonic analysis of fault slip data sets. J. Geophys. Res. Solid Earth 89, 5835–5848.

Armitage, P.J., Worden, R.H., Faulkner, D.R., Aplin, A.C., Butcher, A.R., Iliffe, J., 2010. Diagenetic and sedimentary controls on porosity in Lower Carboniferous fine-grained lithologies, Krechba field, Algeria: A petrological study of a caprock to a carbon capture site. Mar. Pet. Geol. 27, 1395–1410.

Astin, T.R., 1990. The Devonian lacustrine sediments of Orkney, Scotland; implications for climate cyclicity, basin structure and maturation history. J. Geol. Soc. London. 147, 141–151. doi:10.1144/gsjgs.147.1.0141

Astin, T.R., 1985. The palaeogeography of the Middle Devonian Lower Eday Sandstone, Orkney. Scottish J. Geol. 21, 353–375.

Astin, T.R., 1982. The Devonian geology of the Walls peninsula, Shetland. University of Cambridge.

Baba, M., Parnell, J., Muirhead, D., Bowden, S., 2018. Oil charge and biodegradation history in an exhumed fractured reservoir, Devonian, UK. Mar. Pet. Geol.

Barclay, W.., Browne, M.A.., McMillan, A.., Pickett, E.A., Stone, P., Wilby, P.R., 2005. The Old Red Sandstone of Great Britain. Geol. Conserv. Rev. Ser. 31, 393.

Barr, D., Holdsworth, R.E., Roberts, A.M., 1986. Caledonian ductile thrusting in a Precambrian metamorphic complex: The Moine of northwestern Scotland. Geol. Soc. Am. Bull. 97, 754–764.

Barr, D., Savory, K.E., Fowler, S.R., Arman, K., McGarrity, J.P., 2007. Pre-development fracture modelling in the Clair field, west of Shetland. Geol. Soc. London, Spec. Publ. 270, 205–225. doi:10.1144/gsl.sp.2007.270.01.14

Bartholomew, I.D., Peters, J.M., Powell, C.M., 1993. Regional structural evolution of the North Sea: oblique slip and the reactivation of basement lineaments, in: Geological Society, London, Petroleum Geology Conference Series. Geological Society of London, pp. 1109–1122.

Baxter, A.N., Mitchell, J.G., 1984. Camptonite-Monchiquite dyke swarms of Northern Scotland; Age relationships and their implications. Scottish J. Geol. 20, 297–308. doi:10.1144/sjg20030297

Beacom, L.E., Holdsworth, R.E., McCaffrey, K.J.W., Anderson, T.B., 2001. A quantitative study of the influence of pre-existing compositional and fabric heterogeneities upon fracture-zone development during basement reactivation. Geol. Soc. London, Spec. Publ. 186, 195–211. doi:10.1144/GSL.SP.2001.186.01.12

Belaide, A., Trice, R., Walmsley, A., Penman, A., 2016. Integrated drilling and evaluation of a horizontal granitic basement producer, in: SPE Europec Featured at 78th EAGE Conference and Exhibition. Society of Petroleum Engineers.

Belaidi, A., Bonter, D.A., Slightam, C., Trice, R.C., 2018. The Lancaster Field: progress in opening the UK's fractured basement play. Geol. Soc. London, Pet. Geol. Conf. Ser. 8, 385 LP – 398.

Belaidi, A., Bonter, D.A., Slightam, C., Trice, R.C., 2016. The Lancaster Field: progress in opening the UK's fractured basement play. Geol. Soc. London, Pet. Geol. Conf. Ser. 8. doi:10.1144/PGC8.20

Bemis, S.P., Micklethwaite, S., Turner, D., James, M.R., Akciz, S., Thiele, S.T., Bangash, H.A., 2014. Ground-based and UAV-Based photogrammetry: A multi-scale, high-resolution mapping tool for structural geology and paleoseismology. J. Struct. Geol. 69, 163–178. doi:10.1016/j.jsg.2014.10.007

BGS, 2019. British Geological Survey Geoindex Offshore [WWW Document]. Geoindex Offshore. URL http://mapapps2.bgs.ac.uk/geoindex_offshore/home.html

BGS, 2012. Nairn, Scotland Sheet 84E. Bedrock Edition. 1:50,000.

BGS, 2005a. Northmaven, Scotland Sheet 129. Bedrock Edition. 1:50,000.

BGS, 2005b. Unst & Fetlar, Scotland Sheet 131. Solid and Drift Edition. 1:50,000.

BGS, 2004a. Badanloch, Scotland Sheet 109W. Bedrock Edition. 1:50,000.

BGS, 2004b. Evanton, Scotland Sheet 93E. Bedrock Edition. 1:50,000.

BGS, 2003a. Kildonan, Scotland Sheet 109E. Bedrock Edition. 1:50,000.

BGS, 2003b. Reay, Scotland Sheet 115E. Bedrock & Superficial Edition. 1:50,000.

BGS, 2002. Golspie, Scotland Sheet 103W. Solid and Drift Edition. 1:50,000.

BGS, 2001. Strathconon, Scotland Sheet 83W. Solid and Drift Edition. 1:50,000.

BGS, 1999. Orkney Islands 1:100000 Special Provisonal Map Solid and Drift Edition.

BGS, 1998. Helmsdale, Scotland Sheet 103E. Solid and Drift Edition. 1:50,000.

BGS, 1997. Fortrose, Scotland Sheet 84W. Solid & Drift Edition. 1:50,000.

BGS, 1996. Strathy Point, Scotland Sheet 115W. Solid & Drift Edition. 1:50,000.

BGS, 1995. Glenfiddich, Scotland Sheet 85E. Solid Edition. 1:50,000.

BGS, 1994. Yell, Scotland Sheet 130 and parts of 131. Solid & Drift Edition. 1:50,000.

BGS, 1990. Inverness, Scotland Sheet 83. Solid Edition. 1:63,360.

BGS, 1988. Foula Sheet 60 N - 04 W Solid Geology 1:250000 Series.

BGS, 1986. Wick, Scotland Sheet 116E. Solid Edition. 1:50,000.

BGS, 1985a. Thurso, Scotland Sheet 116W. Solid Edition. 1:50,000.

BGS, 1985b. Reay, Scotland Sheet 115E. Solid Edition. 1:50,000.

BGS, 1985c. Latheron, Scotland Sheet 110. Solid Edition. 1:50,000.

BGS, 1985d. Orkney Sheet 59 N - 04 W Solid Geology 1:250000 Series.

BGS, 1984. Shetland Sheet 60 N - 02 W Solid Geology 1:250000 Series.

BGS, 1982. Caithness Sheet 58 N - 04 W Solid Geology 1:250000 Series.

BGS, 1978a. Southern Shetland, Scotland Sheet 126. Solid Edition. 1:63,360.

BGS, 1978b. Central Shetland, Scotland Sheet 128. Solid Edition. 1:63,360.

BGS, 1973. Cromarty, Scotland Sheet 94. Solid Edition. 1:63,360.

BGS, 1971. Western Shetland, Scotland Special Sheet 127 and parts of 125, 126 & 128.

BGS, 1969. Elgin, Scotland Sheet 95. Solid Edition. 1:63,360.

Bird, P.C., 2014. Tectono-stratigraphic Evolution of the West Orkney Basin: Implications for Hydrocarbon Exploration. PhD Thesis, University of Cardiff.

Bird, P.C., Cartwright, J.A., Davies, T.L., 2015. Basement reactivation in the development of rift basins: an example of reactivated Caledonide structures in the West Orkney Basin. J. Geol. Soc. London. 172, 77 LP – 85.

Bjerga, A.D., 2017. The Caledonian tectonomagmatic evolution of the Orkney Islands, Scotland. MSc Thesis, University of Oslo

Blackbourn, G.A., 1987a. Sedimentary environments and stratigraphy of the Late Devonian–Early Carboniferous Clair Basin, west of Shetlands. European Dinantian Environments, 76-91.

Blackbourn, G.A., 1987b. Sedimentary Environments and Stratigraphy of the Late Devonian-Early Carboniferous Clair Basin, West of Shetland. Geol. Journal. Spec. Issue European D, 75–91.

Blackbourn, G.A., 1981a. Correlation of Old Red Sandstone (Devonian) outliers in the Northern Highlands of Scotland. Geol. Mag. 118, 409–414.

Blackbourn, G.A., 1981b. Probable Old Red Sandstone conglomerates around Tongue and adjacent areas, north Sutherland. Scottish J. Geol. 17, 103 LP – 118.

Blackbourn, G.A., Marshall, J.E.A., 1985. The Geology of Foula, Shetland. Geological Field Guide to Foula, Shetland, Britoil Report, 1–46.

Blamey, N.J.F., Conliffe, J., Parnell, J., Ryder, A.G., Feely, M., 2009. Application of fluorescence lifetime measurements on single petroleum-bearing fluid inclusions to demonstrate multicharge history in petroleum reservoirs. Geofluids 9, 330–337. doi:10.1111/j.1468-8123.2009.00265.x

Blumstein, R.D., Elmore, R.D., Engel, M.H., Parnell, J., Baron, M., 2005. Multiple fluid migration events along the Moine Thrust Zone, Scotland. J. Geol. Soc. London. 162,

1031–1045. doi:10.1144/0016-764904-092

Bons, P.D., Elburg, M.A., Gomez-Rivas, E., 2012. A review of the formation of tectonic veins and their microstructures. J. Struct. Geol. 43, 33–62.

Bonter, D., Trice, R., Cavalleri, C., Delius, H., Singh, K., 2018. Giant Oil Discovery West of Shetland-Challenges for Fractured Basement Formation Evaluation, in: SPWLA 59th Annual Logging Symposium. Society of Petrophysicists and Well-Log Analysts.

Bott, M.H.P., 1959. The mechanics of oblique slip faulting. Geol. Mag. 96, 109–117.

Brodu, N., Lague, D., 2012. 3D terrestrial lidar data classification of complex natural scenes using a multi-scale dimensionality criterion: Applications in geomorphology. ISPRS J. Photogramm. Remote Sens. 68, 121–134. doi:10.1016/j.isprsjprs.2012.01.006

Brothers, D.S., Driscoll, N.W., Kent, G.M., Harding, A.J., Babcock, J.M., Baskin, R.L., 2009. Tectonic evolution of the Salton Sea inferred from seismic reflection data. Nat. Geosci. 2, 581.

Brown, J.F., 1975. Potassium-Argon evidence of a Permian age for the camptonite dykes: Orkney. Scottish J. Geol. 11, 259–262.

Brown, J.F., Astin, T.R., Marshall, J.E.A., 2019. The Paleozoic petroleum system in the north of Scotland – outcrop analogues. Geol. Soc. London, Spec. Publ. 471, 253 LP – 280. doi:10.1144/SP471.14

Burns, I.M., 1994. Tectonothermal evolution and petrogenesis of the Navier and Kirtomy Nappes, North Sutherland, Scotland.

Buslov, M.M., De Grave, J., Bataleva, E.A. V, Batalev, V.Y., 2007. Cenozoic tectonic and geodynamic evolution of the Kyrgyz Tien Shan Mountains: A review of geological, thermochronological and geophysical data. J. Asian Earth Sci. 29, 205–214.

Butler, R.W.H., Holdsworth, R.E., Lloyd, G.E., 1997. The role of basement reactivation in continental deformation. J. Geol. Soc. London. 154, 69–71. doi:10.1144/gsjgs.154.1.0069

Caine, J.S., Evans, J.P., Forster, C.B., 1996. Fault zone architechture and permeability structure. Geology 24, 1025–1028. doi:10.1130/0091-7613(1996)024<1025

Cawood, P.A., Nemchin, A.A., Smith, M., Loewy, S., 2003. Source of the Dalradian Supergroup constrained by U–Pb dating of detrital zircon and implications for the East Laurentian margin. J. Geol. Soc. London. 160, 231–246.

Cawood, P.A., Strachan, R., Cutts, K., Kinny, P.D., Hand, M., Pisarevsky, S., 2010. Neoproterozoic orogeny along the margin of Rodinia: Valhalla orogen, North Atlantic. Geology 38, 99–102.

Chambers, L., Darbyshire, F., Noble, S., Ritchie, D., 2005. NW UK continental margin: chronology and isotope geochemistry. British Geological Survey, 161pp.

(CR/05/095N).

Chapman, N.A., 1975. An experimental study of spinel clinopyroxenite xenoliths from the Duncansby Ness vent, Caithness, Scotland. Contrib. to Mineral. Petrol. 51, 223–230.

Chauvet, A., Séranne, M., 1994. Extension-parallel folding in the Scandinavian Caledonides: Implications for late-orogenic processes. Tectonophysics 238, 31–54. doi:http://dx.doi.org/10.1016/0040-1951(94)90048-5

Clarke, P., Parnell, J., 1999. Facies analysis of a back-tilted lacustrine basin in a strike-slip zone, Lower Devonian, Scotland. Palaeogeogr. Palaeoclimatol. Palaeoecol. 151, 167–190. doi:https://doi.org/10.1016/S0031-0182(99)00020-6

Clifford, P., O'Donovan, A., Savory, K., Smith, G., Barr, D., 2005. Clair Field - Managing Uncertainty in the Development of a Waterflooded Fractured Reservoir. Proc. Offshore Eur. doi:10.2118/96316-MS

Cohen, K.M., Finney, S.C., Gibbard, P.L., Fan, J.-X.X., 2013. The ICS International Chronostratigraphic Chart. Episodes, 36: 199–204.

Collins, A.G., Donovan, R.N., 1977. The age of two Old Red Sandstone sequences in southern Caithness. Scottish J. Geol. 13, 53–57.

Coney, D., Fyfe, T.B.B., Retail, P., Smith, P.J.J., 1993. Clair appraisal: the benefits of a co-operative approach. Geol. Soc. London, Pet. Geol. Conf. Ser. 4, 1409–1420. doi:10.1144/0041409

Coward, M.P., 1993. The effect of Late Caledonian and Variscan continental escape tectonics on basement structure, Paleozoic basin kinematics and subsequent Mesozoic basin development in NW Europe. Geol. Soc. London, Pet. Geol. Conf. Ser. 4, 1095–1108. doi:10.1144/0041095

Coward, M.P., 1990. The Precambrian, Caledonian and Variscan framework to NW Europe. Geol. Soc. London, Spec. Publ. 55, 1–34. doi:10.1144/gsl.sp.1990.055.01.01

Coward, M.P., Enfield, M.A., Fischer, M.W., 1989. Devonian basins of Northern Scotland: extension and inversion related to Late Caledonian—Variscan tectonics. Geol. Soc. London, Spec. Publ. 44, 275–308.

Crampton, C.B., Carruthers, R.G., Horne, J.S., Peach, B.N., Flett, J.S., 1914. The Geology of Caithness:(Sheets 110 and 116, with Parts of 109, 115, and 117.). HM Stationery Office.

Davies, R., Cloke, I., Cartwright, J., Robinson, A., Ferrero, C., 2004. Post-breakup compression of a passive margin and its impact on hydrocarbon prospectivity: An example from the Tertiary of the Faeroe–Shetland Basin, United Kingdom. Am. Assoc. Pet. Geol. Bull. 88, 1–20.

de Paola, N., Holdsworth, R.E., McCaffrey, K.J.W., 2005. The influence of lithology and pre-existing structures on reservoir-scale faulting patterns in transtensional rift zones. J.

Geol. Soc. London. 162, 471–480. doi:10.1144/0016-764904-043

De Paola, N., Holdsworth, R.E., McCaffrey, K.J.W., Barchi, M.R., 2005. Partitioned transtension: an alternative to basin inversion models. J. Struct. Geol. 27, 607–625. doi:https://doi.org/10.1016/j.jsg.2005.01.006

Dean, K., McLachlan, K., Chambers, A., 1999. Rifting and the development of the Faeroe-Shetland Basin. Geol. Soc. London, Pet. Geol. Conf. Ser. 5, 533–544. doi:10.1144/0050533

Dec, T., 1992. Textural characteristics and interpretation of second-cycle, debris-flow-dominated alluvial fans (Devonian of Northern Scotland). Sediment. Geol. 77, 269–296.

Delvaux, D., Sperner, B., 2003. New aspects of tectonic stress inversion with reference to the TENSOR program. Geol. Soc. London, Spec. Publ. 212, 75–100.

Dewey, J.F., Dalziel, I.W.D., Reavy, R.J., Strachan, R.A., 2015. The Neoproterozoic to Mid-Devonian evolution of Scotland: a review and unresolved issues. Scottish J. Geol. 51, 5–30. doi:10.1144/sjg2014-007

Dewey, J.F., Holdsworth, R.E., Strachan, R.A., 1998. Transpression and transtension zones. Geol. Soc. London, Spec. Publ. 135, 1–14. doi:10.1144/GSL.SP.1998.135.01.01

Dewey, J.F., Strachan, R.A., 2003. Changing Silurian–Devonian relative plate motion in the Caledonides: sinistral transpression to sinistral transtension. J. Geol. Soc. London. 160, 219–229. doi:10.1144/0016-764902-085

Dichiarante, A.M., 2017. A reappraisal and 3D characterisation of fracture systems within the Devonian Orcadian Basin and its underlying basement: an onshore analogue for the Clair Group. PhD Thesis, Durham University.

Dichiarante, A.M., Holdsworth, R.E., Dempsey, E.D., Selby, D., McCaffrey, K.J.W., Michie, U.M., Morgan, G., Bonniface, J., 2016. New structural and Re–Os geochronological evidence constraining the age of faulting and associated mineralization in the Devonian Orcadian Basin, Scotland. J. Geol. Soc. London. 173, 457–473. doi:10.1144/jgs2015-118

Dickinson, W.R., 2006. Geotectonic evolution of the Great Basin. Geosphere 2, 353–368.

Dickinson, W.R., Gehrels, G.E., 2009. Use of U–Pb ages of detrital zircons to infer maximum depositional ages of strata: a test against a Colorado Plateau Mesozoic database. Earth Planet. Sci. Lett. 288, 115–125.

Doblas, M., 1998. Slickenside kinematic indicators. Tectonophysics 295, 187–197.

Dodd, T.J., McCarthy, D.J., Stewart, M.A., 2018. Small-Scale Sandstone Injectites Surrounding Oil-Filled Reservoirs–Examples From the North Falkland Basin, South Atlantic and West of Shetland, UKCS, in: ACE 2018 Annual Convention & Exhibition.

Donato, J.A., Martindale, W., Tully, M.C., 1983. Buried granites within the mid North Sea High. J. Geol. Soc. London. 140, 825–837.

Donovan, R.N., 2002. Cyclicity in the Sarclet Group, a conglomerate/arkose facies in the Lower Devonian [Old Red Sandstone Facies] in Northern Scotland. GSA South Central Regional Meeting.

Donovan, R.N., 1993. Evaporites in the Middle Devonian of the Orcadian basin near Berriedale, Caithness. Scottish J. Geol. 29, 45–54. doi:10.1144/sjg29010045

Donovan, R.N., 1975. Devonian lacustrine limestones at the margin of the Orcadian Basin, Scotland. J. Geol. Soc. London. 131, 489–510.

Donovan, R.N., 1973. Basin margin deposits of the Middle Old Red Sandstone at Dirlot Caithness. Scottish J. Geol. 9, 203–211. doi:10.1144/sjg09030203

Donovan, R.N., Archer, R., Turner, P., Tarling, D.H., 1976. Devonian palaeogeography of the Orcadian Basin and the Great Glen Fault. Nature 259, 550–551.

Donovan, R.N., Collins, A., Rowlands, M.A., Archer, R., 1978. The age of sediments on Foula, Shetland. Scottish J. Geol. 14, 87–88. doi:10.1144/sjg14010087

Downie, R.A., 2009. Devonian. Pet. Geol. North Sea Basic Concepts Recent Adv. Fourth Ed. 85–103.

Draper, S., Adcock, T.A.A., Borthwick, A.G.L., Houlsby, G.T., 2014. Estimate of the tidal stream power resource of the Pentland Firth. Renew. Energy 63, 650–657.

Duindam, P., van Hoorn, B., 1987. Structural evolution of the West Shetland continental margin. Pet. Geol. North West Eur. Proc. 3rd Conf. 2, 765–773.

Easton, M.C., Woolf, D.K., Bowyer, P.A., 2012. The dynamics of an energetic tidal channel, the Pentland Firth, Scotland. Cont. Shelf Res. 48, 50–60.

Eldholm, O., Grue, K., 1994. North Atlantic volcanic margins: dimensions and production rates. J. Geophys. Res. Solid Earth 99, 2955–2968.

Ellis, D., Stoker, M.S., 2014. The Faroe-Shetland Basin: a regional perspective from the Paleocene to the present day and its relationship to the opening of the North Atlantic Ocean. Geol. Soc. London, Spec. Publ. 397, 11–31. doi:10.1144/SP397.1

Enfield, M.A., Coward, M.P., 1987. The Structure of the West Orkney Basin, northern Scotland. J. Geol. Soc. London. 144, 871–884. doi:10.1144/gsjgs.144.6.0871

Evans, D.J., 1997. Estimates of the eroded overburden and the Permian–Quaternay subsidence history of the area west of Orkney. Scottish J. Geol. 33, 169–181. doi:10.1144/sjg33020169

Falt, U., Guerin, G., Retail, P., Evans, M., 1992. Clair Discovery : Evaluation of Natural Fracturation in a Horizontal Well. Eur. Pet. Conf.

Fame, M.L., Spotila, J.A., Owen, L.A., Dortch, J.M., Shuster, D.L., 2018. Spatially heterogeneous post-Caledonian burial and exhumation across the Scottish Highlands. Lithosphere 10, 406–425.

Feng, Q., Wang, S., Gao, G., Li, C., 2010. A new approach to thief zone identification based on interference test. J. Pet. Sci. Eng. 75, 13–18.

Finlay, A.J., Selby, D., Osborne, M.J., 2012. Petroleum source rock identification of United Kingdom Atlantic Margin oil fields and the Western Canadian Oil Sands using Platinum, Palladium, Osmium and Rhenium: Implications for global petroleum systems. Earth Planet. Sci. Lett. 313, 95–104.

Finlay, A.J., Selby, D., Osborne, M.J., 2011. Re-Os geochronology and fingerprinting of United Kingdom Atlantic margin oil: Temporal implications for regional petroleum systems. Geology 39, 475–478.

Finlay, T.M., Woodward, A.S., White, E.I., 1926. The Old Red Sandtsone of Shetland. Part I. South-eastern area. With an account of the fossil fishes of the Old Red Sandstone of the Shetland Islands. Trans. R. Soc. Edinb. Earth Sci. 54, 553–572. doi:10.1017/S0080456800016094

Fletcher, A.E.J., 1977. Investigation on Devonian megaspores. PhD Thesis, University of Bristol.

Fleuty, M.J., 1964. The description of folds. Proc. Geol. Assoc. 75, 461–492.

Flinn, D., 1992. The history of the Walls Boundary fault, Shetland: the northward continuation of the Great Glen fault from Scotland. J. Geol. Soc. London. 149, 721–726. doi:10.1144/gsjgs.149.5.0721

Flinn, D., 1979. The Walls Boundary Fault, Shetland, British Isles. United States Geol. Surv. Open File Rep. 79, 181–200.

Flinn, D., 1977. The erosion history of Shetland: a review. Proc. Geol. Assoc. 88, 129–146. doi:10.1016/S0016-7878(77)80023-0

Flinn, D., Frank, P.L., Brook, M., Pringle, I.R., 1979. Basement-cover relations in Shetland. Geol. Soc. London, Spec. Publ. 8, 109–115. doi:10.1144/GSL.SP.1979.008.01.09

Flinn, D., May, F., Roberts, J.L., Treagus, J.E., 1973. A revision of the stratigraphic succession of the East Mainland of Shetland. Scottish J. Geol. 8, 335–343. doi:10.1144/sjg08040335

Flinn, D., Stone, P., Stephenson, D., 2013. The Dalradian rocks of the Shetland Islands, Scotland. Proc. Geol. Assoc. 124, 393–409.

Fossen, H., 2016. Structural geology. Cambridge University Press.

Fossen, H., 2010. Extensional tectonics in the North Atlantic Caledonides: a regional view. Geol. Soc. London, Spec. Publ. 335, 767 LP – 793.

Fossen, H., Khani, H.F., Faleide, J.I., Ksienzyk, A.K., Dunlap, W.J., 2017. Post-Caledonian extension in the West Norway–northern North Sea region: the role of structural inheritance. Geol. Soc. London, Spec. Publ. 439, 465–486.

Fossen, H., Schultz, R.A., Shipton, Z.K., Mair, K., 2007. Deformation bands in sandstone: a review. J. Geol. Soc. London. 164, 755–769. doi:10.1144/0016-76492006-036

Fossen, H., Soliva, R., Ballas, G., Trzaskos, B., Cavalcante, C., Schultz, R.A., 2018. A review of deformation bands in reservoir sandstones: geometries, mechanisms and distribution. Geol. Soc. London, Spec. Publ. 459, 9 LP – 33.

Fossen, H., Teyssier, C., Whitney, D.L., 2013. Transtensional folding. J. Struct. Geol. 56, 89–102. doi:http://dx.doi.org/10.1016/j.jsg.2013.09.004

Fossen, H., Tikoff, B., 1998. Extended models of transpression and transtension, and application to tectonic settings. Geol. Soc. London, Spec. Publ. 135, 15–33.

Fossen, H., Tikoff, B., Teyssier, C., 1994. Strain modeling of transpressional and transtensional deformation. Nor. Geol. Tidsskr. 74, 134–145.

Friend, C.R.L., Strachan, R.A., Kinny, P.D., 2008. U–Pb zircon dating of basement inliers within the Moine Supergroup, Scottish Caledonides: implications of Archaean protolith ages. J. Geol. Soc. London. 165, 807–815.

Friend, P.F., 1981. Devonian sedimentary basins and deep faults of the northernmost Atlantic borderlands. Geology of the North Atlantic Borderlands. Mem. 7, 149-165

Friend, P.F., Williams, B.P.., Ford, M., Williams, E.A., 2000. Kinematics and dynamics of Old Red Sandstone basins. Geol. Soc. Spec. Publ. 180, 29–60.

Gautier, D.L., Stemmerik, L., Christiansen, F.G., Sørensen, K., Bidstrup, T., Bojesen-Koefoed, J.A., Bird, K.J., Charpentier, R.R., Houseknecht, D.W., Klett, T.R., 2011. Assessment of NE Greenland: Prototype for development of circum-Arctic resource appraisal methodology. Geol. Soc. London, Mem. 35, 663–672.

Getech, 2017. UKCS Multi-Satellite Gravity Data. Oil And Gas Authority Open Data.

Girdler, R.W., 1990. The Dead Sea transform fault system. Tectonophysics 180, 1–13.

Grippa, A., Hurst, A., Palladino, G., Iacopini, D., Lecomte, I., Huuse, M., 2019. Seismic imaging of complex geometry: Forward modeling of sandstone intrusions. Earth Planet. Sci. Lett. 513, 51–63. doi:https://doi.org/10.1016/j.epsl.2019.02.011

Gutmanis, J., Batchelor, T., Cotton, L., Baker, J., 2012. Hydrocarbon production from fractured basement formations.

Hall, A., Bishop, P., 2002. Scotland's denudational history: an integrated view of erosion and sedimentation at an uplifted passive margin. Geol. Soc. London, Spec. Publ. 196, 271–290.

Hall, A.J., Donovan, R.N., 1978. Origin of complex sulphide nodules related to diagenesis of

lacustrine sediments of Middle Devonian age from the Shetland Islands. Scottish J. Geol. 14, 289–299.

Hansom, J.D., 2007. FOULA, in: Coastal Geomorpology of Great Britain. JNCC, pp. 1–5.

Harland, W.B., 1971. Tectonic transpression in caledonian Spitsbergen. Geol. Mag. 108, 27–41.

Hartz, E., 2000. Early syndepositional tectonics of East Greenland's Old Red Sandstone basin. Geol. Soc. London, Spec. Publ. 180, 537–555. doi:10.1144/GSL.SP.2000.180.01.28

Healy, D., Rizzo, R., Duffy, M., Farrell, N.J.C., Hole, M.J., Muirhead, D., 2018. Field evidence for the lateral emplacement of igneous dykes: Implications for 3D mechanical models and the plumbing beneath fissure eruptions. Volcanica.

Hillier, S., Marshall, J.E.A., 1992. Organic maturation, thermal history and hydrocarbon generation in the Orcadian Basin, Scotland. J. Geol. Soc. London. 149, 491–502.

Hippler, S.J., 1993. Deformation microstructures and diagenesis in sandstone adjacent to an extensional fault: implications for the flow and entrapment of hydrocarbons. Am. Assoc. Pet. Geol. Bull. 77, 625–637.

Hippler, S.J., 1989. Fault rock evolution and fluid flow in sedimentary basins. PhD Thesis, University of Leeds.

Hitchen, K., Ritchie, J.D., 1987. Geological review of the West Shetland area, Petroleum Geology of North West Europe.

Hodgetts, D., 2019. Virtual Reality Geological Studio [WWW Document]. URL www.vrgeoscience.com (accessed 8.1.19).

Hodgetts, D., 2013. Laser scanning and digital outcrop geology in the petroleum industry: A review. Mar. Pet. Geol. 46, 335–354. doi:10.1016/j.marpetgeo.2013.02.014

Hodgetts, D., Gawthorpe, R.L., Wilson, P., Rarity, F., 2007. Integrating digital and traditional field techniques using Virtual Reality Geological Studio (VRGS), in: 69th EAGE Conference and Exhibition Incorporating SPE EUROPEC 2007.

Holdsworth, B., McCaffrey, K., Dempsey, E., 2017. Cracked and full of sand: microstructural insights into how oil gets into a crystalline basement reservoir, in: EGU General Assembly Conference Abstracts. p. 2110.

Holdsworth, R.E., Alsop, G.I., Strachan, R.A., 2007. Tectonic stratigraphy and structural continuity of the northernmost Moine Thrust Zone and Moine Nappe, Scottish Caledonides. Geol. Soc. London, Spec. Publ. 272, 121–142.

Holdsworth, R.E., Butler, C.A., Roberts, A.M., 1997. The recognition of reactivation during continental deformation. J. Geol. Soc. London. 154, 73–78. doi:10.1144/gsjgs.154.1.0073

Holdsworth, R.E., Morton, A., Frei, D., Gerdes, A., Strachan, R.A., Dempsey, E., Warren, C., Whitham, A., 2019. The nature and significance of the Faroe-Shetland Terrane: linking Archaean basement blocks across the North Atlantic. Precambrian Res. 321, 154–171.

Holdsworth, R.E., Stewart, M., Imber, J., Strachan, R.A., 2001. The structure and rheological evolution of reactivated continental fault zones: a review and case study. Geol. Soc. Spec. Publ. 184, 115–137.

Holford, S.P., Green, P.F., Hillis, R.R., Underhill, J.R., Stoker, M.S., Duddy, I.R., 2010. Multiple post-Caledonian exhumation episodes across NW Scotland revealed by apatite fission-track analysis. J. Geol. Soc. London. 167, 675 LP – 694. doi:10.1144/0016-76492009-167

Holloway, S., Reay, D.M., Donato, J.A., Beddoe-Stephens, B., 1991. Distribution of granite and possible Devonian sediments in part of the East Shetland Platform, North Sea. J. Geol. Soc. London. 148, 635–638.

House, M.R., 2000. Chronostratigraphic framework for the Devonian and Old Red Sandstone. Geol. Soc. London, Spec. Publ. 180, 23–27.

Jahn, I., Strachan, R.A., Fowler, M., Bruand, E., Kinny, P.D., Clark, C., Taylor, R.J.M., 2017. Evidence from U–Pb zircon geochronology for early Neoproterozoic (Tonian) reworking of an Archaean inlier in northeastern Shetland, Scottish Caledonides. J. Geol. Soc. London. 174, 217–232.

Johnston, S.C., Smith, R.I., Underhill, J.R., 1995. The Clair Discovery, west of the Shetland Isles. Scottish J. Geol. 31, 187–190.

Johnstone, G.S., Mykura, W., 1989. British regional geology: the Northern Highlands of Scotland. HM Stationery Office.

Jones, R.R., McCaffrey, K.J.W., Clegg, P., Wilson, R.W., Holliman, N.S., Holdsworth, R.E., Imber, J., Waggott, S., 2009. Integration of regional to outcrop digital data: 3D visualisation of multi-scale geological models. Comput. Geosci. 35, 4–18.

Jones, R.R., Wawrzyniec, T.F., Holliman, N.S., McCaffrey, K.J.W., Imber, J., Holdsworth, R.E., 2008. Describing the dimensionality of geospatial data in the earth sciences—Recommendations for nomenclature. Geosphere 4, 354–359. doi:10.1130/ges00158.1

Kellock, E., 1969. Alkaline basic igneous rocks in the Orkneys. Scottish J. Geol. 5, 140 LP – 153.

Kinny, P.D., Strachan, R.A., Fowler, M., Clark, C., Davis, S., Jahn, I., Taylor, R.J.M., Holdsworth, R.E., Dempsey, E., 2019. The Neoarchaean Uyea Gneiss Complex, Shetland: an onshore fragment of the Rae Craton on the European Plate. J. Geol. Soc. London. jgs2019-017. doi:10.1144/jgs2019-017

Kocks, H., Strachan, R.A., Evans, J.A., 2006. Heterogeneous reworking of Grampian

metamorphic complexes during Scandian thrusting in the Scottish Caledonides: insights from the structural setting and U–Pb geochronology of the Strath Halladale Granite. J. Geol. Soc. London. 163, 525–538.

Krabbendam, M., Dewey, J.F., 1998. Exhumation of UHP rocks by transtension in the Western Gneiss Region, Scandinavian Caledonides. Geol. Soc. London, Spec. Publ. 135, 159–181. doi:10.1144/GSL.SP.1998.135.01.11

Lague, D., Brodu, N., Leroux, J., 2013. Accurate 3D comparison of complex topography with terrestrial laser scanner: Application to the Rangitikei canyon (N-Z). ISPRS J. Photogramm. Remote Sens. 82, 10–26. doi:10.1016/j.isprsjprs.2013.04.009

Lancaster, P.J., Strachan, R.A., Bullen, D., Fowler, M., Jaramillo, M., Saldarriaga, A.M., 2017. U–Pb zircon geochronology and geodynamic significance of 'Newer Granite'plutons in Shetland, northernmost Scottish Caledonides. J. Geol. Soc. London. 174, 486–497.

Leather, D., 2017. Demarcation of the boundary between Middle Devonian Upper Stromness Flagstone and Rousay Flagstone formations in Westray, Orkney. Scottish J. Geol. 53, 53 LP – 61.

Leeder, M., 1987. Sediment deformation structures and the palaeotectonic analysis of sedimentary basins, with a case-study from the Carboniferous of northern England. Geol. Soc. London, Spec. Publ. 29, 137 LP – 146.

Lundmark, A.M., Augland, L.E., Bjerga, A.D., 2018. Timing of strain partitioning and magmatism in the Scottish Scandian collision, evidence from the high Ba-Sr Orkney granite complex. Scottish J. Geol.

Lundmark, A.M., Gabrielsen, R.H., Flett Brown, J., 2011. Zircon U–Pb age for the Orkney lamprophyre dyke swarm, Scotland, and relations to Permo-Carboniferous magmatism in northwestern Europe. J. Geol. Soc. London. 168, 1233–1236. doi:10.1144/0016-76492011-017

Macintyre, R.M., Cliff, R.A., Chapman, N.A., 1981. Geochronological evidence for phased volcanic activity in Fife and Caithness necks, Scotland. Earth Environ. Sci. Trans. R. Soc. Edinburgh 72, 1–7.

Mackin, J.H., 1950. The down-structure method of viewing geologic maps. J. Geol. 58, 55–72.

Magee, C., Maharaj, S.M., Wrona, T., Jackson, C.A.-L., 2015. Controls on the expression of igneous intrusions in seismic reflection data. Geosphere 11, 1024–1041. doi:10.1130/GES01150.1

Mange, M.A., Morton, A.C., 2007. Chapter 13 Geochemistry of Heavy Minerals, in: Sedimentology, M.A.M. and D.T.W.B.T.-D. in (Ed.), Heavy Minerals in Use. Elsevier, pp. 345–391. doi:http://dx.doi.org/10.1016/S0070-4571(07)58013-1

Mark, D.F., Green, P.F., Parnell, J., Kelley, S.P., Lee, M.R., Sherlock, S.C., 2008. Late

Palaeozoic hydrocarbon migration through the Clair field, West of Shetland, UK Atlantic margin. Geochim. Cosmochim. Acta 72, 2510–2533. doi:10.1016/j.gca.2007.11.037

Marshall, J.E.A., 2000. Devonian (Givetian) miospores from the Walls Group, Shetland. Geol. Soc. London, Spec. Publ. 180, 473–483. doi:10.1144/GSL.SP.2000.180.01.25

Marshall, J.E.A., 1988. Devonian miospores from Papa Stour, Shetland. Trans. R. Soc. Edinb. Earth Sci. 79, 13–18. doi:10.1017/S0263593300014073

Marshall, J.E.A., Brown, J.F., Hindmarsh, S., 1985. Hydrocarbon source rock potential of the Devonian rocks of the Orcadian Basin. Scottish J. Geol. 21, 301–320. doi:10.1144/sjg21030301

Marshall, J.E.A., Hewett, A.J., Evans, D., Graham, C., Armour, A., Bathurst, P., 2003. The Millennium Atlas: Petroleum geology of the central and northern North Sea. Geological Society, London.

Martin-Short, R., Hill, J., Kramer, S.C., Avdis, A., Allison, P.A., Piggott, M.D., 2015. Tidal resource extraction in the Pentland Firth, UK: potential impacts on flow regime and sediment transport in the Inner Sound of Stroma. Renew. Energy 76, 596–607.

McBride, J.H., 1994. Structure of a continental strike-slip fault from deep seismic reflection: Walls Boundary fault, northern British Caledonides. J. Geophys. Res. Solid Earth 99, 23985–24005. doi:10.1029/94JB00902

McBride, J.H., England, R.W., 1994. Deep seismic reflection structure of the Caledonian orogenic front west of Shetland. J. Geol. Soc. London. 151, 9–16. doi:10.1144/gsjgs.151.1.0009

McCaffrey, K.J.W., Hodgetts, D., Howell, J.A., Hunt, D., Imber, J., Jones, R.R., Tomasso, M., Thurmond, J., Viseur, S., 2010. Virtual fieldtrips for petroleum geoscientists. Geol. Soc. London, Pet. Geol. Conf. Ser. 7, 19–26. doi:10.1144/0070019

McCaffrey, K.J.W., Jones, R.R., Holdsworth, R.E., Wilson, R.W., Clegg, P., Imber, J., Trinks, I., 2005. Unlocking the spatial dimension : digital technologies and the future of geoscience fieldwork Unlocking the spatial dimension : digital technologies and the future of geoscience fieldwork. Geol. Soc. London, Spec. Publ. 162, 927–938. doi:10.1144/0016-764905-017

McClay, K.R., Norton, M.G., Coney, P., Davis, G.H., 1986. Collapse of the Caledonian orogen and the Old Red Sandstone. Nature.

McGeary, S., 1989. Reflection seismic evidence for a Moho offset beneath the Walls Boundary strike-slip fault. J. Geol. Soc. London. 146, 261–269. doi:10.1144/gsjgs.146.2.0261

McKay, A.G., 1974. A sub-bottom profiling survey of the St. Magnus Bay deep, Shetland. Scottish J. Geol. 10, 31–34. doi:10.1144/sjg10010031

McKie, T., Garden, I.R., 1996. Hierarchical stratigraphic cycles in the non-marine Clair Group (Devonian) UKCS. High Resolut. Seq. Stratigr. Innov. Appl. 104, 139–157. doi:10.1144/GSL.SP.1996.104.01.10

Melvin, J., 1985. Walls Formation, Western Shetland: distal alluvial plain deposits within a tectonically active Devonian basin. Scottish J. Geol. 21, 23–40. doi:10.1144/sjg21010023

Melvin, J., 1977. Sedimentological studies in upper Palaeozoic sandstones near Bude, Cornwall and Walls, Shetland. PhD Thesis, University of Edinburgh

Mendum, J.R., Noble, S.R., 2010. Mid-Devonian sinistral transpressional movements on the Great Glen Fault: the rise of the Rosemarkie Inlier and the Acadian Event in Scotland. Geol. Soc. London, Spec. Publ. 335, 161–187. doi:10.1144/SP335.8

Midland Valley, 2018. MOVE 2018.1.

Monaghan, A.A., Arsenikos, S., Callaghan, E., Ellen, R., Gent, C., Greenhalgh, E., Hannis, S., Henderson, A., Leslie, G., Johnson, K., 2016. Overview of the 21CXRM Palaeozoic Project: a regional petroleum systems analysis of the offshore Carboniferous and Devonian of the UKCS.

Morton, a., Milne, a., 2012. Heavy mineral stratigraphic analysis on the Clair Field, UK, west of Shetlands: a unique real-time solution for red-bed correlation while drilling. Pet. Geosci. 18, 115–128. doi:10.1144/1354-079311-026.1354-0793/12/

Morton, A., O'B. Knox, R.W., Hallsworth, C., 2002. Correlation of reservoir sandstones using quantitative heavy mineral analysis. Pet. Geosci. 8, 251–262.

Morton, A.C., 2007. The role of heavy mineral analysis as a geosteering tool during drilling of high-angle wells. Dev. Sedimentol. 58, 1123–1142.

Morton, A.C., 1991. Geochemical studies of detrital heavy minerals and their application to provenance research. Geol. Soc. London, Spec. Publ. 57, 31–45.

Morton, A.C., Hallsworth, C., 1994. Identifying provenance-specific features of detrital heavy mineral assemblages in sandstones. Sediment. Geol. 90, 241–256. doi:http://dx.doi.org/10.1016/0037-0738(94)90041-8

Morton, A.C., Hallsworth, C.R., 1999. Processes controlling the composition of heavy mineral assemblages in sandstones. Sediment. Geol. 124, 3–29. doi:http://dx.doi.org/10.1016/S0037-0738(98)00118-3

Myers, K., Rouillard, P., Zanella, E., 2019. Exploration Performance in the UK and Norwegian North Sea. Geol. Soc. London, Spec. Publ. 494, SP494-2018.

Mykura, W., 1972a. The Old Red Sandstone sediments of Fair Isle, Shetland Islands. HM Stationery Office.

Mykura, W., 1972b. Tuffisitic breccias, tuffisites and associated carbonate-sulphide

mineralization in SE Shetland. Bull geol Surv GB 40, 51–82.

Mykura, W., Flinn, D., May, F., 1976a. British regional geology: Orkney and Shetland. H.M.S.O, Edinburgh.

Mykura, W., Harrison, R.K., 1972. Igneous intrusions and mineralization in Fair Isle, Shetland Islands. HM Stationery Office.

Mykura, W., Phemister, J., Sabine, P.A., 1976b. The geology of Western Shetland:(explanation of One-inch Geological Sheet Western Shetland, comprising Sheet 127 and parts of 125, 126 and 128). HMSO Books.

Neilson, J.C., Kokelaar, B.P., Crowley, Q.G., 2009. Timing, relations and cause of plutonic and volcanic activity of the Siluro-Devonian post-collision magmatic episode in the Grampian Terrane, Scotland. J. Geol. Soc. London. 166, 545 LP – 561. doi:10.1144/0016-76492008-069

Nelson, R., 2001. Geologic analysis of naturally fractured reservoirs. Gulf Professional Publishing.

Newman, M.J., Den Blaauwen, J.L., 2018. A redescription of the endemic antiarch placoderm Asterolepis thule from the Middle Devonian (Givetian) of Shetland and its biostratigraphical horizon. Scottish J. Geol. sjg2018-005.

Nichols, G.J., 2005. Sedimentary evolution of the Lower Clair Group, Devonian, west of Shetland: climate and sediment supply controls on fluvial, aeolian and lacustrine deposition, in: Geological Society, London, Petroleum Geology Conference Series. Geological Society of London, pp. 957–967.

Norton, M.G., McClay, K.R., Way, N.A., 1987. Tectonic evolution of Devonian basins in northern Scotland and southern Norway. Nor. Geol. Tidsskr. 67, 323–338.

Novak, A., Egenhoff, S., 2019. Soft-sediment deformation structures as a tool to recognize synsedimentary tectonic activity in the middle member of the Bakken Formation, Williston Basin, North Dakota. Mar. Pet. Geol. 105, 124–140.

Nyberg, B., Nixon, C.W., Sanderson, D.J., 2018. NetworkGT: A GIS tool for geometric and topological analysis of two-dimensional fracture networks. Geosphere.

O'leary, D.W., Friedman, J.D., Pohn, H.A., 1976. Lineament, linear, lineation: some proposed new standards for old terms. Geol. Soc. Am. Bull. 87, 1463–1469.

Ogilvie, S., Barr, D., Roylance, P., Dorling, M., 2015. Structural geology and well planning in the Clair Field. Geol. Soc. London, Spec. Publ. 421, 197–212. doi:10.1144/SP421.7

Oil and Gas Authority, 2019a. Oil and Gas Authority Open Data [WWW Document]. URL http://data.ogauthority.opendata.arcgis.com/

Oil and Gas Authority, 2019b. Relinquishment Reports [WWW Document]. URL https://itportal.ogauthority.co.uk/web_files/relinqs/relinqs.htm (accessed 1.25.19).

Osmundsen, P.T., Andersen, T.B., 2001. The middle Devonian basins of western Norway: sedimentary response to large-scale transtensional tectonics? Tectonophysics 332, 51–68. doi:http://dx.doi.org/10.1016/S0040-1951(00)00249-3

Park, R.G., 2013. Foundation of structural geology. Routledge.

Parnell, J., 1996. Alteration of crystalline basement rocks by hydrocarbon-bearing fluids: Moinian of Ross-shire, Scotland. Lithos 37, 281–292. doi:https://doi.org/10.1016/0024-4937(95)00028-3

Parnell, J., 1985. Hydrocarbon source rocks, reservoir rocks and migration in the Orcadian Basin. Scottish J. Geol. 21, 321–336. doi:10.1144/sjg21030321

Parnell, J., 1983. The Summery volcanic 'Neck', Hoy. Scottish J. Geol. 19, 401–403.

Parnell, J., Bowden, S., 2017. Emplacement and biodegradation of oil in fractured basement: the 'coal'deposit in Moinian gneiss at Castle Leod, Ross-shire. Earth Environ. Sci. Trans. R. Soc. Edinburgh 107, 23–32.

Parnell, J., Bowden, S., Bullock, L., 2017. Geochemistry and origin of organic-rich sediment veins in fractured granitic basement, Helmsdale, Sutherlandshire, UK. Mar. Pet. Geol. 88, 107–114.

Parnell, J., Bowden, S., Mark, D., 2018. Petroleum generation and migration in the Cambro-Ordovician Laurentian margin succession of NW Scotland. J. Geol. Soc. London. 175, 33 LP – 43.

Parnell, J., Carey, P., Monson, B., 1998. Timing and temperature of decollement on hydrocarbon source rock beds in cyclic lacustrine successions. Palaeogeogr. Palaeoclimatol. Palaeoecol. 140, 121–134. doi:https://doi.org/10.1016/S0031-0182(98)00035-2

Parnell, J., Carey, P.F., Green, P., Duncan, W.I., 1999. Hydrocarbon migration history, West of Shetland: integrated fluid inclusion and fission track studies. Pet. Geol. Northwest Eur. Proc. 5th Conf. Pet. Geol. Northwest Eur. 1, 613–626. doi:10.1144/0050613

Parnell, J., Green, P.F., Watt, G., Middleton, D., 2005. Thermal history and oil charge on the UK Atlantic margin. Pet. Geosci. 11, 99–112. doi:10.1144/1354-079304-618

Parnell, J., Rogers, D., Astin, T., Marshall, J., 1994. Devonian Orcadian Basin, northern Scotland, UK. Glob. Geol. Rec. Lake Basins 1, 73–79.

Passchier, C.W., Simpson, C., 1986. Porphyroclast systems as kinematic indicators. J. Struct. Geol. 8, 831–843.

Passchier, C.W., Trouw, R.A., 1996. Microtectonics. Springer.

Patruno, S., Reid, W., 2017. New plays on the greater east Shetland platform (UKCS quadrants 3, 8–9, 14–16)—Part 2: Newly reported Permo-Triassic intra-platform basins and their influence on the Devonian-Paleogene prospectivity of the area. First

Break 35, 59–69.

Patruno, S., Reid, W., Berndt, C., Feuilleaubois, L., 2018. Polyphase tectonic inversion and its role in controlling hydrocarbon prospectivity in the Greater East Shetland Platform and Mid North Sea High, UK. Geol. Soc. London, Spec. Publ. 471.

Pay, M.D., Astin, T.R., Parker, a., 2000. Clay mineral distribution in the Devonian-Carboniferous sandstones of the Clair Field, west of Shetland, and its significance for reservoir quality. Clay Miner. 35, 151–151. doi:10.1180/000985500546549

Petr, T., 1992. Lake Balkhash, Kazakhstan. Int. J. Salt Lake Res. 1, 21–46.

Piazolo, S., Passchier, C.W., 2002. Controls on lineation development in low to medium grade shear zones: a study from the Cap de Creus peninsula, NE Spain. J. Struct. Geol. 24, 25–44.

Pless, J.C., 2012. Characterising fractured basement using the Lewisian Gneiss Complex, NW Scotland: Implications for fracture systems in the Clair Field basement.PhD Thesis, Durham University.

Prave, A.R., 1999. The Neoproterozoic Dalradian Supergroup of Scotland: an alternative hypothesis. Geol. Mag. 136, 609–617.

Pringle, J.K., Clark, J.D., Westerman, A.R., Stanbrook, D.A., Gardiner, A.R., Morgan, B.E.F., 2001. Virtual outcrops: 3-D reservoir analogues. J. Virtual Explor. 4. doi:10.3809/jvirtex.2001.00036

Rabbel, O., Galland, O., Mair, K., Lecomte, I., Senger, K., Spacapan, J.B., Manceda, R., 2018. From field analogues to realistic seismic modelling: a case study of an oil-producing andesitic sill complex in the Neuquén Basin, Argentina. J. Geol. Soc. London. 175, 580–593.

Ragan, D.M., 2009. Structural geology: an introduction to geometrical techniques. Cambridge University Press.

Ramsay, J.G., 1967. Folding and fracturing of rocks. Mc Graw Hill B. Co. 568.

Ramsay, J.G., Huber, M.I., 1987. The techniques of modern structural geology: Folds and fractures. Academic press.

Rawnsley, K., Wei, L., 2001. Evaluation of a New Method to Build Geological Models of Fractured Reservoirs Calibrated to Production Data. Pet. Geosci. 7, 23–33. doi:10.1144/petgeo.7.1.23

Reading, H.G., 1980. Characteristics and recognition of strike-slip fault systems. Sedimentation in Oblique Slip Mobile Zones. 4, 7–26.

Rebesco, M., Hernández-Molina, F.J., Van Rooij, D., Wåhlin, A., 2014. Contourites and associated sediments controlled by deep-water circulation processes: State-of-the-art and future considerations. Mar. Geol. 352, 111–154.

doi:https://doi.org/10.1016/j.margeo.2014.03.011

Reches, Z., Dieterich, J.H., 1983. Faulting of rocks in three-dimensional strain fields I. Failure of rocks in polyaxial, servo-control experiments. Tectonophysics 95, 111–132.

Reynolds, A.D., 2017. Paralic reservoirs. Geol. Soc. London, Spec. Publ. 444, 7–34.

Richards, P.C., 1990. Devonian. Introd. to Pet. Geol. North Sea. Blackwell, Oxford 78–89.

Ritchie, J.D., Hitchen, K., 1993. Discussion on the location and history of the Walls Boundary fault and Moine thrust north and south of Shetland. J. Geol. Soc. London. 150, 1003–1008. doi:10.1144/gsjgs.150.5.1003

Ritchie, J.D., Hitchen, K., Mitchell, J.G., 1987a. The offshore continuation of the Moine Thrust north of Shetland as deduced from basement isotopic ages. Scottish J. Geol. 23, 163–173. doi:10.1144/sjg23020163

Ritchie, J.D., Hitchen, K., Mitchell, J.G., 1987b. The offshore continuation of the Moine Thrust north of Shetland as deduced from basement isotopic ages. Scottish J. Geol. 23, 163–173.

Ritchie, J.D., Ziska, H., Johnson, H., Evans, D., 2011. Geology of the Faroe-Shetland Basin and adjacent areas. British Geological Survey, 317pp. (RR/11/001).

Roberts, A.M., Badley, M.E., Price, J.D., Huck, I.W., 1990. The structural history of a transtensional basin: Inner Moray Firth, NE Scotland. J. Geol. Soc. London. 147, 87–103. doi:10.1144/gsjgs.147.1.0087

Roberts, A.M., Holdsworth, R.E., 1999. Linking onshore and offshire structures: Mesozoic extension in the Scottish Highlands J. Geol. Soc. London. 156, 1061–1064.

Robertson, A.., Ball, M., Costaschuk, J., Davidson, J., Guliyev, N., Kennedy, B., Leighton, C., Nash, T., Nicholson, H., 2020. The Clair Field, A Giant Hydrocarbon Accumulation (Blocks 206/7a, 206/8, 206/9a, 206/12a and 206/13a) in prep. Geol. Soc. London, Mem.

Rock, N.M.S., 1983. The Permo-Carboniferous camptonite-monchiquite dyke-suite of the Scottish Highlands and Islands: distribution, field and petrological aspects. Rep. Inst. Geol. Sci.

Rodgers, D.A., 1980. Analysis of pull-apart basin development produced by en echelon strike-slip faults. Sediment. Obliq. Mob. Zo. 4, 27–41.

Rogers, D.A., Marshall, J.E.A., Astin, T.R., 1989. Short Paper: Devonian and later movements on the Great Glen fault system, Scotland. J. Geol. Soc. London. 146, 369–372. doi:10.1144/gsjgs.146.3.0369

Rønningen, A., 2015. The first attempt to correlate the migrated bitumen from the Helgeland Basin cores to Devonian source rocks and oils from the UK Orcadian Basin-Is there a Devonian Orcadian type basin offshore Norway.

Sanderson, D.J., Nixon, C.W., 2015. The use of topology in fracture network characterization. J. Struct. Geol. 72, 55–66. doi:http://dx.doi.org/10.1016/j.jsg.2015.01.005

Sasnowski, A., 2015. Palaeogeographic implications of heavy mineral and detrital zircon provenance of Devonian-Carboniferous sedimentary rocks in the North Atlantic region. PhD Thesis, Royal Holloway University of London

Schmidt, a. S., Morton, a. C., Nichols, G.J., Fanning, C.M., 2012. Interplay of proximal and distal sources in Devonian-Carboniferous sandstones of the Clair Basin, west of Shetland, revealed by detrital zircon U-Pb ages. J. Geol. Soc. London. 169, 691–702. doi:10.1144/jgs2011-148

Schmidt, A.S., Morton, A.C., Nichols, G.J., Fanning, C.M., 2012. Interplay of proximal and distal sources in Devonian–Carboniferous sandstones of the Clair Basin, west of Shetland, revealed by detrital zircon U–Pb ages. J. Geol. Soc. London. 169, 691–702.

Schöpfer, K., Hinsch, R., 2019. Late palaeozoic–Mesozoic tectonostratigraphic development of the eastern Faroe-Shetland Basin: New insights from high-resolution 3D seismic and well data. Mar. Pet. Geol.

Schultz, R.A., Fossen, H., 2008. Terminology for structural discontinuities. Am. Assoc. Pet. Geol. Bull. 92, 853–867.

Searle, M., Cornish, S.B., Heard, A., Charles, J.-H., Branch, J., 2019. Structure of the Northern Moine thrust zone, Loch Eriboll, Scottish Caledonides. Tectonophysics 752, 35–51.

Séguret, M., Séranne, M., Chauvet, A., Brunel, A., 1989. Collapse basin: A new type of extensional sedimentary basin from the Devonian of Norway. Geol. 17, 127–130. doi:10.1130/0091-7613

Seranne, M., 1992. Devonian extensional tectonics versus Carboniferous inversion in the northern Orcadian basin. J. Geol. Soc. London. 149, 27–37. doi:10.1144/gsjgs.149.1.0027

Seranne, Michel, 1992. Late Palaeozoic kinematics of the Møre-Trøndelag Fault Zone and adjacent areas, central Norway. Nor. Geol. Tidsskr. 72, 141–158.

Seranne, M., Chauvet, A., Faure, J.L., 1991. Kinematics of the late-orogenic extensional collapse (devonian) in the scandinavian and british caledonides. COMPTES RENDUS L Acad. DES Sci. Ser. II 313, 1305–1312.

Seranne, M., Seguret, M., 1987. The Devonian basins of western Norway: tectonics and kinematics of an extending crust. Geol. Soc. London, Spec. Publ. 28, 537–548.

Shields, M.A., Dillon, L.J., Woolf, D.K., Ford, A.T., 2009. Strategic priorities for assessing ecological impacts of marine renewable energy devices in the Pentland Firth (Scotland, UK). Mar. Policy 33, 635–642. doi:https://doi.org/10.1016/j.marpol.2008.12.013

Sibson, R.H., 1977. Fault rocks and fault mechanisms. J. Geol. Soc. London. 133, 191–213.

Sircar, A., 2004. Hydrocarbon production from fractured basement formations. Curr. Sci. 87, 147–151.

Smalley, A., 2011. Fluvial Paleotransport Derived From Trough Cross-Bedding: Example From the Lower Clair Group, West of Shetland, Using Oriented Whole-Core Images, in: Davidson, S.K., Leleu, S., North, C.P. (Eds.), From River to Rock Record: The Preservation of Fluvial Sediments and Their Subsequent Interpretation. SEPM Society for Sedimentary Geology.

Snyder, D.B., 1990. The Moine Thrust in the BIRPS data set. J. Geol. Soc. London. 147, 81–86. doi:10.1144/gsjgs.147.1.0081

Spence, G.H., Couples, G.D., Bevan, T.G., Aguilera, R., Cosgrove, J.W., Daniel, J.-M., Redfern, J., 2014. Advances in the study of naturally fractured hydrocarbon reservoirs: a broad integrated interdisciplinary applied topic. Geol. Soc. London, Spec. Publ. 374, 1–22. doi:10.1144/SP374.19

Steel, R., Gloppen, T.G., 1980. Late Caledonian (Devonian) basin formation, western Norway: signs of strike-slip tectonics during infilling. Sediment. Obliq. Mob. Zo. 79–103.

Stephenson, D., 1972. Middle Old Red Sandstone alluvial fan and talus deposits at Foyers, Inverness-shire. Scottish J. Geol. 8, 121–127.

Stevens, V., 1991. The Beatrice Field, Block 11/30a, UK North Sea. Geol. Soc. London, Mem. 14, 245–252.

Stoker, M.S., 1982. Old Red Sandstone sedimentation and deformation in the Great Glen Fault Zone, NW of Loch Linnhe. Scottish J. Geol. 18, 147–156. doi:10.1144/sjg18020147

Stoker, M.S., Hitchen, K., Graham, C.C., 1993. The geology of the Hebrides and West Shetland shelves, and adjacent deep-water areas. The Stationery Office/Tso.

Stoker, M.S., Stewart, M.A., Shannon, P.M., Bjerager, M., Nielsen, T., Blischke, A., Hjelstuen, B.O., Gaina, C., McDermott, K., Ólavsdóttir, J., 2016. An overview of the Upper Palaeozoic–Mesozoic stratigraphy of the NE Atlantic region. Geol. Soc. London, Spec. Publ. 447, SP447-2.

Stow, D.A. V, Faugères, J.-C., Howe, J.A., Pudsey, C.J., Viana, A.R., 2002. Bottom currents, contourites and deep-sea sediment drifts: current state-of-the-art. Geol. Soc. London, Mem. 22, 7–20.

Strachan, R.A., 2003. The metamorphic basement geology of Mainland Orkney and Graemsay. Scottish J. Geol. 39, 145–149.

Strachan, Robin A, Alsop, G.I., Friend, C., Miller, S., 2010. An excursion guide to the Moine geology of the Northern Highlands of Scotland. NMSE-Publishing Ltd. Edinburgh.

Strachan, R A, Holdsworth, R.E., Krabbendam, M., Alsop, G.I., 2010. The Moine Supergroup of NW Scotland: insights into the analysis of polyorogenic supracrustal sequences. Geol. Soc. London, Spec. Publ. 335, 233–254.

Strachan, R.A., Prave, A.R., Kirkland, C.L., Storey, C.D., 2013. U–Pb detrital zircon geochronology of the Dalradian Supergroup, Shetland Islands, Scotland: implications for regional correlations and Neoproterozoic–Palaeozoic basin development. J. Geol. Soc. London. 170, 905 LP – 916.

Surdam, R.C., Wolfbaeur, C.A., 1975. Green River Formation, Wyoming: A Playa-Lake Complex. GSA Bull. 86, 335–345.

Svebo, J.R., 2018. High precision U/Pb dating of the Hoy Volcanic Member and its implications. MSc Thesis, University of Oslo

Tang, L., Jones, S.J., Gluyas, J., 2017. Facies architecture of the Fluvial-Aeolian Buchan formation (Upper Devonian) and its implications on field exploration: a case study from Ardmore Field, Central North Sea, UK. Int. J. Geosci. 8, 902–924.

Tavani, S., Granado, P., Corradetti, A., Girundo, M., Iannace, A., Arbués, P., Muñoz, J.A., Mazzoli, S., 2014. Building a virtual outcrop, extracting geological information from it, and sharing the results in Google Earth via OpenPlot and Photoscan: An example from the Khaviz Anticline (Iran). Comput. Geosci. 63, 44–53. doi:10.1016/j.cageo.2013.10.013

Templeton, J.A., 2015. Structural evolution of the Hornelen Basin (Devonian, Norway) from detrital thermochronology. PhD Thesis, Columbia University.

Thomson, K., Underhill, J.R., Green, P.F., Bray, R.J., Gibson, H.J., 1999. Evidence from apatite fission track analysis for the post-Devonian burial and exhumation history of the northern Highlands, Scotland. Mar. Pet. Geol. 16, 27–39.

Tikoff, B., Fossen, H., 1999. Three-dimensional reference deformations and strain facies. J. Struct. Geol. 21, 1497–1512.

Townsend, C., Firth, I.R., Westerman, R., Kirkevollen, L., Hårde, M., Andersen, T., 1998. Small seismic-scale fault identification and mapping. Geol. Soc. London, Spec. Publ. 147, 1 LP – 25. doi:10.1144/GSL.SP.1998.147.01.02

Trewin, N.H., Hurst, A., 2009. Excursion guide to the geology of East Sutherland and Caithness. Dunedin Academic Press Ltd.

Trewin, N.H., Thirlwall, M.F., 2002. Old Red Sandstone, in: The Geology of Scotland 4th Edition (Ed. Trewin, NH). The Geological Society.

Twiss, R.J., Moores, E.M., 1992. Structural geology. Macmillan Publishers.

Ullman, S., 1979. The Interpretation of Structure from Motion. Proc. R. Soc. London B Biol. Sci. 203, 405–426. doi:10.1098/rspb.1979.0006

Underhill, J.R., Brodie, J.A., 1993. Structural geology of Easter Ross, Scotland: implications for movement on the Great Glen fault zone. J. Geol. Soc. London. 150, 515–527.

Venkat-Ramani, M., Tikoff, B., 2002. Physical models of transtensional folding. Geol. 30, 523–526. doi:10.1130/0091-7613(2002)030<0523:PMOTF>2.0.CO;2

Viana, A.R., Almeida, W., Nunes, M.C. V, Bulhões, E.M., 2007. The economic importance of contourites. Geol. Soc. London, Spec. Publ. 276, 1–23.

Waldron, J.W.F., 2005. Extensional fault arrays in strike-slip and transtension. J. Struct. Geol. 27, 23–34. doi:http://dx.doi.org/10.1016/j.jsg.2004.06.015

Walker, S., Thirlwall, M.F., Strachan, R.A., Bird, A.F., 2016. Evidence from Rb–Sr mineral ages for multiple orogenic events in the Caledonides of Shetland, Scotland. J. Geol. Soc. 173, 489–503. doi:10.1144/jgs2015-034

Wallace, R.E., 1951. Geometry of shearing stress and relation to faulting. J. Geol. 59, 118–130.

Wang, Q.M., Nishidai, T., Coward, M.P., 1992. The Tarim Basin, NW China: formation and aspects of petroleum geology. J. Pet. Geol. 15, 5–34.

Watts, L.M., 2001. The walls boundary fault zone and the Møre Trøndelag fault complex:: a case study of two reactivated fault zones. PhD Thesis, Durham University.

Watts, L.M., Holdsworth, R.E., Sleight, J. a., Strachan, R. a., Smith, S. a. F., 2007. The movement history and fault rock evolution of a reactivated crustal-scale strike-slip fault: the Walls Boundary Fault Zone, Shetland. J. Geol. Soc. London. 164, 1037–1058. doi:10.1144/0016-76492006-156

Webster, M., 2018. Clair Phase 1: The Evolving Development of a Complex Fractured Field, in: Abu Dhabi International Petroleum Exhibition & Conference. Society of Petroleum Engineers.

Wellman, C.H., 2014. Spore assemblages from the Lower Devonian 'Lower Old Red Sandstone'deposits of the Northern Highlands of Scotland: the Berriedale Outlier. Earth Environ. Sci. Trans. R. Soc. Edinburgh 105, 227–238.

Westoby, M.J., Brasington, J., Glasser, N.F., Hambrey, M.J., Reynolds, J.M., 2012. "Structure-from-Motion" photogrammetry: A low-cost, effective tool for geoscience applications. Geomorphology 179, 300–314. doi:10.1016/j.geomorph.2012.08.021

Wilkinson, M., 2017. Cenozoic erosion of the Scottish Highlands–Orkney–Shetland area: implications for uplift and previous sediment cover. J. Geol. Soc. 174, 209–216. doi:10.1144/jgs2016-064

Wilson, G.., Knox, J., 1936. The Geology of the Orkney and Shetland Islands. Proc. Geol. Soc. London 47, 270–282. doi:10.1016/S0016-7878(36)80015-7

Wilson, R.W., 2006. Digital fault mapping and spatial attribute analysis of basement-

influenced oblique extension in Passive margin settings. PhD Thesis, Durham University.

Wilson, R.W., Holdsworth, R.E., Wild, L.E., Mccaffrey, K.J.W., England, R.W., Imber, J., Strachan, R. a., 2010. Basement-influenced rifting and basin development: a reappraisal of post-Caledonian faulting patterns from the North Coast Transfer Zone, Scotland. Geol. Soc. London, Spec. Publ. 335, 795–826. doi:10.1144/SP335.32

Wilson, C.D. V, 1965. A marine magnetic survey near Lerwick, Shetland Isles. Scottish J. Geol. 1, 225–230. doi:10.1144/sjg01030225

Witt, A.J., Fowler, S.R., Kjelstadli, R.M., Draper, L.F., Barr, D., McGarrity, J.P., 2010. Managing the start-up of a fractured oil reservoir: development of the Clair field, West of Shetland. Pet. Geol. From Matur. Basins to New Front. 7th Pet. Geol. Conf. 7, 299–313. doi:10.1144/0070299

Woodcock, N.H., Mort, K., 2008. Classification of fault breccias and related fault rocks. Geol. Mag. 145, 435–440.

Wooldridge, L.J., Worden, R.H., Griffiths, J., Utley, J.E.P., 2019. Clay-coat diversity in marginal marine sediments. Sedimentology 66, 1118–1138. doi:10.1111/sed.12538

Wu, J.E., McClay, K., Whitehouse, P., Dooley, T., 2009. 4D analogue modelling of transtensional pull-apart basins. Mar. Pet. Geol. 26, 1608–1623. doi:https://doi.org/10.1016/j.marpetgeo.2008.06.007

Wylde, J.J., Williams, G.D.M., Cousins, R., 2005. Unlocking The Potential: A North Sea Heavy Oil Success Story. doi:10.2118/97772-MS

Ziegler, P.A., 1988. Evolution of the Arctic-North Atlantic and the Western Tethys: A visual presentation of a series of Paleogeographic-Paleotectonic maps. AAPG Mem. 43, 164–196.

Appendix A

Appendix A1 (PETEX/NERC Poster)

A reservoir-scale structural reappraisal of onshore Devonian analogues of the Clair Group in the Fair Isle-Shetland Region

Thomas A. G. Utley[1], Robert E. Holdsworth[1], Ken J. W. McCaffrey[1], Edward D.Dempsey[1], Robert A. Strachan[2] and Richard R. Jones[3].

thomas.a.utley@durham.ac.uk [1]Department of Earth Sciences, Durham University, Science Labs, Durham, DH1 3LE, UK.
[2]School of Earth and Environmental Sciences, Burnaby Building, Burnaby Road, University of Portsmouth PO1 3QL.
[3]Geospatial Research Limited, Durham University, Science Labs, Durham, DH1 3LE, UK.

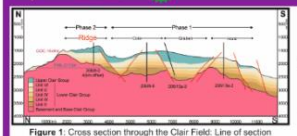

Figure 1: Cross section through the Clair Field: Line of section indicated in Fig.3B (*After* Barr *et al.*, 2007 and Ogilvie *et al.*, 2015).

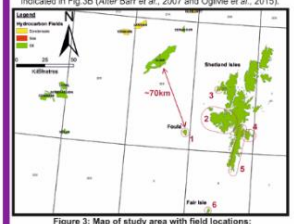

Figure 3: Map of study area with field locations:
1. Foula. 2. Walls Peninsula. 3. Esha ness. 4.Bressay. 5. Southern Shetland. 6. Fair Isle (OGA, 2016).

Project overview:

- The Clair Field, situated to the west of Shetland is comprised of fractured Devonian-Carboniferous sandstones that overlie an up-faulted ridge of fractured Precambrian metamorphic basement (Fig.1).
- The Orcadian Basin has long been used as the classic analogue for the Clair Field (Fig.2), but alternatives exist in Shetland.
- Chosen study area, specifically Foula is the geographically closest onshore analogue (Fig.3), but is relatively poorly studied despite its proximity.

Project aims:

- Produce a new structural and stratigraphic study and model of an alternative onshore analogue in the region closest to the Clair oil field.
- Analyse and study the structural characteristics of faults/fractures and the basement/cover relationships seen throughout the study area.
- Evaluate the role that strike-slip tectonics may have had in the development of the Clair field.
- Production of 3D models of the structure and stratigraphy for use in up-scaling and numerical simulations of fluid flow.
- Comparison to current knowledge/models of Clair, and the regional tectonic setting.

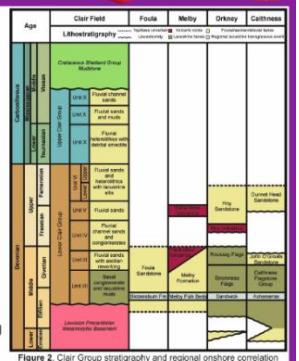

Figure 2. Clair Group stratigraphy and regional onshore correlation with analogue areas. *After* Barr *et al.*, (2007), Johnston, (1995) and Stoker et al., (1993).

The structural geology of Foula, Shetland: an onshore analogue for the top of the Clair Ridge, west of Shetland:

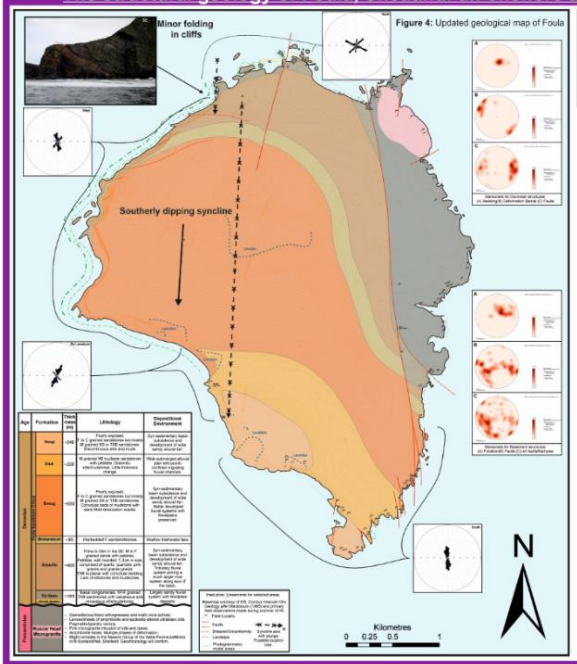

Figure 4: Updated geological map of Foula

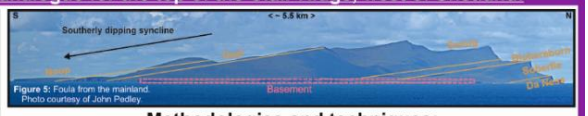

Figure 5: Foula from the mainland. Photo courtesy of John Pedley.

Methodologies and techniques:

- Desk studies and collation of remotely sensed data and literature.
- Photogeology and lineament analysis(Fig. 4 *inset* and Fig.6).
- Primary field observations(Fig.4), data collection and field photography (Fig.5).
- Sampling of fault rocks and basement for dating.
- Photogrammetric reconstruction using(*SfM*) Structure from Motion of archive imagery (Fig.7,8)and images taken in the field.
- Virtual Outrop Model (*VOM*) generation and structural analysis (Fig.7) with the Virtual Reality Geological Studio (VRGS) software package.
- Fracture network characterisation and topology analysis.

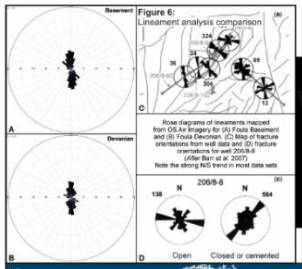

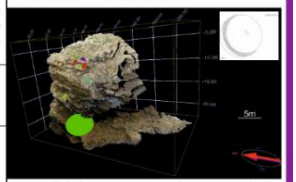

Figure 7 (Above): Point cloud model in VRGS. Da Rippack Stack, Foula. Bedding (green discs), and fractures (red/blue) are exported for analysis. *Inset*, stereonet of bedding measurements.

Figure 8: Low resolution point cloud of Da Kame, Foula. Photos courtesy of BP.

Summary:

- Foula is comprised of ~1600m of gently folded, southerly dipping Middle Devonian clastic sediments unconformably and faulted against a ~1km wide strip of Precambrian metamophic basement.
- Sediments accumulated in a N/S to NE/SW half graben.
- Main structures are N/S dip slip to dextral oblique slip normal faults, and NE/SE to E/W mostly dextral strike-slip faults and discrete fracture corridors with limited offset.
- Folding and faulting is possibly related to Variscan dextral reactivation of pre-existing structures.
- The age and kinematics of folding and faulting not yet clear but further work will establish the relationship between them.
- Structures observed in the Devonian show some similarities to those reported from the Clair Field (see Barr *et al.*, 2007 and Coney *et al.*).

Future work:

- This poster represents *Research In Progress*. Future work will include:
- Fault rock analysis and fracture network modeling.
- Examine related offshore cores and characterise fracture networks.
- Analyse data collected in Shetland, dating of mineralisation and provenace work.
- Reprocessing/reinterpretation of nearby seismic (Fig.9).
- Topological analysis of outcrops, VOMs and lineament analyses to assess connectivity and permeability of fracture networks at multiple scales.
- Fieldwork, data collection and drone work during the summer of 2017.

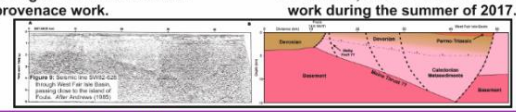

Figure 9: Seismic line SW92-628 through West Fair Isle Basin, passing close to the island of Foula. After Andrews (1985).

References:

Andrews, I., 1985. The Deep Structure of the Stroma Trough (Short Communication). Scottish Journal of Geology, 21(2), pp.213-217.

Barr, D. et al., 2007. Pre-development fracture modelling in the Clair field, west of Shetland. Geological Society, London, Special Publications, 270(1), pp.209-225.

Blackbourn, G.A. 1995. The Geology of Foula, Shetland. Geological Field Guide to Foula, Shetland. BIRAX, Glasgow.

Coney, D. et al., 1995. Clair appraisal: a regional structural framework. Geological Society, London, Petroleum Geology Conference series, 4, pp.1409-1420.

Dichiarante, A.M. et al., 2016. Near-structure and Rietz geochronological evidence constraining the age of faulting and associated mineralisation in the Devonian Orcadian Basin, Scotland. Journal of the Geological Society, 173(3), pp.457473.

Johnston, R.C., 1995. Field Guide to Foula and Mainly with Analogues for the Clair Field.

Mykura, W., Flinn, D. & May, F., 1976. British regional geology: Orkney and Shetland. Stationery Office Books (TSO).

Ogilvie, S. et al., 2015. Structural geology and well planning in the Clair Field. Geological Society, London, Special Publications, 421(1), pp.SP421-13.

Stoker, M.S., Hitchen, K. & Graham, C.C., 1993. The geology of the Hebrides and West Shetland shelves, and adjacent deep-water areas. The Stationery Office/TSO.

Tavani, S. et al., 2014. Building a virtual outcrop, extracting geological information from it, and sharing the results in Google Earth via OpenPlot and Photoscan: An example from the Khaviz Anticline (Iran). Computers & Geosciences, 63(Dekker), pp.44-53.

Will, A.J. et al., 2010. Managing the start-up of a fractured oil reservoir: development of the Clair field, West of Shetland. Petroleum Geology: From Mature Basins to New Frontiers. Proceedings of the 7th Petroleum Geology Conference, 7, pp.1295-1311.

Acknowledgments:

Jim Henderson for assistance in the field and with logistics whilst in Shetland.
Calum Fraser (www.instagram.com/calimists) for capturing drone imagery.
Jim and Richard Scott and the crew of *Lil Jill* for the use of the boat.
Magnus Holbourn and the residents of Foula.

Graham Blackbourn for permission to use information from his unpublished report on the geology of Foula.

Photogrammetric point clouds generated using Agisoft Photoscan and interpreted using the Virtual Reality Geological Studio, courtesy of David Hodgetts, Manchester University.

BP for providing imagery and the Clair JVG for continued interest into research at Durham.

Foula photo reproduced from John Pedley. pangholes.co.uk

Offshore shapefiles from Oil and Gas Authority. Open Data (OGA), 2016.

Durham University

Centre for Doctoral Training (CDT) in Oil and Gas

NERC SCIENCE OF THE ENVIRONMENT

Appendix A1 cont. (PETEX Poster Abstract)

A reservoir-scale structural reappraisal of onshore Devonian analogues of the Clair Group in the Fair Isle-Shetland region.

Thomas A. G. Utley[1], Robert E. Holdsworth[1], Ken J. W. McCaffrey[1], Robert A. Strachan[2] Richard R. Jones[3] and Andy Conway[4].

[1]Department of Earth Sciences, Durham University, Science Labs, Durham, DH1 3LE, UK

[2]School of Earth and Environmental Sciences, Burnaby Building, Burnaby Road, University of Portsmouth, PO1 3QL

[3]Geospatial Research Limited, Durham University, Science Labs, Durham, DH1 3LE, UK

[4]Conoco Phillips (UK) Limited, Aberdeen, AB15 6FZ

Abstract:

The Clair Field, situated to the west of Shetland, represents the largest hydrocarbon resource in the UKCS and is comprised of fractured Devonian-Carboniferous sandstones that overlie an up-faulted ridge of fractured Precambrian metamorphic basement. The onshore, broadly extensional Orcadian Basin has long been used as an analogue for the Clair Field, but it is possible that it formed in a rather different tectonic setting, as it lies in a separate basin to the west with some significant differences. In particular, some of the known complexity in the sub-surface structures, and basement-cover relationships may suggest that strike-slip tectonics played a role in the evolution of the Clair Basin during the Devonian-Carboniferous period. The project will reappraise the stratigraphy, structure and tectonic evolution of an alternative onshore analogue to Clair, using the Devonian basins/sub-basins of Fair Isle-Shetland-Foula region as an analogue for the Palaeozoic tectonics during basin development and later Mesozoic reactivation. This will be achieved through detailed studies of exposed basement-cover contacts and the structure of the overlying sandstone-dominated sequences exposed in large coastal sections.

Fieldwork data will be presented, focusing on the geology and structures of Foula, the Walls Peninsula, Lerwick and Sumburgh with detailed mapping of key localities in the Devonian sequences and associated basement.

Fieldwork will be supplemented by the use of photogrammetry and terrestrial LiDAR to capture the geology of key localities and allow for analysis of structures in difficult to access areas. 3D models of the stratigraphy and structure will be created for use in numerical simulations of fluid flow, modelling of fracture networks, up-scaling and reservoir quality studies. Sampling for heavy mineral analysis will also be carried out in order to determine the provenance and age of the Devonian sequences of Foula and Shetland. All these findings will be compared to previous analogue studies and applied to the current information and models which concern the stratigraphic and structural architecture of the Clair field and its regional tectonic setting.

Appendix A2 (PETEX Presentation Abstract)

Brent Group Petrography and Diagenesis: Implications for Reservoir Quality and Enhanced Oil Recovery

Thomas A. G. Utley[1, 2] and Richard H. Worden[1]

[1]*School of Environmental Sciences, University of Liverpool, Liverpool L69 3GP, UK*

[2] *(Present Address) Department of Earth Sciences, Durham University, Science Labs, Durham, DH1 3LE, UK*

Abstract:

Despite many decades of exploration and oil production there has been no regional assessment of detrital and diagenetic mineralogy and the controls on reservoir quality of the prolific Middle Jurassic Brent Group, Viking Graben, UK. Here we have integrated, evaluated and synthesised a combination of proprietary and publically-available core analysis data and petrographic mineralogical data from the Brent Group. The aim to better understand the regional mineral and petrographic properties of the Brent reservoir units, the distribution of detrital and diagenetic minerals, and how these influence reservoir quality and options for enhanced and improved oil recovery.

Despite the Brent Group being the focus of many studies into sandstone diagenesis in the 80's and 90's, there have been no published reviews of the regional patterns of diagenesis. Furthermore, little effort has been made to develop an overview of how the Brent Group changes both spatially and with depth across the Viking Graben. Using data supplied by four industry partners, together with published data, a data set of over 2500 samples was collated from 169 different wells, representing 27 different fields that are producing or have produced oil from Brent Group reservoirs over the last 40 years. This data set, the largest produced on the Brent, has allowed us to generate and analyse maps of the distribution of the diagenetic minerals that control reservoir quality (quartz, calcite, illite, kaolinite, siderite, etc). We have also compared cement abundances in the various Brent Group formations and examined the effects of depth of burial and different fluid type on cement abundance patterns.

A greater understanding of how the Brent Group varies, spatially, with depth, and between formations, will help in the management of Northern North Sea assets, and in any potential exploration on deeper or satellite structures in the area. A regional understanding of Brent mineralogy will help in appraising the possible effectiveness of EOR approaches such as low salinity water injection. With a drive to reduce costs and maximise economic recovery from the UK Continental Shelf, the encouragement of operators to share information with one another and work more closely with academia, together with the re-examining of legacy data may be the key to future success both in this basin and elsewhere.

Appendix A3 (TSG Presentation Abstract)

The structural geology of Foula, Shetland: an onshore analogue for the top of the Clair Ridge, west of Shetland.

Thomas A. G. Utley1, Robert E. Holdsworth1, Ken J. W. McCaffrey1, Edward D. Dempsey1, Robert A. Strachan2, Richard R. Jones3 and Graham A. Blackbourn4.

[1]Department of Earth Sciences, Durham University, Science Labs, Durham, DH1 3LE, UK

[2]School of Earth and Environmental Sciences, Burnaby Building, Burnaby Road, University of Portsmouth, PO1 3QL, UK

[3]Geospatial Research Limited, Durham University, Science Labs, Durham, DH1 3LE, UK

[4]Blackbourn Geoconsulting, 26 East Pier Street, Bo'ness, West Lothian, EH51 9AB, UK

Abstract:

The Clair Field, situated to the west of Shetland, represents the largest hydrocarbon resource in the UKCS and Europe. It is comprised of fractured Devonian-Carboniferous sandstones that overlie an up-faulted ridge of fractured Precambrian metamorphic basement. The onshore, broadly extensional Orcadian Basin has long been used as an analogue for the Clair Field but it is possible that it formed in a somewhat different tectonic setting, as it lies in a separate basin to the west. On Shetland, evidence of abundant strike-slip events is preserved in both the basement and Devonian-age cover sequences and associated igneous rocks. Indeed, some of the known complexity in the sub-surface structures, and basement-cover relationships can be attributed to deformation associated with this phase of strike-slip tectonics. This suggests that they may have also played a significant role in the evolution of the Clair Basin during the Devonian-Carboniferous period.

Foula, a 13km2 island situated 25km SW of the Shetland Isles is possibly the best onshore analogue to the Clair Ridge which is the second phase development area for the Clair Field. Despite being only ~70km from the Clair Field, the island is relatively poorly studied with regards to its structural evolution. Some 1600m of Middle Devonian sandstones are spectacularly exposed in continuous, kilometre-long cliff sections up to 376m high. These rocks unconformably overlie likely Precambrian-age amphibolite facies basement gneisses and schists intruded by sheeted granites of uncertain age and affinity. Building on earlier studies carried out in the 1980's, the initial results of an ongoing reappraisal of the structure, stratigraphy and tectonic evolution of the island and surrounding area will be presented. This is being achieved through detailed land-, sea- and aerial-(drone) based studies of exposed basement-cover contacts, and the structure and broad stratigraphic architecture of the overlying sandstone dominated sequences exposed in the continuous coastal sections. Samples of the basement have also been collected for radiometric dating using U-Pb geochronology.

Fieldwork data will be presented, supplemented by the use of photogrammetry to capture the geology of key localities and analyse structures in difficult to access areas. 3D models of the stratigraphy and structure are being created for later use in modelling of stratigraphic architecture, fracture networks, numerical simulations of fluid flow, up-

scaling and reservoir quality studies. These findings will be compared to previous analogue studies and applied to the current concepts and models which underpin the stratigraphic and structural architecture of the Clair field and the wider regional tectonic setting.

Appendix A4 (Trans Iapetus Presentation Abstract)

The structural evolution of the Devonian rocks and associated basement in Foula and Shetland: An analogue for the Clair Basin

T. Utley[1], R. Holdsworth[1, 3], E. Dempsey[1], K. McCaffrey[1, 3], R. Strachan[2], R. Jones[3] and G. Blackbourn[4].

[1]Department of Earth Sciences, Durham University, Durham, DH1 3LE. (thomas.a.utley@durham.ac.uk)

[2]School of Earth and Environmental Sciences, University of Portsmouth, PO1 3QL.

[3]Geospatial Research Limited, Durham, DH1 4EL.

[4]Blackbourn Geoconsulting, West Lothian, EH51 9AB.

Abstract:

The Clair Field, west of Shetland, represents the largest remaining hydrocarbon resource in the UKCS. It comprises fractured Devonian-Carboniferous sandstones overlying a fault bounded ridge of Precambrian metamorphic basement. Foula, an island situated 25km SW of the Shetland Isles may represent the nearest and best onshore analogue to the Clair Field, but is relatively little studied. 1600m of gently folded Middle Devonian sandstones correlated with the Lower Clair Group offshore, are exposed in continuous, kilometre-long cliff sections up to 376m high. These rocks unconformably overlie basement gneisses and sheeted granites. On Shetland, the Devonian sandstones of the Walls Peninsula and South-East Shetland again, unconformably overlie metamorphic basement.

Here we present an ongoing reappraisal of the structure, stratigraphy and tectonic evolution of the three Devonian basins in Shetland (Foula, Walls, SE Shetland). Detailed land and aerial (drone) based studies of exposed basement-cover contacts, and the structure and broad stratigraphic architecture of the overlying sandstone dominated sequences are being carried out.

Field data and structural analysis are supplemented by the use of photogrammetry to capture the geology in inaccessible coastal sections. Initial findings show that faulting and folding were contemporaneous with sedimentation during the earliest stages of Mid-Devonian basin development.

The geometries of faults and folding on Foula and Shetland are consistent with models of constrictional strain related to regional sinistral transtension along the Walls Boundary Fault during the Mid-Devonian. Our findings suggest that the transtensional folded Devonian basins of Shetland may represent a better surface analogue for the Clair Basin.

Appendix A5 (AAPG/ICE Presentation Abstract)

The onshore structural geology of Foula, Shetland and implications for the Devonian-Carboniferous development of the offshore Clair Basin

Thomas A. G. Utley[1], Robert E. Holdsworth[1,3,] Edward D. Dempsey[1], Ken J. W. McCaffrey[1,3], Rob A. Strachan[2], Richard R. Jones[3] and Graham A. Blackbourn[4].

[1]Department of Earth Sciences, Durham University, Science Labs, Durham, DH1 3LE, UK

[2]School of Earth and Environmental Sciences, Burnaby Building, Burnaby Road, University of Portsmouth, PO1 3QL, UK

[3]Geospatial Research Limited, Office Suite 7, Harrison House, 1 Hawthorn Terrace, Durham, DH1 4EL, UK

[4]Blackbourn Geoconsulting, 26 East Pier Street, Bo'ness, West Lothian, EH51 9AB, UK

Abstract:

The Clair Field, west of Shetland, represents the largest remaining hydrocarbon resource in the UKCS. It comprises fractured Devonian-Carboniferous sandstones overlying a fault bounded ridge of Precambrian metamorphic basement. The extensional Orcadian Basin in Orkney and Caithness has long been used as an onshore analogue for the Clair Basin, although it has long been recognised that it may have a somewhat different tectonic setting due to its geographical separation from Clair.

Foula, a 13km2 island situated 25km SW of the Shetland Isles may represent the nearest and best onshore analogue to the Clair Ridge, the 2nd phase development of the Clair Field. The island has been relatively little studied with regards to its structural evolution. 1600m of gently folded Middle Devonian sandstones correlated with the Lower Clair Group offshore, are spectacularly exposed in continuous, kilometre-long cliff sections up to 376m high. These rocks unconformably overlie likely Precambrian-age amphibolite facies basement gneisses and schists intruded by sheeted granites of uncertain age and affinity.

Here we present an ongoing reappraisal of the structure, stratigraphy and tectonic evolution of the island and surrounding area. This is being achieved through detailed land and aerial (drone) based studies of exposed basement-cover contacts, and the structure and broad stratigraphic architecture of the overlying sandstone dominated sequences exposed in continuous coastal sections. Field data and structural analysis are supplemented by the use of photogrammetry to capture the geology of the inaccessible cliffs.

Field data show that faulting and folding were contemporaneous with sedimentation during the earliest stages of basin development. The geometries of the faults and folding on Foula are consistent with models of constrictional strain related to regional sinistral transtention along the Walls Boundary Fault during the Middle Devonian. Our findings suggest that the Devonian basins of Shetland may therefore represent a better surface analogue for the Clair Basin. Here there is widespread evidence of strike-slip deformation preserved in both the basement and Devonian-age cover sequences and associated igneous rocks. This suggests that existing tectonic models for the development of the Clair Basin require revision.

Appendix A6 (AAPG/ICE Presentation Abstract)

Brent Group Petrography and Diagenesis: Implications for Reservoir Quality and Enhanced Oil Recovery

Thomas A. G. Utley[1, 2] and Richard H. Worden[1]

[1]*School of Environmental Sciences, University of Liverpool, Liverpool L69 3GP, UK*

[2] *(Present Address) Department of Earth Sciences, Durham University, Science Labs, Durham, DH1 3LE, UK*

Abstract:

Despite many decades of exploration and oil production there has been no regional assessment of detrital and diagenetic mineralogy and controls on reservoir quality of the prolific Middle Jurassic Brent Group, Viking Graben, UK. Here we have integrated, evaluated and synthesised a combination of proprietary and publicly-available core analysis data and petrographic mineralogical data from the Brent Group. The aim to better understand the regional mineral and petrographic properties of the Brent reservoir units, the distribution of detrital and diagenetic minerals, and how these influence reservoir quality and options for enhanced and improved oil recovery.

Despite the Brent Group being the focus of many studies into sandstone diagenesis in the 80's and 90's, there have been no published reviews of the regional patterns of diagenesis. Furthermore, little effort has been made to develop an overview of how the Brent Group changes both spatially and with depth.

Using data supplied by four industry partners, together with published data, a data set of over 2500 samples was collated from 169 wells, representing 27 fields that are producing or have produced oil from Brent Group reservoirs over the last 40 years. This data set, the largest produced on the Brent, has allowed us to generate and analyse maps of the distribution of key diagenetic minerals that control reservoir quality. We have also compared cement abundances in the five formations and examined the effects of burial depth and fluid type on cement abundance patterns.

A greater understanding of how the Brent Group varies, spatially, with depth, and between formations, will help in the management of existing assets, and in any potential exploration on deeper or satellite structures in the area. A regional understanding of Brent mineralogy will help in appraising the effectiveness of EOR approaches such as low salinity water injection. The results of this study suggest that this method is likely to be most effective in the Brent Group as a primary water-flood in favourable reservoir conditions, but in general is not a promising candidate due to the low salinity of formation water and low abundance and type of kaolinite. With a drive to reduce costs and maximise economic recovery from the UKCS, the encouragement of operators to share information with one another and work more closely with academia, along with the re-examining of legacy data may be the key to future success both in this basin and elsewhere.

Appendix A7 (NERC Conference Poster)

The onshore structural geology of Foula, Shetland and implications for the Devonian-Carboniferous development of the offshore Clair Basin

Thomas A. G. Utley[1], Robert E. Holdsworth[1], Ken J. W. McCaffrey[1], Edward D.Dempsey[2], Robert A. Strachan[3], Graham Blackbourn[4], and Richard R. Jones[5].

thomas.a.utley@durham.ac.uk [1]Department of Earth Sciences, Durham University, Science Labs, Durham, DH1 3LE, UK.

[2]School of Environmental Sciences, University of Hull, Hull, HU6 7RX. [3]School of Earth and Environmental Sciences, Burnaby Building, Burnaby Road, University of Portsmouth PO1 3QL.

[4]Blackbourn Geoconsulting, Bo'ness, West Lothian, EH51 9AB. [5]Geospatial Research Limited, Durham University, Science Labs, Durham, DH1 3LE, UK.

1. The Clair Field

- Largest known resource in the UKCS, situated 75km West of the Shetland Isles. An estimated 7-8 Billion BOE in place.
- Comprised of fractured Devonian-Carboniferous sandstones (Clair Group) that overlie an up-faulted ridge of fractured Precambrian metamorphic basement (Rona Ridge) (Fig.1).
- Significant proportion of hydrocarbons are stored within fractures in basement and overlying Devonian sedimentary rocks.
- A greater understanding of Devonian-Basement unconformity and fracture systems is required to produce effectively/efficiently.

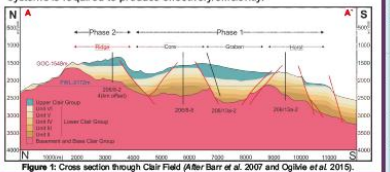

Figure 1: Cross section through Clair Field (*After* Barr *et al.* 2007 and Ogilvie *et al.* 2015).

2. Regional Context and General Geology

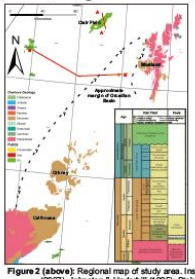

- Clair Basin developed during Mid-Devonian to Early Carboniferous in NE/SW half graben.
- Orcadian Basin of Caithness/Orkney long used as the classic analogue..BUT..
- Alternatives exist in Shetland, and are transtentional (Seranne,1992).
- Foula is the closest onshore analogue. Poorly studied despite its proximity (Fig.2).
- NNE/SSW half graben on NW margin of the Orcadian Basin.
- Comprises Middle (?) Devonian sediments and Precambrian metamorphic basement (Fig.3).
- Correlated regionally based on lacustrine facies and palynology (Fig.2 Inset).

Figure 2 (above): Regional map of study area. Inset-regional stratigraphic chart. *After* Barr *et al.*, (2007), Johnston & Underhill (1995), Stoker *et al.*, (1993) & Coney *et al.* (1993).
Figure 3 (below): Regional cross section through study area. *After* Chesher *et al.*, (1988).

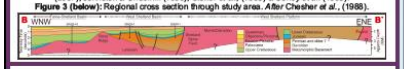

3. General Geology of Foula

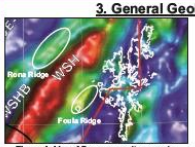

Figure 4: Map of Bouguer gravity anomaly. Red=positive. Blue=negative. (Stoker *et al.*, 1993)

- Foula part of long lived NE/SW trending basement structural high: Foula Ridge (Fig.4) - similar to Clair (Rona Ridge).
- ~1600m of gently folded/dipping Middle Devonian clastics (Fig.5), unconformable and faulted against a ~1km wide strip of basement - similar to Clair.
- Basement and Devonian highly fractured - similar to Clair.

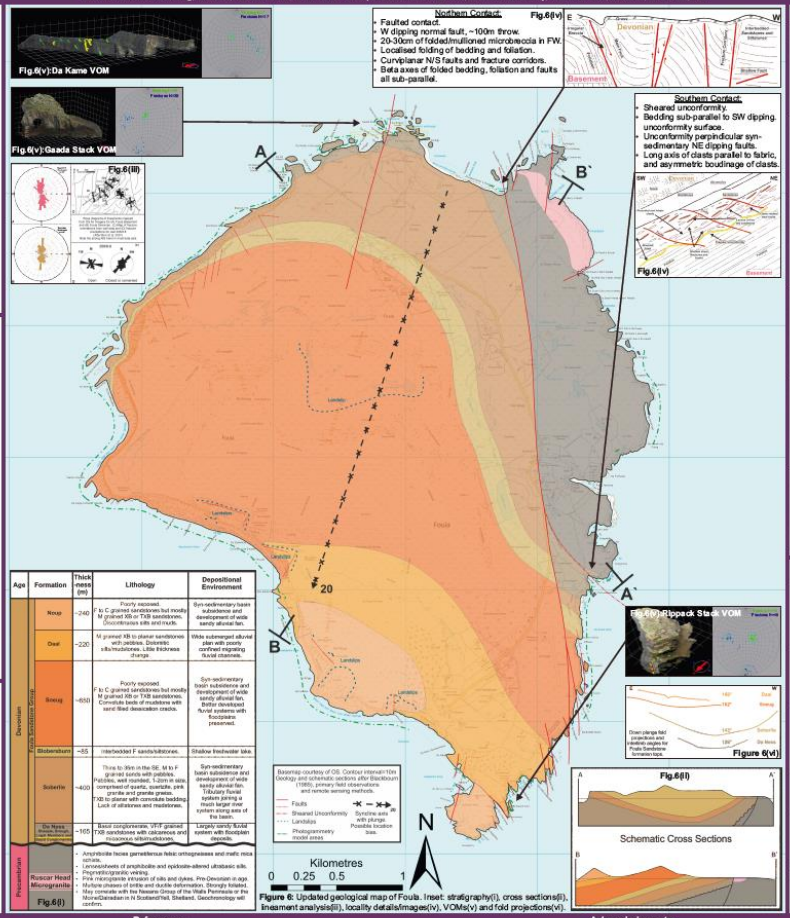

Age	Formation	Thickness (m)	Lithology	Depositional Environment
Devonian	Noup	~240	Poorly exposed. F to C grained sandstones but mostly M grained Xfb or TXB sandstones. Discontinuous soils and mudb.	Syn-sedimentary basin subsidence and development of wide sandy alluvial fan.
	Deal	~220	M grained Xfb to planar sandstones with pebbles. Dolomitic silts/mudstones. Little thickness change.	Wide submerged alluvial plain with poorly confined migrating fluvial channels.
	Sneug	~650	Poorly exposed. F to C grained sandstones but mostly M grained Xfb or TXB sandstones. Comprises beds of mudstone with sand filled desiccation cracks.	Syn-sedimentary basin subsidence and development of wide sandy alluvial fan. Both/or developed fluvial systems with floodplains preserved.
	Blobersburn	~85	Interbedded F sands/siltstones.	Shallow freshwater lake.
	Soberlie	~400	Thins to 35m in the SE. M to F grained sands with pebbles. Pebbles, well rounded, 1-2cm in size, comprised of quartz, quartzite, pink granite and granite gneiss. TXB to planar with cannibale bedding. Lack of siltstones and mudstones.	Syn-sedimentary basin subsidence and development of wide sandy alluvial fan. Tributary fluvial system joining a much larger river system along axis of the basin.
	Da Ness	~165	Basal conglomerate, VFrF grained TXB sandstones with calcareous and micaceous siltstone/mudstones.	Largely sandy fluvial system with floodplain deposits.
Precambrian	Ruscar Head Microgranite		Amphibolite facies garnet/sillimanite felsic orthogneisses and mafic mica schists. Leucosheets of amphibolite and epidiorite-altered ultrabasic sills. Pegmatite/granitic veining. Pink microgranite intrusion of sills and dykes. Pre-Devonian in age. Multiple phases of brittle and ductile deformation. Strongly foliated. May correlate with the Navarre Group of the Walls Peninsula or the Hovie/Glenadam in N Scotland/Fetlar, Shetland. Geochronology will confirm.	
	Fig.6(i)			

Figure 6: Updated geological map of Foula. Inset: stratigraphy(i), cross sections(ii), lineament analysis(iii), locality details/images(iv), VOMs(v) and fold projections(vi).

4. Structural Geology and Basin Development

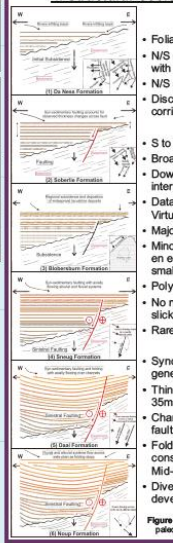

Basement Structures:

- Foliation subtly folded, W through to SW.
- N/S orientated, steeply E dipping normal faults with mineralisation.
- N/S orientated low angle detachments.
- Discrete brittle vertical/sub-vertical N/S fracture corridors (Fig.6).

Devonian Structures:

- S to SSW plunging syncline (Fig.6ii).
- Broad upward opening folds (Fig.7).
- Down plunge projections show an increase in interlimb angle up stratigraphy (Fig.6vi).
- Data supplemented with remote sensing and Virtual Outcrop Models (VOMs) (Fig.6v).
- Major N/S to NNW/SSE trending normal faults.
- Minor N/S to NNW/SSE and E/W to ESE/WNW, en echelon, sub-vertical fracture corridors and small faults (Fig.6).
- Polymodal fracturing, distributed small offsets.
- No mineralisation, and rare sinistral oblique slickenlines.
- Rare dextral reactivation of some N/S faults.

Basin development:

- Synchronous syn-sedimentary faulting and generation of growth folds (Fig.8).
- Thinning of Soberlie Fm. from 400m in HW to 35m in FW and 650 to 220m in Sneug Fm.
- Changing palaeocurrent in response to active faults and folding channelising flow (Fig.8).
- Fold hinges/beta axes of folds consistent with constrictional strain and sinistral transtention in Mid-Devonian.
- Diversity of basement/cover relationships developed (Fig.6iv).

Figure 8 (left): Tectono-stratigraphic evolution of Foula. Inset-paleocurrent maps by formation. *After* Blackbourn (1985).

5. Conclusions

- Basin fill shows synformal growth folding consistent with constrictional extension during regional sinistral transtention during Devonian basin development (Fig.9).
- Similar to structures observed in Shetland, Orkney/Caithness & Inner Moray Firth as well as the Clair Field.
- Folds formed during early basin development & therefore present as potential traps before hydrocarbon generation/or present for subsequent reactivation (Fig.10).
- Possible implications for other petroleum systems elsewhere e.g. East Shetland Platform.
- Diversity of basement/cover relationships = possible drilling hazards, and seismic interpretation/processing challenges (Fig.6iv).
- Is the Clair Basin transtentional? What evidence is there for growth folding in the Clair Group?

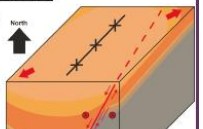

Figure 9: 3D Stuctural model of Foula.

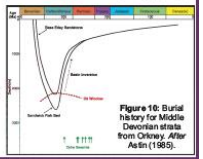

Figure 10: Burial history for Middle Devonian strata from Orkney. *After* Astin (1985).

References:

Astin, TR., 1985. The palaeogeography of the Middle-Devonian Lower Stony Sandstone, Orkney. Scottish Journal of Geology, 21(3), pp.353-370.

Barr, D. et al., 2007. Provenance and facies modelling in the Clair Field area of Shetland. Geological Society, London, Special Publications, 276(1), pp.209235.

Coney, D. et al., 1993. Clair appraisal: the benefits of a co-operative approach. Geological Society, London, Petroleum Geology Conference series, 4, pp.1609-1620.

Chesher, J.A. et al., 1988. Foula Sheet (IDH Anvil Solid Edition 1:250,000 Map Series). British Geological Survey.

Johnston, S.C. & Underhill, J.R., 1995. The Clair Discovery, west of the Shetland Isles. Scottish Journal of Geology, 31(2), pp.167-180.

Ogilvie, S. et al., 2015. Structural geology and weld jointing in the Clair Field. Geological Society, London, Special Publications, 421(1), pp.197-212.

Seranne, M., 1992. Late Paleozoic strike-slip faulting and related basin formation in the northern Orcadian basin, northern North Sea. Tectonics, 11(1), pp.23-37.

Stoker, M.S. et al., 1993. The geology of the Hatton and West Shetland shelves, and adjacent deep-water areas. The Stationery Office/TSO.

Acknowledgements:

Jim Hambleton for assistance in the field and with thin section work in Shetland.

Calum Fraser (www.instagram.com/calmfr) for capturing drone imagery, and Jim and Bill Bissett Scott and the crew of UK24 for the use of the boat.

Graham Blackbourn for permission to use information from his unpublished report on the geology of Foula.

Photogrammetric point clouds generated using Agisoft Photoscan and interpreted using the Virtual Reality Geological Studio, courtesy of David Hodgetts, Manchester University

BP for providing imagery and the Clair 4D time-lapse seismic data interpreted at Durham.

Aerial images courtesy of Cyrrhynx Foula (photo reproduced from John Pratley, pinphotos.co.uk

Bathymetry DTM courtesy of the UK Hydrographic Office (UKHO), Taunton, UK.

Scan the QR code on the right to see more 3D models related to this work.

Centre for Doctoral Training (CDT) in Oil and Gas

NERC SCIENCE OF THE ENVIRONMENT

Appendix A8 (Janet Watson Meeting 2018 and NERC CDT Conference Presentation Abstract)

The use of Virtual Outcrop Models, digital geology and legacy data to reappraise Devonian basin evolution in NE Scotland and Shetland.

Thomas A.G. Utley[1], Robert E. Holdsworth[1,3], Ken J.W. McCaffrey[1, 3], Edward D. Dempsey[2], Rob A. Strachan[3] and Richard R. Jones[4].

thomas.a.utley@durham.ac.uk

[1] Department of Earth Sciences, Durham University, Science Labs, Durham, DH1 3LE, UK

[2] School of Environmental Sciences, University of Hull, Hull, HU6 7RX

[3]School of Earth and Environmental Sciences, Burnaby Building, Burnaby Road, University of Portsmouth, PO1 3QL, UK

[4] Geospatial Research Limited, Office Suite 7, Harrison House, 1 Hawthorn Terrace, Durham, DH1 4EL, UK

Abstract: A virtual outcrop model is a powerful tool for the geosciences due to the inherently 3D nature of the discipline. The extraction of 3D geological information from these three-dimensional models allows for the collection of large quantities of data, quickly and relatively easily, from areas previously inaccessible, overlooked and considered to be 'missing' or 'lost'. Outcrops can be now re-visited at any time and further analysis carried out, producing ever increasing quantities of data which can be now be easily shared and viewed in 3D. These new digital geological methodologies are not a replacement for traditional fieldwork but should be seen as the 'norm' and used to supplement and complement traditional fieldwork, desk studies and geological analysis.

These techniques, in conjunction with the re-interpretation and re-examination of large quantities of legacy data generated by industry and academia is a more cost effective and time efficient approach, avoiding the duplication of datasets. Vast quantities of data can now be collated, interrogated and analysed in new ways highlighting trends and features lost within solitary datasets and in archives.We illustrate this by presenting an ongoing reappraisal of the stratigraphy, structure and tectonic evolution of onshore analogues for the Clair Field through the detailed study of basement/cover contacts, and structure of the overlying Devonian sequences. This is being achieved through desk studies, reappraisal and analysis of legacy and new onshore and offshore datasets, fieldwork, structural analysis and the production of Virtual Outcrop Models.

Our analysis from Shetland, Orkney and Caithness show synchronous faulting and synformal growth folding. These observations are consistent with models of constrictional extension during regional sinistral transtentional Devonian basin development. This in combination with the diversity of basement/cover relationships apparent in the Orcadian Basin could lead to difficulties in exploration and appraisal of resources offshore, and that the established models for Devonian basin development may require revision.

Appendix A9 (PETEX 2018 Presentation Abstract)

Awarded best student presentation

The use of Virtual Outcrop Models, digital geology and legacy data to reappraise Devonian basin evolution in NE Scotland and Shetland: Analogues for the offshore Clair Basin and Clair Oil Field, West of Shetland.

Thomas A. G. Utley[1], Robert E. Holdsworth[1,3], Edward D. Dempsey[2], Ken J. W. McCaffrey[1,3,] Rob A. Strachan[3], Andrew C. Morton[4] and Richard R. Jones[5]

[1]Department of Earth Sciences, Durham University, Science Labs, Durham, DH1 3LE, UK

[2] School of Environmental Sciences, University of Hull, Hull, HU6 7RX

[3]School of Earth and Environmental Sciences, Burnaby Building, Burnaby Road, University of Portsmouth, PO1 3QL, UK

[4]HM Research Associates, Giddanmu, Musselwick Road, St Ishmaels, Pembrokeshire, SA62 3TJ

[5]Geospatial Research Limited, Office Suite 7, Harrison House, 1 Hawthorn Terrace, Durham, DH1 4EL, UK

Extended Abstract:

The Clair Field, west of Shetland, represents the largest hydrocarbon resource in the UKCS. It comprises fractured Devonian-Carboniferous sandstones, overlying a fault bounded ridge of Precambrian metamorphic basement. The onshore, broadly extensional Orcadian Basin, has long been used as an analogue for the Clair Field, but it is possible that it formed in a rather different tectonic setting, as it lies in a separate basin to the west with some significant differences.

Some of the known complexity in sub-surface structures and basement-cover relationships may suggest that strike-slip tectonics played a role in the evolution of the Clair Basin during the Devonian-Carboniferous period. The role of strike-slip tectonics has been linked to the development of the Devonian basins of Norway (Seranne & Seguret 1987; Osmundsen & Andersen 2001; Séguret et al. 1989; Fossen 2010; Fossen et al. 2017), with similar structures having also been recognised in Shetland (Seranne 1992). Thus, our aim is to try to better understand how strike-slip tectonics may have influenced the development of the Devonian basins of Northeast Scotland and Shetland.

The Digital Geological Age

The extraction of 3D geological information from virtual outcrop models created using drone-based photogrammetry allows for the collection of fully geospatially referenced and valuable geological data, quickly and with relative ease, from areas previously inaccessible, overlooked and considered to be 'missing' or 'lost' (See Fig.1). Outcrops can then be re-visited at any time, on 'virtual' fieldtrips, allowing for improved geological, spatial

understanding and further geological analysis, producing data and knowledge which can be now be more easily shared and viewed in 3D.

New digital geological methodologies are not a replacement for traditional fieldwork, but should be seen as the 'norm' and used to supplement and complement traditional fieldwork, desk-based studies and geological data analyses. The integration of these techniques with the results of re-interpretation and re-examination of large quantities of onshore and offshore legacy data generated by industry and academia represents a more cost-effective and time efficient approach. Vast quantities of data can now be collated, interrogated and analysed in new ways, deriving new value, and highlighting trends and features hidden away within solitary datasets and in archives.

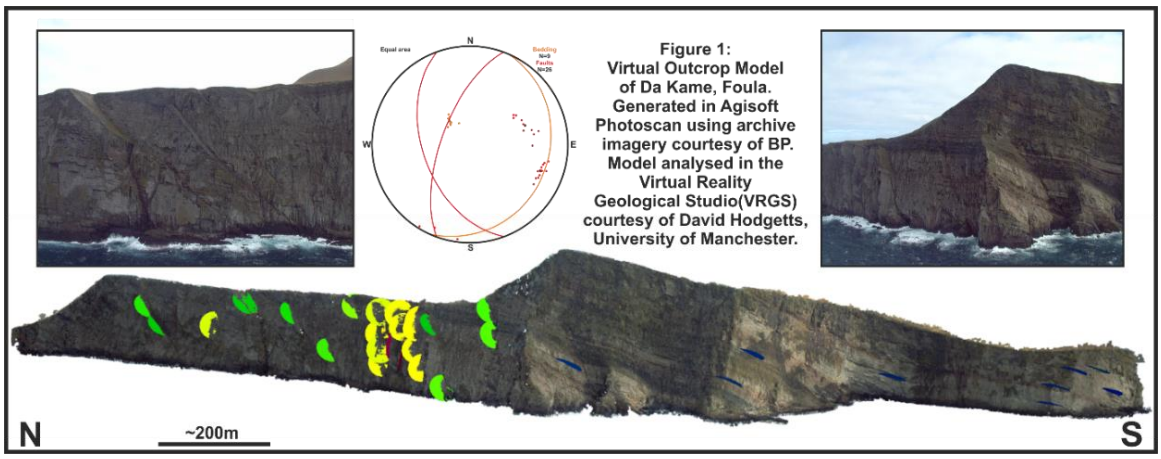

Figure 1: Virtual Outcrop Model of Da Kame, Foula. Generated in Agisoft Photoscan using archive imagery courtesy of BP. Model analysed in the Virtual Reality Geological Studio(VRGS) courtesy of David Hodgetts, University of Manchester.

Reappraisal of Devonian Basin Development

We illustrate this using a reappraisal of the stratigraphy, structure and tectonic evolution of onshore analogues for the Devonian-Carboniferous Clair Basin that includes detailed analysis of basement/cover contacts, and the structural architecture of the overlying Devonian sequences. This is achieved through the integration of multiscale, topographic, photogrammetric, bathymetric, geological and geophysical data. Both legacy and new, onshore and offshore data has been collated and is used in conjunction with fieldwork, structural analysis, heavy mineral provenance analysis, detrital zircon geochronology and the production of Virtual Outcrop Models (VOMs).

Our new synthesis extends from Shetland, Orkney and Caithness, and consistently reveals evidence for synchronous Devonian-age growth faulting and growth folding in all areas. These observations are consistent with models of constrictional extension during regional sinistral transtension along the Walls Boundary and Great Glen Fault Zones. The presence of folds that formed during early basin development, synchronous with basin filling and not due to later reactivation, is important for the assessment of petroleum systems. This is primarily due to the formation of potential hydrocarbon trapping geometries created during basin formation in proximity to potential Devonian lacustrine source rocks, which in the Orcadian basin were mature during the Carboniferous (Astin 1985; Astin 1990; Hillier & Marshall 1992; Marshall et al. 1985). Importantly, this is before basin inversion and exhumation in the Permo-Carboniferous, to which many of these folds have traditionally

been attributed. Furthermore, these structures may be present for later reactivation and/or act as traps for hydrocarbon accumulations in other petroleum systems.

Analysis of offshore data from Caithness/Orkney has also provided new insights into some of the large scale structures present within the Orcadian Basin, which are poorly exposed onshore. Large scale folds and significant numbers of faults and fracture zones can be observed at the sub-seismic scale, and allow the linking of what is seen at outcrop in coastal section, to what is imaged in subcrop the subsurface (Figure 2).

New heavy mineral analysis has revealed subtle differences in sediment provenance between the Devonian Basins of Shetland and Foula, an island 25km to the Southwest. The similarity in provenance signature of Foula, to the Devonian sediments of the Clair Basin and Orkney, suggest similarities in source region, and a large-scale, linked depositional system. This hypothesis is supported by detrital zircon geochronology which has identified the East Greenland continental margin, as the source of sediment into the Clair Basin. More mixed provenance signatures in Caithness/Moray Firth and Shetland reflect both distal, and local sources in Northern Scotland and Shetland respectively. (Schmidt et al. 2012; Sasnowski 2015). The contrasting provenance signatures reflect the complex interplay of climate and tectonics controlling the source of sediment into the Orcadian and Clair Basins.

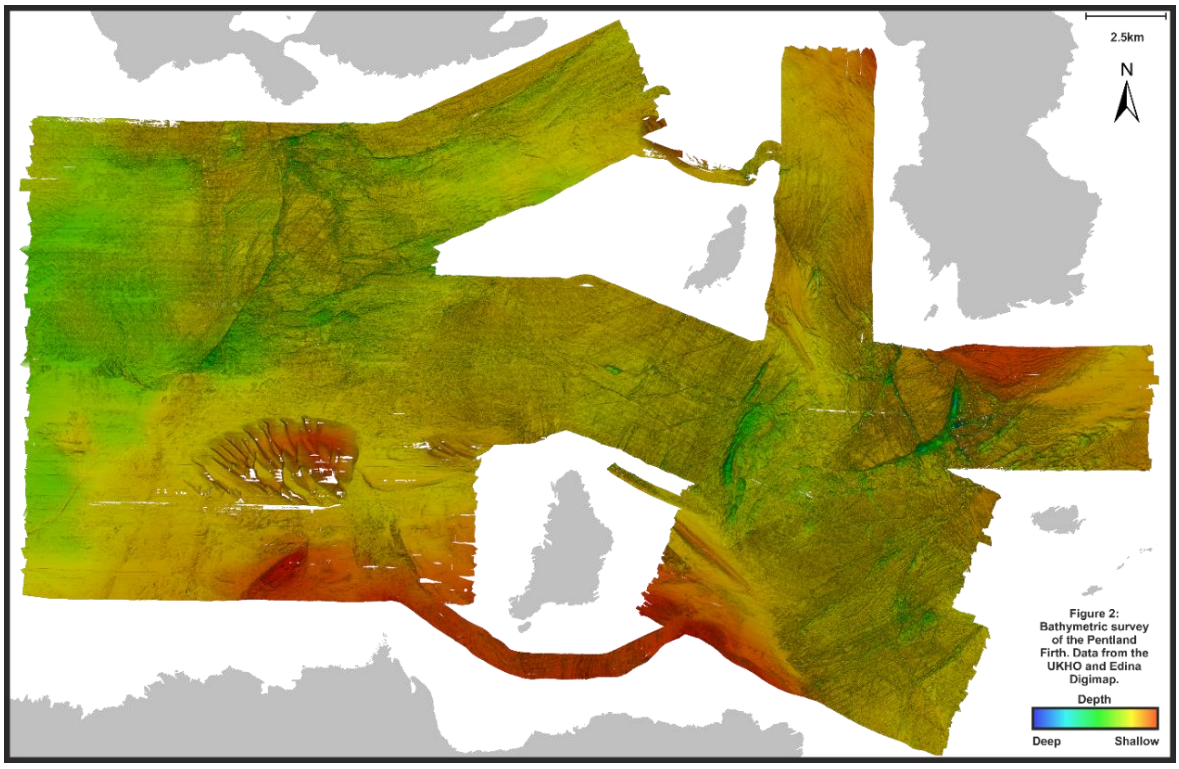

Figure 2: Bathymetric survey of the Pentland Firth. Data from the UKHO and Edina Digimap.

Conclusions

The unusual basin architecture, diversity of basement/cover relationships, together with the distribution, type, and size of structures apparent in the Orcadian Basin could lead to difficulties in exploration and appraisal of resources offshore. This knowledge can be taken further for exploration in offshore settings such as the developing fractured basement play, West of Shetland (Belaidi et al. 2016; Trice 2014) where an improved knowledge of the

nature of the unconformity and fracture systems in the basement and cover sequences could improve seismic imaging and direct drilling campaigns, saving costs, minimising downtime and improving safety.

We propose that the established models for Devonian basin development used offshore may require further revision and that some analogues in Shetland, such as the island of Foula, may represent the missing link between the Clair Basin and the larger Orcadian Basin, preserving a snapshot in the structural and stratigraphic evolution of the Devonian basins of Northeast Scotland.

Appendix A10 Shell Research Day Presentation Abstract

Invited Speaker

The use of Virtual Outcrop Models, digital geology and legacy data to reappraise Devonian basin evolution in NE Scotland and Shetland: Analogues for the offshore Clair Basin and Clair Oil Field, West of Shetland.

Thomas Utley[1], Robert Holdsworth[1,2], Edward Dempsey[3], Ken McCaffrey[1,2], Rob Strachan[4], Andrew Morton[5], and Richard Jones[2]

[1]Department of Earth Sciences Durham University, Durham, United Kingdom.
[2]Geospatial Research Limited, Durham, United Kingdom.
[3]School of Environmental Sciences, University of Hull, Hull, United Kingdom.
[4]School of Earth and Environmental Sciences, University of Portsmouth, Portsmouth, United Kingdom.
[5]HM Research Associates, St Ishmaels, United Kingdom

Abstract

The extraction of 3D geological information from virtual outcrop models created using drone-based photogrammetry allows for the collection of useful and valuable geological data, quickly and relatively easily, from areas previously inaccessible, overlooked and considered to be 'missing' or 'lost' (See Fig.1). Outcrops can be now re-visited at any time and further geological analysis carried out, producing data and knowledge which can be now be easily shared and viewed in 3D. These new digital geological methodologies are not a replacement for traditional fieldwork but should be seen as the 'norm' and used to supplement and complement traditional fieldwork, desk-based studies and geological data analysis.

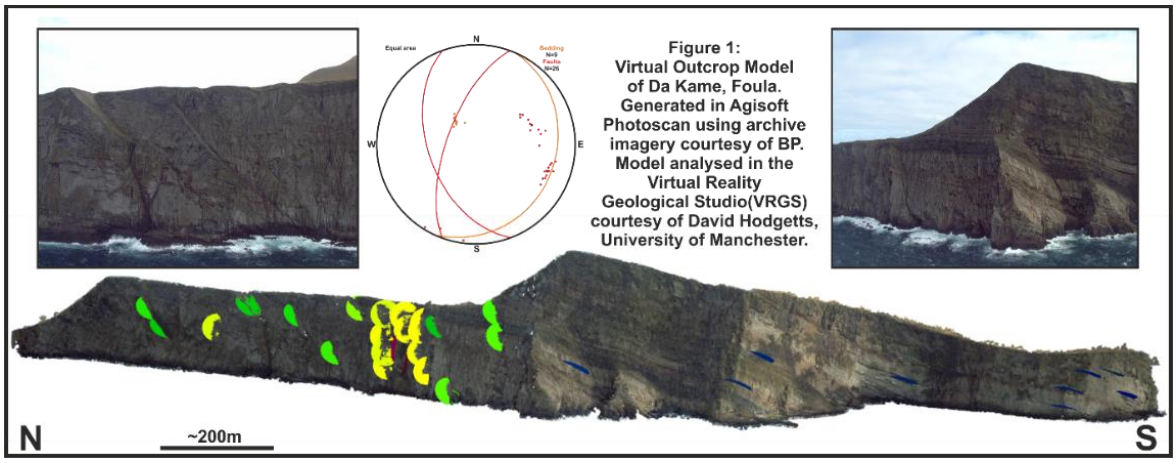

Figure 1: Virtual Outcrop Model of Da Kame, Foula. Generated in Agisoft Photoscan using archive imagery courtesy of BP. Model analysed in the Virtual Reality Geological Studio(VRGS) courtesy of David Hodgetts, University of Manchester.

Use of these models, in conjunction with the re-interpretation and re-examination of large quantities of onshore and offshore legacy data generated by industry and academia is a more cost effective and time efficient approach, avoiding the duplication of datasets. Vast quantities of data can now be collated, interrogated and analysed in new ways, deriving new value, and highlighting trends and features hidden away within solitary datasets and in archives.

We illustrate this using a reappraisal of the stratigraphy, structure and tectonic evolution of onshore analogues for the Devonian-Carboniferous Clair Basin that includes detailed analysis of basement/cover contacts, and the structure of the overlying Devonian sequences. This is achieved through mixture of desk-based study, reappraisal and analysis of legacy and new onshore and offshore datasets, fieldwork, structural analysis and the production of Virtual Outcrop Models.

Our new synthesis extends from Shetland, Orkney and Caithness and consistently reveals synchronous faulting and synformal growth folding in all areas. These observations are consistent with models of constrictional extension during regional sinistral transtentional Devonian basin development. This unusual basin architecture together with the diversity of basement/cover relationships apparent in the Orcadian Basin could lead to difficulties in exploration and appraisal of resources offshore. Thus, established models for Devonian basin development used offshore may require revision.

Presenter Biography

Tom is a graduate of Keele University, where he obtained a Master of Geoscience Degree in 2013 with a final year thesis titled: '3D architecture of vein and flat type mineralisation in the North Pennine Orefield'. He gained industry experience working as geophysicist and surveyor before starting an industry funded research position at the University of Liverpool in 2014, looking at diagenesis and reservoir quality in the Brent Group of the Northern North Sea. At present he is working towards a PhD at Durham University titled: 'A reservoir scale structural reappraisal of onshore Devonian analogues of the Clair Group in the Fair Isle-Shetland region' which is funded by the NERC CDT in Oil & Gas and supported by the Clair JVG. His project reappraises the stratigraphy, structure and tectonic evolution of alternative onshore analogues for the Clair Field through the detailed study of basement/cover contacts, and the structure of the overlying Devonian sequences.

Appendix A11 Joint Meeting of the Yorkshire Geological Society and North Eastern Geological Society Presentation Abstract

Invited Speaker January 2019

The use of Virtual Outcrop Models, digital geology and legacy data to reappraise Devonian basin evolution in NE Scotland and Shetland.

Thomas Utley[1], Robert Holdsworth[1,2], Edward Dempsey[3], Ken McCaffrey[1,2], Rob Strachan[4], Andrew Morton[5], and Richard Jones[2]

[1]Department of Earth Sciences Durham University, Durham, United Kingdom.

[2]Geospatial Research Limited, Durham, United Kingdom.

[3]School of Environmental Sciences, University of Hull, Hull, United Kingdom.

[4]School of Earth and Environmental Sciences, University of Portsmouth, Portsmouth, United Kingdom.

[5]HM Research Associates, St Ishmaels, United Kingdom

The extraction of 3D geological information from virtual outcrop models created using drone-based photogrammetry allows for the collection of useful and valuable geological data, quickly and relatively easily, from areas previously inaccessible, overlooked and considered to be 'missing' or 'lost'. Outcrops can be now re-visited at any time and further geological analysis carried out, producing data and knowledge which can be now be easily shared and viewed in 3D. These new digital geological methodologies are not a replacement for traditional fieldwork, but should be seen as the 'norm' and used to supplement and complement traditional fieldwork, desk-based studies and geological data analysis.

Use of these models, in conjunction with the re-interpretation and re-examination of large quantities of onshore and offshore legacy data generated by industry and academia is a more cost effective and time efficient approach, avoiding the duplication of datasets. Vast quantities of data can now be collated, interrogated and analysed in new ways, deriving new value, and highlighting trends and features hidden away within solitary datasets and in archives.

We illustrate this using a reappraisal of the stratigraphy, structure and tectonic evolution of onshore analogues for the Devonian-Carboniferous Clair Basin that includes detailed analysis of basement/cover contacts, and the structure of the overlying Devonian sequences. This is achieved through mixture of desk-based study, reappraisal and analysis of legacy and new onshore and offshore datasets, fieldwork, structural analysis and the production of Virtual Outcrop Models.

Our new synthesis extends from Shetland, Orkney and Caithness and consistently reveals synchronous faulting and synformal growth folding in all areas. These observations are consistent with models of constrictional extension during regional sinistral transtentional Devonian basin development. This unusual basin architecture together with the diversity of basement/cover relationships apparent in the Orcadian Basin could lead to difficulties in exploration and appraisal of resources offshore. Thus, established models for Devonian basin development used offshore may require revision.

Appendix A12 (TSG 2018 Poster)

Co-author and project supervisor

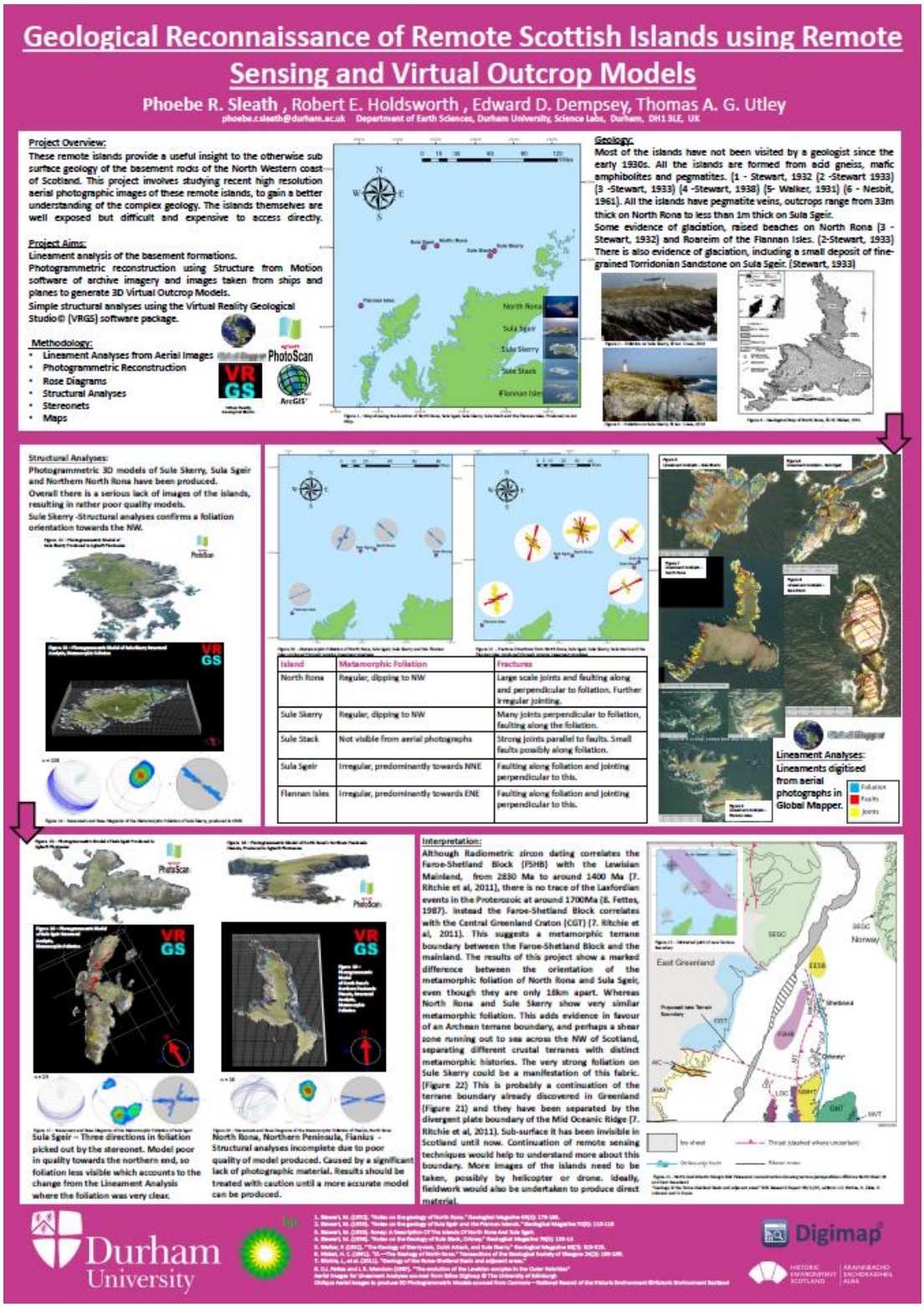

Appendix B

B1: Exploration, Appraisal and Development History of the Clair Oil Field

The Clair Field was first discovered in 1977 by well 208/8-1A in 1977 when BP was exploratory drilling a potential broad anticlinal trap of Jurassic/Cretaceous sands overlying basement (Clifford et al., 2005; Coney et al., 1993; Johnston et al., 1995; Webster, 2018), and 25° API oil was discovered at a rate of 1500 BOPD from Devonian age continental clastic sedimentary rocks at the crest of this structure. This well was followed by 206/7-1 which produced 960 BOPD from a thin Devonian section overlying fractured basement. 12 further wells were drilled and in 1985 well 206/8-7 was drilled close to the original discovery well, but proved as disappointing as the others, with test flow rates of less than 500 BOPD due to poor reservoir quality and closed fractures. Furthermore the reservoir interval was cut by two significant faults, which had been missed on seismic (Coney et al., 1993).

At the time of discovery, licences were held by eleven separate companies (Amoco, BP, British Gas, Britoil/BNOC, Chevron, Conoco, Elf, Enterprise, Esso, ICI and Mobil), which straddled 5 UKCS blocks, in 4 competing licence groups, but none had been able to demonstrate that the Clair Field was commercially viable (Coney et al., 1993). Drilling had proven a hydrocarbon column of over 800m with two separate gas caps. It had also demonstrated the significant size of the field, but had shown the reservoir interval to have poor reservoir quality, that seismic was too poor to image below the base Cretaceous unconformity adequately and that commercial flow rates were not sustainable (Sircar, 2004).

Changes in ownership in the 1980s allowed for greater collaboration and in 1990 a joint 3D seismic survey was carried out, along with several sub-surface and engineering studies. By 1991 eight companies were now working together as part of a Joint Appraisal Agreement (Coney et al., 1993). The Clair Joint venture was formed in order to ensure that best job was done to understand the Clair area. A 28-year appraisal programme was undertaken before sanction of the Phase 1 development in 2001. An extended well test in 1996 demonstrated well rates of 15-20 mbd from horizontal wells that targeted high productivity and permeable fracture zones associated with faults(Webster, 2018)

First production from the field was on the 1st February 2005. Due to the large extent of the field a phased development plan was implemented, with Phase 1 targeting the Core, Graben and Horst areas and approximately 300 million BOE recoverable. Phase 2 will target

the Ridge section of the field and will see the field scale implementation of LoSAL EOR technology. To date the Clair field has produced approximately 135 MBOE at an average flow of 30,000 BOEPD. A total of 61 vertical, deviated and horizontal wells have been drilled with further drilling planned with the completion of the Clair Ridge platform.

The Clair Ridge platform was installed in 2016 and is comprised of two bridge linked platforms with the capacity for 36 wells and production of 120 mbd of oil. The development came on stream in November 2018 from 2 pre-drilled wells which were tied back to the platform, and will target 640 million BOE of recoverable reserves, with a continued drilling programme over ten years to drill and complete the further 34 well slots. Peak production capacity will be 120000 BOEPD and at peak will provide up to 10% of UKCS production (BP, 2018). A third phase is currently in development, which will target the SW Clair Ridge and an area known as Clair South with additional nearfield exploration being undertaken (Figure 1.1) with several small, yet undeveloped discoveries being made.

Unfortunately, at the time of discovery. the technology required to produce from such a challenging field did not exist (Smith et al., 1995), and Clair was left isolated. Significant breakthroughs in technology over its 40 year history have overcome the geological complexities and allowed development of the field to take place along with many subsequent discoveries West of Shetland (Austin et al., 2014). In particular the advent of 3D seismic, improvements in survey design/processing and interpretation (Sircar, 2004) and subsequent use of 3D/4C seismic and 4D seismic (Maultzsch et al., 2007; Qian et al., 2006; Stewart et al., 1991) has enabled a much better understanding of the finer scale structure of the Clair Field, imaging of fault zones and for improved monitoring during operations (Slightam, 2012). Recently acquired 3D broadband seismic, and a permanent OBC and 4D seismic analysis has transformed how much is now known about Clair. Combined with improvements in drilling technology such as deviated and horizontal wells (Ogilvie et al., 2015), extended reach drilling (Narayanasamy et al., 2010) and 'geosteering' (Morton and Milne, 2012) has meant that new wells have been drilled with greater precision into target areas with the greatest number of fractures. New Enhanced Oil Recovery (EOR) techniques during waterflood operations will increase the amount of oil produced and the second phase development (Clair Ridge) will see the first field scale offshore deployment of BP's LoSAL, low salinity water injection technology (Robbana et al., 2011). This technology aims to release an additional 40 million BOE through the alteration

of the wetting state of the reservoir, via the injection of low salinity brine instead of conventional sea water. This is possible due to advances in membrane technologies (Henthorne et al., 2012), a greater understanding of the reservoir and continued research into how the LoSAL effect works.

B2: Overview of Previous Clair Field Analogue Research

Melvin (1977)

Thesis Title - Walls Formation, Western Shetland: distal alluvial plain deposits within a tectonically active Devonian basin

Melvin (1977; 1985) studies two Palaeozoic sedimentary sequences which represent the youngest preserved tectonically deformed sedimentary deposits respective to the orogenic belt they are adjacent to and aims to understand how different sedimentary deposits and processes are influenced by tectonics. In SW England the Upper Carboniferous Crackington and Bude Formation, and in Shetland the Walls Formation are studied in detail using sedimentary analyses such as facies analysis, petrography, and paleocurrent analysis. This analysis of the Walls Formation was the first detailed examination of this unit and was interpreted to have been deposited by fluvial and alluvial processes in a 'molasse-like' sequence within a Caledonian intermontane basin. Subsequent studies by Astin (1982) build on this work

Craigie (1989)

Thesis Title - Chemostratigraphy of Middle Devonian lacustrine sediments in the Orcadian Basin, north-east Scotland

Craigie (1998) takes a multidisciplinary approach to assess the chemostratigraphy and petroleum potential of the Middle Devonian lacustrine sediments in the Orcadian Basin. This is achieved through a combination of sedimentological analysis, petrography, SEM analysis, XRF (X-ray Fluorescence), GC (Gas Chromatography), and GC-MS (Gas Chromatography-Mass Spectrometry), along with the examination of offshore core material and wireline. The purpose of this study was to be able to better correlate onshore and offshore material and understand the development of key stratigraphic horizons such as the fish bed facies and how these may be best identified, in addition to understanding source rock potential.

Hippler (1989)

Thesis Title – Fault rock evolution and fluid flow in sedimentary basins.

Hippler (1989; 1993) uses a combination of detailed field mapping and microstructural analysis to understand fault rock evolution and fluid flow associated with extensional faulting in post-Caledonian basin forming events in Northern Scotland. Studies were carried out on intrabasinal faults in the Orcadian Basin, in the Orkney area to better understand the structural development of the Orcadian Basin. Studies were also carried out on the NW Scottish mainland, in the Durness region, examining faults likely related to the development of the offshore Minch Basin. Three major events are identified in the Orcadian Basin: 1) Devonian basin forming structures, 2) Carboniferous Inversion and 3) Permian dyke emplacement.

Pay (1989)

Thesis Title - Diagenesis and reservoir quality of the Devonian-carboniferous sandstones of the Clair Field, west of Scotland, UK.

Pay (1998) and Pay et al. (2000) studies core material from three wells in the Clair Field to examine and understand the distribution and evolution of reservoir quality. The paragenetic sequence for the Clair Group is established as being similar to that of onshore Devonian sequences. Early diagenetic calcite cements associated with rapid burial and dissolution of calcretes during the Carboniferous are identified as the predominant control on reservoir quality. The distribution of this cement is partly dependent on facies but also due to early fractures which acted as fluid flow conduits. Structurally high areas are further affected by pore filling authigenic kaolinite associated with weathering during the Permo-Triassic.

Davies (1993)

Thesis Title - The radiochemical evolution of the Devonian Orcadian Basin, NE Scotland and comparison with coeval clastic systems from Wales, Norway and the Clair Field

Davies (1993) uses sedimentological and geochemical techniques to understand the radiochemistry of the Devonian sediments of the Orcadian Basin, Hornelen Basin and sequences in SW Wales. In the Orcadian Basin the analysis reveals no systematic stratigraphic relationship in the abundance of K, U and Th and the ratios of Th/K and Th/U for either lacustrine or non-lacustrine sediments. Spatial variations are related to specific

lithologies and source chemistry and more important for characterising the provenance of basin fill. Uranium enrichment is associated with sediments in close proximity to Caledonian age granites and to lacustrine intervals due to syndepositional fixation within algal sediments.

Forbes (1993)

Thesis Title - Reservoir characterization and potential of the old red sandstone around the inner moray firth, NE Scotland

Forbes (1993) uses ORS sediments onshore in the Moray Firth as analogues to offshore sediments, characterise the reservoirs in terms of porosity and permeability, assess their reservoir potential and understand the diagenetic history. The following paragenetic sequence for the ORS sandstones was established. Dissolution of lithic fragments and development of clay/Fe Oxide rims is attributed to early eodiagenesis, at or near the surface, and during initial burial. This is followed by blocky, irregularly distributed calcite cements associated with mesodiagenesis during further burial with later telodiagenesis and dissolution of calcite cements, feldspars and lithic fragments and precipitation of kaolinite, associated with inversion and uplift. Further burial in the Mesozoic and uplift to the present day has led to a complex diagenetic history and largely poor reservoir quality. Initial reservoir quality associated with depositional facies and lithology still play some role in controlling production with Middle ORS deposits being more heterogeneous with sandbodies being separated by significant thicknesses of non-reservoir lacustrine sediments. In the Upper ORS a higher net to gross ratio is associated with stacked fluvial sandbodies and only thin discontinuous mudstones.

Owen (1994)

Thesis Title - The controls on reservoir properties of Devonian sandstones in the Orcadian Basin, north east Scotland.

Owen (1994) analyses 402 core plugs collected from outcrops of Lower, Middle and Upper Devonian age aeolian and fluvial facies. The primary aims were to describe and understand the controls on porosity and permeability and understand the relationship between rock texture and compressional wave velocity. The major controls on reservoir quality were calcite and quartz overgrowths, clay minerals and the dissolution of carbonate cements and detrital grains. It was also discovered that porosity and permeability have a strong

influence of compressional wave velocity which could have an important influence on mapping these units in the subsurface.

Johnston (~1995)

A thesis was not submitted as part of this research due to the project not being continued. A single article (Johnston et al., 1995) was published as an overview of the Clair Field in addition to an industry field trip itinerary and guide to the island of Foula (Johnston and Spicer, 1995). A basic overview of the geology of Foula is presented which builds on some of the early work by Blackbourn & Marshall (1985).

Phillips (1995)

Thesis Title - Fracture cements and cementation processes in the Devonian-Carboniferous Clair group and underlying Lewisian basement, West of Shetland

Phillips (1995) examined cores and other subsurface data to understand fractures within both the Clair Group and metamorphic basement. The main types of structures found were cataclastic faults, cement sealed faults/veins and open fractures. The main cement types discovered were calcite and pyrite (and marcasite), as well as minor fluorite in some Clair Group fractures. Basement fractures also contain epidote/chlorite and quartz/feldspar/hematite. Calcite cements were attributed to the remobilisation of calcium from calcretes, and predated oil charge, with localised volcanic activity perhaps contributing fluorite. Some calcite cements were associated with oil charge or from meteoric/basinal brines. Minor bacterial activity could have also contributed bicarbonate from oxidation of organic matter and methanogenisis from the in-situ breakdown of hydrocarbons. Authigenic iron sulphides may have come from externally sourced H_2S or from bacterial sulphate reduction.

Speed (1999)

Thesis Title - Kerogen variation in a Devonian half graben system

Speed (1999) used fieldwork and laboratory analysis to understand the sedimentary facies and organic matter of Middle Devonian lacustrine rocks in Orkney. The main aims were to understand basin wide stratigraphy allowing for better lithostratigraphic correlation, the influence of tectonics and sedimentology on the quality and distribution of organic matter, and ultimately quantify the hydrocarbon potential of source rocks on Orkney. The study focussed on the Rousay Flagstone Formation, a 200m thick lacustrine succession and the

influence of major basin wide structures such as the East Scapa Fault. Key findings include the high Total Organic Carbon (TOC) value and higher Hydrocarbon Index (HI) values in uplifted footwall blocks due to the quiescent environment formed as a result of the channelling of oxygen and sediment rich turbidity currents into the hangingwall depocentre. The average quantity of TOC was 1.55% and thermal maturity indicators suggest generally uniform burial into the oil window across the study area.

Sleight (2001)

Thesis Title - Fracture characteristics from two reactivated basement fault zones: examples from Norway and Shetland

Sleight (2001) and Watts et al.(2007) carried out detailed analysis of fracture attributes developed in basement rocks adjacent to two major crustal scale faults; the Møre-Trondelag Fault Complex and Walls Boundary Fault System. This study was important as both structures extend offshore into hydrocarbon rich provinces. This study was able to identify multiple periods of fault activity and 'type' the associated structures. A greater understanding of the movement history of these faults in addition the fractures associated with their motions is important for fluid flow in the sub-surface and their influence on petroleum systems e.g. trap formation, reservoir distribution, migration pathways etc.

Watts (2001)

Thesis Title - The walls boundary fault zone and the Møre Trøndelag fault complex: a case study of two reactivated fault zones

Watts (2001) and Watts et al. (2007) study in detail the tectonic history of Walls Boundary Fault Zone and the Møre Trøndelag fault complex, in particular looking at the role of fault reactivation. A detailed history of both fault zones is developed, through the detailed study of their kinematic, geometric and textural evolution. Their role in basin development is evaluated and linked to major structural events during the Caledonian Orogeny and subsequent development of sedimentary basins such as the Orcadian Basin.

Wilson (2006)

Thesis Title - Digital fault mapping and spatial attribute analysis of basement-influenced oblique extension in Passive margin settings

Wilson (2006) and (Wilson et al., 2010, 2006b, 2006a) used a digital mapping methodology to systematically collect fault and fracture information (attributes, kinematics, stress inversion), perform spatial analysis and build 3D models to visualise relationships at different scales. The aims of this study were to understand the role of pre-existing basement fabrics on rift geometry in extensional settings, using the passive margins of the North Atlantic to explore this aim. The results of this study show the complexity in rifted margins is related to changes in the obliquity of pre-existing structures relative to the regional extension direction. Pre-existing structures also lead to localised variations in stress and strain orientations, which if analysed in isolation can be misleading. Onshore studies of basement structures are therefore key to understanding how offshore structures may behave, due to being poorly resolved in offshore datasets. In the West Orkney Basin, it's shown that basement reactivation is not apparent everywhere, but has an influence which can lead to complex fault patterns. A prominent ENE-WSW fault is mapped that runs parallel to the coast and acts as a sinistral transfer zone that was active during the Devonian and/or Permo-Triassic times. In West Greenland, the influence of transform structures in sedimentary basins leads to transtensional strains, as well as localised complex fault patterns and regions of transpression. In Lofoten, a regional model of transtension along the Lofoten Ridge is developed, and examines the role of pre-existing basement fabrics, and buoyancy effects associated with granites influences the type of structures developed during oblique rifting.

Moy (2010)

Thesis Title - The architecture, growth and tectono-stratigraphic significance of rift-oblique lineaments on the NE Atlantic Margin

Moy (2010) studied the NE Atlantic volcanic margin using 2D and 3D seismic reflection data to better understand the nature of fault domain boundaries in segmented rift systems. Two end member conceptual models are proposed; accommodation zones of overlapping normal faults, trending obliquely to the rift axis or transfer zones comprised of sub vertical fault systems that link en-echelon normal fault zones. A series of rift-oblique lineaments broadly described as transfer zones are studied in detail in order to better identify and understand their origin. In summary he concludes that rift-oblique lineaments must be identified and studied individually, as they may have very different influences on basin development and may not be the significant basin-wide structures originally proposed.

Walker (2010)

Thesis Title - The structural evolution of the Faroe Islands, NE Atlantic margin

Walker (2010) and Walker et al. (2011) carried out detailed fieldwork in the Faroe Islands in order to better understand the Mesozoic development of the North Atlantic and the role of 'transfer zones' in controlling the development and distribution of sedimentary basins. The nature of structures developed in brittle basaltic rocks were explored and evaluated in terms of fluid flow and potential role in petroleum systems, as an analogue to brittle structures developed in carbonates and crystalline basement rocks, such as the Rona Ridge.

Pless (2012)

Thesis Title - Characterising fractured basement using the Lewisian Gneiss Complex, NW Scotland: Implications for fracture systems in the Clair Field basement

Pless (2012) and Pless et al. (2015) studies 1,2 and 3-dimensional fracture network characteristics of the Lewisian Gneiss Complex of mainland Scotland as an analogue for fracture systems within the offshore Clair Field basement of the Rona Ridge. This study was required due to limited well penetration in the Rona Ridge and poorly understood fracture systems within crystalline basement rocks. This was achieved through analysis of fractures at outcrop, using terrestrial laser scanning, remotely sensed DEM's (Digital Elevation Models) and offshore core and seismic data. The key findings of this study were the identification of a strong power-law distribution of fracture spacing over at least three orders of magnitude within the outcrop data, and a dominant NE/SW and/or NW/SE fault and fracture trend. This trend was attributed to the reactivation of older ductile basement shear zones and may explain the orientation of the major ridge, and Shetland Spine faults. In the offshore data a comparable trend was identified but within a core a subordinate NNE/SSW trend was also identified which was not apparent in outcrop. The smaller dataset from offshore meant that the power-law relationship was much weaker. The Lewisian Gneiss Complex was identified as being a suitable analogue but with some limitations and should only be used as a model for the sensitivity testing and statistical assessment of other models.

Wilson (2012)

Thesis Title - A high-resolution record of environmental and climatic change in a lacustrine sequence from the Devonian Orcadian Basin, Scotland

Wilson (2012) develops new methodologies to capture high resolution paleoenvironmental and paleoclimate data over a ≤55-year period from within Middle Devonian lacustrine sediments of the Orcadian Basin. Geological and geochemical analysis of varve sets (clastic/carbonate pairs) capture annual, and short-term climatic variations. 12-year cycles previously attributed to sunspot solar forcing also show compositional differences associated with a shift in dominance from allochthonous clastic material to authochthonous carbonate precipitation indicating variations in climatic wetness. Biomarkers indicate hypersaline conditions, which varied both seasonally and cyclically and stable isotope data also show that temperature and primary productivity also varied seasonally and cyclically. Rate of carbon burial exhibits cyclical variation, and an antithetic relationship between the burial efficiency and temperature exists.

Franklin (2013)

Thesis Title - Characterising fracture systems within upfaulted basement highs in the Hebridean Islands: an onshore analogue for the Clair Field

Franklin (2013), through a combination of detailed structural studies in the field, fracture analysis and examination of offshore core material was able to characterise fractures and attributes in the onshore Lewisian Complex of the Hebridean Islands, assess the controls on fracture patterns, and do detailed characterisation of fractures and fracture fills as an analogue to structures observed in the Clair Field. He also compares fracture styles in different lithologies to understand deformation processes at the basement/cover interface and understand how the Clair reservoir units may behave during production. It was identified that lithological variations in the Clair Group have some control on the deformation style with gouges forming in mudstones, and granulation in porous oil-bearing sandstones. Calcite cemented breccias are present in well cemented host rocks. Pyrite and calcite mineralisation are found in association with oil. Scalability studies from the basement rocks of the Hebrides

Bird (2014)

Thesis Title - Tectono-stratigraphic Evolution of the West Orkney Basin: Implications for Hydrocarbon Exploration

Bird (2014) uses reprocessed 2D seismic reflection data from the West Orkney Basin to better understand basin development from the Devonian to the Permian. Burial history modelling is carried out in order to better constrain hydrocarbon generation, understand key risks for hydrocarbon exploration and establish the basins potential for discoveries. This project was supported by Premier Oil and formed the basis of an exploration licence and subsequent relinquishment based upon some of the conclusions of this project. The key conclusions of this study were the identification of Devonian syn-rift reservoir and source rock packages within the basin which are correlateable onshore. This is truncated by an unconformity due to Carboniferous inversion. A second phase of rifting in the Permian is identified with new faults being generated and reactivation of pre-existing structures. Extensive exhumation events have led to the removal of potentially 2.5km of Upper Triassic to Mid-Jurassic sediments and up to 1km of Upper Cretaceous sediments. Basin modelling was performed with the majority of hydrocarbons being expelled during the second phase of rifting. Major risks to a working petroleum system are seal integrity due to multiple, prolonged uplift events.

Saßnowski (2015)

Thesis Title - Palaeogeographic implications of heavy mineral and detrital zircon provenance of Devonian-Carboniferous sedimentary rocks in the North Atlantic region

Sasnowski (2015) uses heavy mineral and detrital zircon geochronology data to better understand the paleogeography and development of sedimentary basins in the North Atlantic region during the Devonian and Carboniferous. Facies analysis and sedimentary logging was carried out on sediments from the Clair and Orcadian Basins, East Greenland and Southwest Norway. The key outcomes from this study are that the Clair Basin is sourced from both local metamorphic basement and from a basin to the North and in the Northern part of the Orcadian Basin, the high proportion of Archaean basement material indicates a connection with the Clair Basin to the North and West, whereas in the Southern part of the basin sediment is largely sourced from Northern Scotland. Sediments from Norway and Greenland show largely locally derived sediment sources.

Dichiarante (2016)

Thesis Title – A reappraisal and 3D characterisation of fracture systems within the Devonian Orcadian Basin and its underlying basement: an onshore analogue for the Clair Group

Dichiarante (2017) and Dichiarante et al. (2016) through a combination of detailed fieldwork, and structural analysis, fracture analysis, and geochronology was able to reappraise the deformation history of the Orcadian Basin. The key findings of this study were the identification and study of the following distinct sets of structures related to regional scale events (Figure 1.5):

1) Devonian transtension associated with NW to NNW trending faults with typically dip-slip slickenlines with a poor component of shear and N/S trending faults with a sinistral sense of shear. These faults have little or no mineralisation or veining and minor quantities of fault gouge. This deformation can be related to regional scale transtension associated with the Devonian age development of the Orcadian Basin.

2) Late Carboniferous to Early Permian inversion associated with metre to kilometre scale N/S trending folds and thrust faults with little or no mineralisation or veining. This deformation is related to regional scale inversion and reactivation of early structures.

3) Permian to Triassic transtension associated with preferential reactivation of N trending faults. NE/SW and NNE/SSW trending faults are developed with mainly oblique dextral sense of shear and E/W trending faults with sinistral sense of shear. These faults are associated with abundant carbonate mineralisation, base metal sulphides and bitumen. This deformation is related to second basin forming event and reactivation and inversion of many earlier structures.

Despite the disparity in age of some key structures in the Orcadian Basin and in Clair Field, the study was a significant breakthrough in the understanding of the structural history of the Orcadian Basin and understanding its limitations as an analogue. Other key findings include the identification of a clear power-law distribution over 8 and 4 orders of magnitude for the fracture attributes of length and aperture. 2D fracture connectivity is highly variable, but with the best connectivity being associated with major faults and

fracture corridors. As such, a horizontal drilling orientation is recommended for the development of these sorts of rocks as a reservoir.

Bjerga (2017)

Thesis Title - The Caledonian tectonomagmatic evolution of the Orkney Islands, Scotland

Bjerga (2017) uses geochronological, geochemical and structural geological techniques to study contact relationships within the metamorphic basement and overlying Old Red Sandstone in the Orkney Isles. This work builds on that of Strachan (2003) and develops a tectonic and magmatic history for the Orkney Isles and early development of the Orcadian Basin. Metasedimentary gneisses of Moine affinity are intruded by two granites at 431±Ma and 430±Ma respectively. These ages are consistent with Scandian deformation during the Caledonian orogeny and the emplacement of Caledonian granites throughout the British Isles as result of continental collision and development of crustal melts. Both basement and the granites are cut by numerous ductile and brittle structures and reflect the processes of uplift, exhumation and erosion before deposition of the basal Devonian Hara Ebb formation and intraformational rhyolites which are dated to 390±0.41Ma.

Svebo (2018)

Thesis Title - High precision U/Pb dating of the Hoy Volcanic Member and its implications

Svebo (2018) uses a combination of fieldwork, structural analysis and geochemical techniques to better understand the deposition of the Devonian age Hoy Volcanic Member, and better place it in a regional stratigraphic context. A combination of fieldwork examining the depositional and structural relationships of the sequence, geochemical analyses and detrital zircon geochronology are employed. A Givetian age of between 381.88±0.22 Ma to 382.88±0.22 Ma for the Hoy Volcanic Member is proposed based upon these analyses with stratigraphic continuity between the Lower Eday Sandstone and not an unconformity as originally proposed.

Tang (2018)

Thesis title - Reservoir Quality Evolution in Upper Devonian Strata of the North Sea

Tang (2018) and Tang et al. (2017; 2018) working in conjunction with EnQuest, aimed to understand the regional reservoir quality distribution in the Upper Devonian sequences offshore, with particular focus on trying to understand anomalously high reservoir quality

within the Buchan Formation in the Alma Field. A combination of field analogue studies, core analysis, petrography, SEM and geochemistry was used to study offshore material and onshore samples from Caithness and Orkney. The key findings were the presence of grain coating illite/smectite formed early due to mechanical infiltration into aeolian deposits from overlying fluvial deposits. These early grain coating clays inhibited later quartz cementation during burial and preserve porosity and permeability, even at the great depths these reservoirs are now buried too. Like many other studies, carbonate cementation was common, but highly variable, and in offshore areas dolomite cements are likely sourced from the overlying Permian Zechstein dolomite.

B3: References

Astin, T.R., 1982. The Devonian geology of the Walls peninsula, Shetland. PhD Thesis, University of Durham.

Austin, J.A., Cannon, S.J.C., Ellis, D., 2014. Hydrocarbon exploration and exploitation West of Shetlands. Geol. Soc. London, Spec. Publ. 397, 1–10. doi:10.1144/SP397.13

Bird, P.C., 2014. Tectono-stratigraphic Evolution of the West Orkney Basin: Implications for Hydrocarbon Exploration. PhD Thesis, Cardiff University.

Bjerga, A.D., 2017. The Caledonian tectonomagmatic evolution of the Orkney Islands, Scotland. MSc Thesis, University of Oslo

Blackbourn, G.A., Marshall, J.E.A., 1985. The Geology of Foula, Shetland. Geological Field. Guide to Foula, Shetland. Britoil Report.

BP, 2018. Clair Ridge [WWW Document]. BP Website. URL https://www.bp.com/Clair-ridge (accessed 12.8.18).

Clifford, P., O'Donovan, A., Savory, K., Smith, G., Barr, D., 2005. Clair Field - Managing Uncertainty in the Development of a Waterflooded Fractured Reservoir. Proc. Offshore Eur. doi:10.2118/96316-MS

Coney, D., Fyfe, T.B.B., Retail, P., Smith, P.J.J., 1993. Clair appraisal: the benefits of a co-operative approach. Geol. Soc. London, Pet. Geol. Conf. Ser. 4, 1409–1420. doi:10.1144/0041409

Craigie, N.W., 1998. Chemostratigraphy of Middle Devonian lacustrine sediments in the Orcadian Basin, north-east Scotland. PhD Thesis, University of Aberdeen.

Davies, S.J., 1993. The radiochemical evolution of the Devonian Orcadian Basin, NE Scotland and comparison with coeval clastic systems from Wales, Norway and the Clair Field. PhD Thesis, University of Leicester.

Dichiarante, A.M., 2017. A reappraisal and 3D characterisation of fracture systems within the Devonian Orcadian Basin and its underlying basement: an onshore analogue for

the Clair Group. PhD Thesis, Durham University.

Dichiarante, A.M., Holdsworth, R.E., Dempsey, E.D., Selby, D., McCaffrey, K.J.W., Michie, U.M., Morgan, G., Bonniface, J., 2016. New structural and Re–Os geochronological evidence constraining the age of faulting and associated mineralization in the Devonian Orcadian Basin, Scotland. J. Geol. Soc. London. 173, 457–473. doi:10.1144/jgs2015-118

Forbes, D., 1993. Reservoir characterization and potential of the old red sandstone around the inner moray firth, NE Scotland. PhD Thesis, Durham University.

Franklin, B.J.S., 2013. Characterising fracture systems within upfaulted basement highs in the Hebridean Islands: an onshore analogue for the Clair Field. PhD Thesis, Durham University..

Henthorne, L., Wodehouse, J., Standard, W., 2012. The Science of Membrane Technology to Further Enhance Oil Recovery. Eighteenth SPE Improv. Oil Recover. Symp. SPE 154281, 14–18.

Hippler, S.J., 1993. Deformation microstructures and diagenesis in sandstone adjacent to an extensional fault: implications for the flow and entrapment of hydrocarbons. Am. Assoc. Pet. Geol. Bull. 77, 625–637.

Hippler, S.J., 1989. Fault rock evolution and fluid flow in sedimentary basins. PhD Thesis, Leeds University.

Johnston, S.C., Smith, R.I., Underhill, J.R., 1995. The Clair Discovery, west of the Shetland Isles. Scottish J. Geol. 31, 187–190.

Johnston, S.C., Spicer, P., 1995. BP Field Guide to Foula and Melby with Analogues for the Clair Field.

Maultzsch, S., Chapman, M., Liu, E., Li, X.-Y., 2007. Modelling and analysis of attenuation anisotropy in multi-azimuth VSP data from the Clair field. Geophys. Prospect. 55, 627–642. doi:10.1111/j.1365-2478.2007.00645.x

Melvin, J., 1985. Walls Formation, Western Shetland: distal alluvial plain deposits within a tectonically active Devonian basin. Scottish J. Geol. 21, 23–40. doi:10.1144/sjg21010023

Melvin, J., 1977. Sedimentological studies in upper Palaeozoic sandstones near Bude, Cornwall and Walls, Shetland. PhD Thesis, Edinburgh University.

Morton, a., Milne, a., 2012. Heavy mineral stratigraphic analysis on the Clair Field, UK, west of Shetlands: a unique real-time solution for red-bed correlation while drilling. Pet. Geosci. 18, 115–128. doi:10.1144/1354-079311-026.1354-0793/12/

Moy, D., 2010. The architecture, growth and tectono-stratigraphic significance of rift-oblique lineaments on the NE Atlantic Margin. PhD Thesis, Durham University.

Narayanasamy, R., Barr, D., Mine, A., 2010. Wellbore-Instability Predictions Within the Cretaceous Mudstones, Clair Field, West of Shetlands. SPE Drill. Complet. 25, 8–11. doi:10.2118/124464-PA

Ogilvie, S., Barr, D., Roylance, P., Dorling, M., 2015. Structural geology and well planning in the Clair Field. Geol. Soc. London, Spec. Publ. 421, 197–212. doi:10.1144/SP421.7

Owen, M.A., 1994. The controls on reservoir properties of Devonian sandstones in the Orcadian Basin, north east Scotland.

Pay, M.D., 1998. Diagenesis and reservoir quality of the Devonian-carboniferous sandstones of the Clair Field, west of Scotland, UK. PhD Thesis, University of Reading.

Pay, M.D., Astin, T.R., Parker, a., 2000. Clay mineral distribution in the Devonian-Carboniferous sandstones of the Clair Field, west of Shetland, and its significance for reservoir quality. Clay Miner. 35, 151–151. doi:10.1180/000985500546549

Phillips, G.M., 1995. Fracture cements and cementation processes in the Devonian-Carboniferous Clair group and underlying Lewisian basement, West of Shetland. University of Aberdeen

Pless, J.C., 2012. Characterising fractured basement using the Lewisian Gneiss Complex, NW Scotland: Implications for fracture systems in the Clair Field basement. PhD Thesis, Durham University.

Pless, J.C., McCaffrey, K.J.W., Jones, R.R., Holdsworth, R.E., Conway, A., Krabbendam, M., 2015. 3D characterization of fracture systems using Terrestrial Laser Scanning: an example from the Lewisian basement of NW Scotland. Geol. Soc. London, Spec. Publ. 421, 125–141. doi:10.1144/SP421.14

Qian, Z., Li, X.Y., Liu, E., 2006. Fracture characterization at clair - Analysis of P-wave azimuthal anisotropy in 2D & 3D ocean-bottom data, in: Society of Petroleum Engineers, 68th European Association of Geoscientists and Engineers Conference and Exhibition, Incorporating SPE EUROPEC 2006, EAGE 2006: Opportunities in Mature Areas. pp. 1592–1596.

Robbana, E., Buikema, T., Mair, C., Williams, D., Mercer, D., Webb, K.J., Hewson, A., Reddick, C., 2011. Low Salinity Enhanced Oil Recovery – Laboratory to Day One Field Implementation – LoSal EOR into the Clair Ridge Project. Proc. EAGE IOR Symp. Cambridge, UK 12–14. doi:10.2118/161750-MS

Sasnowski, A., 2015. Palaeogeographic implications of heavy mineral and detrital zircon provenance of Devonian-Carboniferous sedimentary rocks in the North Atlantic region. PhD Thesis, Royal Holloway University of London.

Sircar, A., 2004. Hydrocarbon production from fractured basement formations. Curr. Sci. 87, 147–151.

Sleight, J.M., 2001. Fracture characteristics from two reactivated basement fault zones:

examples from Norway and Shetland. PhD Thesis, Durham University.

Slightam, C., 2012. Characterizing seismic-scale faults pre- and post-drilling; Lewisian Basement, West of Shetlands, UK. Geol. Soc. London, Spec. Publ. 374. doi:10.1144/SP374.6

Smith, P.J., Daly, M., Stump, M., 1995. The Paradox of a New Oil Province - Foinaven and Clair. doi:10.2118/30354-MS

Speed, R.G., 1999. Kerogen variation in a Devonian half graben system. PhD Thesis, University of Southampton.

Stewart, R.C.S., Huyghues-Despointes, T., Henry, W.J., 1991. The impact of modern interpretation techniques on the evaluation of the Clair discovery, west of Shetlands, UKCS. 61st Ann. Internat. Mtg 268–270.

Strachan, R.A., 2003. The metamorphic basement geology of Mainland Orkney and Graemsay. Scottish J. Geol. 39, 145–149.

Svebo, J.R., 2018. High precision U/Pb dating of the Hoy Volcanic Member and its implications. MSc Thesis, University of Oslo

Tang, L.-X., Gluyas, J., Jones, S., Bowen, L., 2018. Diagenetic and geochemical studies of the Buchan Formation (Upper Devonian) in the Central North Sea. Pet. Sci. 1–19.

Tang, L., 2018. Reservoir Quality Evolution in Upper Devonian Strata of the North Sea. PhD Thesis, Durham University.

Tang, L., Gluyas, J., Jones, S., 2018. Porosity preservation due to grain coating illite/smectite: evidence from Buchan Formation (Upper Devonian) of the Ardmore Field, UK North Sea. Proc. Geol. Assoc.

Tang, L., Jones, S.J., Gluyas, J., 2017. Facies architecture of the Fluvial-Aeolian Buchan formation (Upper Devonian) and its implications on field exploration: a case study from Ardmore Field, Central North Sea, UK. Int. J. Geosci. 8, 902–924.

Walker, R., 2010. The structural evolution of the Faroe Islands, NE Atlantic margin. PhD Thesis, Durham University.

Walker, R.J., Holdsworth, R.E., Imber, J., Ellis, D., 2011. The development of cavities and clastic infills along fault-related fractures in Tertiary basalts on the NE Atlantic margin. J. Struct. Geol. 33, 92–106. doi:http://dx.doi.org/10.1016/j.jsg.2010.12.001

Watts, L.M., 2001. The walls boundary fault zone and the Møre Trøndelag fault complex:: a case study of two reactivated fault zones. PhD Thesis, Durham University.

Watts, L.M., Holdsworth, R.E., Sleight, J. a., Strachan, R. a., Smith, S. a. F., 2007. The movement history and fault rock evolution of a reactivated crustal-scale strike-slip fault: the Walls Boundary Fault Zone, Shetland. J. Geol. Soc. London. 164, 1037–1058. doi:10.1144/0016-76492006-156

Webster, M., 2018. Clair Phase 1: The Evolving Development of a Complex Fractured Field, in: Abu Dhabi International Petroleum Exhibition & Conference. Society of Petroleum Engineers.

Wilson, A.O., 2012. A high-resolution record of environmental and climatic change in a lacustrine sequence from the Devonian Orcadian Basin, Scotland. PhD Thesis, University of Aberdeen.

Wilson, R.W., 2006. Digital fault mapping and spatial attribute analysis of basement-influenced oblique extension in Passive margin settings. PhD Thesis, Durham University.

Wilson, R.W., Holdsworth, R.E., Wild, L.E., Mccaffrey, K.J.W., England, R.W., Imber, J., Strachan, R. a., 2010. Basement-influenced rifting and basin development: a reappraisal of post-Caledonian faulting patterns from the North Coast Transfer Zone, Scotland. Geol. Soc. London, Spec. Publ. 335, 795–826. doi:10.1144/SP335.32

Wilson, R.W., Klint, K.E.S., Gool, J. a M. Van, Mcca, K.J.W., Holdsworth, R.E., Chalmers, J. a, 2006a. Faults and fractures in central West Greenland : onshore expression of continental break-up and sea-floor spreading in the Labrador – Baffin Bay Sea. Geol. Surv. Denmark Greenl. Bull. 11, 185–204.

Wilson, R.W., McCaffrey, K.J.W., Holdsworth, R.E., Imber, J., Jones, R.R., Welbon, A.I.F., Roberts, D., 2006b. Complex fault patterns, transtension and structural segmentation of the Lofoten Ridge, Norwegian margin: Using digital mapping to link onshore and offshore geology . Tectonics 25, TC4018. doi:10.1029/2005TC001895

Appendix C - Sample Information, Data Tables, Analytical Results and Other Methods

C1-Paleostress Inversion

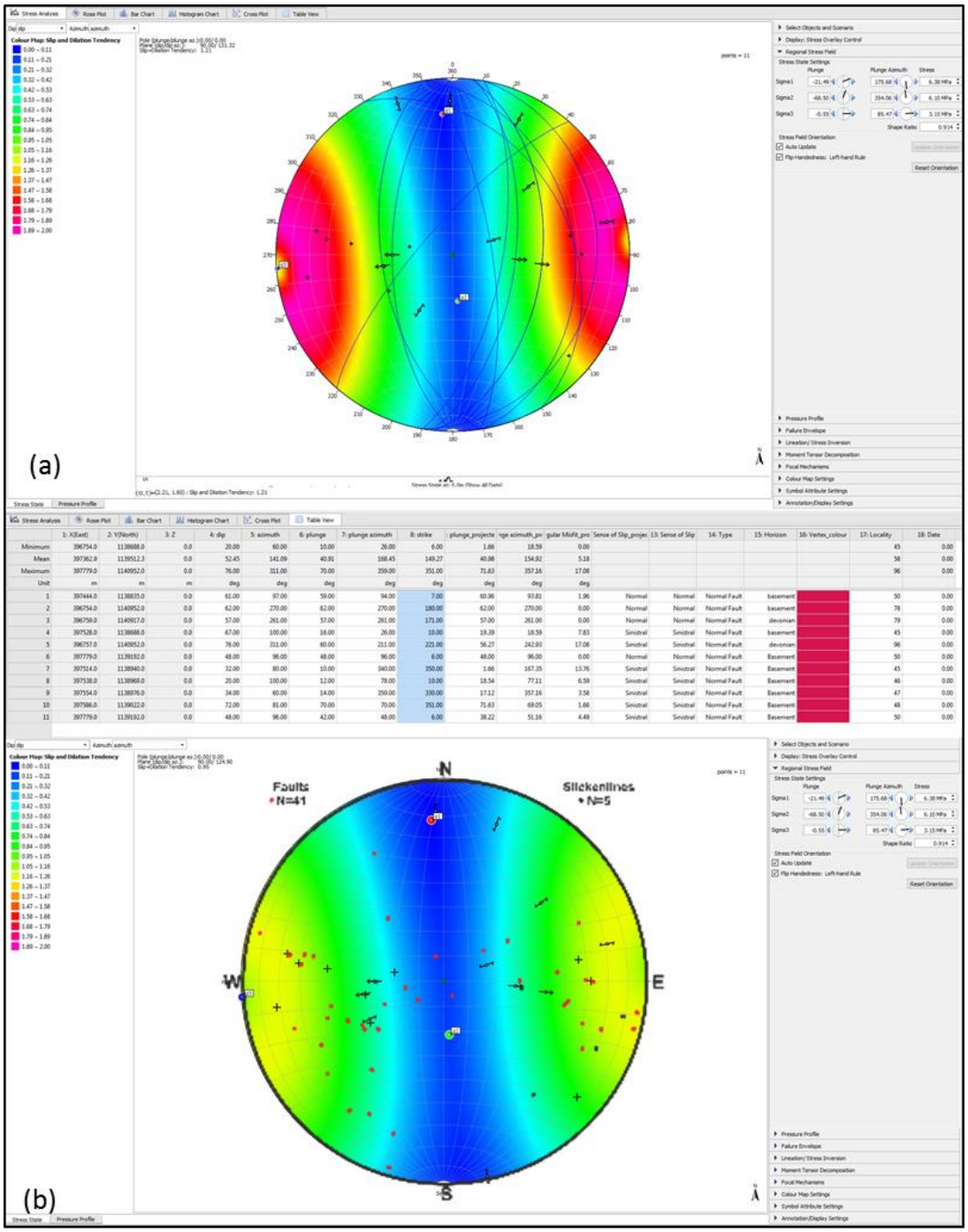

Figure C1: (a) Stress inversion for faults on Foula. (b) Slip and dilation tendency for basement faults on Foula.

C2-Sample Information

Sample No	Original Sample No	Location No	Sheet	X	Y	Field Season	Area	Rock Type Age	Analysis Done
REC-021	REC021	21	HU	443262	1135375	Easter 2016	East Voe	Devonian	Thin Section+QS
REC-031	REC031	31	HT	397744	1139114	Easter 2016	Foula	Basement	
REC-035	REC035	35	HT	397539	1138642	Easter 2016	Foula	Basement	Thin Section
REC-050	REC050	50	HU	428379	1158002	Easter 2016	Walls	Basement	Thin Section+QS
P17-036	036	036	ND	326036	974464	Spring 2017	Caithness	Devonian	Thin Section+QS
P17-036A	036A	036	ND	326036	974464	Spring 2017	Caithness	Devonian	
P17-036B	036B	037	ND	326036	974464	Spring 2017	Caithness	Devonian	
S16-021A	021A	21	HT	397092	1138306	Summer 2016	Foula	Devonian	
S16-021B	021B	21	HT	397092	1138306	Summer 2016	Foula	Devonian	
S16-024	024	24	HT	397412	1138120	Summer 2016	Foula	Devonian	Thin Section+QS
S16-030	030	30	HT	395046	1137987	Summer 2016	Foula	Devonian	Heavy Mineral
S16-036A	036A	36	HT	396524	1136578	Summer 2016	Foula	Devonian	Thin Section + QS
S16-036B	036B	36	HT	396524	1136578	Summer 2016	Foula	Devonian	Thin Section + Heavy Mineral
S16-036C	036C	36	HT	396524	1136578	Summer 2016	Foula	Devonian	Heavy Mineral
S16-037	037	37	HT	396458	1136635	Summer 2016	Foula	Devonian	Thin Section+QS
S16-040	040	40	HT	396051	1137126	Summer 2016	Foula	Devonian	Heavy Mineral
S16-050	050	50	HT	397444	1138835	Summer 2016	Foula	Basement	
S16-054A	054A	54	HT	397210	1136906	Summer 2016	Foula	Devonian	Heavy Mineral
S16-054B	054B	54	HT	397210	1136906	Summer 2016	Foula	Devonian	Heavy Mineral
S16-067A	067A	67	HT	396618	1136207	Summer 2016	Foula	Devonian	Heavy Mineral
S16-067B	067B	67	HT	396618	1136207	Summer 2016	Foula	Devonian	
S16-069	069	69	HT	397543	1138543	Summer 2016	Foula	Basement	Thin Section + QS

S16-072A	072A	72	HT	397598	1139049	Summer 2016	Foula	Basement	
S16-072B	072B	72	HT	397598	1139049	Summer 2016	Foula	Basement	Thin Section
S16-073	073	73	HT	397600	1139056	Summer 2016	Foula	Basement	
S16-078A	078A	78	HT	396754	1140952	Summer 2016	Foula	Basement	Thin Section + QS
S16-078B	078B	78	HT	396754	1140952	Summer 2016	Foula	Basement	Thin Section + QS
S16-093A	093A	93	HT	397038	1141252	Summer 2016	Foula	Basement	Thin Section
S16-093B	093B	93	HT	397038	1141252	Summer 2016	Foula	Basement	Thin Section
S16-102	102	102	HT	397330	1140652	Summer 2016	Foula	Basement	Thin Section + QS
S16-110A	110A	110	HU	452505	1139864	Summer 2016	Bressay	Devonian	Thin Section+QS+Re/Os
S16-110B	110B	110	HU	452505	1139864	Summer 2016	Bressay	Devonian	Thin Section + QS
S16-110C	110C	110	HU	452505	1139864	Summer 2016	Bressay	Devonian	Thin Section + QS
S16-111A	111A	111	HU	452522	1139933	Summer 2016	Bressay	Devonian	Thin Section + QS
S16-113A	113A	113	HU	452571	1140004	Summer 2016	Bressay	Devonian	Thin Section +QS
S16-113B	113B	113	HU	452571	1140004	Summer 2016	Bressay	Devonian	Thin Section + QS+Re/Os
S16-113C	113C	113	HU	452571	1140004	Summer 2016	Bressay	Devonian	
S16-113D	113D	113	HU	452571	1140004	Summer 2016	Bressay	Devonian	Re/Os
S16-117	117	117	HU	442916	1126922	Summer 2016	S Shetland	Basement	Thin Section + QS
S16-118	118	118	HU	441525	1121538	Summer 2016	S Shetland	Devonian	
S16-120	120	120	HU	441618	1121485	Summer 2016	S Shetland	Devonian	
S16-122A	122A	122	HU	436401	1111277	Summer 2016	Garths Ness	Devonian	
S16-122B	122B	122	HU	436401	1111277	Summer 2016	Garths Ness	Devonian	
S16-128A	128A	128	HU	416630	1150180	Summer 2016	Melby	Devonian	Thin Section + QS
S16-128B	128B	128	HU	416630	1150180	Summer 2016	Melby	Devonian	
S16-128C	128C	128	HU	416630	1150180	Summer 2016	Melby	Devonian	Heavy Mineral
S16-128D	128D	128	HU	416630	1150180	Summer 2016	Melby	Devonian	Heavy Mineral

S16-134A	134A	134	HU	426223	1183729	Summer 2016	Esha Ness	Devonian	
S16-134B	134B	134	HU	426223	1183729	Summer 2016	Esha Ness	Devonian	
S16-136	136	136	HU	426297	1183775	Summer 2016	Esha Ness	Devonian	
S16-137A	137A	137	HU	426252	1183779	Summer 2016	Esha Ness	Devonian	
S16-137B	137B	137	HU	426252	1183779	Summer 2016	Esha Ness	Devonian	
S16-139	139	139	HU	426540	1179282	Summer 2016	Esha Ness	Devonian	Heavy Mineral
S16-141A	141A	141	HU	424118	1156862	Summer 2016	Walls	Basement	
S16-143A	143A	143	HU	443325	1125945	Summer 2016	S Shetland	Basement	
S16-143B	143B	143	HU	443325	1125945	Summer 2016	S Shetland	Basement	
S17-004A	004A	004	HU	416667	1156019	Summer 2017	Melby	Devonian	
S17-004B	004B	004	HU	416667	1156019	Summer 2017	Melby	Devonian	
S17-004C	004C	005	HU	417385	1155455	Summer 2017	Melby	Devonian	
S17-011	011	011	HU	416909	1156685	Summer 2017	Melby	Devonian	Heavy Mineral
S17-043A	043A	043	HT	395445	1140631	Summer 2017	Foula	Devonian	
S17-043B	043B	043	HT	395445	1140631	Summer 2017	Foula	Devonian	
S17-044A	044A	044	HT	395581	1140694	Summer 2017	Foula	Devonian	Heavy Mineral
S17-044B	044B	044	HT	395581	1140694	Summer 2017	Foula	Devonian	Heavy Mineral
S17-051A	051A	051	HT	397790	1139225	Summer 2017	Foula	Basement	Thin Section+QS+Re/Os
S17-051B	051B	051	HT	397790	1139225	Summer 2017	Foula	Basement	Thin Section+QS+Re/Os
S17-052A	052A	052	HT	397806	1139277	Summer 2017	Foula	Basement	Thin Section+QS+Re/Os

Table C1: Sample Information and Location

C2-Re/Os Geochronology

Selected samples were analysed utilising Rhenium-Osmium (Re-Os) geochronology in the Source Rock and Sulfide Geochronology and Geochemistry Laboratory, Durham University. Pyrite and/or chalcopyrite from fault rock samples was isolated from the host material by crushing to approximately <5mm grain size before being sieved through 210 micron (70 US Mesh) and 74 micron (200 US Mesh) sieves. If an insufficient quantity of sample was obtained the coarsest fraction (>5mm) was crushed further, or was isolated from the carbonate host sample by dissolution in HCL acid. Samples were then washed and dried before isolation using traditional techniques (hand picking, magnetic and/or heavy liquid separation) and further cleaning with HCL to remove oxidation. Samples then underwent a Re test to ascertain if further analysis was possible. Samples yielding less than 100 ppt are unlikely to yield reliable results and unfortunately the samples collected from Shetland had insufficient quantities of Re to yield reliable results. The samples from Foula contained sufficient Re, but priority for funding was given to zircon geochronology.

Sample Number	Re (ppb)	Re (ppt)
051 (Foula Basement Faults)	29	29000
052 (Foula Basement Faults)	8.1	8100
110A (Shetland Steep Belt	0.023	23
113B (Shetland Steep Belt)	0.11	110
113D (Shetland Steep Belt)	0.021	21

Table C2: Results of Re abundance test.

C3-Heavy Mineral Analysis

Sample No	Formation	Comments
S16-030	Daal Sandstone	Thickly(~1m) bedded, M/C sandstone, grey/buff, well sorted, sub rounded with pebbly layers. XB and TXB.
S16-036C	Daal Sandstone	Thickly(~1m) bedded, M/C sandstone, grey/buff, well sorted, sub rounded. Faint XB.
S16-036B	Daal Sandstone	Thickly(~1m) bedded, M/C sandstone, grey/buff, well sorted, sub rounded. Faint XB.
S16-040	Daal Sandstone	M/C sandstone interbedded with thin beds of fine sandstone. XB and TXB, Buff to yellow.
S16-054A	Sneug Sandstone	M/C sandstone, mod well sorted, sub angular to sub rounded. Grey to pink. Faint XB
S16-054B	Sneug Sandstone	M/C sandstone, mod well sorted, sub angular to sub rounded. Grey to pink. Faint XB
S16-067A	Noup Sandstone	C grained sandstones, mod/poor sorting. Immature. Large scale XB and TXB. Pebbly/cobbly lags.
S17-044A	Soberlie Sandstone	M grained, well sorted, sub angular sandstone. Grey to buff grey, micaceous. XB to TXB.
S17-044B	Soberlie Sandstone	M grained, well sorted, sub angular sandstone. Grey to buff grey, micaceous. XB to TXB.
S16-128C	Melby Sandstone	F to VC sandstone,fining up grading, mod sorting, sub rounded, buff to pink, ~10cm beds, mud cracks. Coarse lags. Some large XB, mostly bedded.
S16-128D	Melby Sandstone	M to VC sandstone,graded, mod sorting, sub rounded, buff to pink, ~10cm beds, mud cracks. Coarse lags.
S17-011	Melby Sandstone	M to C sandstone, well sorted, buff to yellow. Qtz rich, with fdspr. XB and planar thinner interbeds above.
S16-139	Melby Sandstone	M sandstone, angular/sub angular to sub rounded, mod sorting, pinky/red. <10cm beds.

Table C3: Heavy Mineral Sample Information

Sample No	detrital non-opaque heavy minerals	Opaques	Goethite/ Hematite	Carbonate	Anatase (authigenic)	Mica+ Chlorite	Total
S16-030	5	16	64	9		6	100.0
S16-036C	30	38	2		3	27	100.0
S16-036B	34	30	8		5	23	100.0
S16-040	11	71	10		5	3	100.0
S16-054A	7	30	41		1	21	100.0
S16-054B	3	19	48			30	100.0
S16-067A	35	43	4		3	15	100.0
S17-044A	48	2	6		3	41	100.0
S17-044B	43	6	9		2	40	100.0
S16-128C	5	19	32			44	100.0
S16-128D	30	13	32			25	100.0
S17-011	58	2	7			33	100.0
S16-139	1	26	50	1		22	100.0

Table C4: Heavy Mineral Analysis Results

ATi	**apatite:tourmaline index**	**% apatite in total apatite plus tourmaline**
GZi	garnet:zircon index	% garnet in total garnet plus zircon
RuZi	rutile:zircon index	% rutile in total rutile plus zircon
MZi	monazite:zircon index	% monazite in total monazite plus zircon
CZi	chrome spinel:zircon index	% chrome spinel in total chrome spinel plus zircon
SZi	staurolite:zircon index	% staurolite in total staurolite plus zircon
UTi	unstables:tourmaline index	% unstables in total unstables plus tourmaline
unst	unstables	% epidote plus titanite
ARi	apatite roundness index	% rounded apatite in apatite population

Table C5: Heavy Mineral Index Calculations

Sample No	S16-067A	S16-030	S16-036C	S16-036B	S16-040	S16-054A	S16-054B	S17-044A	S17-044B	S16-128C	S16-128D	S17-011	S16-139
Area	Foula	Foula	Foula	Foula	Foula	Foula	Foula	Foula	Foula	Melby	Melby	Melby	Esha Ness
Unit	Noup Fm	Daal Fm	Daal Fm	Daal Fm	Daal Fm	Sneug Fm	Sneug Fm	Soberlie Fm	Soberlie Fm	Melby Fm	Melby Fm	Melby Fm	Melby Fm
Anatase		R			1.5		0.5	R		R		R	0.5
Apatite	52.0	43.0	40.0	33.0	1.0	60.5	57.5	16.0	13.5	31.5	13.0	37.5	36.5
Calcic Amphibole									1.5				
Chrome Spinel			R	R	0.5			0.5	R				R
Epidote							R		1.5				
Garnet		0.5	6.0					27.0	36.5	56.5	77.0	38.0	41.5
Monazite		1.0	0.5	R	2.5	1.0		1.0	0.5	0.5	0.5	1.5	
Rutile	R	4.5	1.0	2.5	7.5	4.5	4.0	7.0	5.5	1.5	0.5	3.5	4.5
Titanite									R				
Staurolite											1.0		
Tourmaline	12.5	13.5	9.5	7.5	12.0	12.0	17.0	21.5	13.0	4.5	0.5	6.5	3.5
Zircon	35.5	37.5	43.0	57.0	75.0	22.0	21.0	27.0	28.0	5.5	7.5	13.0	13.5
Total	100.0	100.0	100.0	100.0	100.0	100.0	100.0	100.0	100.0	100.0	100.0	100.0	100.0
Count	200	200	200	200	200	200	200	200	200	200	200	200	200

Sample No	Area	Group	Formation	ATi	tot	GZi	tot	RuZi	tot	MZi	tot	CZi	tot	SZi	tot	UTi	tot	unst	ARi	tot
S16-030	Foula	Foula Sandstone	Daal Sandstone	76.0	200	1.0	200	11.5	22	1.5	200	0.0	200	0.0	200	0.0	100	0.0	0.0	100
S16-036C	Foula	Foula Sandstone	Daal Sandstone	84.5	200	1.5	200	2.9	60	1.0	200	0.5	200	0.0	200	0.0	500	0.0	3.0	100
S16-036B	Foula	Foula Sandstone	Daal Sandstone	82.0	200	0.0	200	3.4	70	1.0	200	0.5	200	0.0	200	0.0	500	0.0	9.0	100
S16-040	Foula	Foula Sandstone	Daal Sandstone	15.0	100	0.0	200	9.5	220	3.4	200	0.5	200	0.0	100	0.0	500	0.0	5.0	200
S16-054A	Foula	Foula Sandstone	Sneug Sandstone	85.0	200	0.0	100	11.5	110	2.0	200	0.0	100	0.0	100	0.0	500	0.0	3.0	100
S16-054B	Foula	Foula Sandstone	Sneug Sandstone	77.0	200	0.0	100	15.3	110	0.0	100	0.0	100	0.0	100	0.0	500	0.0	3.0	100
S16-067A	Foula	Foula Sandstone	Noup Sandstone	79.5	200	0.0	200	0.5	200	0.0	200	0.0	200	0.0	200	0.0	500	0.0	2.0	100
S17-044A	Foula	Foula Sandstone	Soberlie Sandstone	49.0	200	54.5	220	15.3	230	3.4	200	1.0	200	0.0	200	0.0	100	0.0	2.0	100
S17-044B	Foula	Foula Sandstone	Soberlie Sandstone	38.5	200	59.8	240	17.7	240	2.4	200	0.5	200	0.0	200	8.0	100	1.5	1.0	100
S16-128C	Melby	St Magnus Bay	Melby Sandstone	88.5	200	92.2	210	13.0	110	5.7	100	0.0	100	0.0	100	0.0	250	0.0	6.0	100
S16-128D	Melby	St Magnus Bay	Melby Sandstone	94.0	200	90.5	220	12.3	110	3.8	100	0.0	100	2.4	200	0.0	250	0.0	12.0	100
S17-011	Melby	St Magnus Bay	Melby Sandstone	85.5	200	74.3	200	22.2	250	5.7	210	0.0	200	0.0	200	0.0	500	0.0	1.0	100
S16-139	Esha Ness	St Magnus Bay	Melby Sandstone	88.0	100	76.3	170	29.3	580	0.0	410	2.4	420	0.0	410	0.0	250	0.0	2.0	100

Table C6: Heavy Mineral Analysis Results

C4-QEMSCAN ANALYSIS

Sample No	078A	111A	111A-182	111A-183	117-13	REC021	036A	37	REC050	69	102	110B	110C	113B	128A	P17036	S16024A	S16110A	S16110C	S16113A	S17051A	S17051B	S17052A
Background/porosity	0.43	5.28	1.82	6.16	0.29	0.08	4.08	7.74	0.29	1.93	0.1	1.24	1.12	2.07	7.61	16.8	3.57	3.68	1.79	3.43	1.37	2.69	3.87
Quartz	52.49	34.14	40.9	25.04	61.3	31.38	75.78	82.31	18.58	28.65	21.02	50.31	31.05	21.18	71.01	51.96	30.35	23.84	40.29	69.35	3.69	4.3	13.39
Plagioclase	32.94	30.13	25.33	6.8	0	24.63	4.26	1.36	11.04	44.77	67.33	2.38	2.21	1.3	12.05	12.29	41.64	0.92	2.14	0.08	43.26	33.56	16.94
K-Feldspar	2.9	0.14	0.04	0.01	0.05	2.18	12.83	11.14	2.67	3.45	8.72	0	0.01	0.04	11.14	7.29	16.38	0.02	0	0.01	1.04	17.96	4.62
Calcite	1.1	13.48	7.82	16	0.18	2.1	0.01	0.01	58.44	0.01	0	5.53	17.84	0.01	0.01	0.18	0	2.12	4.66	0	11.24	1.44	6.74
Dolomite	0.04	5.21	5.93	16.72	1.37	0.3	0	0	2.56	0	0	19.14	21.24	0	0	6.57	0	22.34	28.71	0.16	0.19	0.04	0.29
Siderite / Fe-oxides	0.15	0.22	0.1	0.2	0	0.47	0	0	0.01	0.07	0.02	0.07	0.03	0.01	0	0	0	0.03	0.01	0.01	0.11	0.07	0.09
Dolomite-Fe / Ankerite	0	11.14	15.45	32.07	31.64	0.01	0	0	0.11	0	0	17.97	23.61	0	0	8.19	0	38.32	16.16	4.58	0	0	0
Other carbonates	0	0.34	0.2	0.44	0.04	0	0	0	0	0	0	2.64	2.42	0	0	0	0	0.24	1.13	0	0	0	0
Illite	0.23	1.13	1.1	0.27	1.43	0.63	1.4	1.64	0.24	1.65	0.29	0.21	0.39	2.4	1.03	3.64	1.63	0.71	0.19	1.3	0.04	0.12	0.01
Illite-Fe / Glauconite	0.12	0.15	0.16	0.04	0.12	0.53	2.89	1.14	0.01	1.75	0.12	0.09	0.07	0.33	2.56	1.49	1.97	0.34	0.04	0.32	0.02	0.11	0.04
Glauconite	0.01	0	0	0	0	0.02	0.01	0	0	0.02	0	0	0	0	0.01	0	0.01	0	0	0	0	0.02	0.01
Smectite	0.38	0.17	0.16	0.06	0	0.48	0.06	0.03	0.05	0.42	0.61	0.17	0.12	0.02	0.13	0.64	1.15	0.04	0.23	0.01	0.38	0.78	0.38
Chlorite total	7.64	0.02	0.01	0	0.01	33.76	0.26	0.04	4.41	1.24	1.1	0.04	0.04	0.03	0.32	0.24	0.44	0	0.06	0.01	2.68	0.89	2.73
Kaolinite total	0	0.03	0.02	0.03	0	0	0.09	0.76	0	0.12	0	0	0	0.03	0.1	1.04	0.03	0	0	0	0	0	0
Muscovite	0.08	1.56	1.5	0.28	3.07	0.2	0.73	0.91	0.08	1.24	0	0.02	0.06	32.14	0.47	0.58	0.25	0.86	0.03	14.9	0.08	0.07	0.01
Biotite	0.5	0.07	0.04	0.02	0.03	1.11	1.15	0.31	0.1	11.68	0.31	0.05	0.03	0.19	0.55	0.56	4.94	0.05	0.02	0.05	0.08	0.53	0.15
Pyrite	0.03	0	0.01	0	0.38	0	0	0	0.07	0.01	0	0.01	0.03	41.04	0	2.23	0	0.17	0.03	6.66	0.01	0.26	14.55
Chalcopyrite	0	0	0	0	0	0	0	0	0	0	0	0	0	0	0	0	0	1.99	0	0	0	0	0
Rutile	0.45	0.13	0.24	0.04	0.1	0.61	0.15	0.05	0.16	0.39	0.05	0.01	0.01	0.6	0.08	0.18	0.16	0.02	0.02	0.12	0.45	1.03	2.71
Ilmenite	0	0	0	0	0	0.01	0.01	0	0	0.01	0	0	0	0	0.02	0	0	0	0	0	0	0	0
Fe Oxides	0.17	0.05	0.03	0.01	0	0.43	0.03	0.01	0.02	0.19	0.14	0.01	0.01	0.1	0	0	0.09	0.06	0.01	0.02	0.45	0.26	1.05
Zircon	0.03	0	0.01	0	0	0	0.02	0	0.01	0.02	0.01	0	0	0.02	0.01	0.01	0.01	0	0	0	0	0	0.05
Apatite	0.35	0.07	0.08	0.04	0.06	0.35	0.05	0	0.25	0.19	0.05	0.06	0.07	0.19	0.05	0.17	0.17	0.06	0.1	0.12	0.37	0.25	0.91
Dawsonite	0	0	0	0	0	0	0	0	0	0	0	0	0	0	0	0	0	0	0	0	0	0	0
Gypsum / Bassanite / Anhydrite	0	0	0	0	0.01	0	0	0	0	0	0	0.01	0.01	0.01	0	0.27	0	0.03	0.02	0	0	0	0.07
Barite	0	0	0	0	0	0	0	0	0	0.01	0	0	0	0	0	0	0	0	0	0	0	0	0
Epidote	0.02	0.01	0	0	0	0.01	0	0	0.12	3.61	0	0.01	0.01	0	0	0	0	0	0.01	0	27.56	5.16	12.4
Titanite/Rutile	0	0	0	0	0	0	0	0	0.32	0	0	0	0	0	0	0	0	0	0	0	0.36	0.84	1.62
Diopside	0	0.01	0.01	0	0	0	0	0	0.03	0	0	0	0	0	0	0.05	0	0.02	0.01	0	4.77	4.86	6.65
Magnesiohornblende	0	0	0	0	0	0	0	0	0.02	0	0	0	0	0	0	0	0	0	0	0	0.67	2.84	1.97
Ferrohornblende	0	0	0	0	0	0.02	0	0	0.02	0	0	0.07	0.03	0	0	0.03	0	0	0.04	0	0.02	15.61	1.93
Actinolite	0	0	0	0	0	0	0	0	0.16	0	0	0	0	0	0	0	0	0	0	0	0.16	2.86	0.27
Others	0.04	0.06	0.03	0.01	0.01	0.03	0.07	0.08	0	0.09	0.01	0.02	0.01	0.05	0.07	0.14	0.06	0.01	0	0.01	0.02	0.02	0.02
Salts / 'salt muds'	0.05	0.07	0.03	0.06	0.1	0.08	0.12	0.12	0.2	0.14	0.08	0.09	0.22	0.19	0.05	0	0.22	0.05	0.04	0.14	0.05	0.03	0.02
Unclassified	0.26	1.64	0.8	1.83	0.09	0.65	0.1	0.08	0.33	0.27	0.12	1.05	0.45	0.12	0.33	2.24	0.48	7.72	6.05	2.12	2.29	6.1	10.39

Table C7: Results of QEMSCAN Analysis

C5-Detrital Zircon Geochronology

Laboratory and Sample Preparation	
Laboratory name	Geography, Geology and Environment, University of Hull
Sample type/mineral	zircons mounted in resin
Sample preparation	Polished sections
Imaging	None

Laser ablation system	
Make, Model and type	Applied Spectra, RESOlution-SE 193nm
Ablation cell and volume	Laurin Technic S155 two volumn cell
Laser wavelength	193 nm
Pulse width (ns)	5 ns
Fluence (J cm-2)	2.5 J sm-2
Repition rate (Hz)	10 Hz
Ablation duration (s)	30s
Spot diameter	30 microns
Sample mode/pattern	Static spot ablation
Carrier gas	He + N2 in the cell, Ar carrier gas to torch

ICP-MS Instrument	
Make, Model and type	Agilent 8800
Sample introdution	Ablation aerosol mixed with Ar and sent to ICP-Ms
RF power (w)	1170 W
Nebuliser gas flow	Ar 0.86 l min-1
Detection system	Electron multiplier in counts per second mode
Masses measured	204, 206, 207, 208, 232, 235, 238
Integration time	208, 235, 232 = 0.01; 204, 238 = 0.015; 206, 207 = 0.025

Data Processing	
Calibration strategy	Plešovice used as primary reference material, 91500 and 612 used as secondaries/validation
Reference Material Information	(See Standard Ref Sheets) 91500 (Wiedenbeck et al. 1995) Plešovice (Sláma et al. 2008)
Data processing package	Iolite v3, Data Reduction Scheme - X_U_Pb_Geochron4 (Paton et al., 2011)
Common Pb correction	No common Pb correction applied to this data

Table C8: Analytical standards and settings used for zircon geochronology

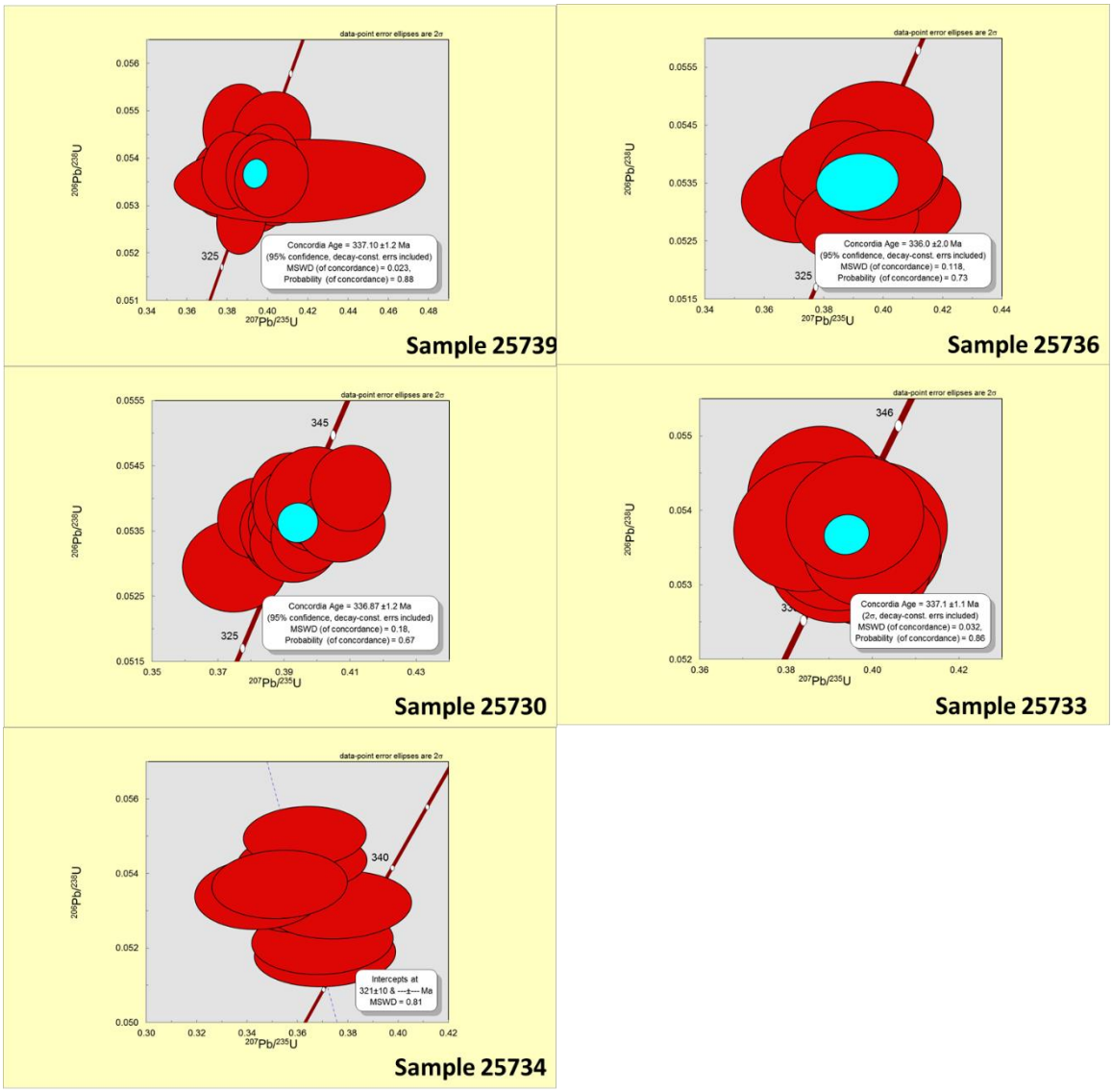

Figure C2: Concordia diagrams for Plesovice zircon standard

Sample	Hg204 CPS	Pb206 CPS	Pb208 CPS	Th232 CPS	U235 CPS	U238 CPS	Weighted Terra-Wasserburg plot $^{207}Pb/^{206}Pb$	2σ	$^{206}Pb/^{238}U$	2σ	Error Correlation 5_38 vs7_45	$^{254}U/^{206}Pb$	2σ	$^{207}Pb/^{206}Pb$	2σ	Error Correlation 38/6 vs 7/6	Final $^{206}Pb/^{238}U$	2σ	Final Age $^{207}Pb/^{235}U$	2σ	Final Age $^{206}Pb/^{238}U$	2σ	Final Age $^{207}Pb/^{206}Pb$	2σ	Approx U ppm	2σ	Approx Th ppm	2σ	Approx Pb ppm	2σ	Final U/Th Ratio	2σ	Preferred Age	Calculated Discordance 6-38/7-6	6-38/7-35
HM25739_154	91200	29150	14900	167300	3540	416000	2.67900	0.07900	2.27400	0.06410	0.10	4.66	0.09	0.08	0.00	0.20	4.24	0.08	1248	20	1220	21	1213	67	33600	2400	187.00	4.60	59.40	2.20	200.00	20.00	1213	-3.8	-1.3
HM25739_97	264400	29320	49500	512000	5220	1021000	2.61700	0.07000	0.15800	0.00340	0.15	5.03	0.09	0.08	0.00	0.27	1.46	0.04	1148	12	1146	18	1076	67	19000	1300	187.00	4.60	59.40	2.20	180.00	8.90	1146	-4.4	-1.6
HM25739_107	123100	11450	21470	375000	5430	752000	2.62400	0.04900	0.15930	0.00230	0.15	5.12	0.06	0.08	0.00	0.35	-0.09	0.34	1112	15	1140	12	1065	48	73200	1400	267.10	5.30	105.00	1.30	196.40	8.10	1140	-8.3	-3.3
HM25739_5	279800	38600	36500	446200	6240	1051000	2.71700	0.05600	0.23900	0.00270	0.07	4.17	0.05	0.08	0.00	0.32	-0.52	0.02	1325	15	1384	14	1280	42	66400	1700	268.30	7.40	198.70	5.40	499.00	18.00	1280	-8.1	-4.5
HM25739_88	590000	59400	73000	967000	17900	2800000	2.62400	0.04500	0.19530	0.00230	0.15	5.12	0.06	0.08	0.00	0.40	-0.09	0.34	1112	15	1149	12	1065	48	73200	1400	267.10	5.30	105.00	1.30	196.40	8.10	1149	-8.3	-1.8
HM25739_8	373600	45460	98200	1152000	8730	1357000	2.62200	0.07300	0.23070	0.00360	0.22	3.29	0.04	0.08	0.00	0.34	-0.20	0.01	1635	14	1711	17	1587	34	78700	2400	203.20	5.90	336.80	5.00	1079.00	22.00	1587	-7.8	-4.6
HM25739_109	139200	13310	20700	298000	5780	823900	2.62400	0.05900	0.23060	0.00310	0.11	3.26	0.03	0.10	0.00	0.27	-1.32	0.07	1637	11	1717	15	1599	27	198700	4400	442.00	12.00	120.20	2.20	352.00	12.00	1599	-7.4	-4.9
HM25739_102	409700	7270	32500	331400	1660	264000	2.62400	0.06700	0.23480	0.00270	0.10	3.08	0.03	0.10	0.00	0.45	-0.37	0.01	1742	12	1814	13	1690	30	118800	1900	282.90	4.30	248.30	3.60	751.00	18.00	1690	-7.3	-4.1
HM25739_33	1053000	110800	48700	608800	26300	3963000	2.62400	0.08600	0.30190	0.00400	0.14	3.31	0.04	0.10	0.00	0.42	-0.51	0.31	1652	17	1697	20	1584	42	67200	3700	180.00	11.00	78.70	1.20	261.00	10.00	1584	-7.1	-2.7
HM25739_50	3255000	364400	58900	684000	16730	2387000	3.02800	0.05600	0.24940	0.00240	0.04	4.01	0.04	0.09	0.00	0.27	-0.91	0.04	1399	13	1435	12	1343	36	106400	1300	269.50	3.40	129.10	2.40	311.00	10.00	1343	-6.9	-2.6
HM25739_48	24680	3900	7600	107000	513	145100	5.02000	0.11000	0.33700	0.00500	0.11	2.97	0.04	0.11	0.00	0.34	-0.39	0.02	1798	17	1868	24	1753	41	57500	2400	139.60	5.60	465.00	21.00	1753	-6.6	-3.9
HM25739_46	74200	9770	15700	137100	1550	258000	2.95800	0.04300	0.24540	0.00200	-0.02	4.07	0.03	0.09	0.00	0.13	-0.79	0.03	1386	10	1414	10	1391	30	206900	2000	526.00	5.70	237.50	3.50	591.00	16.00	1331	-6.2	-2.0
HM25739_110	122000	16080	25900	329000	6270	1039000	3.34800	0.06200	0.27390	0.00310	0.36	3.65	0.04	0.09	0.00	0.17	-0.82	0.04	1490	14	1599	16	1474	33	157600	4400	328.00	13.00	157.60	5.10	369.00	14.00	1474	-5.8	-4.6
HM25739_112	383100	62300	40500	482800	13660	2064000	3.88200	0.05300	0.31790	0.00230	0.00	5.69	0.07	0.08	0.00	0.18	-0.29	0.01	1033	17	1044	13	992	58	48400	820	188.60	3.30	234.80	3.00	404.00	11.00	1044	-5.2	-1.1
HM25739_38	293200	31680	45100	354000	7740	804700	3.03900	0.04900	0.33530	0.00210	0.27	3.00	0.02	0.11	0.00	0.38	-0.29	0.00	1823	7	1895	10	1780	16	334400	3900	743.00	9.80	822.90	5.90	2600.00	34.00	1780	-4.2	-1.8
HM25739_99	1376000	153500	93500	1452000	29010	4150000	3.07100	0.04500	0.32490	0.00210	0.09	3.08	0.03	0.09	0.00	0.34	-0.88	0.05	1816	11	1808	11	1801	28	167000	3300	409.30	9.30	196.30	3.80	1030.00	31.00	1801	-4.2	-2.5
HM25739_28	2300	1378000	287700	2602000	31590	4825000	3.24900	0.04200	0.25900	0.00200	0.07	3.86	0.03	0.09	0.00	0.43	-0.76	0.04	1464	10	1485	10	1427	27	156600	1700	363.50	4.10	205.80	2.70	564.00	15.00	1427	-4.1	-1.4
HM25739_78	53100	6020	12240	161300	1900	308400	2.57100	0.04300	0.22600	0.00240	0.17	4.42	0.05	0.08	0.00	0.11	-0.70	0.05	1286	12	1330	13	1269	31	147700	2400	448.60	5.10	273.20	3.80	586.00	16.00	1269	-3.2	-1.9
HM25739_82	13700	31200	1830400	13090	1823000	0.96700	0.07000	0.08870	0.00240	0.15	11.27	0.31	0.11	0.01	0.01	0.24	2.80	0.28	555	34	547	14	530	140	8000	700	75.21	0.58	62.90	1.10	65.80	4.80	1.20	0.02	547	-3.2	1.4
HM25739_10	157000	97400	138200	1108000	29600	4390000	4.65900	0.06800	0.32140	0.00300	0.23	3.11	0.03	0.11	0.00	0.03	-0.58	0.03	1753	12	1796	15	1743	29	103600	1700	276.00	6.60	179.80	3.90	982.00	15.00	1743	-3.0	-2.5
HM25739_66	24910	2540	6790	138300	428	190400	3.47500	0.06200	0.26750	0.00270	0.08	3.74	0.04	0.09	0.00	0.43	-0.64	0.03	1514	14	1526	14	1483	39	81800	1400	217.40	4.00	167.70	5.20	395.00	14.00	1483	-2.9	-0.8
HM25739_22	183500	18600	19810	224500	4830	701000	4.53900	0.04700	0.31530	0.00200	0.07	3.17	0.02	0.11	0.00	0.41	-1.37	0.06	1736	8	1766	10	1721	21	240500	3700	542.60	8.30	167.50	2.90	538.00	16.00	1721	-2.6	-1.7
HM25739_3	5440000	58700	66400	708000	13140	1847000	12.17000	0.25000	0.50260	0.00650	0.04	1.99	0.03	0.18	0.00	0.07	-0.42	0.04	2577	18	2616	27	2562	38	39780	950	59.43	0.67	56.80	1.00	242.00	8.80	2562	-2.1	-1.5
HM25739_15	136100	11810	14940	299000	5480	820000	2.13900	0.06600	0.18460	0.00190	0.01	5.42	0.06	0.09	0.00	0.10	0.18	0.33	1094	16	1091	10	1069	53	48000	1400	221.90	4.90	103.90	2.80	276.00	17.00	1091	-2.1	0.3
HM25739_45	180400	10390	9680	319000	19110	2916000	2.77000	0.11000	0.15980	0.00330	-0.03	5.01	0.08	0.11	0.01	0.10	5.56	0.56	1253	26	1172	18	1149	85	24370	470	79.30	1.40	42.80	1.30	135.00	11.00	1172	-2.0	6.5
HM25739_53	455100	51450	54700	696000	11450	1764000	3.35000	0.03900	0.26300	0.00210	0.48	3.80	0.03	0.09	0.00	0.15	-0.71	0.01	1491	8	1508	11	1479	19	374100	2900	870.60	9.50	396.30	4.00	1048.00	19.00	1479	-2.0	-1.2
HM25739_34	298100	27840	39400	484000	7630	1178000	5.05100	0.05300	0.33670	0.00350	0.26	2.97	0.03	0.11	0.00	0.70	-0.71	0.03	1826	9	1872	17	1837	24	182800	7900	476.00	20.00	249.00	12.00	876.00	40.00	1837	-1.9	-2.5
HM25739_25	71500	8940	44900	672000	2430	424200	4.52700	0.07900	0.31190	0.00340	0.35	3.21	0.03	0.11	0.00	0.08	-1.04	0.06	1726	13	1790	17	1719	27	122400	1400	302.20	4.00	149.00	2.40	426.00	14.00	1719	-3.8	-1.4
HM25739_80	369500	51590	50900	690200	19420	2772000	11.94000	0.13900	0.50240	0.00460	0.27	1.99	0.02	0.17	0.00	0.39	-0.62	0.03	2597	10	2624	20	2592	21	132100	1800	160.80	2.60	124.90	1.80	591.00	15.00	1145	0.02	-1.0
HM25739_83	1.00	80900	8600	1090000	1490	1.00	3.47100	0.05800	0.26120	0.00230	0.03	3.83	0.03	0.10	0.00	0.26	-0.24	0.00	1488	12	1504	13	1156600	1700	299.10	4.20	386.00	5.40	942.00	22.00	0.75	0.01	1504	0.5	-0.5
HM25739_92	207300	18380	23800	345400	6140	934400	3.31000	0.10000	0.25690	0.00590	0.72	3.89	0.09	0.09	0.00	0.18	-0.55	0.10	1460	26	1474	31	1462	41	79600	2700	263.40	7.80	132.00	3.40	385.00	14.00	1462	0.5	-1.0
HM25739_89	108	186200	11920	210000	401000	7050	896000	4.58100	0.04700	0.30980	0.00200	0.13	3.23	0.02	0.11	0.00	-0.92	0.05	1742	9	1740	10	1753	21	207700	3700	517.90	8.90	230.30	5.40	685.00	20.00	1753	0.8	0.1
HM25739_85	200000	16150	8990	132100	7180	1073000	3.88400	0.05700	0.28320	0.00320	0.40	3.53	0.04	0.10	0.00	0.26	-0.52	0.02	1604	12	1604	16	1618	26	149400	5800	515.00	19.00	345.00	8.40	898.00	21.00	1618	0.9	0.0
HM25739_95	695400	64280	80300	1052000	19470	2959000	4.20700	0.06000	0.32970	0.00360	0.09	3.38	0.03	0.09	0.00	0.43	-0.48	0.02	1674	12	1684	29	1680	31	206800	1500	255.00	3.60	228.50	4.20	634.00	17.00	1684	0.9	0.3
HM25739_96	1056000	131300	300800	880000	34500	5140000	3.24800	0.03900	0.25450	0.00210	-0.01	3.93	0.03	0.09	0.00	0.36	-0.80	0.03	1461	8	1460	11	1477	24	206700	8600	726.00	29.00	338.00	11.00	975.00	38.00	1477	1.2	0.1
HM25739_65	748300	81420	109500	2174000	16220	2497000	3.08900	0.08900	0.28680	0.00320	0.06	3.49	0.04	0.10	0.00	0.25	-0.64	0.04	1632	15	1622	16	1643	38	81000	3100	244.40	9.00	104.50	1.70	428.00	11.00	1638	0.05	0.6
HM25739_14	890	655000	1684000	1325000	2704000	8430	1.38E+06	21360000	0.19000	0.26260	0.00420	0.42	3.81	0.01	0.25	0.00	0.46	7.22	0.15	3172	8	3134	17	3155	13	40310	880	244.50	3.20	260.00	2.00	1043.00	28.00	3155	1.3	1.8
HM25739_9	660	317000	2880000	34800	1037000	8200	1.38E+06	21360000	0.19000	0.26260	0.00	3.79	0.03	0.10	0.00	0.18	5.94	0.27	3196	10	3196	16	3211	36	14100	980	241.10	3.80	306.60	5.20	836.00	30.00	3211	0.72	0.1
HM25739_17	89	287200	31960	348000	8540	1293300	4.30900	0.03800	0.29610	0.00200	0.21	3.38	0.02	0.11	0.00	0.42	-1.87	0.09	1693	7	1673	10	1715	18	309500	4900	1066.00	19.00	212.00	3.50	648.00	19.00	1715	2.5	1.2
HM25739_4	300	165700	15580	177200	6090	1038000	2.16700	0.02700	0.19910	0.00150	0.10	5.02	0.04	0.08	0.00	0.43	19.30	3.30	1169	9	1171	8	1208	27	155100	2900	682.00	14.00	56.40	1.30	165.00	10.00	1208	12.89	0.22
HM25739_75	45210	8570	4850	32800	280	97800	2.12900	0.03400	0.19350	0.00160	0.10	5.17	0.04	0.08	0.00	0.36	0.03	0.81	1153	11	1140	9	1180	35	144200	2300	492.10	7.50	120.50	2.20	207.00	9.90	1140	3.4	1.1
HM25739_43	172700	17970	22810	303900	4230	693000	4.99200	0.06200	0.31740	0.00340	-0.01	3.15	0.03	0.09	0.00	0.12	-0.86	0.04	1809	10	1776	17	1842	25	153800	1900	359.80	7.60	182.20	6.10	644.00	28.00	1842	3.6	1.8
HM25739_11	304000	33600	47500	566000	9750	1.37E+06	4.01900	0.07900	0.27230	0.00310	0.20	3.67	0.04	0.11	0.00	0.40	11.55	0.49	1606	14	1547	15	1600	37	134500	1500	284.00	13.00	150.10	6.30	374.00	22.00	1600	3.3	3.7
HM25739_12	131700	14380	30100	348500	4760	701000	3.03900	0.16000	0.21260	0.00260	0.12	4.70	0.06	0.10	0.00	0.07	10.11	0.48	1322	22	1239	14	1317	60	19950	260	145.20	3.10	92.60	1.40	236.00	40.00	1317	5.9	6.3
HM25739_60	531500	55400	23870	343000	13230	2066000	4.16500	0.04500	0.29010	0.00240	0.18	3.45	0.03	0.11	0.00	0.45	-2.04	0.37	1661	9	1641	12	1712	22	248100	4200	631.00	13.00	131.40	4.00	310.00	13.00	1712	4.1	1.2
HM25739_67	406300	42180	51210	1521000	11260	1678000	4.67400	0.07400	0.30440	0.00300	-0.03	3.29	0.04	0.11	0.00	0.22	-0.66	0.03	1744	12	1715	16	1790	33	95200	2200	269.30	6.90	205.10	8.10	497.00	19.00	1790	4.2	1.7
HM25739_23	145300	13940	23800	286600	3910	639900	2.22700	0.03800	0.15480	0.00180	-0.01	5.13	0.05	0.08	0.00	0.21	55.50	3.80	1171	11	1146	10	1197	33	121900	1800	457.50	7.80	64.30	2.90	126.00	13.00	1146	4.3	2.2
HM25739_40	307800	23970	23910	495900	13790	2001000	2.83500	0.03900	0.23100	0.00160	0.01	4.33	0.03	0.10	0.00	0.51	-1.16	0.06	1365	8	1389	8	1402	23	266800	3500	738.20	9.40	247.90	2.80	669.00	20.00	1402	4.5	1.9
HM25739_35	482300	95300	121700	1819000	7870	1260000	2.18700	0.05300	0.15920	0.00280	0.09	5.20	0.08	0.09	0.00	0.22	-0.20	0.30	1142	16	1131	15	1204	48	66700	900	211.70	3.90	102.10	2.40	196.90	8.40	1131	6.1	1.0
HM25739_42	193300	20670	28100	294000	4260	476000	2.28100	0.04900	0.28190	0.00170	0.12	3.55	0.02	0.11	0.00	0.29	-0.39	0.01	1642	8	1600	9	1708	21	343100	4100	798.90	9.30	697.70	6.40	1956.00	29.00	1708	1.15	0.01
HM25739_7	1761000	186100	30500	4340000	4220	712000	3.07900	0.05200	0.24360	0.00270	0.21	4.11	0.05	0.09	0.00	0.34	-0.42	0.02	1424	13	1408	14	1498	34	71100	2700	306.00	11.00	309.80	5.70	732.00	28.00	1498	6.3	1.5
HM25739_24	234900	24800	31100	384000	5140	866000	3.11900	0.05100	0.24610	0.00190	0.10	3.14	0.03	0.10	0.00	0.36	-0.38	0.01	1580	10	1586	15	1590	26	84200	2400	466.20	7.80	191.60	2.80	491.00	15.00	1590	6.6	3.0
HM25739_26	156600	17500	18530	228500	9490	1327000	0.46350	0.00380	0.06108	0.00027	0.08	16.37	0.07	0.06	0.00	0.38	-0.04	0.03	382	2	382	2	419	17	802600	8100	18000.00	100.00	8450.00	860.00	59503.00	460.00	382	7.7	9.7
HM25739_15	236300	24440	68800	1142000	10660	1680000	4.23800	0.06000	0.28620	0.00310	0.21	3.49	0.04	0.11	0.00	0.42	-0.87	0.48	1679	12	1619	15	1760	28	268000	13000	742.00	20.00	183.40	7.00	456.00	23.00	1760	8.0	3.6
HM25739_115	1316000	80500	3172000	1600000	15720	2340000	9.49000	0.14000	0.42420	0.00660	0.18	2.37	0.04	0.17	0.00	0.75	-0.46	0.03	2381	13	2330	24	2536	29	84100	2000	154.00	3.00	126.50	3.00	512.00	18.00	2536	8.1	2.1
HM25739_16	333900	31200	71100	851000	9510	1.36E+06	3.83000	0.05900	0.28220	0.00230	0.10	3.54	0.03	0.10	0.00	0.27	7.27	0.22	1578	12	1599	11	1464	32	220000	680	278.90	8.00	227.60	4.30	561.00	46.00	1464	1.13	0.01
HM25739_19	156500	16830	25900	313800	4990	699900	3.87000	0.11000	0.26510	0.00370	0.21	3.77	0.05	0.10	0.00	0.29	11.43	0.57	1550	20	1508	18	1505	47	-21190	900	142.20	3.80	84.30	1.30	205.00	8.00	1505	0.03	2.7
HM25739_23	231500	23230	97900	1.08E+06	6760	930000	4.04900	0.07900	0.27540	0.00230	0.10	3.63	0.04	0.11	0.00	0.14	4.12	0.14	1564	14	1584	15	1590	39	-17320	1000	391.00	7.80	297.80	4.80	1080.00	21.00	1580	0.67	0.01
HM25739_27	54800	5300	23840	330000	3560	464000	3.54E+06	2.25200	0.03300	0.00250	0.52	3.31	0.04	0.08	0.00	0.34	17.81	0.68	1187	9	1175	7	1094	26	62400	1200	700.80	23.00	255.50	2.30	474.00	11.00	1175	2.78	0.63
HM25739_28	119200	14300	20100	275000	3890	550000	3.94000	0.16000	0.27060	0.00440	0.03	3.70	0.06	0.11	0.01	0.39	12.68	0.62	1545	21	1533	21	1478	60	13550	380	109.50	4.40	75.10	6.10	161.00	18.00	1478	-3.7	0.8
HM25739_31	460100	43900	49700	998500	14230	1.97E+06	4.45800	0.09000	0.30220	0.00350	0.52	3.31	0.04	0.10	0.00	0.25	19.25	0.89	1683	13	1615	26	1840	30	81000	1000	391.00	16.00	271.00	20.00	397.00	15.00	1615	-4.8	-0.6
HM25739_32	94300	8590	34700	537000	4820	697000	3.81100	0.12000	0.31060	0.00380	0.15	3.09	0.03	0.10	0.00	0.37	6.95	0.44	966	27	954	19	922	89	54000	1200	1582.00	70.00	279.00	70.00	1.01	0.01	954	-3.5	1.2
HM25739_52	27300	3960	7000	87500	333	108000	2.64800	0.06900	0.22830	0.00310	0.26	4.38	0.06	0.08	0.00	0.07	32.10	4.00	1276	17	1322	16	1215	40	95100	4400	3140.00	17.00	49.40	2.20	117.40	7.40	-640000.00	840000.00	1215	4.8	-3.6

Table C9: Zircon Geochronology results for sample 25739 Melby Sandstone (S17-011)

Table C10: Zircon Geochronology results for sample 25730 Daal Sandstone (S16-036B)

									Wetherill				Tera-Wasserberg plot																		Calculated Discordance	
Sample	Hg204 CPS	Pb206 CPS	Pb207 CPS	Pb208 CPS	Th232 CPS	U235 CPS	U238 CPS	$^{207}Pb/^{235}U$	2σ	$^{206}Pb/^{238}U$	2σ	ErrorCorrelation_6_38vs7_35	$^{238}U/^{206}Pb$	2σ	$^{207}Pb/^{206}Pb$	2σ	ErrorCorrelation 38/6 vs 7/6	Final 206Pb/238 U	2σ	Final Age 207Pb/235 U	2σ	Final Age 206Pb/238 U	2σ	Final Age 207Pb/206Pb	2σ	Final 206Pb/204Pb	2σ	Approx U ppm	2σ	Approx Th ppm	2σ	Approx Pb ppm	2σ	Final U/Th Ratio	2σ	Preferred Age	6-38/7-6	6-38/7-35
HM25730_2	-1.39	3.9900	59.70	1.4200	1.65000	15.70	2.33000	2.65.000	0.16.000	0.21.540	0.00.640	0.02	4.64	0.14	0.12	0.01	0.00	4.89	0.52	1103	42	1236	33	1130	120	15520	690	46.5	2.8	34.6	3.5	86	11	1.961	0.059	1236	-9.4	8.6
HM25730_61	-2.79	4.4600	46.10	1.3700	2.24000	16.40	2.95000	1.75.000	0.42.000	0.17.030	0.00.430	0.01	5.87	0.15	0.10	0.01	0.12	1.42	0.27	1020	46	1003	23	930	120	14050	730	64.7	3.3	66.4	3.2	155	13	0.94	0.018	100.3	-7.8	7.3
HM25730_16	-1.56	2.7910	38.60	9.810	3.09000	14.50	2.40000	1.70.000	0.14.000	0.15.500	0.00.500	-0.04	6.45	0.21	0.12	0.01	0.08	2.12	0.30	782	40	920	28	860	140	9110	340	44.8	2.5	71.6	7.3	66.3	4.9	0.827	0.02	920	-7.0	6.5
HM25730_34	-1.52	1.9730	26.90	7.220	1.55000	4.48	1.25700	3.06.000	0.24.000	0.24.000	0.01.000	0.03	4.17	0.17	0.16	0.02	0.58	3.17	0.29	1050	57	1320	49	1250	190	5370	210	23.1	1.6	35.6	4.3	58.9	5.7	1.32	0.28	1250	-5.6	5.3
HM25730_15	-2.38	2.20000	20.80	2.7400	5.69000	89.80	1.25600	2.20.000	0.68.000	0.19.760	0.00.230	0.00	5.06	0.06	0.08	0.00	0.08	0.01	0.27	1177	24	1161	12	1109	54	59100	4100	284	19	170.8	9.7	287	16	1.665	0.026	1161	-4.7	4.5
HM25730_7	-1.92	5.45000	46500	5.3700	9.83000	191.70	3.09000	2.31.400	0.05.700	0.23.260	0.00.220	0.53	4.30	0.04	0.08	0.00	0.40	-1.02	0.05	1213	17	1347	12	1289	27	198300	6700	648	24	222.1	6.8	334	12	2.642	0.034	1289	-4.5	4.3
HM25730_7	-3.34	4.3400	88.00	1.6200	1.04500	64.10	8.72000	16.23.000	0.23.000	0.57.570	0.00.480	0.12	1.74	0.01	0.20	0.00	0.33	9.00	2.70	2875	13	2930	20	2810	21	122000	6400	185	11	29.39	0.94	153.3	9.8	7.2	0.31	2810	-4.3	4.1
HM25730_45	-1.52	4.5600	42.70	5.2700	9.72000	129.70	2.15500	2.74.500	0.07.300	0.26.710	0.00.300	0.43	3.74	0.04	0.09	0.00	0.35	-0.98	0.05	1313	20	1525	15	1469	30	287600	7500	701	23	404	22	489	17	1.924	0.026	1469	-3.8	3.7
HM25730_74	180	1.13800	79.90	2.3600	14.80000	154.00	2.15000	0.68.700	0.08.100	0.06.460	0.00.140	0.05	15.48	0.34	0.06	0.00	0.31	1.53	0.34	444	20	403	9	390	96	30800	2200	452	35	414	34	254	19	1.17	0.013	403	-3.4	3.2
HM25730_42	-4.95	1.78100	14.360	2.3760	4.98000	76.50	1.07700	1.76.500	0.05.700	0.19.620	0.00.260	0.11	5.10	0.07	0.08	0.00	0.13	-0.86	0.05	984	19	1153	14	1117	51	85100	1200	332	5.4	191	6.7	214.6	8.3	1.835	0.026	1153	-3.2	3.1
HM25730_3	-8.7	6.5800	83.80	1.6600	2.01000	24.70	3.09900	3.36.000	0.14.000	0.26.170	0.00.580	0.06	3.82	0.08	0.12	0.01	0.39	3.50	0.71	1405	29	1506	29	1465	85	28080	540	62.5	1.7	42.9	2.7	100.6	9.6	1.741	0.04	1465	-2.8	2.7
HM25730_17	-8.4	4.4600	94.80	5.3500	3.05900	64.90	9.59000	12.79.000	0.27.000	0.55.690	0.00.500	0.25	1.80	0.02	0.20	0.00	0.47	-0.83	0.06	2637	20	2853	20	2779	21	146900	7900	175	9.1	70.2	1.1	364	15	2.55	0.11	2779	-2.7	2.6
HM25730	-4.93	4.5900	59.70	6.450	9.6000	102.0	1.76300	4.80.000	0.57.000	0.30.150	0.00.830	0.00	3.32	0.09	0.14	0.01	0.05	7.46	0.56	1807	40	1671	41	1630	110	14160	560	37	1.9	26.7	4.1	57.3	8	4.65	0.36	1630	-2.5	2.5
HM25730_37	-2.36	1.68900	18.510	2.1140	3.47000	50.50	7.02000	3.51.000	0.12.000	0.29.180	0.00.400	0.06	3.43	0.05	0.11	0.00	0.09	-0.47	0.17	1449	24	1650	20	1611	48	61800	1600	148	5.2	90.6	5.6	177	7.8	1.888	0.032	1611	-2.4	2.4
HM25730_10	-4.40	3.64900	37.400	1.0610	2.38000	95.10	1.50200	3.50.100	0.08.400	0.29.120	0.00.340	0.33	3.43	0.04	0.10	0.00	0.33	37.10	4.70	1514	19	1651	16	1614	30	132600	1700	311.3	5.8	56.6	6.5	68.8	4.8	10.82	0.4	1614	-2.3	2.2
HM25730_36	-1.72	2.2660	17.380	2.0900	4.55000	102.10	1.70300	1.42.500	0.04.300	0.17.440	0.00.220	0.22	5.73	0.07	0.07	0.00	0.46	2.25	0.75	876	17	1035	12	1014	48	65500	3000	341	15	113.4	7.2	173	10	3.186	0.056	1035	-2.1	2.0
HM25730_39	60	2.0460	18.300	4.5800	8.09000	74.60	1.16900	2.17.000	0.29.000	0.20.170	0.00.220	0.05	4.96	0.05	0.09	0.00	0.01	-0.31	0.02	1222	22	1184	12	1177	58	85500	1100	321.4	4	294.7	4.9	593	18	1.076	0.01	1184	-0.6	0.6
HM25730_21	-5.38	4.7200	52.000	3.2400	3.73000	104.80	1.69900	4.87.300	0.09.700	0.31.040	0.00.240	0.03	3.22	0.02	0.11	0.00	0.13	-1.07	0.07	1759	13	1745	12	1737	27	158000	4000	426	12	123.3	4.9	372	17	3.487	0.054	1737	-0.5	0.5
HM25730_24	-2.68	3.4250	33.640	4.3900	5.94800	86.00	1.35000	4.01.000	0.31.000	0.27.870	0.00.250	0.09	3.59	0.03	0.10	0.00	0.37	-0.50	0.02	1627	16	1584	12	1577	30	129900	1500	351.8	4	203.7	2.7	517	17	1.728	0.022	1577	-0.4	0.4
HM25730_3	-5.08	3.4490	36.790	3.3600	4.27500	82.70	1.24100	4.57.500	0.07.300	0.30.900	0.00.260	-0.03	3.24	0.03	0.11	0.00	0.37	-0.65	0.04	1739	13	1735	13	1740	30	109000	1300	261.5	3.6	119.1	2.6	306.7	9.9	2.246	0.026	1740	0.3	-0.3
HM25730_78	-4.82	3.1500	67.300	4.5500	3.41000	39.20	6.85000	19.30.000	1.10.000	0.58.880	0.00.650	0.05	1.70	0.02	0.23	0.00	0.17	-0.37	0.02	3059	17	2991	26	2999	25	329000	4400	141.2	6.2	93.1	4.3	487	20	1.454	0.021	2999	0.3	-0.3
HM25730_8	-1.27	5.5080	111.500	9.3000	6.28000	79.80	1.23200	13.36.000	0.28.000	0.54.360	0.00.450	0.27	1.84	0.02	0.20	0.00	0.34	-0.52	0.01	2674	19	2800	19	2810	18	225400	2800	259.9	3.8	143.6	2.3	582	16	1.752	0.016	2810	0.4	-0.4
HM25730_52	-5.32	1.91000	1.0490	2.3400	11.95000	210.00	3.26700	0.47.900	0.01.600	0.06.394	0.00.084	0.04	15.64	0.21	0.06	0.00	0.35	-0.52	0.04	397	11	400	5	401	71	66100	1000	744.7	6	372.1	3.6	281	14	2.006	0.016	400	0.4	-0.4
HM25730_15	-2.52	2.3240	25.730	2.8800	4.88000	59.50	9.75000	3.90.000	0.12.000	0.29.970	0.00.370	0.11	3.34	0.04	0.11	0.00	0.04	-0.78	0.05	1554	23	1691	18	1700	38	77500	1700	185.5	5.6	114	7.2	193.1	7.9	1.966	0.04	1700	0.5	-0.5
HM25730_46	-4.16	1.48000	20.800	1.2860	1.64000	32.80	5.52000	9.41.000	0.45.000	0.46.300	0.01.200	0.44	2.16	0.06	0.17	0.01	0.05	7.50	1.20	2214	48	2397	51	2415	50	80700	6300	181	16	69	6.6	120.6	9.1	2.59	0.11	2415	0.7	-0.8
HM25730_20	110	1.9700	1.8200	1.6600	2.71000	48.60	7.15000	2.11.000	0.25.800	0.40.410	0.00.410	0.16	3.86	0.06	0.10	0.00	0.14	4.71	0.94	1355	26	1486	21	1501	52	35000	2000	115	8	57.3	4.5	118	13	2.251	0.053	1502	1.1	-1.1
HM25730_34	-5.02	8.4000	87.200	1.2850	15.33000	215.00	3.12300	4.49.700	0.05.200	0.29.840	0.00.240	-0.16	3.35	0.03	0.10	0.00	0.09	-0.35	0.01	1723	9	1683	12	1706	21	375000	6900	882	24	569.1	9.6	1648	33	1.519	0.023	1706	1.3	-1.4
HM25730_64	-2.06	7.0670	81.700	1.570	6.2700	162.40	2.47500	5.39.000	0.66.000	0.33.680	0.00.220	0.00	2.97	0.02	0.12	0.00	0.31	213.00	7.80	1904	15	1871	10	1897	19	276000	3200	539.6	8.4	18.5	2.4	17.5	3.5	-2.61E+07	2.40E+06	1897	1.4	-1.4
HM25730_4	250	1.6800	1.8090	4.5600	7.36000	51.40	7.34000	3.67.000	0.12.000	0.28.290	0.00.420	0.08	3.53	0.05	0.11	0.00	0.10	-0.40	0.02	1512	24	1602	21	1628	48	68170	940	149.9	3	159	7.2	276.3	8	1.048	0.013	1628	1.6	-1.6
HM25730_12	170	3.2630	3.5060	2.6500	3.29100	87.10	1.21000	4.58.000	0.18.000	0.30.400	0.00.300	0.11	3.29	0.03	0.11	0.00	0.25	-0.85	0.05	1762	16	1712	15	1740	31	108000	1200	267.3	3.5	96.4	2.5	271	10	2.82	0.044	1740	1.6	-1.6
HM25730_16	-1.12	2.5010	2.6600	2.6600	4.10000	98.40	1.27700	3.13.500	0.07.100	0.24.240	0.00.370	-0.04	4.13	0.06	0.09	0.00	0.10	-0.68	0.15	1414	17	1399	19	1429	44	81100	3900	292	19	124.1	3.4	282	11	2.203	0.075	1429	2.1	-2.1
HM25730_65	-5.00	1.5670	9990	6.2000	34.53000	169.30	2.66800	0.58.700	0.04.400	0.06.731	0.00.076	-0.02	14.86	0.17	0.07	0.01	0.03	-0.12	0.00	435	13	420	5	430	71	58110	890	580.7	6.7	1015	11	690	17	0.5706	0.0032	420	2.4	-2.4
HM25730_76	70	3.4620	3.7900	3.8700	4.56000	82.00	1.41400	4.72.000	0.42.000	0.30.710	0.00.280	0.07	3.26	0.03	0.11	0.00	0.27	-0.55	0.03	1770	17	1724	14	1767	30	105000	3800	294	11	125.9	4.5	415	36	2.101	0.044	1767	2.4	-2.5
HM25730_49	-2.69	2.8230	2.3220	4.0100	9.33000	120.00	1.83100	1.67.300	0.04.500	0.19.140	0.00.190	0.17	5.22	0.05	0.08	0.00	0.31	-0.89	0.05	971	17	1128	10	1159	42	152500	4600	588	20	397	13	387	14	1.53	0.036	1128	2.7	-2.7
HM25730_19	-2.61	4.1800	3.7970	9.9400	7.18000	55.40	8.71000	15.30.000	1.30.000	0.52.610	0.00.520	-0.01	1.90	0.02	0.20	0.00	0.55	-0.23	0.01	2811	15	2715	22	2789	21	125000	3900	205.1	5.4	223.7	8.6	1084	37	0.93	0.012	2789	2.7	-2.7
HM25730_5	-1.09	3.7200	2.9600	5.1800	11.38000	178.00	2.36000	2.27.000	0.24.000	0.18.160	0.00.180	0.07	5.51	0.05	0.08	0.00	0.43	-0.44	0.02	1105	15	1075	10	1106	36	130000	5500	499	21	318	13	481	18	1.575	0.014	1075	2.8	-2.9
HM25730_50	-1.67	2.6070	2.6700	4.9200	7.02000	73.60	1.11000	4.08.000	0.31.000	0.28.420	0.00.300	0.04	3.52	0.04	0.11	0.00	0.20	-0.27	0.01	1670	18	1613	15	1659	35	103000	2000	256.2	5.5	221.4	5.7	596	17	1.165	0.012	1659	2.8	-2.9
HM25730_80	-2.34	2.9230	2.6060	3.9000	6.40000	93.80	1.47700	2.60.000	0.37.000	0.23.060	0.00.180	-0.06	4.34	0.03	0.09	0.00	0.25	-0.44	0.02	1350	19	1338	10	1378	37	97100	2200	299.3	8.1	170.3	4.6	417	15	1.757	0.02	1378	2.9	-3
HM25730_53	-2.39	7.3300	81.70	1.8680	2.89000	23.30	3.24000	3.82.000	0.42.000	0.26.680	0.00.530	0.03	3.75	0.07	0.11	0.00	0.19	-0.20	0.07	1600	33	1516	27	1565	72	25420	810	73.5	2.5	89.4	3.7	222.8	9.9	0.843	0.013	1565	3.1	-3.2
HM25730_13	-2.88	1.9610	2.1170	3.1600	3.94000	43.50	7.23000	4.58.000	0.48.000	0.30.400	0.00.360	0.01	3.29	0.04	0.11	0.00	0.42	-0.44	0.03	1769	20	1711	18	1767	37	56250	690	161	2.2	116.4	3.7	326	12	1.474	0.023	1767	3.2	-3.3
HM25730_33	210	4.1200	7.7900	2.5800	2.60000	61.00	1.03100	10.76.000	0.27.000	0.49.130	0.00.660	0.03	2.04	0.03	0.19	0.00	0.04	-1.74	0.16	2472	22	2613	24	2704	21	109500	2800	182	2	57.7	3.1	208.9	8.7	3.808	0.084	2704	3.4	-3.5
HM25730_23	-4.72	1.8850	1.5550	2.1710	6.11000	70.30	1.11800	2.34.000	0.24.000	0.19.430	0.00.240	0.00	5.15	0.06	0.08	0.00	0.13	-0.68	0.05	1197	20	1142	13	1182	49	66100	1900	287.5	4.5	206.9	5.1	253	11	1.394	0.018	1142	3.4	-3.5
HM25730_44	30	1.1440	1.3390	1.3500	2.01000	24.80	4.52000	3.91.000	0.13.000	0.30.820	0.00.600	0.06	3.24	0.06	0.12	0.00	0.29	7.80	1.40	1556	26	1741	28	1804	52	64700	1900	145.4	4.2	81.8	7.6	124	10	2.628	0.083	1804	3.5	-3.6
HM25730_95	-5.69	8.2880	8.5800	5.1500	6.68000	21.70	3.28400	4.33.000	0.51.000	0.29.510	0.00.180	0.00	3.39	0.02	0.11	0.00	0.36	-1.03	0.05	1721	14	1668	9	1729	20	297000	3100	766	10	195.7	3.4	584	16	3.875	0.041	1729	3.5	-3.6
HM25730_98	-5.70	1.1780	1.0360	1.7000	2.90000	52.30	7.70000	2.18.000	0.62.000	0.17.620	0.00.240	0.02	5.68	0.08	0.09	0.00	0.15	2.30	0.79	1075	24	1045	13	1085	72	48340	870	189.8	3.6	88.8	4.9	196	25	2.465	0.055	1045	3.7	-3.8
HM25730_33	-2.27	1.3070	1.1530	1.6450	2.93100	43.00	7.11200	3.17.000	0.27.000	0.20.430	0.00.270	-0.01	4.89	0.06	0.09	0.00	0.09	-0.33	0.23	1245	26	1197	14	1246	62	57710	830	201.3	2.3	108.9	3.4	210	11	1.939	0.034	1246	3.9	-4.1
HM25730_96	-1.99	2.6870	5.8100	6.1200	4.62000	36.10	5.89000	16.10.000	1.30.000	0.55.040	0.00.650	0.07	1.82	0.02	0.22	0.00	0.17	-0.27	0.01	2930	16	2823	27	2938	26	111000	1400	140.1	3.3	137.3	5.1	697	21	1.059	0.015	2938	3.9	-4.1
HM25730_35	-4.53	1.3240	1.0670	1.6270	4.06000	68.90	9.75000	1.34.500	0.04.500	0.16.140	0.00.330	0.40	6.20	0.13	0.08	0.00	0.64	-0.24	0.32	845	20	966	18	1006	61	38560	540	186.9	4.8	97	4.5	133.9	6.8	2.08	0.036	966	4.0	-4.1
HM25730_45	-4.0	3.3760	6.7400	6.9800	4.39000	43.40	7.64000	12.50.000	1.80.000	0.51.500	0.00.550	0.00	1.94	0.02	0.20	0.00	0.15	-0.35	0.02	2759	16	2673	24	2792	27	150000	1600	192.9	3.4	149.6	4.3	890	40	1.348	0.019	2792	4.3	-4.5
HM25730_27	-2.93	3.6850	3.2470	3.9000	7.08000	131.40	2.01700	2.38.000	0.23.000	0.20.990	0.00.190	0.11	4.76	0.04	0.09	0.00	0.20	-0.69	0.04	1295	16	1228	10	1284	36	150000	3600	545	11	250.6	6.3	471	18	2.261	0.025	1284	4.4	-4.6
HM25730_107	-1.73	3.2590	3.3870	6.0800	7.44000	87.80	1.26600	5.37.000	0.37.000	0.29.450	0.00.270	0.00	3.40	0.03	0.11	0.00	0.42	-0.32	0.01	1712	18	1663	14	1740	32	198000	2800	359.4	5.6	250.5	4.7	749	22	1.421	0.013	1740	4.4	-4.6
HM25730_52	-2.14	4.5100	5.0800	1.4130	2.59200	14.200	2.49000	3.68.000	0.13.000	0.29.450	0.00.480	0.35	3.40	0.06	0.11	0.00	0.03	9.90	3.50	1530	29	1663	24	1741	31	203200	6100	674	33	95.6	3.6	145.8	7.4	6.29	0.2	1741	4.5	-4.7
HM25730_40	-1.80	4.3970	8.9600	4.3700	3.40800	57.70	9.53000	14.32.000	0.19.000	0.52.110	0.00.500	0.19	1.92	0.02	0.20	0.00	0.23	-0.73	0.06	2762	12	2701	21	2828	23	195000	3600	252.4	6.1	120.7	2.1	565	21	2.103	0.066	2828	4.5	-4.7
HM25730_34	110	1.0770	1.1110	9.3200	12.92000	267.50	4.12700	4.13.000	0.24.000	0.29.230	0.00.180	0.01	3.42	0.02	0.11	0.00	0.13	-0.76	0.05	1727	13	1652	9	1733	19	429000	6400	1031.6	8.8	436.9	6.2	1184	36	2.406	0.035	1733	4.7	-4.9
HM25730_23	-2.14	1.0140	8810	8700	2.93000	49.10	7.40000	1.50.900	0.05.600	0.16.500	0.00.330	0.09	6.06	0.12	0.09	0.00	0.51	21.20	1.50	882	21	986	18	1035	73	27030	440	113.9	2.5	59.6	7.5	63.4	7.9	6.61	0.34	986	4.7	-5.0
HM25730_21	-1.07	2.1630	2.8740	2.9200	2.62000	53.90	7.93000	4.73.000	0.13.000	0.32.840	0.00.500	0.00	3.05	0.05	0.13	0.00	0.16	-0.90	0.14	1714	19	1819	24	1912	43	52800	1600	125.4	2.3	54.6	2.3	209	13	2.469	0.046	1912	4.9	-5.1
HM25730_30	-4.73	4.3600	4750	7500	1.17000	1290	2.13000	3.67.000	0.27.000	0.24.820	0.00.740	0.08	4.03	0.12	0.11	0.01	0.60	5.01	0.57	1567	37	1415	38	1491	90	18310	740	60.2	3.8	43.4	3.9	94.5	8.4	1.588	0.044	1491	5.1	-5.4
HM25730_72	-2.08	1.0340	1.0830	2.9800	4.18000	212.0	4.44500	4.08.000	0.40.000	0.27.690	0.00.520	0.04	3.61	0.07	0.11	0.00	0.24	-0.22	0.02	1650	26	1582	24	1668	56	35500	1200	94.1	1.8	118.1	3.3	322	14	0.811	0.012	1668	5.2	-5.4
HM25730_94	-2.95	1.2610	2.3480	1.3750	11.63000	194.30	3.01.900	13.10.000	1.10.000	0.49.410	0.00.280	0.07	2.02	0.01	0.19	0.00	0.49	-0.50	0.03	2712	13	2588	12	2744	12	432000	7300	692	12	336.1	4.2	1551	36	1.991	0.035	2744	5.7	-6
HM25730_10	-8.0	2.6150	2.9210	2.9700	5.35000	69.50	9.82000	4.71.000	0.33.000	0.29.680	0.00.370	0.03	3.37	0.04	0.11	0.00	0.07	-0.63	0.05	1773	18	1672	19	1778	36	74200	1900	214	4.3	154.5	6.5	297	11	1.511	0.024	1778	6	-6.3
HM25730_55	-2.05	3.1550	6.6000	6.6700	5.32000	46.00	7.12000	14.60.000	1.30.000	0.52.650	0.00.610	0.09	1.90	0.02	0.21	0.00	0.42	-0.26	0.01	2860	17	2722	26	2895	24	105000	2100	160	5.1	163.2	7.5	787	35	1.036	0.015	2895	6	-6.4
HM25730_109	-2.76	1.5120	9320	1.5600	8.71000	171.70	2.62900	0.64.600	0.03.300	0.07.016	0.00.084	0.04	14.25	0.17	0.06	0.00	0.09	1.69	0.72	460	14	437	5	465	67	69300	2400	751	24	293	8.6	194	11	2.45	0.022	437	6	-6.4
HM25730_70	-2.59	1.5200	1.4930	1.9820	3.04000	42.30	6.95000	3.43.000	0.52.000	0.25.370	0.00.320	-0.01	3.94	0.05	0.10	0.00	0.30	-0.51	0.03	1520	22	1457	16	1552	48	52400	650	148.3	1.4	86.7	2.9	215	10	1.821	0.035	1552	6.1	-6.5
HM25730_106	-2.09	2.3000	2.3830	4.9600	6.94000	62.20	9.46700	4.17.000	0.31.000	0.28.180	0.00.340	0.07	3.55	0.04	0.11	0.00	0.49	-0.28	0.01	1674	19	1599	17	1703	40	131000	1700	267.6	2.6	233.3	4.5	609	18	1.167	0.013	1703	6.1	-6.5
HM25730_9	70	7.2700	1.4050	9.4300	9.45000	113.30	1.81000	11.62.000	0.34.000	0.49.360	0.00.630	0.79	2.03	0.03	0.19	0.00	0.19	-0.62	0.01	2559	27	2576	28	2744	15	292200	5700	382.7	3.9	218.7	4	594	17	1.754	0.019	2744	6.1	-6.5
HM25730_30	-1.30	1.0790	1.7940	1.4830	1.32600	172.10	2.72900	8.40.000	0.17.000	0.44.260	0.00.340	0.46	2.26	0.02	0.17	0.00	0.24	-0.47	0.01	2264	19	2358	15	2514	15	263800	3200	437.6	6.3	270.7	2.2	1171	20	1.654	0.017	2514	6.2	-6.6
HM25730_41	640	1.1670	1.9360	1.6790	1.40400	197.70	3.09000	8.13.000	0.11.000	0.43.710	0.00.260	0.02	2.29	0.01	0.17

Sample	Hg204 CPS	Pb206 CPS	Pb207 CPS	Pb208 CPS	Th232 CPS	U235 CPS	U238 CPS	Wetherill				Tera-Wasserburg plot				ErrorCorrelation_6_38v s7_35	Final 238U/206Pb	2σ	Final Age 207Pb/235U	2σ	Final Age 207Pb/238U	2σ	Final 206Pb/204Pb	2σ	Approx U ppm	2σ	Approx Th ppm	2σ	Approx Pb ppm	2σ	Final U/Th Ratio	2σ	Preferred Age	2σ	Calculated Discordance	
								207Pb/206Pb	2σ	207Pb/235U	2σ	238U/206Pb	2σ	207Pb/206Pb	2σ																			6-38/7-6	6-38/7-35
HM25734_26	177	81900	5190	18910	859000	8840	1217000	0.60000	0.22000	0.00110	-0.05	14.03	0.22	0.07	0.00	0.12	13.40	0.57	419	21	443	6	407	73	49600	1200	531	7	452	6	340	14	1.12	0.01	448	-8.9	8.2
HM25734_64	0	50100	5880	45000	498500	530	160100	6.00000	7.50000	0.36840	0.01	2.97	0.06	0.13	0.00	0.19	3.25	0.11	1548	45	1843	29	1716	70	26820	690	70	1	263	4	814	22	0.26	0.00	1716	-7.4	6.9
HM25734_51	178	74800	7540	16100	281000	2880	498100	0.07000	0.09000	0.07580	0.03	5.69	0.08	0.09	0.00	NaN	13.91	0.57	918	35	1043	14	978	77	44400	1900	217	9	148	7	289	18	1.51	0.03	1043	-6.6	6.2
HM25734_3	0	47000	4810	14200	165300	557	177800	4.20000	0.61000	0.08350	-0.01	3.53	0.07	0.11	0.00	0.32	9.62	0.47	1405	42	1606	27	1511	74	28200	1200	78	3	87	2	255	12	0.82	0.02	1511	-6.3	5.9
HM25734_83	0	71100	6270	11410	155400	2530	420100	0.06500	0.16070	0.09280	0.00	5.89	0.10	0.09	0.00	0.26	24.41	0.99	1094	20	1099	15	958	67	59800	7900	240	6	112	2	236	16	2.15	0.04	1099	-5.3	5.1
HM25734_15	342	60000	5720	14790	222400	2100	353900	2.47000	0.11000	0.18810	0.06	5.32	0.09	0.10	0.00	0.08	9.98	0.40	1110	26	1100	16	1046	77	34700	4900	117	1	87	1	235	12	1.32	0.02	1100	-5.2	4.9
HM25734_68	0	180600	17870	34100	447300	4450	742900	3.28700	0.06500	0.25310	0.09260	-0.06	3.95	0.04	0.10	0.00	20.35	0.66	1457	13	1453	13	1434	39	139000	10000	404	4	319	7	661	20	1.30	0.02	1434	-1.3	1.3
HM25734_28	0	26820	1950	5410	198500	2210	416200	0.37000	0.40000	0.06860	0.00180	0.00	14.58	0.38	0.08	0.00	NaN	7.75	0.40	402	28	422	10	420	120	15940	490	182	2	104	2	95	8	1.70	0.02	422	-0.5	0.5
HM25734_57	204	87000	83200	27600	231000	3830	705600	9.40000	4.80000	0.58400	0.00450	0.03	1.71	0.01	0.22	0.00	0.51	40.50	1.40	2704	37	2963	18	2954	16	238000	4500	307	7	122	4	498	20	2.42	0.03	2954	-0.3	0.3
HM25734_31	0	126600	14750	34100	397100	3120	438000	3.40000	1.10000	0.36140	0.00460	0.04	3.32	0.05	0.11	0.00	0.16	11.19	0.39	1541	35	1699	23	1696	43	70000	2200	191	7	209	5	615	20	0.90	0.02	1696	-0.2	0.2
HM25734_21	0	74200	8960	19200	217600	1730	263500	4.94000	0.13000	0.38940	0.00480	0.02	3.26	0.05	0.12	0.00	0.23	10.56	0.40	1735	21	1720	23	1717	57	49000	3800	91	2	90	4	311	14	1.10	0.02	1717	-0.2	0.2
HM25734_69	0	167600	13850	7960	128300	6600	106400	0.55000	0.51000	0.17030	0.00170	0.02	5.87	0.06	0.08	0.00	0.22	48.00	2.10	864	28	1012	9	1012	49	94910	970	464	3	68	3	134	10	7.55	0.17	1012	0.0	0.0
HM25734_23	204	286400	50670	54400	431300	4000	626500	0.06500	0.20000	0.59310	0.00550	0.60	1.69	0.02	0.18	0.00	0.00	13.77	0.48	2648	15	2622	24	2625	22	143000	2200	220	5	183	4	886	23	1.18	0.02	2625	0.1	-0.1
HM25734_38	490	372700	381.90	56600	685000	9310	1463000	1.60000	1.10000	0.28960	0.00210	0.05	3.56	0.03	0.10	0.00	0.30	19.76	0.50	1371	31	1591	11	1594	25	216000	3900	638	9	361	7	1024	33	1.72	0.02	1594	0.2	-0.2
HM25734_56	411	411100	80000	138000	991000	9350	863300	13.87000	0.13000	0.59950	0.00400	0.31	1.96	0.02	0.18	0.00	0.22	9.15	0.26	2666	9	2650	17	2665	16	282000	29000	460	11	713	12	2920	53	0.64	0.02	2665	0.6	-0.6
HM25734_86	0	99300	10870	25200	287100	2110	366800	4.16800	0.09600	0.28510	0.00420	0.01	3.51	0.05	0.11	0.00	0.25	14.15	0.65	1605	18	1611	20	1618	48	57900	5300	152	2	154	5	428	19	1.07	0.02	1618	0.4	-0.4
HM25734_74	0	375500	16440	19030	293800	5670	865100	2.70300	0.06200	0.21880	0.00290	0.12	4.57	0.06	0.09	0.00	0.30	34.40	1.60	1291	16	1273	15	1284	42	138000	18000	476	14	210	5	377	15	2.11	0.03	1284	0.9	-0.9
HM25734_21	135	208600	40240	11290	84700	2400	428400	13.72000	0.18000	0.59050	0.00520	0.21	1.98	0.02	0.19	0.00	0.35	66.00	2.70	2648	13	2636	22	2667	23	138000	18000	239	5	61	4	229	14	4.96	0.14	2667	1.2	-1.2
HM25734_71	0	287700	53880	64700	483400	3400	547900	9.80000	3.40000	0.53750	0.00500	0.01	1.86	0.02	0.20	0.00	0.25	11.16	0.23	2519	38	2768	21	2801	20	151200	1600	239	3	255	4	1172	24	0.90	0.01	2801	1.2	-1.2
HM25734_32	0	67600	6960	18800	233800	1510	284800	3.21500	0.09100	0.26530	0.00430	0.01	4.08	0.07	0.10	0.00	0.42	12.48	0.48	1419	21	1391	21	1411	62	47900	5300	130	4	169	5	342	18	0.93	0.01	1411	1.4	-1.4
HM25734_3	0	200700	47790	28770	203700	2200	368300	20.15000	0.25000	0.69980	0.00650	0.45	1.64	0.02	0.24	0.00	0.36	16.26	0.54	3089	12	3061	26	3112	20	91400	8900	117	2	78	3	438	13	1.67	0.03	3112	1.6	-1.7
HM25734_33	0	383900	90560	27520	454700	15830	2342000	0.77000	0.50000	0.17960	0.00120	0.04	5.57	0.04	0.08	0.00	0.34	43.50	1.50	913	26	1064	7	1084	30	226700	2900	1021	16	240	3	496	18	3.97	0.05	1064	1.8	-1.8
HM25734_29	0	208700	20600	27400	347000	5610	880500	1.57000	0.87000	0.25860	0.00250	-0.02	3.87	0.04	0.10	0.00	0.45	29.96	0.86	1287	32	1485	12	1514	34	131400	2200	384	7	183	6	495	24	2.12	0.03	1514	1.9	-2.0
HM25734_40	218	32280	3990	7970	84800	660	196900	2.37000	0.13000	0.17040	0.00390	0.02	5.87	0.13	0.12	0.01	0.10	9.69	0.55	1040	34	999	21	1020	110	18700	2300	89	2	51	3	138	16	2.18	0.06	999	2.1	-2.1
HM25734_45	0	135800	12270	30500	420000	4140	668500	1.14000	0.63000	0.22290	0.00240	0.05	4.49	0.05	0.09	0.00	0.51	14.46	0.52	1106	31	1295	13	1323	46	82200	1900	292	6	221	6	550	23	1.28	0.01	1323	2.2	-2.2
HM25734_8	191	48800	4830	11130	173600	1900	294700	0.65000	0.09000	0.16890	0.00310	0.01	5.92	0.11	0.11	0.01	0.20	11.17	0.48	870	37	995	17	1019	92	27900	860	129	3	91	4	199	15	1.48	0.03	995	2.4	-2.4
HM25734_52	0	67600	6960	18800	233800	1510	284800	3.21500	0.09100	0.26530	0.00430	0.01	4.08	0.07	0.10	0.00	0.42	12.48	0.48	1419	21	1391	21	1411	62	47900	5300	130	4	169	5	342	18	0.93	0.01	1411	1.4	-1.4
HM25734_3	0	200700	47790	28770	203700	2200	368300	20.15000	0.25000	0.69980	0.00650	0.45	1.64	0.02	0.24	0.00	0.36	16.26	0.54	3089	12	3061	26	3112	20	91400	8900	117	2	78	3	438	13	1.67	0.03	3112	1.6	-1.7
HM25734_33	0	383900	90560	27520	454700	15830	2342000	0.77000	0.50000	0.17960	0.00120	0.04	5.57	0.04	0.08	0.00	0.34	43.50	1.50	913	26	1064	7	1084	30	226700	2900	1021	16	240	3	496	18	3.97	0.05	1064	1.8	-1.8
HM25734_29	0	208700	20600	27400	347000	5610	880500	1.57000	0.87000	0.25860	0.00250	-0.02	3.87	0.04	0.10	0.00	0.45	29.96	0.86	1287	32	1485	12	1514	34	131400	2200	384	7	183	6	495	24	2.12	0.03	1514	1.9	-2.0
HM25734_40	218	32280	3990	7970	84800	660	196900	2.37000	0.13000	0.17040	0.00390	0.02	5.87	0.13	0.12	0.01	0.10	9.69	0.55	1040	34	999	21	1020	110	18700	2300	89	2	51	3	138	16	2.18	0.06	999	2.1	-2.1
HM25734_45	0	135800	12270	30500	420000	4140	668500	1.14000	0.63000	0.22290	0.00240	0.05	4.49	0.05	0.09	0.00	0.51	14.46	0.52	1106	31	1295	13	1323	46	82200	1900	292	6	221	6	550	23	1.28	0.01	1323	2.2	-2.2
HM25734_8	191	48800	4830	11130	173600	1900	294700	0.65000	0.09000	0.16890	0.00310	0.01	5.92	0.11	0.11	0.01	0.20	11.17	0.48	870	37	995	17	1019	92	27900	860	129	3	91	4	199	15	1.48	0.03	995	2.4	-2.4
HM25734_52	232	237500	25990	31850	351700	5970	874700	2.30000	1.10000	0.29050	0.00270	0.03	3.44	0.03	0.12	0.00	0.15	22.55	0.79	1460	32	1442	14	1721	37	142400	1900	381	2	185	3	574	18	2.09	0.03	1721	4.6	-4.6
HM25734_31	214	334800	36780	64200	760000	9140	1267000	4.10100	0.05100	0.28410	0.00260	0.21	3.52	0.03	0.11	0.00	0.52	13.71	0.29	1646	10	1611	13	1689	25	206000	18000	503	11	274	5	1080	24	1.38	0.02	1689	4.6	-4.8
HM25734_32	0	634600	1005100	31200	431300	11080	1093400	7.60000	1.30000	0.43680	0.00490	0.01	2.34	0.03	0.16	0.00	-0.07	32.46	0.81	2172	31	2284	22	2401	16	404100	8100	739	12	227	4	927	22	3.05	0.03	2401	4.9	-5.1
HM25734_70	297	611900	132100	88200	756000	8980	1237000	3.10000	3.40000	0.52000	0.00330	0.05	1.92	0.01	0.20	0.00	0.27	20.72	0.64	2344	31	2708	14	2852	15	302600	8700	540	10	398	7	1598	38	1.37	0.02	2852	5.0	-5.3
HM25734_77	144	122500	14160	31800	340000	2480	469500	1.80000	1.10000	0.27960	0.00260	-0.02	3.58	0.04	0.12	0.00	0.34	13.72	0.51	1393	35	1580	17	1675	46	97900	1900	205	3	179	6	574	38	1.19	0.02	1675	5.1	-5.4
HM25734_37	211	386900	189700	32800	495000	13440	2092000	13.05700	0.09100	0.49400	0.00330	0.47	2.02	0.01	0.19	0.00	0.51	48.40	1.20	2084	7	2590	14	2733	12	515000	68500	968	18	281	6	965	23	3.31	0.07	2733	5.2	-5.5
HM25734_36	239	171900	33750	49700	350000	2820	378500	13.24000	0.17000	0.49480	0.00490	0.07	2.02	0.02	0.20	0.00	0.62	9.42	0.28	2689	12	2598	24	2742	25	98800	7700	162	2	195	3	849	22	0.84	0.01	2742	5.3	-5.5
HM25734_2	236	268900	34580	56600	535000	3470	601300	14.45000	0.19000	0.53790	0.00370	0.09	1.93	0.02	0.21	0.00	0.33	10.59	0.33	2766	12	2688	24	2840	23	101000	11000	190	2	204	6	860	22	1.03	0.02	2840	5.4	-5.7
HM25734_43	264	1366000	2090100	177100	1305000	14070	2113000	14.45000	0.18000	0.53410	0.00390	0.04	1.95	0.02	0.20	0.00	0.08	15.36	0.25	2771	11	2679	25	2831	13	185000	54000	1602	24	871	23	3095	81	1.22	0.02	2831	5.4	-5.7
HM25734_26	107	89900	17720	44800	322900	596	159400	12.46000	0.25000	0.47770	0.00480	0.00	2.09	0.03	0.20	0.00	0.22	7.90	0.22	2803	18	2510	29	2655	37	63800	6900	108	1	231	4	904	24	0.45	0.01	2655	5.5	-5.8
HM25734_12	140	421800	81400	64900	460400	5090	907100	12.46000	3.20000	0.49450	0.00360	0.01	2.02	0.01	0.20	0.00	0.43	18.96	0.57	2397	36	2590	16	2740	18	256700	4900	395	6	243	5	1175	28	1.70	0.04	2740	5.5	-5.8
HM25734_3	0	312800	51770	30990	318000	5150	805500	1.70000	0.43110	0.05290	0.00270	0.03	2.32	0.03	0.16	0.00	0.10	17.73	0.52	2190	32	2309	26	2445	22	132500	3100	351	11	273	9	930	21	1.27	0.02	2445	5.6	-5.9
HM25734_17	184	158000	33830	34990	242500	1870	325000	14.63000	0.15000	0.50740	0.00790	0.03	1.97	0.03	0.12	0.00	0.11	10.56	0.42	2736	18	2658	43	2818	43	94000	5900	104	4	92	2	534	20	1.11	0.03	2818	5.6	-5.9
HM25734_27	0	341500	39820	35950	673000	8680	1395000	4.75400	0.06010	0.39650	0.00290	0.05	3.26	0.03	0.12	0.00	0.15	14.75	0.46	1746	12	1721	14	1833	29	144000	18500	469	12	268	7	935	26	1.69	0.02	1833	6.1	-6.5
HM25734_11	0	74200	8970	27900	283300	1640	392400	4.09000	0.12000	0.38470	0.00290	0.00	3.78	0.06	0.12	0.00	0.42	13.70	0.56	1986	22	1904	21	1977	61	65700	5900	159	3	203	5	590	27	0.76	0.01	1977	6.4	-6.9
HM25734_47	186	59600	13970	32900	724000	701	1317000	2.50000	0.48720	0.06750	0.00	2.05	0.03	0.20	0.00	0.48	2.54	0.07	2414	38	2567	32	2798	34	63900	970	95	2	381	9	1683	32	0.24	0.00	2798	6.9	-7.4
HM25734_20	180	124800	30670	9980	172100	5100	788000	0.79000	0.17120	0.09190	0.00	5.44	0.06	0.08	0.00	0.36	15.44	0.33	1501	34	1706	16	1859	46	89810	9900	318	7	169	4	533	17	1.43	0.04	1859	8.2	-9.0
HM25734_14	330	46500	5470	12700	145500	1730	271000	0.59000	0.63000	0.13770	0.00370	0.19	3.24	0.04	0.13	0.01	NaN	34.70	1.80	1302	21	1775	31	1788	43	87900	18000	318	5	76	3	135	10	1.43	0.04	1788	8.2	-9.0
HM25734_55	221	202500	41890	28400	353000	3270	1052000	3.51000	0.63000	0.20770	0.00	4.82	0.04	0.09	0.00	0.36	12.12	0.75	1647	10	1815	38	1820	30	112000	8900	295	8	188	4	508	22	1.51	0.01	1815	8.7	-8.3
HM25734_46	780	823800	161000	63100	1053000	9980	1552000	3.30000	0.47720	0.06240	0.00	4.23	0.03	0.09	0.00	0.20	11.38	0.30	1593	12	1489	12	1594	15	143000	8900	386	5	277	5	1357	33	3.51	0.07	1594	8.0	-8.6
HM25734_41	415	132800	11170	29400	206200	1400	197300	3.63000	0.51100	0.06410	0.00	4.15	0.02	0.11	0.00	0.28	14.98	0.37	1502	21	1495	15	1485	15	143000	8800	466	2	165	2	887	17	3.21	0.11	1485	8.0	-8.7
HM25734_24	236	54100	6710	13400	331000	3650	507300	4.20000	1.40000	0.38210	0.00	3.05	0.03	0.11	0.00	0.32	15.64	0.33	1501	34	1706	16	1859	46	89810	9900	318	7	169	4	533	17	3.21	0.11	1859	8.2	-9.0
HM25734_9	0	54100	6710	7910	105700	937	232700	11.23000	0.29000	0.04650	0.00790	0.19	2.24	0.04	0.13	0.01	NaN	34.70	1.80	1302	21	1775	31	1788	43	87900	18000	318	5	76	3	135	10	1.43	0.04	1788	8.2	-9.0
HM25734_67	343	545400	65120	67700	866200	13160	1268000	11.67000	0.50000	0.06210	0.00	4.15	0.02	0.11	0.00	0.32	14.98	0.37	1502	21	1495	15	1485	15	143000	8800	466	2	165	2	887	17	3.21	0.11	1485	8.0	-8.7
HM25734_35	0	505900	96600	12700	96020	7820	1172000	6.79000	0.32000	0.06200	0.00	4.16	0.01	0.13	0.00	0.25	104.70	4.50	2218	29	2452	13	2494	16	208500	3200	511	5	47	1	239	12	13.89	0.25	2494	9.0	-9.9

Table C11: Zircon Geochronology results for sample 25734 Noup Sandstone (S16-067A)

Table C12: Zircon Geochronology results for sample 25736 Soberlie Sandstone (S17-044B)

	Weth erill											Tera-Wasserberg plot																				Calculated Discordance	
Sample	Hg204 CPS	Pb206 CPS	Pb207 CPS	Pb208 CPS	Th232 CPS	U235 CPS	U238 CPS	$^{207}Pb/^{235}U$	2s	$^{206}Pb/^{238}U$	2s	ErrorCorrelation_6_38vs7_35	$^{238}U/^{206}Pb$	2s	$^{207}Pb/^{206}Pb$	2s	ErrorCorrelation 38/6 vs 7/6	Final 206Pb/238U	2s	Final Age 207Pb/235U	2s	Final Age 206Pb/238U	2s	Final Age 207Pb/206Pb	2s	Final 206Pb/204Pb	2s	Approx U ppm	2s	Approx Th ppm	2s	Approx Pb ppm	2s	Final U/Th Ratio	2s	Preferred Age	6-38/7-6	6-38/7-35
HM25736_3	-168	45200	4370	11880	384000	1800	319400	1.93000	0.11000	0.15730	0.00270	0.00	6.36	0.11	0.10	0.01	0.17	4	0.45	887	33	939	15	856	92	24470	740	133.70	3.80	202.00	11.00	244.00	16.00	1.02	0.03	939	-9.7	8.8
HM25736_95	-197	93300	6400	24500	1135000	9380	1625000	0.55500	0.02700	0.06574	0.00086	-0.01	15.21	0.20	0.07	0.00	0.27	1.04	0.31	392	14	411	5	378	73	41600	1400	568.00	17.00	426.00	14.00	372.00	17.00	1.31	0.01	411	-8.7	8.0
HM25736_44	-363	105800	9610	29900	470800	3900	644300	2.25300	0.09400	0.18320	0.00220	0.14	5.46	0.07	0.09	0.00	0.01	-0.361	0.018	1066	24	1084	12	1021	60	59980	920	232.40	3.40	172.70	2.80	373.00	16.00	1.38	0.01	1084	-6.2	5.8
HM25736_23	-190	93400	8600	14470	325000	3770	609100	1.99000	0.11000	0.16330	0.00210	0.00	6.12	0.08	0.09	0.01	0.01	0.82	0.4	931	24	970	11	917	66	45530	660	224.10	2.90	134.00	6.30	183.10	9.40	2.01	0.03	970	-5.8	5.5
HM25736_21	-171	100900	8550	9910	494000	4610	691000	1.60300	0.06800	0.16310	0.00200	0.03	6.13	0.08	0.08	0.00	0.29	10.8	1	887	24	975	11	929	63	45300	1700	257.00	10.00	208.00	19.00	129.10	9.60	2.75	0.10	975	-5.0	4.7
HM25736_75	-317	96300	8380	18710	361000	2680	558600	2.41000	0.10000	0.16330	0.00220	0.01	5.17	0.06	0.09	0.00	0.08	-0.17	0.16	1100	25	1141	12	1102	59	66850	990	229.90	3.10	175.50	6.20	391.00	15.00	1.46	0.02	1141	-3.5	3.4
HM25736_111	-192	94500	8130	10010	194100	3720	499000	2.29000	0.10000	0.19470	0.00310	0.15	5.14	0.08	0.09	0.00	0.32	7.66	0.95	1105	30	1146	16	1111	57	44900	1700	174.10	8.20	67.90	3.20	126.70	6.80	2.71	0.07	1146	-3.2	3.1
HM25736_120	-393	29040	4930	6330	52900	0	58670	1743000	0.82000	0.52900	0.01600	-0.02	1.89	0.06	0.20	0.01	0.64	4.28	0.51	2872	50	2637	61	2569	86	15280	490	22.47	0.29	20.98	0.57	100.00	7.00	1.25	0.05	2569	-2.6	2.6
HM25736_146	-191	157700	17050	17540	268600	3640	635000	4.25000	0.16000	0.29420	0.00290	0.09	3.40	0.03	0.10	0.00	0.35	5	1.3	1581	29	1663	14	1627	37	101300	2700	276.30	8.60	137.60	3.90	332.00	16.00	1.96	0.08	1627	-2.2	2.2
HM25736_109	-421	128900	10600	32400	680000	5200	824000	2.01100	0.07300	0.17690	0.00180	-0.03	5.65	0.06	0.08	0.00	0.18	-0.374	0.017	1040	24	1049	10	1032	48	63300	1300	285.90	5.00	236.40	6.20	404.00	14.00	1.28	0.01	1049	-1.7	1.6
HM25736_61	-385	67000	5830	15290	317000	2110	384600	2.10800	0.09100	0.18890	0.00310	-0.01	5.29	0.09	0.09	0.00	0.38	0.19	0.2	1050	28	1107	17	1094	69	41300	970	174.70	3.20	176.40	6.90	304.00	12.00	1.13	0.02	1107	-1.2	1.2
HM25736_78	-103	65200	13130	93500	747200	8050	1259900	16.18000	0.50000	0.56350	0.00310	-0.10	1.77	0.01	0.20	0.00	0.50	-0.558	0.032	2807	30	2881	13	2856	12	379300	3200	503.70	3.80	347.80	3.70	1902.00	42.00	1.45	0.02	2856	-0.9	0.9
HM25736	260	115100	9320	14210	318000	5330	819000	1.59600	0.06100	0.15500	0.00190	-0.05	6.45	0.08	0.08	0.00	0.21	4.69	0.88	887	21	925	10	918	57	64100	1500	349.00	5.70	172.00	10.00	316.00	19.00	2.61	0.04	925	-0.8	0.8
HM25736_42	-359	137400	8050	14510	646000	14190	2095000	0.59900	0.02400	0.06992	0.00074	0.02	14.30	0.15	0.06	0.00	0.36	2.27	0.73	453	14	435	5	434	61	72900	2200	748.00	22.00	234.30	8.20	178.00	9.00	3.19	0.03	435	-0.3	0.3
HM25736_30	-180	112800	9910	15060	243400	3310	533600	2.80000	0.11000	0.23170	0.00260	-0.02	4.32	0.05	0.09	0.00	0.40	-0.01	0.29	1274	26	1344	14	1343	47	59370	810	189.10	2.40	91.70	1.50	176.50	6.90	2.11	0.02	1343	-0.1	0.1
HM25736_121	-149	31010	4600	9610	214000	628	204800	2.53000	0.22000	0.16270	0.00350	-0.02	6.15	0.13	0.15	0.03	0.01	3.27	0.37	909	37	967	19	970	130	17250	420	79.50	1.60	86.70	5.00	155.10	9.60	1.08	0.02	967	0.3	-0.3
HM25736_90	-142	242700	26520	23930	325000	5790	874000	4.83000	0.15000	0.31330	0.00250	-0.05	3.19	0.03	0.11	0.00	0.34	-0.914	0.042	1710	25	1754	12	1760	29	132800	2100	312.10	5.30	126.90	6.50	395.00	15.00	2.90	0.04	1760	0.3	-0.3
HM25736_54	-108	1082000	205800	33450	267000	14950	2327000	14.67000	0.49000	0.53310	0.00260	0.20	1.88	0.01	0.19	0.00	0.51	-2.87	0.15	2696	32	2754	11	2764	10	725000	13000	961.00	21.00	121.90	3.80	529.00	15.00	8.02	0.17	2764	0.4	-0.4
HM25736_16	-168	275900	22510	46400	949000	10610	1529000	2.24800	0.07400	0.19910	0.00140	-0.09	5.02	0.04	0.08	0.00	0.13	-0.504	0.023	1123	21	1170	8	1175	33	146600	1600	582.80	7.10	421.10	7.70	660.00	17.00	1.43	0.02	1170	0.4	-0.4
HM25736_143	-409	74800	4700	14310	689000	8210	1217500	0.59300	0.02600	0.06792	0.00093	-0.02	14.72	0.20	0.07	0.00	0.15	1.74	0.48	429	14	423	6	425	71	40780	840	562.50	2.80	384.40	8.80	295.00	14.00	1.59	0.02	423	0.5	-0.5
HM25736_151	-324	271300	19700	36300	774000	11120	1798000	1.77900	0.06000	0.16830	0.00120	0.04	5.94	0.04	0.07	0.00	0.33	-0.614	0.026	979	20	1003	7	1008	34	181000	2300	747.00	11.00	369.80	7.70	634.00	17.00	2.04	0.02	1003	0.5	-0.5
HM25736_105	-381	79900	17280	13290	112200	544	159600	18.73000	0.84000	0.53560	0.00800	0.06	1.87	0.03	0.22	0.01	0.07	2.45	0.55	2768	38	2769	33	2790	42	41340	680	54.73	0.95	39.20	2.30	167.10	8.70	1.72	0.04	2790	0.8	-0.8
HM25736_11	-350	95700	5220	10930	512000	9820	1575000	0.53100	0.02400	0.06853	0.00090	0.05	14.59	0.19	0.06	0.00	0.40	6.32	0.88	397	14	427	5	431	63	52300	1400	629.00	16.00	247.60	8.00	185.00	11.00	2.59	0.03	427	0.9	-0.9
HM25736_77	-154	90000	7600	21300	426000	3440	556000	2.20000	0.11000	0.17710	0.00320	0.00	5.65	0.10	0.09	0.00	0.15	-0.01	0.16	1020	26	1039	16	1049	65	53200	1400	224.60	6.40	201.50	8.20	388.00	15.00	1.14	0.02	1039	1.0	-1.0
HM25736_116	240	125200	11760	18600	301000	5240	842000	2.28000	0.11000	0.17550	0.00190	-0.02	5.70	0.06	0.09	0.00	0.03	2.76	0.71	1040	23	1042	10	1056	58	78000	1700	301.20	7.60	108.50	4.20	252.00	28.00	2.81	0.04	1042	1.3	-1.3
HM25736_18	-370	57100	4790	19180	394000	2080	361000	1.73700	0.07900	0.17170	0.00310	0.01	5.82	0.11	0.09	0.00	0.39	-0.127	0.086	916	28	1013	17	1027	74	26990	720	136.20	2.90	171.30	6.50	263.00	12.00	0.87	0.01	1013	1.4	-1.4
HM25736_138	-215	104500	21090	11900	98300	1410	210200	16.59000	0.66000	0.53350	0.00820	0.03	1.87	0.03	0.21	0.00	0.13	5.32	0.89	2737	36	2722	32	2761	35	66200	2400	101.20	4.10	57.80	2.40	260.00	12.00	1.91	0.06	2761	1.4	-1.4
HM25736_76	-116	83300	17490	7300	93000	504	180900	15.15000	0.55000	0.53850	0.00770	0.09	1.86	0.03	0.20	0.00	0.48	11.1	1	2713	34	2773	32	2815	35	51100	2400	73.80	3.00	44.60	5.40	192.00	9.90	3.44	0.17	2815	1.5	-1.5
HM25736_70	-355	85200	7500	26650	595000	2640	497000	2.10700	0.08200	0.18510	0.00260	-0.02	5.40	0.08	0.09	0.00	0.38	-0.282	0.014	1066	25	1095	13	1113	64	55650	960	219.60	2.90	323.00	17.00	572.00	18.00	0.85	0.01	1095	1.6	-1.6
HM25736_86	-348	324800	69130	35690	264000	3860	615900	18.79000	0.55000	0.56310	0.00440	0.03	1.78	0.01	0.22	0.00	0.46	-0.748	0.038	2979	29	2880	18	2936	18	184300	1500	224.80	1.10	106.90	2.40	628.00	17.00	2.19	0.03	2936	1.9	-1.9
HM25736_83	-442	131100	7900	1780	144500	12760	1935000	0.78300	0.03900	0.07279	0.00084	-0.02	13.74	0.16	0.06	0.00	0.14	47.2	2.5	510	17	453	5	462	62	61100	1400	739.00	18.00	62.70	1.90	34.20	4.30	11.39	0.20	453	2.0	-2.0
HM25736_35	-135	12320	20430	54700	496900	1740	302900	10.59000	0.38000	0.45880	0.00590	0.13	2.18	0.03	0.17	0.00	0.37	-0.1821	0.0091	2377	33	2429	25	2482	32	64380	950	106.40	1.60	181.40	2.80	639.00	14.00	0.58	0.01	2482	2.1	-2.2
HM25736_92	-143	69800	6930	7390	189600	3120	456900	2.16000	0.11000	0.16630	0.00250	-0.03	6.01	0.09	0.09	0.00	0.06	11.59	0.98	994	27	991	14	1016	72	35980	810	161.20	3.60	72.80	3.40	117.90	8.00	2.46	0.05	991	2.5	-2.5
HM25736_88	-169	139100	18290	71600	693000	2350	426000	6.48000	0.23000	0.36190	0.00420	0.18	2.76	0.03	0.13	0.00	0.48	-0.1653	0.007	1950	32	1990	19	2042	35	75200	1800	153.80	4.30	275.00	10.00	1222.00	47.00	0.58	0.01	2042	2.5	-2.6
HM25736_142	-407	49880	53300	30900	420000	12320	1779000	4.92000	0.17000	0.30620	0.00220	0.13	3.27	0.02	0.11	0.00	0.39	-1.487	0.067	1703	29	1721	11	1767	21	294200	5800	830.00	21.00	237.00	15.00	646.00	25.00	4.38	0.06	1767	2.6	-2.7
HM25736_148	-119	283100	25040	40100	674000	8500	1393000	3.01000	0.10000	0.22950	0.00170	0.01	4.36	0.03	0.09	0.00	0.14	-0.581	0.027	1305	24	1332	9	1368	31	194500	2500	595.30	9.00	336.00	10.00	736.00	20.00	1.87	0.02	1368	2.7	-2.7
HM25736_27	-152	1426000	232400	26150	399000	22070	3310000	10.59000	0.36000	0.45980	0.00270	0.26	2.17	0.01	0.16	0.00	0.33	-4.84	0.45	2421	33	2434	12	2501	10	1190000	11000	1183.00	24.00	154.00	14.00	1220.00	31.00	12.74	0.34	2501	2.7	-2.8
HM25736_133	-102	1624000	296200	169100	1371000	22850	3556000	13.61000	0.45000	0.50370	0.00230	0.01	1.99	0.01	0.19	0.00	0.38	-0.6135	0.0076	2630	31	2629	10	2704	10	1128000	11000	1732.00	20.00	809.00	15.00	3752.00	51.00	2.23	0.02	2704	2.8	-2.9
HM25736_157	-347	281400	54060	105900	1104000	3810	603200	14.78000	0.50000	0.52200	0.00430	0.09	1.92	0.02	0.20	0.00	0.54	-0.1729	0.003	2705	33	2704	18	2784	18	169900	1900	232.30	2.50	462.70	8.00	1551.00	25.00	0.51	0.00	2784	2.9	-3.0
HM25736_63	-363	116000	8370	15320	493000	7340	1266000	1.56200	0.08900	0.12530	0.00300	0.62	7.98	0.19	0.08	0.00	0.09	0.7	0.46	817	33	756	17	781	58	81100	1000	577.00	18.00	278.00	13.00	314.00	14.00	2.28	0.03	756	3.2	-3.3
HM25736_64	-365	74700	13090	17260	196000	534	177300	11.63000	0.44000	0.46650	0.00720	0.16	2.14	0.03	0.19	0.01	0.32	-0.16	0.14	2459	38	2465	32	2547	42	51340	780	80.70	1.40	110.60	8.50	358.00	15.00	1.04	0.02	2547	3.2	-3.3
HM25736_50	-387	593400	133600	87500	720600	7540	1104000	18.64000	0.61000	0.57360	0.00330	-0.01	1.74	0.01	0.23	0.00	0.41	-0.802	0.076	2940	33	2921	14	3019	12	347400	3700	432.50	5.30	299.30	2.50	1261.00	30.00	1.48	0.02	3019	3.2	-3.4
HM25736_73	-334	60300	6120	23590	330000	790	271400	3.20000	0.13000	0.24020	0.00370	-0.03	4.16	0.06	0.11	0.00	0.50	-0.213	0.035	1360	30	1383	19	1430	70	40270	720	113.80	1.90	165.30	4.10	499.00	19.00	0.71	0.01	1430	3.3	-3.4
HM25736_33	-348	234900	22320	46400	673000	6210	1037000	3.35000	0.12000	0.25570	0.00210	0.01	3.91	0.03	0.10	0.00	0.48	-0.397	0.017	1404	25	1467	11	1517	32	120800	3700	365.00	11.00	248.30	4.00	541.00	15.00	1.39	0.03	1517	3.3	-3.4
HM25736_20	-143	177600	21610	16000	186000	3520	582400	5.57000	0.19000	0.33590	0.00370	-0.02	2.98	0.03	0.13	0.00	0.23	1.49	0.75	1825	28	1866	17	1930	34	81000	1700	217.40	2.90	79.20	4.90	212.00	11.00	3.52	0.07	1930	3.3	-3.4
HM25736_123	60	232700	44280	53100	467000	2520	877900	15.58000	0.57000	0.52980	0.00530	0.33	1.89	0.02	0.21	0.00	0.25	-0.308	0.013	2784	35	2731	23	2827	24	136800	2600	191.00	2.90	197.10	5.30	900.00	23.00	1.08	0.01	2827	3.4	-3.5
HM25736_147	-329	295500	59300	2330	34100	3620	605000	15.76000	0.51000	0.53420	0.00410	-0.05	1.87	0.01	0.21	0.00	0.28	124.9	4.2	2769	31	2754	17	2851	18	199500	1700	260.90	1.60	17.20	2.90	43.40	6.00	-109700000.00	990000.00	2851	3.4	-3.5
HM25736_94	-201	148200	26610	51700	412600	1920	340600	12.54000	0.44000	0.48290	0.00570	0.09	2.07	0.02	0.19	0.00	0.28	-0.2215	0.0074	2546	34	2541	24	2641	29	73570	920	119.50	1.80	156.10	3.60	797.00	18.00	0.78	0.01	2641	3.8	-3.9
HM25736_38	-368	111300	21030	10620	148000	1570	250200	12.94000	0.45000	0.49690	0.00670	0.11	2.01	0.03	0.19	0.00	0.35	9	1.1	2569	33	2600	27	2704	31	56400	1300	88.20	2.10	53.20	6.20	126.70	7.20	3.48	0.14	2704	3.8	-4.0
HM25736_160	-164	197700	40440	58200	444000	2250	416500	15.62000	0.54000	0.53260	0.00510	0.12	1.88	0.02	0.21	0.00	0.26	-0.2367	0.0055	2771	33	2749	22	2859	22	117500	1400	156.80	2.20	78.30	4.20	797.00	17.00	0.93	0.01	2859	3.8	-4.0
HM25736_34	-352	171800	17430	36400	551000	4170	685300	4.00000	0.14000	0.27550	0.00290	0.05	3.63	0.04	0.11	0.00	0.36	-0.409	0.022	1549	28	1566	14	1629	37	91700	1500	241.00	2.20	202.20	3.70	425.00	12.00	1.25	0.02	1629	3.9	-4.0
HM25736_28	-349	956000	180000	146200	1144000	13590	2199000	12.80000	0.33000	0.50330	0.00390	-0.38	1.99	0.02	0.19	0.00	0.17	-0.4502	0.0099	2595	26	2628	17	2734	11	505600	7600	784.00	11.00	437.60	7.80	1725.00	42.00	1.83	0.04	2734	3.9	-4.0
HM25736_113	-362	135200	13680	18100	300000	4000	606000	3.40000	0.13000	0.24500	0.00290	0.10	4.08	0.05	0.10	0.00	0.43	3.45	0.73	1413	30	1409	15	1476	43	68500	2500	213.20	8.80	106.00	7.30	235.00	13.00	2.52	0.04	1476	4.5	-4.8
HM25736_62	-369	829000	237400	106500	866000	8260	1352000	31.10000	1.44000	0.65310	0.00600	0.60	1.53	0.01	0.29	0.00	-0.07	-0.771	0.051	3293	49	3234	24	3397	18	560700	8100	615.00	13.00	486.10	7.00	2153.00	64.00	1.30	0.03	3397	4.8	-5.0
HM25736_117	-152	77300	7220	10550	301000	3320	491000	1.96300	0.08500	0.16890	0.00240	-0.02	5.92	0.08	0.09	0.00	0.24	8.47	0.87	1002	26	1004	13	1055	71	45000	1100	177.00	4.40	110.00	11.00	145.90	9.90	2.67	0.07	1004	4.8	-5.1
HM25736_36	-389	67400	13590	40200	305000	434	148700	14.28000	0.56000	0.49600	0.00740	0.07	2.02	0.03	0.21	0.01	0.24	-0.1415	0.0064	2600	35	2591	32	2723	43	33550	530	52.24	0.88	109.90	2.70	475.00	12.00	0.49	0.01	2723	4.8	-5.1
HM25736_45	-372	102200	6180	30720	1583000	9520	1538200	0.57900	0.02100	0.07113	0.00079	-0.02	14.06	0.16	0.06	0.00	0.24	-0.288	0.014	444	14	443	5	466	65	56590	710	558.40	2.10	585.10	5.50	388.00	11.00	0.98	0.01	443	5.0	-5.3
HM25736_150	-105	540400	130200	16700	506000	6270	1049000	21.72000	0.83000	0.58380	0.00420	0.45	1.71	0.01	0.25	0.00	0.21	21.5	4.1	3028	38	2966	17	3135	14	373100	5800	440.00	10.00	245.30	9.00	296.00	22.00	1.95	0.05	3135	5.4	-5.7
HM25736_124	-367	98200	19220	105200	1103000	13400	2127000	14.40000	0.48000	0.50860	0.00260	0.11	1.97	0.01	0.20	0.00	0.36	-0.5999	0.0096	2694	32	2650	11	2806	11	601700	8300	863.00	14.00	477.00	11.00	1828.00	33.00	1.90	0.02	2806	5.6	-5.9
HM25736_108	-231	338600	65000	69100	743000	4390	812000	13.47000	0.49000	0.49440	0.00450	0.39	2.02	0.02	0.20	0.00	0.26	-0.394	0.017	2653	35	2591	20	2750	19	160700	3500	280.80	5.70	257.90	9.30	857.00	25.00	1.16	0.02	2750	5.8	-6.1
HM25736_29	-219	32740	6270	7200	117000	333	82500	11.84000	0.54000	0.46800	0.01300	0.04	2.14	0.06	0.23	0.01	0.68	6.63	0.51	2413	46	2374	52	2520	81	16340	450	29.30	1.10	44.60	5.90	84.60	5.90	1.72	0.08	2520	5.8	-6.1
HM25736_125	-372	32260	58420	51300	569000	4420	766000	12.63000	0.41000	0.47370	0.00420	-0.05	2.11	0.02	0.19	0.00	0.29	0.5	0.022	2587	31	2510	17	2670	19	197800	2500	315.70	4.20	251.90	8.40	912.00	21.00	1.36	0.02	2670	6.0	-6.4
HM25736_89	-352	72700	15940	10840	216000	2220	413300	2.79000	0.14000	0.19260	0.00310	-0.03	5.19	0.08	0.11	0.01	0.25	4.89	0.72	1143	29	1127	16	1200	76	38060	790	148.30	2.30	85.00	6.40	181.90	9.20	2.07	0.04	1127	6.1	-6.5
HM25736_55	-358	148100	15210	39040	553000	3650	588100	4.13000	0.14000	0.27670	0.00340	0.04	3.61	0.04	0.11	0.00	0.51	-0.312	0.016	1574	28	1582	16	1685	37	100300	1300	246.10	1.80	258.90	4.90	635.00	16.00	1.02	0.01	1685	6.1	-6.5
HM25736_74	-321	205900	18760	7440	101100	6280	1046500	2.94000	0.10000	0.21940	0.00190	-0.11	4.56	0.04	0.10	0.00	0.05	36.5	3	1283	22	1277	10	1362	38	139800	1700	434.90	3.80	49.89	0.96	157.00	10.00	8.70	0.16	1362	6.2	-6.7
HM25736_82	-269	42400	4540	12600	255000	1930	322900	1.75100	0.09900	0.14300	0.00250	0.01	6.99	0.12	0.11	0.01	0.76	3.25	0.4	828	31	862	14	920	110	18500	590	124.50	3.10	112.30	4.40	246.00	21.00	1.16	0.02	862	6.3	-6.7
HM25736_26	-346	280900	22990	5420	155000	10550	1720000	11.45000	0.42000	0.46050	0.00160	0.47	5.33	0.05	0.08	0.00	0.15	84.6	4.6	3101	29	3107	9	1184	33	513300	2400	521.00	17.00	60.30	1.60	372.00	9.60	32.00	2.20	1107	6.5	-6.9
HM25736_41	-359	72800	6820	9900	216000	2090	354300	2.77000	0.11000	0.22500	0.00340	0.10	4.44	0.07	0.10	0.00	0.61	6.46	0.8	1260	28	1308	18	1400	63	40530	760	126.00	2.80	78.10	6.10	120.40	6.70	2.30	0.06	1400	6.6	-7.0
HM25736_17	-364	66700	13040	36700	296400	506	150400	13.03000	0.48000	0.48910	0.00830	0.05	2.04	0.03	0.20	0.01	0.35	-0.1616	0.0081	2566	35	2551	33	2735	40	34430	560	57.04	0.99	130.20	3.40	511.00	15.00	0.45	0.01	2735	6.7	-7.2
HM25736_71	-373	315400	94600	26640	250500	2640	535800	28.69000	0.98000	0.65710	0.00570	0.20	1.52	0.01	0.30	0.00	0.12	-1.097	0.05	3394	37	3248	22	3483	16	195600	3000	235.00	3.20	134.30	2.90

Table C13: Zircon Geochronology results for sample 25733 Sneug Sandstone (S16-054A)

												Tera-Wasserburg plot																		Calculated Discordance	
								Wetherill																							
Sample	Hg204 CPS	Pb206 CPS	Pb207 CPS	Pb208 CPS	Th232 CPS	U235 CPS	U238 CPS	$^{207}Pb/^{235}U$	2σ	$^{206}Pb/^{238}U$	2σ	Error Correlation 6_38vs 7_35	$^{208}U/^{206}Pb$	2σ	$^{207}Pb/^{206}Pb$	2σ	Error Correlation 38/6 vs 7/6	Final 206Pb/238U	2σ	Final Age 207Pb/235U	2σ	Final Age 206Pb/238U	2σ	Final Age 207Pb/206Pb	2σ	Final 206Pb/204Pb	2σ	Approx U ppm	2σ	Approx Th ppm	2σ	Approx Pb ppm	2σ	Final U/Th Ratio	2σ	Preferred Age	6-38/7-6	6-38/7-35
HM25733_11	-161	134600	10970	25210	451300	5990	872000	1.77000	0.13000	0.16840	0.00200	-0.01	5.94	0.07	0.08	0.00	0.33	-0.63	0.09	1031	17	1001	11	911	52	75600	1500	338.80	5.20	218.70	3.00	442.00	16.00	1.68	0.02	1001	-9.9	9.0
HM25733_51	-172	140700	11940	21500	351300	5170	737000	2.41000	0.12000	0.20410	0.00250	0.03	4.90	0.06	0.08	0.00	0.45	0.17	0.40	1235	17	1193	14	1094	50	96900	2400	361.80	9.40	221.40	5.50	417.00	16.00	1.65	0.02	1193	-9.0	8.3
HM25733_82	-233	48200	5250	6490	73000	1330	203300	4.02000	0.24000	0.26330	0.00550	-0.01	3.80	0.08	0.12	0.00	0.18	8.40	0.67	1511	34	1491	28	1368	80	25910	660	76.40	2.10	32.53	0.87	103.30	6.70	2.72	0.11	1368	-9.0	8.2
HM25733_24	-186	188900	14860	20600	371000	7570	1137000	1.98000	0.19000	0.17920	0.00170	0.07	5.58	0.05	0.08	0.00	0.35	8.20	1.40	1087	15	1062	9	979	46	126600	3100	480.60	9.60	195.40	9.00	374.00	19.00	4.64	0.41	1062	-8.5	7.8
HM25733_7	170	152500	12160	14900	254600	7910	1238000	1.75400	0.08300	0.16450	0.00230	0.03	6.08	0.08	0.08	0.00	0.42	4.75	0.87	1018	18	979	13	905	54	81200	3500	494.00	27.00	127.20	3.40	263.00	12.00	3.68	0.19	979	-8.2	7.6
HM25733_48	-151	203600	16330	13800	256700	8840	1232000	2.11000	0.12000	0.18630	0.00180	0.02	5.37	0.05	0.08	0.00	0.41	12.40	1.70	1151	16	1099	10	1031	46	132500	4400	608.00	21.00	163.20	6.00	269.00	14.00	3.77	0.05	1099	-6.6	6.2
HM25733_1	-146	167500	14310	25580	429000	6340	930200	2.26000	0.13000	0.19800	0.00230	0.04	5.05	0.06	0.08	0.00	0.46	-0.91	0.04	1201	15	1162	12	1094	43	106200	1100	395.50	2.60	229.30	2.40	458.00	16.00	1.68	0.02	1162	-6.2	5.9
HM25733_75	-220	99880	9070	18720	278900	3570	476000	2.90000	0.18000	0.22340	0.00300	0.01	4.48	0.06	0.09	0.00	0.30	0.60	0.38	1335	22	1294	16	1219	57	59500	1200	188.40	2.90	132.90	2.40	310.00	12.00	1.42	0.02	1219	-6.2	5.8
HM25733_92	-251	79900	7670	14470	188800	2200	357800	3.30000	0.16000	0.24130	0.00360	0.03	4.14	0.06	0.10	0.00	0.51	3.68	0.65	1439	24	1387	19	1312	64	40100	820	124.80	2.20	76.80	1.30	217.60	9.60	1.71	0.03	1312	-5.7	5.4
HM25733_123	-198	102600	8110	30600	596000	4840	708000	1.71000	0.33000	0.15950	0.00210	-0.01	6.27	0.08	0.08	0.00	0.32	-0.45	0.04	976	20	951	12	900	67	63600	1500	305.60	5.10	304.40	5.50	494.00	16.00	0.96	0.02	951	-5.7	5.4
HM25733_3	-167	145600	13710	22030	327400	5210	734000	2.76000	0.19000	0.22240	0.00250	0.03	4.50	0.05	0.09	0.00	0.09	-0.21	0.31	1330	18	1293	13	1226	48	80500	1800	304.90	4.90	170.80	3.20	393.00	15.00	1.79	0.02	1226	-5.5	5.2
HM25733_44	-178	304300	25050	37000	608000	11530	1646000	2.34400	0.09800	0.20390	0.00190	0.05	4.90	0.05	0.08	0.00	0.57	-1.12	0.09	1239	13	1195	10	1134	35	226700	5500	814.00	18.00	387.00	10.00	721.00	23.00	2.09	0.02	1195	-5.4	5.1
HM25733_95	-60	58200	6150	7690	91400	1500	240000	4.06000	0.28000	0.26480	0.00480	0.01	3.78	0.07	0.11	0.00	0.49	8.58	0.77	1550	29	1501	24	1430	73	27810	680	83.00	1.80	36.78	0.96	114.70	7.00	2.54	0.05	1430	-5.0	4.7
HM25733_43	-112	54900	5790	20480	300300	2340	342000	2.61000	0.25000	0.19890	0.00380	0.03	5.03	0.10	0.10	0.00	0.28	0.55	0.22	1212	34	1163	20	1108	89	40700	1700	168.90	8.60	190.60	5.60	399.00	19.00	0.73	0.02	1163	-5.0	4.7
HM25733_27	-98	283000	31400	17400	206000	7080	1110000	4.84000	0.25000	0.31300	0.00320	0.02	3.19	0.03	0.11	0.00	0.46	12.70	1.70	1784	17	1751	16	1669	37	178000	11000	48.30	32.00	112.00	6.90	320.00	22.00	3.74	0.06	1669	-4.9	4.7
HM25733_6	-214	251300	21000	14230	284700	10320	1522000	2.17000	0.29000	0.18270	0.00150	0.03	5.47	0.04	0.08	0.00	0.08	12.70	2.20	1124	13	1080	8	1035	39	144400	1500	613.10	6.50	143.60	3.10	252.00	11.00	4.54	0.06	1080	-4.3	4.2
HM25733_15	-103	286800	22410	43500	833000	13910	1912000	1.69000	0.18000	0.16400	0.00140	-0.06	6.10	0.05	0.08	0.00	0.11	-0.83	0.04	1007	13	978	8	942	40	173000	3700	739.10	8.90	400.50	6.10	765.00	22.00	1.97	0.02	978	-3.8	3.7
HM25733_90	150	41670	3280	7170	171800	4340	640000	0.49000	0.02000	0.07020	0.00140	-0.02	14.25	0.28	0.08	0.01	0.12	8.94	0.59	443	20	436	8	420	100	20810	570	225.20	3.10	70.60	2.00	108.00	10.00	3.60	0.07	436	-3.8	3.6
HM25733_142	380	89200	8760	10800	142300	4100	598900	2.08000	0.40000	0.16100	0.00230	-0.10	6.21	0.09	0.10	0.01	0.12	16.30	1.30	979	22	958	13	927	76	64500	1500	267.90	3.70	77.70	2.10	182.00	24.00	3.64	0.07	958	-3.3	3.2
HM25733_34	-240	226900	18630	13180	229500	11200	1748000	2.12600	0.09200	0.18420	0.00430	0.12	5.43	0.13	0.08	0.00	0.23	9.20	1.80	1115	23	1077	24	1047	52	141900	6800	813.00	41.00	134.80	2.40	249.00	11.00	5.81	0.32	1077	-2.9	2.8
HM25733_65	-177	140400	12120	21510	342000	4770	753000	2.40000	0.21000	0.19410	0.00280	-0.01	5.15	0.07	0.09	0.00	0.30	1.64	0.49	1185	23	1139	15	1113	63	90100	3400	334.00	10.00	188.40	5.80	388.00	16.00	1.72	0.02	1139	-2.3	2.3
HM25733_111	-252	52300	5550	7350	101500	1390	233100	3.78000	0.18000	0.24930	0.00480	0.01	4.01	0.08	0.11	0.00	0.41	9.25	0.76	1482	31	1421	25	1394	75	28160	700	88.60	2.40	44.80	1.70	112.60	7.70	2.10	0.05	1394	-1.9	1.9
HM25733_67	-211	228400	25700	21400	225000	6000	863000	4.89000	0.31000	0.30920	0.00390	-0.01	3.23	0.04	0.11	0.00	0.39	4.58	0.86	1773	20	1723	19	1691	42	143900	6500	376.00	17.00	121.20	5.50	380.00	25.00	2.99	0.05	1691	-1.9	1.9
HM25733_87	-173	44400	4850	16530	207300	1210	202700	3.51000	0.20000	0.23520	0.00460	0.00	4.25	0.08	0.12	0.01	0.19	1.06	0.26	1409	33	1351	24	1327	84	23260	620	72.40	1.60	86.80	1.90	253.00	12.00	0.87	0.01	1327	-1.8	1.8
HM25733_14	-143	121200	13080	20240	237400	3540	502000	3.95000	0.25000	0.27040	0.00360	-0.01	3.70	0.05	0.11	0.00	0.33	-0.26	0.25	1597	19	1537	18	1513	48	73400	1700	193.70	4.80	113.80	1.70	355.00	13.00	1.80	0.03	1513	-1.6	1.6
HM25733_32	-179	147900	11660	23000	447000	6710	953000	1.78100	0.05200	0.15950	0.00220	0.02	6.27	0.09	0.08	0.00	0.27	1.15	0.45	1015	18	954	12	941	66	96000	4000	436.00	15.00	257.10	7.50	430.00	20.00	1.51	0.02	954	-1.4	1.4
HM25733_22	-180	86800	8260	22340	254500	4110	610000	2.99000	0.18000	0.21700	0.00580	0.10	4.61	0.12	0.10	0.00	0.23	2.91	0.60	1301	31	1243	31	1231	65	46300	1200	246.00	10.00	127.70	3.80	399.00	17.00	9.40	1.60	1231	-1.0	1.0
HM25733_12	55	275900	29330	50200	632700	7730	1089000	3.94000	0.25000	0.27950	0.00250	0.05	3.58	0.03	0.10	0.00	0.22	-0.68	0.04	1635	14	1586	13	1572	31	167900	1600	418.80	4.60	303.00	4.20	880.00	23.00	1.49	0.01	1572	-0.9	0.9
HM25733_53	-188	101500	8980	12730	201600	3660	549100	2.45000	0.24000	0.19340	0.00240	-0.04	5.17	0.06	0.09	0.00	0.31	5.40	1.00	1192	22	1137	13	1128	63	71600	2000	268.00	4.70	126.00	1.70	246.00	11.00	2.06	0.04	1137	-0.8	0.8
HM25733_136	-223	244600	45300	49300	341800	3090	511000	13.73000	0.82000	0.51760	0.00490	-0.04	1.93	0.02	0.19	0.00	0.50	-0.71	0.12	2722	15	2682	21	2664	23	155600	4800	232.40	5.70	188.30	4.70	829.00	26.00	1.49	0.07	2664	-0.7	0.7
HM25733_58	-186	104100	10280	14830	245000	4320	693000	3.28000	0.13000	0.23100	0.00510	0.11	4.33	0.10	0.10	0.00	0.22	2.69	0.52	1398	28	1326	27	1318	66	70700	3300	331.00	30.00	148.80	7.30	282.00	13.00	1.80	0.05	1318	-0.6	0.6
HM25733_134	-146	165700	17030	53000	685000	4160	681000	4.14000	0.24000	0.27820	0.00300	0.00	3.59	0.04	0.10	0.00	0.43	-0.40	0.02	1629	17	1577	15	1570	39	107100	3100	310.60	8.90	376.80	9.00	888.00	26.00	0.77	0.01	1570	-0.4	0.4
HM25733_57	-142	413600	47920	52500	537000	9560	1366000	5.48000	0.31000	0.32630	0.00250	0.01	3.06	0.02	0.11	0.00	0.38	-1.01	0.04	1881	12	1817	12	1822	23	288000	5300	655.80	9.50	328.10	5.60	1002.00	26.00	1.93	0.02	1822	0.3	-0.3
HM25733_97	-172	163200	9820	17830	818000	18240	2606000	0.52000	0.01000	0.06794	0.00056	0.01	14.72	0.14	0.06	0.00	0.09	2.15	0.76	453	10	424	4	425	53	83800	1800	899.00	14.00	327.60	6.50	264.00	11.00	2.89	0.02	424	0.3	-0.3
HM25733_20	-168	226000	42690	38600	272800	3100	487200	12.20000	2.70000	0.50510	0.00460	0.03	1.98	0.02	0.18	0.00	0.38	-0.75	0.04	2678	15	2626	20	2635	25	123900	2600	193.60	2.60	134.70	2.30	685.00	19.00	1.47	0.02	2635	0.3	-0.3
HM25733_80	-183	249000	25500	12520	155800	7700	1190000	3.76000	0.23000	0.26090	0.00370	0.01	3.83	0.05	0.10	0.00	0.39	4.02	0.93	1562	22	1489	19	1495	52	141200	8800	454.00	28.00	70.70	1.80	201.50	9.70	5.14	0.27	1495	0.4	-0.4
HM25733_62	-151	207400	19500	15940	187200	7430	1076000	3.47000	0.27000	0.24430	0.00360	-0.03	4.09	0.06	0.10	0.00	0.14	13.20	2.50	1480	19	1402	19	1410	41	133700	4100	490.00	21.00	106.50	3.00	292.00	14.00	7.10	0.55	1410	0.6	-0.6
HM25733_121	-203	226800	17130	16370	354900	10360	1490000	1.78700	0.08300	0.16070	0.00150	0.01	6.22	0.06	0.08	0.00	0.30	14.30	2.50	1013	13	961	8	966	42	142100	3300	634.10	6.60	178.10	4.30	262.00	13.00	4.18	0.14	961	0.6	-0.6
HM25733_60	-178	110400	6870	43100	2016000	12300	1706000	0.64100	0.02300	0.06953	0.00087	0.01	14.38	0.18	0.06	0.00	0.35	-0.28	0.07	472	12	433	5	440	64	73400	2000	789.00	17.00	1172.00	34.00	800.00	29.00	0.73	0.01	433	1.6	-1.6
HM25733_28	-171	130200	9350	37700	747000	9480	1324000	1.11800	0.03700	0.11250	0.00230	0.18	8.89	0.18	0.07	0.00	0.02	-0.49	0.11	721	17	684	13	697	60	85700	2000	583.00	12.00	411.00	14.00	696.00	28.00	2.58	0.18	684	1.9	-1.9
HM25733_110	-288	460400	81700	35160	272300	7530	1044000	12.57000	0.45000	0.48940	0.00390	0.00	2.04	0.02	0.18	0.00	0.29	-1.63	0.08	2565	17	2616	17	2577	25	254600	3100	393.50	6.80	119.20	2.30	537.00	15.00	3.11	0.04	2616	1.9	-2.0
HM25733_146	-185	211800	22750	24450	285500	5960	834000	4.17000	0.28000	0.27940	0.00260	0.02	3.58	0.03	0.11	0.00	0.17	-0.95	0.22	1651	16	1583	13	1618	36	139600	3000	357.50	5.70	149.50	3.20	409.00	16.00	2.37	0.03	1618	2.2	-2.2
HM25733_153	-200	195000	39500	42400	322000	2810	445000	14.14000	0.65000	0.50540	0.00690	0.01	1.98	0.03	0.19	0.00	0.39	-0.33	0.08	2708	21	2624	30	2683	37	115800	8600	18.40	14.00	160.80	6.30	694.00	30.00	0.86	0.04	2683	2.2	-2.2
HM25733_145	-194	80700	13980	6400	46700	1140	201800	11.69000	0.53000	0.45990	0.00760	0.00	2.17	0.04	0.18	0.00	0.43	16.80	1.10	2527	23	2420	34	2482	45	53100	1500	87.00	3.00	24.60	1.40	107.20	9.10	-33000.00	19000.00	2482	2.5	-2.6
HM25733_69	-166	80700	8770	23100	254300	2290	391000	4.36000	0.20000	0.27260	0.00510	0.05	3.67	0.07	0.11	0.00	0.26	0.22	0.34	1652	25	1540	26	1580	60	49200	1800	167.50	8.20	133.80	2.50	406.00	15.00	1.52	0.11	1580	2.5	-2.6
HM25733_18	-199	298300	31370	91300	1201000	8280	1254000	3.90000	0.18000	0.26800	0.00240	0.02	3.73	0.03	0.10	0.00	0.56	-0.41	0.02	1610	15	1530	12	1577	32	175400	5800	49.20	15.00	585.00	22.00	1613.00	61.00	0.95	0.01	1577	3.0	-3.1
HM25733_16	-149	53100	3960	2800	23900	6060	925000	0.57000	0.12000	0.06300	0.00100	0.33	15.87	0.25	0.07	0.00	0.07	20.32	0.75	426	17	393	6	405	87	32430	820	35.90	5.50	11.50	1.20	49.20	9.20	-8800000.00	8800000.00	393	3.0	-3.1
HM25733_25	-133	114400	13840	15530	170100	2620	410900	5.00000	0.26000	0.30550	0.00440	0.01	3.27	0.05	0.12	0.00	0.41	4.25	0.89	1809	20	1710	22	1766	47	77400	1700	17.50	4.20	90.50	3.30	283.00	13.00	1.90	0.03	1766	3.2	-3.3
HM25733	-125	223000	52680	37600	232300	2740	451300	17.90000	0.74000	0.56410	0.00610	0.05	1.77	0.02	0.23	0.00	0.41	-0.76	0.03	3005	12	2876	25	2976	21	132400	2900	194.30	3.60	125.80	2.20	676.00	20.00	1.47	0.02	2976	3.4	-3.5
HM25733_29	-122	485900	92700	90700	647800	7170	1035000	13.08000	0.88000	0.49510	0.00320	-0.01	2.02	0.01	0.19	0.00	0.05	-0.59	0.01	2701	10	2590	14	2681	17	315100	6500	459.80	3.50	360.50	4.90	1678.00	35.00	1.20	0.01	2681	3.4	-3.5
HM25733_17	-90	1029600	117600	19120	220600	26470	3688000	4.65000	0.30000	0.30300	0.00170	0.04	3.30	0.02	0.11	0.00	0.32	27.80	6.80	1784	9	1704	8	1766	16	598000	12000	143.80	16.00	106.90	2.80	337.00	15.00	15.67	0.30	1766	3.5	-3.6
HM25733_81	-183	194400	18820	27500	380500	5790	875000	3.33000	0.22000	0.24160	0.00230	0.02	4.14	0.04	0.10	0.00	0.40	-0.74	0.13	1468	16	1393	12	1444	39	103800	2500	331.10	6.20	171.10	3.20	440.00	15.00	1.85	0.02	1444	3.5	-3.7
HM25733_124	-220	57680	6340	14610	165900	1590	273500	3.20000	1.20000	0.23090	0.00380	-0.01	4.33	0.07	0.11	0.00	0.07	3.79	0.60	1383	32	1329	20	1378	79	34310	770	118.98	0.69	85.50	1.30	237.00	14.00	1.37	0.02	1378	3.6	-3.7
HM25733_144	-175	377400	32410	51300	618000	15070	2194000	2.83000	0.10000	0.21430	0.00310	0.12	4.67	0.07	0.09	0.00	0.01	-1.50	0.12	1334	18	1246	16	1293	32	244900	5800	949.00	28.00	327.00	10.00	861.00	33.00	5.87	0.40	1293	3.6	-3.8
HM25733_23	-197	1885000	107800	3343000	184400000	251000	34830000	0.44100	0.03400	0.05844	0.00025	-0.08	17.11	0.07	0.05	0.00	0.23	-0.05	0.00	395	5	366	2	380	18	106400	15000	141900.00	180.00	93300.00	1100.00	59870.00	570.00	0.15	0.00	366	3.7	-3.8
HM25733_68	-175	369900	30870	12930	190300	1495	214400	2.36000	0.16000	0.19500	0.00180	0.03	5.13	0.05	0.08	0.00	0.25	23.40	3.40	1222	14	1147	10	1195	33	227600	7200	926.00	28.00	101.30	2.60	229.00	14.00	8.59	0.16	1147	4.0	-4.2
HM25733_37	-155	140500	16490	26250	292000	3570	533000	4.96000	0.29000	0.29540	0.00400	-0.05	3.39	0.05	0.12	0.00	0.12	-0.68	0.12	1786	17	1665	20	1737	43	97400	2200	85.40	5.60	180.40	3.50	505.00	17.00	1.36	0.02	1737	4.1	-4.3
HM25733_73	-228	85000	16110	25710	188000	1110	199300	12.62000	0.50000	0.47410	0.00730	0.00	2.11	0.03	0.19	0.00	0.58	-0.40	0.06	2625	21	2482	32	2597	41	46100	1400	80.10	3.10	91.40	1.90	432.00	14.00	0.86	0.02	2597	4.4	-4.6
HM25733_79	15	149100	15750	31910	409200	4130	608000	4.05000	0.17000	0.26690	0.00320	0.01	3.75	0.04	0.11	0.00	0.47	-0.56	0.04	1619	18	1522	16	1594	43	89200	2100	233.60	5.90	187.40	3.20	516.00	15.00	1.19	0.02	1594	4.5	-4.7
HM25733_35	-221	49700	3170	1630	13130	5410	778000	0.91000	0.67000	0.06740	0.00120	-0.02	14.84	0.26	0.10	0.02	0.89	25.28	0.84	428	18	419	7	440	140	30710	920	364.70	7.20	7.79	0.39	30.90	8.30	-7150000.00	810000.00	419	4.8	-5.0
HM25733_66	-145	142300	16190	16880	190800	3580	543000	4.75000	0.27000	0.29300	0.00360	0.00	3.41	0.04	0.12	0.00	0.37	4.18	0.75	1762	20	1653	18	1743	44	89500	3000	239.80	7.70	103.80	3.70	302.00	14.00	2.66	0.11	1743	5.2	-5.4
HM25733_131	-218	260900	26350	15340	225900	7830	1160000	3.60000	0.26000	0.25180	0.00220	0.01	3.97	0.03	0.10	0.00	0.23	9.60	2.00	1533	15	1445	11	1525	33	159600	5000	52.40	17.00	122.10	3.00	254.00	11.00	4.01	0.06	1525	5.2	-5.5
HM25733_120	41	175100	33210	36100	260300	2560	416000	13.19000	0.72000	0.48740	0.00610	-0.02	2.05	0.03	0.19	0.00	0.11	-0.65	0.03	2692	15	2546	26	2688	27	106000	2500	175.40	4.50	129.50	2.10	576.00	16.00	1.24	0.02	2688	5.3	-5.6
HM25733_9	240	241800	21380	30380	458600	9870	1387000	2.33000	0.29000	0.19020	0.00160	0.14	5.26	0.04	0.09	0.00	0.16	-1.06	0.05	1190	14	1120	9	1184	40	133900	2900	545.00	5.40	225.20	4.10	534.00	16.00	2.73	0.07	1120	5.4	-5.7
HM25733_30	-198	670300	73700	56900	708000	18800	2654000	4.45000	0.14000	0.28750	0.00310	0.05	3.48	0.04	0.11	0.00	0.30	-1.50	0.06	1735	10	1624	16	1721	19	469200	4900	1190.00	25.00	398.00	10.00	1057.00	27.00	2.85	0.03	1721	5.6	-6.0
HM25733_93	-189	947000	179000	76200	589000	14580	2030000	13.36000	0.58000	0.48800	0.00290	0.08	2.05	0.01	0.19	0.00	0.34	-1.78	0.12	2706	9	2560	12	2726	12	460800	9600	70.80	7.20	238.30	6.80	1143.00	35.00	4.13	0.16	2726	6.1	-6.5
HM25733_112	-189	227500	28340	37000	368600	5580	759000	6.01000	0.26000	0.33590	0.00400	0.03	2.98	0.04	0.13	0.00	0.44	-0.77	0.04	1973	14	1864	19	1989	30	131000	2100	291.00	6.40	164.40	2.50	568.00	16.00	1.68	0.03	1989	6.3	-6.7
HM25733_13	-136	247600	49630	129800	884000	3720	551400	12.80000	1.20000	0.48450	0.00570	-0.02	2.06	0.02	0.20	0.00	0.56	-0.18	0.00	2692	14	2545	24	2721	29	147200	3600	212.20	3.10	423.10	7.10	2275.00	43.00	0.53	0.01	2721	6.5	-6.9
HM25733_36	70	35900	5890	10500	60800	1000	164600	4.50000	1.90000	0.23170	0.00550	-0.04	4.32	0.10	0.17	0.02	0.55	6.76	0.57	1331	53	1326	29	1420	140	22560	930	79.30	2.40	37.30	1.30	202.00	30.00	-6500.00	3800.00	1420	6.6	-7.1
HM25733_140	170	93700	9110	13300	211600	3840	536500	2.60000	0.33000	0.18990	0.00270	0.00	5.27	0.07	0.10	0.00	0.12	7.20